START

1 of 2

0007791

DOE/RL 82-3
Volume I

Site Characterization Report for the Basalt Waste Isolation Project

November 1982

MAR 1990
RECEIVED
EDMC

9212495051 0

Prepared by Rockwell Hanford Operations
Under Contract DE-AC06-77RLO1030

Prepared For:
U.S. Department of Energy
Assistant Secretary for Nuclear Energy
Office of Terminal Waste Disposal
and Remedial Action
Washington, D.C. 20545

THIS PAGE INTENTIONALLY
LEFT BLANK

EDMC
RECEIVED
MAR 1999

VOLUME I

CONTENTS

EXECUTIVE SUMMARY 1

CHAPTER 1. INTRODUCTION 1.1-1

1.1 Regional Setting 1.1-1
1.2 Background 1.2-1
1.3 The Hanford Site 1.3-1
1.3.1 Geographic Setting 1.3-1
1.3.2 Geologic Setting 1.3-3
1.4 Purpose and Scope. 1.4-1
1.5 Contents 1.5-1
1.5.1 Chapter 1: Introduction 1.5-1
1.5.2 Chapter 2: Decision Process for Choosing a Reference Repository Location and an Alternate Repository Location. 1.5-1
1.5.3 Chapter 3: Geologic Description of the Reference Repository Location and the Surrounding Area 1.5-1
1.5.4 Chapter 4: Geoengineering 1.5-1
1.5.5 Chapter 5: Hydrogeology 1.5-2
1.5.6 Chapter 6: Geochemistry 1.5-2
1.5.7 Chapter 7: Surface Hydrology. 1.5-2
1.5.8 Chapter 8: Climatology, Meteorology, and Air Quality. 1.5-2
1.5.9 Chapter 9: Environmental, Land-Use, and Socio-economic Characteristics 1.5-2
1.5.10 Chapter 10: Repository Design 1.5-3
1.5.11 Chapter 11: Waste Package 1.5-3
1.5.12 Chapter 12: Performance Assessment. 1.5-3
1.5.13 Chapter 13: Site Issues and Plans 1.5-3
1.5.14 Chapter 14: Geoengineering and Repository Design Issues and Plans 1.5-3
1.5.15 Chapter 15: Waste Package and Site Geochemistry Issues and Plans 1.5-4
1.5.16 Chapter 16: Performance-Assessment Issues and Plans . 1.5-4
1.5.17 Chapter 17: Site Characterization Program 1.5-4
1.5.18 Chapter 18: Quality Assurance 1.5-4
1.5.19 Chapter 19: Identification of Alternate Sites 1.5-4
1.6 References 1.5-1

CHAPTER 2. DECISION PROCESS FOR CHOOSING A REFERENCE REPOSITORY LOCATION AND AN ALTERNATE REPOSITORY LOCATION. 2.0-1

2.1 Site-Identification Methodology. 2.1-1
2.1.1 Identification of Siting Objectives and Development of Guidelines. 2.1-1
2.1.2 Screening Process. 2.1-6
2.1.3 Ranking Process. 2.1-7
2.1.4 Development of a Data Base 2.1-13
2.2 Technical Factors. 2.2-1
2.3 Environmental Factors. 2.3-1
2.4 Legal and Institutional Factors. 2.4-1
2.4.1 Federal Legal Framework. 2.4-1
2.4.2 State and Local Laws 2.4-1
2.4.3 Public Involvement 2.4-1
2.5 Decision-Making Analysis 2.5-1
2.5.1 Results of the Screening Process 2.5-1
2.5.2 Results of the Ranking Process 2.5-19
2.6 Identification of Principal Borehole/Exploratory Shaft Site. . 2.6-1
2.7 Identification of Candidate Repository Horizons. 2.7-1
2.8 References 2.8-1

CHAPTER 3. GEOLOGIC DESCRIPTION OF THE REFERENCE REPOSITORY LOCATION AND THE SURROUNDING AREA. 3.1-1

3.1 Introduction 3.1-1
3.2 Site Penetrations 3.2-1
3.2.1 Repository Feasibility and Siting Boreholes. 3.2-1
3.2.2 Site Boreholes 3.2-5
3.2.3 Status 3.2-5
3.3 Physiography and Topography. 3.3-1
3.4 Geomorphology. 3.4-1
3.4.1 Application of Geomorphic Information to Site Identification. 3.4-1
3.4.2 Geomorphology of the Reference Repository Location . . 3.4-1
3.5 Stratigraphy and Lithology 3.5-1
3.5.1 Regional Stratigraphic Framework 3.5-1
3.5.2 Relationship of Candidate Area to the Regional Framework 3.5-8
3.5.3 Surface Geology. 3.5-9
3.5.4 Stratigraphic and Lithologic Framework of the Reference Repository Location. 3.5-9
3.5.5 Future Rock Formation and Alteration 3.5-38
3.5.6 Status 3.5-39
3.6 Geophysical Studies of the Hanford Site and the Reference Repository Location. 3.6-1
3.6.1 Seismic Reflection and Refraction. 3.6-1
3.6.2 Magnetics. 3.6-3
3.6.3 Gravity. 3.6-10
3.6.4 Magnetotelluric Surveys. 3.6-13

3.6.5 Regional Heat Flow 3.6-17
3.6.6 Remote Sensing 3.6-20
3.6.7 Borehole Geophysical Logging 3.6-25
3.6.8 Status 3.6-27
3.7 Structural Geology and Tectonics 3.7-1
3.7.1 Tectonic Framework 3.7-1
3.7.2 Tectonic History 3.7-1
3.7.3 Seismicity of the Columbia Plateau 3.7-34
3.7.4 Seismicity of the Reference Repository Location. . . . 3.7-54
3.7.5 Status 3.7-55
3.8 Long-Term Regional Stability 3.8-1
3.8.1 Preliminary Deformation Rate 3.8-1
3.8.2 Synopsis of Current Tectonic Models. 3.8-2
3.8.3 Status 3.8-6
3.9 Mineral Resources. 3.9-1
3.9.1 Subsurface Mining. 3.9-1
3.9.2 Mineral-Resource Values--Reference Repository Location and Vicinity. 3.9-1
3.9.3 Assessment of Comparison Area - Columbia Plateau Region 3.9-6
3.9.4 Analysis of Resources - Relative Attractiveness of the Reference Repository Location for Mineral-Resource Exploration and Development 3.9-6
3.9.5 Status 3.9-6
3.10 Summary of Unresolved Issues 3.10-1
3.11 References 3.11-1

CHAPTER 4. GEOENGINEERING 4.0-1

4.1 Mechanical Properties of Rock Units - Continua 4.1-1
4.1.1 General. 4.1-1
4.1.2 Test Methods and Results 4.1-1
4.1.3 Discussion of Results. 4.1-7
4.1.4 Summary. 4.1-10
4.2 Mechanical Properties of Rock Units - Large Scale. 4.2-1
4.2.1 General. 4.2-1
4.2.2 Borehole Jacking Tests 4.2-2
4.2.3 Jointed Block Test 4.2-5
4.2.4 Discussion of Results. 4.2-11
4.2.5 Summary. 4.2-11
4.3 Mechanical Properties of Rock Units - Discontinua. 4.3-1
4.3.1 General. 4.3-1
4.3.2 Field Investigation. 4.3-1
4.3.3 Laboratory and In Situ Testing 4.3-2
4.3.4 Summary. 4.3-6
4.4 Thermal and Thermomechanical Properties - Laboratory Results . 4.4-1
4.4.1 General. 4.4-1
4.4.2 Results and Discussion 4.4-1
4.4.3 Summary. 4.4-4

4.5 Thermal and Thermomechanical Properties - In Situ. 4.5-1
4.5.1 General. 4.5-1
4.5.2 Full-Scale Heater Tests. 4.5-2
4.5.3 Instrumentation Performance. 4.5-8
4.5.4 Summary. 4.5-9
4.6 Stress Field 4.6-1
4.6.1 General. 4.6-1
4.6.2 Stress Measurements by Hydraulic Fracturing. 4.6-2
4.6.3 Geologic Evidence. 4.6-11
4.6.4 Summary. 4.6-11
4.7 Special Geoengineering Properties. 4.7-1
4.7.1 Potential for Rock Bursts and Sudden Collapse of Mined Openings 4.7-1
4.7.2 Potential for Thermal Degradation and Slabbing 4.7-1
4.8 Excavation Characteristics of the Rock Mass. 4.8-1
4.8.1 General. 4.8-1
4.8.2 Existing Basalt Construction Experience. 4.8-1
4.8.3 Excavation Effects on the Rock Mass. 4.8-3
4.8.4 Summary. 4.8-4
4.9 Summary of Unresolved Issues 4.9-1
4.10 References 4.10-1

CHAPTER 5. HYDROGEOLOGY 5.1-1

5.1 Regional and Site Hydrogeologic Investigations 5.1-1
5.1.1 Introduction 5.1-1
5.1.2 Rock Units 5.1-3
5.1.3 Hydrologic Characteristics 5.1-12
5.1.4 Potentiometric Levels. 5.1-47
5.1.5 Regional Hydrochemistry. 5.1-80
5.1.6 Isotope Hydrochemistry 5.1-140
5.1.7 Interrelationship of Hydrologic Systems. 5.1-181
5.1.8 Groundwater Velocity and Travel Times. 5.1-189
5.1.9 Groundwater Uses 5.1-189
5.1.10 Reexamination of Conceptual Model. 5.1-198
5.2 Site Hydrogeologic System. 5.2-1
5.2.1 Hydrologic Characteristics 5.2-1
5.2.2 Potentiometric Levels. 5.2-4
5.2.3 Groundwater Hydrochemistry 5.2-13
5.3 Summary of Unresolved Issues 5.3-1
5.4 References 5.4-1

FIGURES:

1-1. Location of the Pasco Basin and the Hanford Site, Washington State 1.1-2
1-2. Regions That are Being Considered for Geologic Disposal of Radioactive Waste. 1.2-3
1-3. The Hanford Site 1.3-2
1-4. Stratigraphy of the Columbia River Basalt Group, Yakima Basalt Subgroup, and Intercalated and Suprabasalt Sediments Within the Pasco Basin 1.3-4
1-5. Generalized Cross Section Through the Pasco Basin. . . . 1.3-5
1-6. Repository Siting Process. 1.4-2
2-1. Repository-Site Process. 2.0-1
2-2. Location of the Reference Repository Location and Alternate Repository Location. 2.0-3
2-3. Elements of Site Identification Methodology. 2.1-2
2-4. Relationships of Terms Used in Screening and Ranking . . 2.1-4
2-5. Approach to Guideline Development. 2.1-5
2-6. The Overlay Process Used in Site Screening 2.1-8
2-7. Relationship of Area Designations and Screening Steps. . 2.1-9
2-8. Illustrative Example of the Screening Process. 2.1-10
2-9. Pasco Basin and Hanford Site Boundaries. 2.5-2
2-10. Pasco Basin Candidate Area 2.5-5
2-11. Subareas Within Pasco Basin. 2.5-8
2-12. Hanford Site: Compilation of Available Area and Site Localities. 2.5-11
2-13. Site Localities on the Hanford Site. 2.5-12
2-14. Initial Candidate Sites on the Hanford Site. 2.5-16
2-15. Ten Candidate Sites in the Cold Creek Syncline Area (after eliminating sites Y and Z from further consideration) 2.5-18
2-16. Reference Repository Location, Site A-H, and Alternate Site J 2.6-2
3-1. Location of the Columbia Plateau, Hanford Site, Cold Creek Syncline, and Reference Repository Location. . . 3.1-2
3-2. Stratigraphy of the Columbia River Basalt Group, Yakima Basalt Subgroup, and Intercalated and Suprabasalt Sediments Within the Pasco Basin 3.1-3
3-3. Location Map for Key Boreholes Used in Basalt Waste Isolation Project Studies. 3.2-3
3-4. Stratigraphic Levels Penetrated by Boreholes on the Hanford Site and Vicinity. 3.2-4
3-5. Borehole Location Map, Reference Repository Location . . 3.2-6
3-6. Physiographic Provinces of the Pacific Northwest 3.3-2
3-7. Divisions of the Columbia Intermontane Province. 3.3-3
3-8. Map of Major Landform Systems, Pasco Basin 3.3-4
3-9. Geomorphic Map, Reference Repository Location. 3.4-2
3-10. Regional Columbia River Basalt Group Stratigraphic Nomenclature 3.5-3
3-11. General Stratigraphic Relationship of Suprabasalt Sediments. 3.5-5
3-12. Generalized Locations of The Dalles Group and Their Depositional Basins. 3.5-7

9 1 2 1 2 4 9 5 0 5 1 6

FIGURES (Contd.):

3-13. General Geologic Map of the Pasco Basin. 3.5-10
3-14. Generalized Structure Cross Section. 3.5-11
3-15. Generalized Surficial Geologic Map of the Reference Repository Location. 3.5-12
3-16. Generalized Cross Section Through the Reference Repository Location. 3.5-13
3-17. Stratigraphic Nomenclature, Pasco Basin, Cold Creek Syncline 3.5-14
3-18. Location Map, Pasco Basin and Surrounding Areas (showing location of boreholes pentrating the candidate repository horizons and geologic sections) . 3.5-16
3-19. Isopach Map of the Middle Sentinel Bluffs Flow, Pasco Basin and Vicinity 3.5-17
3-20. General Stratigraphic Relationships Among Grande Ronde Basalt Flow Sequences in the Pasco Basin 3.5-18
3-21. Isopach Map of the Umtanum Flow, Pasco Basin and Vicinity 3.5-20
3-22. Fence Diagram, Upper Grande Ronde Basalt, Crescent Bar to Sentinel Bluffs 3.5-21
3-23. Fence Diagram, Upper Grande Ronde Basalt, Sentinel Bluffs to Borehole DC-6. . . . . 3.5-22
3-24. Fence Diagram, Upper Grande Ronde Basalt, Boreholes DC-4 to DDH-3. . . . . 3.5-23
3-25. Stratigraphic Column, Reference Repository Location. . . 3.5-24
3-26. Typical Intraflow Structures Present in a Grande Ronde Basalt Flow. 3.5-26
3-27. Intraflow Structure Types. 3.5-27
3-28. Fence Diagram, Umtanum Flow. 3.5-29
3-29. Cliff Exposure, Umtanum Flow at Emerson Nipple Section . 3.5-30
3-30. Isopach Map of the Flow Top of the Middle Sentinel Bluffs Flow, Pasco Basin and Vicinity. 3.5-34
3-31. Isopach Map of the Flow Top of the Umtanum Flow. 3.5-36
3-32. Location of 1979 and 1980 Seismic-Reflection Surveys . . 3.6-2
3-33. Seismic-Reflection Anomaly Location Map. 3.6-4
3-34. Aeromagnetic Surveys Including Columbia Plateau Area . . 3.6-5
3-35. Pasco Basin Aeromagnetic Surveys 3.6-8
3-36. Locations of Ground-Magnetic Surveys 3.6-9
3-37. Pasco Basin Ground-Magnetic Surveys. 3.6-11
3-38. Location Map - Regional Gravity: 3.6-12
3-39. Tensor Magnetotelluric-Survey Station Location 3.6-14
3-40. Electrical Strike, Tensor-Magnetotelluric Data from Fiscal Year 1978 and 1979 Surveys. 3.6-16
3-41. Temperature Gradient Measurements and Regional Heat Flow Reported for the Pasco Basin and Vicinity 3.6-19
3-42. Remote-Sensing Studies Conducted Within the Columbia Plateau 3.6-24
3-43. Illustrative Borehole Geophysical Log Response in Columbia River Basalt. 3.6-26
3-44. Gamma-Gamma-Log Response, Grande Ronde Basalt, Sentinel Bluffs Sequence 3.6-28

FIGURES (Contd.):

3-45. Informal Structural Subdivisions of the Columbia Plateau 3.7-2
3-46. Chronology of Igneous Activity in the Pacific Northwest. 3.7-3
3-47. Generalized Tectonic Map of Part of the Columbia Plateau 3.7-5
3-48. Faults of the Pasco Basin. 3.7-9
3-49. Comparison of the Interpreted Strain Geometry of the Umtanum Anticline with a Photomosaic of a Canyon in the Priest Rapids Area 3.7-21
3-50. Folds of the Pasco Basin 3.7-22
3-51. Top-of-Basalt Contour Map. 3.7-27
3-52. Interpretive Bedrock-Structure Map 3.7-29
3-53. Schematic Cross Section, Cold Creek Syncline (illustrating predicted distribution of faults with respect to folds) 3.7-30
3-54. Historical Seismicity of the Columbia Plateau Tectonic Province. 3.7-36
3-55. Instrumental Seismicity (post-1969) above Magnitude 3.0, Columbia Plateau Tectonic Province 3.7-42
3-56. Instrumental Seismicity of the Pasco Basin 3.7-43
3-57. Well-Located Shallow Earthquakes, Pasco Basin and Surrounding Area, 1969-1979. . . . . 3.7-45
3-58. Cumulative Number of Events per Year Versus Magnitude for Entire Region. 3.7-46
3-59. Columbia Plateau Earthquakes Focal-Mechanism Summary . . 3.7-50
3-60. Hanford Seismic Array. 3.7-56
3-61. Simple Translation Model of Oblique-Transform Faulting and Compressional Folding 3.8-4
3-62. Locations of the Reference Repository Location Vicinity, Pasco Basin, Adjacent-Counties, and Columbia Plateau Study Areas 3.9-2
4-1. Strength Versus Confining Stress for Pomona Basalt . . . 4.1-8
4-2. Effects of Confining Stress and Temperature on the Deformation Modulus for Umtanum Basalt Specimens . . . 4.1-9
4-3. Average Modulus Value (uncorrected) Versus Orientation, from Modified Goodman Jack Tests in the Colonnade Zone of Pomona Flow at the Near-Surface Test Facility Site 4.2-4
4-4. Block Test Number 1 Flat Jack and Grouting Boxes 4.2-6
4-5. Heater and Instrumentation Holes - Block Test Step 1 . . 4.2-7
4-6. Individual Stress Cancellation Values for Vibrating Wire Stressmeters in Step 1 of the Block Test. 4.2-8
4-7. Temperature and Flat Jack Pressure Cycles During Step 1 . . . . . 4.2-10
4-8. Plan View of Boreholes Drilled for Full-Scale Heater Test No. 1. . . . . 4.5-3
4-9. Plan View of Boreholes Drilled for Full-Scale Heater Test No. 2. . . . . 4.5-4
4-10. Heater Power Levels for Full-Scale Heater Test No. 1 . . 4.5-5
4-11. Heater Power Levels for Full-Scale Heater Test No. 2 . . 4.5-5

FIGURES (Contd.):

4-12. Comparison of Full-Scale Heater Test No. 2 Actual Data with Predictive Analysis Value. 4.5-6
4-13. Axial Temperature Profile in Basalt at 0.71 Meter (2.3 Feet) from Heater-Hole Axis on Test Day 259 for Full-Scale Heater Test No. 1 . . . . . 4.5-7
4-14. Axial Temperature Profile in Basalt at 0.40 Meter (1.3 Feet) from Heater-Hole Axis on Test Day 259 for Full-Scale Heater Test No. 1 . . . . . 4.5-7
4-15. Map of the Hanford Site Showing Location of Drill Hole DB-15 and DC-12 . . . . . 4.6-3
4-16. Basalt Core Recovered from Borehole DC-12 at Test Depth Between 1,011 and 1,014 Meters (3,317 and 3,325 feet). 4.6-5
4-17. Typical Pressure-Time Curve Obtained in Borehole DC-12 at Test Depth of 1,013 Meters (3,323 feet) 4.6-6
4-18. Pressure-Time Curve Plotted on a Semi-Logarithmic Paper to Determine the Shut-In Pressure at Test Depth of 1,036 Meters (3,400 Feet) 4.6-7
4-19. A Typical Fracture Impression Obtained at Test Depth (1,013 meters (3,323 feet)), Exhibiting Two Vertical Fractures Approximately 180 Degrees Apart. 4.6-8
4-20. Variation of Ratio of Average Horizontal Stress to Vertical Stress with Depth Below Surface 4.6-12
5-1. Geographic Setting of the Pasco Basin. 5.1-2
5-2. Hydrologic Test Sites for Individual Formations Within the Columbia River Basalt Group 5.1-5
5-3. Areal Distribution of Formations Within the Columbia River Basalt Group 5.1-8
5-4. Outcrop Distributions of the Saddle Mountains, Wanapum, and Grande Ronde Basalts and Overburden Sediments. 5.1-9
5-5. Flow Chart of General Procedures Used in Hydrologic Testing. 5.1-15
5-6. Guidelines for Application Range of Test Methods for Test Zones at the Hanford Site 5.1-16
5-7. Borehole Geophysical Log for Borehole DB-15. . . . . 5.1-18
5-8. Borehole Geophysical Log for Borehole DC-6 . . . . . 5.1-19
5-9. Borehole Geophysical Log for Borehole DC-7 . . . . . 5.1-20
5-10. Borehole Geophysical Log for Borehole DC-12. . . . . 5.1-21
5-11. Borehole Geophysical Log for Borehole DC-14. . . . . 5.1-22
5-12. Borehole Geophysical Log for Borehole DC-15. . . . . 5.1-23
5-13. Borehole Geophysical Log for Borehole DC-16. . . . . 5.1-24
5-14. Borehole Geophysical Log for Borehole RRL-2. . . . . 5.1-25
5-15. Areal Distribution of Hydraulic Conductivity Across the Hanford Site for the Unconfined Aquifer. 5.1-26
5-16. Comparison of Equivalent Hydraulic-Conductivity Values for all Flow Tops and Interbeds Tested Within the Columbia River Basalts. 5.1-29
5-17. Comparison of Equivalent Hydraulic Conductivity Values Versus Depth for Flow Interiors (colonnade and entablature) of Selected Columbia River Basalts. . 5.1-32

FIGURES (Contd.):

5-18. Equivalent Hydraulic Conductivity Values for Test Intervals Across Interbeds and Flow Tops in Borehole DB-13 . . . . . 5.1-33
5-19. Equivalent Hydraulic Conductivity Values for Test Intervals Across Interbeds and Flow Tops in Borehole DB-15 . . . . . 5.1-34
5-20. Equivalent Hydraulic Conductivity Values for Test Intervals Across Flow Tops in Borehole DC-6. . . . . 5.1-35
5-21. Equivalent Hydraulic Conductivity Values for Test Intervals Across Flow Tops in Borehole DC-7. . . . . 5.1-36
5-22. Equivalent Hydraulic Conductivity Values for Test Intervals Across Flow Tops and One Interbed in Borehole DC-12 . . . . . 5.1-37
5-23. Equivalent Hydraulic Conductivity Values for Test Intervals Across Flow Tops and Interbeds in Borehole DC-14 . . . . . 5.1-38
5-24. Equivalent Hydraulic Conductivity Values for Test Intervals Across Flow Tops and Interbeds in Borehole DC-15 . . . . . 5.1-39
5-25. Equivalent Hydraulic Conductivity Values for Test Intervals Across Mostly Flow Tops and Interbeds in Borehole DC-16A 5.1-40
5-26. Equivalent Hydraulic Conductivity Values for Test Intervals Across Mostly Flow Tops and Interbeds in Borehole RRL-2. . . . . 5.1-41
5-27. Hydraulic Conductivity of Various Crystalline and Argillaceous Rocks 5.1-48
5-28. Elevation of the Groundwater Table Within the Pasco Basin. 5.1-50
5-29. Estimated 1944 Water-Table Map for the Hanford Site. . . 5.1-51
5-30. Comparison of Hydraulic Heads in the Rattlesnake Ridge Interbed to Water-Table Elevation. 5.1-52
5-31. Potentiometric Map for and Inferred Flow Directions of Groundwater Within the Mabton Interbed Beneath the Hanford Site 5.1-54
5-32. Total Nitrogen-Nitrate (N as NO_3) Concentration for Groundwater Within the Saddle Mountain Basalt in the Pasco Basin 5.1-58
5-33. Hydrograph for Well 10N/30E-19E Located North of Pasco, Washington. 5.1-59
5-34. Hydraulic Head Measurements Within the Saddle Mountains and Wanapum Basalts in Borehole DB-15. . . . 5.1-65
5-35. Hydraulic Head Measurements Within the Grande Ronde Basalt in Borehole DC-6. . . . . 5.1-66
5-36. Hydraulic Head Measurements Within the Grande Ronde Basalt in Borehole DC-7. . . . . 5.1-67
5-37. Hydraulic Head Measurements Within the Wanapum and Grande Ronde Basalts in Borehole DC-12 . . . . . 5.1-68
5-38. Hydraulic Head Measurements Within the Columbia River Basalts in Borehole DC-14. . . . . 5.1-69

FIGURES (Contd.):

5-39. Hydraulic Head Measurements Within the Columbia River Basalts in Borehole DC-15. . . . . 5.1-70
5-40. Hydraulic Head Measurements Within the Saddle Mountains and Wanapum Basalts at Borehole DC-16A 5.1-71
5-41. Hydraulic Head Measurements Within the Columbia River Basalts at Borehole RRL-2. . . . . 5.1-72
5-42. Three-Dimensional Perspective Views Showing Composite Potentiometric Surfaces for Various Strata Within the Columbia River Basalts 5.1-76
5-43. Three-Dimensional Perspective Views Showing the Potentiometric Surface Configuration of the Saddle Mountains and Wanapum Basalt 5.1-77
5-44. Locations and Vertical-Head Distributions of Washington State Department of Ecology Test/ Observation Wells. 5.1-78
5-45. Selected Examples of Hydrographic Data for Wells Within the Columbia Plateau Region. 5.1-81
5-46. Sampling Sites for Groundwater Collected from Columbia River Basalt Zones. 5.1-84
5-47. Chemical Composition of Groundwater Within the Columbia River Basalt Group. 5.1-86
5-48. Nitrate-Ion Distribution in Unconfined Groundwater . . . 5.1-89
5-49. Location of Boreholes on the Hanford Site for Which Groundwater Hydrochemistry is Available from the Saddle Mountains Basalt. 5.1-92
5-50. Hydrochemical Facies Map for Aquifers and Springs in the Saddle Mountains Basalt Within the Pasco Basin . . 5.1-97
5-51. Chemical Composition of Springs and Groundwater Sampled from the Saddle Mountains Basalt 5.1-99
5-52. Saturation Index Data for Calcite and Cristobalite for Selected Saddle Mountains Basalt Groundwaters. . . 5.1-100
5-53. Distribution of Total Dissolved Solids and Inferred Flow Direction of Groundwater Within the Mabton Interbed. 5.1-102
5-54. Mabton Interbed Groundwater Temperature in Boreholes on the Hanford Site. 5.1-106
5-55. Boreholes with Hydrochemical Data from Groundwater Within the Wanapum Basalt on the Hanford Site. 5.1-109
5-56. Major Inorganic Hydrochemistry for Groundwater Zones in Boreholes DC-14 and DB-15 Within the Wanapum Basalt 5.1-113
5-57. Major Inorganic Composition of Wanapum Groundwaters from Inside and Outside the Cold Creek Syncline. . . . 5.1-114
5-58. Calcite and Cristobalite Saturation Index for Selected Groundwaters Within the Wanapum Basalt. . . . 5.1-117
5-59. Borehole Locations Where Hydrochemical Data Are Available from Within the Grande Ronde Basalt. 5.1-123
5-60. Chemical Composition of Groundwater Within the Grande Ronde Basalt Beneath the Hanford Site 5.1-126

FIGURES (Contd.):

5-61. Saturation Index for Calcite and Cristobalite in Selected Groundwater Zones Within the Grande Ronde Basalt 5.1-128
5-62. Stiff Diagrams for Selected Intervals in Borehole DB-15 . . . . . 5.1-134
5-63. Stiff Diagrams for Selected Intervals in Borehole DC-6. . . . . 5.1-135
5-64. Stiff Diagrams for Selected Intervals in Borehole DC-12 . . . . . 5.1-136
5-65. Stiff Diagrams for Selected Intervals in Borehole DC-14 . . . . . 5.1-137
5-66. Stiff Diagrams for Selected Intervals in Borehole DC-15 . . . . . 5.1-138
5-67. Tritium Distribution in the Unconfined Aquifer Beneath the Hanford Site 5.1-143
5-68. Generalized Plot of Delta Oxygen-18 Versus Delta Hydrogen-2, Showing the Meteoric Water Line and Possible Secondary Fractionation Processes 5.1-145
5-69. Plot of Delta Hydrogen-2 Versus Delta Oxygen-18 for the Deep Basalts Beneath the Hanford Site. 5.1-147
5-70. Distribution of Deuterium Within Three Formations of the Columbia River Basalt at the Hanford Site . . . 5.1-148
5-71. Distribution of Oxygen-18 Within Three Formations of the Columbia River Basalt at the Hanford Site . . . 5.1-149
5-72. Deuterium and Oxygen-18 Relationship for Groundwater Within the Saddle Mountains and Wanapum Basalts at Borehole DB-15. . . . . 5.1-150
5-73. Deuterium and Oxygen-18 Relationships for Groundwaters Within the Columbia River Basalts at Borehole DC-14 . . . . . 5.1-151
5-74. Deuterium and Oxygen-18 Relationships for Groundwaters Within the Columbia River Basalts at Borehole DB-15 . . . . . 5.1-152
5-75. Variation of Delta Oxygen-18 and Delta Hydrogen-2 as a Function of Depth in Borehole DB-15 . . . . . 5.1-153
5-76. Variation of Delta Oxygen-18 and Delta Hydrogen-2 as a Function of Depth in Borehole DC-15 . . . . . 5.1-154
5-77. Distribution of Delta Carbon-13 Values of Bicarbonate Within Selected Columbia River Basalt Group Groundwaters at the Hanford Site 5.1-160
5-78. Distribution of Delta Carbon-13 Values of Bicarbonate for Selected Springs in the Vicinity of the Hanford Site 5.1-161
5-79. Relationship of Delta Carbon-13 (HCO_3^-) and Percent of Total Dissolved Gas Versus Depth in Borehole DC-15. . . . . 5.1-162
5-80. Eh-pH Diagram for Stable Sulfur Species at 25°C and 1 Atmosphere Total Pressure. 5.1-163
5-81. Sulfate Versus Delta Sulfur-34 (sulfate) for Basalt Groundwaters at the Hanford Site 5.1-165

FIGURES (Contd.):

5-82. Areal Plot of Corrected Carbon-14 Ages for Groundwater from the Mabton Interbed 5.1-171
5-83. Location of Wells Used by Silar When Studying the Carbon-14 Age of Groundwater in Eastern Washington State. 5.1-175
5-84. Total Uranium Versus Activity Ratio for the Springs and the Columbia River Basalt Groundwaters Beneath the Hanford Site 5.1-177
5-85. Possible Changes of Uranium-234/Uranium-238 as a Function of Time and Position in a Flow System 5.1-178
5-86. Distribution of Chlorine-36 to Total Chlorine with Depth for Selected Intervals Within the Columbia River Basalt Group. 5.1-181
5-87. Comparison of Columbia River Stage Fluctuations with Well Hydrograph Response in Three Unconfined-Aquifer Well Sites at the Hanford Site 5.1-183
5-88. Streamflow Rates for the Yakima and Columbia Rivers Near the Hanford Site and Hydrographs for Two Nearby Boreholes 5.1-185
5-89. Selected Hydrochemistry for Borehole DC-15 . . . . . 5.1-186
5-90. Areal Hydrochemical Data for Groundwater Within the Priest Rapids Member 5.1-188
5-91. Frequency of Well-Use Types Listed by Depth Intervals. . 5.1-193
5-92. Water-Table Rise Beneath the Hanford Site, 1944-1978 . . 5.1-195
5-93. Location of Unconfined-Aquifer Test Sites Within the Reference Repository Location. 5.2-2
5-94. Water-Table Map for the Unconfined Aquifer Within the Reference Repository Location. 5.2-5
5-95. Water-Table Rise Within the Reference Repository Location Attributable to Water-Disposal Activities 5.2-6
5-96. Estimated 1944 Water-Table Map Within the Reference Repository Location Prior to Water-Disposal Activities 5.2-8
5-97. Unconfined Water-Level Responses in Wells Within and Adjacent to the Reference Repository Location. 5.2-9
5-98. Hydrograph of the Water Levels in the DC-1 Piezometers from 1972 Through 1981 . . . . . 5.2-12
5-99. Location of Unconfined-Aquifer Well Sites Within the Reference Repository Location. 5.2-14
5-100. Chemical Composition of Groundwater Within the Unconfined Aquifer in the Reference Repository Location . . 5.2-16
5-101. Nitrate Ion Distribution in Unconfined Groundwater Beneath the Reference Repository Location. 5.2-18
5-102. Temperature Distribution in Unconfined Groundwater . . . 5.2-20
5-103. Tritium Hydrographs for Wells 699-35-66 and 699-37-82A Completed in the Unconfined Aquifer Within the Reference Repository Location 5.2-22

TABLES:

2-1. Area Designations Used in Screening. 2.1-11
2-2. Steps in the Ranking Process 2.1-12
2-3. Summary Description of Technical Factors Considered in the Siting Process 2.2-2
2-4. Summary of Screening Guidelines. 2.2-9
2-5. Summary Description of Environmental Factors Considered in the Siting Process. 2.3-2
2-6. Considerations, Measures, and Guidelines Used in the Candidate-Area Screening of the Pasco Basin. 2.5-3
2-7. Considerations, Measures, and Guidelines Used in Subarea Screening of the Pasco Basin 2.5-7
2-8. Estimated Range of Existing Conditions at Site Localities on the Hanford Site 2.5-13
2-9. Criteria Matrix Descriptors. 2.5-20
2-10. Ranking Criteria 2.5-24
2-11. Candidate Site Measure Matrix. 2.5-25
2-12. Criteria Ranges and Rank Order of Weights. 2.5-26
2-13. Results of Ranking 2.5-27
3-1. Summary and Description of Hanford Site Boreholes. . . . 3.2-2
3-2. Aeromagnetic Surveys 3.6-6
3-3. Gravity Investigations 3.6-13
3-4. Geoelectric Layers and Interpreted Rock Type 3.6-15
3-5. Geothermal Gradients Calculated for Selected Borehole Logs from Wells Within the Hanford Site. 3.6-18
3-6. Remote-Sensing Studies of the Columbia Plateau and Surrounding Area 3.6-21
3-7. Calculated Long-Term Probability of Consequent Volcanic Events. 3.7-6
3-8. Faults Within the Pasco Basin. 3.7-10
3-9. Characteristics of Folds Within the Pasco Basin. 3.7-23
3-10. Felt and Recorded Earthquakes Within the Columbia Plateau and Surrounding Area through 1980. . . . . 3.7-39
3-11. Eastern Washington Focal Mechanism Solutions 3.7-48
3-12. Projected Gross and Net Values and Estimated Present Values of Mineral Resources in the Adjacent Counties Study Area, 1981-2005. . . . . 3.9-4
3-13. Development, Production, and Marketing Costs of Known or Potential Geologic Resources of the Reference Repository Location Vicinity Study Area and the Remainder of the Columbia Plateau. 3.9-5
3-14. Projected Gross and Net Values and Estimated Present Values of Mineral Resources in the Columbia Plateau Study Area, 1981-2005. . . . . 3.9-7
3-15. Economic Comparisons of Mineral-Resource Values-- the Reference Repository Location Vicinity Versus the Remainder of the Columbia Plateau. 3.9-8
4-1. Mechanical Characteristics of Basalts Used for Conceptual Design. 4.1-2
4-2a. Physical and Mechanical Property of Hanford Site Basalt Entablature Zones 4.1-3

TABLES (Contd.):

4-2b. Physical and Mechanical Property of Hanford Site Basalt Colonnade Zones 4.1-4
4-2c. Physical and Mechanical Property of Hanford Site Basalt Interflow Zones 4.1-5
4-3. Physical- and Mechanical-Property Tests. 4.1-6
4-4. Goodman Jack Test: Modulus Values in the Entablature Zone of the Pomona Flow at the Near-Surface Test Facility 4.2-3
4-5. Step 1 - Modulus of Deformation for Pomona Entablature at the Near-Surface Test Facility 4.2-9
4-6. Coefficient of Friction of Joints for Umtanum Entablature Samples Tested in Triaxial Compression at 20°C. . 4.3-4
4-7. Coefficient of Friction of Joints for Umtanum Entablature Samples Tested in Triaxial Compression at Elevated Temperatures. 4.3-5
4-8. Thermal and Thermomechanical Characteristics of Basalts Used for Conceptual Design 4.4-1
4-9. Thermal Properties of Hanford Site Basalts 4.4-2
4-10. Thermal Property Tests 4.4-3
4-11. Summary of In Situ Stess Data Obtained by the Hydrofracturing Method. 4.6-9
4-12. Comparison of the Three Principal Stresses Measured by Overcoring and Hydrofracturing Methods in Pomona Basalt at the Near-Surface Test Facility Level 4.6-10
4-13. Construction Projects Completed in Basalt. 4.8-2
5-1. Principal Groups Involved in Basalt Hydrologic Testing. 5.1-4
5-2. Dimensional Statistics of the Principal Stratigraphic Units Within the Columbia Plateau. 5.1-6
5-3. General Information Regarding Groundwater Hydrology. . . 5.1-11
5-4. General Ranges and Values for Selected Hydrologic Properties 5.1-28
5-5. Equivalent Hydraulic Conductivity for Selected Stratigraphic Intervals. 5.1-30
5-6. Comparison of Equivalent Hydraulic Conductivity Values Between the Middle Sentinel Bluffs and Umtanum Flows. 5.1-43
5-7. Hydraulic Heads Within Selected Stratigraphic Intervals in the Saddle Mountains Basalt 5.1-56
5-8. Areal Head Gradients in Selected Members of the Wanapum Basalt 5.1-62
5-9. Areal Head Gradient in the Middle Sentinel Bluffs and Umtanum Flow Tops of the Grande Ronde Basalt 5.1-63
5-10. Construction Data for Washington State Department of Ecology Test/Observation Wells in Eastern Washington . 5.1-79
5-11. Range in Concentration and Mean Composition of Major Chemical Constituents Within Groundwater of the Columbia River Basalt Group. 5.1-85
5-12. Range and Median Concentrations of Trace Elements for Groundwater Within Columbia River Basalt 5.1-87

TABLES (Contd.):

5-13. Range in Concentration and Mean Composition for Major Chemical Constituents Within Groundwater in the Unconfined Aquifer at Hanford. 5.1-88

5-14. Range and Median Concentrations of Trace Elements for Unconfined Groundwater at Hanford. 5.1-90

5-15. Location, Depth, and Date of Groundwater-Sample Collection for Zones Within the Saddle Mountains Basalt 5.1-93

5-16. Range in Concentration and Mean Composition of Major Chemical Constituents for Groundwater Within the Mabton Interbed and Saddle Mountains Basalt. 5.1-96

5-17. Range and Median Concentrations of Trace Elements for Groundwater Within Saddle Mountains Basalt at the Hanford Site 5.1-103

5-18. Formation Fluid Temperature Within the Saddle Mountains Basalt in Selected Boreholes on the Hanford Site . . . 5.1-104

5-19. Dissolved Gas Content and Makeup for Groundwater Collected from the Saddle Mountains Basalt in Borehole DC-15 . . . . . 5.1-107

5-20. Location, Depth, and Date of Groundwater-Sample Collection for Zones Within the Wanapum Basalt 5.1-111

5-21. Range in Concentration and Mean Composition of Major Inorganic Constituents and Hydrochemical Parameters for Wanapum Basalt Groundwater on the Hanford Site . . 5.1-112

5-22. Total Dissolved Solids and Chloride Concentration in Priest Rapids Groundwater. 5.1-115

5-23. Range and Median Concentrations of Trace Elements for Groundwater Within the Wanapum Basalt. 5.1-116

5-24. Formation Temperature Within the Wanapum Basalt in Selected Boreholes on the Hanford Site 5.1-119

5-25. Potentiometric Measurement of Eh in Groundwaters Collected From Zones Within the Wanapum Basalt 5.1-120

5-26. Distribution of Dissolved Gas-Components in Wanapum Basalt Zones 5.1-121

5-27. Location, Depth, and Date of Groundwater Collection for Selected Zones Within the Grande Ronde Basalt. . . 5.1-124

5-28. Range of Concentration and Mean Composition of Major Inorganic Constituents and Hydrochemical Parameters Within the Groundwater of the Grande Ronde Basalt. . . 5.1-125

5-29. Range and Median Concentrations of Trace Elements for Groundwater Within the Grande Ronde Basalt 5.1-129

5-30. Formation Fluid Temperatures for Groundwater Zones in the Grande Ronde Basalt in Selected Boreholes on the Hanford Site 5.1-130

5-31. Measured Potentiometric Eh Values for Groundwater Collected from Zones Within the Grande Ronde Basalt. . 5.1-131

5-32. Distribution of Dissolved Gas Components in Grande Ronde Basalt Zones. 5.1-133

5-33. Stratigraphic Location of Hydrochemical and Isotopic Breaks Beneath the Hanford Site. 5.1-139

TABLES (Contd.):

5-34. Natural Abundance of Some Isotopes Presently Being Used and/or Considered for Use in Hydrologic Studies. . 5.1-141
5-35. Ranges and Mean Values of Delta Oxygen-18 and Delta Hydrogen-2 for the Three Major Basalt Formations Beneath the Hanford Site 5.1-155
5-36. Ranges and Mean Values of Delta Oxygen-18 and Delta Hydrogen-2 for the Three Major Basalt Formations Both Inside and Outside the Cold Creek Syncline Area, Hanford Site 5.1-157
5-37. Calculated Mean Surface Air Temperature from Delta Oxygen-18 and Delta Hydrogen-2 Values for Basalts Beneath the Hanford Site 5.1-158
5-38. Values of Delta Carbon-13 for Various Natural Materials 5.1-159
5-39. Values of Delta Carbon-13 for Both Bicarbonate and Methane from Various Wells at the Hanford Site 5.1-163
5-40. Sulfur Isotopic Composition for the Principal Sources of Sulfate in Groundwater. 5.1-164
5-41. Mean Tritium Concentrations (in tritium units) for Columbia River Basalts from Selected Boreholes and the Columbia River 5.1-167
5-42. Mean Carbon-14 Age Calculations for the Columbia River Basalt Groundwaters Beneath the Hanford Site 5.1-170
5-43. Range and Mean Values for Activity Ratios and Total Uranium for Spring and Groundwater Samples from Columbia River Basalts at the Hanford Site 5.1-178
5-44. Distribution of Wells According to Major Use Categories Within the Columbia Plateau and the Pasco Basin. . . . 5.1-191
5-45. Distribution of Wells Within the Columbia Plateau and Pasco Basin According to Use 5.1-192
5-46. Groundwater Use in the Pasco Basin 5.1-193
5-47. Primary References for Hydrologic Testing Data and Conceptual Models. 5.1-199
5-48. Hydraulic-Property Values for the Unconfined Aquifer Within the Reference Repository Location and the Entire Hanford Site. 5.2-3
5-49. Expected Range and Mean of Hydraulic-Property Values for the Columbia River Basalt Group Within the Reference Repository Location. 5.2-3
5-50. Anticipated Hydraulic-Head Conditions Within Confined Aquifers of the Columbia River Basalt Group in the Reference Repository Location 5.2-10
5-51. Expected Range in Concentration and Mean Composition for Major Chemical Constituents for Groundwater Within the Unconfined Aquifer in the Reference Repository Location and the Entire Hanford Site. . . . 5.2-15
5-52. Historic Major Inorganic- and Hydrochemical-Parameter Analyses for the Unconfined Aquifer at Well 699-27-8 . . . . . 5.2-19

TABLES (Contd.):

5-53. Anticipated Range in Concentration and Mean Composition of Major Chemical Constituents for Columbia River Basalt Groundwaters Within the Reference Repository Location. 5.2-24
5-54. Historic Major Inorganic and Hydrochemical Parameter Analyses for Groundwater Within the Upper Wanapum Basalt in the Cold Creek Valley. 5.2-25
5-55. Principal Dissolved-Gas Components Anticipated in Columbia River Basalt Groundwater Within the Reference Repository Location. 5.2-27
5-56. Expected Range and Mean Values in Stable Isotopic Content for Columbia River Basalt Groundwater Within the Reference Repository Location 5.2-28
5-57. Expected Range and Mean Radioisotope Content for Columbia River Basalt Groundwaters Within the Reference Repository Location. 5.2-30

9 2 1 2 4 9 5 0 5 2 8

THIS PAGE INTENTIONALLY
LEFT BLANK

92124950529

EXECUTIVE SUMMARY

The reference location for a repository in basalt for the terminal storage of nuclear wastes on the Hanford Site and the candidate horizons within this reference repository location have been identified and the preliminary characterization work in support of the site screening process has been completed. Fifteen technical questions regarding the qualification of the site were identified to be addressed during the detailed site characterization phase of the U.S. Department of Energy-National Waste Terminal Storage Program site selection process. Resolution of these questions will be provided in the final site characterization progress report, currently planned to be issued in 1987, and in the safety analysis report to be submitted with the License Application. The additional information needed to resolve these questions and the plans for obtaining the information have been identified. This Site Characterization Report documents the results of the site screening process, the preliminary site characterization data, the technical issues that need to be addressed, and the plans for resolving these issues.

On the basis of the geotechnical data now available, the following can be concluded for the basalts underlying the Hanford Site:

- Basalt flows located more than 610 meters (2,000 feet) below the ground surface are not subject to significant erosion, and several flows may have thick enough flow interiors and sufficient lateral continuity to accommodate the construction of a nuclear waste repository.

- The present calculated rate of deformation poses no threat to the long-term integrity of a repository in basalt at the Hanford Site.

- The basalt stratigraphy, or sequence of basalt flows, beneath the Hanford Site is well understood and the depth to the flows can be predicted with reasonable accuracy.

- The low permeability measured in boreholes for the basalt-flow interiors indicate these portions of the flows will provide the isolation necessary to prevent the radionuclides reaching the accessible environment in concentrations above established guidelines.

- Preliminary tests indicate that the basalt rock, groundwater, and materials to be placed in terminal storage are compatible under both ambient and expected thermal stress conditions, in that they favor long-term stability.

- There is an extremely low probability of any adverse climatic impact on a repository in basalt at the Hanford Site.

9212495053 0

- No faults have been identified on the Hanford Site that would have an adverse impact on a repository constructed at the reference repository location.

- The potential for renewed volcanism on the Hanford Site is very low.

- There are no economic resources mined from the basalt in the vicinity of the Hanford Site at the present time, other than groundwater pumped from shallow aquifers. The Hanford Site is relatively unattractive to future subsurface mineral exploration and development within the Columbia River Basalt Group compared with other areas of the Columbia Plateau.

- The reference repository location is situated in a favorable position with respect to available transportation modes, support and service facilities, remoteness from population centers, and smoothness of the terrain.

- There is no land conflict with currently planned or existing facilities on the Hanford Site.

Fifteen issues or technical questions have been identified that need to be resolved during detailed site characterization. These issues are in the form of questions that require answers to satisfy regulatory and technical criteria. Three of these issues are designated "key issues." Key issues are those technical questions where engineers cannot substantially and economically alter a negative finding. The three key issues are as follows:

- What is the total amount (activity) of radionuclides potentially releasable to the accessible environment in a 10,000-year period, and is this amount in compliance with appropriate U.S. Environmental Protection Agency regulations?

- Can stability and isolation capability of the repository be maintained in the presence of coupled in situ, excavation-induced, and thermal-induced stresses?

- Can repository shafts, tunnels, and exploratory boreholes be constructed and sealed without causing preferential pathways for groundwater or increasing the potential for radionuclide migration from a nuclear waste repository such that compliance with appropriate U.S. Environmental Protection Agency regulations is not possible?

The additional work needed to resolve the criteria requirements has been identified and the methods, plans, and schedules to support this work have been outlined. All of the data needed to satisfy the criteria would be obtained during the detailed site characterization phase. Where positive resolution of the criteria requirements cannot be satisfied by technical data, risk analyses will be made. Following the completion of

the detailed site characterization phase and prior to submission of a license application for construction, the following work will also be completed:

- Final design requirements for a waste package
- Assessment of the environmental impact of a repository
- Evaluation of the results of in situ testing in the exploratory shaft and Near-Surface Test Facility.

In addition, significant progress will have been made on design and engineering studies in support of repository construction.

SUMMARY OF THE SITING PROCESS

In the U.S. Department of Energy-National Waste Terminal Storage Program national site screening plan (public draft), early consideration was given to the Hanford Site in Washington State because of its prior long-standing use and commitment to nuclear activities and existing government ownership. Although the Hanford Site was selected as the study area, initial screening encompassed the Pasco Basin, which is the smallest physiographic unit with geologic and hydrologic characteristics that would influence the conditions of a repository beneath the Hanford Site.

A methodology was used to systematically and rapidly focus on areas that had a high likelihood of containing a potential repository site. Application of the first screening guidelines reduced the area from about 4,145 square kilometers (1,600 square miles) to an area of about 1,800 square kilometers (700 square miles). Successive screening steps led to the identification of ten candidate sites in the central part of the Hanford Site known as the Cold Creek syncline, an area of about 180 square kilometers (70 square miles). Preliminary evaluation of the ten candidate sites made it clear that the sites were too closely matched to be differentiated between by routine ranking; therefore, a method of dominance analysis was used for this purpose. The dominance analysis showed that two of the ten candidate sites, located in the western portion of the Cold Creek syncline and designated sites A and H, had about the same dominance numerical value, a value which was significantly greater than the values for other sites. These two sites overlapped each other in area, and the combination was selected as the reference repository location. Site J, located east of the A-H site, was selected as the alternate repository location.

Two candidate repository horizons within the reference repository location have been identified for further study: the Umtanum flow and middle Sentinel Bluffs flow in the Grande Ronde Basalt. Due to prior emphasis on the Umtanum flow, it was selected as the reference horizon

for the site identification study. Because of the importance of the location of lineaments and thickness criteria used in the dominance analysis, the substitution of a thick Grande Ronde Basalt flow other than the Umtanum (i.e., the middle Sentinel Bluffs flow) as the reference horizon would not alter the results of the siting process.

The reference repository location is an area of about 48 square kilometers (18 square miles) with nearly flat-lying terrain. An optimization study was made, using selected environmental engineering and design criteria, to identify the specific location for a principal borehole and exploratory shaft within the reference repository location. The location identified was in the west-central part of the reference repository location.

GEOLOGIC DESCRIPTION OF CANDIDATE AREA AND SITE

The Hanford Site is situated in the Pasco Basin, a lowland area on the Columbia Plateau. The Columbia Plateau was formed by more than 100 basalt flows that literally flooded the region lying between the Cascade Range to the west, the Rocky Mountains to the east, the Okanagan Mountains to the north, and the Blue Mountains to the south. The reference repository location is situated in a relatively flat terrain within the Pasco Basin.

In the central portion of the Columbia Plateau, where the Hanford Site is located, no pre-basalt basement rocks are exposed. The basalt flows of the Columbia River Basalt Group have been drilled to a depth of more than 3,250 meters (10,655 feet) in the Pasco Basin and a number of the flows encountered in drilling are more than 100 meters (328 feet) thick and laterally continuous. The internal structures that develop within a flow during the emplacement of the flow over the ground surface and subsequent cooling of the molten lava are termed intraflow structures. Intraflow structures are not uniform from one flow to another or even within a given flow. Intraflow structure may vary in thickness, be absent entirely from any given flow, or occur repeatedly within a single flow. However, the intraflow structure of some of the thicker flows (greater than 30 meters (100 feet)) does show considerable continuity and uniformity within the Pasco Basin.

Although basalt is a fractured and jointed rock, data from rock core show that the great majority of fractures within the flow interiors are filled with multiple generations of secondary minerals, such as clays. The results of laboratory and field testing indicate that the volume of unfilled fractures is small, as attested by the low total fracture porosity and permeability.

Folding and faulting of the Columbia River basalt appear to have developed at about the same time during the past 16 million years. On the basis of existing data, such as fault plane solutions and hydrofracturing tests, the principal direction of the existing stress field for the Pasco Basin is generally indicated by north-south compression. The average rate of uplift of the mountains that form the north and south boundaries of the Pasco Basin is less than 1 meter (3.28 feet) in 10,000 years and appears to have been rather uniform throughout this time period.

No major tectonic structures have been discovered that would preclude development of a repository beneath the Hanford Site. Deformation, once initiated, appears to have continued along the same structures that were developing about 16 million years ago.

The basalt stratigraphy, or sequence of basalt flows within the Pasco Basin, is well understood, and there are no currently known stratigraphic or lithologic factors that would preclude the siting of a repository within the reference repository location.

An evaluation of the erosional processes that have modified the landforms within the Pasco Basin suggest that there is little likelihood that the candidate horizons could be uncovered by either potential glaciation, catastrophic flooding, or stream runoff.

Based on available information, the Pasco Basin may experience effects resulting from distant volcanic activity during the next 10,000 years, but the probability of breach of a repository or of thermally induced disturbance of a repository resulting from volcanic activity is exceedingly low.

Current mineral industry activity within 100 kilometers (62 miles) of the reference repository location is limited to surface mining of diatomaceous earth, sand and gravel, and clay and stone. A small, depleted, low-pressure natural gas field was in production from 1929 to 1941 at the southern edge of the Hanford Site, and a few small gold placers have also been worked along the Columbia River. No other current or past commercial production of minerals has been recorded. Groundwater is used for domestic, agricultural, and industrial purposes. The production of groundwater is primarily from wells less than 300 meters (984 feet) in depth. The poor quality of groundwater in the Grande Ronde Basalts restricts its use for these purposes.

GEOENGINEERING

Geoengineering data on the state of in situ stress show that the ratio of the maximum horizontal stress to the vertical stress is approximately 2, and that the direction of maximum horizontal stress is consistent with the geologic evidence of north-south compression.

Determinations of strength and deformability of basalt, measured both in the laboratory and in situ, indicate that the behavior of a large rock mass measured in situ is generally different from that measured on a small specimen in the laboratory. It was found that for closely jointed rock like basalt, it is necessary to measure the thermal and mechanical properties on a large enough block to include a representative number of fractures and joints.

A large basalt block has been isolated in the Near-Surface Test Facility to determine the thermal and mechanical behavior of the basalt in situ. This block measures 2 meters (6.6 feet) on a side and is cut 4.5 meters (14.8 feet) into the sidewall of the tunnel. The data from this test will be unique, in that this isolated block of basalt represents the largest block of intact basalt rock ever isolated in this manner for in situ determinations.

Preliminary results from two in situ heater tests, which simulate the heat from a nuclear waste package, suggest that basalt responds to thermal loading in a predictable fashion and the walls of the storage borehole for the waste package maintain their structural integrity up to the maximum temperature measured (450°C). Vertical deformation was more predictable than the horizontal deformation due to the large number of vertical joints in the basalt tested.

HYDROGEOLOGY

The Columbia River is the primary surface stream within the Pasco Basin. Its major tributaries include the Yakima, Snake, and Walla Walla Rivers. The reference repository location straddles the drainage divide separating the Columbia and Yakima watersheds. The maximum historical flood and the calculated probable maximum flood of the Columbia River would not reach the central portion of the Hanford Site where the reference repository is located.

Groundwater beneath the Hanford Site from both confined and unconfined aquifers discharges to the Columbia River. The recharge areas are the highlands adjacent to and beyond the Hanford Site to the west. The sediments overlying the basalt and those intercalated with the basalts are hydraulically the most permeable. There are some zones between flows that also transmit large quantities of water; such zones are found primarily in the upper basalt section within the Wanapum and Saddle Mountains Basalts. The flow tops and dense flow interiors of the Grande Ronde are overall hydraulically tighter than the shallower basalts and produce less groundwater than shallow basalts.

The groundwater movement is generally in an east to southeast direction within the Cold Creek syncline beneath the Hanford Site. Data on hydrologic properties, hydraulic heads, and groundwater chemistry indicate that lateral groundwater flow takes place primarily through permeable flow tops and sedimentary interbeds. Vertical groundwater flow or mixing

9 2 1 2 4 9 5 0 5 3 5

between these different permeable layers may occur along geologic structures such as the Umtanum Ridge-Gable Mountain anticline. Some vertical leakage between high-permeability zones may also take place across the low-permeability interiors of individual basalt flows, although the quantity of such leakage is considered quite low compared to the volume of groundwater moving laterally.

Modeling of the near-field groundwater flow system around a repository indicates that the groundwater flow paths are primarily controlled by the more permeable flow tops between successive flows. Results of modeling also indicate that the minimum groundwater travel times from the repository site to the accessible environment, a distance defined by the U.S. Environmental Protection Agency in its draft regulations as 10 kilometers (6.2 miles), would be on the order of 10,000 years or greater. The very small quantities of radionuclides which do ultimately travel to the accessible environment appear to remain small and well below the U.S. Environmental Protection Agency draft regulations.

Over the past several years, a number of far-field hydrologic modeling studies have been conducted by independent organizations. Each study had limiting assumptions and used the most recent data available at the time of the study. Travel times were estimated for groundwater movement between the repository and a discharge point at the Columbia River, a distance of 8 to 60 kilometers (5 to 35 miles) depending upon the assumed flow path. Travel times estimated ranged from 20,000 to over 1 million years. Regardless of the different assumptions used, these estimated pre-waste-emplacement travel times are significantly longer than the U.S. Nuclear Regulatory Commission proposed technical criterion of a 1,000-year minimum travel time between the repository and the accessible environment.

GEOCHEMISTRY

A preliminary assessment of the environmental conditions within the basalts beneath the reference repository location has been made. The parameters measured were temperature, pressure, groundwater composition, basalt mineralogy, Eh, and pH. The results of these studies have established the prevailing geochemical conditions for the candidate repository horizons of the Grande Ronde Basalt. Based on the current knowledge of these environmental conditions, matrix dissolution and leaching (ion exchange) represent the major degradation mechanisms for the waste form. General corrosion is the mechanism that will probably dominate canister degradation. At the end of the waste containment period, precipitation of new, less soluble, mineral phases from saturated solutions is the process that will likely control radionuclide concentrations in the groundwater flow system for all meaningful time periods relative to release criteria.

It was found that the iron oxide in the basalt is only partially oxidized and the equilibrium condition that now exists between the iron oxides in the basalt and the available oxygen present in the groundwater is one of low oxidation potential (Eh). Under these conditions essentially all of the available oxygen in the environment of the emplacement hole will be consumed by reaction with the iron oxide existing in the basalt. Under these reducing conditions many of the radionuclides are extremely insoluble and thus immobile. Corrosion of metals is also significantly reduced in an oxygen-poor environment.

CLIMATOLOGY, METEOROLOGY, AND AIR QUALITY

The Hanford region is classified as a midlatitude semiarid desert, with cool, wet winters and sunny, warm, dry summers.

The Hanford climate is greatly influenced by the surrounding topography. The Hanford Site is in the rain shadow of the Cascade Range, which accounts for the relatively low rainfall of 15 to 18 centimeters (6 to 7 inches), variation in winds, and variation in temperature. In winter, a chinook (warm and dry) wind from the southwest can result in a sudden large temperature rise (11°C per hour), rapid melting of snow (if present), and strong gusty winds. Occasionally, an incursion of cold arctic air will result in low temperatures (less than -18°C) in the region.

During the warm, dry summers, potential evaporation exceeds the precipitation. Potential evaporation has been calculated to be 5 to 9 times the mean annual precipitation, so there is a net loss of moisture from the surficial sediments.

A general evaluation of the reference repository location indicates that there would be no major impact on air quality. The only concern is dust from the rock mined at depth and stored on the ground surface. The large particle size of the basalt fragments will preclude most dust problems. Gas emissions from vents to the repository are expected to contain slightly elevated levels of naturally occurring radon gas.

In the absence of significant counteracting atmospheric effects, it seems likely that the largest climate change in the future will be a continued cooling trend. Precipitation will range from 8 to 32 centimeters (3 to 13 inches) per year and the winds will be more northerly. As a result of the cooling trend, a period of renewed glaciation is estimated to be possible as early as 10,000 years in the future. This would probably mean formation of a continental ice sheet north of the Pasco Basin, and increased stream flow and deposition of sediments within the basin.

ENVIRONMENTAL, LAND-USE, AND SOCIOECONOMIC CHARACTERISTICS

The Hanford Site is a shrub-covered grassy plain with a variety of plant communities. Sagebrush is the dominant shrub, and cheatgrass is the dominant grass over the reference repository location. These plants give food, cover, and shelter to many species of wildlife. Currently, there are no federally recognized threatened or endangered plant or mammal species known to occur on the reference repository location. The most important big-game mammal is the mule deer. Coyotes are the principal predators. The Great Basin pocket mouse is the most abundant small mammal occurring in the Hanford environs, although cottontail rabbits may be found in some areas. The most common upland game birds are chukar partridge and California quail, with ringnecked pheasants being found in limited numbers. Raptors such as Swainson's hawks, red-tailed hawks, golden eagles, American kestrels, and burrowing owls utilize many areas at the Hanford Site as nesting sites. Reptiles and amphibians are relatively scarce, with the bull (gopher) snake and side-blotched lizard being the most common.

There are four major operational areas on the Hanford Site. They are identified by area numbers and generally reflect the types of activities that are conducted within them. The 100 Areas, located along the Columbia River, are the sites of the plutonium production reactors. The 200 Areas are the sites of the fuel reprocessing and waste management activities. The 300 Area is the site of both research and development laboratories and the fuel-fabrication facilities. The 400 Area is the site of the Fast Flux Test Facility. The southern part of the Hanford Site has been dedicated as an Arid Lands Ecology Reserve. The lands within the Hanford Site have been within the jurisdiction of the Federal Government since 1943.

Continued growth in the economy of the communities adjoining the Hanford Site will be largely dependent on federal support for research and waste management programs and utility company construction of nuclear power plants at Hanford.

REPOSITORY DESIGN

The conceptual repository design is based on the capability to store 27,900 waste packages containing a total of 47,400 metric tons of heavy metal equivalent of reprocessed high-level waste and spent fuel declared as waste, and 32,000 packages of solidified low-level transuranic waste. These waste forms will be isolated within the Grande Ronde Basalt below the ground surface.

The repository design includes surface waste receiving and inspection facilities, surface decontamination and packaging facilities, a shaft pillar containing five shafts connecting the surface and the underground workings, underground storage panels, transport facilities, and ancillary service systems including two separate ventilation systems.

The function of the repository is to provide long-term containment and isolation. After the storage rooms have been filled with waste packages, the storage rooms are planned to be filled with engineered backfill intended to act as a chemical and physical barrier against radionuclide migration. At the time of decommissioning of the repository, multiple seals will be placed in accesses between the panel areas and in the shaft pillar and in the shafts above the repository level.

WASTE PACKAGE

The conceptual waste package design for commercial high-level waste forms consists of the waste form sealed in a low-carbon steel canister and surrounded by a tailored backfill composed of 75 percent crushed basalt and 25 percent bentonite clay. The repository conceptual design calls for waste to be emplaced horizontally in long boreholes. Present plans call for delayed backfilling to allow the waste canister to cool, and to readily facilitate the possibility of retrieval as required by the U.S. Nuclear Regulatory Commission proposed technical criteria. Borosilicate glass is the assumed commercial high-level waste form, with spent fuel being an alternate waste form.

The waste package is being designed to provide safe handling of the waste during shipment and emplacement (as well as retrieval), to provide containment of the waste during the thermal period in which heat from fission product decay dominates (300 to 600 years), and, finally, to assure the controlled and slow release of radionuclides during the period of geologic control to meet U.S. Nuclear Regulatory Commission proposed release criteria. During the thermal period (the first 1,000 years after closure), the metallic canister provides a primary function of preventing release of the waste to the general environment or to the repository and site subsystems. During the thermal period the backfill acts also as a secondary barrier by preventing water from reaching the canister and by buffering the water near the canister, thus inhibiting corrosion.

During the period of geologic control, the primary barriers to radionuclide migration are the waste form and the backfill. The waste form functions to limit release of radionuclides and the backfill functions to retard radionuclide migration by sorption or chemical alteration to insoluble nuclide-containing secondary minerals, as well as retarding the rate of groundwater flow in the immediate vicinity of the waste form. The backfill also serves as a redundant barrier in the event that some containment is lost during the first 1,000 years after closure. There are no waste package containment requirements beyond 1,000 years, but it is expected that waste packages designed to prevent release during the period of highest heat output will provide some containment beyond the thermal period.

PERFORMANCE ASSESSMENT

To quantify the degree of isolation afforded by an engineered system in the basalts underlying the Hanford Site, three performance measures are being used. These performance measures consist of groundwater flow paths and travel times, rate of radionuclide release from the repository, and total activity of individual radionuclides reaching the accessible environment. A minimum groundwater transit time of 1,000 years to the accessible environment is the current technical criterion proposed by the U.S. Nuclear Regulatory Commission. The long-term repository performance centers on these performance measures with specific regard to the numerical limits required for compliance with applicable technical criteria and proposed regulations.

Mathematical models have been developed for predicting long-term performance for comparison with the site criteria developed by the federal regulatory agencies. Relevant and site-specific release scenarios have been formulated that have application to a repository constructed in the basalt underlying the Hanford Site. The performance analysis solutions have been broken down into three subregions: the very near field (canister to room scale), near field (repository scale), and far field (accessible environment and immediate surroundings scale).

The primary conclusions from the predictive modeling for both disruptive and nondisruptive scenarios are as follows:

- Solubility of radionuclides from the reference waste forms in a basalt environment limits the repository release rates to levels well below the U.S. Nuclear Regulatory Commission proposed technical criteria.
- There is little or no economic or safety incentive for a complex waste package.
- High-sorptive properties of basalt will significantly retard the movement of radionuclides such as cesium, strontium, radium, and americium.
- Groundwater flow paths from the repository are predominantly horizontal and are restricted to the Grande Ronde Basalt.
- The minimum groundwater travel time from the repository to the accessible environment is in the range of 10,000 years or greater.
- The transport of mobile long-lived radionuclides, such as ^{99}Tc, is limited to about 200 vertical meters (656 feet) and less than a few kilometers (miles) horizontally after 10,000 years.

- Radionuclide release appears to remain well below the U.S. Environmental Protection Agency draft regulations for both disruptive and nondisruptive scenarios.

ISSUES AND PLANS

A review of the information obtained during preliminary site characterization resulted in the identification of fifteen issues or technical questions that require answers to satisfy the proposed regulatory criteria. The work to be accomplished to answer an issue or technical question has also been identified. The four issues related to geology and hydrology or to modeling the groundwater flow system are as follows:

- What is the total amount (activity) of radionuclides potentially releasable to the accessible environment in a 10,000-year period, and is this amount in compliance with appropriate U.S. Environmental Protection Agency regulations?

- What are the geologic, mineralogic, and petrographic characteristics of the candidate repository horizons and surrounding strata within the reference repository location?

- What are the nature and rates of past, present, and projected structural and tectonic processes within the geologic setting and reference repository location?

- Are the pre-waste-emplacement groundwater travel times near the repository sufficient to assure compliance with U.S. Nuclear Regulatory Commission proposed technical criteria?

Four issues related to geoengineering and repository design are as follows:

- Can stability and isolation capability of the repository be maintained in the presence of coupled in situ, excavation-induced, and thermal-induced stresses?

- Can repository shafts, tunnels, and exploratory boreholes be constructed and sealed without causing preferential pathways for groundwater or increasing the potential for radionuclide migration from a nuclear waste repository such that compliance with appropriate U.S. Environmental Protection Agency regulations is not possible?

- Can satisfactory representative measurements or estimates of rock-mass strength be obtained?

- Are current methods of in situ stress measurement used at depth reliable enough to provide satisfactory data for design requirements?

The remaining seven issues are related to waste package, site geochemistry, and waste package testing and performance confirmation. These issues are as follows:

- Does the very near-field interaction between the waste package and its components, the underground facility, and the geologic setting compromise waste package or engineered system performance? (i.e., What is the maximum expected release rate from the engineered system and does the geologic setting prevent the waste package containment objective from being achieved?)

- Is a unique borehole backfill required?

- Are the geochemical and hydrologic properties of the geologic setting (in conjunction with the waste forms) sufficient to meet or exceed U.S. Nuclear Regulatory Commission proposed waste isolation requirements?

- What is the relative importance of waste form leach rates versus solubility of key radionuclides in the near-field environment for controlling release?

- Can valid Eh measurements for the candidate repository horizons in the reference repository location be made either by potentiometric measurement or indirectly by measurement of dissolved redox couples?

- To what degree does the geologic setting retard migration of key radionuclides from the engineered system in meeting U.S. Environmental Protection Agency draft release criteria?

- How can very near-field waste/barrier/rock materials interaction data, as measured experimentally, be extrapolated over time to reasonably assure that overall waste package and repository performance meets regulatory criteria?

A description of the work elements planned during detailed site characterization to resolve all or part of an issue is discussed in this report. Some of the work elements are conducted to provide information to reduce the level of uncertainty associated with a technical question. If all of the work elements are completed and show positive resolution of the criteria requirements, then all of the issues should be resolved with the exception of those that cannot be satisfied by technical data, but which can be mitigated with acceptable cost and risk. In these instances, risk analyses are planned.

The methods to be used for obtaining the needed data include the drilling of boreholes, construction of an exploratory shaft, and in situ testing of the selected candidate repository horizon, geophysical surveys, laboratory and field testing, and numerical modeling.

Logic diagrams and schedules contained in this Site Characterization Report identify the order in which the major work element activities will be conducted, the interface between activities, and the timing for completion of the activities for the detailed site characterization leading to the eventual construction and operation of a repository.

1. INTRODUCTION

1.1 REGIONAL SETTING

The U.S. Department of Energy's (DOE's) Hanford Site is located in the southeastern part of the state of Washington, just north of the confluence of the Columbia, Snake, Walla Walla, and Yakima Rivers. The southeastern part of Washington and adjacent parts of the states of Idaho and Oregon are unique, in that the region is covered by a thick mantle of lava flows called the Columbia River Basalt Group. Successive prehistoric flows of basalt have led to the formation of a broad relatively flat plateau. Near the center of the plateau is a gentle downwarped area called the Pasco Basin. The Hanford Site is centrally located within the Pasco Basin, just north of the city of Richland (Fig. 1-1).

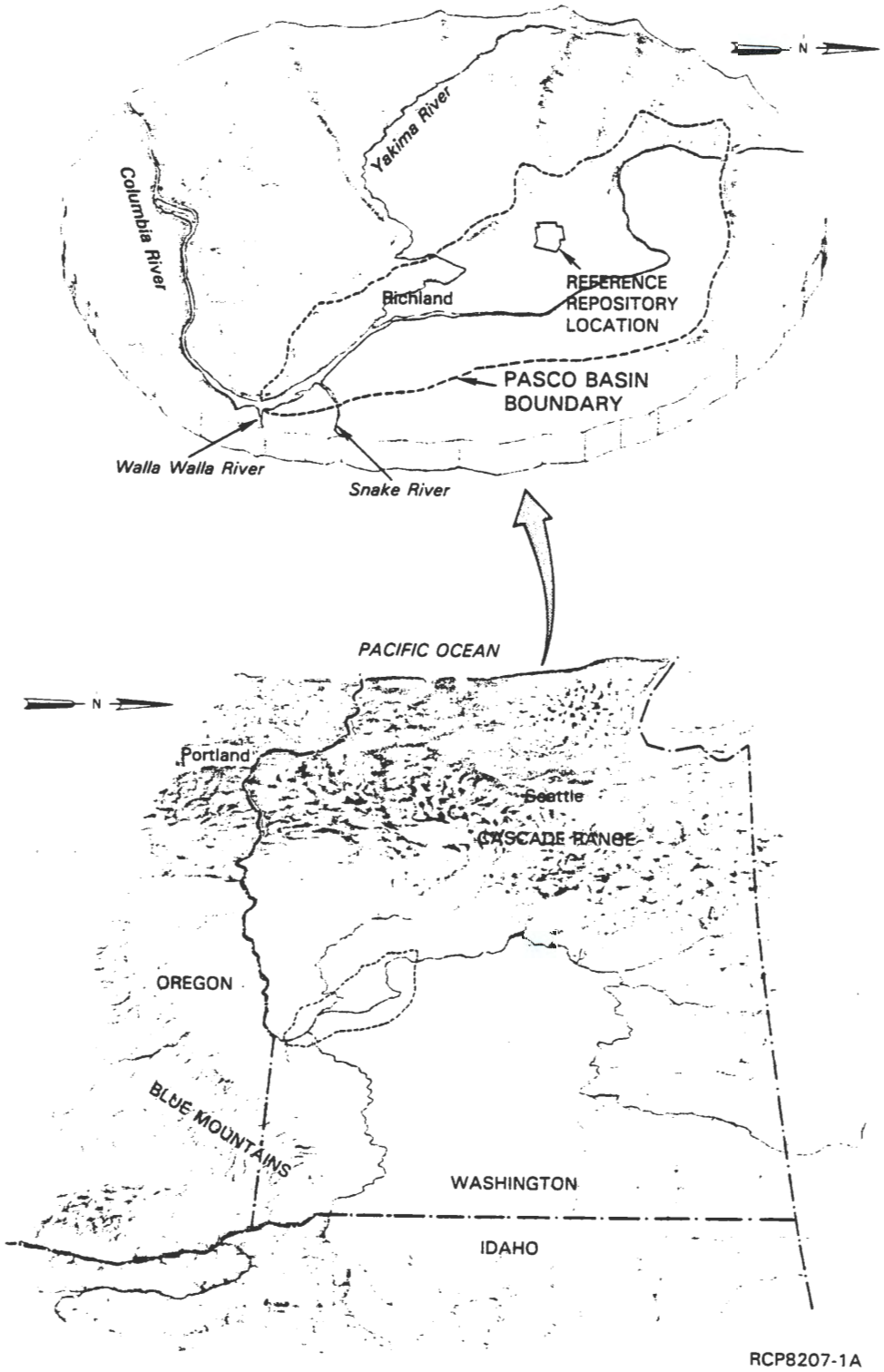

FIGURE 1-1. Location (in perspective) of the Pasco Basin and Hanford Site, Washington State.

1.2 BACKGROUND

At the request of the U.S. Atomic Energy Commission in 1955, the National Academy of Sciences-National Research Council initiated a feasibility study for disposal of high-level radioactive wastes on land within the continental limits of the United States. Among the proposed disposal methods were disposal of solidified wastes in salt, injection of liquid wastes in permeable formations deep underground, and incorporation of all radioactive materials into virtually insoluble silicate blocks and storing them on the ground surface in arid areas or in dry mines.

In the early 1960s a program of studies was undertaken to obtain data on bedded salt, hydraulic fracturing in shale, and bedrock storage in granite rock. By the mid-1960s concern was expressed (1) about the ability to store liquid wastes in underground chambers mined out of the crystalline bedrock and (2) about the long-term capacity of the hydraulic fracturing and grouting technique. It was recommended by the National Academy of Sciences-National Research Council Committee on Geologic Aspects of Radioactive Waste Disposal that a program be implemented to drill and test geologically acceptable basin provinces in the United States and, specifically, to reenter the 3,248-meter (10,655-foot) borehole in the Rattlesnake Hills, located at the southwestern boundary of the Hanford Site. The committee also recommended that detailed geologic investigations of the Rattlesnake Hills be conducted to determine the feasibility of constructing underground storage tunnels in basalt for the disposal of solid nuclear wastes.

As a result of the information obtained from the deep borehole in the Rattlesnake Hills, funding was provided to drill several deep boreholes in the Hanford Site to further characterize the underlying basalt rock. As part of this study, four deep boreholes greater than 1,067 meters (3,500 feet) deep were drilled, and limited hydrologic tests were conducted within the Hanford Site in the late 1960s. Results of the borehole studies were summarized in ARHCO (1976).

Emphasis was placed in the mid-1970s on waste solidification and interim storage in engineered surface storage facilities. The major effort in waste-form technology was devoted to glass.

In 1976, the U.S. Energy Research and Development Administration expanded its commercial radioactive waste management programs and established the National Waste Terminal Storage Program. The U.S. Energy Research and Development Administration's successor, the DOE, has aggressively continued this technical program to meet applicable regulatory requirements and to ensure that nuclear waste management problems will not be deferred to future generations.

The scope of the National Waste Terminal Storage Program includes the identification of potential repository sites in several different types of geologic rock types. The program has called for research and development to support design, licensing, construction, operation, and decommissioning of a repository. The goal of the program is to establish a system of regionally based repositories designed for the disposal of high-level and transuranic nuclear wastes generated by commercial power reactors and unreprocessed spent fuel (if disposal is deemed appropriate).

In July 1978, the National Waste Terminal Storage Program was restructured and expanded. The DOE contracted with Battelle Memorial Institute to develop the technology for mined geologic disposal of nuclear wastes. The Office of Nuclear Waste Isolation was established within the Project Management Division of Battelle Memorial Institute to augment existing programs of the National Waste Terminal Storage Program. As part of this expanded National Waste Terminal Storage Program, three major geologic projects aimed toward the selection of a first repository site were established: (1) the Office of Nuclear Waste Isolation, (2) the Basalt Waste Isolation Project (BWIP), and (3) the Nevada Nuclear Waste Storage Investigations. A fourth National Waste Terminal Storage project, Subseabed Disposal, is studying the feasibility of emplacing packaged high-level waste beneath the seabed in stable regions of the ocean floor.

A detailed evaluation of the National Waste Terminal Storage Program was presented in the Final Environmental Impact Statement: Management of Commercially Generated Wastes (DOE, 1980).

In April 1981, the DOE issued a Record of Decision (DOE, 1981) which formalized the selection of a strategy for the disposal of commercially generated radioactive wastes and the supporting program of research and development. In their formal decision step, the DOE decided to (1) adopt a strategy to develop mined geologic repositories for disposal of commercially generated high-level and transuranic radioactive wastes (while continuing to examine subseabed and very deep hole disposal as potential backup technologies) and (2) conduct a research and development program to develop repositories and the necessary technology to ensure the safe long-term containment and isolation of these wastes.

The National Waste Terminal Storage Program presently emphasizes disposal in mined repositories deep underground in stable geologic formations. The locations of the types of rocks now under study are shown in Figure 1-2. The BWIP is studying basalt formations underlying the DOE's Hanford Site. The Nevada Nuclear Waste Storage Investigations include several different rock types (principally tuff, a volcanic ash) underlying the DOE's Nevada Test Site. The Office of Nuclear Waste Isolation is evaluating other geologic formations within the United States on non-DOE lands, including domed and bedded salt and crystalline rocks (granite).

7 2 1 2 4 9 5 0 5 5 4 7

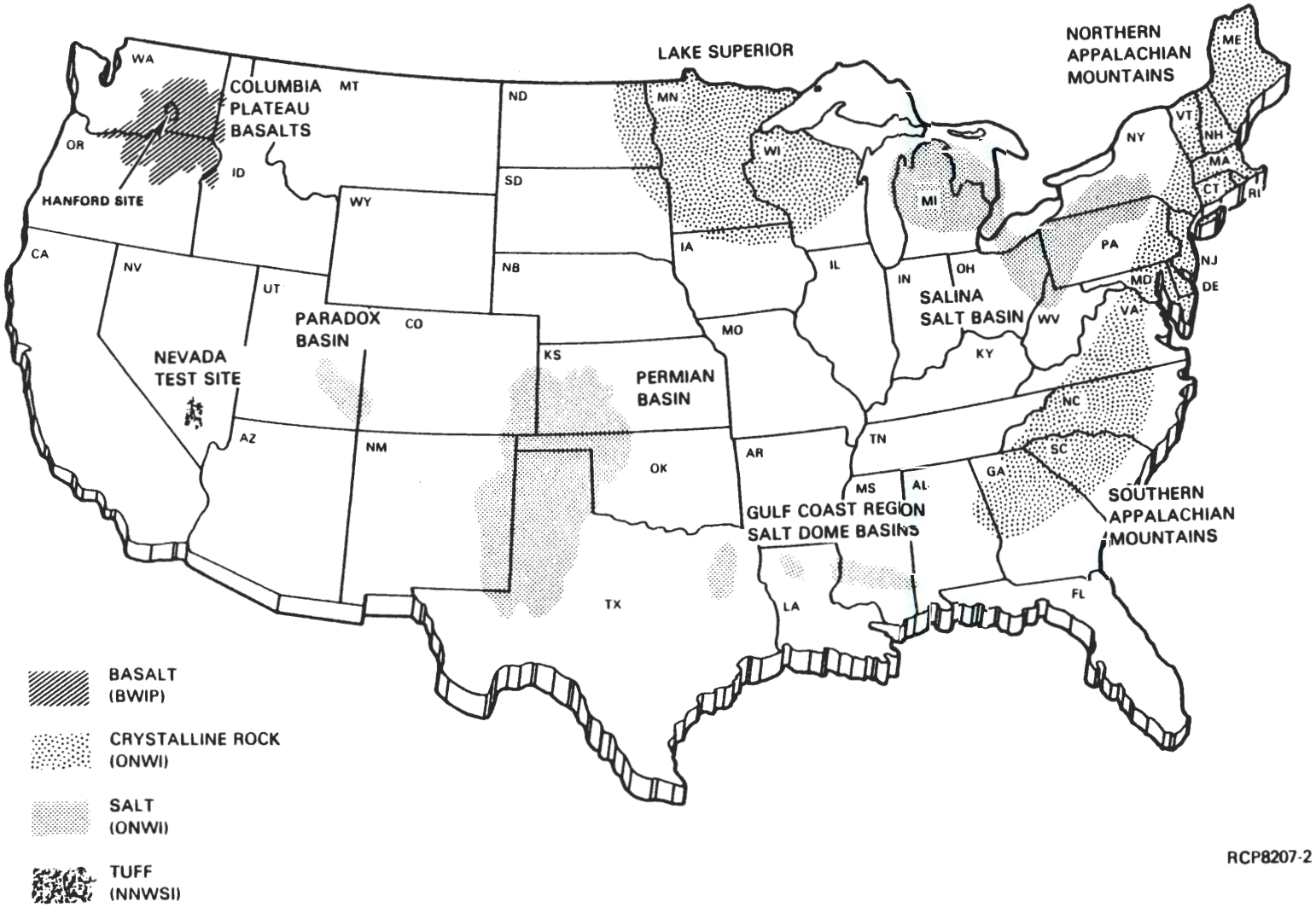

FIGURE 1-2. Regions That are Being Considered for Geologic Disposal of Radioactive Waste.

The Office of Nuclear Waste Isolation was also involved in the development of the technology common to the design, construction, operation, and decommissioning of geologic repositories. The U.S. Geological Survey is assisting the DOE by providing technical expertise in all of these program elements and by screening geohydrologic provinces on a prototypical basis.

Rockwell Hanford Operations (Rockwell) is presently responsible for the investigations of the basalts beneath the Hanford Site for the DOE. The BWIP, operated by Rockwell, has been chartered by the DOE, as part of the National Waste Terminal Storage Program, to conduct this work. The BWIP mission is to identify potential geologic repository sites in basalt within the Hanford Site, to design the facilities associated with such a repository, and to develop technology required for the permanent isolation of radioactive wastes in basalt formations. If feasibility is shown, the DOE may proceed with the detailed design, construction, and operation of such a facility. The BWIP has emphasized the systems approach to integrate diverse program elements including geologic and hydrogeologic studies, development of nuclear waste packages, and repository-engineering studies.

1.3 THE HANFORD SITE

1.3.1 Geographic Setting

The Hanford Site, which occupies approximately 1,500 square kilometers (570 square miles), is located within the Pasco Basin (Fig. 1-1). At the northernmost boundary of the Hanford Site (Fig. 1-3), the Saddle Mountains rise to an elevation of more than 610 meters (2,000 feet). At the southern boundary, the Rattlesnake Hills rise to an elevation of more than 914 meters (3,000 feet). The Columbia River flows through the central part of the Hanford Site at an elevation of less than 122 meters (400 feet). Along the east bank of the Columbia River the land surface rises abruptly more than 122 meters (400 feet), forming the White Bluffs, tan- to chalky-colored sands, silts, and clays. Along the western boundary of the site is a highland area formed by three sinuous ridges that rise more than 1,220 meters (4,000 feet) in elevation at their highest point, but gently dip eastward and terminate at the site boundary. There are more than 460 kilometers (285 miles) of paved roads on the Hanford Site, which connect the seven major areas: the city of Richland, 1100 Area, 300 Area, 400 Area, 200 Areas, 100 Areas, and the Washington Public Power Supply System, Inc. site.

The Hanford Site is approximately 52 kilometers (32 miles) north to south and 42 kilometers (26 miles) east to west. The separations areas (200 East and 200 West Areas) are located near the center of the Hanford Site on what is commonly referred to as the "200 Areas Plateau." This portion of the Hanford Site contains the irradiated-uranium-fuels-processing and plutonium-separation facilities and the major radioactive waste-storage and -disposal facilities. The reactor areas (100-B, -K, -N, -D, -H, and -F) are located along the west bank of the Columbia River where it makes an abrupt swing to the north and then back to the south. The Fast Flux Test Facility is located in the 400 Area in the southeastern part of the Hanford Site; just to the north are the power-reactor sites under construction by the Washington Public Power Supply System, Inc. North of the city of Richland are the 1100 Area and the 300 Area. In the 300 Area, UNC Nuclear Industries, Inc. operates a fuels-production facility, and the Pacific Northwest Laboratory and the Westinghouse Hanford Company operate research laboratories. The Exxon Nuclear Company, Inc., J. A. Jones Construction Services' minor construction services facilities, and the Hanford Site transportation and stores services are located in the 1100 Area.

The nearest population center to the Hanford Site is Richland, Washington, which had a population of 33,478 in 1980 (Bureau of the Census, 1981). Intensive farming is carried out along the Yakima River Valley to the south of Rattlesnake Hills and to the east. West of the Hanford Site is the U.S. Army's Yakima Firing Center, which has restricted access. There are approximately 11,000 workers on the Hanford Site.

9 2 1 2 4 9 5 0 5 5 0

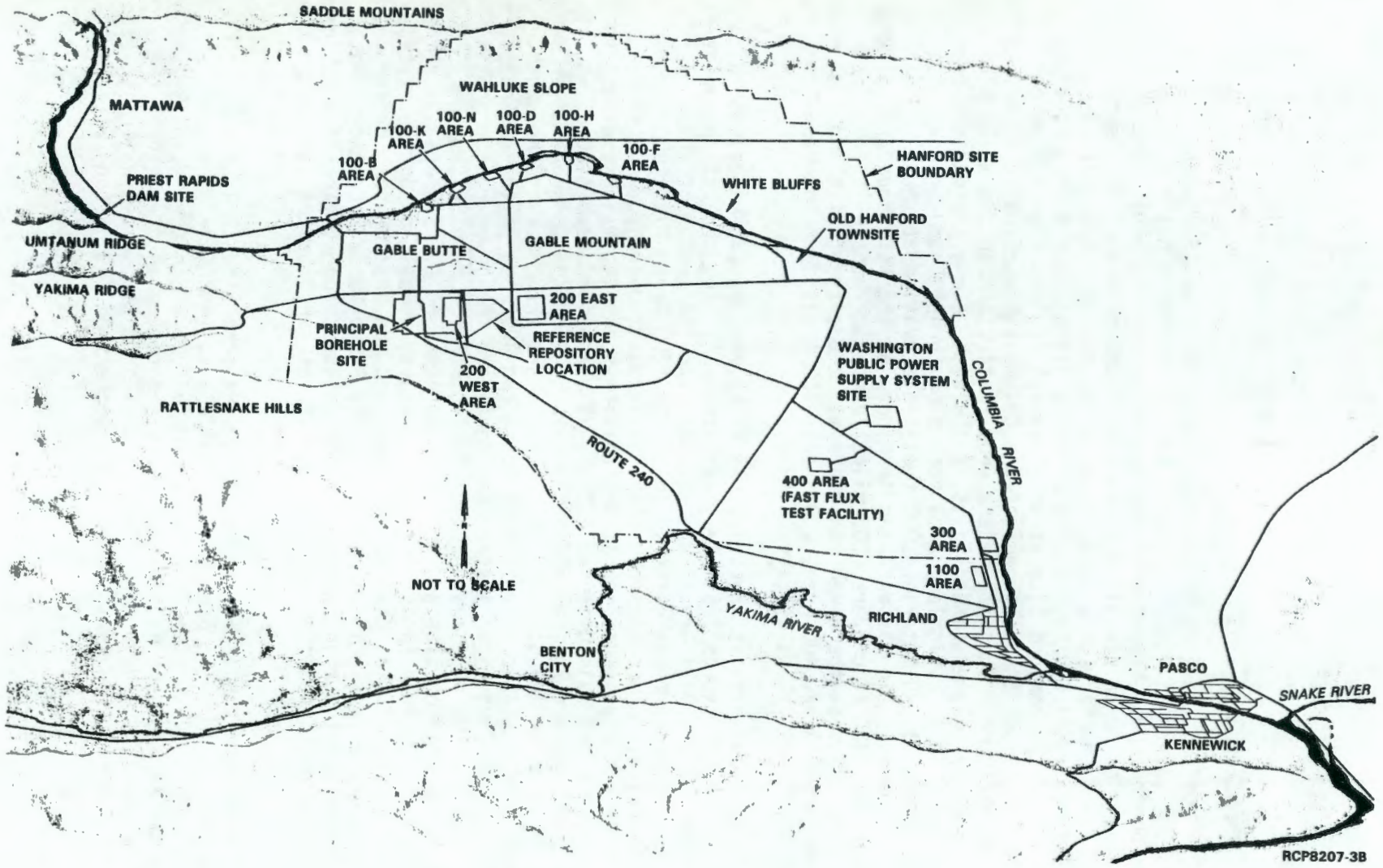

FIGURE 1-3. The Hanford Site.

1.3.2 Geologic Setting

The lava flows that erupted from fissures or fractures in the Earth's surface 6 to 16.5 million years ago in southeastern Washington and adjacent parts of Oregon and Idaho accumulated in several longstanding depressions or downwarped areas. In one of these downwarped areas, the Pasco Basin, the basalt flows (a name given to these igneous rocks based on their chemical composition) attained a thickness of over 3,048 meters (10,000 feet).

These layered basalt flows have been named the Columbia River Basalt Group, which in turn has been subdivided into three formations: the lowermost called the Grande Ronde Basalt, the middle formation called the Wanapum Basalt, and the uppermost formation called the Saddle Mountains Basalt (Fig. 1-4). Intercalated or sandwiched between these basalt flows, especially within the Saddle Mountains Basalt, are sedimentary interbeds of the Ellensburg Formation, which are composed primarily of volcanic debris from the Cascade Range.

The rocks that lie beneath the basalts within the Pasco Basin have not been sampled. Nevertheless, data from geophysical surveys indicate the possible presence of sedimentary rocks below the basalts and above the crystalline basement.

Overlying the Columbia River basalts within the Pasco Basin are two sedimentary formations. The Ringold Formation directly overlies the basalt and the Hanford formation (informal name) overlies the Ringold Formation. Sediments of the Ringold Formation were deposited by streams with some shallow-lake environments and are, for the most part, well bedded. The rocks forming the White Bluffs, along the east bank of the Columbia River, are of the Ringold Formation. The Hanford formation is composed of sediments that were deposited in the Pasco Basin by catastrophic floods during the last Ice Age, floods with flow rates on the order of cubic kilometers of water per hour.

During the past 10,000 years, the ground surface has been modified by erosion and deposition. The most striking depositional feature in the Pasco Basin is the area of sand dunes that covers an area of more than 26 square kilometers (10 square miles) on the Hanford Site.

The total rock mass that makes up the formations within the Pasco Basin has been subjected to stress throughout geologic time. In response to this stress, some areas have been folded or arched upward (anticlines) and some have been folded downward (synclines). Along some of the anticlines, deformation continued beyond the capacity of the rock to fold, and fractures or faults were created. A north-south cross section through the Pasco Basin, showing the general structure of the underlying rocks, is presented in Figure 1-5.

9 2 1 2 4 9 5 0 5 5 2

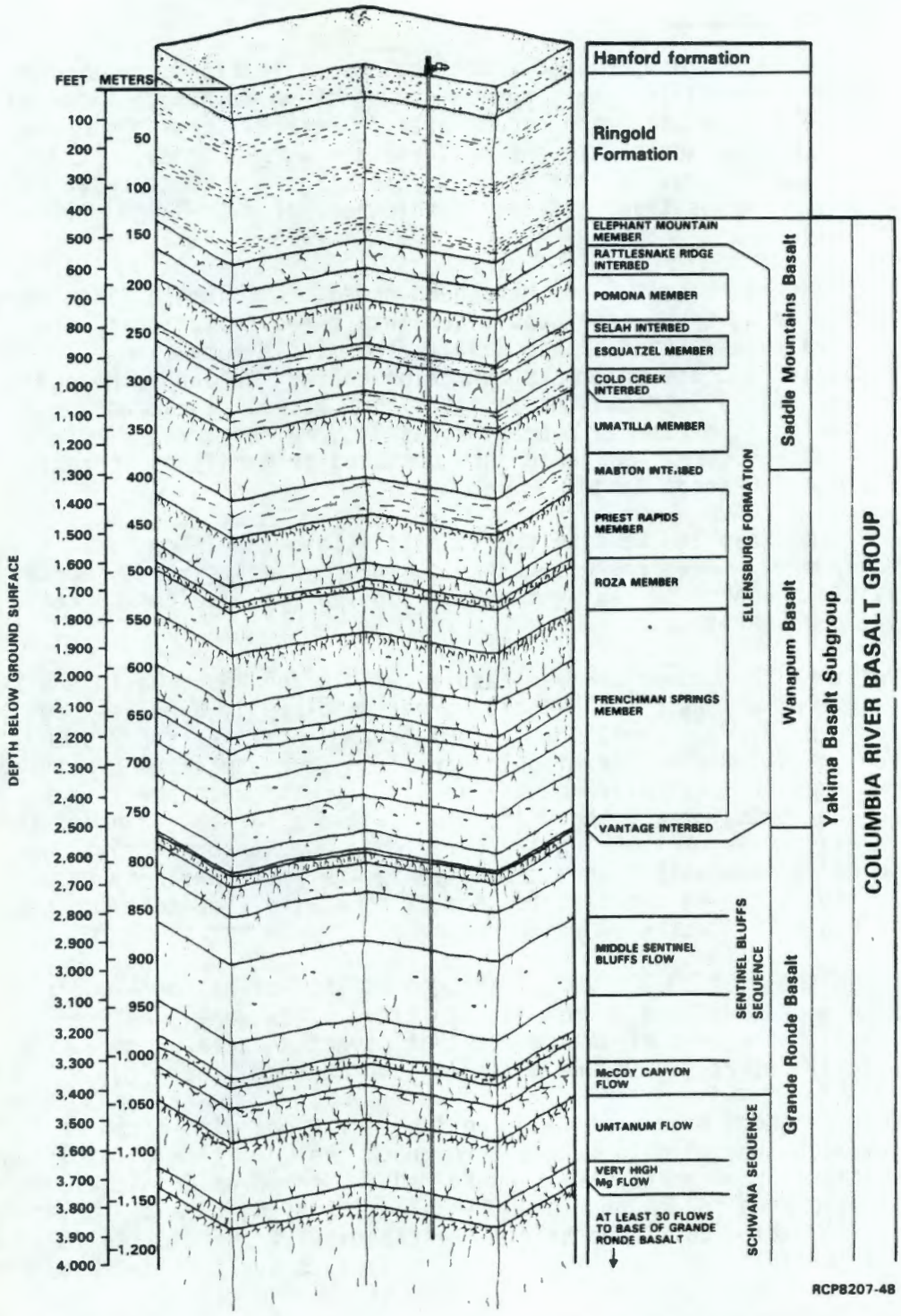

FIGURE 1-4. Stratigraphy of the Columbia River Basalt Group, Yakima Basalt Subgroup, and Intercalated and Suprabasalt Sediments Within the Pasco Basin.

9 2 1 2 4 9 5 0 5 5 3

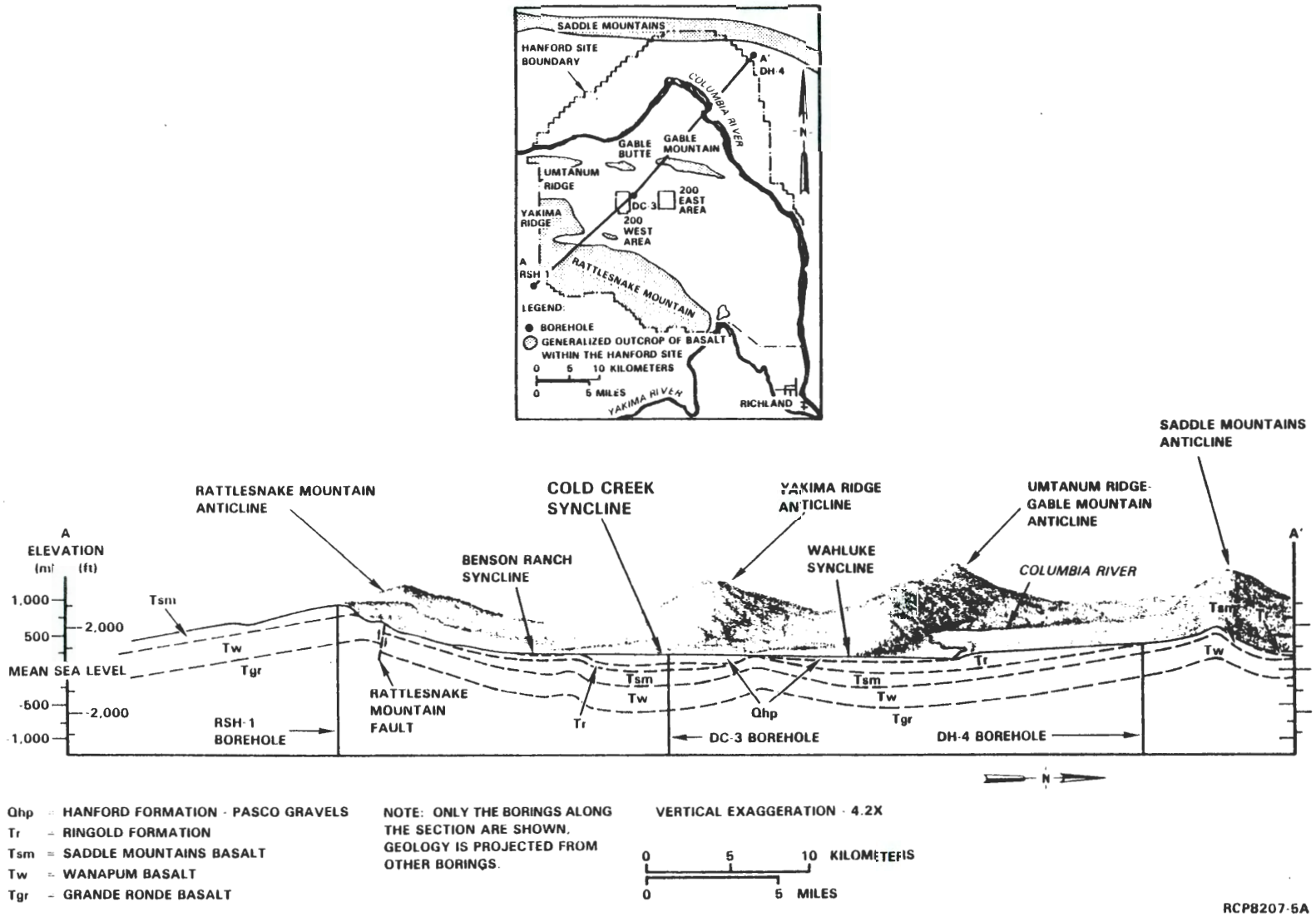

FIGURE 1-5. Generalized Cross Section Through the Pasco Basin.

The reference repository location is situated in the relatively flat-lying Cold Creek syncline, which is bounded on the north by the Gable Butte-Gable Mountain anticline and on the south by the Yakima Ridge anticline (Fig. 1-5). The combined thickness of the Hanford and Ringold sediments overlying the basalts at the reference repository location is about 180 meters (600 feet). The Umtanum and the middle Sentinel Bluffs flows are the candidate horizons (Fig. 1-4). The middle Sentinel Bluffs is three flows higher than the Umtanum flow in the section shown. Eighteen basalt flows encompassing about 700 meters (2,300 feet) overlie the middle Sentinel Bluffs flow.

1.4 PURPOSE AND SCOPE

The DOE siting process includes three phases of work prior to the submission of an application for a license to construct a repository for the terminal storage of nuclear wastes. These phases are the site screening phase, the detailed site studies phase, and the site selection phase (Fig. 1-6). At the conclusion of the site screening phase, a site characterization report is prepared for submission to the U.S. Nuclear Regulatory Commission, which summarizes the site studies to date and delineates the work needed to fully characterize the potential repository site in conformance with 10 CFR 60 (NRC, 1981). This document is the Site Characterization Report for the BWIP. It focuses on the geology and hydrology studies, development of nuclear waste packages, and repository-engineering studies. Special emphasis has been placed on the development of performance standards for radionuclide release that will be required of the geologic, waste package, and repository systems.

The purpose of this report is to provide the status of and identify the data necessary for the detailed site studies phase and the plans for acquiring the data, including construction of an exploratory shaft and in situ testing.

This Site Characterization Report thus serves as a DOE planning document in accordance with 10 CFR 60 (NRC, 1981) and clearly defines specific siting objectives, policies, and criteria and identifies the activities (content and timing) needed to accomplish the objectives, the organizational components responsible for implementation, and the driving forces for conflict resolution.

Through the detailed site studies phase (Fig. 1-6), additional reports will be issued describing site data and analyses that provide an evaluation of the site suitability. The purpose of these reports is to provide geohydrologic and environmental data obtained in accordance with this initial Site Characterization Report sufficient to (1) determine site suitability, (2) prepare licensing documents, (3) perform design trade-off studies, and (4) prepare performance assessments.

Following the completion of the detailed site studies of the basalts underlying Hanford, the basalt reference repository location will be considered along with other candidate sites that have been characterized in the United States as the site recommended for repository construction. Following the selection of one of these sites, a final environmental impact statement and site selection report will be issued. As shown in Figure 1-6, sites not initially selected may be protected and remain candidates for future selection as repository sites. License applications will be prepared for selected sites and filed with the U.S. Nuclear Regulatory Commission after public review of the reports that recommend the site to be selected. When the DOE-selected site is accepted by the U.S. Nuclear Regulatory Commission, the selection decision is confirmed.

9 2 1 2 4 9 5 0 5 5 6

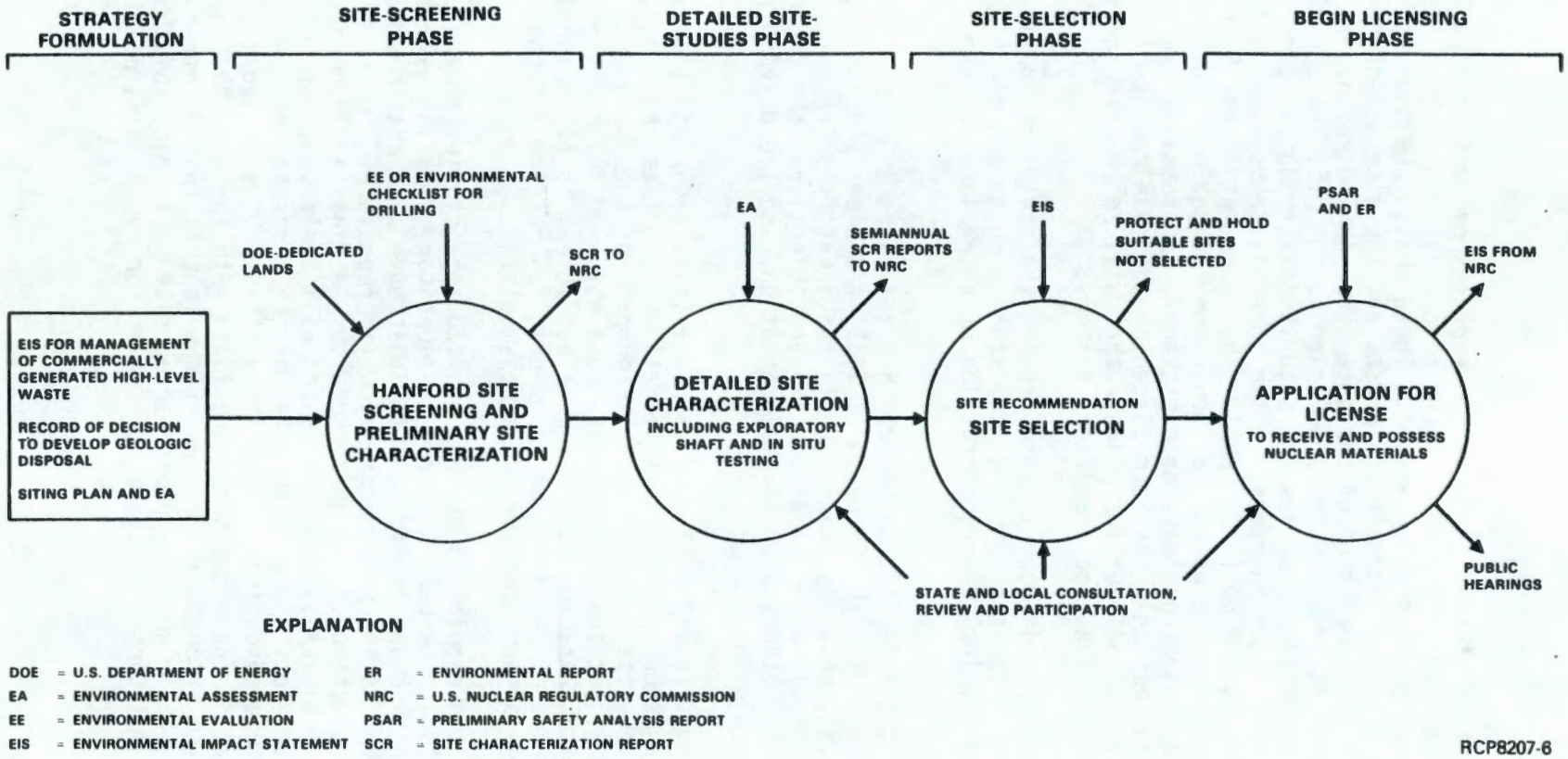

FIGURE 1-6. Repository Siting Process (modified from DOE, 1982).

1.5 CONTENTS

1.5.1 Chapter 1: Introduction

The information presented in this chapter provides an overview of the regional setting of the Hanford Site and a general discussion of the events that led up to the present site screening and site characterization work. The geography and geology of the Hanford Site are presented to provide the reader with some background information for ease in following the more detailed discussion in the subsequent chapters. The purpose of the Site Characterization Report is also put in context within the DOE siting process.

1.5.2 Chapter 2: Decision Process for Choosing a Reference Repository Location and an Alternate Repository Location

The methodology used in the site screening process is described, along with the steps taken in the screening process to identify a reference repository location. The chapter also includes the decision-making analysis that led to the identification of the candidate areas, candidate subareas, site localities, candidate sites, reference repository location, alternate repository location, and candidate repository horizons.

1.5.3 Chapter 3: Geologic Description of the Reference Repository Location and the Surrounding Area

A detailed description is given of the rocks that underlie the Hanford Site and, specifically, the reference repository location. The structure of these rocks is described in detail. Information is also presented on the tectonic history of the region, which produced the existing structure. A review of the seismic history of the region is given and a detailed listing of past earthquakes in the region is included.

1.5.4 Chapter 4: Geoengineering

The mechanical properties of basalt are presented in this chapter. These properties are given for both basalt hand specimens measured in the laboratory and properties measured on large intact blocks in the Near-Surface Test Facility.

9 2 1 2 4 9 5 0 5 5 8

1.5.5 Chapter 5: Hydrogeology

The regional groundwater flow system is described, along with the general groundwater hydrochemistry. The wells, from which the information on hydrologic parameters was obtained, are identified. The groundwater flow system for the site is described and detailed information is presented on the hydrologic parameters measured on the rocks as a function of depth and on the hydrochemistry. Results of age determinations of the groundwater as a function of depth are also presented.

1.5.6 Chapter 6: Geochemistry

The geochemistry of the basalt environment is described, including the mineralogy of the Grande Ronde Basalt. Data on hydrothermal reactions of waste package materials with basalt, under conditions similar to those in a repository in basalt, are assessed. Information is also presented on solubility of materials in a basalt environment and sorption reactions of radionuclides on host-rock minerals. Natural analogs that apply to the stability of a repository in basalt are also discussed.

1.5.7 Chapter 7: Surface Hydrology

Information on the drainage basin in which the Hanford Site is situated is presented, along with more detailed information on the surface-water regimes associated with the reference repository location. Specific information is presented on past and projected flooding of the site, quality of surface waters, and water demand within the Pasco Basin.

1.5.8 Chapter 8: Climatology, Meteorology, and Air Quality

A discussion of the general climate of the Hanford Site is given, along with a detailed summary of the synoptic meteorological data and air quality data. A discussion of the paleoclimate and future climatic variations is also included in this chapter.

1.5.9 Chapter 9: Environmental, Land-Use, and Socioeconomic Characteristics

A summary listing of the plants and animals that exist on the Hanford Site and, specifically, the reference repository location is presented. Attention is given to threatened and endangered species. Information is presented on current land use, the population distribution, and the economy of the area in relation to the reference repository location.

9 2 1 2 4 9 5 0 5 5 9

1.5.10 Chapter 10: Repository Design

A description of the repository conceptual design, including basis of conceptual design, design of underground openings, and a summary of the thermal and rock-stress analyses, is presented in this chapter. A discussion is also included on the method of construction and backfilling/sealing of the shafts, boreholes, panels, and storage rooms.

1.5.11 Chapter 11: Waste Package

The chemical and physical properties of spent fuel and the borosilicate glass waste form are described. A description of the waste package design for basalt is presented, along with a discussion of the research and development work now being done by the BWIP to define the waste package design requirements. Included in the status of the research and development work are the results of preliminary performance-evaluation modeling. A review of the chemical, physical, and radiological emplacement conditions for a repository in basalt is also contained in this chapter.

1.5.12 Chapter 12: Performance Assessment

This chapter describes the BWIP approach to performance modeling and provides a detailed discussion of the various mathematical models used to predict rock stress/strain, heat transfer, groundwater flow, and solute transport. A discussion of the preliminary analyses made of the near field (within 1,000 meters (3,280 feet) of the repository) and the far field (within several tens of kilometers (miles) of the repository) is included.

1.5.13 Chapter 13: Site Issues and Plans

The work elements needed to resolve three site related issues (technical questions about which some uncertainty or controversy exists regarding the resolution of a regulatory or technical requirement) and one key issue (technical question that could either confirm or eliminate the basalts underlying the Hanford Site from further consideration as a repository site) are outlined and discussed in this chapter. For each work element outlined, a status is provided and a discussion of the work planned for the detailed site characterization phase is presented.

1.5.14 Chapter 14: Geoengineering and Repository Design Issues and Plans

The work needed to resolve two engineering issues and two key engineering issues (see definition of issues in Section 1.5.13 above) is outlined and discussed in this chapter. A status of each work element and a discussion of the work planned to be completed during the detailed site characterization phase are also provided.

9 2 1 2 4 9 5 0 5 6 0

1.5.15 Chapter 15: Waste Package and Site Geochemistry Issues and Plans

The work needed to resolve six issues (see definition of issues in Section 1.5.13) is outlined and discussed in this chapter. A concise summary of the status of each work element is presented, together with a plan of the work to be completed during detailed site characterization.

1.5.16 Chapter 16: Performance-Assessment Issues and Plans

The work needed in performance assessment is outlined and discussed in this chapter. A summary of the status of each work element is presented, together with a plan of the work to be completed during detailed site characterization. (The issues discussed in this chapter are not new issues but are issues previously identified in Chapters 13 and 15.)

1.5.17 Chapter 17: Site Characterization Program

This chapter describes the program and schedule for completing the work elements described in Chapters 13 through 16. The exploratory shaft and in situ testing objectives and plans are presented with a breakdown of the supporting work elements (from Chapters 13, 14, and 15). Details are presented on the methods of exploratory shaft construction and testing.

1.5.18 Chapter 18: Quality Assurance

The quality assurance program in support of the BWIP is presented in this chapter. Detailed information is presented on identification and control of items and processes, inspection and control of measuring and test equipment, records, and audits.

1.5.19 Chapter 19: Identification of Alternate Sites

The generic screening process used by the National Waste Terminal Storage Program is presented, along with a general discussion of the alternate sites that have been selected based on this national screening. Domed and bedded salt, tuff, granite, and other crystalline rocks are discussed.

9 2 1 2 4 9 5 0 5 6 1

1.6 REFERENCES

ARHCO, 1976, Preliminary Feasibility Study on Storage of Radioactive Wastes in Columbia River Basalts, ARH-ST-137, Atlantic Richfield Hanford Company, Richland, Washington.

Bureau of the Census, 1981, 1980 Census of Population and Housing, Washington, PHC80-V-49, Advance Reports, Bureau of the Census, U.S. Department of Commerce, Washington, D.C., March 1981.

DOE, 1980, Final Environmental Impact Statement: Management of Commercially Generated Radioactive Waste, DOE/EIS-0046-F, U.S. Department of Energy, Washington, D.C., October 1980.

DOE, 1981, "Program of Research and Development for Management and Disposal of Commercially Generated Wastes; Record of Decision (to adopt a strategy to develop geologic repositories...)," Federal Register, Vol. 46, No. 93, U.S. Department of Energy, Washington D.C., May 1981.

DOE, 1982, Public Draft, National Plan for Siting High-Level Radioactive Waste Repositories and Environmental Assessment, DOE/NWTS-4, DOE/EA-151, National Waste Terminal Storage Program, U.S. Department of Energy, Washington, D.C., February 1982.

NRC, 1981, Disposal of High-Level Radioactive Wastes in Geologic Repositories: Licensing Procedures, Title 10, Chapter 1, Code of Federal Regulations-Energy, Part 60, U.S. Nuclear Regulatory Commission, Washington, D.C., February 25, 1981.

9 2 1 2 4 9 5 0 5 6 2

THIS PAGE INTENTIONALLY
LEFT BLANK

2. DECISION PROCESS FOR CHOOSING A REFERENCE REPOSITORY LOCATION AND AN ALTERNATE REPOSITORY LOCATION

The U.S. Department of Energy's (DOE) overall plan for selecting sites for high-level radioactive waste repositories is set forth in its public draft national siting plan (DOE, 1982). The siting process proposed in that plan is basically a three-phase process: site screening, detailed site studies, and site selection (Fig. 2-1).

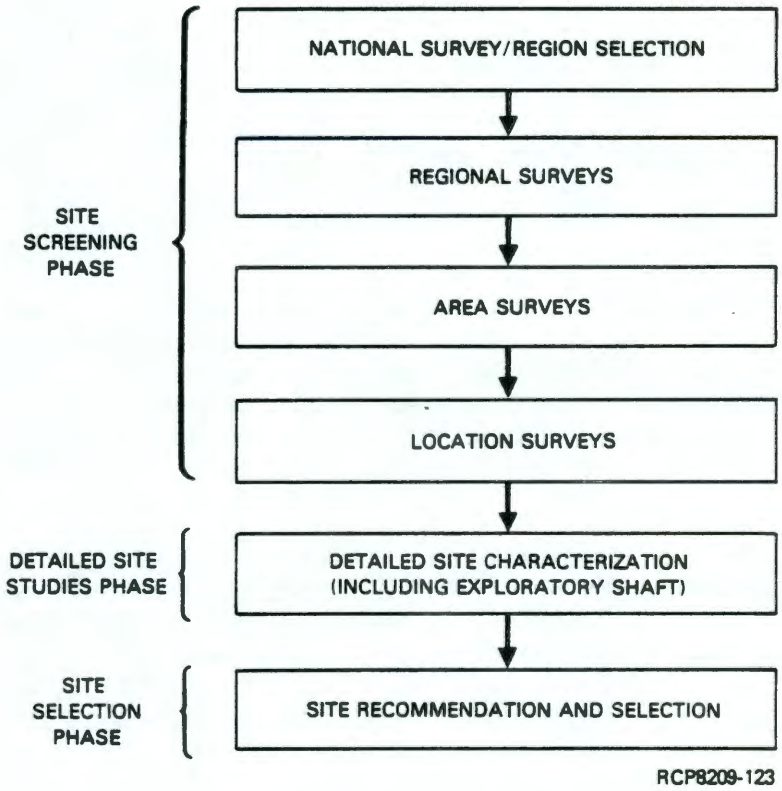

FIGURE 2-1. Repository Siting Process (DOE, 1982).

"Site screening" describes a decision process. The site screening phase consists of a set of decisions made sequentially to identify sites from vast land areas favorable for waste disposal. Several approaches to site screening are being used by the DOE. All use a stepwise method that may proceed through national, region, area, and location surveys. These surveys narrow the land areas considered from region, to area, to location, and to site (these terms being defined in relatively decreasing sizes of land areas). Decisions to continue or discontinue study of each alternative land area can be made after any of the survey steps.

9 2 1 2 4 9 5 0 5 6 4

Multiple approaches to site screening result from the choice of variables to use for initial screening. The DOE has used several approaches to identify starting points for screening studies (e.g., identifying regions containing potentially suitable host rock types and identifying federally owned lands that have been committed to nuclear activities and may have suitable host rocks). For example, early consideration of prior compatible land use has resulted in screening the DOE lands at the Nevada Test Site and at the Hanford Site in Washington State for potential repository sites. The rationale was (and is) that after many years of commitment to nuclear activities extensive portions of these sites would never be returned to unrestricted land use; thus, these sites are considered to be highly appropriate for continued equivalent use.

The detailed site study phase (Fig. 2-1) consists of scientifically collecting and evaluating information about the physical, chemical, geologic, and human environment necessary to judge site suitability. Detailed surface and subsurface studies will be performed at a small number of sites. The studies will include the construction of an exploratory shaft and testing of rock at repository depth as required by the U.S. Nuclear Regulatory Commission's (NRC) procedural rule, 10 CFR 60 (NRC, 1981a).

"Site selection" (Fig. 2-1) is the decision to choose a site for a repository. The site selection phase will include those events, after detailed site studies, that preceded the final selection decision. In this phase alternative sites will be compared and one or more will be recommended for a repository. Public review of the recommended site will occur before DOE makes the final selection and prepares a license application.

A discussion of the results of the site screening process carried out by the Basalt Waste Isolation Project (BWIP) is the subject of this chapter. The overall goal was to identify a reference repository location (i.e., preferred site) and an alternate repository location within the Hanford Site (Fig. 2-2). To achieve the stated goal, a methodology was employed that could be used to systematically and rapidly focus on areas where there would be a high likelihood of finding potential repository sites.

Basically, this methodology entailed the development of guidelines and the application of these guidelines through the processes of screening and ranking. The screening process was used to reduce the area under consideration to candidate sites, while the ranking process was used to discriminate or rank the order of these candidate sites. The highest and second highest ranked candidate sites were subsequently designated as the reference repository location and alternate repository location, respectively (Fig. 2-2).

9 2 1 2 4 9 5 0 5 6 5

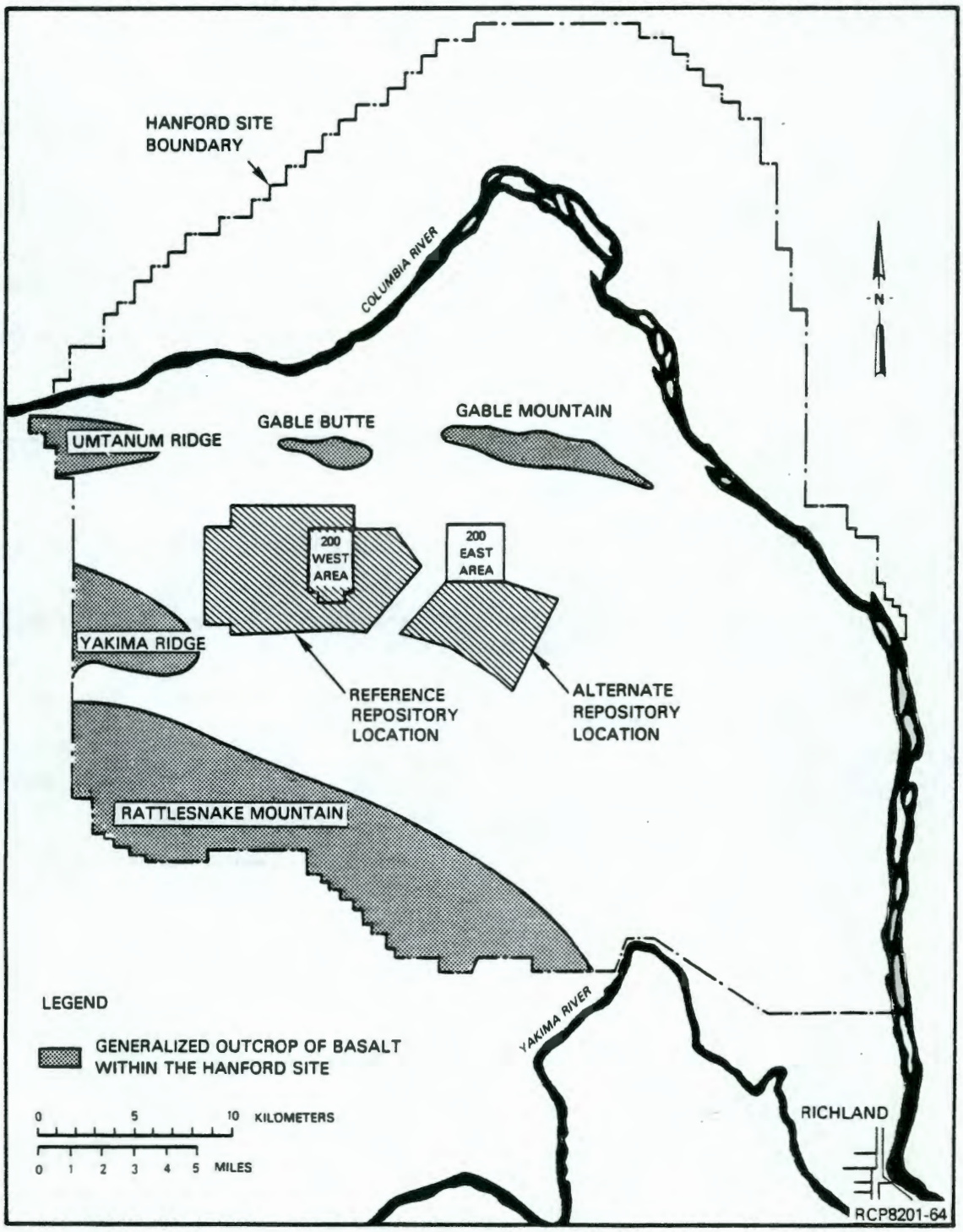

FIGURE 2-2. Location of the Reference Repository Location and Alternate Repository Location.

The site identification study was guided by the following key assumptions:

- The repository will require licensing by the NRC.
- The design and operation of surface facilities will be governed by existing safety and environmental licensing requirements.
- Nominal design and performance characteristics of the repository can be estimated.
- The long-term, safety-related characteristics of the host rock system can be evaluated and can be used in the selection of guidelines; similarly, appropriate judgments can be made regarding long-term social, economic, and political considerations applicable to repository siting.
- The repository will be designed for two time frames: a relatively short emplacement and retrievability phase and a much longer isolation phase.
- The site identification study will be based on data available at the time of the study.
- The repository licensing requirements will be written in the style of other nuclear fuel cycle facilities.

Interim results of site identification work, initiated in September 1978, are detailed in two reports: Site Locality Identification Study: Hanford Site (WCC, 1980) and Identification of Candidate Sites Suitable for a Geologic Repository in Basalt Within Hanford (BWIP, 1980). A third report, Study to Identify a Reference Repository Location for a Nuclear Waste Repository on the Hanford Site (WCC, 1981), details the final results of the siting study. The content of this chapter is basically a summary of information contained in these reports.

9 2 1 2 4 9 5 0 5 6 7

2.1 SITE IDENTIFICATION METHODOLOGY

The methodology used in the siting study was designed to provide a logical approach to the overall goal of identifying a reference repository location and an alternate repository location by systematically and rapidly focusing on areas where there is a high likelihood of finding repository sites. For this purpose the selected methodology was designed to:

- Allow a reevaluation of site identification results in light of changes in technology, regulatory requirements, and social values
- Meet anticipated licensing requirements
- Enable technically and nontechnically interested parties to understand the essential concepts involved in site identification.

The application of the site identification methodology to the Hanford Site basically consisted of the following steps:

- Identification of the objectives of siting and development of screening and ranking guidelines that form the basis for area identification
- Development of a data base of appropriate scope and detail that could be utilized for defining the conditions within the areas defined in each step of the siting process
- Implementation of a multistep screening process that permitted the application of guidelines to smaller and smaller areas until candidate sites were identified
- Utilization of a uniform ranking process to preferentially order the candidate sites, based on the application of ranking guidelines, to ultimately identify the reference repository location and an alternate repository location.

A flow diagram summarizing the elements of the site identification methodology is shown in Figure 2-3. Although the diagram implies a once-through approach, each step generally had more than one iteration.

2.1.1 Identification of Siting Objectives and Development of Guidelines

The first step in the siting methodology was to establish the basis on which areas could be identified and recommended for further investigation. The approach used was to develop a broad statement of objectives responding to the overall goal of site identification and from there to systematically refine the objectives and identify means of measuring achievement of the objectives through the use of guidelines. The guidelines provided the tools and the rules by which the entire siting process (both screening and ranking) was governed.

9 2 1 2 4 9 5 0 5 6 8

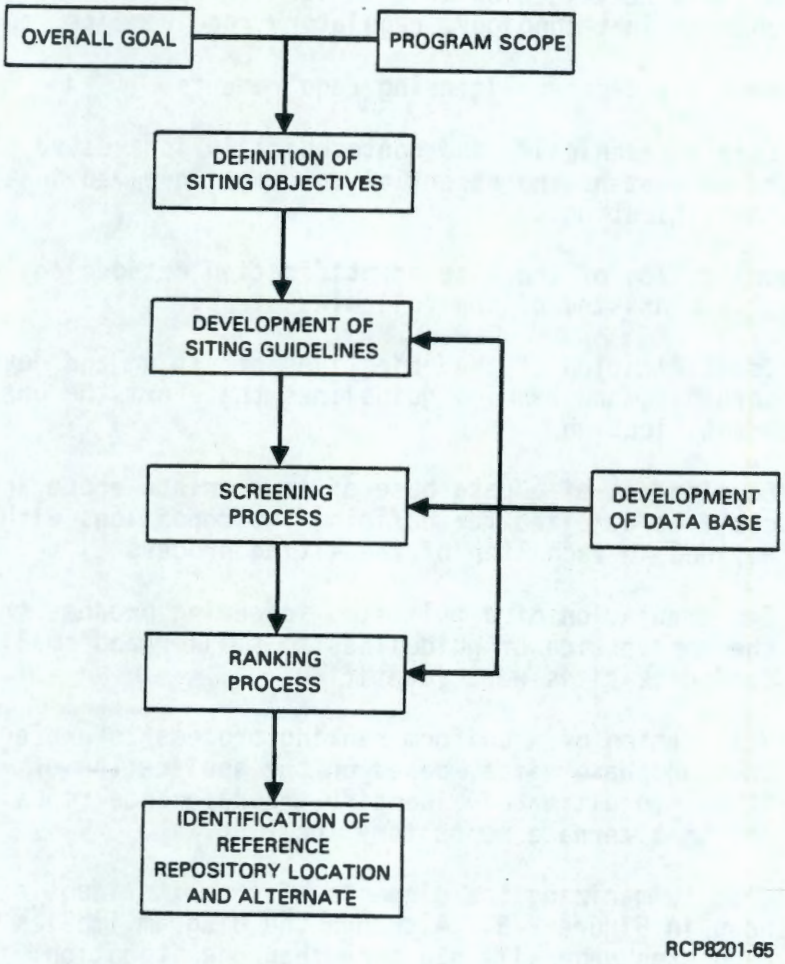

FIGURE 2-3. Elements of Site Identification Methodology (WCC, 1981).

The results of the first step of the methodology were development of two sets of guidelines: one for identifying candidate sites in a screening process and another for ranking these sites. The approach used to accomplish this step of the methodology consists of the following:

- Defining the overall goal of the study and developing a formal statement of objectives for the proposed repository (e.g., to minimize adverse conditions affecting public health and safety)

- Defining and establishing the considerations that described the concerns of each objective; e.g., fault rupture and groundwater contamination were established as considerations that describe the objective of public health and safety

- Defining specific measures for each consideration and establishing the appropriate numerical guidelines for each measure; e.g., the distance to faults was established as a measure defined for the consideration of fault rupture; a numerical guideline was to include areas for further study that occur greater than 8 kilometers (5 miles) from active faults

- Reviewing the guidelines with respect to completeness, relevancy, practicability, applicability, and sensitivity to changes in basic information used to develop the guidelines

- Identifying guidelines for use in the siting study.

A flow diagram summarizing the guideline development approach is shown in Figure 2-4.

In the development of the guidelines, a set of terms unique to the siting methodology was established. These terms are: overall goal, objectives, considerations, measures, and guidelines. As discussed below, each term represents a more detailed and specific articulation in response to the overall goal of the siting study.

2.1.1.1 Development of Siting Objectives, Considerations, and Measures. The first step in developing guidelines was the establishment of sound objectives for the siting decision. Existing and anticipated regulations, national and state environmental legislation, and principles of sound engineering practice provided basic guidance for the articulation of the siting objectives:

- Maximize public health and safety

- Minimize adverse environmental and socioeconomic impacts

- Minimize costs necessary to attain the requisite level of safety, as well as costs of mitigation.

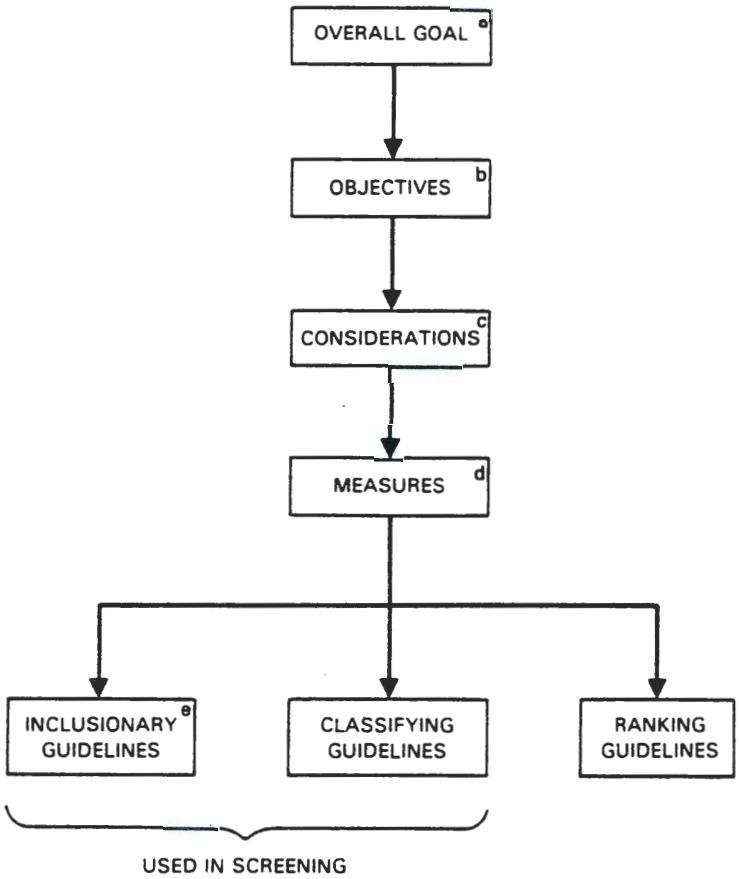

[a]OVERALL GOAL: A FORMAL STATEMENT OF THE AIMS OF THE SITING PROCESS; THAT IS, IDENTIFYING ACCEPTABLE SITES FOR A NUCLEAR WASTE REPOSITORY (WCC, 1981).

[b]OBJECTIVE: A CONDITION THAT IS TO BE ADDRESSED IN ORDER TO MEET THE OVERALL GOAL OF THE SITING PROCESS (e.g., MAXIMIZING PUBLIC HEALTH AND SAFETY) (WCC, 1981).

[c]CONSIDERATION: A CONDITION OR STATEMENT OF THE SPECIFIC ASPECT OF OBJECTIVES DESCRIBED TO MEET THE OVERALL GOAL OF THE SITING PROCESS (e.g., FAULT RUPTURE IS A CONSIDERATION OF THE SAFETY OBJECTIVE) (WCC, 1981).

[d]MEASURE: A LEVEL OF ACHIEVEMENT FOR A CONSIDERATION THAT IS IDENTIFIED AND REQUIRED. DISTANCE TO A CAPABLE FAULT (NRC, 1975) IS A MEASURE OF THE FAULT RUPTURE CONSIDERATION (WCC, 1981).

[e]GUIDELINE: A QUANTITATIVE OR QUALITATIVE STATEMENT THAT DEFINES A REQUIRED LEVEL OF ACHIEVEMENT IN THE SITING PROCESS. GUIDELINES MAY CHANGE WITH TIME, SINCE THEY DEPEND ON SOCIAL, POLITICAL, TECHNOLOGICAL, AND FINANCIAL CONDITIONS (WCC, 1981). FOR DEFINITION OF SPECIFIC TYPES OF GUIDELINES, SEE GLOSSARY.

RCP8201-66

FIGURE 2-4. Relationships of Terms Used in Screening and Ranking (WCC, 1981).

For each objective described above, a set of considerations and the means to measure them were developed. The selection of considerations was based on assumed repository design and performance estimates, the pertinent regulatory guidance, and assessment of the natural and man-made characteristics of the study area. The considerations were further limited to those that might be expected to differ from one location to another.

The choice of measures for these considerations was based on past NRC licensing experience and relevant regulatory decisions, on the availability of data, and on the need to portray as many measures as possible on maps.

2.1.1.2 Development of Siting Guidelines. The approach to the development of siting guidelines consisted of the following steps, which are illustrated in Figure 2-5:

- Identify and evaluate the baseline conditions
- Develop screening guidelines using the baseline information
- Review and revise the guidelines for use in the siting process.

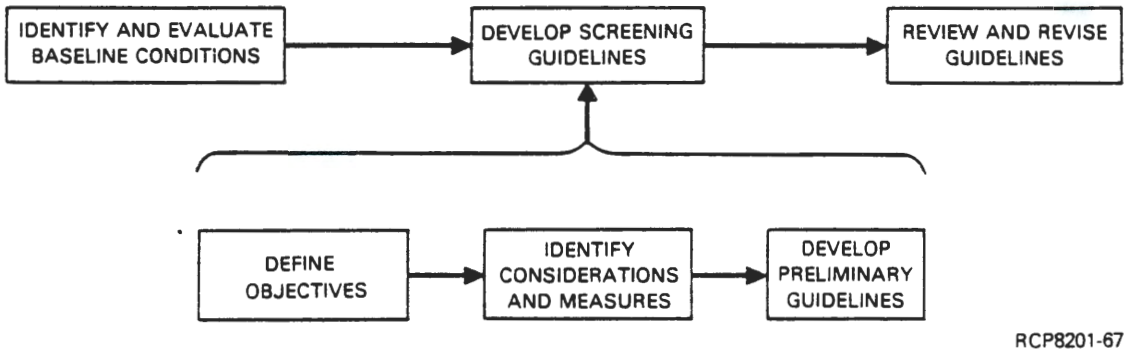

FIGURE 2-5. Approach to Guideline Development (WCC, 1981).

2.1.1.2.1 Baseline Conditions Used in Guideline Development. An essential part of the development of siting guidelines was the identification and selection of basic information or data that established baseline conditions describing a reference nuclear waste repository (WCC, 1981, Table III-1). This information provided qualitative and quantitative information, in addition to descriptive and facility performance information which provided a basis for establishing numerical guidelines in the siting process.

2.1.1.2.2 Development of Guidelines. The development of the guidelines began with the articulation of the siting objectives (see Section 2.1.1) and proceeded systematically to refine these objectives and identify a means of measuring the achievement of the objectives. The results of this process were the guidelines. Sites identified by the guidelines can be shown to meet minimum levels of achievement for the siting objectives used.

Two types of screening guidelines were established: inclusionary and classifying. An inclusionary guideline was defined as one for which a finite level of achievement must be reached to meet siting objectives. This level of achievement was required or implied by statute, regulation, technological limitations, or gross economic considerations. In such a case, a limit was established for the appropriate measure. A classifying guideline was defined as one for which a finite level of achievement was not required or could not be established, but that could provide a basis for differentiating between areas. In such a case, the measure itself was established as the guideline. A classifying guideline was used to identify groups of areas or localities with similar characteristics. (For examples of guidelines, see Section 2.2.)

2.1.1.2.3 Review and Revision of Guidelines. The final step in guideline development was to review the established guidelines. At the outset of the siting study, the emphasis on guideline review was (1) consistency within the set of guidelines, (2) compatibility with emerging repository design concepts and repository systems development, (3) compliance with regulations, (4) completeness and reasonableness in comparison to previous or concurrent repository siting guideline development efforts, and (5) the ability to portray guidelines on maps. Review was accomplished through an examination of pertinent literature, comparison with successfully applied guidelines that had been used to site similar large facilities, meetings with experts in engineering and geosciences, and test applications of selected guidelines on a portion of the study area.

2.1.2 Screening Process

The screening process was used to systematically and rapidly focus on portions of the study area where the likelihood of finding conditions favorable to a given purpose (e.g., siting a repository) was high, relative to other parts of the study area. The process was designed to ultimately identify a set of candidate sites from which a reference repository location could be identified.

Basically, the screening process involved the compilation, analysis, and transfer of data to maps reflecting the applicable guidelines through a series of repeatable steps. Each step of the screening process consisted of two substeps: selection of the guidelines to apply in that step and manual application of the guidelines on overlay maps.

The selection of guidelines used in a particular step of screening was governed primarily by the map scale, completeness of data base, and ease of application of the individual guidelines. The screening guidelines were applied through an overlay process, shown schematically in Figure 2-6. The superimposing of overlays (each showing a different set of mapped guidelines) enables areas failing to meet the inclusionary guidelines to be identified and removed from further consideration. The distinct and successively smaller areas defined using the four-step screening process are shown in Figures 2-7 and 2-8. Definitions of the area designations are given in Table 2-1.

In site identification studies for the BWIP, a distinction was drawn between screening guidelines that applied only to surface facilities during the operation phase and those that applied to subsurface facilities during the operation and/or isolation phase.

This distinction led to identification of relatively small land areas (localities) having a variety of surface/subsurface siting options. The surface/subsurface distinction recognizes that portions of the subsurface facility (e.g., horizontal galleries) may be located logically and safely beneath a portion of the surface that may not of itself be suitable for siting a nuclear materials handling facility. For the purpose of siting, subsurface guidelines take precedence over surface guidelines. That is, a portion of an area screened from consideration on the basis of surface guidelines was considered usable if subsurface conditions were deemed favorable.

2.1.3 Ranking Process

The ranking process was used to differentiate among the candidate sites in terms of the siting objectives developed for the study. Ranking of the candidate sites was based on a decision analysis approach. The decision analysis approach separates a problem into parts that are easier to analyze than the whole, then puts the parts back together using a logical and systematic procedure.

The decision analysis approach used in the identification of the reference repository location and alternate repository location is termed dominance analysis. The dominance analysis was conducted by a Siting Committee formed of technical representatives from Woodward-Clyde Consultants and Rockwell Hanford Operations. The steps followed in the ranking process are summarized in Table 2-2.

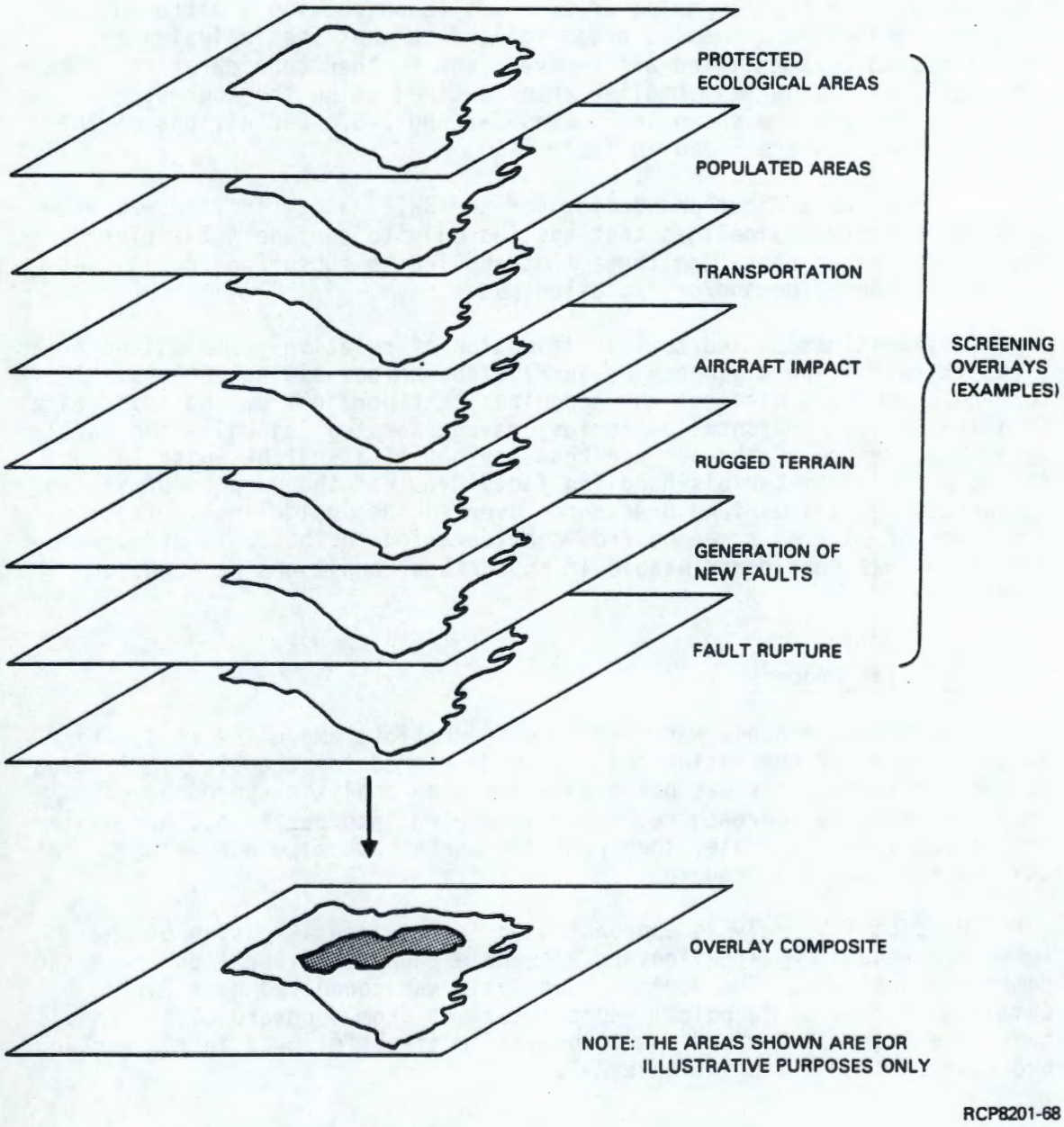

FIGURE 2-6. The Overlay Process Used in Site Screening (WCC, 1981).

9 2 1 2 4 9 5 0 5 7 5

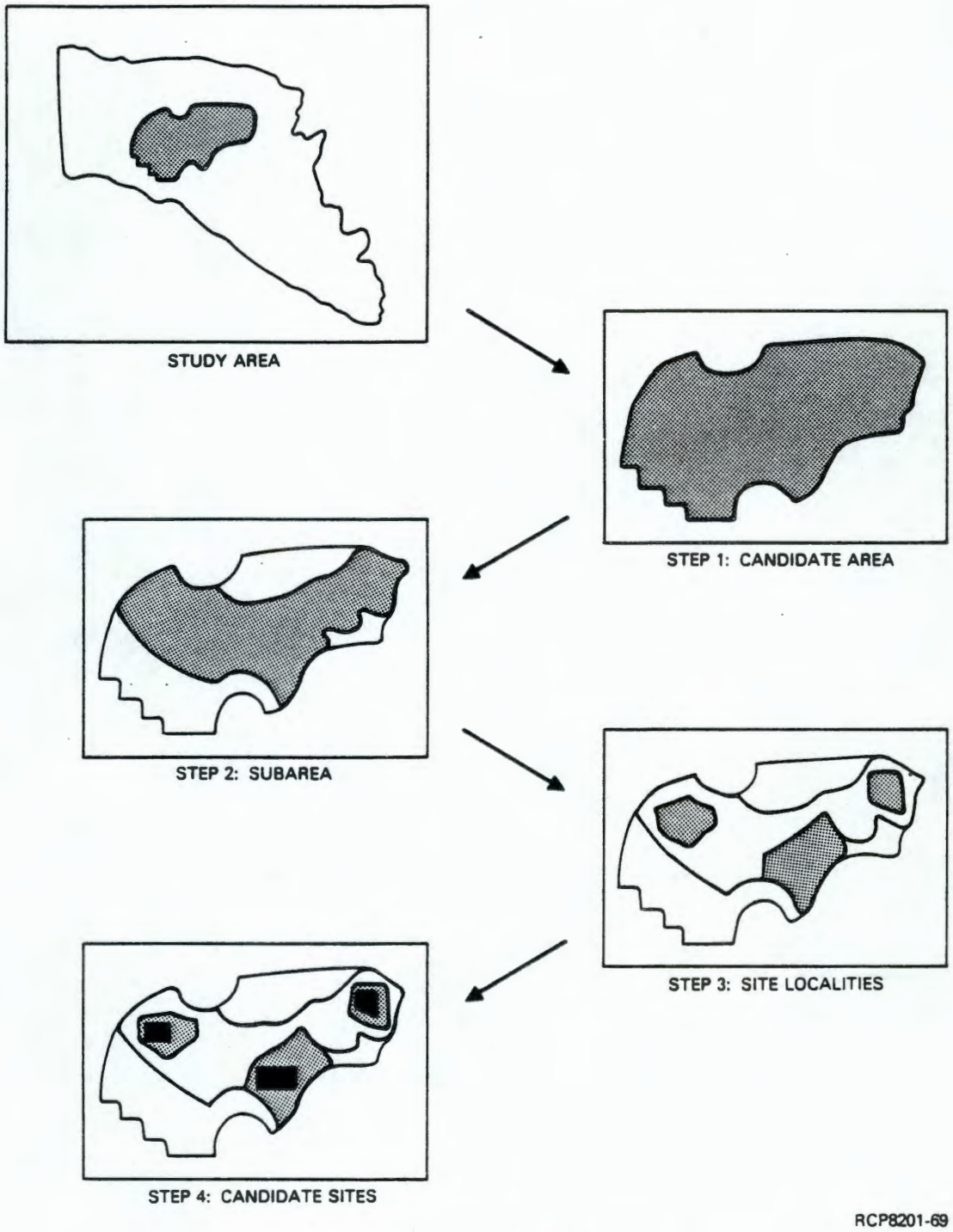

FIGURE 2-7. Relationship of Area Designations and Screening Steps (WCC, 1981).

9 2 1 2 4 9 5 0 5 7 6

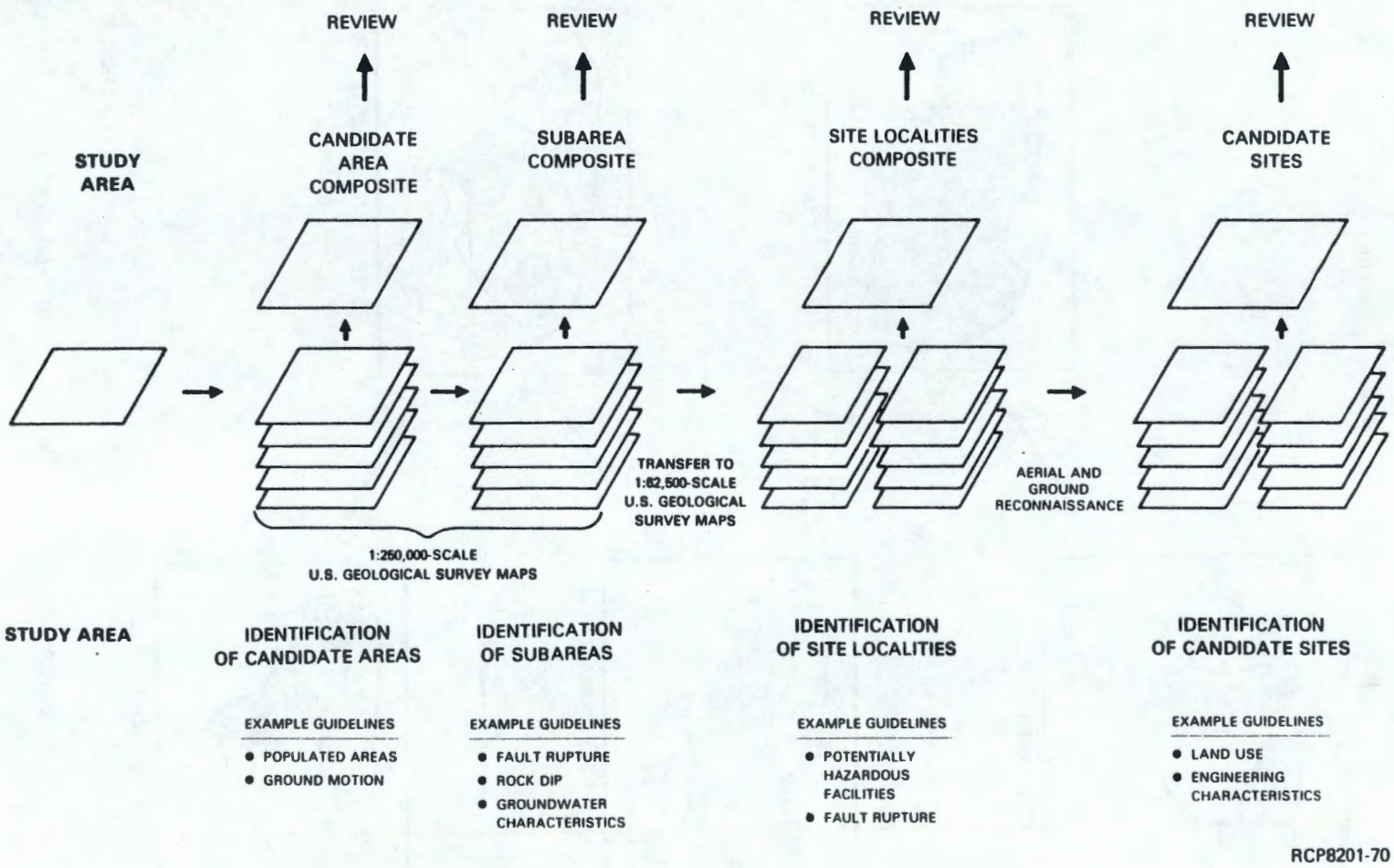

FIGURE 2-8. Illustrative Example of the Screening Process (WCC, 1981).

TABLE 2-1. Area Designations Used in Screening.

Study area: The Pasco Basin, which is approximately 4,145 km^2 (1,600 mi^2).

Candidate area: A portion of the study area that has a higher potential of containing suitable sites for a waste repository than the rest of the study area. Generally, a candidate area covers several hundred square kilometers (several hundred square miles) and was derived by the application of inclusionary guidelines.

Subarea: A portion of a candidate area having a higher potential of containing sites than other portions. The subarea was defined on a larger scale map than that used to identify candidate areas and was derived by the application of inclusionary guidelines. Subareas generally cover more than 260 km^2 (100 mi^2).

Site localities: Portions of subareas that have a higher potential of containing suitable sites for a waste repository than the rest of the subarea. Generally, a site locality covers an area up to 150 km^2 (50 mi^2).

Candidate sites: Specific locations within a site locality considered to be suitable for locating a repository. Generally, a candidate site covers an area up to 26 km^2 (10 mi^2).

Reference repository location: The highest ranking candidate site determined by the screening process.

Alternate repository location: The candidate site that ranked second to the reference repository location in the ranking process.

9 2 1 2 4 9 5 0 5 7 8

TABLE 2-2. Steps in the Ranking Process.

Steps	Action
1	Structure the problem: Definition of the scope of the problem or task for ranking. Development of measures for those ranking guidelines (criteria) that can be used to differentiate among the candidate sites. Development of ranking criteria from the criteria matrix established during this step.
2	Describe the consequences: Determination of the consequences (e.g., costs, environmental impacts) for each candidate site in terms of the measures developed in Step 1. Development of a site measure matrix.
3	Determine the preferences of different consequences: Assessment of the relative importance of different levels of the same impact, or of the relative importance of one impact versus another. Assessment of the role of uncertainties in the decision process. This assessment establishes the framework and rules whereby the consequences of choosing one candidate site over another are evaluated. Assessment includes ordinal dominance analysis, requiring the assessment of trade-offs to determine which measures are of relatively more importance in differentiating among the candidate sites. Dominance analysis results in criteria ranges and rank order of the weights.
4	Synthesize the information to rank order the candidate sites: Information from the preceding steps is combined into a formal analysis that results in a rank order of the candidate sites using dominance analysis. This rank order reflects the impacts and uncertainty surrounding a particular site choice, seen in the context of the preference structure assessed in Step 3. Sensitivity analysis of the ranking is performed by varying the inputs to the evaluation and noting changes in the resultant rank order.

9 2 1 2 4 9 5 0 5 7 9

2.1.4 Development of a Data Base

A necessary part of siting methodology that had a significant impact on each step followed in the ranking process was the collection, review, and cataloging of available published and unpublished data. This procedure was tailored to be applicable to each specific aspect of siting (guideline development, screening, ranking). Published and unpublished reports describing the geology, tectonics, hydrology, land use, etc. of the study area provided the necessary information to complete the steps of the siting process. Of particular use were reports summarizing geologic (Myers/Price et al., 1979) and hydrologic (Gephart et al., 1979) data gathered through surface mapping, drilling and testing, and geophysical surveys. Data collection and review were based on the following assumptions:

- Data reviewed were readily available
- Data review and evaluation were for use in a siting process with applications of present-day technology
- Data coverage and detail varied depending on the area in question and the step in the siting process.

THIS PAGE INTENTIONALLY
LEFT BLANK

9 2 1 2 4 9 5 0 5 8 1

2.2 TECHNICAL FACTORS

The technical factors considered in the identification of a reference repository location and alternate repository location within the Hanford Site were obtained from both existing and pending criteria and regulations (i.e., NWTS-33(2), NWTS, 1981; 10 CFR 60, NRC, 1981b). Major categories of factors derived from this review are listed as follows:

- Geologic and tectonic
- Hydrologic
- Meteorologic
- Geochemical
- Geomechanical
- Resource evaluation
- Human activity
- Site conditions potentially affecting system costs.

Summarized in Table 2-3 is information regarding these categories as it pertains to site selection. Technical factors within this summary table are compared to NWTS-33(2) (NWTS, 1981) criteria in BWIP (1981). Detailed descriptions of the data base for each of these technical factor categories are contained in Chapters 3 through 9 of this report and are not repeated here.

A review of the technical factors listed in Table 2-3 and the overall siting objectives (Section 2.1.1) served as the basis for the formulation of considerations, measures, and guidelines. The relationship between these elements is summarized in Table 2-4. The specific application of the guidelines contained in this table to each step of the site identification process is presented in Section 2.5.

9 2 1 2 4 9 5 0 5 8 2

TABLE 2-3. Summary Description of Technical Factors Considered in the Siting Process (WCC, 1981).[a] (Sheet 1 of 7)

Factor	Conditions evaluated	Description
GEOLOGIC AND TECTONIC		
Structural geology: Evaluate long-term repository stability and rock-medium integrity.		
Known faults within 8 km (5 mi) of the subsurface limits of the candidate site.	Weak zones[b] in the rock medium (all faults), repository facility rupture, seismic sources, ground motion (capable faults).	Location, orientation, type, length, age of movement, capability, closest distance to site boundary.
Bedrock fracturing and jointing within 2.4 km (1.5 mi) of the subsurface limits of the candidate site.	Weak zones in the rock medium.[b]	Location, orientation, type, patterns, density of spacing, inferred origin, closest distance to site boundary.
Lineaments and postulated faults within 8 km (5 mi) of the subsurface limits of the candidate site.	Possible seismic sources,[c] ground motion, weak zones in the rock medium,[b] steep bedrock dip.[c]	Location within site. Lineaments are those delineated on gravity and aeromagnetic surveys, aerial photographs, LANDSAT imagery, and/or seismic reflection profiles.
Anticlines within 8 km (5 mi) of the subsurface limits of the candidate site.[d]	Steep bedrock dip, possible seismic sources, weak zones in the rock medium.[b]	Location, orientation, type, length, closest distance from axial trace to site boundary.
Seismicity: Evaluate the short-term stability of the repository; identify and/or predict sources of future seismicity.		
Microearthquakes within 26.7 km (16 mi) of the subsurface limits of the candidate site center.	Historic seismic sources, possible hidden structure, probable sources of future seismicity.	Spatial and temporal distribution, nature (swarm vs. nonswarm), focal depth, magnitude, closest distance to site.

9 2 1 2 4 9 5 0 5 8 3

TABLE 2-3. Summary Description of Technical Factors Considered in the Siting Process (WCC, 1981).[a] (Sheet 2 of 7)

Factor	Conditions evaluated	Description
Potential earthquake sources within 48.3 km (30 mi) of subsurface limits of the candidate site center.	Short-term past seismicity, possible hidden structure, probable sources of future seismicity.	Location, orientation, type, length, faulted segments, rupture length, possible earthquake magnitude, closest distance to site center.
Potential sources of induced seismicity.[e]	Sources of ground motion.	Closest distance to site center.
Tectonics: Assess short-term tectonic activity, its effect on the present structural geologic regime, and its effect on repository stability.		
Identified Quaternary and neotectonic crustal movement within 8 km (5 mi) of the subsurface limits of the candidate site.	Recent seismic activity.	Location, type of movement, rate and magnitude of movement, closest distance to site center.
Tectonic stress field.	Possible sources and orientation of tectonic movement.	Orientation, vertical and lateral changes, residual stresses.
Comparison and possible relationships of known faults, fractures, and tectonic joints within 8 km (5 mi) of the candidate site with respect to tectonic stress regime.	Fit of present structures into stress regime; possible new sources of tectonic movement and/or renewal of fracturing along structurally weak zones.[b]	See above.
Potential volcanism.	Possible short-term or future volcanic events.	Location of volcanic sources, closest distance to site center; volcanic effects.
Stratigraphy: Characterize the rock medium's resistance to stress, identify suitable host flow dimensions,[f] and determine geologic history (long-term past, short-term past, and future).		
Stratigraphic unit at the proposed repository level.	Structural conditions within host flow at repository level.	Lithology, structure, stratigraphic anomalies and discontinuities.

9 2 1 2 4 9 5 0 5 8 4

TABLE 2-3. Summary Description of Technical Factors Considered in the Siting Process (WCC, 1981).[a] (Sheet 3 of 7)

Factor	Conditions evaluated	Description
Ringold Formation and Quaternary stratigraphy.	Near-surface conditions, post-Tertiary geologic history, possible short-term or future geologic, climatic, and surface hydrologic events; erosion/denudation potential; landslide potential.	Lithology, structure, age, thickness and lateral extent, marker beds, presence and thickness in site; relationship of repository elevation to base level; location with respect to landslides.
HYDROLOGIC		
Geohydrology: Evaluate the consequences of possible radionuclide release, its projected path to the biosphere, the rock volume's mitigating properties, and the effect of hydrologic events on surface facilities.		
Natural or man-made groundwater discharge areas.	Direction of possible radionuclide release from proposed repository to and probable emergence location to biosphere.	Hydrologic characteristics, closest distance from site center.
Groundwater flow travel time to closest natural or man-made discharge areas.	Direction of possible radionuclide release time in transit, probable location of emergence to biosphere.	Flow path direction, length, time to discharge area center measured from site center.
Aquifers and aquitards above and below the proposed repository.	Possible long- and short-term groundwater transfer and storage areas.	Distance to relatively transmissive zones.
Groundwater recharge rates.	Sources and rate of groundwater input at repository level.	Hydrologic characteristics at repository level.
Vertical and horizontal gradients.	Rate of groundwater movement input at repository level.	Distance to known hydraulic gradients from site center.

TABLE 2-3. Summary Description of Technical Factors Considered in the Siting Process (WCC, 1981).[a] (Sheet 4 of 7)

Factor	Conditions evaluated	Description
Groundwater geochemical characteristics at and surrounding the proposed repository.	Reducing/oxidizing or otherwise chemical bonding and retaining conditions for radionuclides in fluid/rock medium; groundwater residence times; age of groundwater.	Groundwater radiometric age.
Host-rock geohydrologic characteristics.	Movement of groundwater in immediate vicinity of repository.	Effective porosity, water content, permeability, transmissivity.
Surface flooding.	Possible hazards to surface facilities from natural or man-induced floods.	Published maximum flood levels, height above and distance to candidate site.
METEOROLOGIC		
In general, meteorologic conditions act uniformly over the candidate area, hence no descriptive factors were employed in the screening process. Site-specific meteorologic conditions pertaining to ambient air quality and wind direction with regard to stack plumes or potentially contaminated airborne dust from existing activities were considered.		
GEOCHEMICAL		
Geochemical factors are considered uniformly operable across the entire candidate area and no screening factors were required in this category.		
GEOMECHANICAL		
Host rock characteristics: Evaluate the host flow's resistance to stress induced by physical conditions at depth or by the radioactive waste and its ability to act as a barrier to radionuclide propagation; determine repository geometric constraints.		
Host-flow structural characteristics.	Physical conditions at repository level, areas of steep dip, host-flow geometry.	Thickness, lateral extent, bedrock dip at repository level.

9 2 1 2 4 9 5 0 5 8 6

TABLE 2-3. Summary Description of Technical Factors Considered in the Siting Process (WCC, 1981).[a] (Sheet 5 of 7)

Factor	Conditions evaluated	Description
Thickness of buffer zone vertically and laterally around the proposed repository.[g]	Repository geometric constraints.	Flow thickness, repository conceptual design conditions.
Thermal and mechanical properties of the proposed repository host rock.	Host flow physical properties, short- and long-term behavior of rock medium under expected repository conditions.	Thermal conductivity, thermal expansion, fracture density, compressive tensile strength.
Horizontal and vertical lithostatic stress at the proposed repository depth.	Expected stress regime at the proposed repository level.	Stress regime, repository conceptual design conditions.
RESOURCE EVALUATION		
Potential, significant, specialty, and incompatible land uses.	Areas set aside for uses conflicting with waste disposal/storage or outside federal jurisdiction.	Description, location with respect to sites.
HUMAN ACTIVITY		
Potentially hazardous facilities, possible missile generators, and possible vapor sources.	Conditions and facilities adverse to repository surface facilities during repository construction and operation.	Description, percent site area, location of surface facilities with respect to such sources.
Transportation corridors.	Surface access to repository; aircraft corridors.	Distance to highways, railroads, waterways; distance to airports, location with respect to aircraft routes.
Radiation contaminated soil and groundwater.	Contaminated soil volume, near-surface contaminated groundwater dispersion.	Location with respect to site, percent of site area, description of radionuclides involved.

9 2 1 2 4 9 5 0 5 8 7

TABLE 2-3. Summary Description of Technical Factors Considered in the Siting Process (WCC, 1981).[a] (Sheet 6 of 7)

Factor	Conditions evaluated	Description
Facilities or areas interpreted to be possible defense or security risks.	Potentially hazardous facilities or areas.	Location with respect to site or percent of site area.
Boreholes penetrating basalt and boreholes within 2.4 km (1.5 mi) of the subsurface limits of the candidate site.	Disruption to integrity of host flow and/or rock volume.	Number, location on-site, number outside site, depth, (for boreholes >300 m (>1,000 ft)).
SITE CONDITIONS POTENTIALLY AFFECTING SYSTEM COSTS		
Thickness of unconsolidated material.	Depth of sediments to be excavated for repository construction.	Ringold Formation; glaciofluvial sediments (Hanford formation), top-of-basalt elevation, ground surface elevation.
Depth to the unconfined aquifer.	Saturated and unsaturated sediment thickness.	Elevation of top of saturated zone, ground surface elevation.
Depth to the proposed repository (shaft length).	Rock volume.	Depth to repository host flow.
Candidate site topographic characteristics.	Site surface relief.	Description, minimum, maximum, and average elevation.
Candidate site preparation and construction costs.	Regolith and rock volume, surface relief, saturated soil volume, groundwater dispersion, construction personnel protective measures.	Surface topography, thickness of unconsolidated material, depth to aquifer and to repository flow.

TABLE 2-3. Summary Description of Technical Factors Considered in the Siting Process (WCC, 1981).[a] (Sheet 7 of 7)

Factor	Conditions evaluated	Description
Candidate site operation cost.	Rock volume, environmental baseline conditions, groundwater dispersion.	Repository depth, backfill rock volume, monitoring, site restoration.

[a]Factors were identified and applied based on available surface mapping, surface cored boreholes, geophysical investigations, and other data outlined in WCC (1981); e.g., parameters under structural geology were used to the level known when the site identification study was conducted. Rationale for selected "setback distances" is given in WCC (1980; 1981).

[b]Faulted, fractured, folded, brecciated, or otherwise weakened zones in the rock medium may act as shortcuts to postulated groundwater flow paths from the proposed repository to the biosphere. They also constitute zones where renewed fracturing may occur as a result of motion in a seismic event.

[c]Lineaments considered may represent, among other features, faults of undetermined capability and folds.

[d]Geologic studies in the Yakima fold belt of the Columbia Plateau indicate that the more prominent faulting is associated with the larger, more strongly folded anticlines.

[e]Potential sources of induced seismicity may be man-made reservoirs, the effects of irrigation (groundwater withdrawal and recharge), and construction of the proposed repository shafts and tunnels.

[f]Suitable conditions are based on conceptual design conditions. Host flow dimensions and conditions are defined utilizing the Umtanum flow as the reference horizon (see Section 2.7 for further discussion of candidate repository horizons, including the Umtanum flow).

[g]The buffer zone is that zone in which the host rock characteristics remain the same as within the actual repository without crossing anomalies, discontinuities, or into another rock type.

9 2 1 2 4 9 5 0 5 8 9

TABLE 2-4. Summary of Screening Guidelines (WCC, 1981). (Sheet 1 of 5)

Consideration	Measure	Guideline*
OBJECTIVE: MAXIMIZE PUBLIC HEALTH AND SAFETY		
Natural hazards		
1. Fault rupture	a. Horizontal and vertical distance from known faults interpreted to be capable	a. Include areas >8 km (>5 mi), horizontally and vertically, from known faults interpreted to be capable b. Include areas >8 km (>5 mi), horizontally and vertically, from known faults whose capability is unknown, which have low potential for a capability evaluation
	b. Horizontal and vertical distance from known faults interpreted to be not capable and zones of fracturing and jointing	a. Include areas >0.8 km (>0.5 mi) from known faults interpreted to be not capable and from zones of fracturing and jointing b. Include areas >0.8 km (>0.5 mi) from known faults whose capability is unknown but which have a high potential for a capability evaluation
	c. Location with respect to lineaments and postulated faults	Evaluate areas on basis of proximity to linear features (lineaments), as interpreted from remote sensing and geophysical data, and postulated faults
2. Generation of new faults	Location with respect to future potentially capable tectonic structures	Include areas >8 km (>5 mi) from folds interpreted to be capable of forming new faults
3. Ground motion	Location with respect to potential earthquake sources and estimated levels of ground motion	a. Include areas that may be subject to <40% g peak surface acceleration from known and interpreted earthquake sources b. Include areas >19.3 km (>12 mi) from fault epicenters >MM V and >9.7 km (>6 mi) from instrumental epicenters magnitude >4.0 that occur in concentrations or clusters as interpreted from historical-earthquake-epicenter plot maps c. Evaluate areas and their locations with respect to isolated earthquakes of epicenter intensities >MM V and magnitude >4.0, based on estimated location errors and geologic and tectonic setting d. Evaluate areas and their locations with respect to shallow (<56.3 km (<35 mi) depth) microearthquakes based on location error, geologic and tectonic setting, and local and regional stress regime

TABLE 2-4. Summary of Screening Guidelines (WCC, 1981). (Sheet 2 of 5)

Consideration	Measure	Guideline*
4. Tectonic movement	Location with respect to potential bedrock folding	Evaluate areas on basis of proximity to bedrock folds (anticlines, synclines, or monoclines)
5. Groundwater contamination	Location with respect to natural and man-made discharge areas	Evaluate areas on basis of distance from discharge areas and interpreted contaminant travel time
6. Flooding	Height above selected flood level	a. Include areas outside of primary floodplains and published maximum flood levels b. Evaluate areas on basis of height above primary floodplains and estimated published maximum flood levels c. Evaluate areas on basis of location with respect to areas where catastrophic flooding (i.e., Spokane Floods) has occurred in Quaternary time
7. Volcanic effects	Distance from Quaternary ashfall sources	Evaluate areas on basis of exposure to tephra fall from Quaternary stratovolcanoes: A = >241.4 km (>150 mi) to source B = 64.4 to 241.4 km (40 to 150 mi) to source C = <64.4 km (<40 mi) to source
8. Future new volcanic activity	Location with respect to probability of new volcanic sources	Evaluate areas on basis of probability and proximity to areas of interpreted new volcanic sources and effects
9. Ground failure	a. Location with respect to landslides and potential landslides	a. Include areas not on mapped landslides b. Evaluate areas on basis of probability of landsliding: A = Low probability of a landslide B = Slight probability of a landslide C = Higher probability of a landslide
	b. Characteristics of foundation conditions	Evaluate general foundation conditions: A = Bedrock area (0 to 6.1 m (0 to 20 ft) consolidated material) B = Shallow alluvial area (6.1 to 30 m (20 to 100 ft) unconsolidated material) C = Deep alluvial area (>30 m (>100 ft) unconsolidated material)
10. Erosion/ denudation	Location with respect to potential areas of erosion or denudation	a. Include areas >0.8 km (>0.5 mi) from steep-walled canyons or slopes b. Evaluate areas on basis of height of underground repository above base level: A = Repository elevation below base level (sea level) B = Repository elevation above base level (sea level)

TABLE 2-4. Summary of Screening Guidelines (WCC, 1981). (Sheet 3 of 5)

Consideration	Measure	Guideline*
11. Stratigraphic characteristics	a. Bedrock dip	Evaluate areas on basis of bedrock dip: A = 0 to 5 degrees B = 5 to 10 degrees C = >10 degrees
	b. Presence of suitable stratigraphic characteristics	Include areas where basalt flows with desirable internal-flow structure, density, porosity, extent, continuity, etc., are >30 m (>100 ft) thick within the proposed repository depth zone
	c. Thickness of underlying basalt	Include areas where thickness of underlying repository host-rock-type material at the repository depth is >152.4 m (>500 ft)
Man-made hazards		
1. Aircraft impact	a. Distance from airports	a. Include areas >8 km (>5 mi) from airports shown on state airport plans, accommodating aircraft >5,670 kg (>12,500 lb) gross weight or any military airport b. For airports with >12,500 yearly operations, but with 50,000, include areas >d kilometers from airport: distance (d) = $\sqrt{0.0051 \times \text{total operations}}$ [d miles from airport: d = $\sqrt{0.002 \times \text{total operations}}$]. c. For airports with 50,000 to 100,000 operations per year, include 16 km (10 miles) from airport. For airports with 100,000 operations per year, include areas >d kilometers from airport: distance (d) = $\sqrt{0.0026 \times \text{total operations}}$ [d miles from airport: d = $\sqrt{0.001 \times \text{total operations}}$].
	b. Locations with respect to commercial jet routes and military routes	Evaluate areas with respect to proximity to high-frequency routes
	c. Location with respect to restricted airspace	Include areas away from the limits of restricted airspace defining military airspace usage
2. Hazardous facilities	Location with respect to hazardous facilities, possible missile generators, and possible vapor sources	a. Include areas away from facilities occupying 7,284 ha (18,000 acres) or more b. Include areas >0.97 km (>0.6 mi) from potential explosion, fire, missile hazards c. Include areas >0.97 km (>0.6 mi) from potential sources of noxious or flammable vapors d. Evaluate areas on basis of proximity to hazardous facilities

TABLE 2-4. Summary of Screening Guidelines (WCC, 1981). (Sheet 4 of 5)

Consideration	Measure	Guideline*
3. Transportation	Distance from transportation corridors	a. Include areas >0.97 km (>0.6 mi) from U.S. highways, interstate highways, railroads, and navigable waterways b. Evaluate areas on basis of proximity to transportation corridors
4. Induced seismicity	Location with respect to sources of induced seismicity and potential future earthquake sources	a. Include areas >8 km (>5 mi) from existing reservoirs >30 m (>100 ft) deep b. Evaluate areas on basis of proximity to future reservoirs and interpreted sources of induced seismicity A = >8 km (>5 mi) B = 0 to 8 km (0 to 5 mi)
5. Subsurface mineral exploration and extraction	Location with respect to existing and potential future mineral exploration and extraction	a. Include areas away from existing subsurface mineral extraction b. Evaluate areas on basis of proximity to potential future mineral exploration or extraction
6. National defense and security	Proximity to facilities or areas interpreted to be possible defense or security risks	Evaluate areas on basis of proximity to facilities or areas interpreted to be attractive military targets
Repository induced events		
1. Thermo-mechanical effects	Thickness of host-rock flow and general rock characteristics	Evaluate flow thicknesses and characteristics of potential host rock
2. Operational radiation release	Distance from population	a. Include areas >4.8 km (>3 mi) from populations of >2,500 b. Include areas >1.6 km (>1 mi) from any incorporated community c. Include areas >1.6 km (>1 mi) from any urbanized area
OBJECTIVE: MINIMIZE ADVERSE ENVIRONMENTAL AND SOCIOECONOMIC IMPACTS		
1. Protected ecological areas	Location with respect to protected ecological areas	Include areas outside of designated protected ecological areas of: ≥7,284 ha (≥18,000 acres) 2,023 to 7,284 ha (5,000 to 18,000 acres) <2,023 ha (<5,000 acres)

TABLE 2-4. Summary of Screening Guidelines (WCC, 1981). (Sheet 5 of 5)

Consideration	Measure	Guideline*
2. Culturally important areas: Indian reservations, parks, monuments, wilderness, primitive areas, roadless area of national forest, Bureau of Land Management roadless recreation area, archaeological sites	a. Location with respect to designated scenic areas	Include areas greater than a calculated distance based on height of surface repository
	b. Location with respect to all designated areas	Include areas outside of designated culturally important areas of: ≥7,284 ha (≥18,000 acres) 2,023 to 7,284 ha (5,000 to 18,000 acres) <2,023 ha (<5,000 acres)
3. Protected and endangered species	Location with respect to protected and endangered species	Include areas outside of known locations of protected and endangered species
4. Biologically important areas	Location with respect to biologically important areas	Evaluate areas based on proximity to biologically important areas
5. Existing significant, specialty, or incompatible land uses	Location with respect to significant, specialty, or incompatible land uses	Include areas outside of mapped extent of specialty agriculture, irrigated agriculture, incompatible facilities, other land uses that are locally limited and regionally significant
6. Potential significant or incompatible land uses	Location with respect to potential future significant or incompatible land uses	Evaluate areas with respect to potential future uses. The evaluation will focus on agriculture: A. Potentially irrigable lands B. Arable soils C. Marginal soils C. Submarginal soils
OBJECTIVE: MINIMIZE SYSTEM COSTS		
1. Site preparation (surface)	a. Terrain ruggedness	Subjective evaluation for terrain characteristics (i.e., slope >15%, relief and degree of dissection)
	b. Usable land area	Evaluate available land area for dominant site-preparation costs, slope, local relief, degree of dissection, size of area, location and juxtaposition of relatively level areas, water supply, access, and amount of excavation and fill necessary to fit 971 ha (2,400 acres) of surface facilities
2. Site preparation (subsurface)	Mining and excavation costs	Evaluate areas on basis of thickness of overburden, depth of shafts, host-rock characteristics, configuration and length of tunnels (spoil, etc.), excavated volume, water handling, ventilation, etc.

*Rationale for "setback distances" given in WCC (1980; 1981).

THIS PAGE INTENTIONALLY
LEFT BLANK

9 2 1 2 4 9 5 0 5 9 5

2.3 ENVIRONMENTAL FACTORS

The environmental factors considered in the identification of a reference repository location and an alternate repository location within the Hanford Site were also obtained from both existing and pending criteria and regulations (i.e., NWTS-33(2), NWTS, 1981; 10 CFR 60, NRC, 1981b). Major categories of factors derived from this review are listed as follows:

- Radiological
- Ecological
- Air quality
- Water quality
- Land resources and use
- Aesthetics
- Historic, archaeological, and cultural resources
- Socioeconomic impacts.

Summarized in Table 2-5 is information regarding these categories as it pertains to site identification. Environmental factors within this summary table are compared to NWTS-33(2) (NWTS, 1981) criteria in BWIP (1981). Detailed descriptions of the data base for each of these environmental factor categories are contained in Chapters 7, 8, and 9 of this report and are not repeated here.

A review of the environmental factors listed in Table 2-5 and the overall siting objectives (Section 2.1.1) served as the basis for the formulation of considerations, measures, and guidelines. The relationship between these elements is summarized in Table 2-4. The specific application of the guidelines contained in this table to each step of the site identification process is presented in Section 2.6.

TABLE 2-5. Summary Description of Environmental Factors Considered in the Siting Process (WCC, 1981).* (Sheet 1 of 2)

Factor	Conditions evaluated	Description
	RADIOLOGICAL	
Radiation contaminated soil.	Contaminated soil volume.	Location with respect to site, percent of site area, description of radionuclides involved.
	ECOLOGICAL	
Critical wildlife habitats within 2.4 km (1.5 mi) of the candidate site boundaries.	Ecologically diverse areas, unique habitats, critical wintering ranges, relatively undisturbed areas.	Critical wildlife habitat characteristics, distribution within site, percent of site area.
Important vegetative natural communities within 2.4 km (1.5 mi) of the candidate site boundaries.	Areas that are distinctive or representative of the regional ecology.	Vegetative community characteristics, distribution within site, percent of site area.
Unique, fragile, or restricted microhabitat within 2.4 km (1.5 mi) of the candidate site boundaries.	Areas that are highly valued, areally restricted, contain unique or uncommon species, or are relatively susceptible to disturbance.	Microhabitat characteristics, location, distribution within site, percent of site area.
Threatened, endangered, or otherwise protected species and plant communities within 2.4 km (1.5 mi) of the candidate site boundaries.	Species that are exemplary of a particular environment, unique, or endangered (and thus protected) on a regional or national basis.	Species name, number, location, and status.
	AIR QUALITY	
Ambient air quality.	Expected meteorologic conditions for construction and operational phases.	Meteorologic description, particulates, and pollutants in the air.

9 2 1 2 4 9 5 0 5 9 7

TABLE 2-5. Summary Description of Environmental Factors Considered in the Siting Process (WCC, 1981).* (Sheet 2 of 2)

Factor	Conditions evaluated	Description
WATER QUALITY		
Radiation contaminated groundwater.	Near-surface contaminated groundwater dispersion.	Location with respect to site, percent of site area, description of radionucides involved.
LAND RESOURCES AND USE		
Security areas, defense-related structures within 1.0 km (0.6 mi) of the acceptable siting area.	All existing security areas, 200 Areas, defense-related and restricted land-use areas.	Location with respect to site.
AESTHETICS		
Aesthetic factors were not used in the reference repository location site screening or ranking process; any detrimental effects could be mitigated by architectural design.		
HISTORIC, ARCHAEOLOGICAL, AND CULTURAL RESOURCES		
Archaeological sites within 2.4 km (1.5 mi) of the candidate site boundaries.	Recent human activity of historic or socioeconomic value.	Location, type, age, or date of historic, prehistoric, and/or protohistoric sites.
SOCIOECONOMIC IMPACTS		
Candidate site human-population projection.	Population distribution surrounding site during operational phase, momentary peak population, and average daily population at site during construction and operational phases. Other socioeconomic impacts were not used during the screening process as these factors did not discriminate between discrete subdivisions.	Projected number by compass sector and set-distance radii.

*Factors were identified and applied based on available data outlined in WCC (1981).

9 2 1 2 4 9 5 0 5 9 8

THIS PAGE INTENTIONALLY
LEFT BLANK

9 2 1 2 4 9 5 0 5 9 9

2.4 LEGAL AND INSTITUTIONAL FACTORS

The siting process involved a review of federal, state, and local laws and reflects national policy regarding the management of nuclear wastes as expressed in the Presidential Directive of February 12, 1980 (Presidential Message to Congress, 1980), which states in concept that the siting process must:

- Be open and accessible to the public
- Include efforts to inform and educate the public
- Involve a variety of interest groups to build acceptance as well as technical consensus.

2.4.1 Federal Legal Framework

As specified in 10 CFR 60 (NRC, 1981a), licensing is required for the proposed repository under authority of the NRC, with the DOE as license applicant. Requirements for safety and environmental concerns are to guide the design of repository facilities, and these concerns are expressed in the major objectives of the BWIP siting study (see Section 2.1.1). Promulgation of 10 CFR 60 (NRC, 1981a) places responsibility for supervision of safety, transportation, and environment within the context of a DOE/NRC interface with the appropriate federal agencies.

2.4.2 State and Local Laws

As part of the siting study, a review of state and local regulations was performed based on data provided by the Washington Public Power Supply System, Inc. No existing state or local regulations were found to affect the siting process.

2.4.3 Public Involvement

It is anticipated that the licensing process will involve review by a number of agencies with jurisdiction in the vicinity of the repository location. As such, periodic briefing sessions have been held with Washington State officials regarding the status of the siting process.

Involvement of the general public has been accomplished to date by instituting open program review meetings held in the late fall and winter of 1978, 1979, and 1980 in Richland, Washington and in the winter of 1980 and 1981 in Columbus, Ohio. At each of these meetings, a summary of the status of the BWIP siting effort was presented and questions solicited

9 2 1 2 4 9 5 0 6 0 0

from the audience. Public information meetings involving siting discussions were also held in Richland, and Seattle, Washington and Portland, Oregon on August 6, 8, and 9, 1979, respectively. In addition, press releases have been prepared at frequent intervals and project personnel have described the progress of siting studies at a variety of organizational meetings held throughout the Pacific Northwest.

Involvement of the technical community has been accomplished through presentations at professional meetings. Such presentations have provided a direct contact for peer review. In addition, BWIP technical publications pertinent to the site identification effort have been distributed through the Technical Information Center, Oak Ridge, Tennessee.

2.5 DECISION-MAKING ANALYSIS

This section describes the results of the application of the site identification methodology to the study area. To provide a clearly defined physiographic boundary for this process, the study area was defined as the Pasco Basin. This broader study area was also considered to determine whether there were any apparent, obviously superior, siting areas within a naturally bounded region but outside of the Hanford Site. The relationship of the Hanford Site to the Pasco Basin is illustrated in Figure 2-9.

2.5.1 Results of the Screening Process

A summary of the results of the step-by-step screening of the Pasco Basin follows. The summary description of each step includes the specific guidelines applied and the resulting map.

2.5.1.1 Identification of Candidate Areas. The first step in screening the Pasco Basin resulted in the identification of candidate areas. Screening involved the use of inclusionary guidelines reflecting these key considerations:

- Fault rupture
- Generation of new faults
- Ground motion
- Aircraft impact
- Transportation
- Operational radiation release
- Protected ecological areas
- Culturally important areas
- Site preparation costs.

These guidelines (Table 2-6) were selected because the data were available over the study area, and they could be readily and easily depicted on overlay maps at a 1:250,000 scale. Hydrologic guidelines and the other remaining guidelines were not applied during this step of the screening because they were more readily applicable to the increasing levels of detail used in later screening steps.

The portion of the Pasco Basin remaining, after the application of guidelines in this first step, was termed the candidate area, shown in Figure 2-10.

9 2 1 2 4 9 5 0 6 0 2

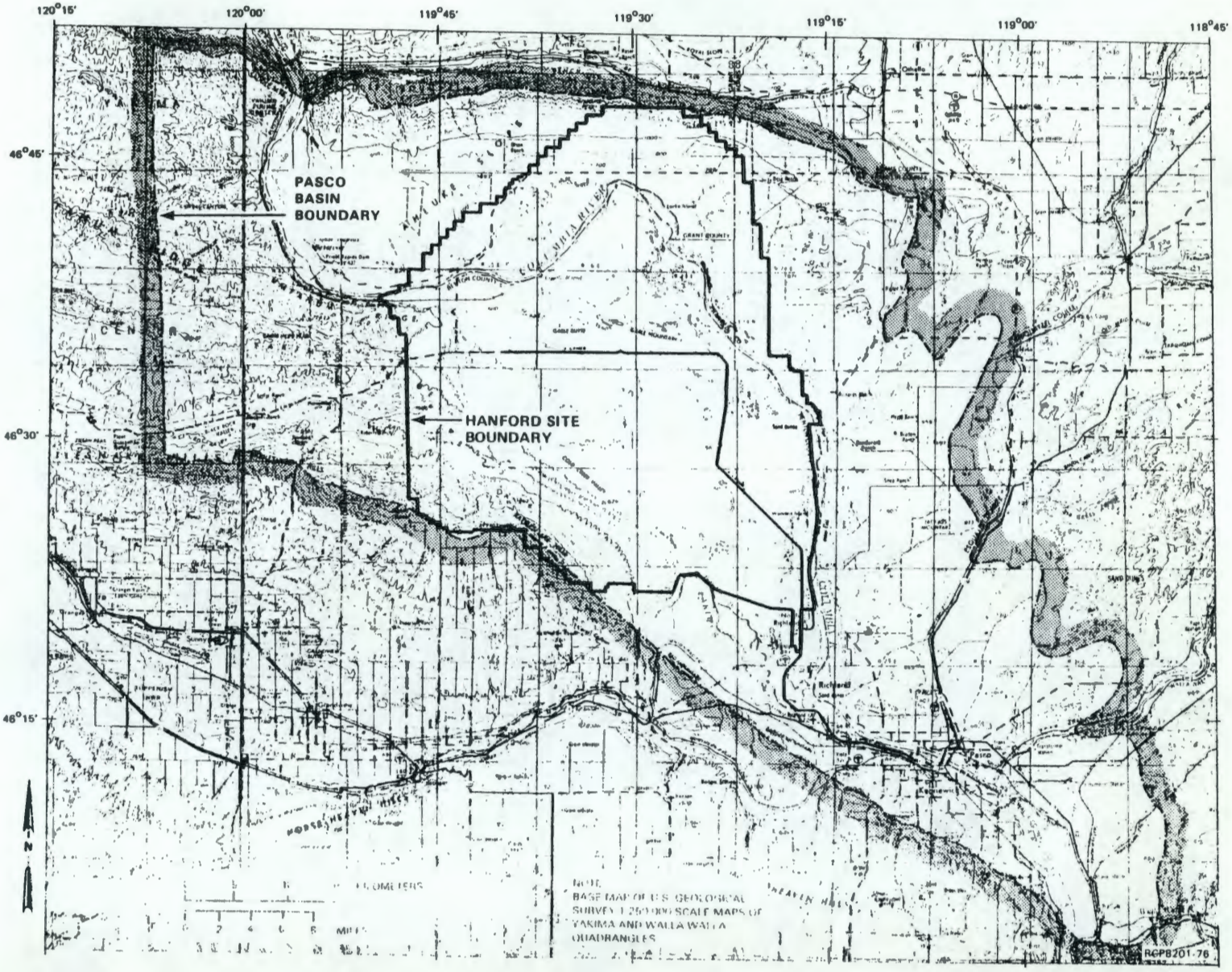

FIGURE 2-9. Pasco Basin and Hanford Site Boundaries (WCC, 1981). (Western boundary of the Pasco Basin, for purposes of the screening study, was considered to be a straight line. See Chapter 3 for comparison of this boundary with interpreted physiographic boundary of the Pasco Basin.)

9212495060 3

TABLE 2-6. Considerations, Measures, and Guidelines Used in the Candidate-Area Screening of the Pasco Basin (WCC, 1981).[a] (Sheet 1 of 2)

Consideration	Measure	Guideline
OBJECTIVE: MAXIMIZE PUBLIC HEALTH AND SAFETY		
Fault rupture	Distance from known faults interpreted to be capable	Include areas >8 km (>5 mi) from known faults interpreted to be capable and known faults whose capability is unknown
Generation of new faults	Location with respect to future potentially capable tectonic structures	Include areas >8 km (>5 mi) from folds interpreted to be capable of forming new faults
Ground motion	Location with respect to earthquake sources and estimated levels of ground motion	a. Include areas that may be subject to <40% g peak surface acceleration from known and interpreted earthquake sources b. Include areas >19.3 km (>12 mi) from felt epicenters >MM V[b] and >9.7 km (>6 mi) from instrumental epicenters magnitude >4.0 that occur in concentrations or clusters as interpreted from historical-earthquake-epicenter plot maps
Aircraft impact	a. Distance from airports	a. Include areas >8 km (>5 mi) from airports shown on state airport plans, accommodating aircraft ≥ 5,670 kg (≥12,500 lb) gross weight, or any military airport b. For airports with >12,500 yearly operations, but with <50,000, include areas >d kilometers from airport: distance (d) = $\sqrt{0.0051 \times \text{total operations}}$ [d miles from airport: distance (d) = $\sqrt{0.002 \times \text{total operations}}$].
	b. Location with respect to restricted airspace	Include areas away from the limits of restricted airspace defining intense military usage

9 2 1 2 4 9 5 0 6 0 4

TABLE 2-6. Considerations, Measures, and Guidelines Used in the Candidate-Area Screening of the Pasco Basin (WCC, 1981).[a] (Sheet 2 of 2)

Consideration	Measure	Guideline
Transportation	Distance from transportation corridors	Include areas >0.97 km (>0.6 mi) from U.S. highways, interstate highways, major railroads, and navigable waterways
Operational radiation release	Distance from population	a. Include areas >4.8 km (>3 mi) from populations of >2,500 b. Include areas >1.6 km (>1 mi) from any incorporated community
OBJECTIVE: MINIMIZE ADVERSE ENVIRONMENTAL AND SOCIOECONOMIC IMPACTS		
Protected ecological areas	Location with respect to protected ecological areas	Include areas outside of designated protected ecological areas
Culturally important areas	Location with respect to all designated areas >2,025 ha (>5,000 acres)	Include areas outside of designated culturally important areas >2,023 ha (>5,000 acres)
OBJECTIVE: MINIMIZE SYSTEM COSTS		
Site preparation costs (surface)	Terrain ruggedness	Include areas outside of rugged terrain

[a]See Table 2-4 for source of considerations, measures, and guidelines.

[b]Modified Mercalli (MM) on a scale of >V.

9 2 1 2 4 9 5 0 6 0 5

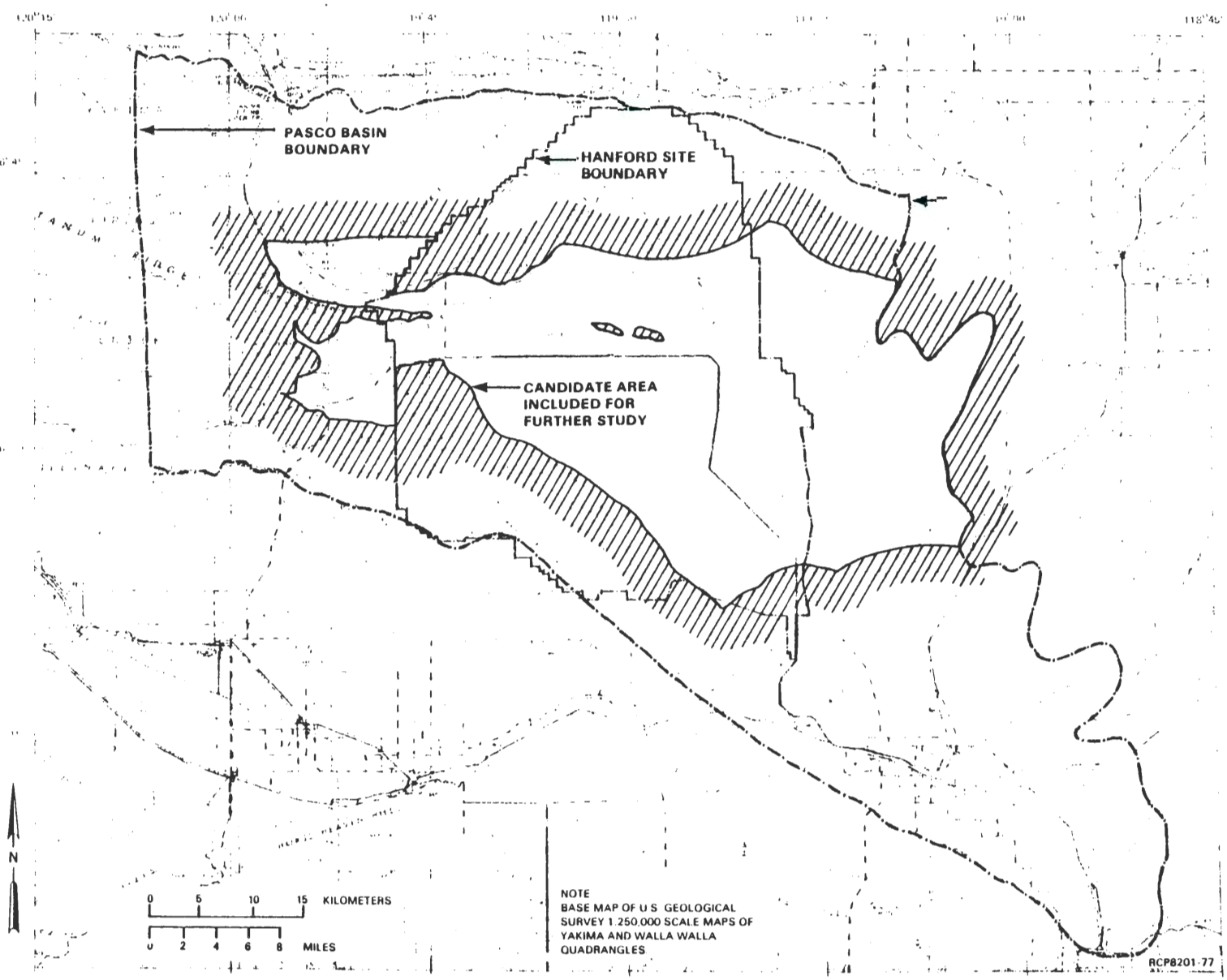

FIGURE 2-10. Pasco Basin Candidate Area (WCC, 1981).

2.5.1.2 Identification of Subareas. The second step in the screening of the Pasco Basin was to identify subareas. This involved the use of inclusionary guidelines, which represent a total of seven considerations under the three siting objectives. The considerations used to identify subareas from within the candidate area were:

- Fault rupture
- Flooding
- Ground failure
- Erosion/denudation
- Hazardous facilities
- Induced seismicity
- Site preparation (surface).

The measures and guidelines developed from these considerations are listed in Table 2-7. The subareas identified as a result of applying those guidelines are illustrated in Figure 2-11.

The guidelines in this screening step were selected because the data were available over the study area, and they could be readily and easily depicted on the screening overlays at a scale of 1:62,500.

2.5.1.3 Identification of Site Localities. Site localities on the Hanford Site were identified through an evaluation of the subareas, based on the guidelines presented in Table 2-4. The evaluation was conducted in two steps: evaluation of subareas within the Pasco Basin, but outside the Hanford Site; and evaluation of subareas within the Hanford Site.

The first step in the identification of site localities was designed to determine whether any obviously superior site localities occur in the subareas within the Pasco Basin, but outside the Hanford Site (Fig. 2-11). Two subareas were located in the Pasco Basin totally outside the Hanford Site, and two others were located partly inside and partly outside the Hanford Site.

One subarea outside the Hanford Site (Priest Rapids subarea) was located just east of Priest Rapids Dam, adjacent to the Columbia River. The area is used for irrigated farming and is adjacent to the Saddle Mountain National Wildlife Refuge. On the basis of land use and hydrology, this area is not considered obviously superior to subareas on the Hanford Site.

The second subarea (Umtanum Ridge subarea) is located south of Umtanum Ridge and west of the Hanford Site. This subarea is contiguous to the Hanford Site. The soil was found to be suitable for irrigated farming.

3 2 1 2 4 9 5 0 6 0 7

TABLE 2-7. Considerations, Measures, and Guidelines Used in Subarea Screening of the Pasco Basin (WCC, 1981).

Consideration	Measure	Guideline
OBJECTIVE: MAXIMIZE PUBLIC HEALTH AND SAFETY		
Fault rupture	Horizontal and vertical distance from known faults interpreted to be not capable, and from zones of fracturing and jointing	Include areas >0.8 km (>0.5 mi) from known faults interpreted to be not capable, known faults of unknown capability that have a high potential for a capability evaluation, and from zones of fracturing and jointing
Flooding	Height above selected flood level	Include areas outside primary floodplain and estimated probable maximum flood levels
Ground failure	Location with respect to landslides and potential landslides	Include areas not on mapped landslides
Erosion/ denudation	Location with respect to potential areas of erosion and denudation	Include areas >0.8 km (>0.5 mi) from steep-walled canyons or slopes
Hazardous facilities	Distance from possible missile or noxious-vapor generators	Include areas >0.97 km (0.6 mi) from facilities with potential explosion, fire, or missile hazards
Induced seismicity	Location with respect to sources of induced seismicity and potential earthquake sources	Include areas >8 km (>5 mi) from existing reservoirs >30 m (>100 ft) deep
OBJECTIVE: MINIMIZE SYSTEM COSTS		
Site preparation (surface)	Terrain ruggedness	Subjective evaluation for terrain characteristics (i.e., topography, slope, relief, and degree of dissection)

EXPLANATION:

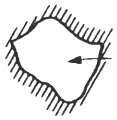

Subareas included for further study *

* These areas may be considered if favorable subsurface conditions exist.

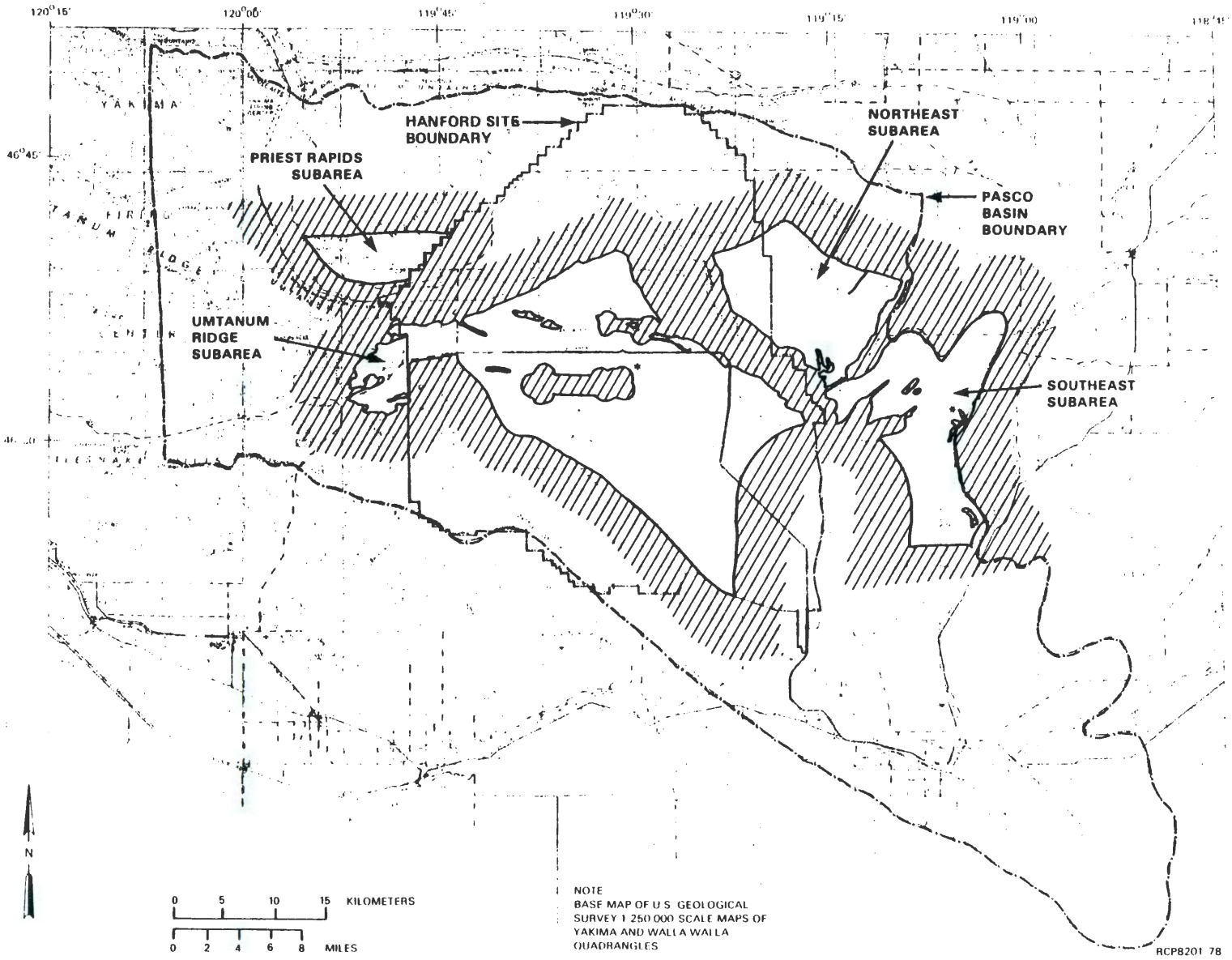

FIGURE 2-11. Subareas Within Pasco Basin (WCC, 1981).

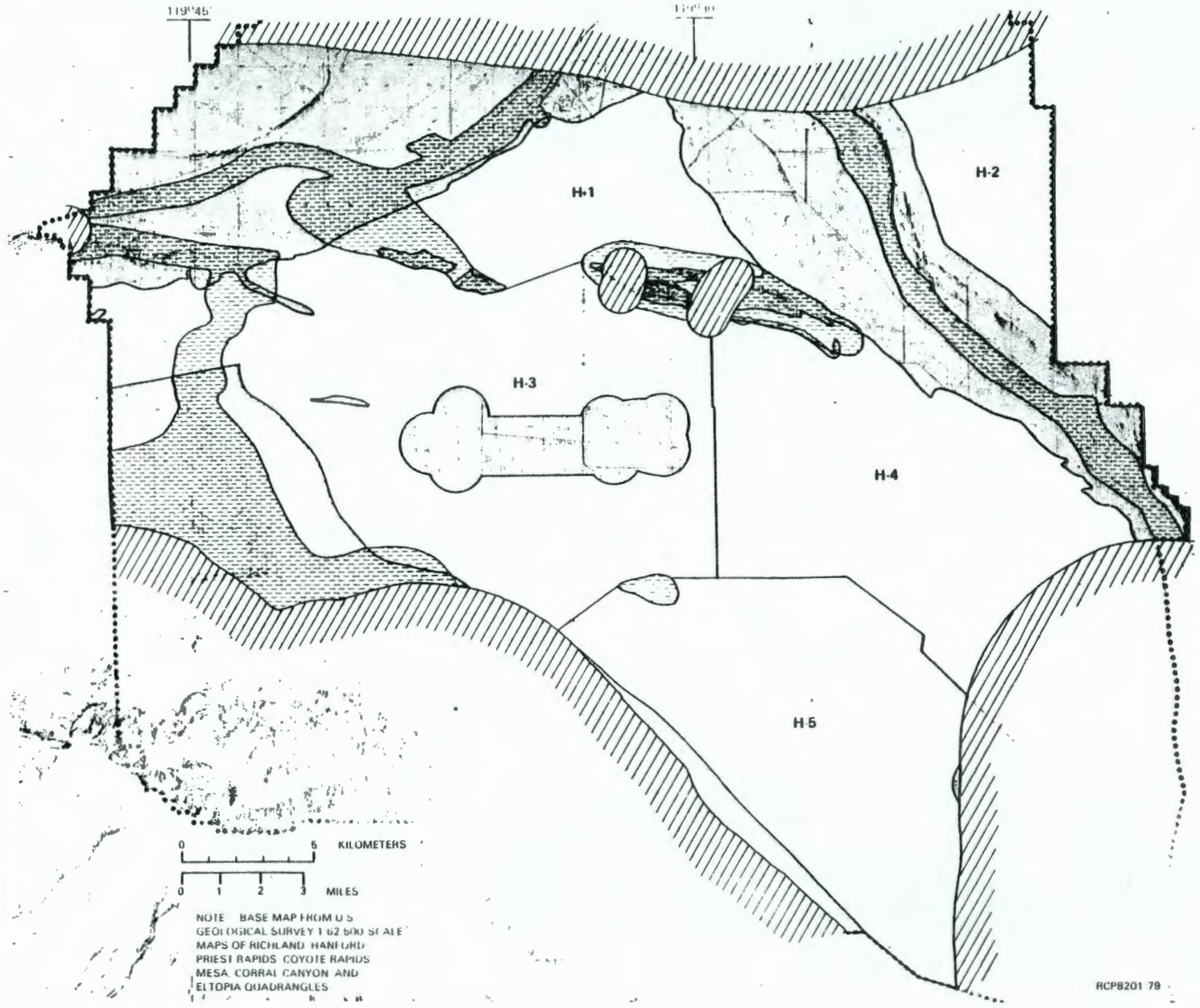

AREA SCREENED BASED ON INCLUSIONARY GUIDELINES OF:
- Fault Rupture
- Generation of Faults
- Ground Motion
- Aircraft Impact
- Transportation
- Operational Radiation Release
- Protected Ecological Areas
- Culturally Important Areas
- Site Preparation Costs

AREA SCREENED BASED ON SUBSURFACE GUIDELINES OF:
- Bedrock Dip
- Microearthquake Activity
- Hydrology
- Subarea Size

*AREAS NOT AVAILABLE FOR SURFACE FACILITIES BASED ON INCLUSIONARY GUIDELINES OF:
- Hazardous Facilities
- Flooding
- Rugged Terrain
- Erosion/Denudation
- Landslides
- Protected Ecological Areas

•••••• HANFORD SITE BOUNDARY

H-3 SITE LOCALITY DESIGNATION

* These areas may be considered if favorable subsurface conditions exist.

FIGURE 2-12. Hanford Site: Compilation of Available Area and Site Localities (WCC, 1981).

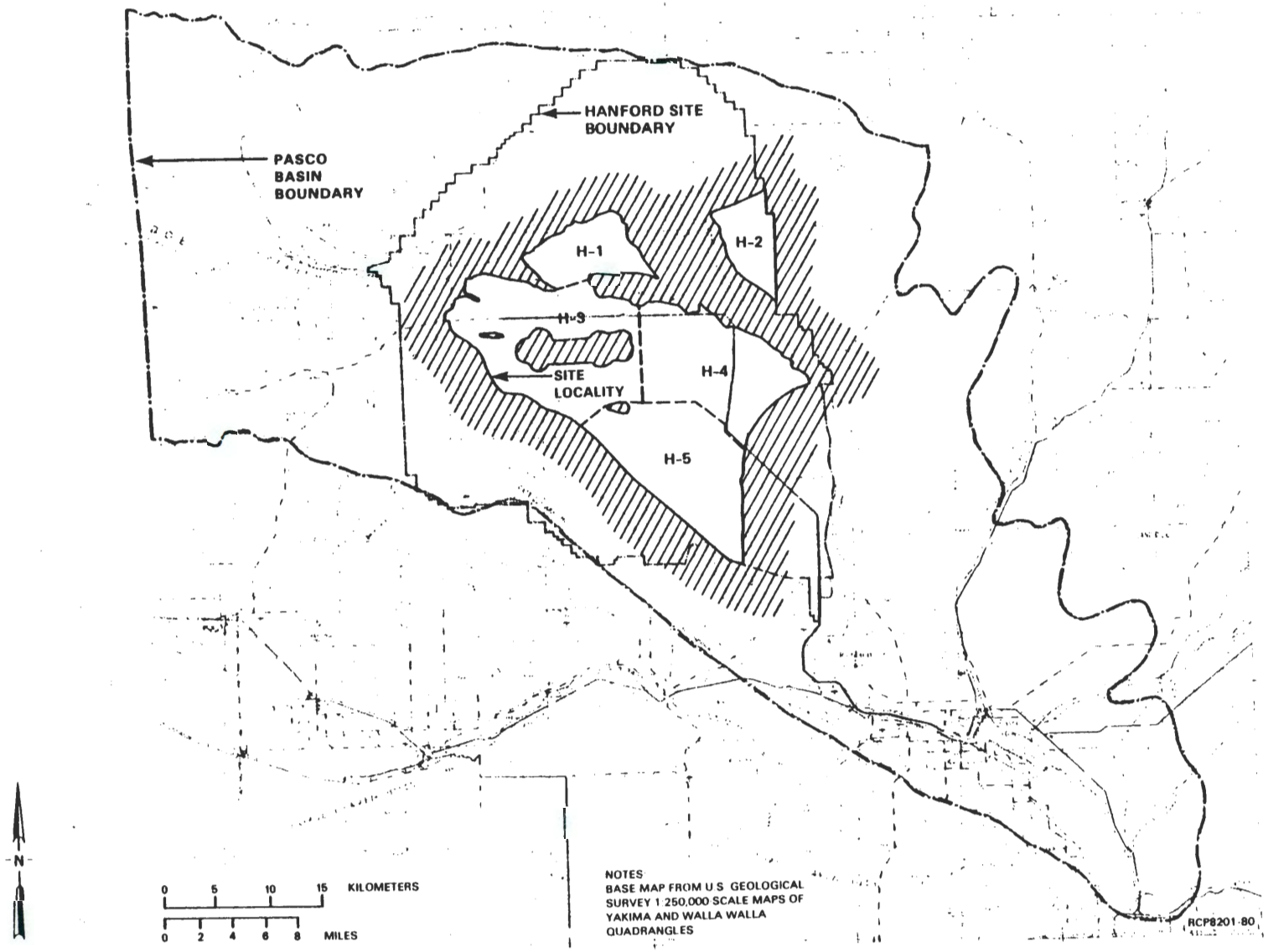

FIGURE 2-13. Site Localities on the Hanford Site (WCC, 1981).

Several deep wells have already been drilled within the subarea, and it is close to the Columbia River. Yakima Ridge traverses the subarea and appears to contain areas where the bedrock dip is greater than 5 degrees. Umtanum Ridge and Rattlesnake Hills are close to the subarea. On the basis of land use, hydrology, bedrock dip, and tectonic stability, this subarea outside the Hanford Site was not considered superior to subareas within the Hanford Site.

A third subarea (Northeast subarea) was located adjacent to and continuous with the northeastern part of the Hanford Site. This subarea is underlain by loess and is presently used for intensive irrigated agriculture. It is also near the Columbia River. On the basis of land use and hydrology, this subarea was not considered obviously superior to subareas on the Hanford Site.

The fourth subarea (Southeast subarea) is located east of the Hanford Site east of and close to the Columbia River. This land is part of the Columbia Basin Irrigation Project and is used for irrigated agriculture. Several irrigation canals and pumping stations are located within this subarea. On the basis of land use and hydrologic evaluations, this subarea was not considered superior to subareas on the Hanford Site.

As a result of this evaluation, no subareas in the Pasco Basin outside the Hanford Site were found to be obviously superior to subareas within the Hanford Site. Consequently, further study to identify site localities was concentrated on the subareas totally within the Hanford Site.

The second step, the evaluation of subareas on the Hanford Site, was an examination of the results from the application of the guidelines (Table 2-4) as they affect the subsurface, compared to those that affect the surface.

Subsurface conditions on the Hanford Site were evaluated based on inclusionary and classifying guidelines employing screening overlays for:

- Bedrock dip
- Microearthquake activity
- Hydrology.

The available surface area was defined by the inclusionary guidelines using the screening overlays for:

- Potentially hazardous facilities
- Flooding
- Terrain ruggedness
- Erosion/denudation

9 2 1 2 4 9 5 0 6 1 2

- Landslides
- Protected ecological areas.

The area screened in this step is illustrated in Figure 2-12 and reflects the boundaries defined during the identification of subareas, except for the Hanford Site boundary to the west and east.

The results of applying both surface and subsurface screens indicated that the area resulting from the combined effect of the screens was more suitable and had a higher likelihood of containing suitable waste-repository sites than the area identified in either step separately.

Three general areas were defined by the combined screens: east of the Columbia River, north of Gable Mountain, and south of Gable Mountain. Using the general size of a site locality as less than 130 square kilometers (50 square miles) and more than 26 square kilometers (10 square miles), five site localities (H-1 through H-5) were identified in the three areas, as indicated in Figure 2-12. The site localities are shown in the regional context of the Pasco Basin screening area in Figure 2-13. The boundaries describing site localities H-1 and H-2 were defined by screening boundaries. The three site localities south of Gable Mountain were defined somewhat arbitrarily to maintain equal size. A small area west of site locality H-3 was not considered further due to its small size, which would preclude a repository based on a subsurface area of 26 square kilometers (10 square miles). Favorable subsurface conditions took precedence over unfavorable surface conditions; i.e., areas were not removed from further consideration merely on the basis of inclusionary guidelines for surface facilities (see Fig. 2-12).

To characterize the existing conditions within each site locality and to provide a basis for evaluating the site localities with respect to identifying candidate sites in future steps of the siting process, 23 descriptive parameters were selected representing geology, hydrology, seismology, land use, ecology, and man-made hazards. These parameters were derived from the considerations shown in Table 2-7. The estimated ranges of the existing conditions for each of these categories, for each site locality, are presented in Table 2-8. Further documentation of the site locality identification study is found in WCC (1980).

2.5.1.4 Identification of Candidate Sites. The identification of candidate sites on the Hanford Site was the fourth step in the screening process. Nine candidate sites (A through G, Y and Z, Fig. 2-14) were identified within the five site localities.

The identification of candidate sites was based on a selective and successive examination and evaluation of the range of existing geologic, hydrologic, seismologic, land use, and ecologic conditions that characterize each of the five site localities. The 23 parameters that describe the existing conditions at the site localities, summarized in Table 2-8, were used in the evaluation. The parameters provide information that was used for the identification of candidate sites. In addition, the parameters were selected to reflect the objectives of the siting study.

9 2 1 2 4 9 5 0 6 1 3

TABLE 2-8. Estimated Range of Existing Conditions at Site Localities on the Hanford Site (WCC, 1981). (Sheet 1 of 3)

Parameter	Site locality				
	H-1	H-2	H-3	H-4	H-5
Geology/hydrology					
Estimated depth to basalt within site locality	120 to 215 m (400 to 700 ft)	140 to 245 m (450 to 800 ft)	0 m (Gable Butte) to ~215 m (0 to 700 ft)	0 m (Gable Mountain) to ~213.4 m (0 to ~700 ft)	0 m (south) to ~213.4 m (north) (0 to ~700 ft)
Estimated depth to Ringold Formation within site locality	~3 to ~20 m (~10 to ~60 ft)	0 to ~15 m (0 to ~50 ft)	~8 to ~30 m (~25 to ~100 ft)	~15.2 to ~45.7 m (~50 to ~150 ft)	~15.2 to ~38.1 m (~50 to ~125 ft)
Estimated basalt stratigraphic characteristics within site locality	Approximately flat-lying except at south boundary	Approximately flat-lying; uniform; no apparent structure; beds thin to north	All edges dip slightly toward center. Structural low near wells DC-4 and -5. Yakima Ridge anticline crosses southern part	Dipping slightly to southern tip of site locality near wells DC-7 and -8; northwest area is structurally complex	Southern 2/3 dips slightly to north; northern 1/3 dips slightly south; Yakima Ridge anticline may affect western parts
Estimated depth to Umtanum marker flow	>915 m (>3,000 ft)	>915 m (>3,000 ft)	~915 to 1,160 m (~3,000 to 3,800 ft)	~914.4 to 1,158.2 m (~3,000 to 3,800 ft)	~914.4 to 1,158.2 m (~3,000 to 3,800 ft)
Formations in repository zone 610- to 1,220-m (2,000- to 4,000-ft) depth	Upper part of Grande Ronde	Lower Wanapum and upper Grande Ronde	Lower Wanapum and upper Grande Ronde	Lower Wanapum and upper Grande Ronde	Lower Wanapum and upper Grande Ronde
Distance to nearest anticlines and faults	Measured from Gable Mountain anticline and associated faults: 0.2 to 5.2 km (0.25 to 3.25 mi)	Measured from Gable Mountain and Saddle Mountain anticlines: 5.6 to 11.6 km (3.5 to 7.25 mi)	Measured from Gable Mountain anticline and faults and Umtanum and Yakima Ridge anticlines: 0 to 6.4 km (0 to 4 mi)	Measured from Gable Mountain anticline and faults and Yakima Ridge anticline: 0 to 12.9 km (0 to 8 mi)	Measured from Yakima Ridge anticline: 0 to 8 km (0 to 5 mi)
Distance to rivers	0.8 to 7.2 km (0.5 to 4.5 mi)	1.6 to 6.4 km (1 to 4 mi)	2.8 to 16.8 km (1.75 to 10.5 mi)	2.0 to 12.9 km (0.25 to 8 mi)	0 to 16 km (0 to 10 mi)
Estimated depth to water table	<30 to >45 m (<50 to >150 ft)	~90 m (~300 ft)	<15 to >106 m (<50 to >350 ft)	<15.2 to >45.7 m (<50 to >150 ft)	<39.6 to >57.9 m (<130 to >190 ft)
Estimated distance to irrigation wells	12.8 to 17.6 km (8 to 11 mi)	1.6 to 8 km (1 to 5 mi)	4.8 to 20.8 km (3 to 13 mi)	3.2 to 19.3 km (2 to 12 mi)	9.6 to 18.5 km (6 to 11.5 mi)

TABLE 2-8. Estimated Range of Existing Conditions at Site Localities on the Hanford Site (WCC, 1981). (Sheet 2 of 3)

Parameter	Site locality				
	H-1	H-2	H-3	H-4	H-5
Seismology (Based on historical seismicity)					
Microearthquake: (Magnitude 1.0 from 1969 to 1977)					
a. Spatial distribution (trends)	No trend	No trend	Some trend northwest	No trend	No trend
b. Seismographic instrument coverage within or near site locality (USGS or UW)	3 instruments	No instruments	4 instruments	2 instruments	1 instrument
c. Focal depth distribution	≤13.7 km (≤8.5 mi)	≤29.0 km (≤18 mi)	≤29.0 km (≤18 mi)	No recorded events	≤29.0 km (≤18 mi)
d. Temporal distribution of events in or near site locality	Swarm behavior	Swarm behavior	Random occurrences	No recorded events $M_L \geq 1$	Swarm behavior
e. Magnitude distribution	M_L 1 to 3; $M_L \leq 2.5$ for swarms	M_L 1 to 3; $M_L \leq 2.5$ for swarms	M_L 1 to 2	Not applicable	M_L 1 to 3; $M_L \leq 2.5$ for swarms
f. Possible association with irrigation	Yes	Yes	Not applicable	Not applicable	Yes
Estimated horizontal bedrock accelerations from offsite historical earthquakes and distances for >MM V and/or magnitude >4.0	3.2 to 12.9 km (2 to 8 mi); ≤0.02 g	8 to 17.7 km (5 to 11 mi); ≤0.02 g	11.3 to 20.9 km (7 to 13 mi); ≤0.02 g	20.9 to 38.6 km (13 to 24 mi); ≤0.02 g	12.9 to 38.6 km (8 to 24 mi); ≤0.02 g

TABLE 2-8. Estimated Range of Existing Conditions at Site Localities on the Hanford Site (WCC, 1981). (Sheet 3 of 3)

Parameter	Site locality				
	H-1	H-2	H-3	H-4	H-5
Land use/ecology					
Amount of surface area underlain by irrigable soil	~35% (center of H-1 from north to south)	~20% (all in southern part of H-2)	~20% (all along and east edges of H-3)	~4%	0%
Estimated amount of site locality with important wildlife habitat	10%	55%	75%	65%	80%
Estimated distance from protected ecological areas	1.2 to 11.3 km (0.75 to 7 mi)	8 to 17.7 km (5 to 11 mi)	0 to 12.1 km (0 to 7.5 mi)	5.6 to 17.6 km (3.5 to 11 mi)	0 to 9.2 km (0 to 5.75 mi)
Man-made hazards					
Distance to hazardous facilities	N Reactor and 200 West Area: 1.2 to 8 km (0.75 to 5 mi)	N Reactor and 200 East Area: 12.9 to 18.5 km (8 to 11.5 mi)	200 West Area and 200 East Area: 0.97 to 8 km (0.6 to 5 mi)	200 East Area FFTF and WPPSS sites: 0.4 to 10.4 km (0.25 to 6.5 mi)	200 East Area FFTF and WPPSS sites: 0.96 to 10.8 km (0.6 to 6.75 mi)
Low-altitude military routes and high-altitude jet routes	Almost entire site locality within limits of jet route J143; only the ~1.2-km (0.75-mi) strip in northwest part lies outside; outside the limits of low-altitude military routes	Almost entire site locality within limits of jet route J143; only southeastern tip lies outside; outside the limits of low-altitude military routes	Almost entire site locality within limits of jet route J143; only the southeastern and northwestern corners lie outside; outside the limits of low-altitude military routes	The northwestern 1/3 of site locality is within limits of jet route J143; outside the limits of low-altitude military routes	Entire site locality lies outside the limits of jet route J143 and low-altitude military routes
Contaminated soil and water: area/extent/level	Not applicable	Not applicable	Surface soil: Some contamination. Unconfined groundwater: Some contamination	Surface soil: None. Unconfined groundwater: Some contamination	Surface soil: None. Unconfined groundwater: Some contamination
Deep wells (>305 m) (>1,000 ft); distance and depth	Distance: 4.8 to 10.5 km (3 to 6.5 mi) Depth: None in site locality	Distance: 2.4 km (1.5 mi) Depth: None in site locality	Distance: 0 to 6.4 km (0 to 4 mi) Depth: 318.8 to 1,737.4 m (1,046 to 5,700 ft) (4 wells)	Distance: 0 to 8.9 km (0 to 5.5 mi) Depth: 427.6 to 1,249.7 m (1,403 to 4,100 ft) (2 wells)	Distance: 0 to 9.6 km (0 to 6 mi) Depth: 393.8 to 454.2 m (1,292 to 1,490 ft) (2 wells)

FFTF = Fast Flux Test Facility
M_L = local magnitude
MM = modified Mercalli
USGS = U.S. Geological Survey
UW = University of Washington
WPPSS = Washington Public Power Supply System, Inc.

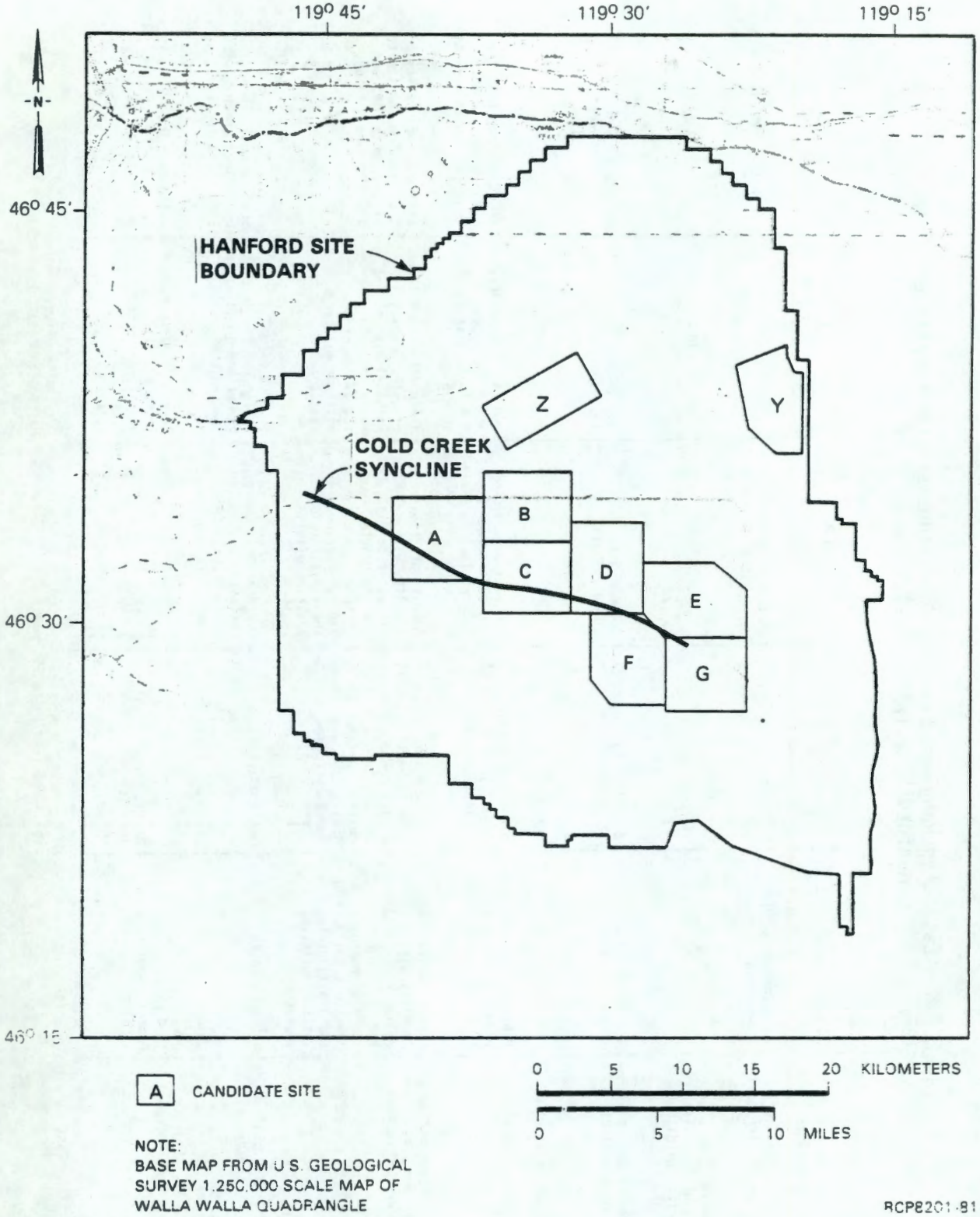

FIGURE 2-14. Initial Candidate Sites on the Hanford Site (WCC, 1981).

To identify the candidate sites, screening overlays representing the range of conditions and area affected by each parameter under consideration were superimposed. The results of this overlay process were used to identify the portion within each locality that tended to maximize the desirable characteristics. Seven of the identified candidate sites (A through G) were located in a group within the Cold Creek syncline, a major structural feature of the Pasco Basin. Two other candidate sites (Y and Z) lie just outside this structure (Fig. 2-14).

To identify a subset that appeared favorable for more detailed analysis, preliminary ranking of the nine candidate sites was conducted. Five attributes were used to provide a means of comparing and eventually differentiating among the sites. The identification and development of these attributes proceeded from a review and evaluation of the considerations and guidelines used in the screening process and the 23 parameters that describe the existing conditions at the site localities (Table 2-8). The attributes included:

- Distance to discharge areas
- Structural geologic considerations
- Site biologic impact
- Distance to potentially hazardous facilities
- Potential for repository expansion.

These attributes were used to quantitatively measure a condition or characteristic of the candidate site by means of an actual unit scale, such as distance, or a constructed scale that quantified the conditions.

The results of the preliminary evaluation of the candidate sites showed that the central portion of the Cold Creek syncline area (Fig. 2-15) represented by candidate sites A through G was the most attractive (BWIP, 1980). The preliminary ranking process revealed that decisions based on the data did not provide a clear-cut dominance of some sites by others. It became apparent that the addition of more recently acquired technical data (particularly geophysical) could affect the ranking. Subsequent evaluation and ranking were carried out with an updated data base to identify a reference repository location and possible alternate repository location. The remaining seven contiguous candidate sites in the Cold Creek syncline were retained (Fig. 2-14) for further evaluation to identify a reference repository location and an alternate repository location.

Lineament mapping resulting from geophysical studies, and the possible structural geologic significance of the lineaments, made it useful to reevaluate the boundaries of the seven candidate sites. For comparison with previous work, the original candidate site boundaries were maintained and three additional candidate sites established. These three additional sites, H, J, and K (see Fig. 2-15), overlapped portions of the original seven sites. Site H incorporates much of original site A and part of

9 2 1 2 4 9 5 0 6 1 8

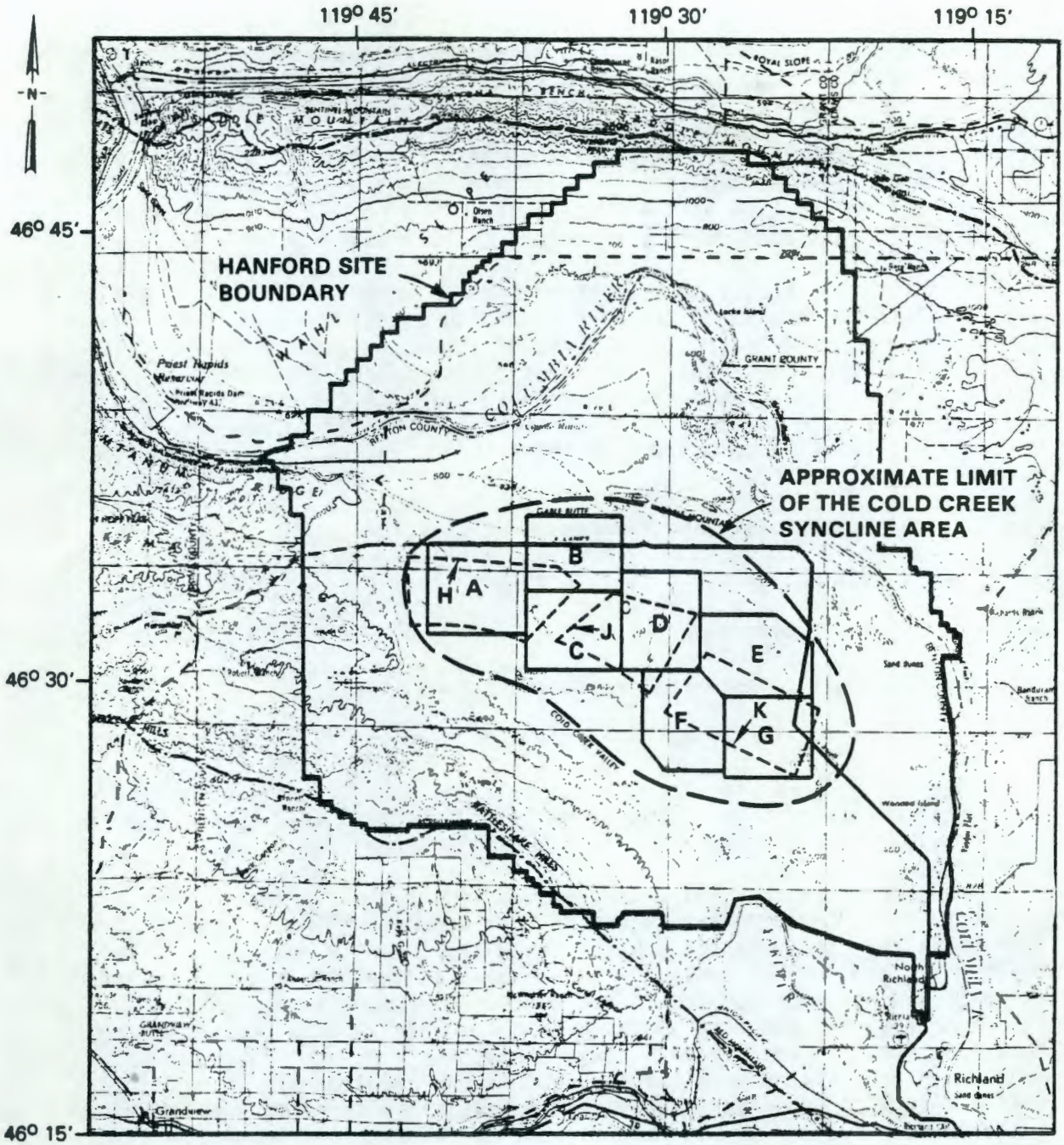

E ORIGINAL CANDIDATE SITE

H NEW SITE ADDED AS A RESULT OF GEOPHYSICAL SURVEY

NOTE:
BASE MAP FROM U.S. GEOLOGICAL SURVEY 1:250,000 SCALE MAP OF WALLA WALLA QUADRANGLE

0 5 10 15 20 KILOMETERS

0 5 10 MILES

RCP8201-82

FIGURE 2-15. Ten Candidate Sites in the Cold Creek Syncline Area (after eliminating sites Y and Z from further consideration) (WCC, 1981).

site B that was not influenced by the Gable Mountain structure. Site J overlies sites C and D. Site K overlapped the southeastern three sites. Incorporation of the three new sites provided a total of ten candidate sites ranging from 26 to 39 square kilometers (10 to 15 square miles) in area, which were evaluated for the identification of the reference repository location and alternate repository location.

2.5.2 Results of the Ranking Process

Each candidate site in the Cold Creek syncline area (Fig. 2-15) included sufficient space for surface and subsurface facilities. Preliminary evaluation made it clear that the sites were too closely matched to be separable by routine ranking. The modified approach was to compile an enlarged and updated data base from which descriptions of the geology, hydrology, land use, ecology, etc. could be formulated in a format amenable to comparison. The construction of a criteria matrix to accommodate this data base resulted in an enlarged set of descriptors derived from the parameters used for screening (Table 2-8). The descriptors (Table 2-9) were reviewed and revised to form a set of ranking criteria on which to base the decision analysis approach used to identify the reference repository location and alternate repository location. The relationship between criteria matrix descriptors and NWTS-33(2) criteria (NWTS, 1981) is summarized in BWIP (1981).

The identification of a reference repository location and an alternate repository location from among the ten sites in the Cold Creek syncline area (Fig. 2-15) was conducted in four steps:

- Structuring the problem
- Describing the consequences
- Determining preferences for different consequences
- Synthesizing the information and performing ordinal dominance analysis.

The following discussion describes the ranking procedure undertaken at each step and the results obtained by the Siting Committee (comprised of Woodward-Clyde Consultants' and Rockwell Hanford Operations' technical personnel) in identifying a reference repository location and an alternate repository location.

2.5.2.1 Structuring the Problem. The key element of this step was the development of measures for those ranking criteria (guidelines) that could be used to differentiate the candidate sites. The ranking criteria and their measures were derived from a detailed evaluation of criteria and data comprising the criteria matrix. A list of all possible attributes drawn from the criteria matrix was screened to eliminate redundancies. Criteria having similar consequences for all sites, and therefore (regardless of absolute importance) not useful for differentiation, were removed

TABLE 2-9. Criteria Matrix Descriptors (WCC, 1981). (Sheet 1 of 3)

Category	Descriptor title
Structural geology	Known faults within 8 km (5 mi) of the subsurface limits of the candidate site.
	Bedrock fracturing and jointing within 2.4 km (1.5 mi) of the subsurface limits of the candidate site.
	Lineaments and postulated faults within 8 km (5 mi) of the subsurface limits of the candidate site.
	Anticlines within 8 km (5 mi) of the subsurface limits of the candidate site.
Seismicity	Microearthquakes within 25.7 km (16 mi) of the candidate site center.
	Potential earthquake sources within 48.3 km (30 mi) of the candidate site center.
	Potential sources of induced seismicity.
Tectonics	Identified Quaternary and neotectonic crustal movement within 8 km (5 mi) of the subsurface limits of the candidate site.
	Tectonic stress field.
	Comparison and possible relationships of known faults, fractures, and tectonic joints within 8 km (5 mi) of the candidate site with respect to the tectonic-stress regime.
Stratigraphy	Stratigraphic unit at the proposed repository level.
	Ringold Formation and Quaternary stratigraphy.
Host rock characteristics	Host flow structural characteristics.
	Thickness of buffer zone vertically and laterally around the proposed repository.
	Thermal and mechanical properties of the proposed repository host rock.
	Horizontal and vertical lithostatic stress at the proposed repository depth.

TABLE 2-9. Criteria Matrix Descriptors (WCC, 1981). (Sheet 2 of 3)

Category	Descriptor title
Geohydrology	Natural or man-made groundwater discharge areas.
	Groundwater travel time to closest natural or man-made discharge areas.
	Aquifers and aquitards above and below the proposed repository horizon.
	Groundwater recharge rates at the proposed repository level.
	Vertical and horizontal hydraulic gradients.
	Groundwater geochemical characteristics at and surrounding the proposed repository.
	Host rock geohydrologic characteristics.
	Surface flooding.
Environment	Critical wildlife habitats within 2.4 km (1.5 mi) of the candidate site boundaries.
	Important vegetative natural communities within 2.4 km (1.5 mi) of the candidate site boundaries.
	Unique, fragile, or restricted microhabitats within 2.4 km (1.5 mi) of the candidate site boundaries.
	Threatened, endangered, or otherwise protected species and plant communities within 2.4 km (1.5 mi) of the candidate site boundaries.
	Candidate site human population projection.
	Ambient air quality.
	Potential, significant, specialty, and incompatible land uses.
	Archaeological sites within 2.4 km (1.5 mi) of the candidate site boundaries.

TABLE 2-9. Criteria Matrix Descriptors (WCC, 1981). (Sheet 3 of 3)

Category	Descriptor title
Man's activities	Potentially hazardous facilities, possible missile generators, and possible vapor sources.
	Transportation corridors.
	Radiation contaminated soil and groundwater.
	Facilities or areas interpreted to be possible defense or security risks.
	Possible areas of future mineral resource exploration and extraction within 2.4 km (1.5 mi) of the candidate site boundaries.
	Boreholes penetrating basalt and boreholes deeper than 304.8 m (1,000 ft) within 2.4 km (1.5 mi) of the subsurface limits of the candidate site.
Engineering and systems costs	Thickness of unconsolidated material.
	Depth to the unconfined aquifer.
	Depth to the proposed repository horizon (shaft length).
	Candidate site topographic characteristics.
	Candidate site preparation costs.
	Candidate site operation costs.

from further consideration. Some criteria were considered or redefined to form more realistic measures. The result was a list of preliminary ranking criteria refined during the Siting Committee meeting, including redefinition of terms, deletions, and additions. The final list was the ranking criteria (Table 2-10).

2.5.2.2 Describing the Consequences. Once the ranking criteria and measures were established, they were applied to each candidate site in the Cold Creek syncline area by utilizing the available published and unpublished data and the professional judgment of the members of the Siting Committee. The results of the process can be summarized in the site-measure matrix (Table 2-11).

2.5.2.3 Determining Preferences for Different Consequences. An examination of the site measure matrix indicated that no one site was superior with respect to all criteria. Furthermore, because there were a number of criteria and alternatives, simple dominance analysis was difficult to perform. Therefore, ordinal dominance analysis assuming a linear additive value function was used to proceed with ranking.

Ordinal dominance required the assessment of trade-offs to determine which measures were of relatively more importance in differentiating among the candidate sites. Trade-offs were assessed by the Siting Committee. The trade-offs were examined in two ways to provide consistency checks. First, the Siting Committee was asked the following type of question: "Given a hypothetical site with all the criteria at their most desirable levels and given that one criterion had to be changed to its least desirable level, which one could be changed?" The criterion selected for this question would have the least importance or smallest weight. (Notice that the question is defined in terms of the most and the least desirable levels spanned by the candidate sites and is thus geared to determining how important a criterion is in differentiating among the sites.) The question was repeated with the provision that another criterion must now be picked and was repeated successively until the weights were rank ordered.

An alternate procedure was to ask the Siting Committee how much they were willing to give up on one criterion to gain on another. For example, how many meters (feet) of host flow interior thickness would they give up to improve from a less preferred level of another criterion (e.g., bedrock fractures) to a more preferred level. The rank ordering of weight provided by this procedure agreed with that provided by the first procedure discussed.

A list of the criteria, their most and least desirable or preferred levels, and the constraints on the weights that represented the strong consensus of the Siting Committee are given in Table 2-12. In examining this table, two points should be noted. First, it was the strong consensus of the Siting Committee that the environmental criteria and the man's activities criterion were useful only to differentiate among sites that were identical in all other respects. The Committee was unwilling to trade off any interior flow thickness to move from the worst levels of

TABLE 2-10. Ranking Criteria.

Criteria	Site characteristics
Structural geology	Bedrock fractures and faults: Closest distance to known faults and bedrock fractures of consequence from subsurface limits of the candidate site.
	Lineaments: Number and distribution of lineaments of consequence within the subsurface limits of the candidate site.
Seismicity	Potential earthquake sources: Closest distance to the nearest potential earthquake source from site center.
Geohydrology	Groundwater travel time: Shortest relative groundwater flow travel time from site center to nearest discharge area.
Man's activities	Contaminated soil/contaminated groundwater/surface facilities: Largest contiguous site area available without contaminated soil, contaminated groundwater, or incompatible surface facilities.
Host rock characteristics	Host flow interior: Thickness of repository host flow interior.
	Tiers: Degree of development of tiers or internal flow discontinuities within repository host flow.
Environment	Vegetative natural communities: Percent of candidate site area made up of important vegetative natural communities.
	Unique microhabitats: Extent of unique, fragile, or restricted microhabitats within candidate site boundaries.
	Special species: Number of threatened, protected, or endangered species within candidate site boundaries.

TABLE 2-11. Candidate Site Measure Matrix.

Candidate site	Structural geology			Seismicity		Geohydrology	Man's activities		Host rock characteristics			Environment		
	Bedrock fractures, faults (distance)		Lineaments (constructed scale)[a]	Earthquake sources (distance)		Groundwater travel time (constructed scale)[b]	Contamination, surface facilities (areas available)		Host flow interior (thickness)*		Tiers (constructed scale)[c]*	Vegetative natural communities (% site area)	Unique microhabitats (constructed scale)[d]	Special species (number in site)
	km	mi		km	mi		km^2	mi^2	m	ft				
A	3.2	2.0	1	5.0	3.1	2	16.8	6.5	36.6	120	1	100	3	2
B	1.1	0.7	9	4.3	2.7	3	16.8	6.5	42.7	140	2	25	3	1
C	6.0	3.7	6	3.5	2.2	3	13.0	5.0	35.1	115	2	95	2	2
D	1.9	1.2	8	5.6	3.5	5	16.8	6.5	38.1	125	3	10	3	1
E	1.4	0.9	8	6.3	3.9	5	11.7	4.5	36.6	120	4	0	1	0
F	5.5	3.4	12	1.1	0.7	2	27.2	10.5	24.4	80	3	35	1	0
G	0.0	0.0	7	3.2	2.0	1	25.9	10.0	24.4	80	4	0	1	0
H	2.3	1.4	0	4.7	2.9	2	11.7	4.5	36.6	120	1	100	3	3
J	4.8	3.0	5	4.3	2.7	5	11.7	4.5	36.6	120	3	40	1	2
K	0.0	0.0	5	3.1	1.9	2	35.0	13.5	27.4	90	4	0	1	0

*Umtanum horizon used as a reference.

Constructed scale values

	Most desirable	Least desirable
a	0	12
b	5	1
c	1	4
d	1	3

TABLE 2-12. Criteria Ranges and Rank Order of Weights.

Criterion	Value measured	Preference level		Importance weight (best estimate)*
		Most	Least	
Lineaments	Constructed scale	0	12	$k_l = 0.48$
Umtanum flow interior	Thickness	42.7 m (140 ft)	24.4 m (80 ft)	$k_i = 0.16$
Tiering within the Umtanum flow	Constructed scale	1	4	$k_t = 0.16$
Potential earthquake sources	Distance	6.3 km (3.9 mi)	1.1 km (0.7 mi)	$k_p = 0.13$
Groundwater travel time	Constructed scale	5	1	$k_g = 0.04$
Bedrock fractures, faults	Distance	6.0 km (3.7 mi)	0.0 km (0.0 mi)	$k_b = 0.03$
Contaminated soil/ground-water/surface facilities	Site area	35.0 km^2 (13.5 mi^2	11.7 km^2 (4.5 mi^2)	$k_c = 0+$
Special species	Number in site	0	3	$k_s = 0+$
Vegetative natural communities	Percent site area	1	3	$k_u = 0+$
Unique microhabitats	Constructed scale	0	100	$k_v = 0+$

*Consensus constraints on weights: $k_l \geq 2k_i \geq 2k_t \geq 2k_p \geq 4k_g \geq 4k_b$.

environmental or man's activities to the best for these criteria. Second, the Siting Committee could not easily agree as to the relative importance of tiers versus thickness given their ranges. The ordinal dominance analysis allowed for the examination of both cases.

2.5.2.4 Synthesizing the Information and Performing Ordinal Dominance Analysis. Given the preference information, the sites were ranked using ordinal dominance analysis. The results of this dominance analysis are shown in Table 2-13.

TABLE 2-13. Results of Ranking* (WCC, 1981).

Candidate site	Dominated by
A	H
B	A, H, J
C	A, H
D	A, H, J
E	A, C, D, H, J
F	A, C, D, E, G, H, J, K
G	A, C, H, J, K
H	--
J	A, H
K	A, H, J

*For site ranking values, see WCC (1981, Vol. II).

The ordinal dominance analysis showed that H was the preferred candidate site dominating all other sites. Site A dominated all others except site H. Site J was dominated only by sites A and H. Site C was ranked fourth after site J by virtue of preferential weighting of the ranking criteria.

Since site A overlapped most of site H, the reference repository location was considered to be a combination of sites A and H. Site J was the alternate to the reference repository location A-H.

The results of the dominance analysis were tested by adding potential criteria such as one of the environmental measures, man's activities, or microearthquakes. The identification of candidate sites H, A, J, and C for highest consideration still resulted. Further documentation of the reference repository location identification study is contained in WCC (1981).

1 2 1 2 4 9 5 0 6 2 8

THIS PAGE INTENTIONALLY
LEFT BLANK

9 2 1 2 4 9 5 0 6 2 9

2.6 IDENTIFICATION OF PRINCIPAL BOREHOLE/ EXPLORATORY SHAFT SITE

With the identification of the A-H site as the reference repository location, the BWIP undertook an investigation to select the recommended area within the reference repository location for construction of an exploratory shaft. To support this decision, six boreholes were drilled to locate the top of basalt to determine the dip of bedrock throughout the site. The dip was determined to be less than 1 degree across the 46.7-square-kilometer (18-square-mile) reference repository location. Composite overlays were also utilized based on selection criteria to locate the suitable exploratory shaft area. These criteria included avoidance of previously contaminated areas, distance from A-H peripheral geologic anomalies, and Hanford Site planned utilization. Following location of a suitable area, optimization features were utilized to pick the specific recommended location for a principal borehole and exploratory shaft. These included proximity to roads, services, and utilities, and ease of placement of surface facilities. The location selected for a principal borehole and exploratory shaft is shown in Figure 2-16. The principal borehole (RRL-2), at the location designated in this figure, has been cored to a depth of 1,211 meters (3,973 feet).

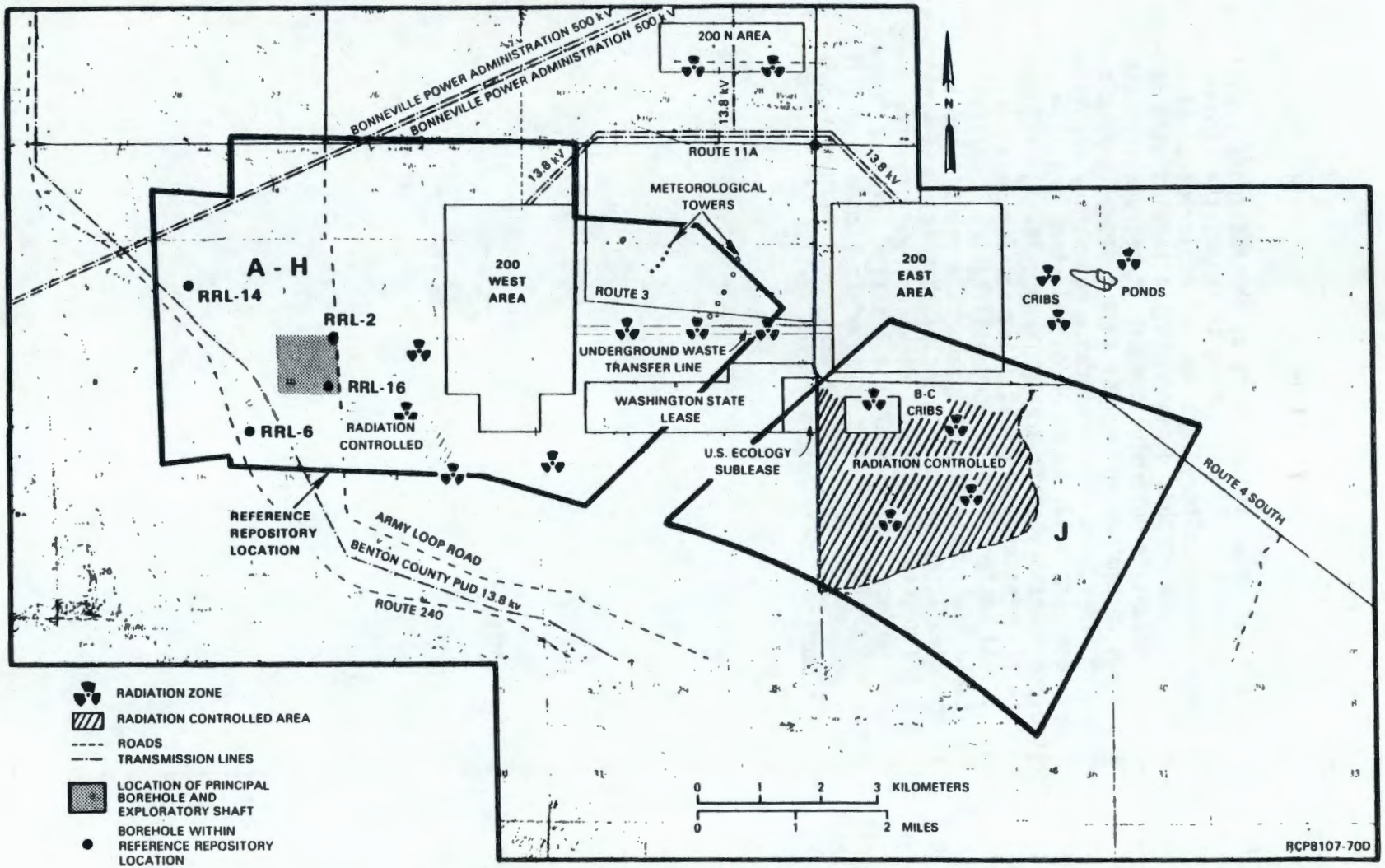

FIGURE 2-16. Reference Repository Location, Site A-H, and Alternate Site J.

2.7 IDENTIFICATION OF CANDIDATE REPOSITORY HORIZONS

During the feasibility phase of the BWIP, geotechnical and engineering studies focused on the Umtanum flow as the most promising repository horizon (Myers/Price et al., 1979; Gephart et al., 1979; Smith et al., 1979; Myers and Price, 1981). This focus was based on a progressive accumulation and analysis of technical data starting as early as 1968.

Preliminary investigations into the possibility of using the Hanford Site as a nuclear waste repository site started in 1968 with reentry of an abandoned 3,250-meter (10,660-foot) deep exploration well, Rattlesnake Hills Well No. 1, located near the southwest corner of the Hanford Site. As a result of this investigation, Raymond and Tillson (1968) identified four potential repository horizons, which were interpreted on the basis of geophysical logs to be relatively thick, unfractured basalt flows. One of these zones, located at a depth of approximately 830 meters (2,722.4 feet), was later termed the Umtanum flow (ARHCO, 1976). Another of the zones, located at a depth of approximately 650 meters (2,132 feet), was later termed the middle Sentinel Bluffs flow.

In 1969, waste isolation studies continued with the drilling of borehole DC-1 within the central Hanford Site. Evaluation of geophysical data from this borehole resulted in the identification of 10 horizons that might serve as repository host flows (Isaacson, 1969). One of these horizons was considered to have the most promising characteristics; i.e., high density, low porosity and permeability, adequate thickness and surface (Isaacson and Tomlinson, 1969a; 1969b). The name "Umtanum" was given to this "most promising" borehole DC-1 interval. Another promising flow identified in this evaluation, with similar characteristics to the Umtanum, was the middle Sentinel Bluffs flow. Studies beginning in 1976 continued to show that the Umtanum flow exhibited promising repository host rock characteristics--thick, dense interior, lateral continuity, low porosity and hydraulic conductivity, low structural dip, and favorable waste-rock interaction potential (Myers/Price et al., 1979; Gephart et al., 1979; Smith et al., 1980).

With the continued recognition that the Umtanum flow appeared to optimize both thickness and depth (i.e., provide the greatest degree of radionuclide isolation at an achievable mining depth), the site identification study described in Sections 2.1 through 2.5 utilized the Umtanum flow as the reference horizon. Because of the heavy weighting of the "lineament" and "thickness" criteria (Table 2-12), the substitution of a thick Grande Ronde Basalt flow other than the Umtanum as the reference horizon (e.g., the middle Sentinel Bluffs flow) would not be expected to alter the results of the previously discussed site identification study.

Over the past year as the BWIP has moved toward construction of an exploratory shaft, it has become increasingly apparent that the actual identification of the horizon or flow in which shaft breakout (or repository construction) would occur should be subject to more rigorous analysis similar to the decision analysis technique utilized to identify the

reference repository location. For example, as the repository conceptual design progressed, the economic and engineering advantages of decreasing the depth of the repository became more apparent. In addition, the data obtained from the principal borehole (RRL-2) showed that the Umtanum flow-top thickness was significantly more variable than previously observed in other boreholes.

Steps have been taken to assemble the data matric needed to complete this decision analysis. Preliminary screening, based primarily on flow thickness, groundwater, and radionuclide travel times, continues to identify two Grande Ronde Basalt flows, the Umtanum and middle Sentinel Bluffs, as candidate repository horizons. Identification of the preferred candidate repository horizon will be based on a detailed comparison of these two flows. In order for the identification process to be optimized, the data matrix will include comparable data sets on characteristics significant to construction and performance for both candidate repository horizons. As part of this work, data obtained from the principal borehole and three additional boreholes, RRL-6, RRL-14, and RRL-16 (Fig. 2-16), will be input into the data matrix. Also the quantity of the data available for the middle Sentinel Bluffs flow will be brought up to an equivalent level as that for the Umtanum flow. The lack of middle Sentinel Bluffs flow data is due to the previous focus on only the Umtanum flow. Completion of the decision analysis and identification of the candidate repository horizon for exploratory shaft breakout is currently scheduled for May 1983. The results of this study will be reported in future reports.

1 2 1 2 4 9 5 0 6 3 3

2.8 REFERENCES

ARHCO, 1976, Preliminary Feasibility Study on Storage of Radioactive Wastes in Columbia River Basalts, ARH-ST-137, Atlantic Richfield Hanford Company, Richland, Washington.

BWIP, 1980, Identification of Candidate Sites Suitable for a Geologic Repository in Basalt Within Hanford, RHO-BWI-LD-24, Rockwell Hanford Operations, Richland, Washington, February 1980.

BWIP, 1981, Comparison of NWTS-33(2) Criteria and Basalt Waste Isolation Project Screening Considerations, RHO-BW-EV-1 P, Rockwell Hanford Operations, Richland, Washington, August 1981.

DOE, 1982, Public Draft National Plan for Siting High-Level Radioactive Waste Repositories and Environmental Assessment, DOE/NWTS-4, DOE/EA-151, National Waste Terminal Storage Program, U.S. Department of Energy, Washington, D.C., February 1982.

Gephart, R. E., Arnett, R. C., Baca, R. G., Leonhart, L. S., and Spane, F. A., Jr., 1979, Hydrologic Studies Within the Columbia Plateau, Washington: An Integration of Current Knowledge, RHO-BWI-ST-5, Rockwell Hanford Operations, Richland, Washington, October 1979.

Isaacson, R. E., 1969, Hanford Exploratory Deep Well, ARH-SA-47, Atlantic Richfield Hanford Company, Richland, Washington.

Isaacson, R. E. and Tomlinson, R. E., 1969a, Atlantic Richfield Hanford Company Semiannual Report, Research and Development, November 1, 1968 through April 30, 1969, ARH-1299, Atlantic Richfield Hanford Company, Richland, Washington.

Isaacson, R. E. and Tomlinson, R. E., 1969b, Atlantic Richfield Hanford Company Semiannual Report, Research and Development, May 1, 1969 through October 31, 1969, ARH-1515, Atlantic Richfield Hanford Company, Richland, Washington.

Myers, C. W./Price, S. M., and Caggiano, J. A., Cochran, M. P., Czimer, W. J., Davidson, N. J., Edwards, R. C., Fecht, K. R., Holmes, G. E., Jones, M. G., Kunk, J. R., Landon, R. D., Ledgerwood, R. K., Lillie, J. T., Long, P. E., Mitchell, T. H., Price, E. H., Reidel, S. P., and Tallman, A. M., 1979, Geologic Studies of the Columbia Plateau: A Status Report, RHO-BWI-ST-4, Rockwell Hanford Operations, Richland, Washington, October 1979.

Myers, C. W. and Price, S. M., eds., 1981, Subsurface Geology of the Cold Creek Syncline, RHO-BWI-ST-14, Rockwell Hanford Operations, Richland, Washington, July 1981.

NRC, 1981a, Disposal of High-Level Radioactive Wastes in Geologic Repositories: Licensing Procedures, Title 10, Chapter 1, Code of Federal Regulations-Energy, Part 60, U.S. Nuclear Regulatory Commission, Washington, D.C., February 25, 1981.

NRC, 1981b, "Nuclear Regulatory Commission, 10 CFR 60, Disposal of High-Level Radioactive Wastes in Geologic Repositories," Federal Register, Vol. 46, No. 130, July 8, 1981, Proposed Rules.

NWTS, 1981, NWTS Program Criteria for Mined Geologic Disposal of Nuclear Waste, Site Performance Criteria, NWTS-33(2), National Waste Terminal Storage Program, U.S. Department of Energy, Washington, D.C.

Presidential Message to Congress, 1980, "Comprehensive Radioactive Waste Management Program," Weekly Compilation of Presidential Documents, Vol. 16, No. 71, Washington, D.C.

Raymond, J. R. and Tillson, D. D., 1968, Evaluation of a Thick Basalt Sequence in South-Central Washington, Geophysical and Hydrological Exploration of the Rattlesnake Hills Deep Stratigraphic Test Well, BNWL-776, Battelle, Pacific Northwest Laboratories, Richland, Washington.

Smith, M. J., Anttonen, G. J., Barney, G. S., Coons, W. E., Hodges, F. N., Johnston, R. G., Kaser, J. D., Manabe, R. M., McCarel, S. C., Moore, E. L., Noonan, A. F., O'Rourke, J. E., Schulz, W. W., Taylor, C. L., Wood, B. J., and Wood, M. I., 1980, Engineered Barrier Development for a Nuclear Waste Repository Located in Basalt: An Integration of Current Knowledge, RHO-BWI-ST-7, Rockwell Hanford Operations, Richland, Washington, May 1980.

WCC, 1980, Site Locality Identification Study: Hanford Site, Vol. I: Methodology, Guidelines, and Screening; Vol. II: Data Cataloging, RHO-BWI-C-62, Woodward-Clyde Consultants for Rockwell Hanford Operations, Richland, Washington, July 1980.

WCC, 1981, Study to Identify a Reference Repository Location for a Nuclear Waste Repository on the Hanford Site, Vol. I: Text; Vol. II: Appendixes, RHO-BWI-C-107, Woodward-Clyde Consultants for Rockwell Hanford Operations, Richland, Washington, May 1981.

1 2 1 2 4 9 5 0 6 3 5

CHAPTER 3

THIS PAGE INTENTIONALLY
LEFT BLANK

3. GEOLOGIC DESCRIPTION OF THE REFERENCE REPOSITORY LOCATION AND THE SURROUNDING AREA

3.1 INTRODUCTION

The Basalt Waste Isolation Project (BWIP) geologic studies to date have provided geologic information necessary to identify areas beneath the Hanford Site that have a high probability of containing bedrock suitable for a nuclear waste repository. Geologic activities thus far completed include reconnaissance studies throughout much of the area covered by the Columbia River Basalt Group, herein referred to as the Columbia Plateau, and detailed investigations in the vicinity of the Hanford Site (Fig. 3-1). These investigations have emphasized the stratigraphy, lithology, structure, and tectonic setting of the study area relating not only to geologic considerations for repository site identification, but also to site characterization.

Geologic studies have shown that the central Hanford Site contains laterally continuous basalt flows with thick dense interiors (Myers/Price et al., 1979). Furthermore, within the Cold Creek syncline (Fig. 3-1), these flows appear to be nearly flat-lying across areas in excess of tens of square kilometers and located within an area of likely tectonic stability (Myers and Price, 1981). As pointed out in the previous chapter, two such flows, the Umtanum and the middle Sentinel Bluffs, are the leading host-rock candidates within the reference repository location (Fig. 3-1). Both flows are interpreted to have sufficiently thick dense interior to meet design and isolation requirements.

The Cold Creek syncline is a subdivision of the Pasco Basin, one of several structural and topographic basins within the western Columbia Plateau. The basin is underlain primarily by a Miocene volcanic sequence, the Columbia River Basalt Group (Fig. 3-2). Lava flows of this group were erupted from a linear vent system, remnants of which are exposed as dikes primarily in the eastern and southeastern portions of the plateau. Because of their high fluidity and large volume, the lavas spread considerable distances from their source fissures. In so doing, they covered vast areas, inundated older rocks and structures within the plateau interior, and onlapped highlands around the plateau margin. Flows of the Columbia Plateau are interbedded with and overlain by sediments. Within the Pasco Basin, the upper basalt sequence is interbedded with clastic sediments of the Ellensburg Formation and overlain by the fluvial-lacustrine Ringold Formation and catastrophic flood deposits of the Hanford formation (Fig. 3-2). Much of the discussion contained in this chapter is a condensation of data contained in two documents, Myers/Price et al. (1979) and Myers and Price (1981).

8 9 0 6 5 0 9 4 2 1

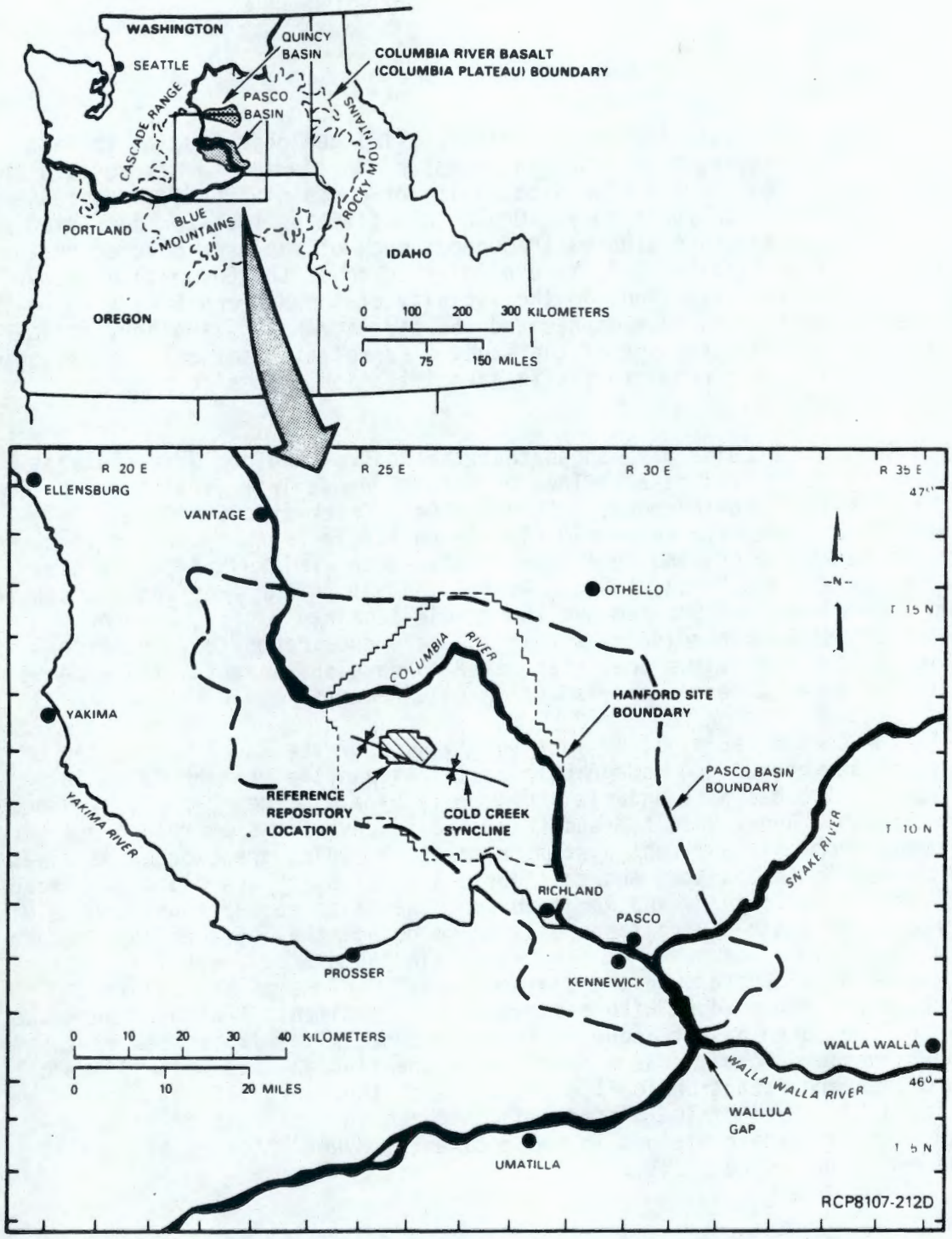

FIGURE 3-1. Location of the Columbia Plateau, Hanford Site, Cold Creek Syncline, and Reference Repository Location.

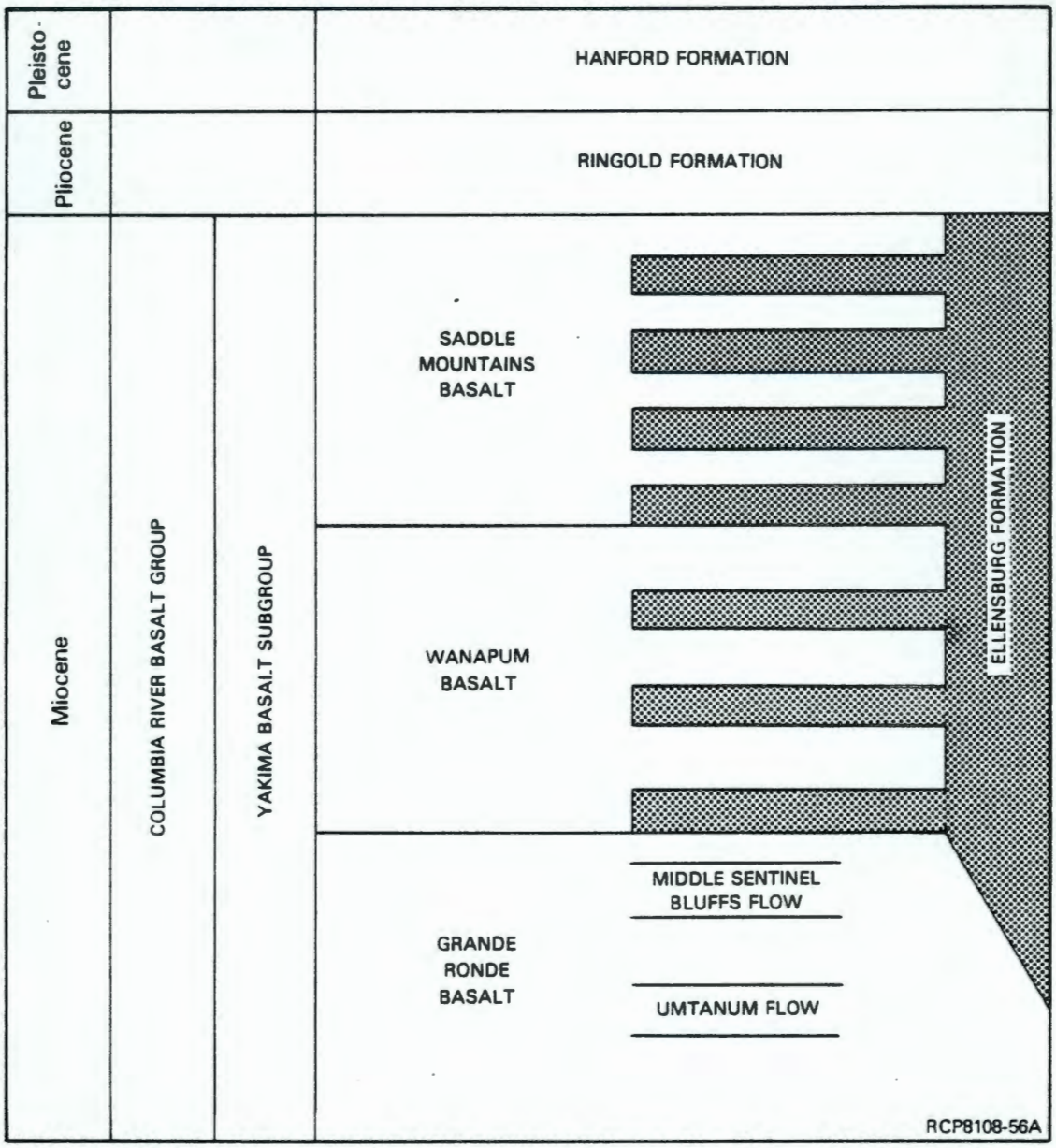

FIGURE 3-2. Stratigraphy of the Columbia River Basalt Group, Yakima Basalt Subgroup, and Intercalated and Suprabasalt Sediments Within the Pasco Basin.

THIS PAGE INTENTIONALLY
LEFT BLANK

3.2 SITE PENETRATIONS

The primary subsurface penetrations of basalt within the Hanford Site are boreholes and the Near-Surface Test Facility (see Chapter 4). Publications that document the approximately 2,200 boreholes drilled prior to and after the establishment of the Hanford Site include those by Jenkins (1922), Walters and Grolier (1960), Newcomb et al. (1972), McGhan and Damschen (1979), and Fecht and Lillie (1981). Drillers logs are summarized in Fecht and Lillie (1981). Boreholes included in these references are divisible on the basis of general purpose into five broad categories: (1) water supply, (2) gas exploration and production, (3) surveillance, (4) nuclear power plant siting, and (5) repository feasibility and siting. Pertinent boreholes in the first four categories are summarized in Table 3-1 and located, along with category (5) wells, in Figure 3-3. The fifth category is discussed below.

3.2.1 Repository Feasibility and Siting Boreholes

Information regarding the boreholes drilled and/or used to assess the feasibility of constructing a nuclear waste repository in basalt at Hanford is summarized in Figure 3-4 and in Moak (1981b, Table A-2).

The first boreholes to assess the feasibility of a nuclear waste repository in basalt were drilled between 1969 and 1973. Data from five core holes (DDH-1, -3, DH-2, -4, and -5) and one rotary borehole (DC-1) (Fig. 3-3 and 3-4) were used to establish a stratigraphic framework for the basalt underlying the Hanford Site and to identify potential repository host-rock horizons (Myers, 1973; Myers and Brown, 1973; ARHCO, 1976). "Deep" core and rotary boreholes (approximately 550 to 800 meters) that penetrate the Grande Ronde Basalt within the Hanford Site area include the initial deep boreholes mentioned above in addition to deep core holes drilled since 1977 (DC-2, -4, -6, -8, -12, -14, and -15) (Fig. 3-3). Boreholes DC-5 and -7 are companion rotary boreholes drilled within 33 meters of DC-4 and -8, respectively. One additional rotary borehole (DC-3) penetrated into the Umtanum. All are vertical boreholes, with the exception of two slant core holes (DC-2A1 and -2A2), which were drilled from DC-2 through the Umtanum flow at an angle of 25° from vertical. Only DC-2A2 is now accessible, as DC-2 and -2A1 were successively filled with cement to facilitate slant-hole drilling.

Twenty-two DH-series core holes (Fig. 3-4) were drilled to define the stratigraphy of the Ringold Formation. The results of analyses of samples from this suprabasalt sedimentary sequence are discussed in Tallman et al. (1981) and summarized in Section 3.5.

TABLE 3-1. Summary and Description of Hanford Site Boreholes.

Borehole category	Description
Water supply	Includes approximately 200 water-supply wells that were hand dug into suprabasalt sediments along the Columbia River by turn-of-the-century homesteaders. Earliest recorded boreholes into basalt include approximately 7 water-supply wells drilled between 1918 and 1927, all to depths of less than 300 meters. The borehole nearest to the reference repository location is the Haynes stock well, a 295-meter-deep well located approximately 6.5 kilometers to the north-east. Water supply wells constructed after the establishment of the Hanford Site include those constructed primarily to provide water for outlying installations.
Gas exploration and production	Includes wells drilled into basalt between 1917 and 1931 in a small gasfield located on the northern limb of Rattlesnake Mountain, approximately 10 kilometers south of the reference repository location. A discussion of this gasfield and the 26 associated boreholes is presented by Hammer (1934) and McFarland (1979). Only seven of the boreholes were drilled deeper than 300 meters, the deepest being WW-6 (Fig. 3-3), which originally penetrated to a depth of 1,116 meters. The original driller's log and geologic cross sections and interpretations (Hammer, 1934) indicate that WW-6 penetrated the Grande Ronde Basalt and probably the Umtanum flow. The nearest of the Rattlesnake gasfield boreholes to the site is the 610-meter-deep Benson Ranch well, located 2.5 kilometers to the south (Fig. 3-3). The only gas exploration well drilled since 1942 is Rattlesnake Hills Well No. 1 (RSH-1), located approximately 13 kilometers southwest of the reference repository location near the crest of Rattlesnake Mountain (Fig. 3-3). The well was drilled between 1956 and 1957 to a depth of 3,250 meters (Raymond and Tillson, 1968) into lower Grande Ronde Basalt flows (Reidel et al., 1981). The hole was terminated approximately 2,400 meters below the Umtanum flow.
Surveillance	Includes approximately 2,000 boreholes drilled in conjunction with the production and reprocessing of nuclear materials at Hanford. These primarily include dry wells to characterize and monitor waste-disposal facilities and deeper boreholes to monitor potential groundwater contamination. These boreholes generally terminate within sediments overlying basalt and more than half are located within the 200 East and 200 West Areas of the Hanford Site (Fig. 3-3). Also includes 15 boreholes drilled since 1973 for the purpose of characterization and surveillance of confined aquifers in the Saddle Mountains Basalt. These core holes, prefaced by DB (Fig. 3-3), average 300 meters in depth and generally penetrate into or through the Mabton interbed (located at the Saddle Mountains-Wanapum Basalt contact).
Nuclear-power-plant siting	Includes boreholes that have been drilled to support the siting and construction of nuclear power plants on the Hanford Site. These include the 100 core and rotary boreholes drilled since 1968 by WPPSS (1981) and an additional 175 boreholes drilled by Northwest Energy Services Company (PSPL, 1982). Of these boreholes, only 42 penetrate the uppermost confined aquifer system, the Rattlesnake Ridge interbed.

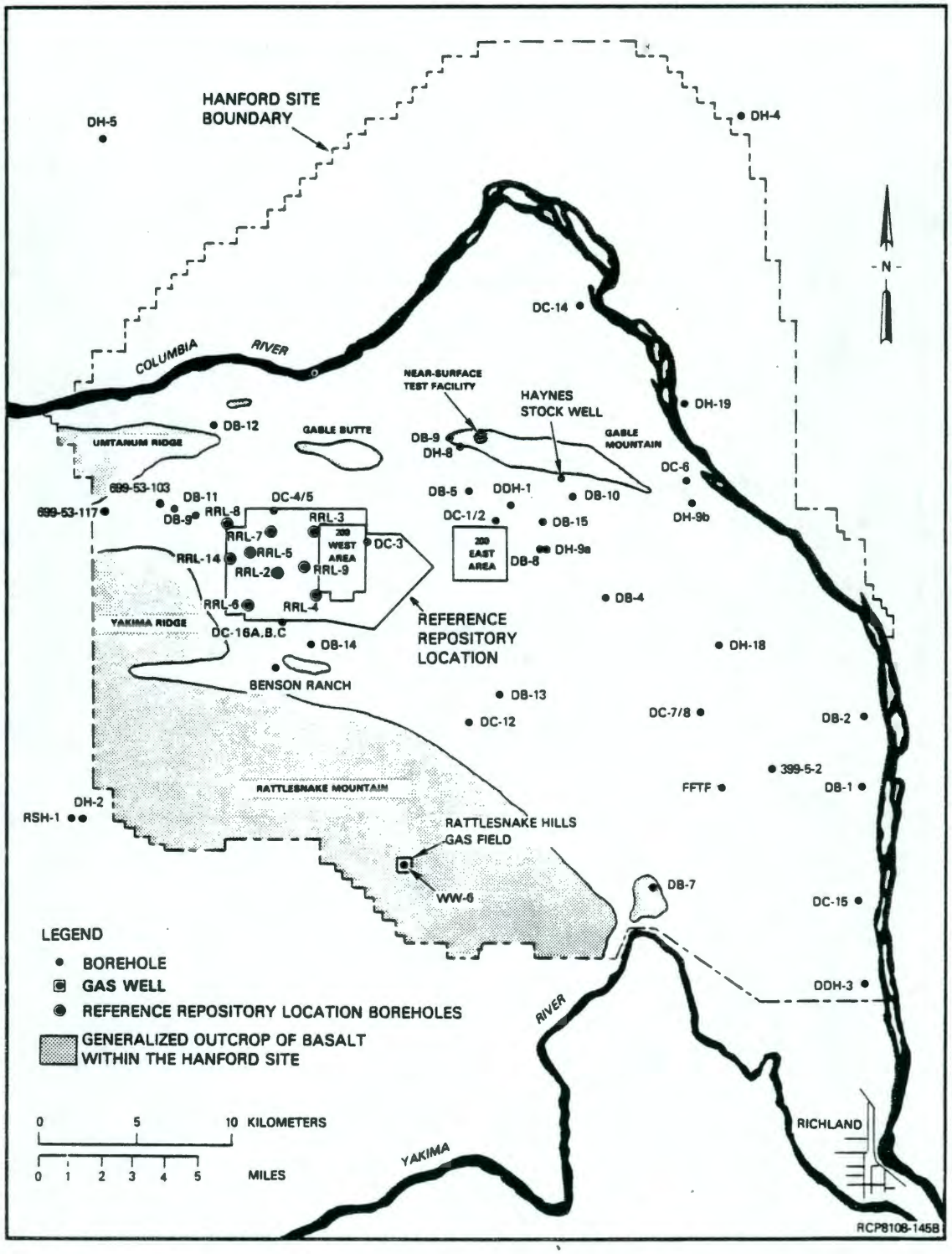

FIGURE 3-3. Location Map for Key Boreholes Used in Basalt Waste Isolation Project Studies.

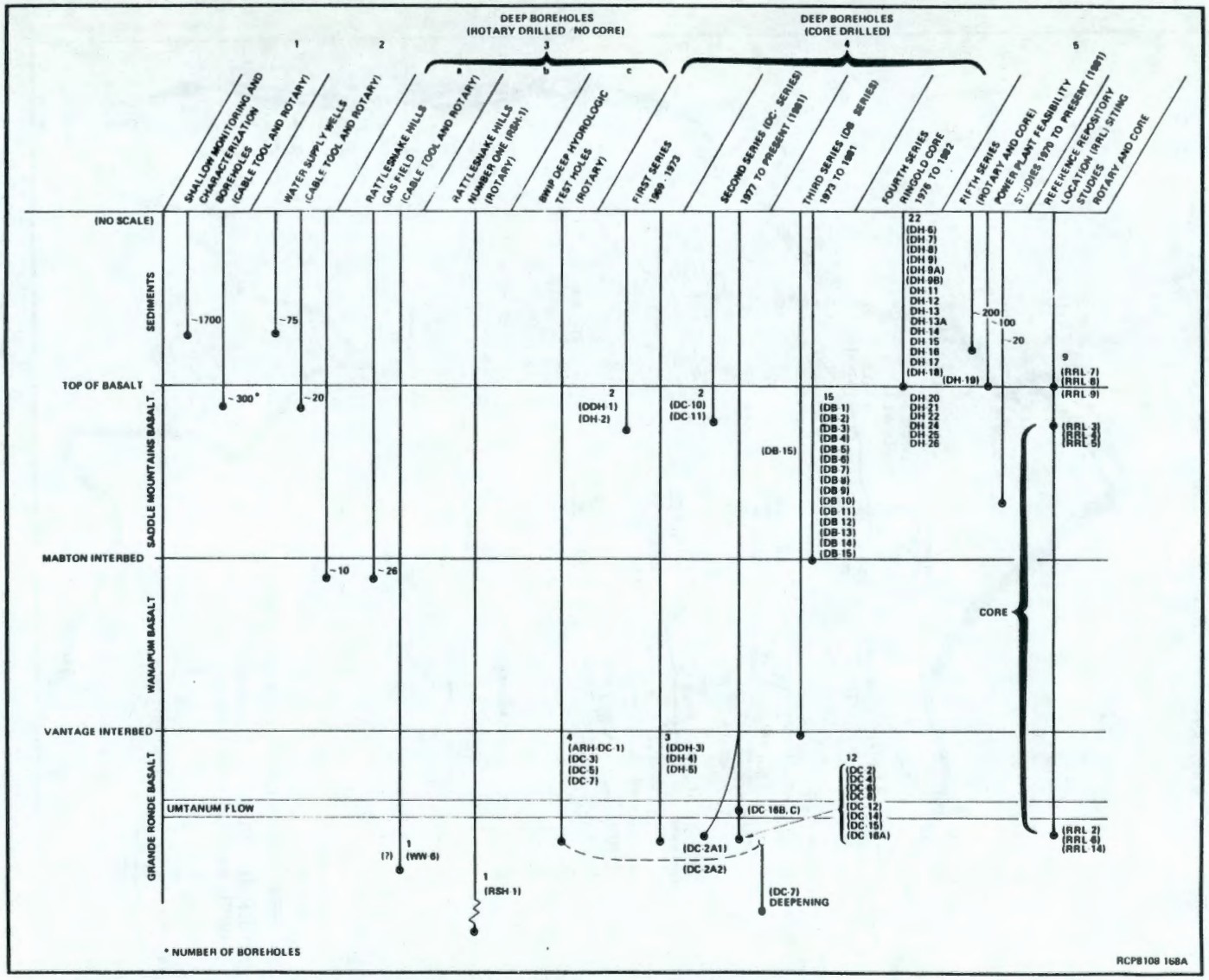

FIGURE 3-4. Stratigraphic Levels Penetrated by Boreholes on the Hanford Site and Vicinity. Locations of boreholes in parentheses are shown in Figure 3-3; DH-20, -21, -22, -24, -25, and -26 are shown in Figure 3-3.

3.2.2 Site Boreholes

The locations of the 38 boreholes within the reference repository location (or within several hundred meters of its boundaries) that penetrate basalt are shown in Figure 3-5; also shown in this figure is the configuration of the repository conceptual design, centered about a reference shaft-pillar area. Only 12 of the 38 boreholes penetrate the upper confined aquifer systems (interbedded sediments) of the Saddle Mountains Basalt. Other boreholes terminate within the suprabasalt sediments and are primarily located within the 200 West Area of the Hanford Site. Although five boreholes (699-29-78, -32-72, -34-88, -38-65, and -44-64 in Fig. 3-5) have been partially plugged with cement to permit installation of sample pumps, no borehole is abandoned or has been plugged back to the surface.

Nine boreholes within the candidate site (RRL-2, -3, -4, -5, -6, -7, -8, -9, and -14) were designed and constructed solely to obtain geologic and geophysical data to support identification of an exploratory shaft site. These six boreholes penetrate into or through the Saddle Mountains Basalt. Borehole RRL-2, -6, -14, and DC-16A penetrate through the Umtanum flow and DC-16B and -16C penetrate into the Umtanum flow.

3.2.3 Status

No subsurface penetrations of consequence, other than boreholes, exist within the Hanford Site. The locations and status of these boreholes are well-documented. Of the 38 boreholes located within the reference repository location, only 12 boreholes penetrate the uppermost confined aquifer (Rattlesnake Ridge interbed). Of these boreholes, three (RRL-3, -4, and -5) penetrate into or just through the uppermost confined aquifer, two (DC-16B and -16C) penetrate into the Umtanum flow, and seven (RRL-2, -6, -14, DC-3, -4, -5, and -16A) penetrate through the Umtanum flow. Borehole RRL-2 is the principal borehole used in siting the exploratory shaft.

1 2 1 2 4 9 5 0 6 4 6

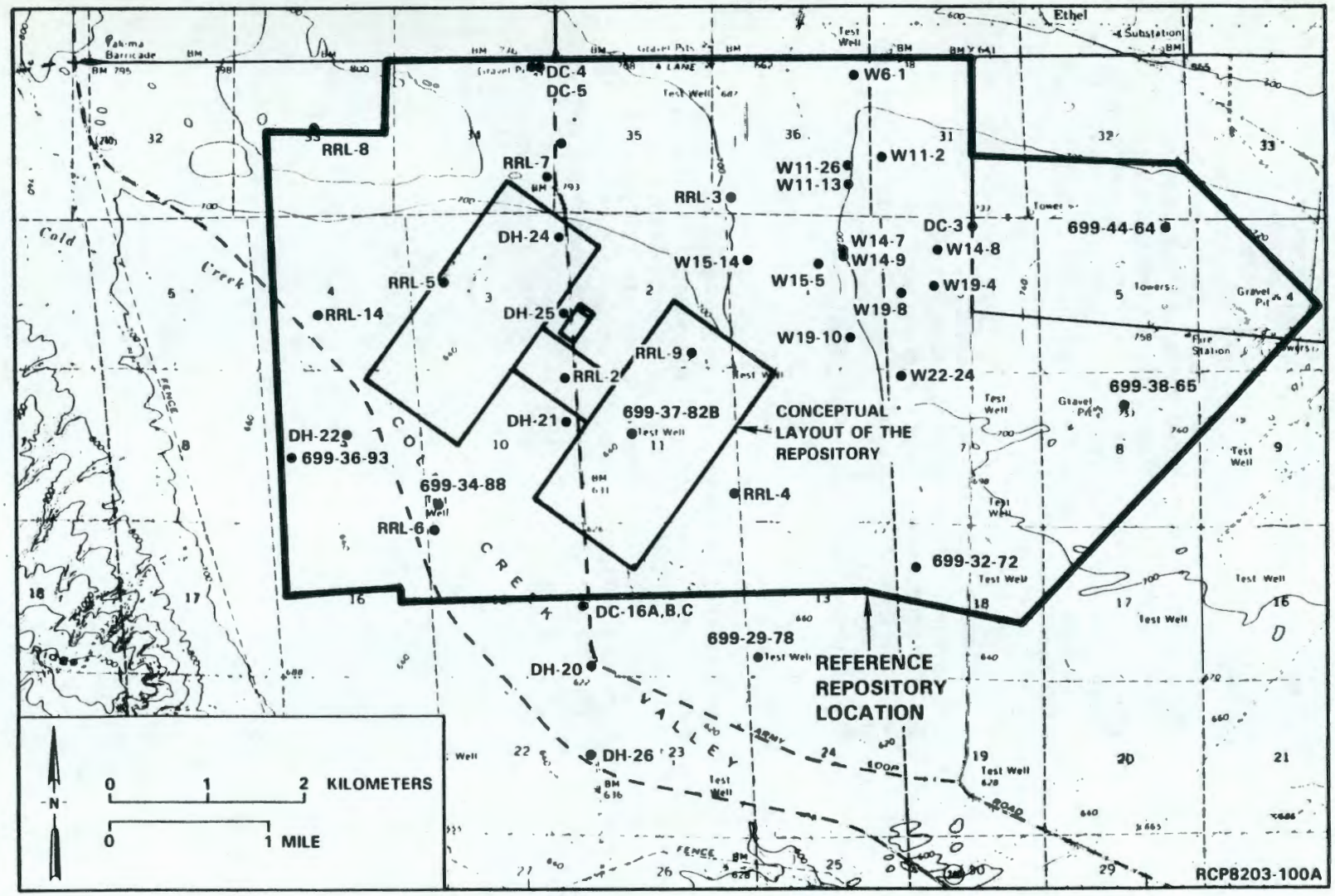

FIGURE 3-5. Borehole Location Map, Reference Repository Location.

3.3 PHYSIOGRAPHY AND TOPOGRAPHY

The physiographic provinces of the Pacific Northwest are shown in Figure 3-6 (Freeman et al., 1945). The regional physiography is characterized by north-south-trending mountain ranges separated by elongate lowlands. Between the Cascade and Rocky Mountains provinces lies the Columbia Intermontane province, which contains several physiographically diverse subprovinces, including the area defined as the Columbia Plateau (Section 3.1). The Columbia Intermontane province is subdivided into the following four subprovinces (Fig. 3-7): (1) Columbia Basin, (2) Central Highlands, (3) High Lava Plains, and (4) Owyhee Upland. The Columbia Basin and Central Highlands subprovinces contain thick sequences of Columbia River basalt. The reference repository location is located in the Columbia Basin subprovince.

The Columbia Basin subprovince of the Columbia Intermontane province is divided into six sections on the basis of general morphology: (1) Central Plains, (2) Yakima Folds, (3) Waterville Plateau, (4) Channeled Scablands, (5) Palouse Hills, and (6) North Central Oregon Plateau (Fig. 3-7). A general discussion of landforms and currently active geomorphic processes, with the exception of the North Central Oregon plateau, is contained in Myers/Price et al. (1979).

The reference repository location is located in the western part of the Pasco Basin, which occupies the south-western part of the Central Plains section of the Columbia Basin subprovince of the Columbia Intermontane physiographic province (Fig. 3-7). The Pasco Basin is divided into three major landform systems or areas of recurring landforms, processes, and effects. These are the ridge, lower slope, and basin and valley terrains (Fig. 3-8). The ridge terrain consists of prominent anticlinal basalt ridges and is located in the Yakima Folds section of the Columbia Basin subprovince. The lower slope terrain consists primarily of middle and lower slopes of anticlinal basaltic ridges of the Yakima Folds section, but also includes minor portions of the bounding Central Plains section. The basin and valley terrain, including the reference repository location, consists of the low sediment-filled portion of the Pasco Basin in the Central Plains section and the synclinal valleys of the Yakima Folds section. A more detailed description of these three landform systems is given in Myers/Price et al. (1979); geomorphic processes specific to the site are given in Section 3.4 of this report.

8 4 0 6 5 9 4 2 1

FIGURE 3-6. Physiographic Provinces of the Pacific Northwest.

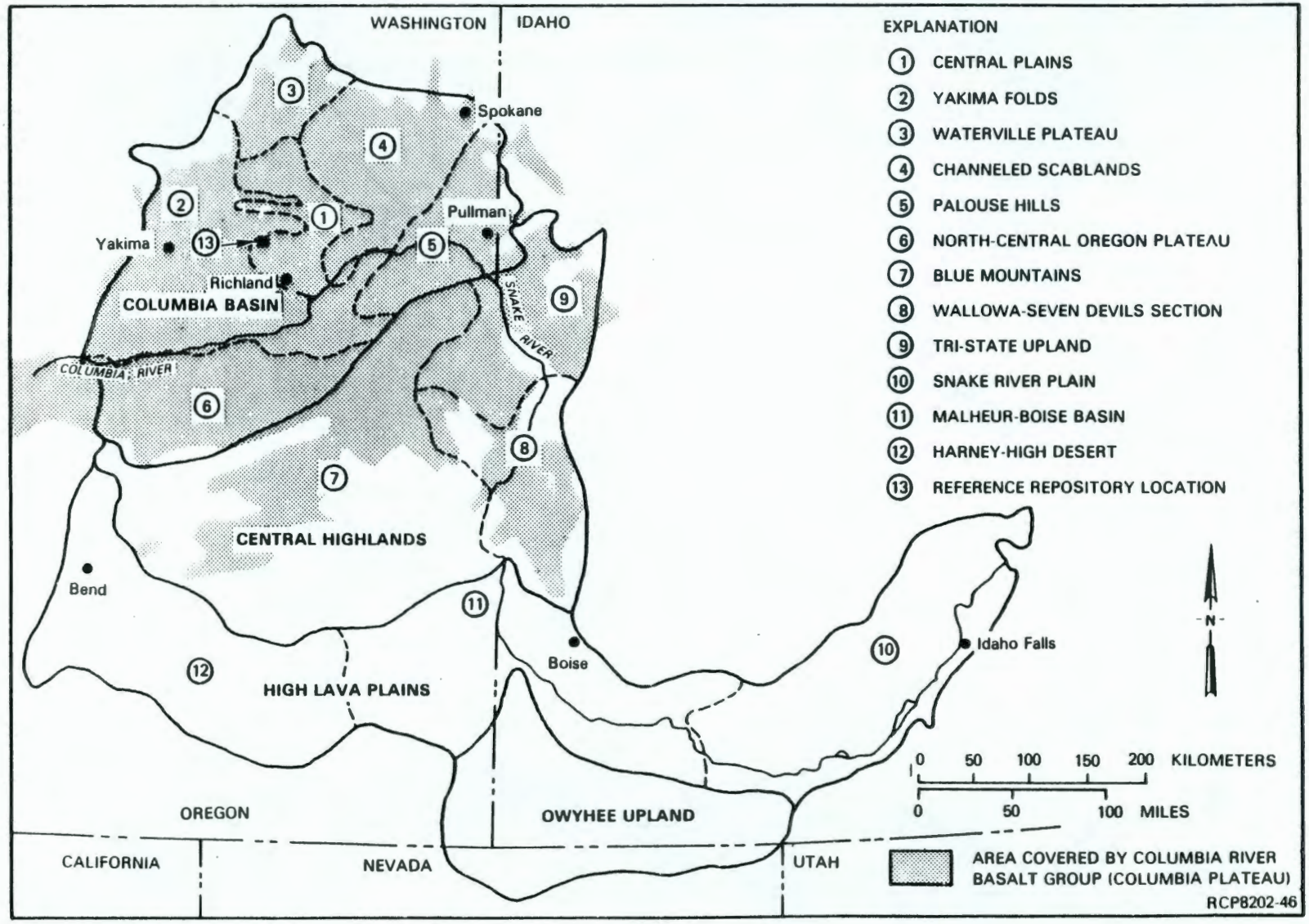

FIGURE 3-7. Divisions of the Columbia Intermontane Province (after Freeman et al., 1945).

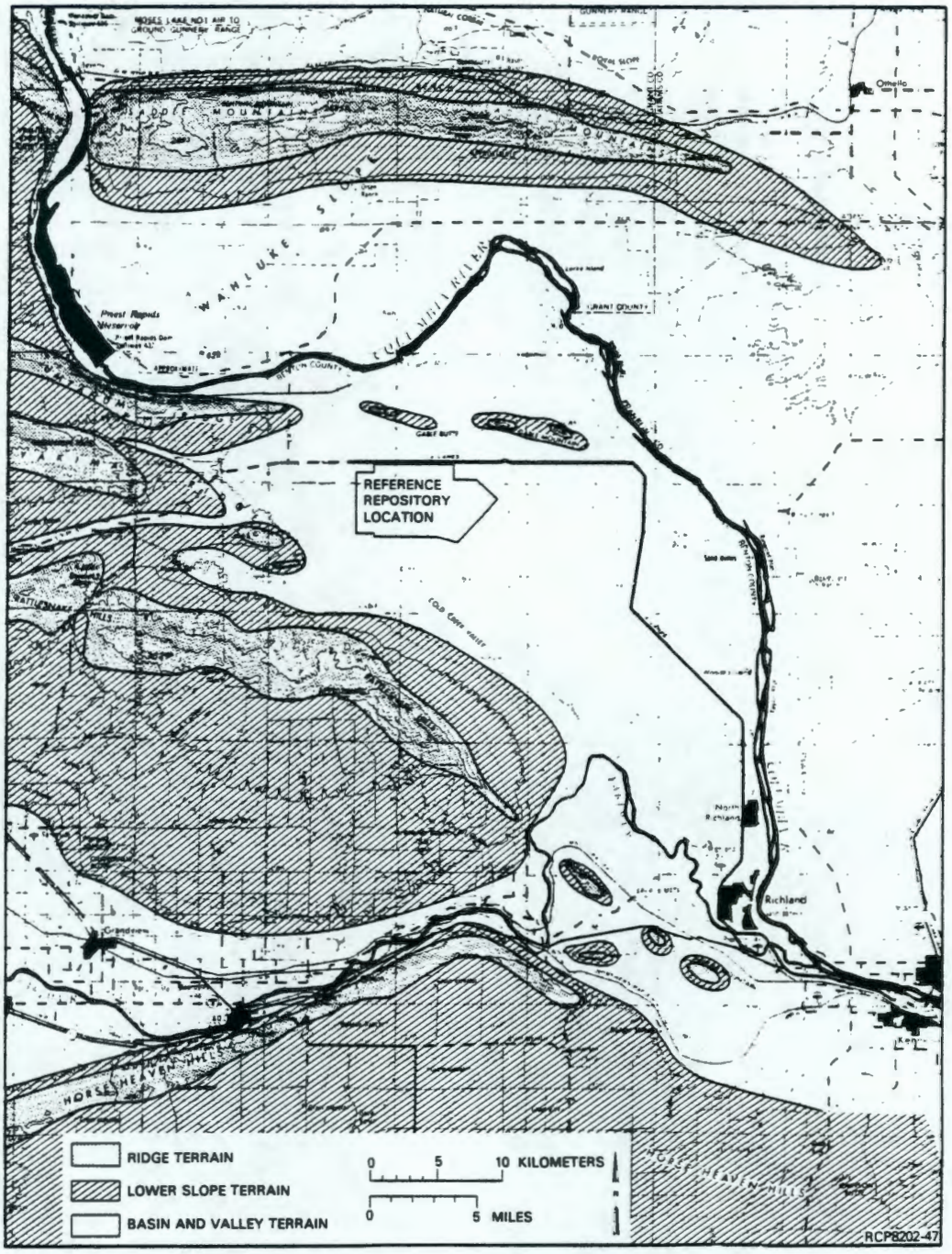

FIGURE 3-8. Map of Major Landform Systems, Pasco Basin.

3.4 GEOMORPHOLOGY

This section contains a discussion of landforms and general geomorphic processes, past and present, within the Pasco Basin. A detailed discussion of the effects of surficial geologic processes in the Pasco Basin is contained in WCC (1980c).

3.4.1 Application of Geomorphic Information to Site Identification

Geomorphology was used in site screening (see Chapter 2) within the Hanford Site by avoiding areas of mass wasting, high-velocity runoff, and major alluviation. High slope gradients were avoided because of additional costs of surface-engineered structures. Anticlinal ridges of the Yakima folds were avoided, based on structural geology, by adopting an 8-kilometer offset from fold hinge lines (Chapter 2). In avoiding the anticlinal ridges, the areas of large slope gradients and mass wasting were also avoided.

The geomorphic units, processes, and effects within the area of the Cold Creek syncline (Fig. 3-1) are essentially the same throughout the entire area and were not used as discriminators in the identification of the reference repository location. Within the syncline, only minor differences in slope are present (between 0.5 and 2 percent), the exception being the edge of catastrophic flood bars where slopes locally reach a maximum of 15 percent. Only minor ephemeral streams occur west of the reference repository location, where runoff, if any, generally infiltrates into the permeable sand and gravel.

3.4.2 Geomorphology of the Reference Repository Location

3.4.2.1 Geomorphic Units. The reference repository location is in the western part of the basin and valley terrain (Section 3.3) and is divided into four geomorphic units: (1) Umtanum Ridge bar, (2) 200 Areas bar, (3) central Hanford sand plain, and (4) Cold Creek alluvial plain (Fig. 3-9). These geomorphic units, with the exception of the Cold Creek alluvial plain, have remained virtually unchanged since deposition in the late Pleistocene.

The southeast-extending Umtanum Ridge bar covers about 6 square kilometers and is the highest feature in the reference repository location. It is a late Pleistocene eddy bar built by catastrophic floodwaters behind the east end of Umtanum Ridge on the north slope of Cold Creek Valley. The bar is relatively flat and streamlined in shape. The steep (15 percent) south slope of the bar is in the northernmost part of the reference repository location. The relief on the bar within the reference repository location is about 30 meters and the bar varies in elevation from about 215 meters at the base of the south slope to about 245 meters at the crest of the bar. The bar is composed of cobble gravel in a sand matrix.

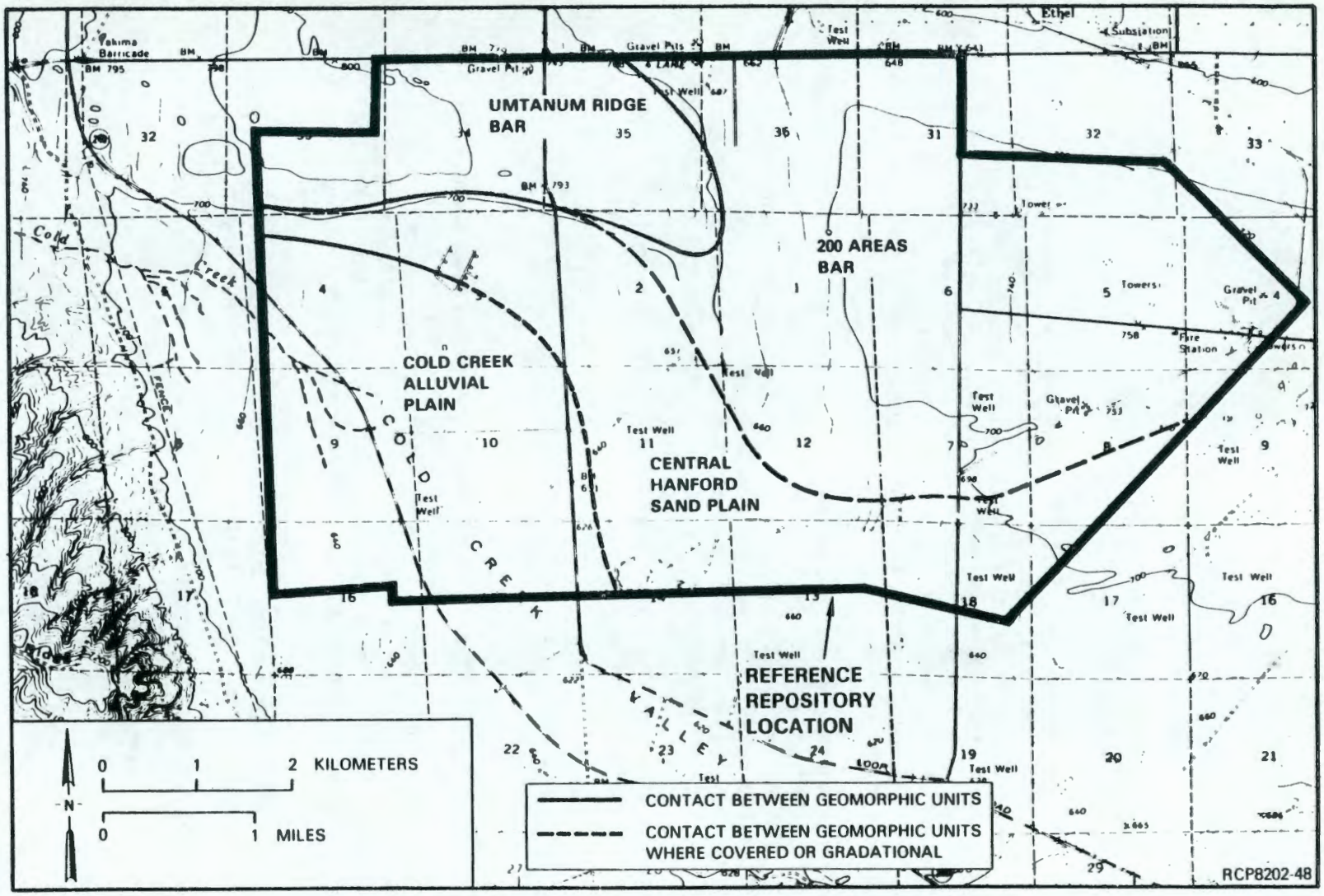

FIGURE 3-9. Geomorphic Map, Reference Repository Location.

The 200 Areas bar is the continuation of the Umtanum Ridge bar, trending southeast. This bar is the most extensive geomorphic unit in the reference repository location, covering about 20 square kilometers. The 200 Areas bar is an expansion bar formed as the result of decelerating flow of catastrophic floodwaters in the expanded reach south of the Umtanum Ridge-Gable Mountain structure. The general form of the bar is very broad and relatively flat, but is not streamlined like the Umtanum Ridge bar. The maximum elevation of the bar is about 230 meters and the lowest elevation in the reference repository location is about 200 meters along the north slope of the bar. The bar is composed of coarse sand and gravel in the north and east parts of the reference repository location and grades to silty medium-to-coarse sand at the southwestern limit of the bar. Modification of the bar by Holocene geomorphic processes are minor and mainly from wind action.

The central Hanford sand plain is located south of the flood bars in the southern part of the reference repository location. This plain was formed during Pleistocene flooding, when fine-grained sediments were deposited on the lee of the Umtanum Ridge bar. The sand plain, which covers about 15 square kilometers of the reference repository location, is relatively flat, sloping gently into the Cold Creek Valley. The elevation of the sand plain ranges from about 215 meters on the northern boundary of the plain to about 190 meters near the southern boundary of the reference repository location. The central Hanford sand plain is composed mainly of silty coarse-to-fine sand with a slight fining in grain size to the west and southwest. Winds have modified the plain, forming sand sheets in the west that change to longitudinal dunes in the east. These sheets and dunes are now largely stabilized.

The Cold Creek alluvial plain forms the western part of the reference repository location and covers about 13 square kilometers. It was deposited by intermittent Holocene streams flowing from the lower slope and ridge terrain of the upper Cold Creek Valley. The alluvial plain is superimposed on the western portion of the late-Pleistocene central Hanford sand plain. Sloping slightly to the southeast down Cold Creek Valley, the alluvial plain ranges in elevation from about 205 meters to the northwest to 190 meters to the southeast. The plain is composed of granules of fine sand and silt. The active portions of the alluvial plain are represented by dendritic patterns. Much of the inactive part of the alluvial plain has been slightly modified by winds that have formed a thin sand sheet.

3.4.2.2 Geomorphic Processes. A study of geomorphic processes relevant to waste isolation in an underground repository within the Pasco Basin was conducted by Woodward-Clyde Consultants (WCC, 1980c). The geomorphic process that is considered most relevant to waste isolation is the possible occurrence of large floods resulting from ice-dam failure in a future continental glaciation. The most recent major catastrophic flood is dated at about 13,000 years before present. During this event, water was impounded behind the underfit Wallula Gap (Fig. 3-1) to an elevation of approximately 365 meters, resulting in a lake 170 meters deep at the reference repository location.

9 2 1 2 4 9 5 0 6 5 4

The impact of such an event on the confined aquifer and groundwater flow paths is not known. The short duration (weeks) of such floods suggests that the impact on the recharge of confined aquifers would be minor. Such an event would be preceded by a very long period of ice buildup and advance in the northern latitudes and alpine regions.

The presence of alluvium (Fig. 3-9) indicates that Cold Creek has flooded to elevations above the surface of part of the reference repository location since the last major catastrophic flood (approximately 13,000 years before present). A discussion of the potential impact of surface flooding on the site is contained in Chapter 7.

3.4.2.3 Geomorphic Effects. From a waste isolation standpoint, the geomorphic effects of catastrophic flooding are considered to be negligible, as the net effect within the reference repository location would be sediment deposition. Relatively minor cut-and-fill sequences have been observed within and around the reference repository location, but none have incised more than several meters. Approximately 175 to 200 meters of sediments overlie the top of the basalt in the reference repository location. Less than 50 meters are flood deposits; the remainder is the Miocene-Pliocene Ringold Formation, which was not eroded during multiple Pleistocene catastrophic floods.

The main channels of Pleistocene floodwater are located north and east of the reference repository location (Tallman et al., 1979; Myers/Price et al., 1979). The topographic control on the position of these channels (basalt ridges) would remain the same for potential future floods; therefore, major incision within the reference repository location would not be likely.

3.4.2.4 Status. There are no geologic data that suggest potential incision of the candidate host rock in the reference repository location by either potential catastrophic flooding or stream runoff. The net effect of both processes is anticipated to be depositional.

In the Pasco Basin, the Columbia River system is about 120 meters above the present sea level, and in the reference repository location the candidate host rock is greater than 900 meters below present sea level. The thick sequence of rock below sea level and the synclinal position of the reference repository location within a larger basin essentially preclude the possibility of host-rock incision under the present tectonic regime (see Section 3.7).

3.5 STRATIGRAPHY AND LITHOLOGY

The Columbia Plateau is underlain by tholeiitic flood basalts of the Columbia River Basalt Group and intercalated sediments. The sediments that overlie the basalt flows are thickest in the numerous structural and topographic basins located throughout the plateau. Field mapping and lithologic studies have led to a detailed stratigraphic framework necessary to determine the structural setting of the region, to assess the tectonic stability of the reference repository location, and to evaluate the suitability of the potential host rock for a nuclear waste repository.

3.5.1 Regional Stratigraphic Framework

The region is defined as the outcrop extent of the Columbia River Basalt Group (see Fig. 3-1). The stratigraphy for the region was developed from regional reconnaissance mapping using standard field techniques. For the Columbia River Basalt Group, paleomagnetic properties and chemical compositions were used to verify the identification of map units and thus to place regional units within their proper stratigraphic framework (Myers/Price et al., 1979; Swanson et al., 1979c; 1980; 1981).

The principal rocks comprising the region are divided into four broad divisions: (1) "basement rock," (2) Columbia River Basalt Group, (3) intercalated and suprabasalt sediments, and (4) other late Cenozoic volcanic deposits.

3.5.1.1 Basement Rock. Rock older than the Columbia River Basalt Group is primarily exposed along the margin of the plateau and as isolated exposures in the basalt (Swanson et al., 1979b; 1980). No pre-basalt rock is exposed in the central portion of the Columbia Plateau. Along the western margin of the plateau, the basalt flows overlie an irregular, eroded, pre-Miocene or early Miocene surface composed of folded metasedimentary and volcanic rocks that have been intruded by later igneous rock. To the north, basalt is underlain by crystalline gneisses, plutonic complexes, and schists, which comprise a former surface of moderately low relief. Along the northeastern and eastern margins of the plateau, basalt rests upon an irregular surface of Precambrian metasedimentary rocks and Mesozoic intrusive rocks. In the southeastern part of the plateau, chiefly low-grade metasedimentary and metavolcanic rocks of Permian, Triassic, and Jurassic age occur. Along the southern margin, the basalt overlies Mesozoic and early Tertiary sediments and volcanics.

3.5.1.2 Columbia River Basalt Group. The tholeiitic Columbia River Basalt Group was extruded between about 16.5 and 6 million years before present. The basalt covers an area of about 200,000 square kilometers and has an estimated volume of 375,000 cubic kilometers (Reidel et al., 1981). Individual flows range from a few tens of centimeters (rarely) to more than 100 meters thick, averaging 30 to 40 meters (Swanson and Wright, 1978). Flows exhibit a characteristic jointing pattern, reflective of the solidification of lava upon cooling.

9 2 1 2 4 9 5 0 6 5 6

The Columbia River Basalt Group consists of 5 formations and 19 members (Swanson et al., 1979c; Camp, 1981) (Fig. 3-10). General characteristics, including petrographic, chemical, and paleomagnetic properties of each formation and most members, are contained in Myers/Price et al. (1979, Tables II-2 through II-6 and III-2), Swanson et al. (1979c), Myers and Price (1981), and Camp (1981).

3.5.1.2.1 Imnaha and Picture Gorge Basalt. The basal formation of the Columbia River Basalt Group is the Imnaha Basalt (Fig. 3-10) (Swanson et al., 1979c; Reidel, 1981). This formation comprises approximately 6 volume percent of the group and is not known to occur in the Pasco Basin. Exposures of this formation and known feeder dikes (Taubeneck, 1970; Kleck, 1976) are confined to northeastern Oregon, southeastern Washington, and adjacent Idaho (Myers/Price et al., 1979, Fig. II-5). This formation is generally coarse-grained and plagioclase-phyric, with phenocrysts ranging from 5 to 25 millimeters in length (Myers/Price et al., 1979, Table II-2).

The Picture Gorge Basalt is coeval with basal (R_1 and N_1) Grande Ronde Basalt flows (Fig. 3-10) (Swanson et al., 1979c), comprises approximately 5 volume percent of the Columbia River Basalt Group (Reidel et al., 1981), and is not known to occur in the Pasco Basin. The Picture Gorge Basalt and feeder dikes crop out only in north-central Oregon (Waters, 1961; Fruchter and Baldwin, 1975). The flows of the Picture Gorge Basalt are both plagioclase-phyric and aphyric and generally medium- to coarse-grained (Myers/Price et al., 1979, Table II-2).

3.5.1.2.2 The Grande Ronde Basalt. Grande Ronde Basalt is the oldest formation of the Yakima Basalt Subgroup (Fig. 3-10) and comprises approximately 85 volume percent of the Columbia River Basalt Group (Reidel et al., 1981). This formation underlies virtually the entire plateau and is divisible into four magnetostratigraphic units (Fig. 3-10). The Grande Ronde Basalt reaches its greatest known thickness in the Pasco Basin. Grande Ronde flows are aphyric to sparsely plagioclase-phyric and are generally fine grained (Myers/Price et al., 1979, Tables II-3 and III-2).

3.5.1.2.3 Wanapum Basalt. The Wanapum Basalt comprises approximately 3 volume percent of the Columbia River Basalt Group and forms much of the plateau surface (Myers/Price et al., 1979, Fig. II-11). The formation has been divided into five members (Swanson et al., 1979c; Camp, 1981) (Fig. 3-10). The characteristics and distribution of individual members have been summarized by Swanson et al. (1979c), Camp (1981), and Myers/Price et al. (1979, Tables II-5 and III-2). These members consist of lavas that were erupted in the eastern and southeastern part of the plateau and flowed to the west (Swanson et al., 1979c). Wanapum Basalt flows are generally medium-grained, olivine-bearing, and slightly to moderately plagioclase-phyric.

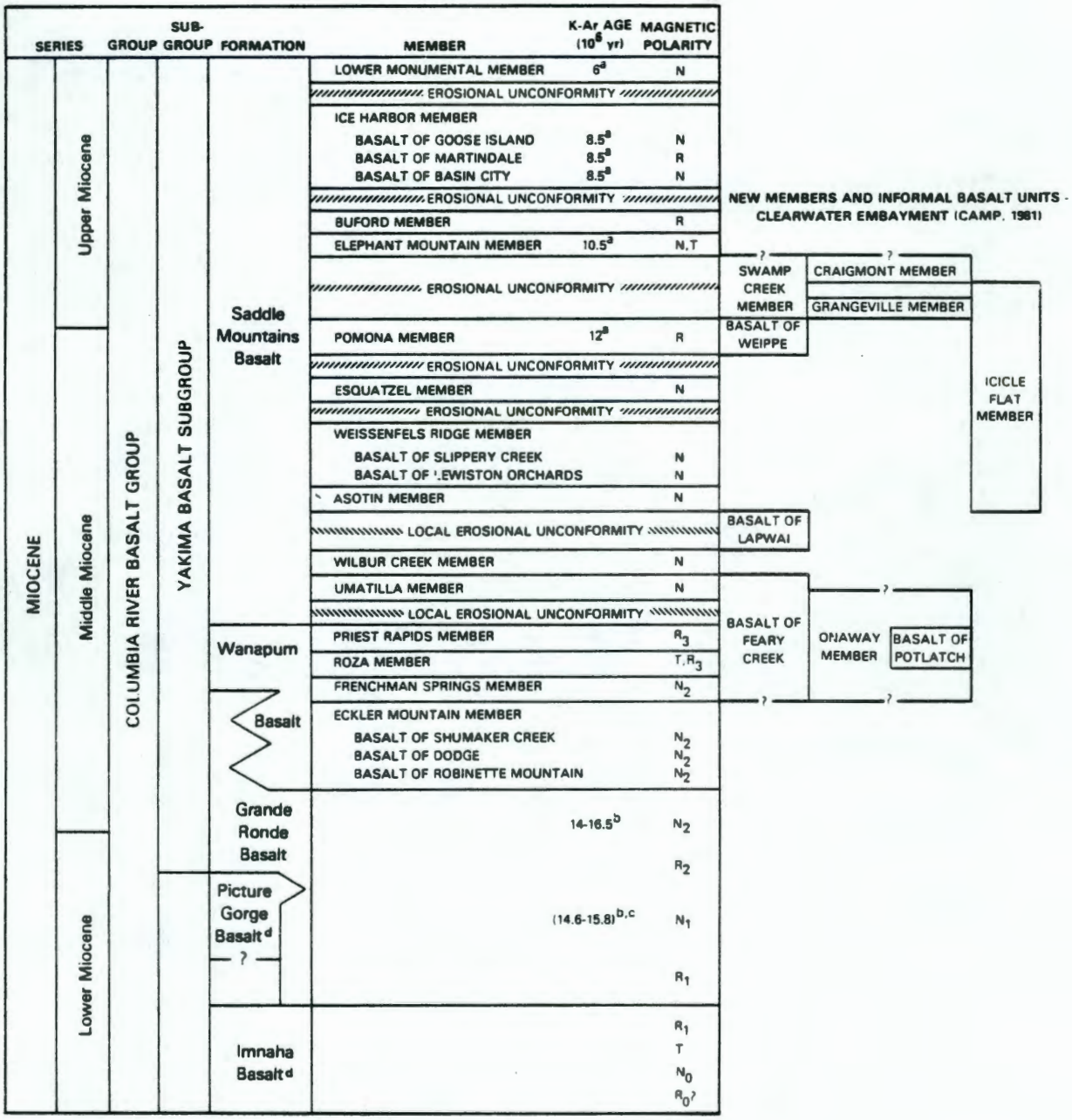

[a]DATA FROM McKEE et al. (1977)
[b]DATA MOSTLY FROM WATKINS AND BAKSI (1974)
[c]INFORMATION IN PARENTHESES REFERS TO PICTURE GORGE BASALT
[d]THE IMNAHA AND PICTURE GORGE BASALTS ARE NOWHERE KNOWN TO BE IN CONTACT. INTERPRETATION OF PRELIMINARY MAGNETOSTRATIGRAPHIC DATA SUGGESTS THAT THE IMNAHA IS OLDER

RCP8202-49

FIGURE 3-10. Regional Columbia River Basalt Group Stratigraphic Nomenclature (after Swanson et al., 1979c).

3.5.1.2.4 The Saddle Mountains Basalt. The Saddle Mountains Basalt is the youngest formation of the Columbia River Basalt Group and consists of 14 members (Swanson et al., 1979c; Camp, 1981) (Fig. 3-10) totaling less than 1 percent of the Columbia River Basalt. These flows occur primarily in the east and central part of the plateau (Myers/Price et al., 1979; Fig. II-16), where they were erupted from vents during a period of waning volcanism. Saddle Mountains time is marked by the development of thick local sedimentary deposits between flows, as well as more apparent folding, faulting, and canyon cutting. The contact between most flows of the Saddle Mountains Basalt are paraconformities and generally only in paleochannels are unconformities found.

The general characteristics and distributions of each member are given in Myers/Price et al. (1979; Tables II-6 and III-2), Swanson et al. (1979c; 1980; 1981), Camp (1981), and Reidel and Fecht (1981).

3.5.1.3 Intercalated and Suprabasalt Sediments. The Miocene to Holocene sedimentary units of the Columbia Plateau are made up of four general groups. These are (1) the sediments interbedded with Columbia River basalt flows, (2) the Miocene-Pliocene suprabasalt sediments that are in part coeval with Columbia River basalt elsewhere on the plateau, (3) the Pleistocene sediments, many of which are the result of catastrophic flooding, and (4) the Holocene sediments, chiefly alluvium and eolian deposits. The general stratigraphic relationship of the sediments discussed in this section is illustrated in Figure 3-11.

3.5.1.3.1 Ellensburg Formation and Equivalents. The Ellensburg Formation (Russell, 1893) includes clastic and volcaniclastic sediments that are mainly concentrated in the western and central part of the plateau. Units of the formation underlie, interfinger, and overlie Wanapum and Saddle Mountains Basalts (Swanson et al., 1979c). Waitt (1979) included all sedimentary interbeds of the Yakima Basalt Subgroup (Fig. 3-10) in the Ellensburg Formation. The general properties of the formation are given in Myers/Price et al. (1979, Table III-2 and Fig. II-27).

All major sedimentary interbeds in the northeastern part of the plateau are assigned to the Latah Formation (Griggs, 1976); the Mascall Formation in central Oregon is locally interbedded with Columbia River basalt (Thayer and Brown, 1966). Elsewhere in the plateau the interbeds are not clearly defined formations.

3.5.1.3.2 Ringold Formation. The Ringold Formation is confined principally to the Pasco and Quincy Basins (Fig. 3-1), where it overlies the Columbia River basalt. Based on fossils and paleomagnetic data in the Pasco Basin, the Ringold is interpreted to range from 8.5 million years (post-Ice Harbor Basalt, Fig. 3-10) to 3.7 million years in age (Tallman et al., 1981). A general description of the unit is given in Myers/Price et al. (1979, Table III-2). Ringold sediments were deposited in a fluvial environment with some lacustrine facies. Clast lithologies represent both the Columbia and the Snake River drainages.

9 2 1 2 4 9 5 0 6 5 9

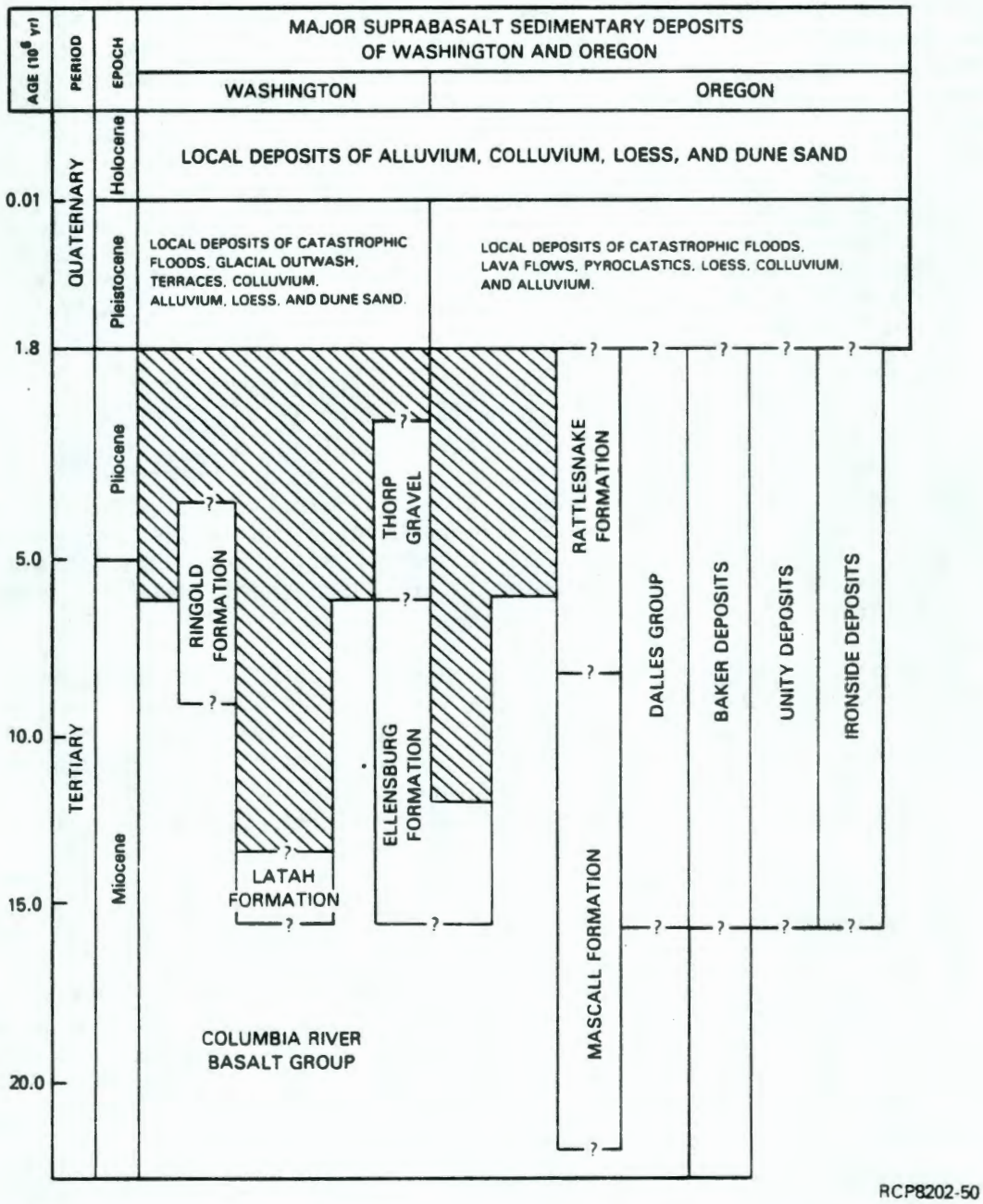

FIGURE 3-11. General Stratigraphic Relationship of Suprabasalt Sediments.

3.5.1.3.3 Dalles Group. The Dalles Group (Fig. 3-11) has been recently defined by Farooqui et al. (1981a; 1981b) to include Miocene and Pliocene deposits consisting chiefly of fluvial silt, sand and gravel, lahar and tuff, airfall tuff, and basalt flows that overlie the Columbia River basalt in Oregon and extreme southern Washington. These deposits extend along the northern flank of the Blue Mountains from the Cascade Range to nearly 118° W. longitude. They were laid down in northeasterly trending, probably isolated, discrete basins (Fig. 3-12) of tectonic origin.

The Dalles Group is composed of five formations: the Chenoweth (The Dalles Basin), Alkali Canyon (Arlington-Boardman Basin), Deschutes (Madras Basin), Tygh Valley (Tygh Valley Basin), and Makay Formations (Agency Basin). The group overlies the Columbia River basalt and is overlain by a variety of Quaternary deposits. The age is estimated to be middle Miocene to Pliocene.

3.5.1.3.4 Other Miocene-Pliocene Suprabasalt Units of Oregon. The Rattlesnake Formation of the John Day Valley of north-central Oregon (Merriam, 1901) overlies the Mascall Formation (Fig. 3-10), Columbia River basalt, and locally, Paleozoic rocks. The Rattlesnake Formation is late Miocene to Pliocene in age (Farooqui et al., 1981b). Baker, Unity, Ironside, and LeRoux deposits (Fig. 3-11) are Miocene and Pliocene in age and all are at least, in part, suprabasalt sedimentary units in basins and valleys of eastern Oregon. These units are discussed in detail in Farooqui et al. (1981b).

3.5.1.3.5 Thorp Gravel. The Thorp Gravel of Pliocene age (Waitt, 1979) (Fig. 3-11) is restricted to the Kittitas Valley on the west side of the Columbia Plateau. It is approximately time-equivalent with the upper part of the Ringold Formation and occurs as high terraces along the Yakima River and its tributaries (Rigby and Othberg, 1979). The deposit is a moderately weathered, weakly cemented, well-rounded, fluvial gravel and coarse sand.

3.5.1.3.6 Glacial Deposits. Glacial deposits include till, ice-contact-stratified drift, and outwash. The most extensive glacial deposits occur on the northwestern portion of the plateau and were deposited by the Okanogan Lobe of the Cordilleran ice sheet. The terminal position of this late Wisconsin ice sheet is marked by the Withrow Moraine. Glacial drift resulting from alpine glaciation occurs in the northwestern plateau in the Kittitas, Wenatchee, and Chelan Valleys (Rigby and Othberg, 1979) and in the highlands of Oregon (Farooqui et al., 1981b) and Idaho in the southeastern portion of the plateau.

3.5.1.3.7 Catastrophic Flood Deposits. Catastrophic flood deposits are widespread in the Columbia Plateau. They were deposited when ice dams in western Montana and northern Idaho were breached, allowing large volumes of water to spill across eastern and central Washington (Bretz, 1959). The number of floods is undetermined. Most of the sediments are

9 2 1 2 4 9 5 0 6 6 1

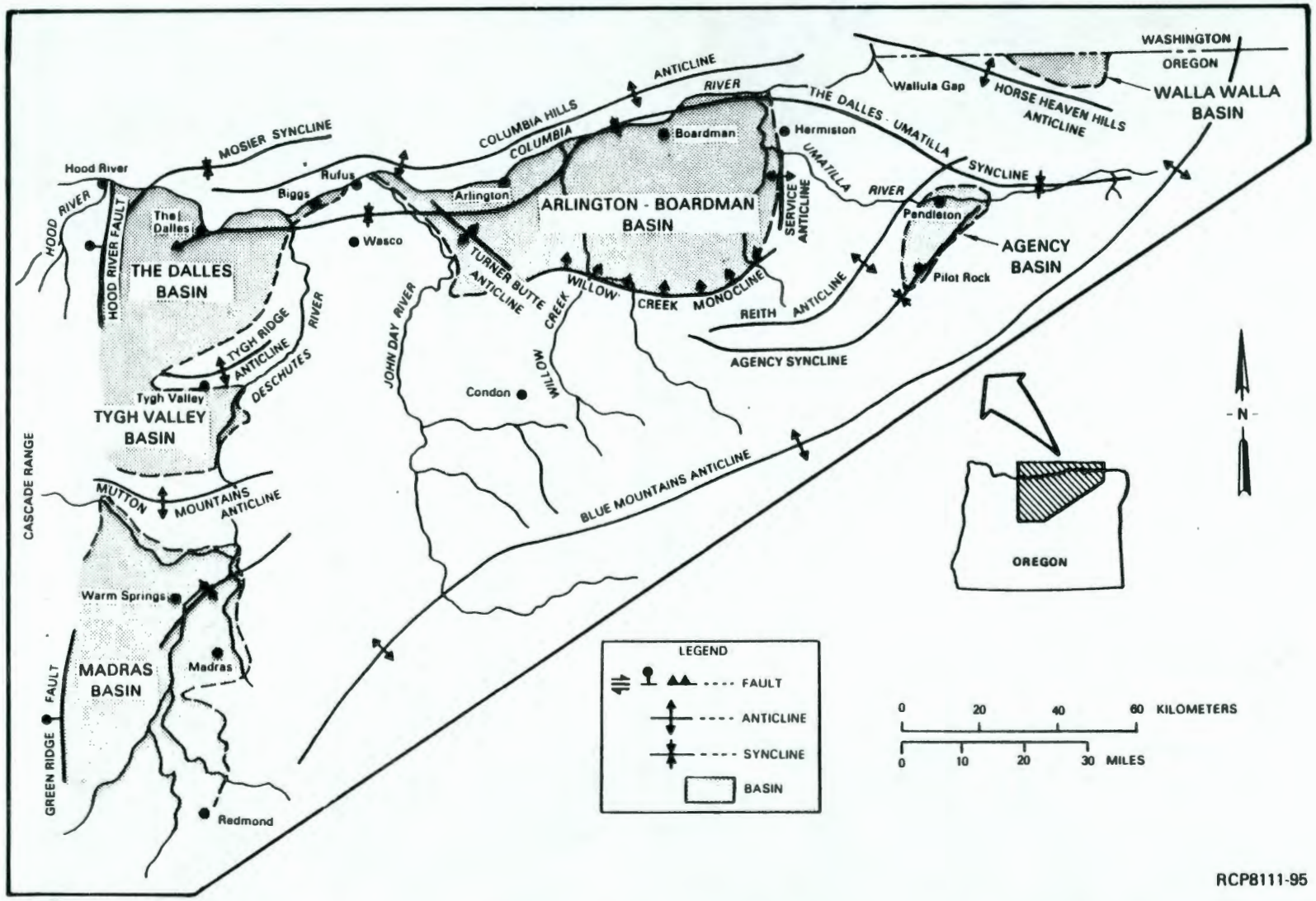

FIGURE 3-12. Generalized Locations of the Dalles Group and Their Depositional Basins (after Farooqui et al., 1981a).

late Pleistocene, with the last major flood sequence dated at about 13,000 years before present (Mullineaux et al., 1977). These deposits (referred to as the Hanford formation in the Pasco Basin) are composed of two facies, a flood facies (sand and gravel) and slack-water facies (sand to silt) (Myers/Price et al., 1979, Tables II-7 and III-2).

3.5.1.3.8 Loess. Loess mantles much of the Columbia Plateau in varying thickness. At least four different ages are recognized (Richmond et al., 1965). The oldest is greater than 125,000 years before present and the youngest is late Wisconsin to Holocene.

3.5.1.3.9 Other Surficial Deposits. Alluvium, colluvium, sand dunes, and landslide deposits occur throughout the area. Alluvium is primarily Holocene, as are local lacustrine, paludal, and eolian deposits. Mazama and Glacier Peak ash horizons (Section 3.5.1.4) are commonly found in alluvium and sand dunes. Older, probably Pleistocene, alluvium is present as fan deposits and is usually capped with a petrocalcic horizon. Colluvium, primarily Holocene talus deposits, is common at the base of steep slopes, particularly in coulees. Landslide deposits are of variable age and genesis.

3.5.1.4 Late Cenozoic Volcanics. Post-Columbia River basalt volcanics are present on the western margin of the plateau and tephra deposits are interbedded with Pliocene to Holocene sedimentary deposits in much of the western and central Columbia Plateau. These units are associated with Cascade volcanic activity and include Simcoe lavas (4.5 to 1 million years before present) (Shannon and Wilson, 1973) and Tieton andesite (Pleistocene) (Swanson, 1967). Undifferentiated volcanics are also present in north-central and northeastern Oregon.

Pliocene to Holocene tephras are intercalated with sediments throughout the Columbia Plateau. Of these horizons, ashes from Mount St. Helens, Glacier Peak, and Mount Mazama are important Pleistocene and Holocene time-stratigraphic units. At least eight major ashes were erupted from Mount St. Helens between 35,000 and 150 years before present (Mullineaux et al., 1975), excluding the May 18, 1980 eruption which blanketed eastern Washington. The Mount St. Helens S set has been dated at about 13,000 years before present (Mullineaux et al., 1977) and is associated with deposits of the last major scablands flood. Glacier Peak erupted numerous times between about 11,000 and 13,000 years before present (Smith et al., 1977; Westgate and Evans, 1978; Porter, 1978). Mazama ash deposits are dated at 6,600 years before present (Wilcox, 1965).

3.5.2 Relationship of Candidate Area to the Regional Framework

The candidate area is defined as the Pasco Basin. This basin contains the thickest known accumulation of Columbia River basalt. Many flows of the Columbia River Basalt Group cover large areas of the Columbia Plateau and can be individually identified on the basis of chemical and physical properties. The fact that flows can be recognized enables them to be traced over a regional extent, including the Pasco Basin.

9 2 1 2 4 9 5 0 6 6 3

The suprabasalt sedimentary units are less continuous than basalt flows and are generally restricted to local basins. Time-stratigraphic correlations are more difficult and are based on paleontology, radiometric dating, and stratigraphic position.

3.5.3 Surface Geology

A detailed surficial geologic map of the Pasco Basin (scale 1:62,500) is included in Myers/Price et al. (1979, Plate III-1). A general geologic map of the Pasco Basin is shown in Figure 3-13. The general structure cross section (Fig. 3-14) illustrates the relationship of surface rock units to those in the subsurface. The generalized surficial geologic map of the reference repository location is shown in Figure 3-15.

Three rock-stratigraphic units are exposed on the broad, relatively flat plains of the proposed reference repository location. The most extensive unit is the Pleistocene Hanford formation composed of two major facies of unconsolidated sediments, the Pasco gravels and the Touchet beds (Fig. 3-15). The two other rock-stratigraphic units, Cold Creek alluvium and dune sand, are of Holocene age and locally veneer the Hanford formation.

The relationship of surface geologic units to the subsurface geology of the reference repository location is illustrated in Figure 3-16. The Hanford formation is the only surficial unit that is extensive enough to correlate in the subsurface. The Cold Creek alluvium and sand dunes veneer the Pleistocene Hanford formation, which unconformably overlies the Miocene-Pliocene Ringold Formation.

3.5.4 Stratigraphic and Lithologic Framework of the Reference Repository Location

The bedrock of the Pasco Basin, including the Cold Creek syncline, consists of flows belonging to three formations of the Columbia River Basalt Group: (1) Grande Ronde Basalt, (2) Wanapum Basalt, and (3) Saddle Mountains Basalt (Fig. 3-17). The basalt section is interbedded with sediments of the Ellensburg Formation and is overlain by up to 220 meters of the chiefly fluvial Miocene-Pliocene Ringold Formation and catastrophic flood deposits of the Pleistocene Hanford formation. Holocene loess and sand dunes mantle much of the surface. Alluvium is present in flood plains. The stratigraphic relationships among these units are shown in Figure 3-16. Radiometric ages for units are given where available. The five formations shown in this figure are present in the site.

3.5.4.1 Grande Ronde Basalt. The interpretation of Grande Ronde Basalt stratigraphy in the Cold Creek syncline and the reference repository location is based on an integration of surface and subsurface data (Myers, 1973; ARHCO, 1976; Long, 1978; Myers/Price et al., 1979; Long and Landon, 1981). Grande Ronde Basalt outcrops in the vicinity of the reference repository location, particularly along the western margin of the Pasco Basin, have been studied in some detail (Long and Davidson, 1981). Geophysical logs have been used as an aid in determining contacts between

9 2 1 2 4 9 5 0 6 6 4

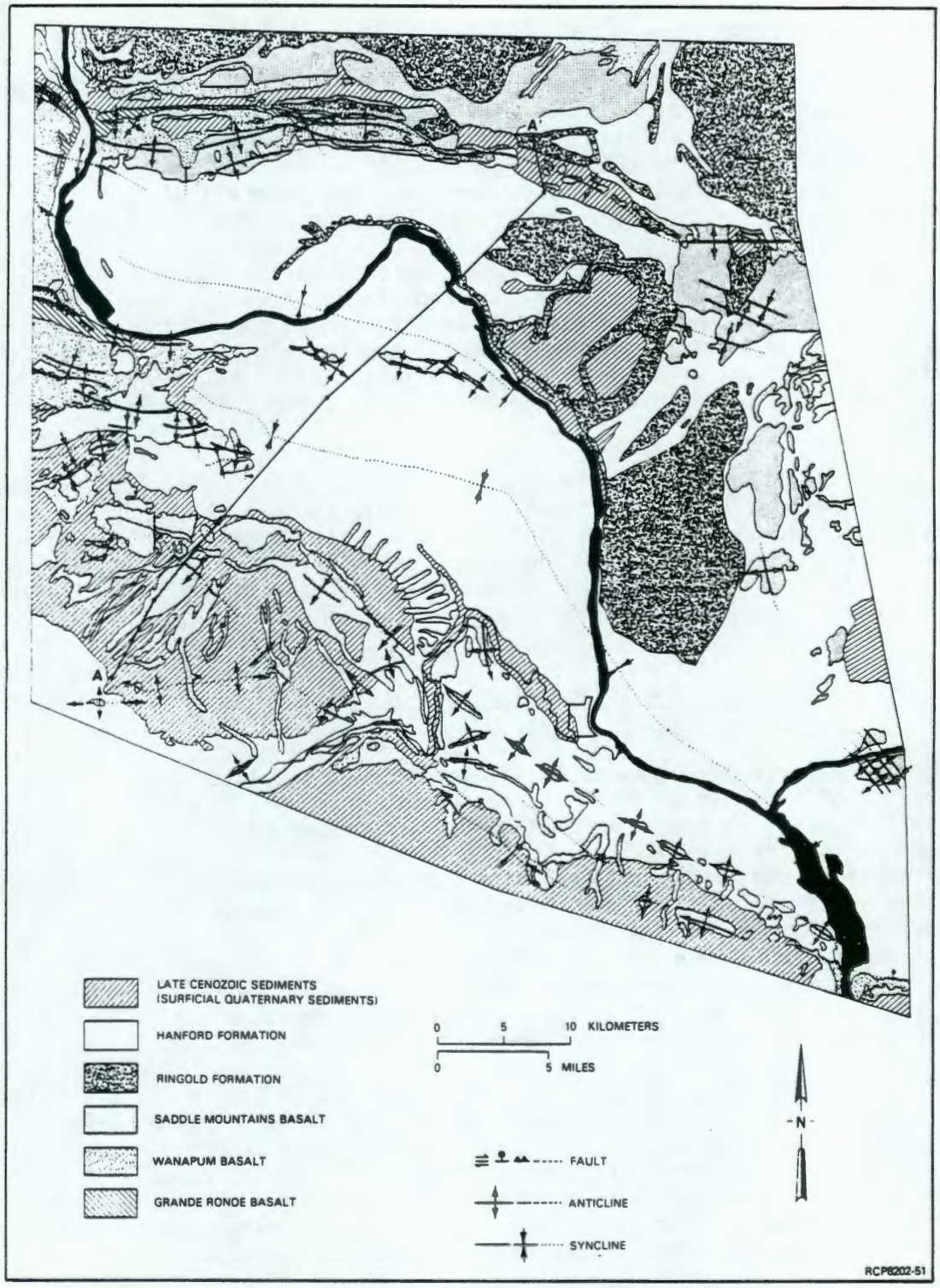

FIGURE 3-13. General Geologic Map of the Pasco Basin. Cross section A-A' is shown in Figure 3-14.

9 2 1 2 4 9 5 0 6 6 5

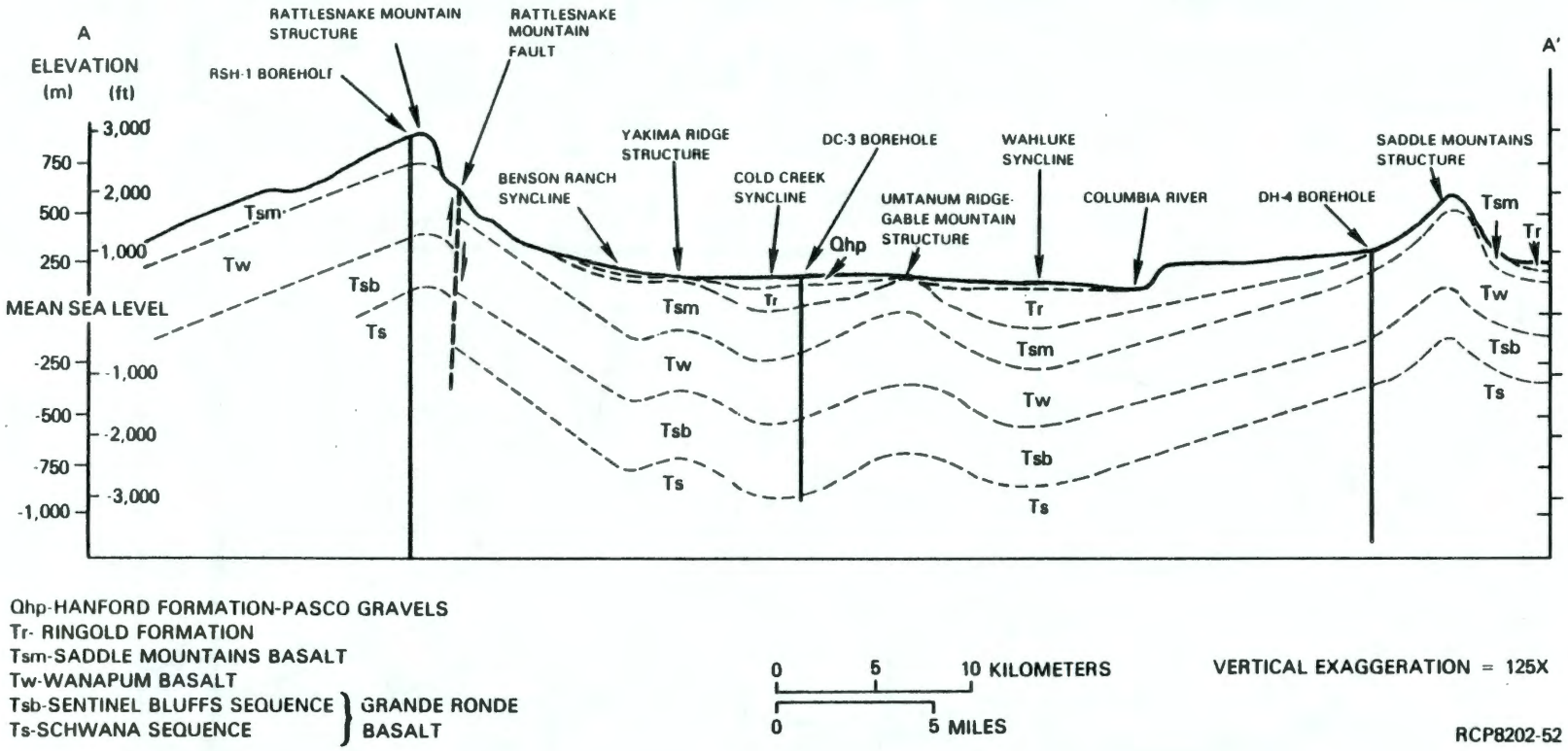

Qhp-HANFORD FORMATION-PASCO GRAVELS
Tr- RINGOLD FORMATION
Tsm-SADDLE MOUNTAINS BASALT
Tw-WANAPUM BASALT
Tsb-SENTINEL BLUFFS SEQUENCE } GRANDE RONDE
Ts-SCHWANA SEQUENCE } BASALT

0 5 10 KILOMETERS
0 5 MILES

VERTICAL EXAGGERATION = 125X

RCP8202-52

FIGURE 3-14. Generalized Structure Cross Section. (See Fig. 3-13 for location.)

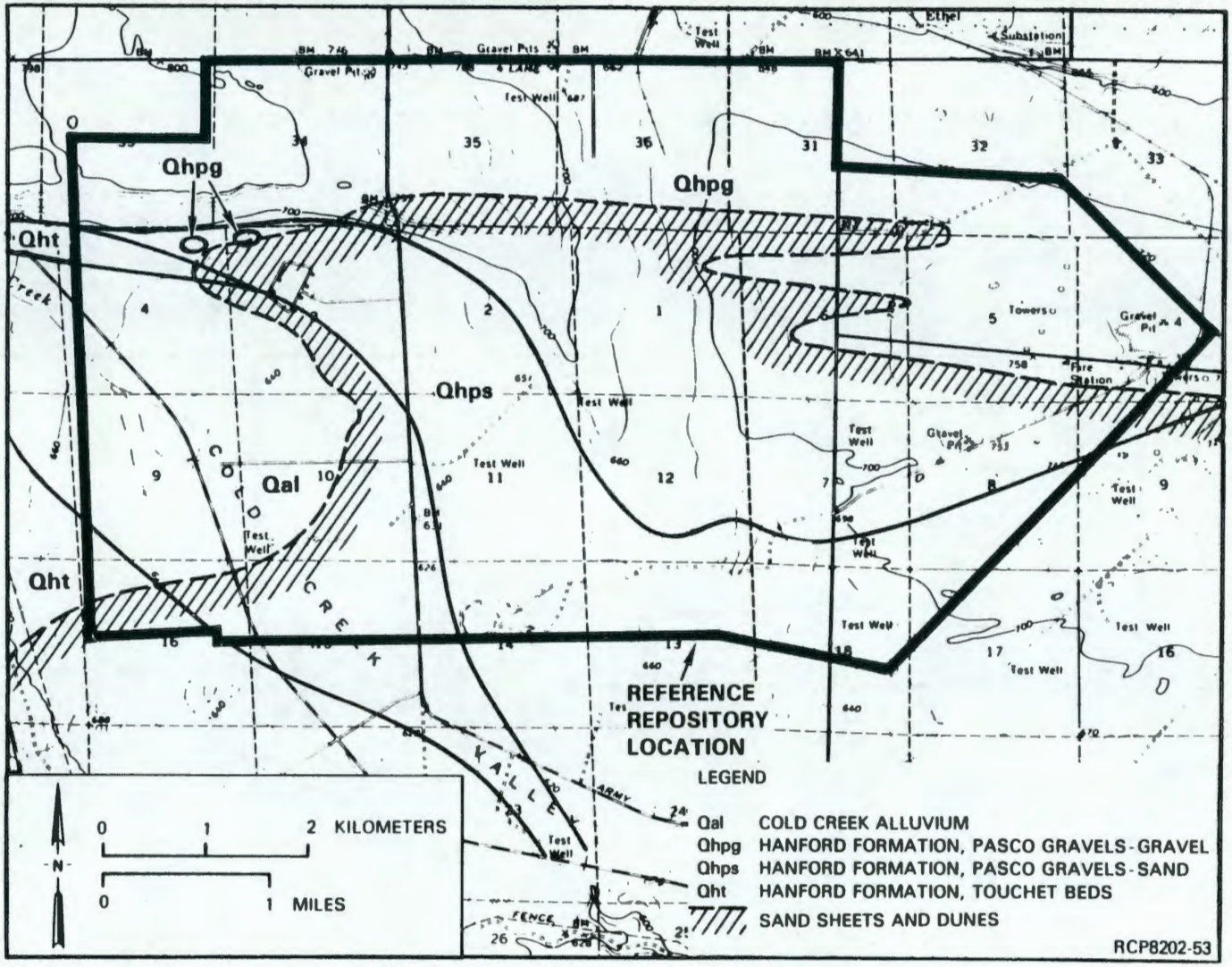

FIGURE 3-15. Generalized Surficial Geologic Map of the Reference Repository Location.

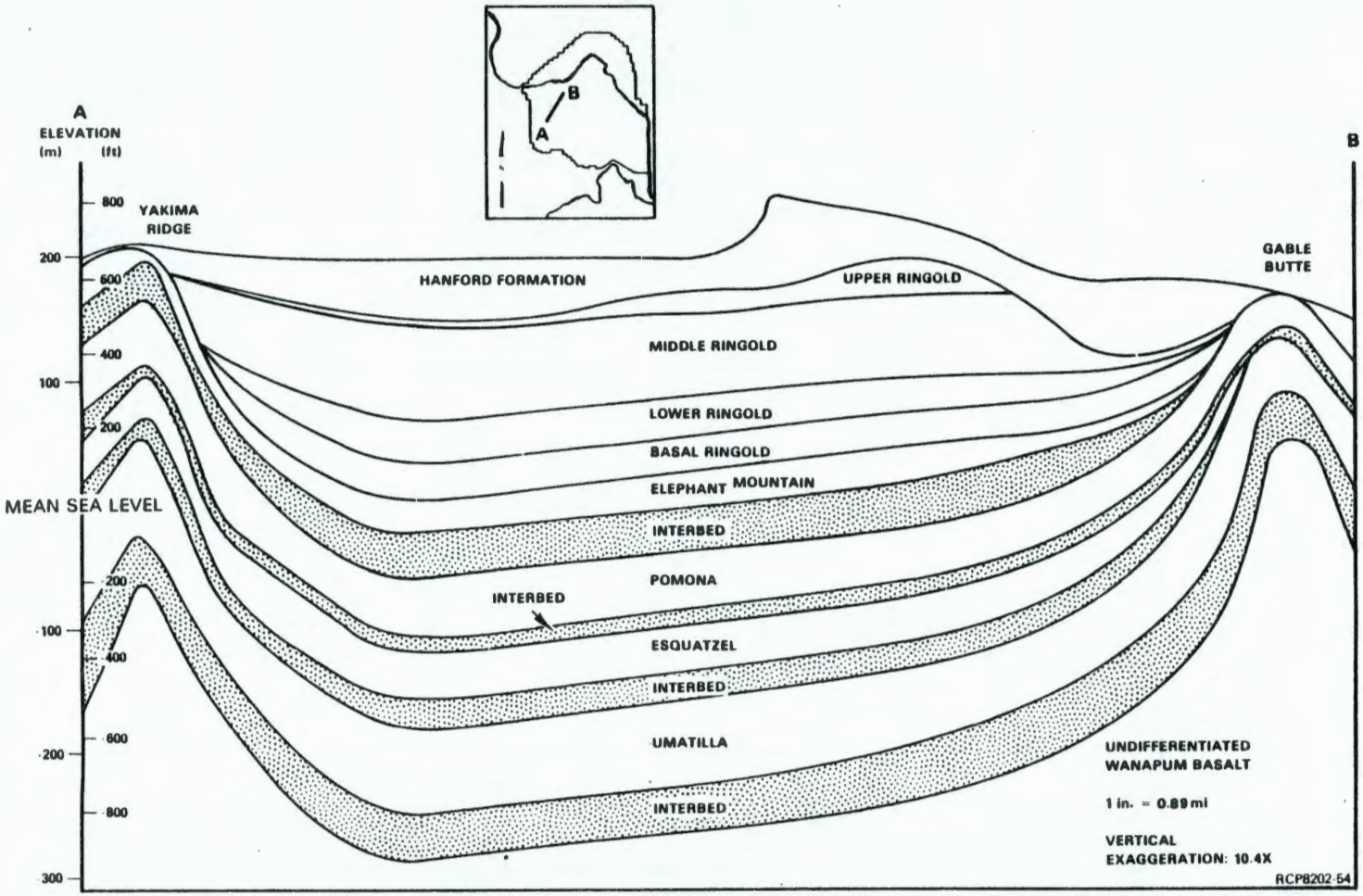

FIGURE 3-16. General Cross Section Through the Reference Repository Location.

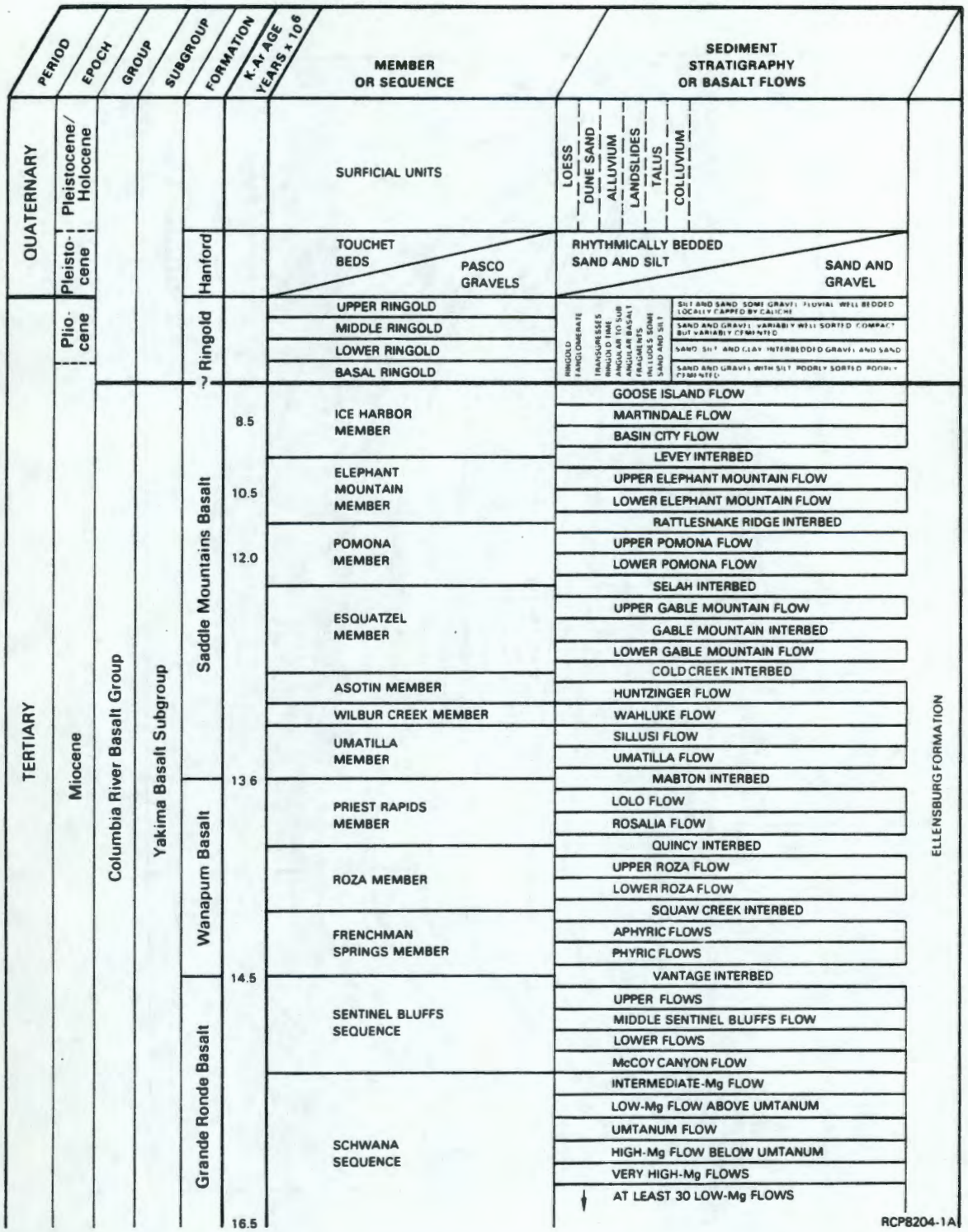

FIGURE 3-17. Stratigraphic Nomenclature, Pasco Basin, Cold Creek Syncline.

flows in boreholes, particularly where no core is available (e.g., RSH-1, DC-3; Fig. 3-18). Core has been sampled for major element analysis (Long et al., 1980), trace element analysis (Long et al., 1981), and paleomagnetic analysis (Coe et al., 1978; Beck et al., 1978; Packer and Petty, 1979; Van Alstine and Gillett, 1981). The positions of contacts between individual flows, coupled with the data obtained from core analyses, are the basis of correlations of the Grande Ronde Basalt (Long and Landon, 1981). A more detailed description of analytical methods used in stratigraphic interpretations is given in Long and Landon (1981) and Long and Davidson (1981).

3.5.4.1.1 Stratigraphy. Within the Pasco Basin, the Grande Ronde Basalt consists of more than 50 flows extending to a depth of at least 3.2 kilometers (Reidel et al., 1981). The general stratigraphic subdivisions and nomenclature of Grande Ronde Basalt are illustrated in Figure 3-17. Core holes and surface exposures in the vicinity of the Pasco Basin include the normal (N_2) and uppermost reversed (R_2) paleomagnetic units (Fig. 3-10). The N_2-R_2 horizon thus provides an important stratigraphic horizon within the Pasco Basin.

In addition to the broad subdivisions based on paleomagnetic polarity, two major sequences of flows based on bulk chemistry have been recognized within the Grande Ronde Basalt in the Pasco Basin: (1) the Schwana sequence, consisting almost entirely of flows with relatively low-magnesium content (low-magnesium chemical type) and (2) the Sentinel Bluffs sequence, consisting entirely of flows with higher magnesium content (high-magnesium chemical type) (Fig. 3-19). The Schwana sequence lies stratigraphically below the Sentinel Bluffs flows and contains the Umtanum flow (Fig. 3-20). The contact between these two sequences is known as the magnesium horizon (Fig. 3-20). Details of the stratigraphy of the Schwana and Sentinel Bluffs sequences are given in Long and Landon (1981).

From borehole data, the Umtanum flow at the reference repository location is known to lie directly below the magnesium horizon. The Umtanum flow is recognized on the basis of unusual thickness, major- and trace-element chemistry, and paleomagnetic inclination. It has distinctly higher TiO_2 content (Long and Landon, 1981, Fig. 4-4) than other low-magnesium flows in the upper portion of the Schwana sequence; hence, it is considered a chemical subtype of the low-magnesium chemical type.

Thickness variations for the Sentinel Bluffs sequence and for flows which lie stratigraphically close to the Umtanum flow are discussed in Long and Landon (1981, Fig. 4-10, 4-11, 4-15, and 4-16). The middle Sentinel Bluffs flow is found throughout the Pasco Basin. It is thickest in the central portion and thins slightly to the northeast and more so to the south (Fig. 3-19). The Umtanum flow is found throughout the Pasco Basin, but thins to the northeast and is not present in surface sections

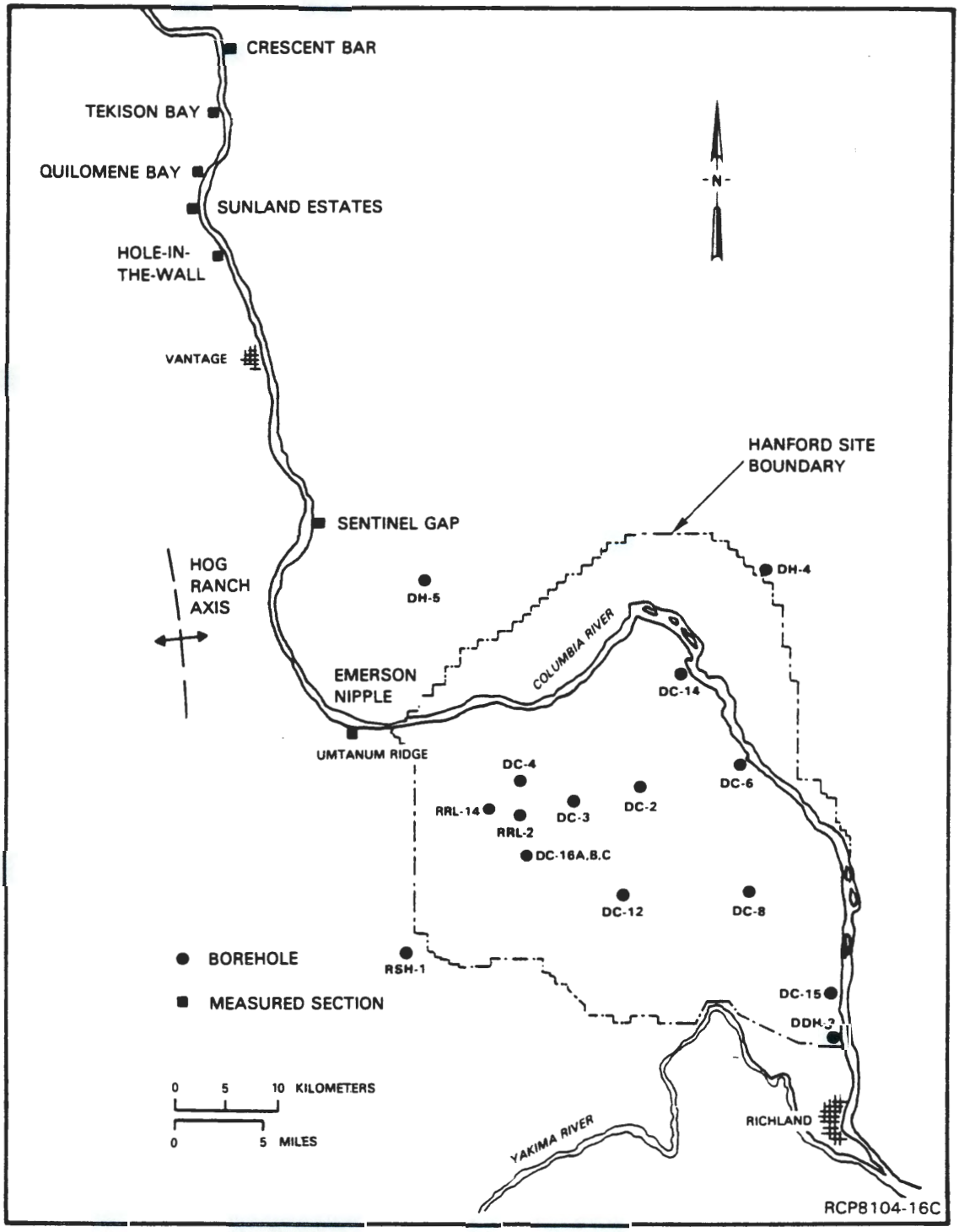

FIGURE 3-18. Location Map, Pasco Basin and Surrounding Areas (showing location of boreholes penetrating the candidate repository horizons and geologic sections).

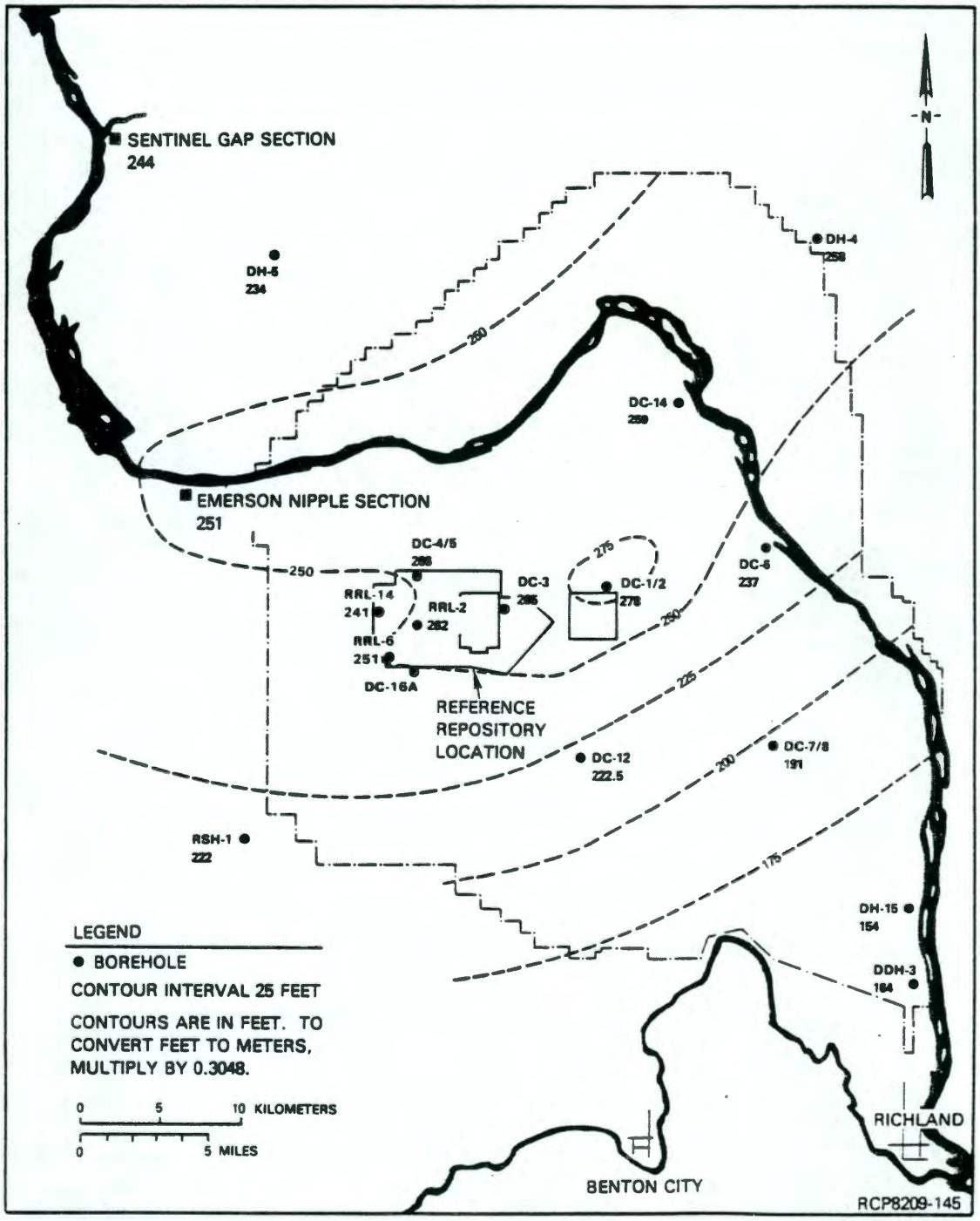

FIGURE 3-19. Isopach Map of the Middle Sentinel Bluffs Flow, Pasco Basin and Vicinity.

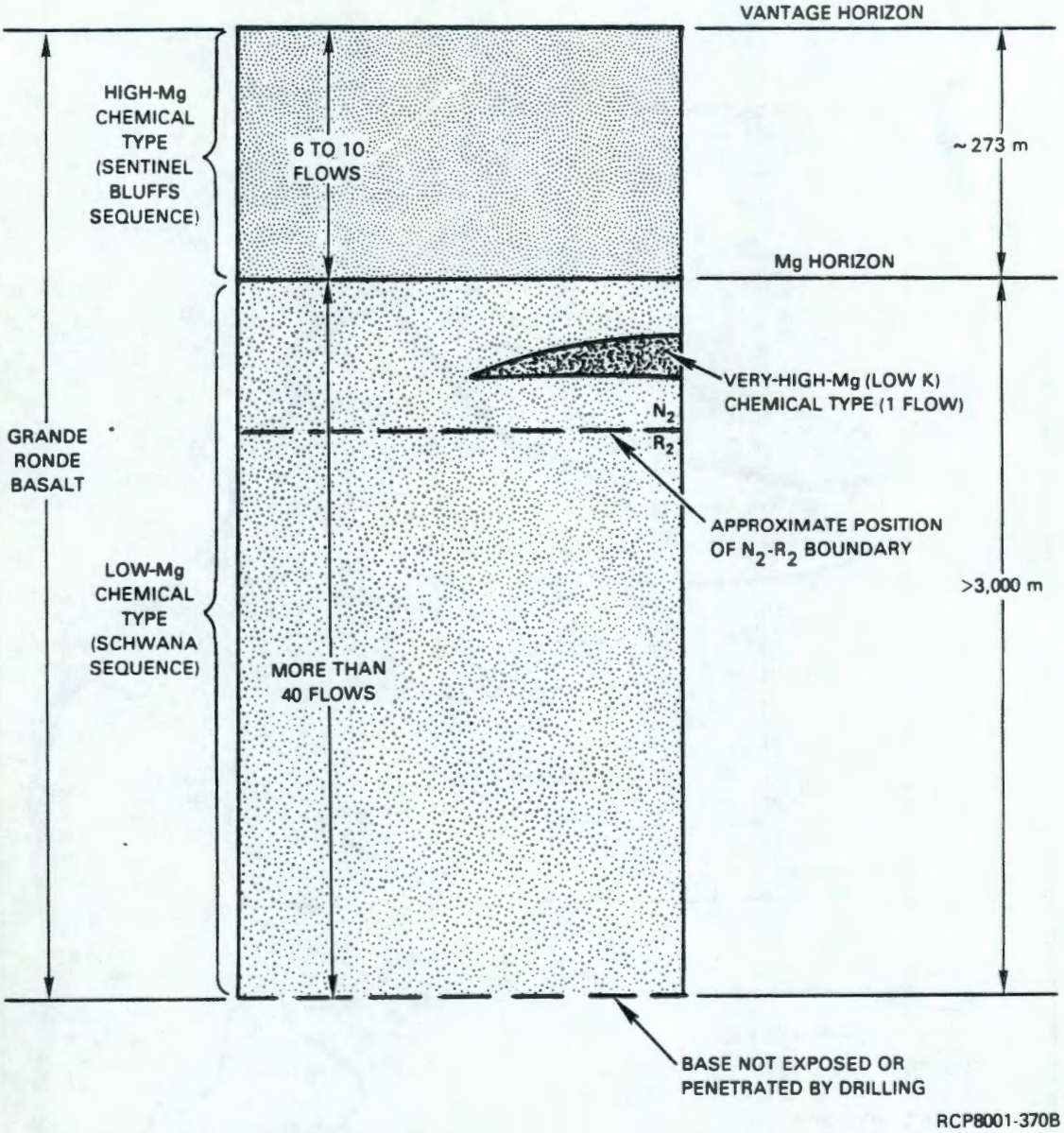

FIGURE 3-20. General Stratigraphic Relationships Among Grande Ronde Basalt Flow Sequences in the Pasco Basin. Thickness figures and number of flows are based on drilling results in the Pasco Basin and vicinity. Analysis of chip samples from a deep, rotary-drilled well (RSH-1) indicates that Grande Ronde Basalt extends to a depth of at least 3.2 kilometers.

north of Sentinel Gap. It also thins dramatically west of the Emerson Nipple section and to a lesser degree to the southwest. It is thickest in the area of Emerson Nipple and Sentinel Gap and in the southeast near DC-15 and DDH-3 (Fig. 3-21). A broad zone of relatively constant thickness occurs in the central Pasco Basin.

General thickness variations for all flows are depicted in Figures 3-22, 3-23, and 3-24. These fence diagrams also provide an overall summary of the stratigraphic interpretations for Grande Ronde Basalt in the Pasco Basin subsurface.

Available Grande Ronde Basalt data suggest that the thickness of flows is controlled by the interacting effects of tectonic deformation, limited volume, and constructional topography. A more detailed discussion of factors controlling flow distribution of the Grande Ronde Basalt in the central Pasco Basin is contained in Long and Landon (1981, pp. 4-20 to 4-41).

Flows of the Grande Ronde Basalt were erupted in very rapid succession with an average of less than 50,000 years between flows. During the time between emplacement of the flows, minor weathering occurred, although it was not well developed and is not evident in either the drill core recovered, or in borehole geophysical logs. Significant paleosols were not developed and no significant sedimentation occurred within the reference repository location. In rotary borehole RSH-1 (Fig. 3-3), however, organic-rich cuttings were encountered in the vicinity of the projected N_2-R_2 paleomagnetic horizon and near the middle Sentinel Bluffs and Umtanum flows. These interbeds have not been encountered in any other borehole that has penetrated to these depths. These interbeds are interpreted to have resulted from the diversion of the regional drainage system to the west of the present day Pasco Basin, allowing deposition, or to small lakes that may have formed in depressions on the tops of flows.

The stratigraphy of the reference repository location is depicted in Figure 3-25. As deep basalts in the reference repository location have not been drilled, the thickness is inferred from isopach maps and interpolation between boreholes (Long and Landon, 1981). For flows that may pinch out within the reference repository location, the pinch-out is depicted diagrammatically. Further borehole data within and adjacent to the reference repository location will be required to define thickness variations and pinchouts more precisely.

3.5.4.1.2 Lithology - Intraflow Structure. Intraflow structures and petrographic textures have been studied in a general way for a number of Grande Ronde flows and in considerable detail for two flows: the Umtanum and McCoy Canyon flows. The McCoy Canyon flow overlies the Umtanum flow and is accessible in surface sections north of the Pasco Basin. The results of this work are discussed in detail in Long (1978), Myers/Price et al. (1979), and Long and Davidson (1981). These references, as well as previous work by others (Waters, 1961; Mackin, 1961; Camp, 1976; Holden and Hooper, 1976; Price, 1977; Reidel, 1978b; Ross, 1978; and Swanson et al., 1979c), are the primary data sources for the material presented here.

9 2 1 2 4 9 5 0 6 7 4

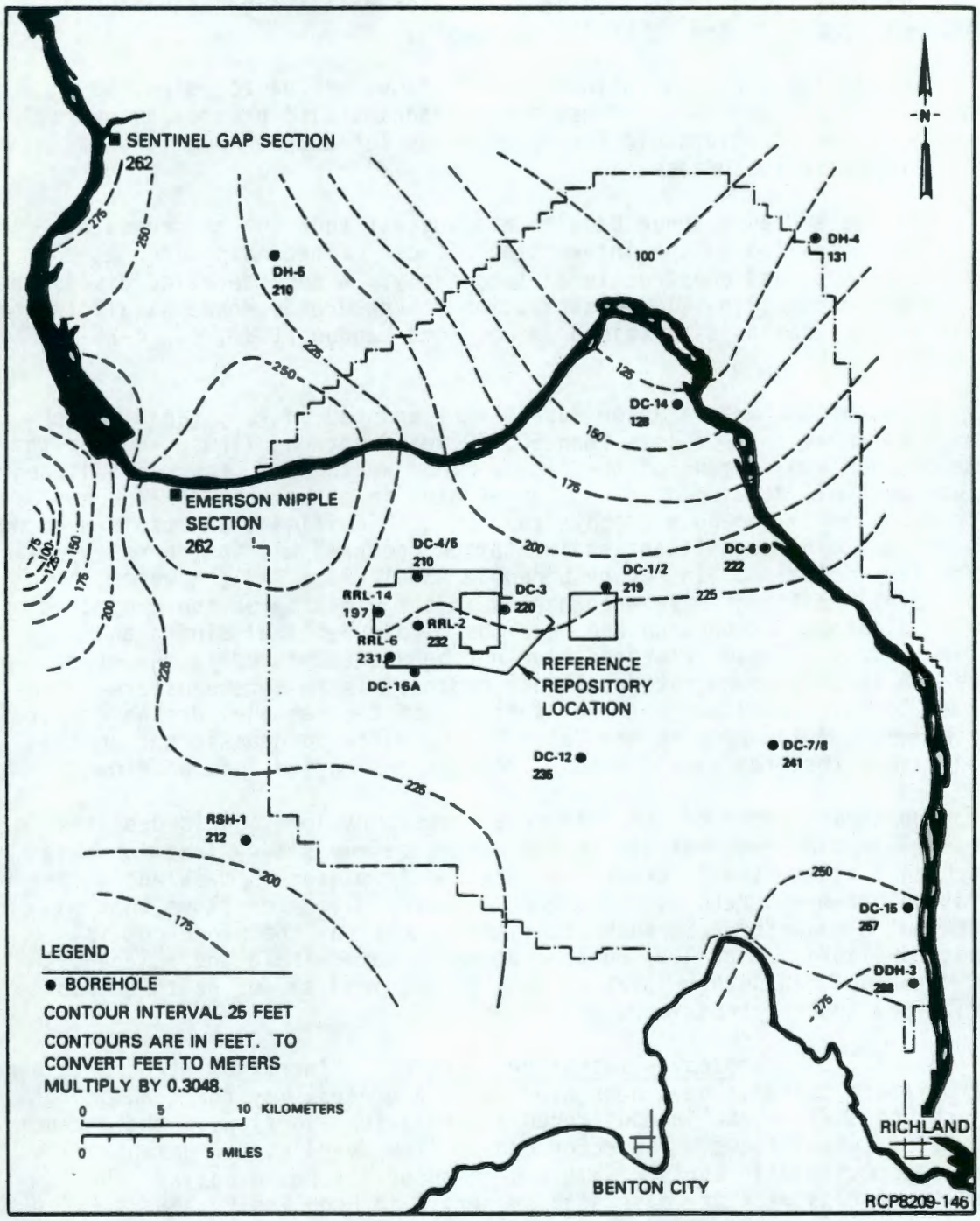

FIGURE 3-21. Isopach Map of the Umtanum Flow, Pasco Basin and Vicinity.

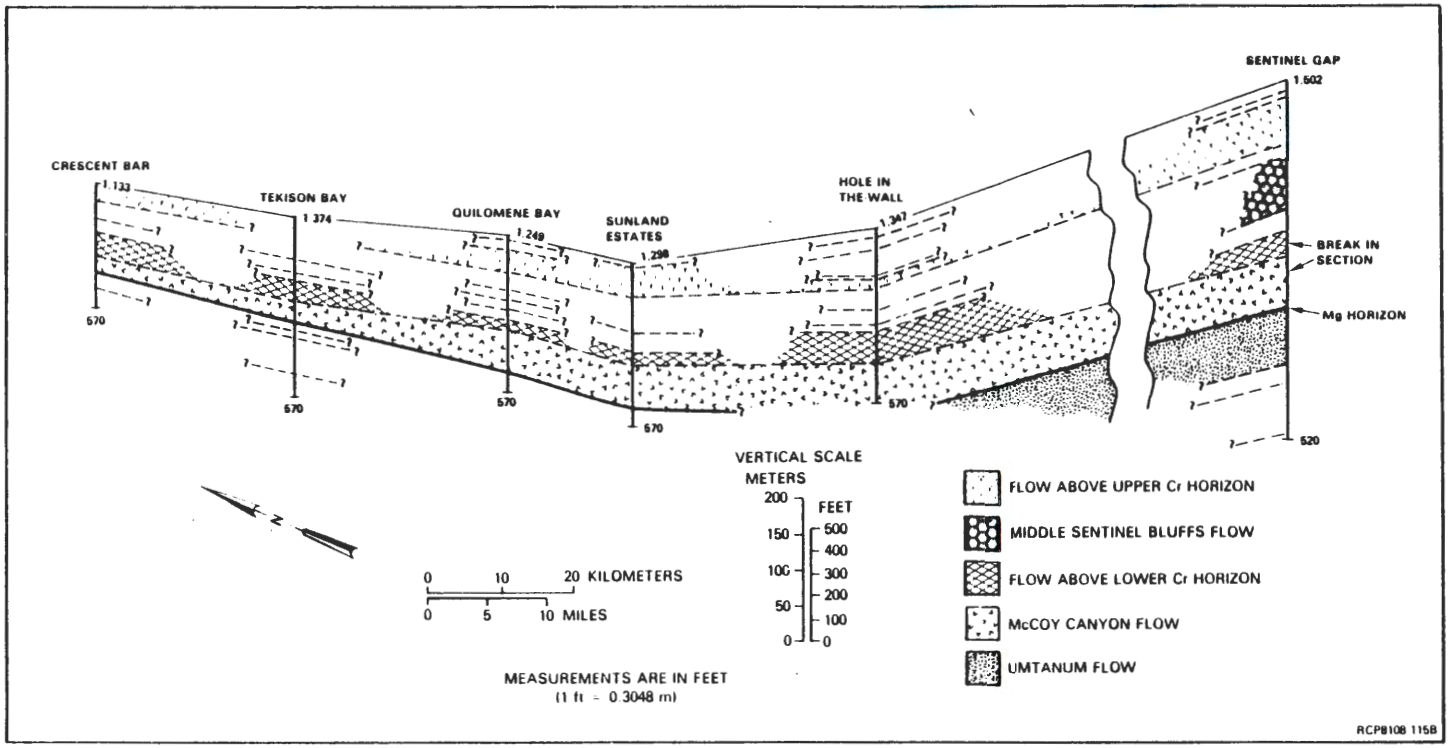

FIGURE 3-22. Fence Diagram, Upper Grande Ronde Basalt, Crecent Bar to Sentinel Bluffs. (See Fig. 3-18 for location.)

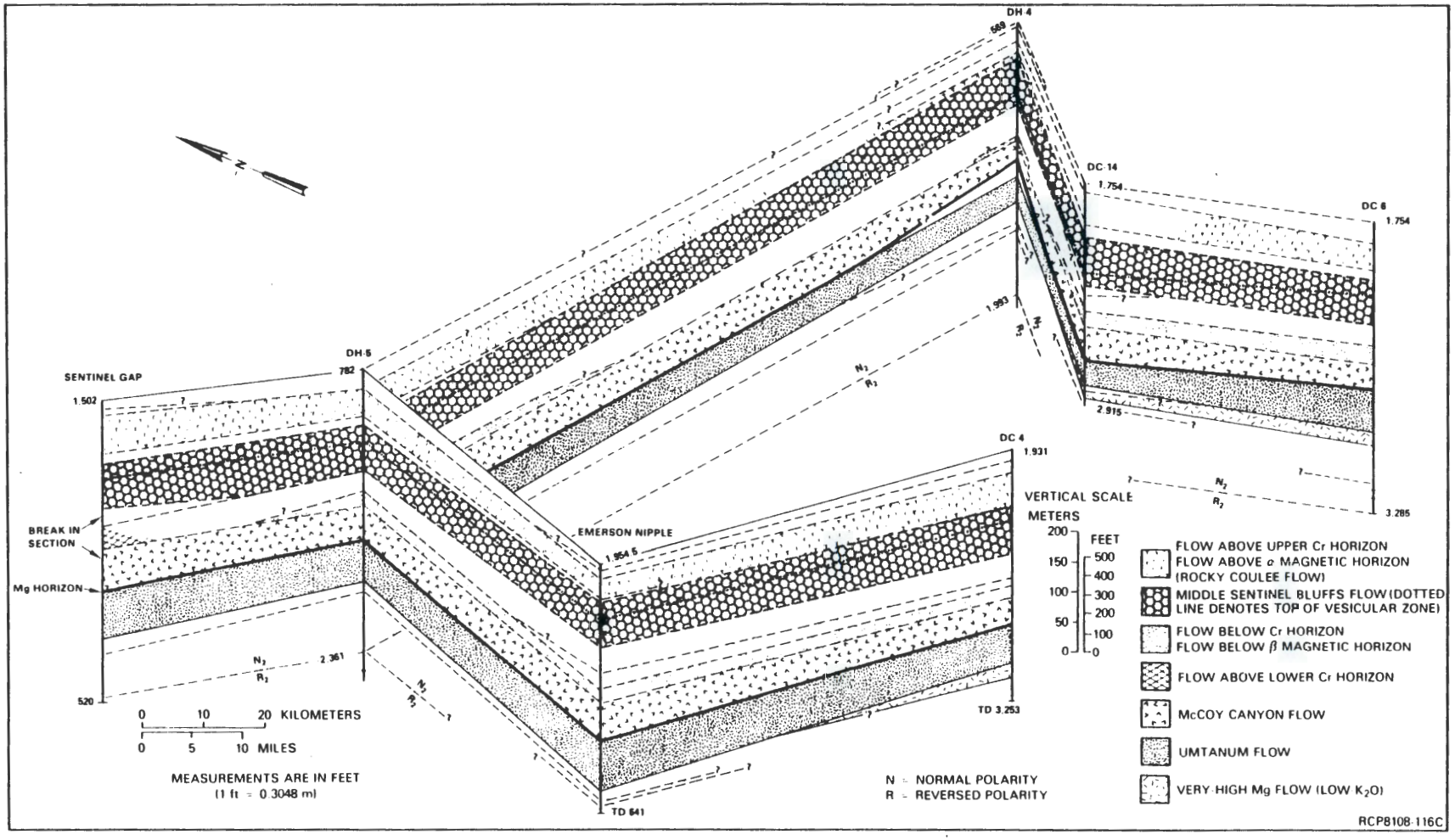

FIGURE 3-23. Fence Diagram, Upper Grande Ronde Basalt, Sentinel Bluffs to Borehole DC-6. (See Fig. 3-18 for location.)

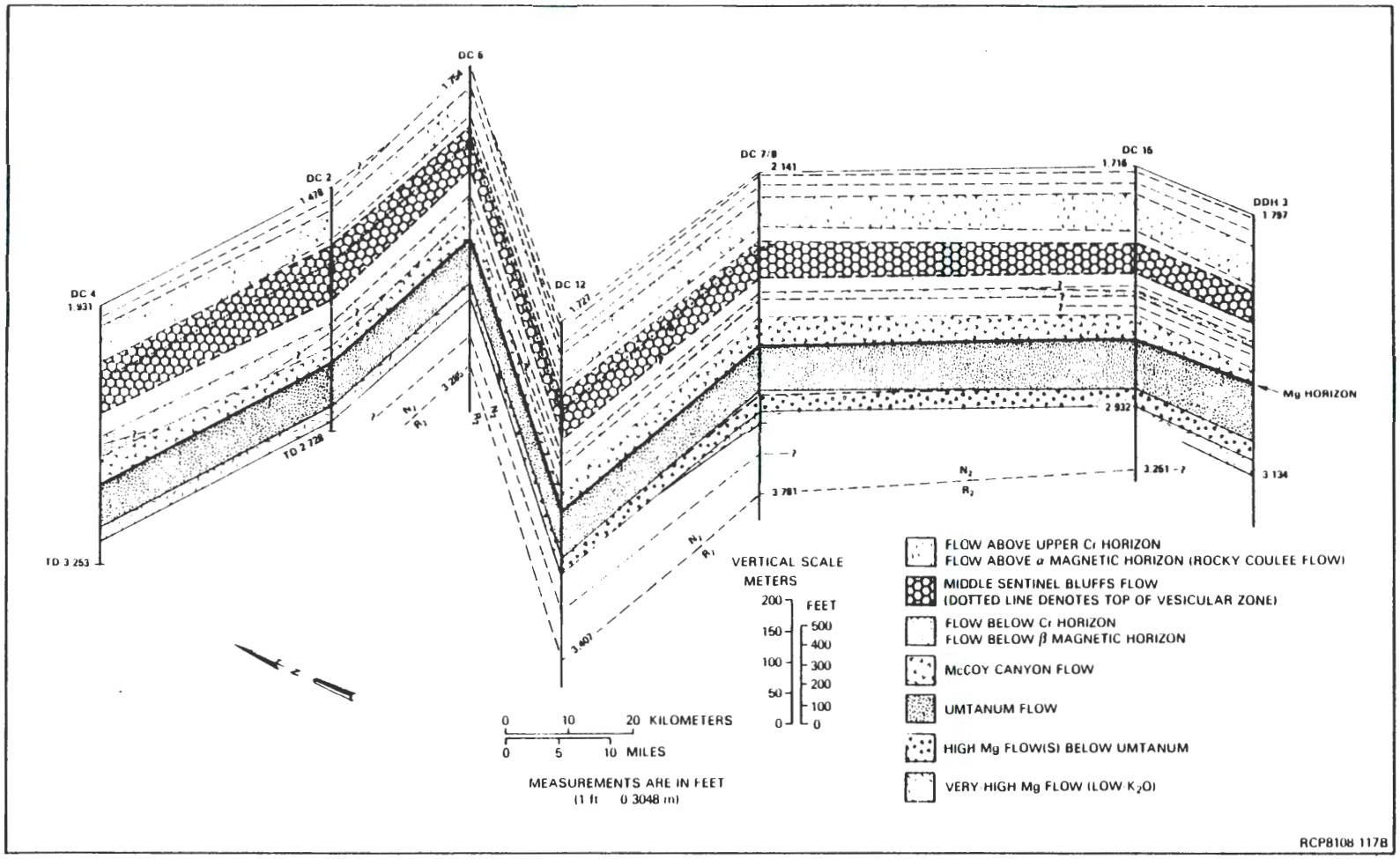

FIGURE 3-24. Fence Diagram, Upper Grande Ronde Basalt, Boreholes DC-4 to DDH-3. (See Fig. 3-18 for location.)

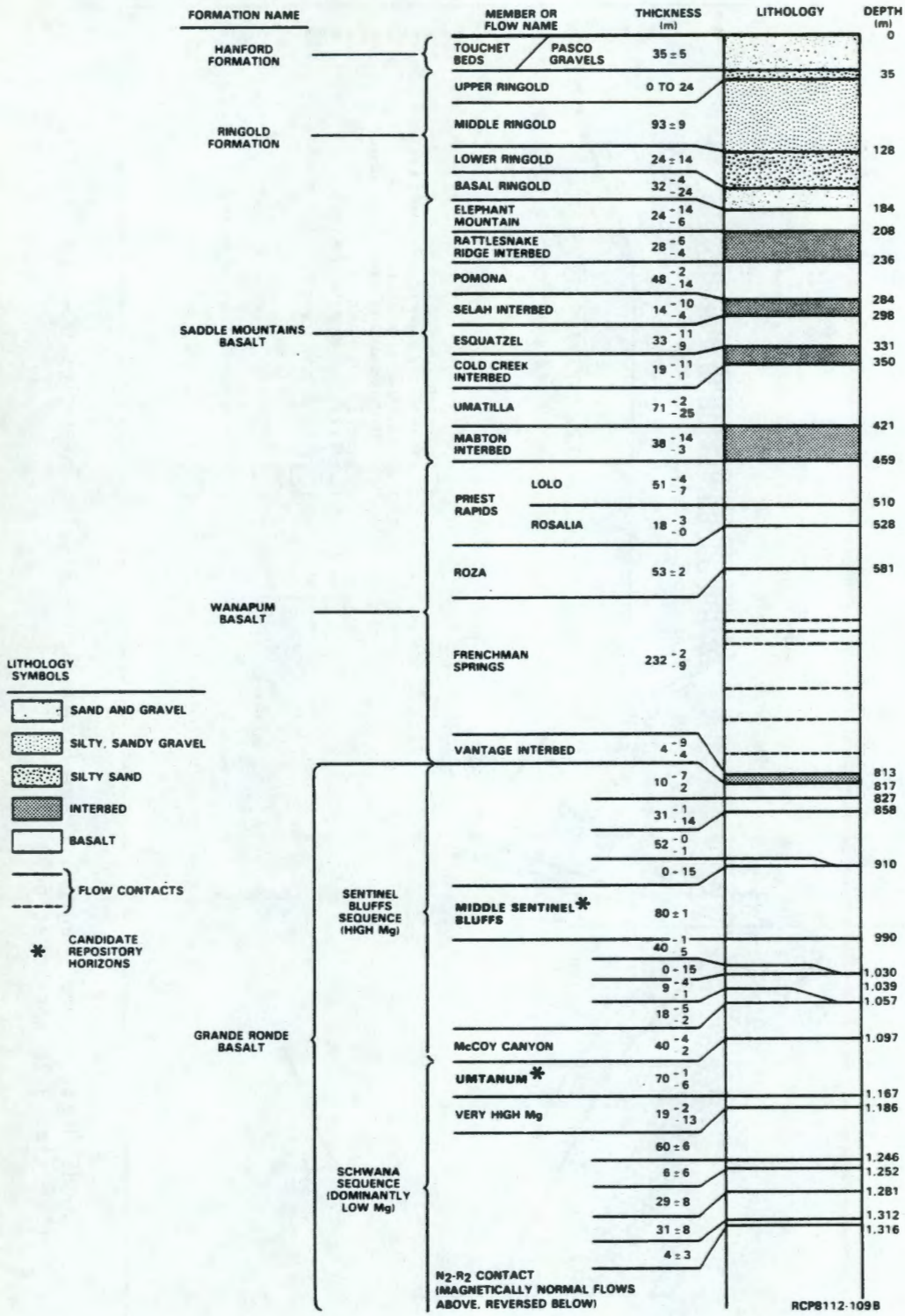

FIGURE 3-25. Stratigraphic Column, Reference Repository Location.

The term intraflow structure is used here to refer to internal units within the flow with relatively uniform macroscopic features. These features are principally defined by the abundance and geometry of fractures, but also include size and abundance of vesicles, flow-top breccia, and the occurrence of pillows. Intraflow structures which may be present within a flow are shown in Figure 3-26. The intraflow structures may vary greatly in thickness, be absent entirely from any given flow, or occur repeatedly within a single flow. Patterns in the way intraflow structures occur, however, allow classification of flows into three general intraflow structure types (Fig. 3-27) (Long, 1978). These types are best thought of as end members with nearly continuous gradations between all three types.

Type I flows lack a distinct entablature and have a poorly developed vesicular flow top. Such flows are invariably diktytaxitic, commonly contain vesicle cylinders, and are relatively thin (10 to 30 meters in thickness), consisting primarily of irregular, tapering columns 1 to 2 meters in diameter. Type II flows are very thick (45 to 75 meters in thickness), exhibiting columnar tiers of alternating entablature and colonnade-type columns in the lower half of the flow that grade upward into a hackly entablature. An oxidized flow top with large, frothy blocks is common and vesicles are abundant in the upper third of the flow. Fanning of columns in the entablature occurs locally. Type III flows are moderately to very thick (30 to 80 meters), exhibiting a sharp break between entablature and colonnade. This break defines a marked difference in fracture abundance and column size. The colonnade in these flows commonly shows pinch-and-swell structure in the columns, and the entablature is a complex pattern of smaller, radiating columns. A crude upper colonnade caps the entablature along parts of many type III flows.

The relationship between internal structures and petrographic textures has been investigated by detailed sampling and petrographic analysis of individual flows (Long and Davidson, 1981).

Type I flows show consistent intersertal to intergranular textures throughout the flow thickness, except for somewhat glassy basalt in the flow top. Morphology of opaques, glass abundance, and glass texture are similar in all parts of the flow beneath the flow top.

Type II flows exhibit textural differences that are spatially associated with the repeated entablature and colonnade tiers (Fig. 3-27). Samples from the lower colonnade have intersertal to intergranular textures and octahedral to cruciform magnetite grains. The entablature portions are characterized by a hyalocrystalline texture, a dendritic morphology of titaniferous magnetite, and an inclusion-charged glassy mesostasis. In addition, the colonnade typically has 15 to 25 volume percent mesostatis, whereas the entablature has 35 to 70 volume percent mesostasis. The middle Sentinel Bluffs flow exhibits characteristics of a type II flow.

9 2 1 2 4 9 5 0 6 8 1

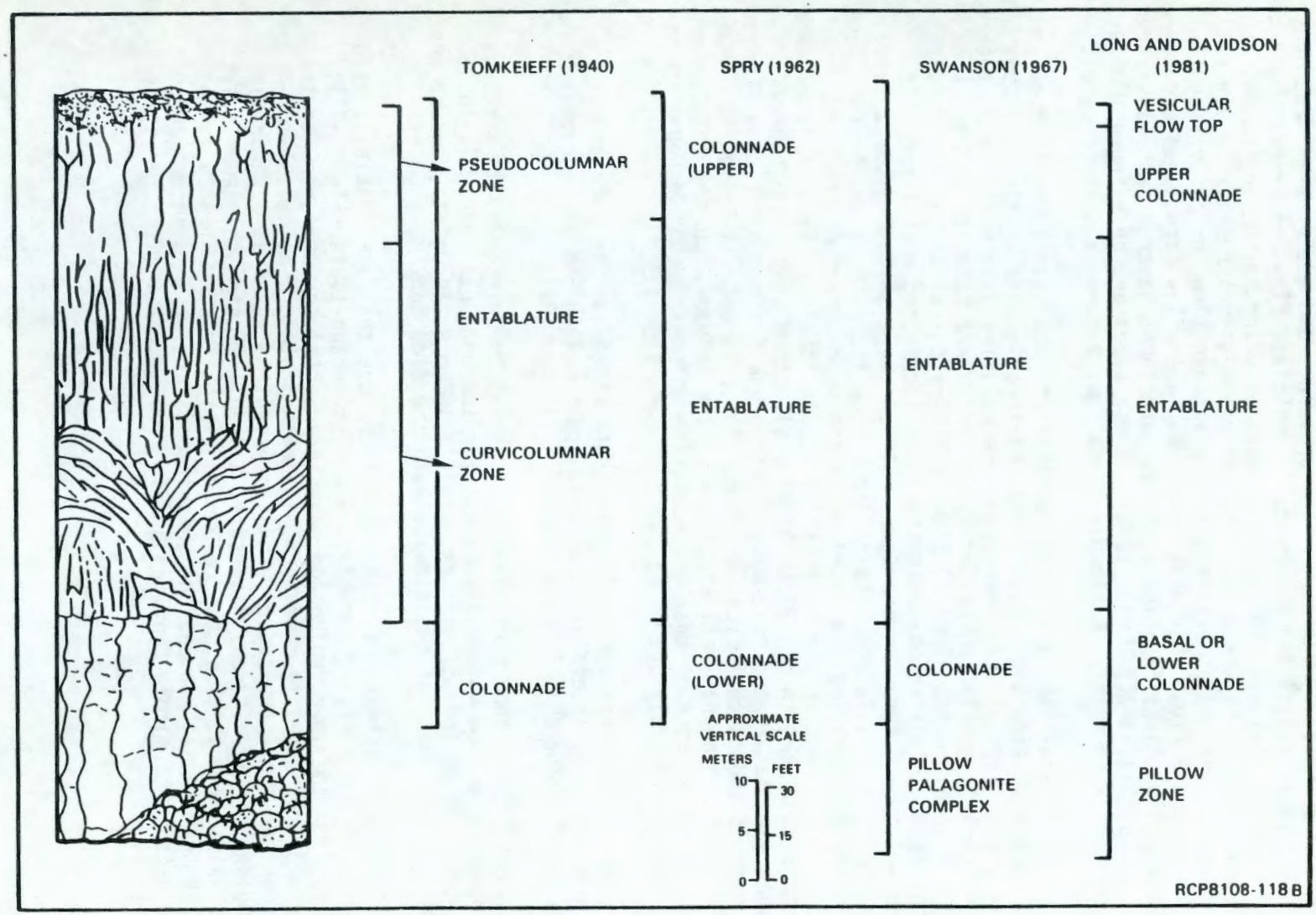

FIGURE 3-26. Typical Intraflow Structures Present in a Grande Ronde Basalt Flow. Nomenclature used in various studies is compared.

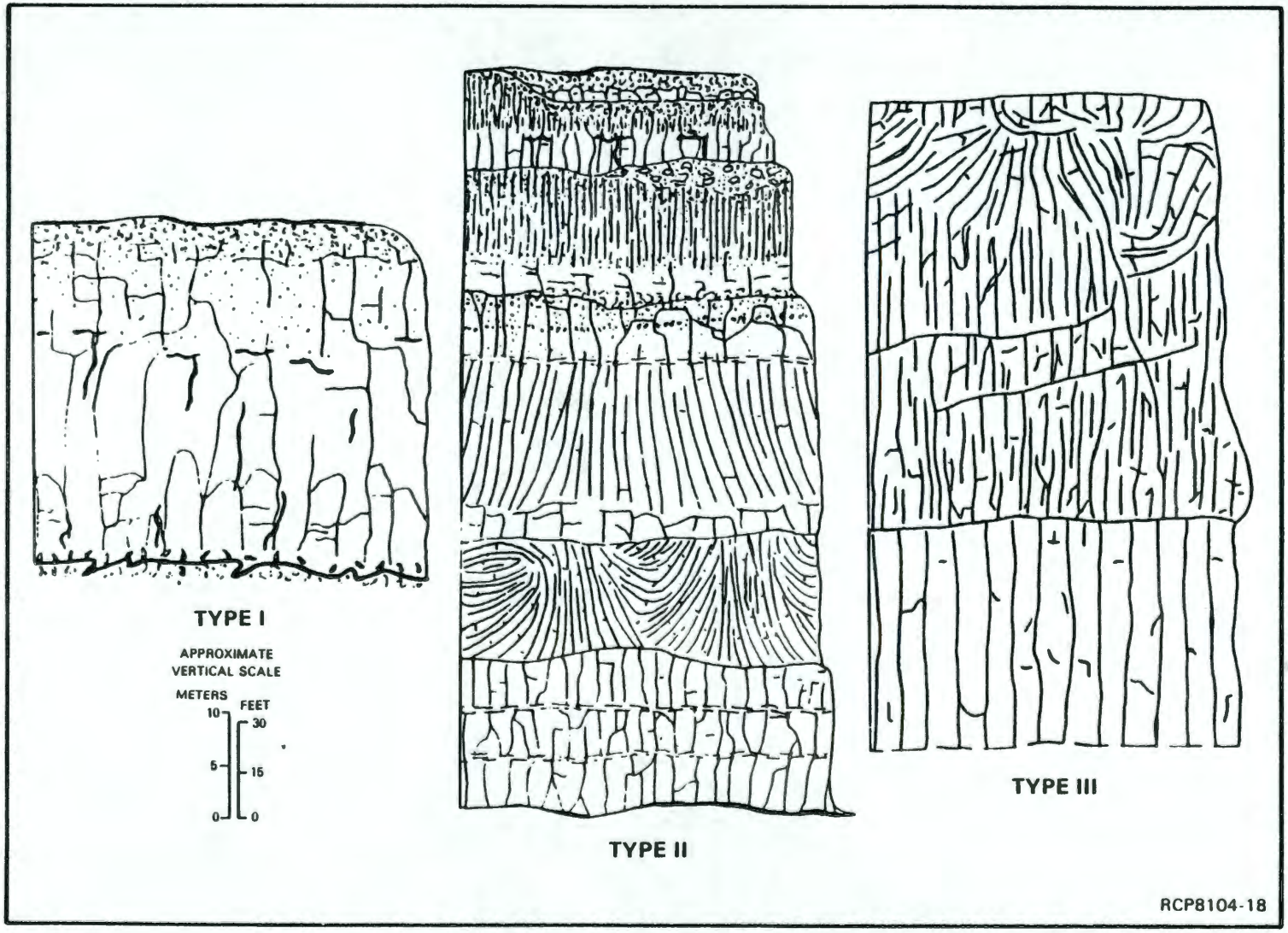

FIGURE 3-27. Intraflow Structure Types (after Long, 1978). (See text for explanation.)

Type III flows exhibit textures associated with entablature and colonnade that are similar to those in type II flows. In type III flows, however, the entablature and colonnade sequence is not repeated. Instead, a single, sharp, entablature-colonnade contact occurs in the lower half of the flow. The Umtanum flow is generally a type III flow; however, boreholes have encountered textural variations in the Umtanum flow that may be type II features (Fig. 3-28).

The petrographic characteristics of entablature and colonnade indicate that the entablature cooled at a more rapid rate than the colonnade. The abundance of mesostasis, the texture of the mesostasis, and the morphology and texture of titaniferous magnetite relative to that of the colonnade all point to a more rapid cooling rate for the entablature.

Significant differences in cooling rate apparently occurred adjacent to one another across the entablature-colonnade contact. Thermal properties of silicate rocks suggest that this cannot occur if thermal conduction alone controls the cooling of the flow (Jaeger, 1961). For this reason, the cooling history of flows has been investigated by a simple, one-dimensional thermal model which mimics the effects of convective removal of heat by ingress of water along cooling joints. The results of the model (Wood and Long, 1981) show that it is possible to quench the interior of a flow if the depth of water ingress is controlled by the position of the solidification front in the flow. Thus, if the flow exterior had solidified slowly and the flow interior was inundated by water from deranged drainage or perhaps heavy rainfall, the interior of the flow would cool at a much higher rate than the previously crystallized outer parts of the flow.

3.5.4.1.3 Lateral Variation. Intraflow structures are generally not constant over distances greater than 1 kilometer (Swanson et al., 1979c), although considerable continuity exists in some flows such as the Umtanum (Long and Davidson, 1981). The previously discussed relationship between internal structures and petrographic textures has been used to determine the internal structures of the McCoy Canyon and Umtanum flows. Data from surface exposures and drill core have been used to construct fence diagrams that illustrate the lateral variations in internal structures of these flows (Long and Davidson, 1981). The fence diagram for the Umtanum flow is included as Figure 3-29.

The thickness of the basal colonnade of the Umtanum flow is not consistently correlatable with total flow thickness; in most core holes, however, it constitutes about 10 percent of the total flow thickness. The entablature is also variable in its thickness, but in general it is relatively thick (approximately 50 meters). It exhibits tiering in the southeastern portion of the Pasco Basin and in DH-5 and displays a relatively thick flow-top breccia in the Emerson Nipple section, RRL-2, DC-8, and DDH-3.

9 2 1 2 4 9 5 0 6 8 3

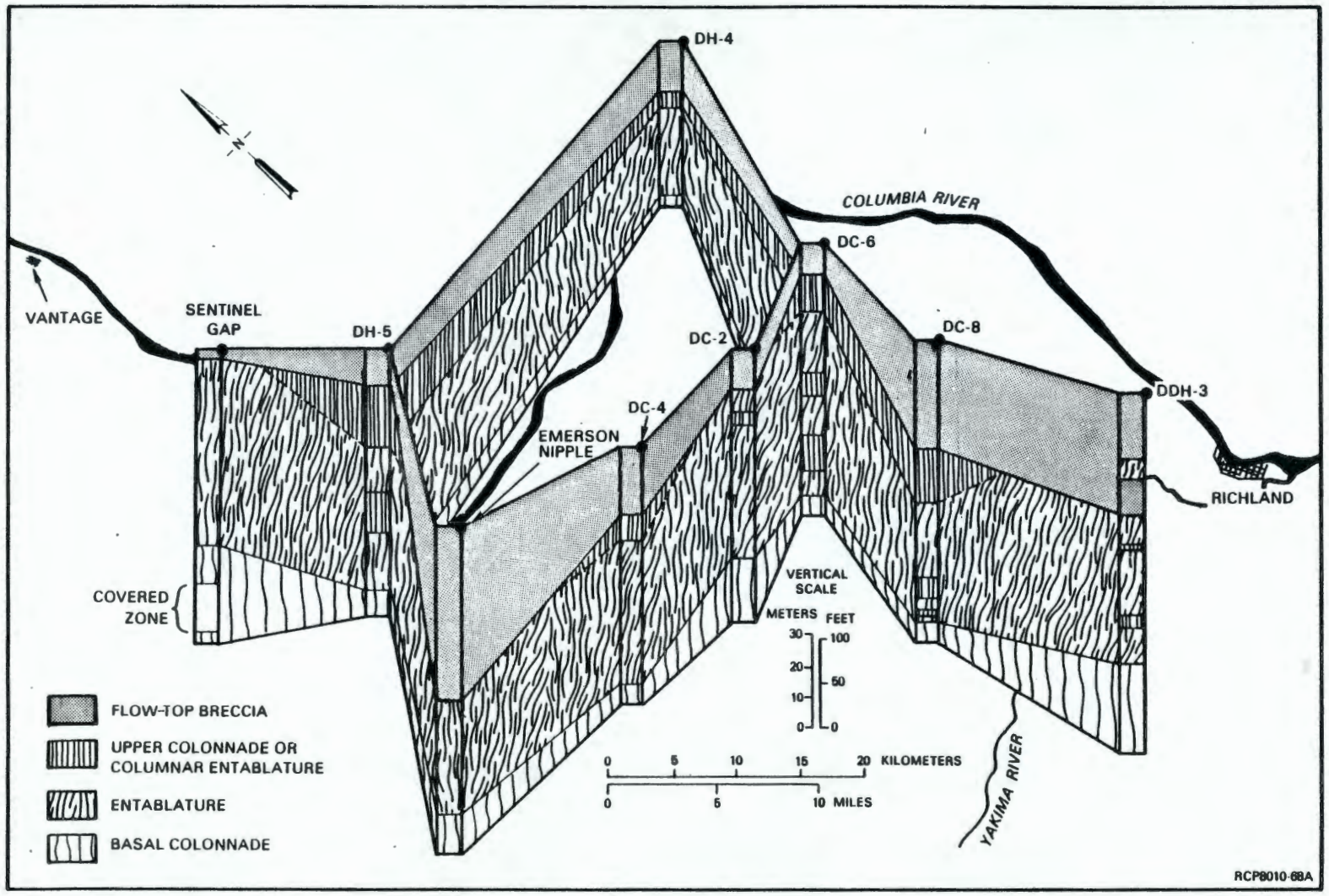

FIGURE 3-28. Fence Diagram, Umtanum Flow. This figure is an illustration of the lateral variation of internal structures of the flow in subsurface borings and surface exposures. (See Fig. 3-18 for location.)

9 2 1 2 4 9 5 0 6 8 5

FIGURE 3-29. Cliff Exposure, Umtanum Flow at Emerson Nipple Section. Note the thick flow breccia and thin colonnade. Prominent fanning arrays occur in the entablatures and these features are spatially associated with areas of thickening of the overlying flow top. The radiating columns of the fan in conjunction with the flow top and lower colonnade may be of hydrologic significance.

The well-defined upper colonnade of the Umtanum flow occurs in five of the boreholes but, as in most type III flows, it is highly irregular in its thickness.

Actual field exposures of the Umtanum flow are limited to two localities: (1) Emerson Nipple area and vicinity and (2) Sentinel Gap area. The flow pinches out to the north, somewhere between Sentinel Gap and Sunland Estates (Fig. 3-18); hence, laterally extensive exposures are not available for study. Exposures that are available, however, provide considerable information about intraflow structures. One exposure has been photographed and mapped in order to illustrate the types of internal differences that occur across this exposure (Fig. 3-29). At the Emerson Nipple section, the Umtanum flow has an anomalously thick flow top that comprises approximately 50 percent of the flow and has a thickness of 40 meters. This flow top is principally a flow-top breccia with clasts of vesicular and nonvesicular basalt cemented by basalt or palagonite. These clasts range in size from approximately 2 to approximately 30 centimeters with a mean size of approximately 10 centimeters. Across approximately 400 meters of exposure at the Emerson Nipple section, the flow top maintains a great thickness, although it is somewhat variable (Fig. 3-29). In contrast, the Umtanum flow at the Sentinel Gap section has a thin (approximate 5 meter) flow top which is vesicular, but has little or no breccia.

The entablature at both localities is thick relative to the colonnade. At Emerson Nipple, the colonnade is 5 to 8 meters thick; whereas, the entablature is 30 to 75 meters thick. The entablature at Sentinel Gap is 40 meters thick; whereas, the colonnade is at least 15 meters thick. Poor exposure may conceal a second, lower entablature that would make the Umtanum flow here a type II flow.

Evidence from limited exposure of the Umtanum flow suggests, then, that a major intraflow structure, the flow-top breccia, thins markedly in the 20 kilometers from Emerson Nipple to Sentinel Gap. It is also possible that the flow changes from a type III to a type II flow over that same distance.

The details of fracture patterns within the entablature also vary significantly between the two exposures of the Umtanum flow. At the river-level exposure at Sentinel Gap, the entablature exhibits a distructive, hackly fracture pattern with only a suggestion of a columnar structure. At Emerson Nipple, columnar structure is well developed as well-formed, slender columns. Locally, these columns radiate as inverted fans (Fig. 3-29) with centers spaced at intervals ranging from a few to 160 meters. From these observations, it is predicted that orientation of column-defining fractures, especially in the entablature, will vary considerably. On the other hand, parts of the Umtanum flow interior are expected to have a very hackly character with approximately random orientation of fractures.

Figure 3-29 also illustrates that the radiating fans in this particular exposure have flow-top breccia at their apices. This breccia is connected to the main body of flow-top breccia and, thus, it forms a dimple on the interface between the flow-top breccia and the underlying entablature. The origin of the dimple is uncertain, but it has apparently affected the formation of cooling joints locally, thus creating the inverted fans. The occurrence of the dimples is particularly significant because the relatively porous nature of the flow top combined with the well-developed columnar fractures of the inverted fans may significantly reduce the amount of hydrologic isolation provided by the host flow itself. In order to check this possibility, it will be necessary to hydrologically test these features, this probably can only be accomplished in a test facility at repository depths.

Basal colonnade at the Emerson Nipple locality ranges from approximately 7 to 12 meters in thickness. As previously stated, there may be two colonnades at Sentinel Gap. The exact way in which the transition from one to two colonnades takes place is uncertain, but judging from exposures north of Vantage, the transition would be gradual rather than abrupt. The lower colonnade at Emerson Nipple may correlate with the lowest colonnade at Sentinel Gap. This means that major changes in fracture abundance or average column diameter are to be expected in at least some parts of the Umtanum flow interior; that is, colonnade may occur in what would otherwise be homogeneous entablature. Evidence for such occurrence has been obtained from subsurface cores as illustrated in Figure 3-28.

Studies of laterally extensive surface exposures of Grande Ronde Basalt indicate that intraflow structures of flows change laterally. They do so, however, within certain limits. Some of the changes, such as appearance or disappearance of pillowed zones, can be predicted if paleogeography is known or can be assumed. The locations of other features, such as thinning of colonnade, multiple tiers of entablature or colonnade, fanning of entablature columns, and thickening of flow-top breccia probably cannot be predicted with any certainty. These features should, however, be anticipated in the Umtanum and other Grande Ronde flows, and they can be objectives for hydrologic testing at depth in an exploratory test facility. With additional data from field observations and from deep boreholes, the number and spacing of these features that might occur in any given volume of the Umtanum flow could be predicted.

3.5.4.1.4 Fracture Characteristics. A summary of fracture studies in Grande Ronde Basalt is contained in Long and Davidson (1981). The vast majority of fractures in Grande Ronde Basalt are joints created by thermal contraction during cooling of individual flows. Qualitatively, the dominant fractures range from those that define well-formed, regular, polygonal solids to those that define irregular, elongate to equant blocks. There is nearly an entire spectrum from regular, well-formed columns to irregular (hackly) blocks.

9 2 1 2 4 9 5 0 6 8 7

The great majority of fractures in drill core have narrow "apertures" (less than 0.5 millimeter) filled with multiple generations of secondary minerals (see Section 6.1). Information from fracture logging of drill cores was used to calculate the volume percent of fracture openings (filled or unfilled) in the core. The total volume percent of all fractures is less than 0.4 volume percent. The volume of unfilled fractures ranges from 0.025 to 0.059 volume percent. These results suggest that the volume of unfilled fractures, particularly in the dense interior of Grande Ronde flows, is small, and thus the total fracture porosity of these rocks is comparably small. Hydrologic testing of such zones is required to assess their hydraulic conductivity.

3.5.4.1.5 Lithology at the Reference Repository Location. Mineralogy, fracture abundance, degree of fracture filling, characteristic fracture patterns, and character of flow-top breccias in the reference repository location are all expected to be similar to those features in Grande Ronde Basalt (Long and Davidson, 1981), except for a predicted lack of associated pillow zones and associated palagonite. Additional exploratory drilling will be required to confirm this prediction.

For the middle Sentinel Bluffs flow, isopachs of the flow top (Fig. 3-30) and total flow (Fig. 3-19) indicate that, within the reference repository location, the flow top is less than 6 meters in thickness and that the total flow is greater than 76 meters in thickness. Surface exposures and boreholes show that the flow top of the middle Sentinel Bluffs flow is relatively constant throughout the Pasco Basin and does not exceed 12 meters.

The interior of the middle Sentinel Bluffs flow is expected to consist of repeated tiers of entablature and colonnade. Entablature sections will be relatively fine-grained basalt with abundant mesostasis, whereas the colonnade sections will be medium-grained basalt with relatively low mesostasis (Long and Davidson, 1981, Fig. 5-26). These tiers are not anticipated to impact long-term repository performance, except that slight differences in sorption may occur between entablature and colonnade. Slight differences in the rock machanics characteristics of entablature and colonnade may also exist (see Chapter 4).

A vesicular zone occurs in the upper third of the middle Sentinel Bluffs flow. This zone consists of abundant vesicles in otherwise intact basalt and is traceable from one borehole to another (see Fig. 3-22, 3-23, and 3-24). Cooling joints pass through this zone uninterrupted and vesicles do not appear to be interconnected. Within the reference repository location, there is adequate thickness below the vesicular zone for repository construction. Indeed, the vesicular zone may serve as a guide for positioning of the repository tunnels; short boreholes could be drilled upward to intersect the vesicular zone as a marker horizon. This would avoid penetration of the flow top or bottom.

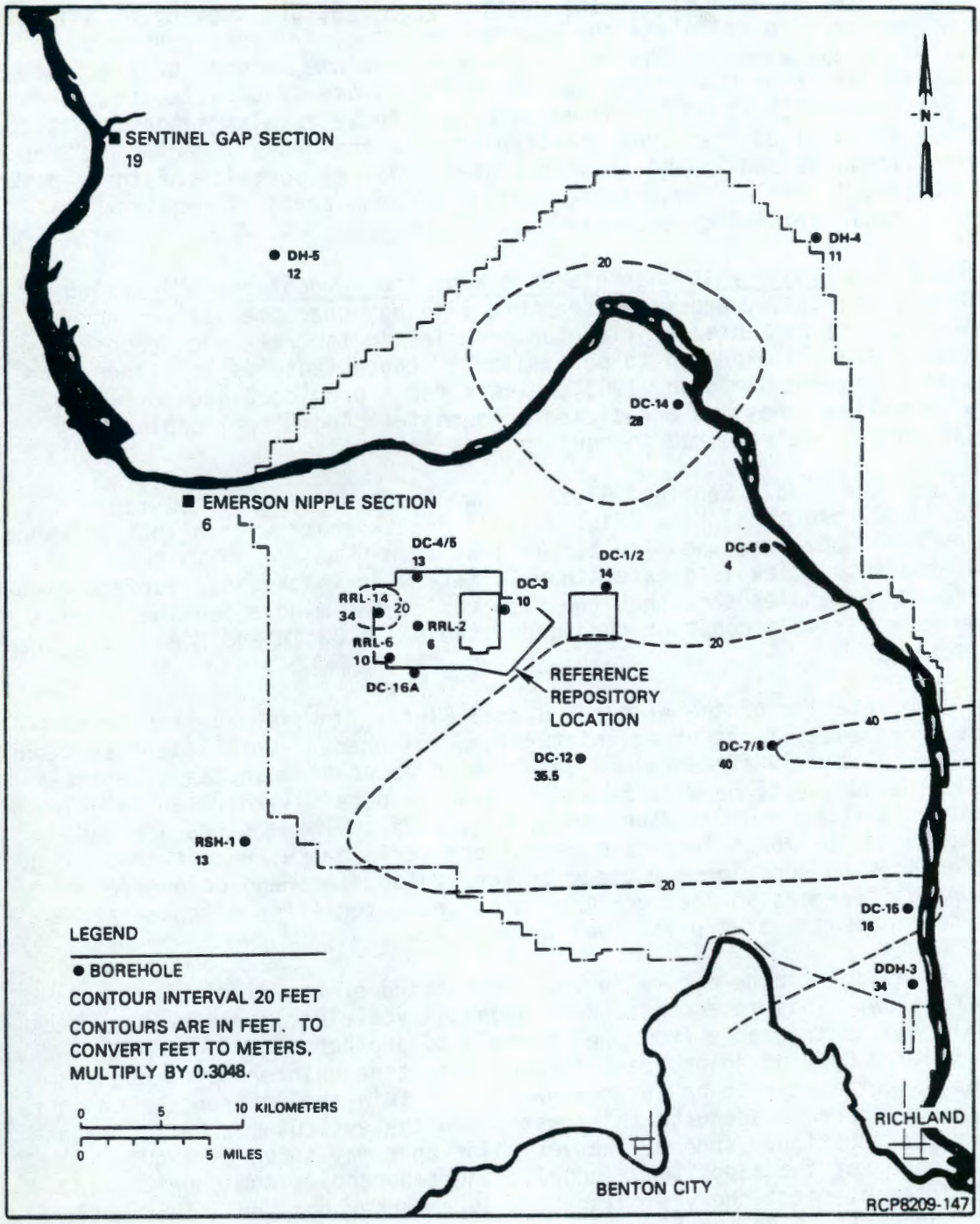

FIGURE 3-30. Isopach Map of the Flow Top of the Middle Sentinel Bluffs Flow, Pasco Basin and Vicinity.

Fractures in the middle Sentinel Bluffs flow are expected to be filled with secondary minerals. As with any basalt flow, there is the possibility of encountering areas of vesiculation and/or brecciation associated with the intersection of two emplacement lobes. Available data on the middle Sentinel Bluffs flow suggests that the probability of such occurrences is very low.

For the Umtanum flow itself, isopachs of the flow top (Fig. 3-31) and total flow suggest that the flow top in the reference repository location ranges from 17 meters thick to at least 45 meters thick. Recently obtained borehole data (RRL-2) indicate that localized increase or decrease in the flow-top thickness and related fanning joints occurs in the Umtanum flow in the reference repository location.

Examination of the Umtanum flow top indicates that it is a quench breccia that probably formed when the Umtanum flow was emplaced into relatively deep water. Evidence for such an origin includes rinds of quenched basaltic glass on breccia clasts and the very fine grain size of the Umtanum flow. Thermal shock and convection resulting from interaction of the magma with the water apparently brecciated and mixed the outer carapace of the flow to form the flow top. The implication of this mode of origin of the Umtanum flow top is that significant differences in flow top thickness can be expected to occur within the reference repository location. This is because the exact thickness of breccia is probably controlled by a combination of variable conditions such as eruption rate of the flow, density of the initially formed breccia, and water depth.

The dense interior portion of the Umtanum flow in the reference repository location is expected to be dominantly a fine-grained basalt with abundant mesostasis (Long and Davidson, 1981). Locally, colonnade-type textures will also occur in the flow interior, possibly in association with fanning columns. Fractures are expected to be filled with secondary minerals. Vesicular zones could locally occur in the flow interior due to overlapping emplacement lobes. Borehole data and observations of surface exposures of the Umtanum flow suggest that the probability of such occurrence is low (less than 15 percent). The flow top of the Umtanum flow is expected to be similar in character to that described in Section 3.5.4.1.3.

3.5.4.2 Wanapum Basalt. The Wanapum Basalt consists of three members in the Pasco Basin: Frenchman Springs, Roza, and Priest Rapids. The Vantage interbed, or where absent, a minor saprolite zone, separates this formation from the underlying Grande Ronde Basalt; the Mabton interbed separates the Wanapum Basalt from the overlying Saddle Mountains Basalt (Fig. 3-17). Wanapum Basalt is thickest (about 350 meters) in the central area of the Cold Creek syncline. It thins from west to east and over the Rattlesnake Mountain and Umtanum Ridge-Gable Mountain structures. A detailed discussion of Wanapum Basalt members within the Pasco Basin and Cold Creek syncline is given in Myers/Price et al. (1979) and Reidel and Fecht (1981).

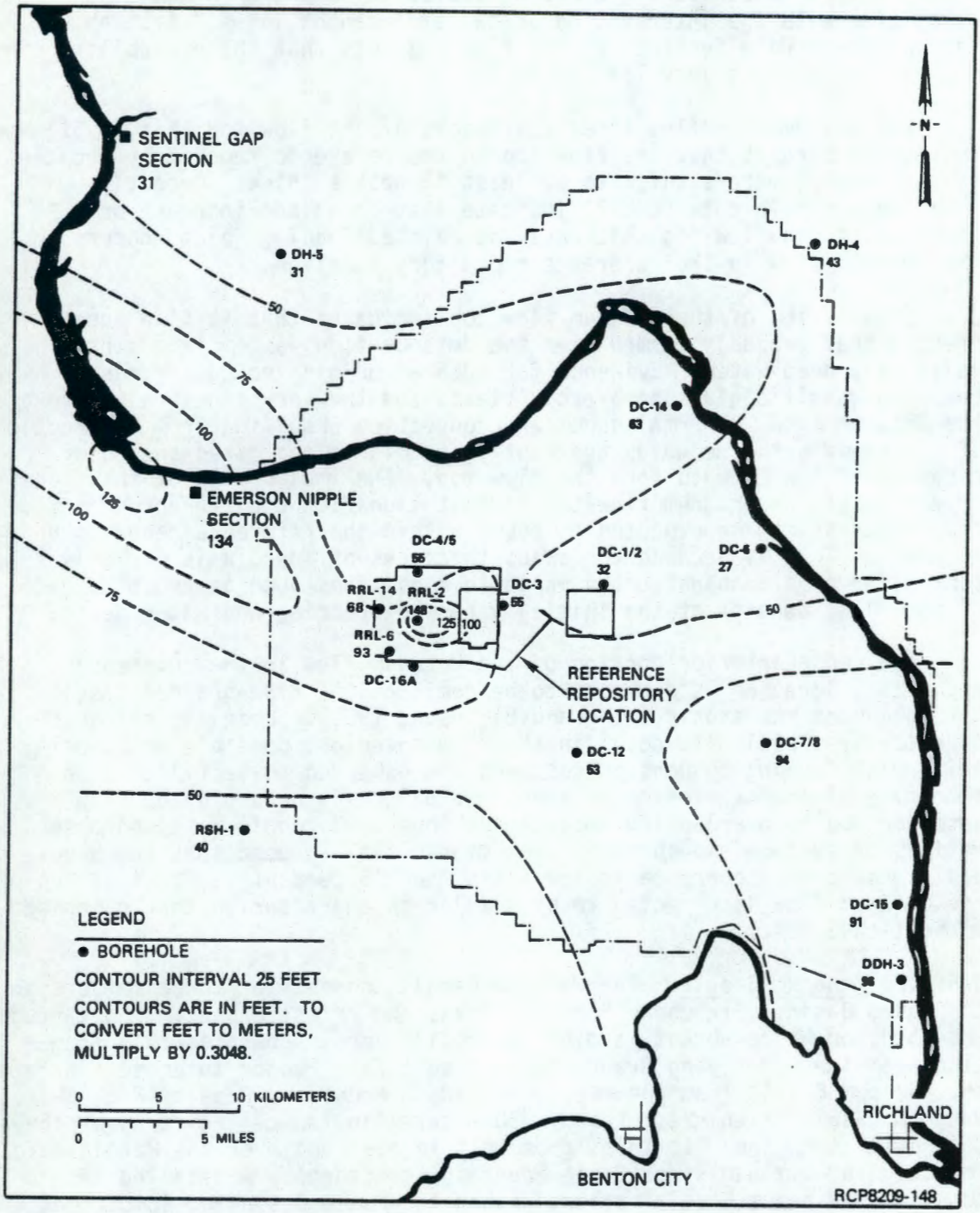

FIGURE 3-31. Isopach Map of the Flow Top of the Umtanum Flow.

3.5.4.3 Saddle Mountains Basalt. The Saddle Mountains Basalt consists of seven members (Fig. 3-17) in the Pasco Basin: the Umatilla, Wilbur Creek, Asotin, Esquatzel, Pomona, Elephant Mountain, and Ice Harbor. With the exception of the Wilbur Creek, all members are present in the Cold Creek syncline area. The general characteristics of these members are discussed in Myers/Price et al. (1979, Table III-2) and Reidel and Fecht (1981). Thickness variations are greater and more complex in the Saddle Mountains Basalt than in the Wanapum Basalt because of (1) thinning over topographic highs, (2) a greater time between eruptions, and (3) the limited volume of many flows (Reidel and Fecht, 1981, Table 3-4).

3.5.4.4 Ellensburg Formation. Within the Pasco Basin, sediments of the Ellensburg Formation are primarily interbedded in the Wanapum and Saddle Mountains Basalts (Fig. 3-17), but occur in the Grande Ronde Basalt in one borehole, RSH-1 (Fig. 3-18). The lateral extent and thickness of these sediments generally increase upward in the section due to increased time between eruptions. Two major facies, volcaniclastic and fluvial, occur either as distinct or mixed deposits. A detailed discussion of the Ellensburg Formation within the Pasco Basin is contained in Myers/Price et al. (1979) and Reidel and Fecht (1981).

3.5.4.5 Ringold Formation. The Ringold Formation overlies the Columbia River Basalt Group within most of the Pasco Basin (Fig. 3-17), except where (1) basalt crops out, (2) the glaciofluvial Hanford formation onlaps ridges above the margin of the Ringold Formation, or (3) it has been eroded and Hanford sediments were deposited directly on basalt. The Miocene-Pliocene Ringold Formation is a fluvial sedimentary unit with some lacustrine and fanglomerate facies. The stratigraphy of the Ringold Formation within the site is presented in Tallman et al. (1981).

3.5.4.6 Hanford Formation. A discussion of the Hanford formation within the Pasco Basin and Cold Creek syncline is contained in Myers/Price et al. (1979) and Tallman et al. (1981). The Hanford formation, chiefly the Pasco gravels, overlies the Ringold Formation throughout the reference repository location (Fig. 3-17). The sediments primarily consist of gravel to sand with varied bed forms and represent relatively high-energy, fluvial deposition during Pleistocene flooding. The Pasco gravels have been subdivided into the Missoula and Pre-Missoula gravels by the Puget Sound Power and Light Company (PSPL, 1982).

3.5.4.7 Surficial Deposits. Alluvium, dune sand, loess, talus, colluvium, and landslide debris occur in the Pasco Basin. Most of these deposits are Holocene, but some are Pleistocene (Lillie et al., 1978; Myers/Price et al., 1979). The surficial deposits of the reference repository location are shown in Figure 3-15.

9 2 1 2 4 9 5 0 6 9 2

3.5.5 Future Rock Formation and Alteration

Future rock formation and alteration likely to occur over the next 10,000 years in the Pasco Basin are minimal. The most likely rock formation processes are deposition of volcanic ash, deposition of fluvial sand and gravel, and possible deposition of sand and gravel by catastrophic flooding related to glaciation. Eruption and deposition of additional flows of Columbia River basalt are extremely unlikely (Section 3.7.2). Eruption of lava outside the reference repository location and consequent deposition on the surface of the reference repository location would not adversely impact a repository. Eruption along a linear vent system through the reference repository location would breach repository containment. Such an event is much less likely than eruption on the plateau in general and is not considered a significant threat to repository performance. None of these processes are therefore likely to have a significant impact on the isolation capabilities of the reference repository location.

The dominant rock-alteration process is continued alteration of mesostasis glass along fractures in basalt; this results in deposition of silica, smectite, and zeolite in open fractures or vugs. The most recent material filling the vugs and fractures is most commonly silica (see Section 6.1); it seems highly probable that such deposition will continue over the next 10,000 years. Filling of fractures and vugs in this manner will act to decrease permeability of the basalts. It is conceivable that a change in the groundwater composition could result in partial dissolution of fracture fillings. However, the thermodynamic instability of the mesostasis glass in the basalts means that reaction, hydration, and ion exchange between glass and groundwater will determine the groundwater geochemistry under a given pressure-temperature regime. These reactions will tend to maintain saturation of stable silicate phases. (See Section 5.1.5 for groundwater chemistry and saturation data.) Dissolution of fracture fillings is then likely to be volumetrically insignificant and, in any case, would probably be counterbalanced by deposition elsewhere in the system.

The length of time over which diagenesis has occurred is also significant. The exact rate at which it has occurred is not known, but it probably has been distributed over much of the 15 million years since emplacement of Grande Ronde Basalt. During any given 10,000-year increment of that time, alteration of the rock would be very slight.

Diagenesis is also occurring in the interbeds and in the Ringold and Hanford Formations and is expected to result primarily in increased silica and calcium-carbonate cementation of the sedimentary rocks of the site. Such additional cementation, as well as any additional compaction, will generally act to decrease the porosity and permeability of the sediments.

9212495069 3

Alteration processes for both sediments and basalts at the reference repository location thus apparently tend to decrease the permeability of the rocks involved. Local increases in permeability due to dissolution of fracture fillings or cements cannot be entirely ruled out, but the inherent instability of phases undergoing alteration relative to the phase being formed suggest that dissolution of alteration and cementation products will not be volumetrically significant.

3.5.6 Status

The general stratigraphic setting of the Pasco Basin and Cold Creek syncline is well understood, and there are no currently known stratigraphic or lithologic factors that would preclude the siting of a repository in one of two candidate horizons within the reference repository location. Additional detailed stratigraphic and lithologic investigations are required to adequately assess the candidate repository horizons and surrounding strata within the reference repository location and to refine the stratigraphy of the Ringold and Hanford Formations to determine more precisely the late-Miocene to Holocene deformation rate. These studies are further detailed in Chapter 13.

THIS PAGE INTENTIONALLY
LEFT BLANK

9 2 1 2 4 9 5 0 6 9 5

3.6 GEOPHYSICAL STUDIES OF THE HANFORD SITE AND THE REFERENCE REPOSITORY LOCATION

Geophysical surveys that have been conducted in the Pasco Basin include ground-magnetic and gravity surveys designed to locate faults, folds, erosional channels, and related geologic structures in the uppermost Saddle Mountains Basalt flows and the overlying 50 to 150 meters of sediments. In addition, reflection-seismic, gravity, aeromagnetic, and magnetotelluric surveys have been conducted to obtain geologic information from the basalt surface to depths as great as the crust-mantle boundary. Other areas addressed in this section include remote sensing, heat flow, and borehole geophysics.

3.6.1 Seismic Reflection and Refraction

The only regional seismic survey was conducted by Hill (1972; 1978). He obtained deep seismic refraction data from explosions in Greenbush, British Columbia, recorded on a due-south profile across the Columbia Plateau. Using quarry-blast data in conjunction with the Greenbush explosions, Hill (1978) interpreted a crustal thinning from 35 kilometers beneath the mountain terrain of northeastern Washington to about 25 kilometers beneath the Pasco Basin. He also suggested a general thickening of the crust below the Blue Mountains southeast of the Pasco Basin.

Exploration-seismic surveys conducted on the Hanford Site between 1959 and 1975 are discussed in Myers/Price et al. (1979) and Holmes and Mitchell (1981). Early surveys consisted mainly of short (less than 2 kilometers) seismic-reflection and -refraction profiles conducted primarily to test methodology, measure the thickness of sediments overlying the basalt, and determine seismic velocities in different sediment layers.

In 1978, the seismic-reflection technique was tested by the BWIP to determine whether it was possible to obtain penetration of the seismic signal down to and reflection from the level of the Umtanum flow (Heineck and Beggs, 1978). The test showed that the reflection method could give a rapid determination of the attitudes of some basalt layers, especially the uppermost basalt flow. The ability of the technique to obtain reflections from the Umtanum flow was not successful. However, the technique was found to be useful for detecting the top of basalt.

During 1979 and 1980, 195 line kilometers (121 line miles) of seismic reflection profiling were completed using the VIBROSEIS energy source. Details for these surveys, including field techniques, data processing, and interpretations are discussed in Heineck and Beggs (1978), Myers/Price et al. (1979), and Holmes and Mitchell (1981). The primary purpose of these surveys was to locate structural features; therefore, most of the seismic lines were run across the projected strike of Yakima folds (Fig. 3-32).

9 2 1 2 4 9 5 0 6 9 6

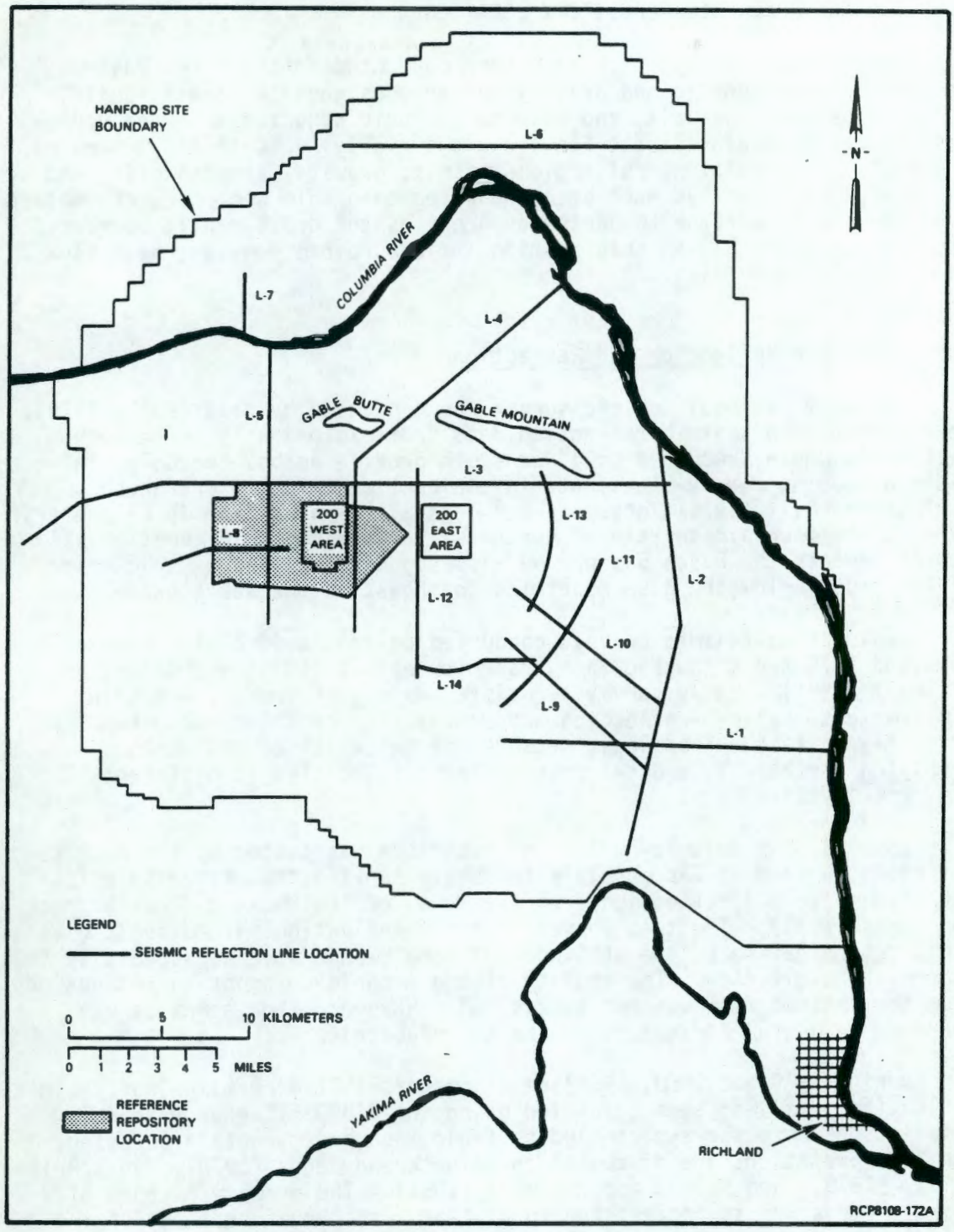

FIGURE 3-32. Location of 1979 and 1980 Seismic-Reflection Surveys.

Seismic-reflection anomalies identified in preliminary interpretations made by Seismograph Services Corporation are shown in Figure 3-33. Seismograph Services Corporation established several criteria for anomaly detection, such as severe and radical character changes, reflection-time offsets, rapid changes in reflector dip, reflection discontinuities, and apparent diffraction patterns. All Seismograph Services Corporation anomalies were considered in delineating potential repository sites during the site-identification process (see Chapter 2).

Using additional geophysical and geologic information, the BWIP qualitatively classified the anomalies identified by Seismograph Services Corporation into general categories (Fig. 3-33) ranging from a "real" bedrock or geologic structure to a data-processing phenomenon (Holmes and Mitchell, 1981). Many anomalies identified appear to be related to near-surface phenomena. A more detailed quantitative assessment of the seismic reflection data is planned for future work (Chapter 13). Interpretations of seismic-reflection-survey data were used to prepare the top-of-basalt map contained in Section 3.7.2.3.2.

3.6.2 Magnetics

Aeromagnetic and ground-magnetic surveys have been used on the Columbia Plateau to support structural studies. Due to the relative ease of data collection for the aeromagnetic survey, this exploration technique has received wider use than the ground method. Aeromagnetic surveys in the plateau were primarily designed to explore structures within the youngest units of the basalt sequence and, thus, are predominantly low-level surveys. Ground-magnetic studies have been used to provide detailed studies of small-scale geologic structures that are not easily detected by aerial surveys and to further define aeromagnetic anomalies. Interpreted sources of aeromagnetic anomalies include (1) structurally controlled topography (e.g., anticlines), (2) basalt dikes, (3) faults, and (4) valley-filling basalt flows.

3.6.2.1 Aeromagnetic Surveys. Ten aeromagnetic surveys have been performed over parts of the Columbia Plateau (Fig. 3-34). Parameters for these surveys are tabulated in Table 3-2. Three of these surveys (H, E, and C, Fig. 3-26) are regional, while the remaining surveys were designed to investigate localized areas of the plateau. In addition, the compilation survey map of Idaho (USGS, 1978) covers parts of the eastern Columbia Plateau.

Regional survey H (Fig. 3-34 and Table 3-2) was designed to investigate very large regional sturctures. Along the western margin of the plateau, mapped structures in the basalt correspond, in places, with magnetic trends; these trends continue eastward beyond recognized deformation in the basalts. Swanson (in Zietz et al., 1971) suggested this may be evidence of locally reactivated basement structures which deformed the western margin of the plateau.

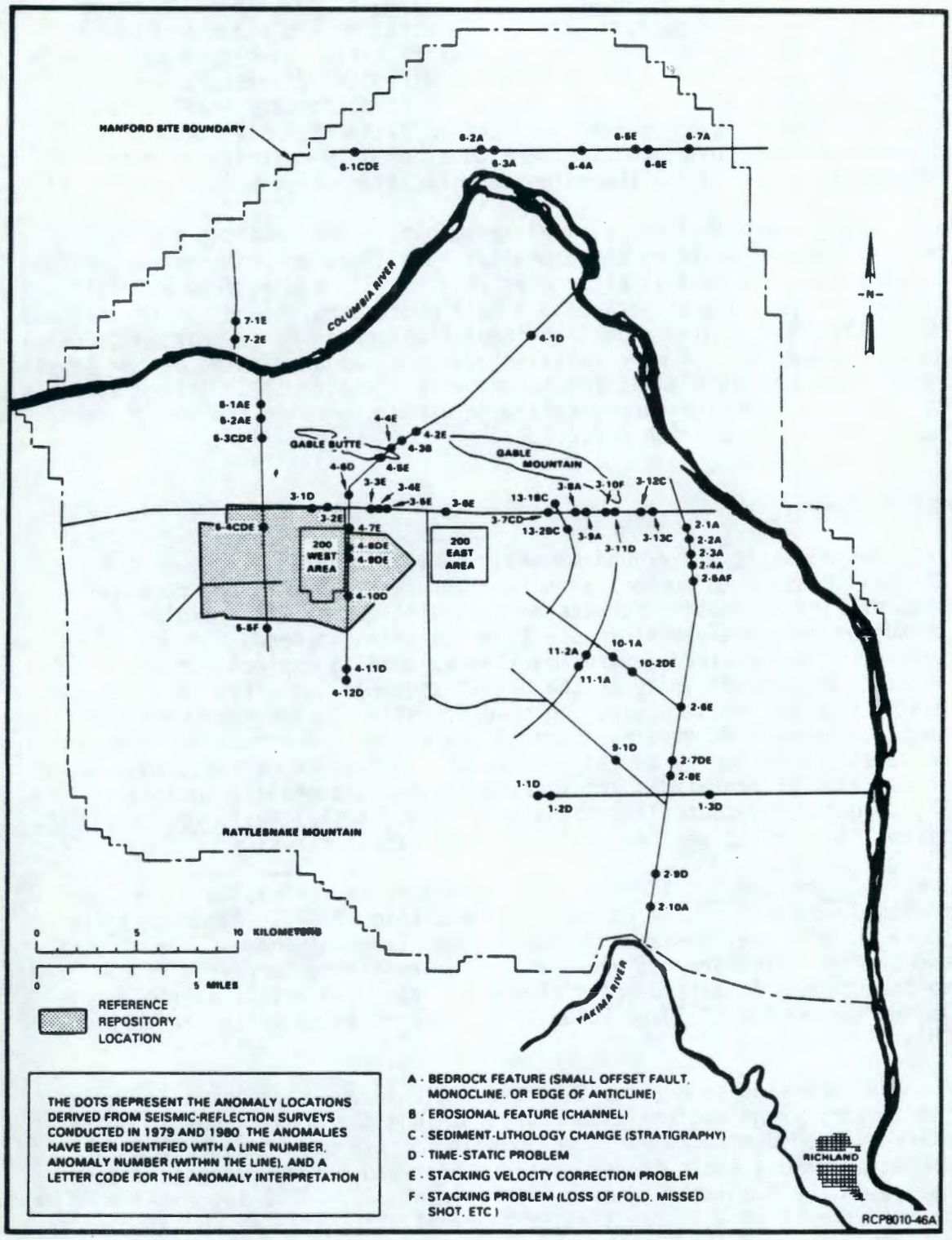

FIGURE 3-33. Seismic-Reflection Anomaly Location Map.

9 2 1 2 4 9 5 0 6 9 9

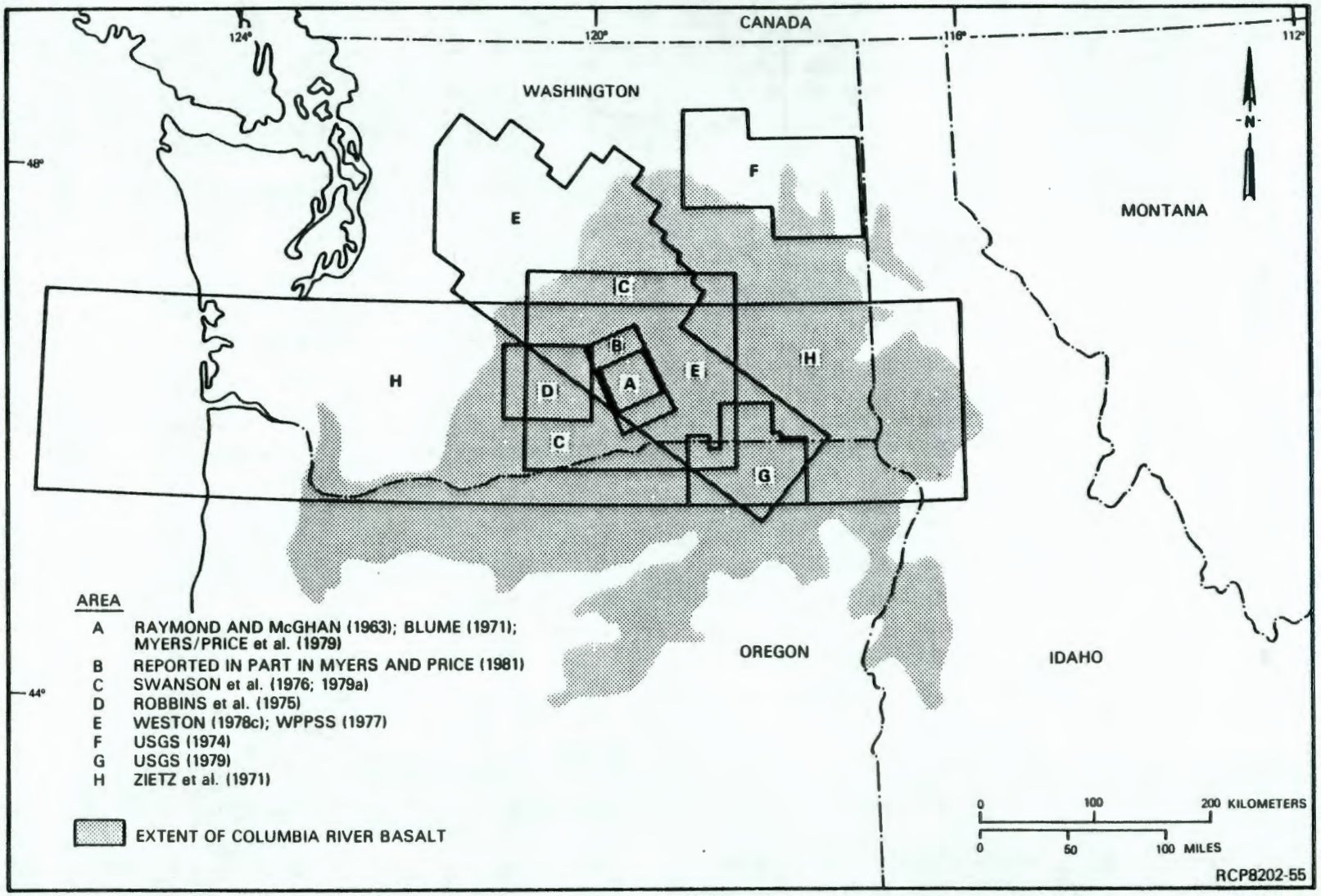

FIGURE 3-34. Aeromagnetic Surveys Including Columbia Plateau Area.

TABLE 3-2. Aeromagnetic Surveys.

Area in Figure 3-34	Survey reference	Survey altitude	Survey line spacing and orientation	Magnetometer
A	Raymond and McGhan (1963)	150-m terrain clearance	1.6 km north-south	Fluxgate
H	Zietz et al. (1971)	4,575-m constant elevation above sea level (barometric)	8.0 km east-west	Alkali vapor and fluxgate
A	Blume (1971)	275 and 455 m barometric	3.2 x 3.2 km northeast-southwest northwest-southeast	Proton precession
F	USGS (1974)	2,134 m above sea level	1.6 km, east-west, the lines north-south	Unspecified
D	Robbins et al. (1975)	150 m	3.1 km north-south traverses, 1.6 km flight line spacing	Modified AN-ASQ/3A
E	Weston (1978c) and WPPSS (1977)	305- and 450-m terrain clearance	0.8 x 0.8 km northeast-southwest traverse lines, northwest-southwest tie lines	Optically pumped cesium vapor
C	Swanson et al. (1979a)	150-m terrain clearance	1.6 km north-south	Fluxgate
A	Myers/Price et al. (1979)	1,220 m barometric	0.8 x 0.8 km northeast-southwest northwest-southeast	Proton precession
G	USGS (1979)	150 m	1.6 km, north-south	Proton precession
B	Holmes and Mitchell (1981)	760, 990, 1,220, 1,450, and 1,680 m	0.8 x 0.8 km northeast-southwest northwest-southeast	Optically pumped cesium vapor

Regional survey E (Fig. 3-34) is the most widespread low-level survey on the plateau. Data from this survey have been utilized in a number of interpretive studies (Weston, 1978a; 1978c; 1979; WPPSS, 1977; 1980) of structures located within and peripheral to the Columbia Plateau (see Section 3.7).

Surveys performed over the Pasco Basin are shown in Figure 3-35. Surveys performed specifically for the BWIP include those discussed in Myers/Price et al. (1979) and Holmes and Mitchell (1981). These surveys, and surveys interpreted by Weston (1978c), WPPSS (1977), and Swanson et al. (1979a) (Fig. 3-34 and Table 3-2) will be briefly discussed.

Weston's aeromagnetic coverage of the Pasco Basin revealed anomalies that were primarily related to structurally controlled topography (i.e., anticlines and synclines) (Weston, 1978b, 1978c; WPPSS, 1977). However, qualitative examination of the data reveals alignments of anomalies that often cross-cut the topography. Some areas of anomalously high intensity that do not correlate with topography have been interpreted as evidence of dipping or intracanyon basalt flows. Swanson et al. (1976; 1979a) also noted anomalies related to structurally controlled topography, as well as anomalies associated with intracanyon basalts, dikes, and faults within the Pasco Basin.

Details of a constant-elevation (1,220 meters) aeromagnetic survey of a portion of the Pasco Basin, including a magnetic-features map, are reported in Myers/Price et al. (1979, Plate III-6). Features noted from the total field map were described in terms of linears (which indicate strikes of moderate-to-high horizontal gradients in the total field) and axes of symmetry for high and low enclosures of total-field intensity.

To provide high-resolution aeromagnetic data within the central Pasco Basin (i.e., Cold Creek syncline), a multilevel aeromagnetic survey was conducted for the BWIP (Fig. 3-35) (Holmes and Mitchell, 1981). The survey was flown at five different altitudes: 760, 990, 1,220, 1,450, and 1,680 meters constant elevation above mean sea level. In addition to the total-field, gradient, and residual maps, Werner deconvolution profiles were generated for each flight line from all five survey levels. Aeromagnetic interpretive maps for the 760- and 1,220-meter levels, and a discussion of selected Werner deconvolution solutions, are included in Holmes and Mitchell (1981, Fig. B-11 and B-12) and Myers (1981). Multilevel aeromagnetic-survey results were considered during the siting process (Chapter 2) and during the preparation of the top-of-basalt map for the Cold Creek syncline (see Section 3.7.2.3.2).

3.6.2.2 Ground-Magnetic Surveys. Ground-magnetic coverage is restricted to specific study areas and has been used mainly for detailed exploration of small-scale features discovered by other geologic or geophysical means. The locations of ground-magnetic surveys within the Columbia Plateau are shown in Figure 3-36. The surveys outside of the Pasco Basin are discussed by Weston (1978a).

9 2 1 2 4 9 5 0 7 0 2

9 2 1 2 4 9 5 0 7 0 3

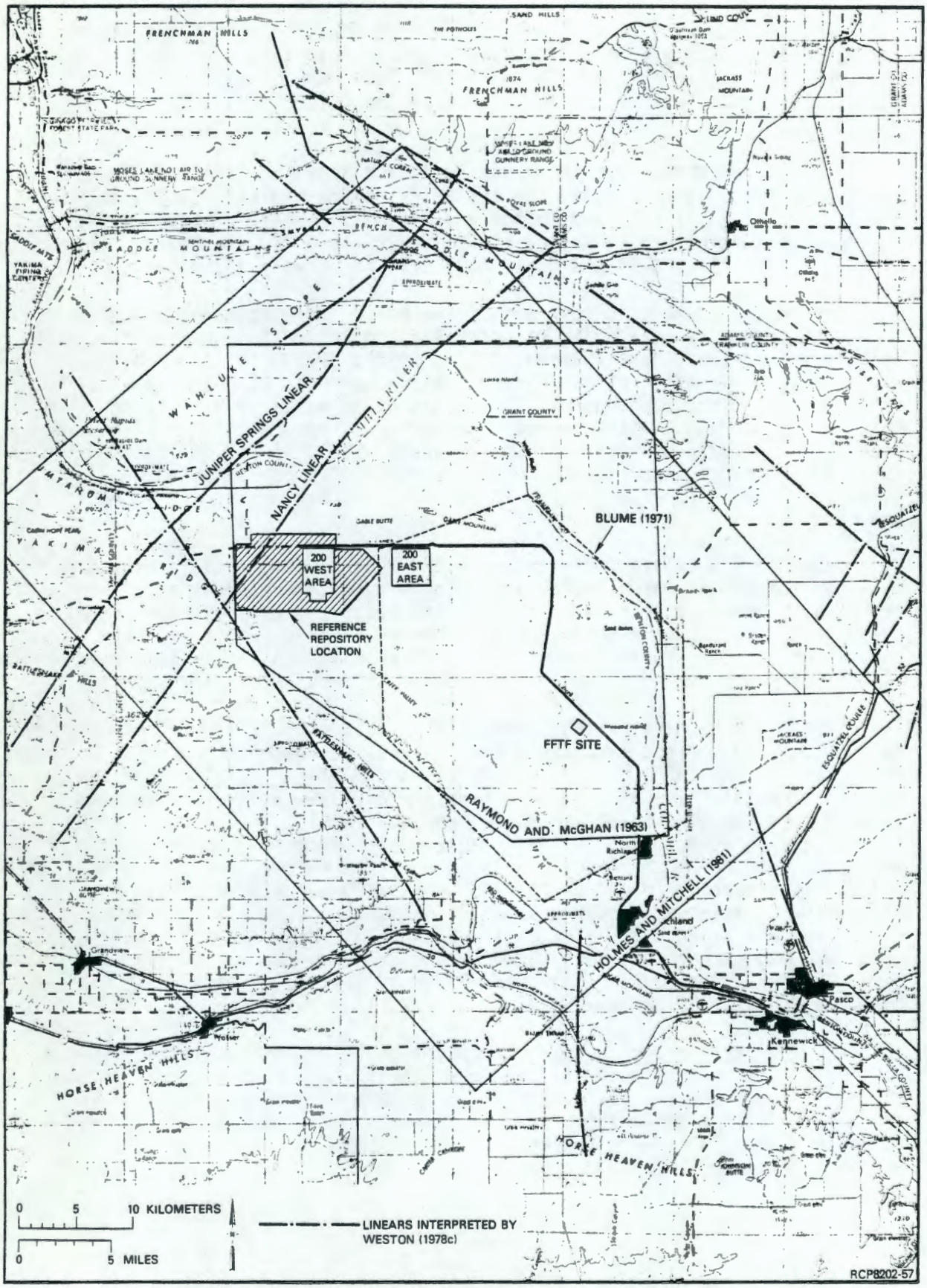

FIGURE 3-35. Pasco Basin Aeromagnetic Surveys.

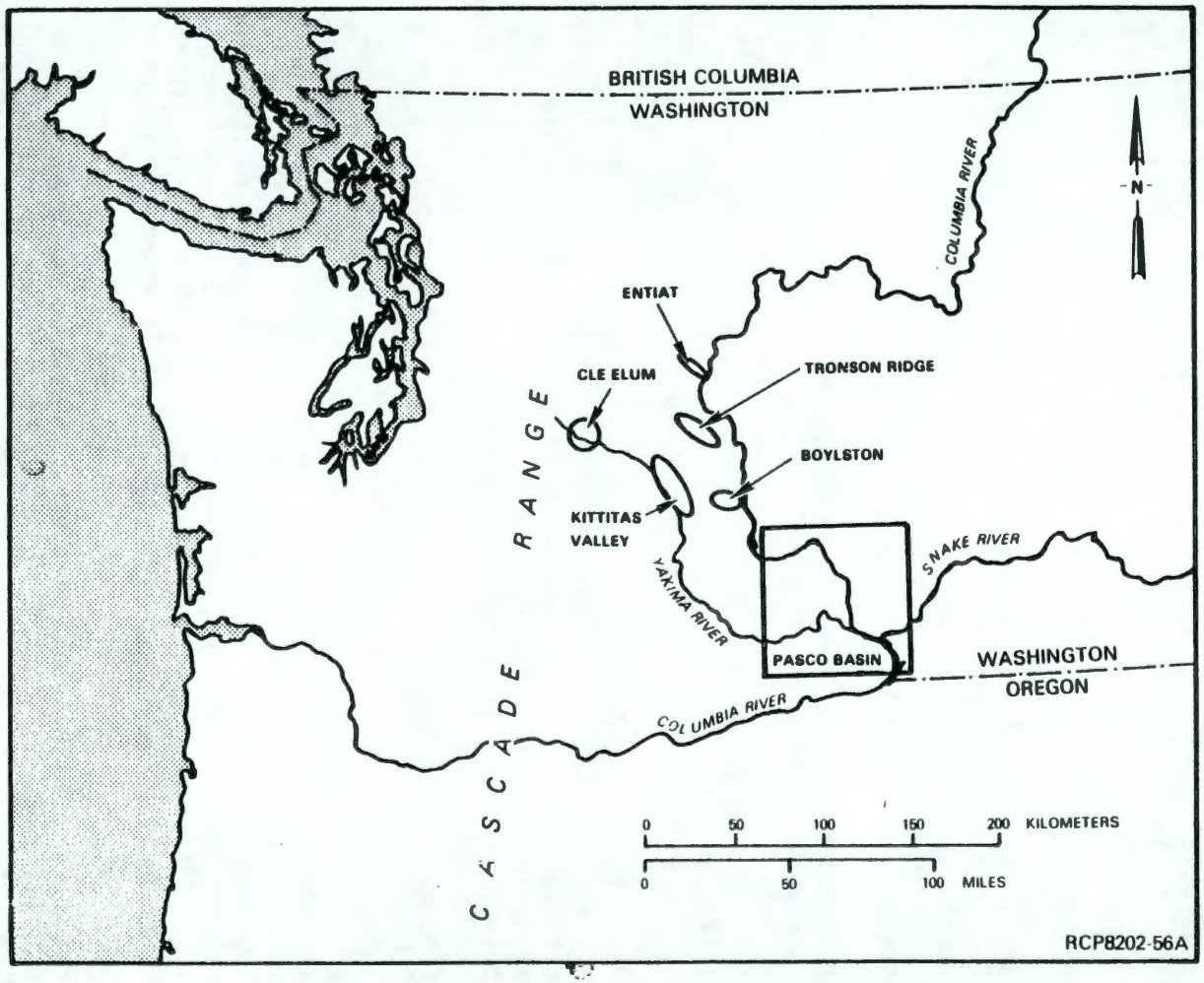

FIGURE 3-36. Locations of Ground-Magnetic Surveys.

Within the Pasco Basin, ground-geophysical studies conducted for the BWIP have generally been concentrated along shallow bedrock areas near the crests of the Yakima folds. Ground-magnetic studies, run in conjunction with such surveys, are shown in Figure 3-37. These surveys are discussed in Myers/Price et al. (1979), Kunk (1981), Ault (1981), and Cochran (1981a) and were factored into the top-of-basalt map for the Cold Creek syncline, discussed in Section 3.7.2.3.2. Interpretation of ground-magnetic data obtained from an investigation of a segment of the Rattlesnake Hills lineament (Fig. 3-37) is discussed in Cochran (1981b).

3.6.3 Gravity

The areal coverage of recent regional gravity surveys is shown in Figure 3-38. These investigations, their station spacing, and the aeromagnetic survey used in evaluation of the gravity data are listed in Table 3-3. Where station spacings were not specifically reported, they were measured from station-location maps.

The most comprehensive gravity investigation covering the Pacific Northwest has been reported by WPPSS (1977) (Fig. 3-38). This compilation of gravity data, which included most of the investigations listed in Table 3-3, focused on the determination of regional gravity trends, the correlation of the trends with areas of high seismicity, and the evaluation of a stress model based on gravity and seismic data.

The Pasco Basin is expressed as a regional gravity high (WPPSS, 1977). This was interpreted by Koníček (1975) and Robbins et al. (1975) to be attributable to a thick accumulation of Columbia River basalt that reaches maximum thickness in the Pasco Basin. Peterson (1966) attributed the high to both a thick basalt sequence and an upwarp in the mantle-crust contact. An upwarp in the mantle-crust contact is further supported by crustal-velocity studies (Section 3.6.1) and recent magnetotelluric data (Section 3.6.4).

Gravity investigations in the Pasco Basin have been continuing since the initial work by Peterson (1965; 1966), with increasing emphasis in recent years. Deju and Richard (1975) and Richard and Deju (1977) used the data acquired by Peterson (1965; 1966) to project the subsurface orientations of the Wahluke syncline, Umtanum Ridge, and Cold Creek syncline in the Pasco Basin. Their work indicated that these folds change strike from east-west to more north-south just east of Gable Mountain and lose amplitude.

Gravity profiles within the Pasco Basin have been reported by Blume (1971), Richard (1976), Lillie and Richard (1977), WPPSS (1977), Weston (1978a), Myers/Price et al. (1979), Ault (1981), Cochran (1981a) and Kunk (1981). The results of these profiles were used primarily to evaluate the subsurface extent and continuity of Umtanum Ridge and the Rattlesnake Hills-Wallula Gap trend (see Section 3.7).

9 2 1 2 4 9 5 0 7 0 5

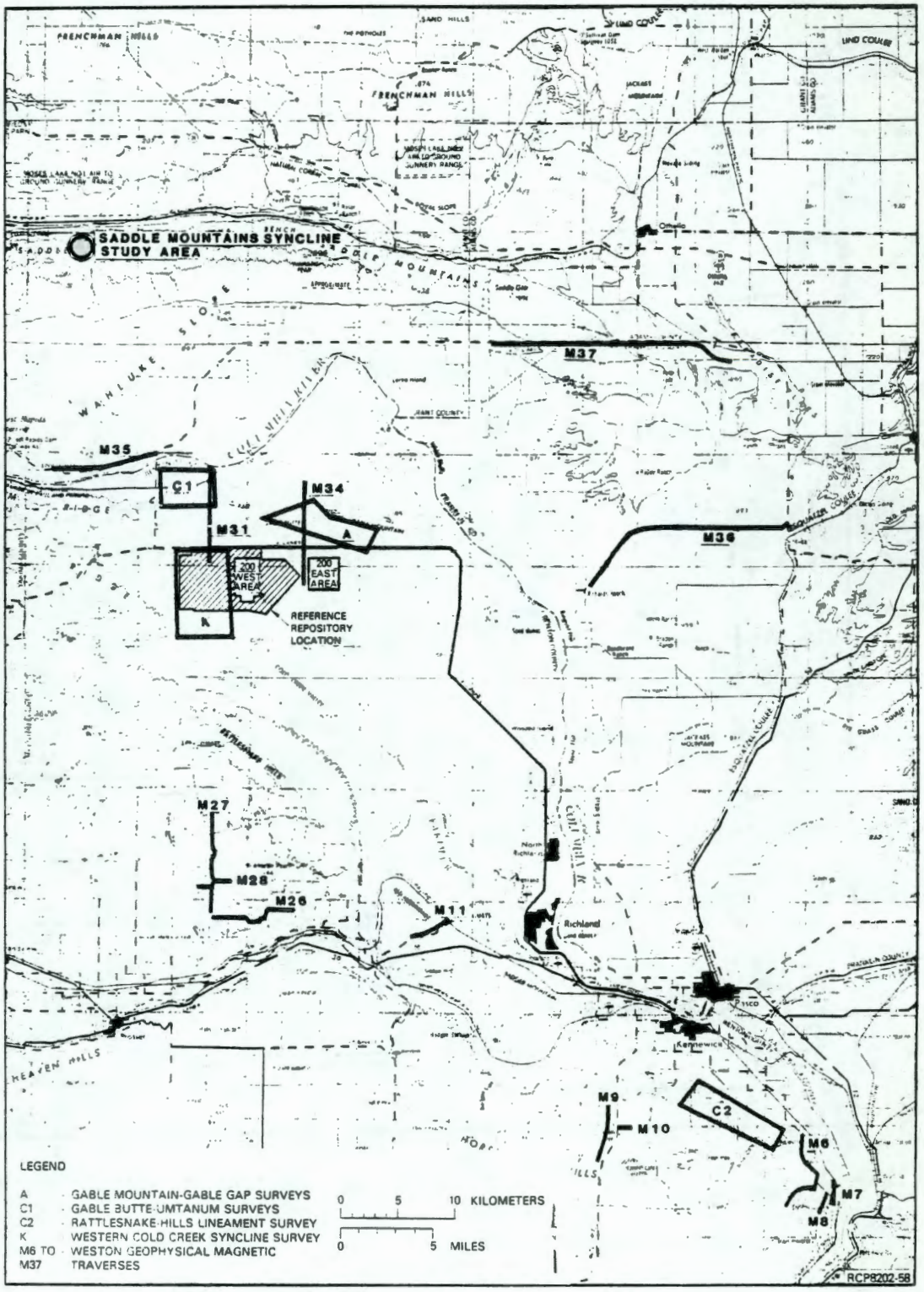

FIGURE 3-37. Pasco Basin Ground-Magnetic Surveys.

9-2124950706

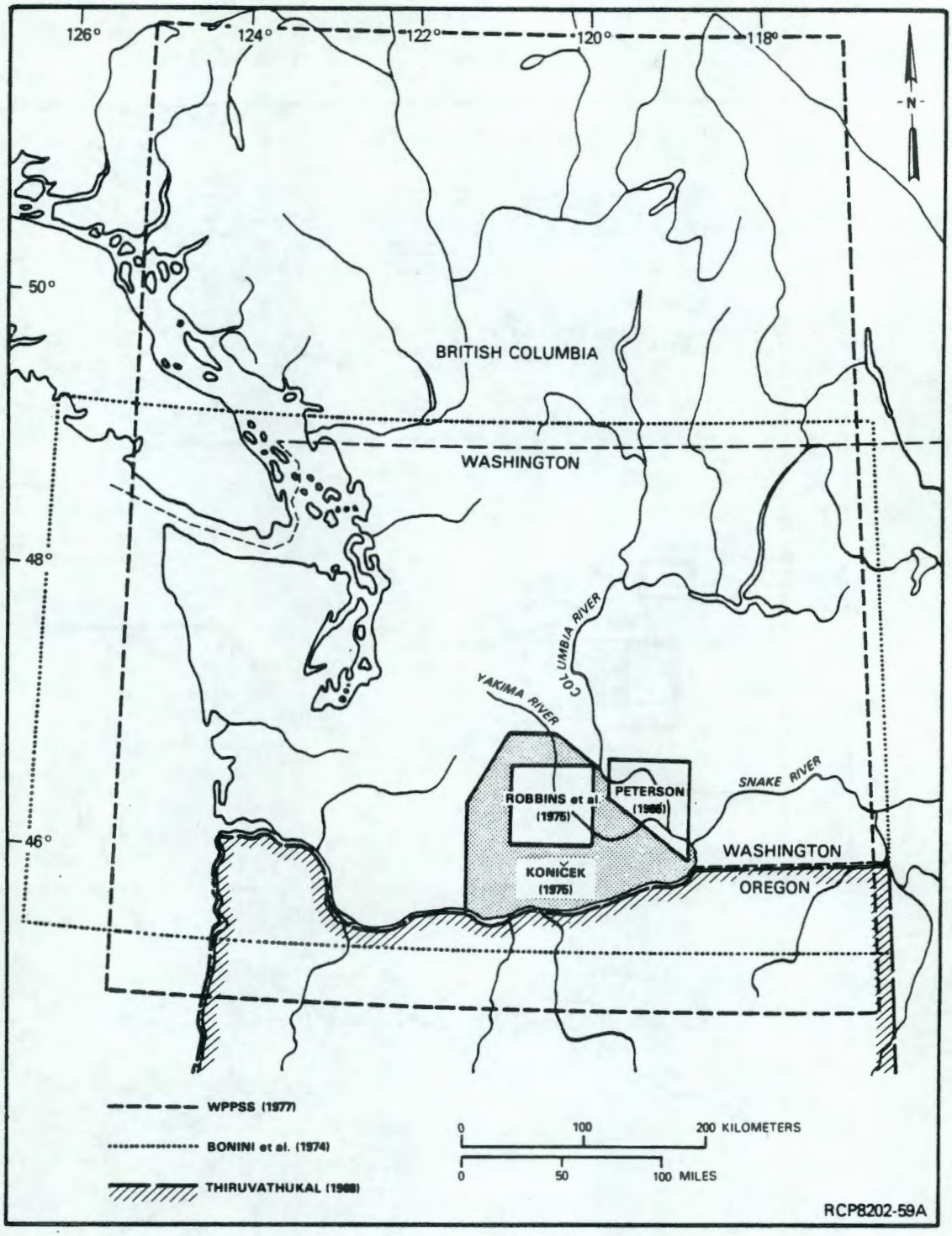

FIGURE 3-38. Location Map - Regional Gravity.

9 2 1 2 4 9 5 0 7 0 7

TABLE 3-3. Gravity Investigations.

Source	Station interval
WPPSS (1977)	60 m to 75 km
Robbins et al. (1975)	3 km
Koniček (1975)	5 to 6 km
Bonini et al. (1974)	0.3 to 20 km
Thiruvathukal (1968)	4 to 160 km
Peterson (1965; 1966)	1.5 km

Gravity investigations in the reference repository location have been reported by Peterson (1965; 1966), Weston (1978a), Richard and Deju (1977), Koniček (1975), Deju and Richard (1975), Lillie and Richard (1977), Richard (1976) and Kunk (1981). Results of these studies have shown that the reference repository location is dominated by a westward-dipping regional trend of approximately 1 milligal per 1.6 kilometers (1 mile). This regional trend continues westward to the city of Yakima on regional gravity maps of WPPSS (1977), Koniček (1975), and Bonini et al. (1974). Two residual anomalies existing near the site are due to (1) the known, east-west trending, subsurface extension of Yakima Ridge (see Section 3.7.2.3.2) and (2) a large gravel bar in the northern portion of the site (see Section 3.4.2.1) (Kunk, 1981).

Because of station spacing and incomplete coverage, existing surveys cannot be used to construct a meaningful gravity-contour map of the reference repository location. Data are presently being collected on a 152- by 152-meter grid to enable preparation of such a map (Kunk, 1981).

3.6.4 Magnetotelluric Surveys

Tensor-magnetotelluric surveying has been utilized by the BWIP to obtain deep subsurface data in the Pasco Basin. Initial surveys conducted in fiscal year 1978 tested the magnetotelluric technique and consisted of 4 tensor-magnetotelluric stations and 18 scalar-magnetotelluric stations (Edwards, 1978). These preliminary investigations showed that magnetotellurics could aid in the definition of the deep crustal structure beneath the Pasco Basin.

A subsequent magnetotelluric survey conducted in fiscal year 1979 consisted of 26 tensor-magnetotelluric stations in an approximate 10- by 10-kilometer grid (Fig. 3-39). These new stations were located to supplement existing data and to expand the coverage from the fiscal

9 2 1 2 4 9 5 0 7 0 8

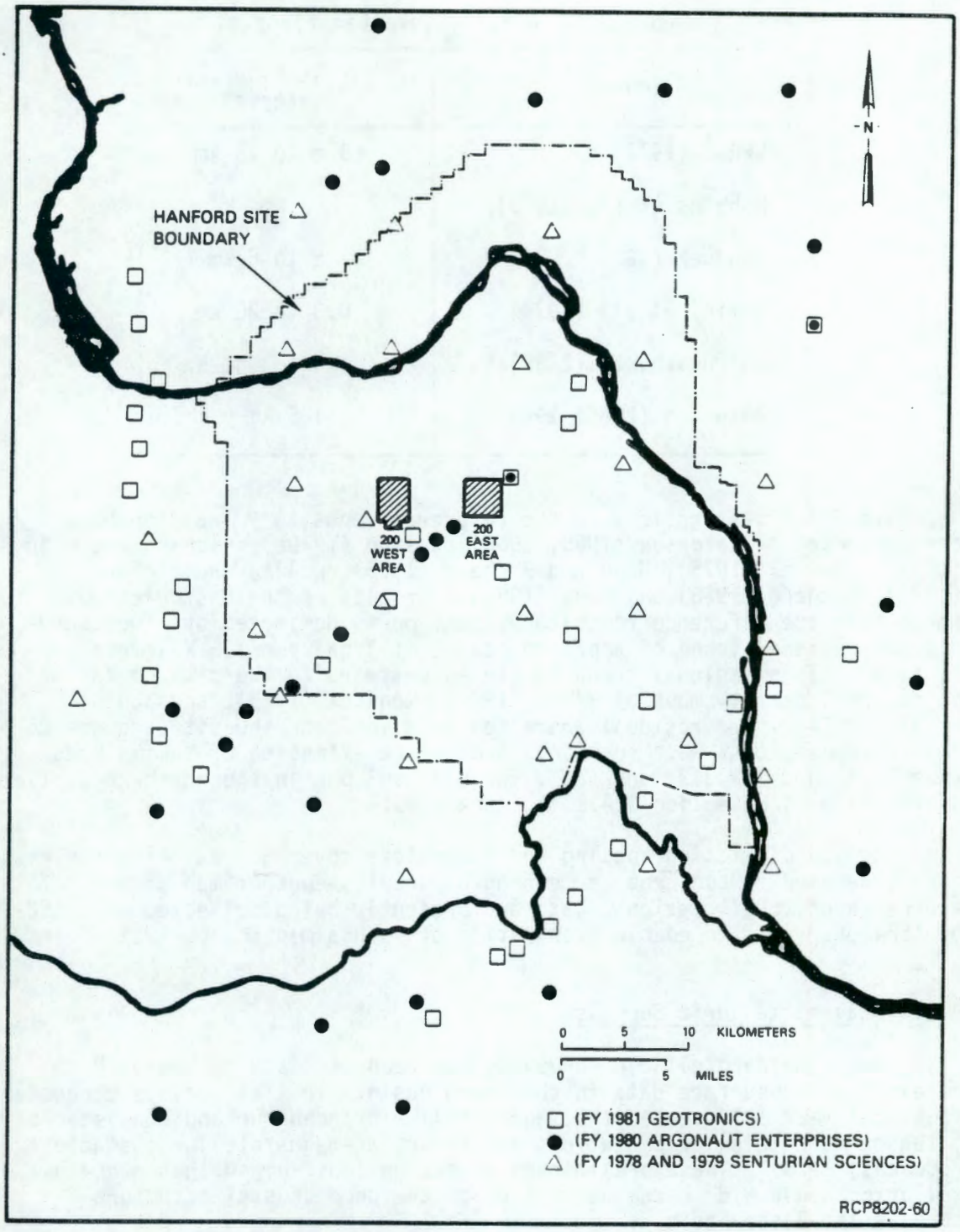

FIGURE 3-39. Tensor Magnetotelluric-Survey Station Location.

9 2 1 2 4 9 5 0 7 0 9

year 1978 survey. The 1979 tensor-magnetotelluric technique measured electrical strike at all locations; survey results indicated that electrical strike varies within the Pasco Basin, making the measurement of this parameter a basic requirement for obtaining subsurface resistivity models (Fig. 3-40). Thus, the fiscal year 1978 scalar-magnetotelluric data (which assumed a uniform strike) have been used only as a gross indicator of subsurface conditions.

In fiscal year 1980, 34 tensor-magnetotelluric stations were added to the previous coverage (Fig. 3-39). Twenty-seven tensor-magnetotelluric stations (Fig. 3-39), including two primary profiles across the Rattlesnake Mountain structure and the eastern expression of Yakima and Umtanum Ridges, were collected in late fiscal year 1981.

Current interpretation of magnetotelluric data (Myers/Price et al., 1979) indicates that the Pasco Basin is characterized by five geoelectric layers (Table 3-4). The conductive zone (layer 3) persists throughout the survey area and suggests a lithologic change below the basalt. This is supported by information from deep boreholes located approximately 100 kilometers to the north and east of the Pasco Basin (Williams, 1961; Brown, 1978).

TABLE 3-4. Geoelectric Layers and Interpreted Rock Type.

Geoelectric layer	Rock type
1 (conductive)	Surficial sediments
2 (resistive)	Basalt (includes Columbia River Basalt Group, interbeds, and any volcanic rocks underlying Columbia River Basalt Group)
3 (conductive)	Unknown (probably a layer of Mesozoic or early Tertiary sedimentary rocks)
4 (high resistive)	Unknown (probably crystalline basement rocks)
5 (conductive)	Unknown (probably within subcrust or upper mantle)

Fiscal year 1979 survey data show corresponding elevation highs in geoelectric layers 3, 4, and 5 that trend northeast beneath the Pasco Basin. Zones of thinning in geoelectric layers 2, 3, and 4 generally coincide with the elevation highs. If the elevation highs in geoelectric layers 3, 4, and 5 represent structural highs, then northeast trends of the deep geoelectric layers contrast sharply with the northwest trends

9 2 1 2 4 9 5 0 7 1 0

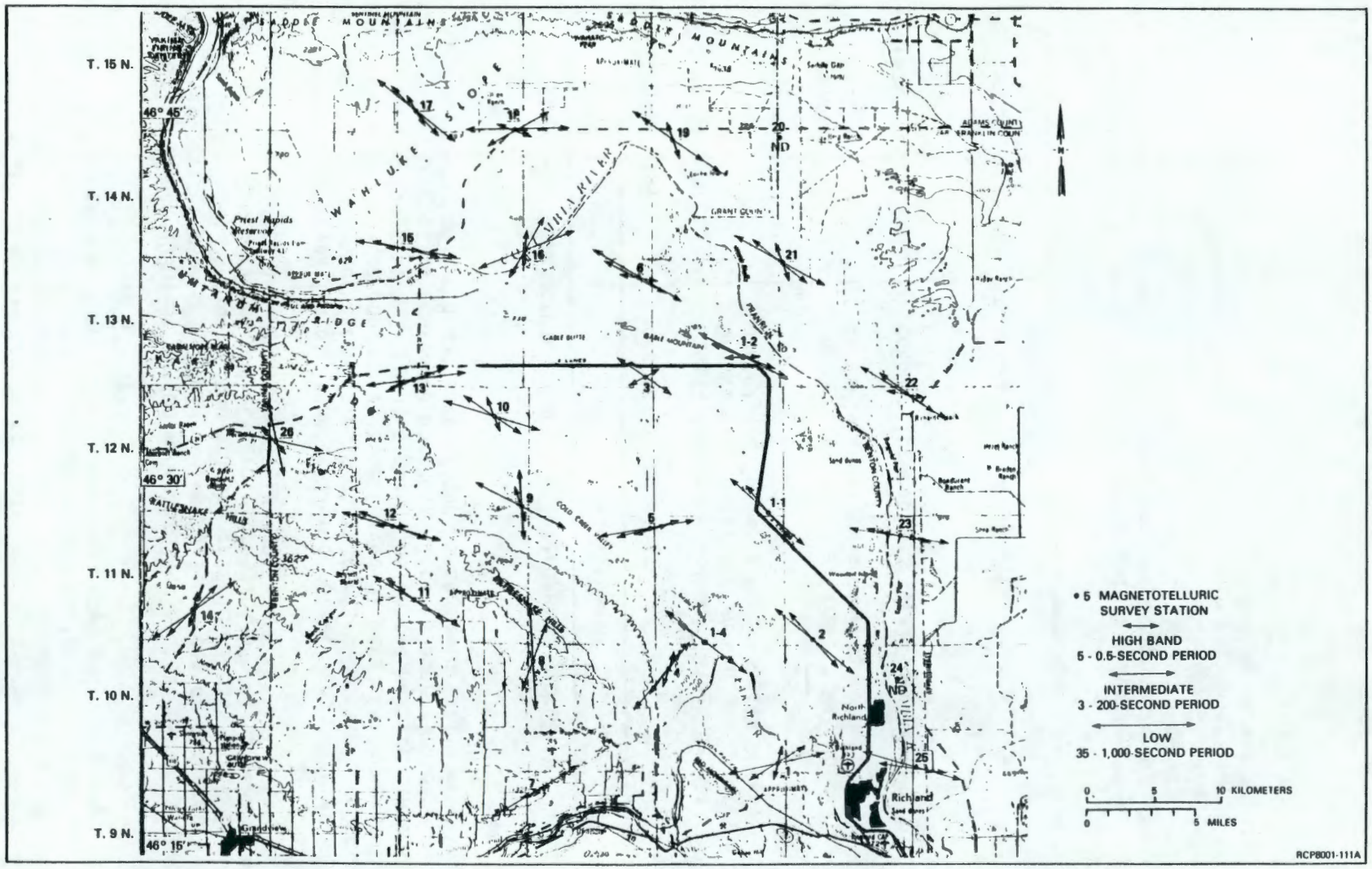

FIGURE 3-40. Electrical Strike, Tensor-Magnetotelluric Data from Fiscal Year 1978 and 1979 Surveys. (In a two-dimensional electric structure, conductivity varies along a horizontal and vertical coordinate. The horizontal direction normal to measured gradient is the electrical strike.)

9 2 1 2 4 9 5 0 7 1 1

of structural highs in the basalt surface (with the exception of the Rattlesnake Hills area). The results of the fiscal year 1980 survey also show northeast structural trends in deep layers and the presence of several northwest trends. The interpretations of the fiscal-year-1981 survey shown in Figure 3-39 support the five-layer case.

A comparison of magnetotelluric data, gravity data (Deju and Richard, 1975; WPPSS, 1977; Section 3.6.3), and seismic refraction data (Hill, 1972; Section 3.6.1) suggests that an area of crustal thinning with a south strike occurs along the horn of the Columbia River. This interpretation is consistent with the crustal-thinning interpretation of Eaton et al. (1978).

3.6.5 Regional Heat Flow

Basalt of the Columbia Plateau is believed by Swanson (1979) to have originated in the mantle or deep crust and to have risen rapidly to the surface through fissures and vents. Because intrusive rocks derived from basaltic-magma systems typically consist of only relatively small, rapidly chilled dikes at shallow depths, the potential for heat sources in the upper crust within the Columbia Plateau, including the Pasco Basin, is considered very low. Most of the Columbia River Basalt Group was erupted 13 to 16 million years ago during extrusion of Grande Ronde Basalts, but the youngest flood-basalt volcanism, volumetrically much smaller, ended approximately 6 million years ago with eruption of the Lower Monumental Member to the east of the Pasco Basin.

Thermal-gradient and heat-flow measurements presently available for the Pasco Basin are not measurements of simple convective heat transfer. Currently available fluid-temperature measurements reflect heat transfer within a flowing groundwater system. Locally, lateral and vertical groundwater flow can alter thermal gradients (see Chapter 5). In addition, the thermal regime of the unconfined aquifer has been altered by artificial recharge on the Hanford Site over the past 35 years. Shallow boreholes from which high gradients have been reported (Korosec and Schuster, 1980) are located near cooling-water disposal sites at Hanford reactor areas. Measured and calculated geothermal gradients and heat flow based on data from shallow measurements within the unconfined aquifer in areas of groundwater recharge or discharge are, therefore, difficult to analyze.

Thermal data available for the Pasco Basin were geologically evaluated. In this analysis we (1) excluded the unconfined aquifer, (2) excluded wells not allowed to thermally reequilibrate prior to logging, and (3) avoided wells in which crossflow was apparent. Data were selected on the basis of lithologic logs, known distribution of cooling-water recharge, and knowledge of downhole conditions during logging. Nevertheless, relatively large thermal variations remain and suggest the need for borehole logging in specific areas for the express purpose of careful thermal measurement. Data used in this assessment are presented in Table 3-5, Korosec and Schuster (1980), and Blackwell (1980). Wells from which data were obtained are shown in Figure 3-41.

9 2 1 2 4 9 5 0 7 1 2

TABLE 3-5. Geothermal Gradients Calculated for Selected Borehole Logs from Wells Within the Hanford Site.

Hole number	Town-ship	Range	Section	Hanford Site designation[a]	Depth (m)	Gradient (°C/km)	Bottom hole temperature (°C)	Geophysical log company[b]	Lithology
1	10	28	14	DDH-3	998	49.9	55.4	WSU	Grande Ronde Basalt
2	11	24	15	RSH-1	2,890	37.7	96.7	Schlumberger	Grande Ronde Basalt
3	11	26	3	DC-12	1,018	41.7	53.7	PNL	Grande Ronde Basalt
4	11	28	35	DC-15	945	41.0	51.5	PNL	Grande Ronde Basalt
5	12	27	6	DB-8	244	42.0	24.8	PNL	Cold Creek interbed
6	12	27	36	DC-7	1,243	48.9	72.2	WELEX	Grande Ronde Basalt
7	13	24	25	699-53-117[c]	213	44.6	20.6	PNL	Priest Rapids Member
8	13	25	16	DB-12	215	28.9	20.5	PNL	Priest Rapids Member
9	13	25	30	699-53-103	299	49.2	28.7	PNL	Priest Rapids Member
10	13	25	34	DC-5	945	37.1	62.8	WELEX	Grande Ronde Basalt
11	13	26	35	DC-1	1,692	38.1	75.3	WSU	Grande Ronde Basalt
12	13	27	29	DB-10	257	43.0	26.4	PNL	Umatilla Member
13	14	27	29	DC-14	1,017	44.6	57.2	PNL	Mabton interbed
14	15	24	28	DH-5	1,525	40.7	73.5	WSU	Frenchman Springs Member
15	15	28	30	DH-4	1,456	43.0	75.2	WSU	Frenchman Springs Member
16	10	28	10	399-5-2	128	35.4	19.6	PNL	Elephant Mountain Member
17	12	25	10	RRL-2	1,211	37.0	58.5	PNL	Grande Ronde Basalt

[a]Well locations shown in Figure 3-3.

[b]WSU = Washington State University, Pullman, Washington
PNL = Pacific Northwest Laboratory, Richland, Washington
WELEX = WELEX, Bakersfield, California
Schlumberger = Schlumberger Limited, Houston, Texas

[c]Formerly 699-52-115.

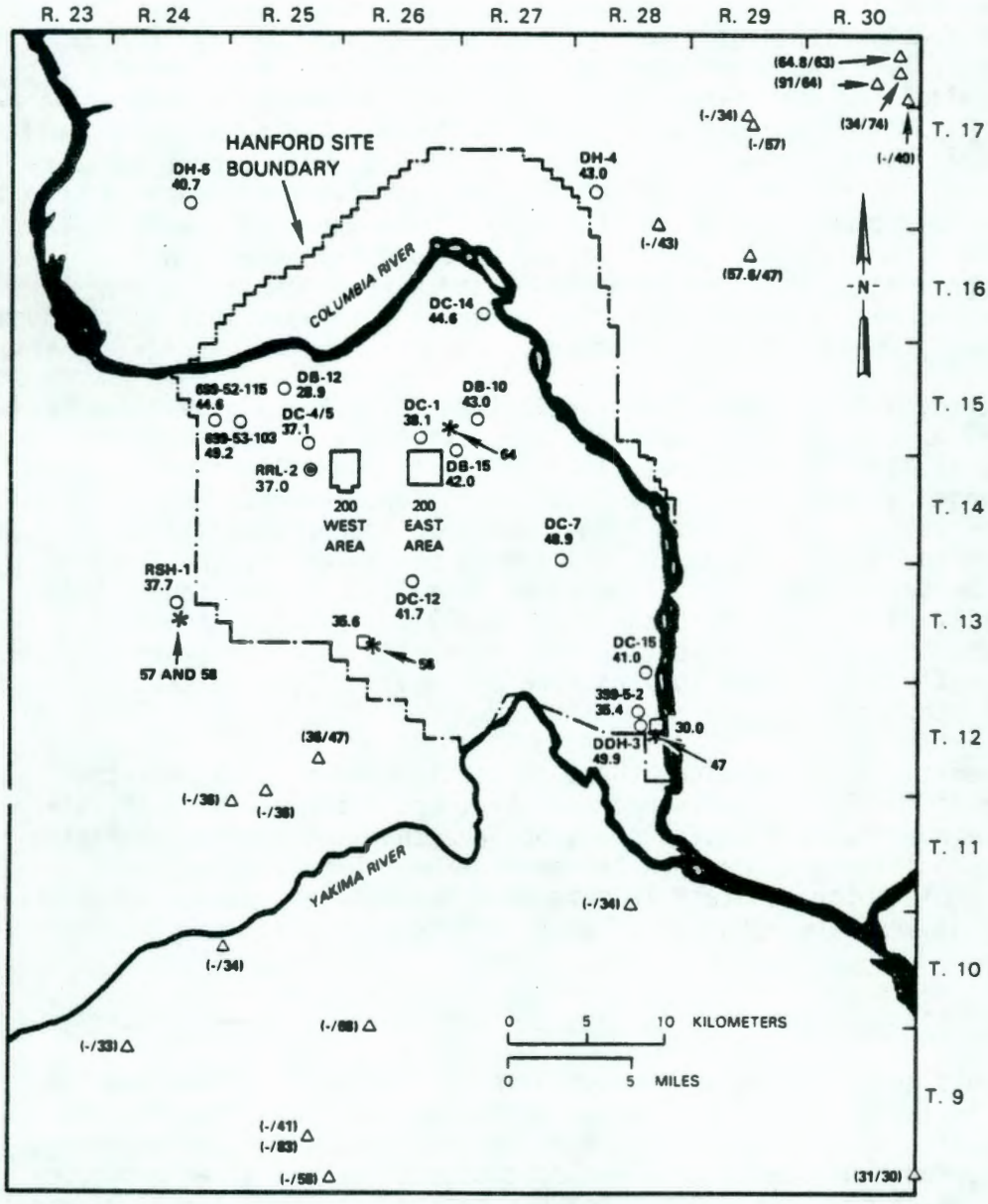

□ BLACKWELL (1980)

△ KOROSEC AND SCHUSTER (1980) (MEASURED GRADIENT/CALCULATED GRADIENT)

○ ROCKWELL DATA IN MURPHY AND JOHNEER (1981)

◉ ROCKWELL DATA IN THIS REPORT

DC-12 BOREHOLE NUMBER
41.7 TEMPERATURE GRADIENT

ALL ABOVE VALUES IN °C/km

✱ REGIONAL HEAT-FLOW VALUES (mW/m²) (BLACKWELL, 1980)

RCP8202-61A

FIGURE 3-41. Temperature Gradient Measurements and Regional Heat Flow Reported for the Pasco Basin and Vicinity.

9 2 1 2 4 9 5 0 7 1 4

Available data suggest that heat flow (calculated from gradient and thermal-conductivity data) and geothermal gradient in the Pasco Basin are not appreciably different from the remainder of the Columbia Plateau (Blackwell, 1978) and that shallow crustal sources of heat are not present. Calculated heat flows (Blackwell, 1980) and measured thermal gradients (Fig. 3-41) range from 47 to 64 milliwatts per square meter and 35° to 50°C per kilometer, respectively. Heat flow is generally near the lower limit of the 55 to 70 milliwatts per square meter range reported as normal by Korosec and Schuster (1980). Most measured gradients are also within the normal range of 35° to 45°C per kilometer. Calculated gradients, based on bottom-hole and surface-ambient temperatures, tend to vary over a wider range than measured gradients, but most values are between 33° to 47°C per kilometer.

Sparse heat-flow data (Blackwell, 1980; Fig. 3-41) provide no indication of a localized shallow heat source within the Pasco Basin or anomalously high regional heat flow. A 55- to 70-milliwatt-per-square-meter range is reported for the Columbia Plateau, whereas regions of high heat flow such as the Cascade Range, southern Idaho, Imperial Valley, and the Rio Grande rift average 100 milliwatts per square meter. Much of the western United States ranges from 60 to 90 milliwatts per square meter (Blackwell, 1981; Sass and Lachenbruch, 1979). In the presence of a local, shallow, intrusive heat source, heat flow would be expected to be significantly greater and to vary more systematically than that observed in the Pasco Basin.

Given the existing data, there is little reason to suspect the presence of localized heat sources within, or in the vicinity of, the reference repository location or to believe that the area is characterized by heat flow greater than the average heat flow for the Earth's crust. Radioisotope content in reference repository location host-rock minerals is very low compared to most continental-crust rocks.

3.6.6 Remote Sensing

Remote sensing studies conducted in the Columbia Plateau are summarized in Table 3-6 and Figure 3-42. The studies have involved the analysis of satellite imagery, aerial photography, and topographic maps for the purpose of identifying geologic structures and other geologic features which may bear on the tectonic setting of the Columbia Plateau.

9 2 1 2 4 9 5 0 7 1 5

TABLE 3-6. Remote-Sensing Studies of the Columbia Plateau and Surrounding Area. (Sheet 1 of 3)

Title	Reference	Location	Purpose	Lineaments or faults cited	Comments
Lineament map of the state of Washington; overlay to Landsat space imagery, 1:500,000, 1977	Brewer (1977)	Washington State	Lineament mapping	X	Lineament map of the entire state of Washington at 1:500,000 scale
Lower Monumental Lock and Dam, Snake River, Washington, Design Memorandum No. 1, General Design Memorandum, Appendix D - Geology, 1959	COE (1959)	Immediate vicinity of Lower Monumental Dam	Geology of dam site	X	Plate 1 is an aerial photo of dam site with geology; 1,600 ft northeast of dam site a large regional fault is inferred trending approximately N. 25° W.
Tectonic map of Idaho from ERTS imagery, 1973	Day and Hall (1973)	Idaho	Structure and tectonics	X	Tectonic map of state of Idaho from ERTS imagery
WPPSS, WNP No. 1, PSAR Amendment 23, Appendix 2RK, remote-sensing analysis of the Columbia Plateau, 1977	Glass (1977)	Much of the Yakima River Valley and the Pasco Basin (see Fig. 3-42)	Geologic studies	X	Conducted aerial photo analysis to identify and characterize faulting. Discusses Moxee and Wenas fault zones
WPPSS, WNP No. 1, PSAR, Amendment 23, Appendix 2RF, imagery and topographic interpretation of geologic structures in central Washington, 1977	Glass and Slemmons (1977)	Area of 45° to 49° latitude, 118° to 123° longitude (see Fig. 3-42)	Geologic studies	X	Lineaments and known faults in the presumed (at that time) epicentral region for the 1872 earthquake were analyzed on remote-sensing imagery and topographic maps to determine whether recent surface rupture had occurred
Analysis and interpretation of remote-sensing data applied to the Columbia Plateau, Washington and Oregon 1980	Glass (1980)	Washington and Oregon (see Fig. 3-42)	Lineament mapping	X	Reports results of study of lineament in southeastern Washington and northeastern Oregon and presents tectonic model

TABLE 3-6. Remote-Sensing Studies of the Columbia Plateau and Surrounding Area. (Sheet 2 of 3)

Title	Reference	Location	Purpose	Lineaments or faults cited	Comments
Remote sensing of southeastern Washington; Part I, infrared scanning imagery	Godfrey et al. (1972)	15,000 mi^2 area centered around Hanford Site	Geologic mapping		Attempts to answer question of whether faults and geologic structures can be mapped using infrared imagery
A lineament analysis of the United States, 1975	Haman (1975)	Entire contiguous United States	Lineament mapping	X	1:10,000,000 scale. Only one lineament shown in Columbia Plateau
Geology and tectonic history of the Hanford area and its relation to the geologic and tectonic history of the State of Washington and the active seismic zones of western Washington and western Montana, 1966	Jones and Deacon (1966)	Hanford area and parts of western Washington and western Montana	Earthquake studies of Hanford area	X	Review of geology and tectonics of Hanford area, western Washington, and western Montana. Many photos and lineament interpretations. Lineament map scale is 1 in. = 19 mi
An evaluation of the ERTS-1 system imagery in a structural study and a map application of ERTS-1 imagery in southeastern Washington, northeastern Oregon, and parts of western Idaho, 1974	Klosterman (1974)	Basically the area covered by the Grangeville and Pullman quadrangles, 1:250,000	Geologic application of remote sensing	X	Discusses methods of using ERTS-1 imagery products to map geologic structures, then applies techniques in study area. Many photos and some field checking
Lineament map of Oregon, 1974	Lawrence and Carter (1974)	Oregon	Lineament mapping	X	Lineament map on ERTS mosaic of the State of Oregon, 1:1,000,000
Tectonic significance of regional jointing in Columbia River basalts, north-central Oregon, 1979	Lawrence (1979)	Oregon (see Fig. 3-42)	Tectonic jointing study	X	Reports results of remote-sensing study on tectonic joints in two areas of north-central Oregon

TABLE 3-6. Remote-Sensing Studies of the Columbia Plateau and Surrounding Area. (Sheet 3 of 3)

Title	Reference	Location	Purpose	Lineaments or faults cited	Comments
Multispectral remote-sensing techniques applied to salinity and drainage problems in the Columbia Basin, Washington, 1972	Prentice (1972)	Columbia Basin Project (U.S. Bureau of Reclamation)	Apply remote sensing to salinity and drainage problems		Multispectral scanner data, aerial photography, and ground data used to study soil moisture and soil salinity as it relates to agricultural problems
Geologic remote sensing of the Columbia Plateau	Sandness et al. (1981)	Columbia Plateau in Washington, Oregon, and Idaho (see Fig. 3-42)	Remote-sensing analysis of the Columbia Plateau and surrounding areas	X	Results from analysis of Landsat, Skylab, and U-2 photos. 20 lineament maps at 1:250,000 scale
WPPSS, WNP No. 1, PSAR, Amendment 23, Appendix 2RG, remote-sensing analysis of the 1872 earthquake epicentral region, 1977	Slemmons et al. (1977)	Aerial reconnaissance routes in central Washington and British Columbia (see Fig. 3-42)	Geologic studies	X	Analyzed remote-sensing imagery, took low sun-angle aerial photos of major faults, and searched for faults with surface offsets from 1872 earthquake. Emphasis on Straight Creek fault
Fault and earthquake hazard evaluation of five Corps of Engineers dams in southwestern Washington, 1979	Slemmons and O'Malley (1979)	Washington (see Fig. 3-42)	Earthquake hazard evaluation	X	Reports results of remote sensing used in earthquake hazard evaluation
WPPSS, WNP No. 1 and 4, remote-sensing analysis of geologic structures, 1872 earthquake studies, 1979	Slemmons (1979)	Washington	Remote-sensing analysis of Columbia Plateau and much of Washington state	X	Presents remote-sensing analysis of most of Washington state, including azimuthal analysis

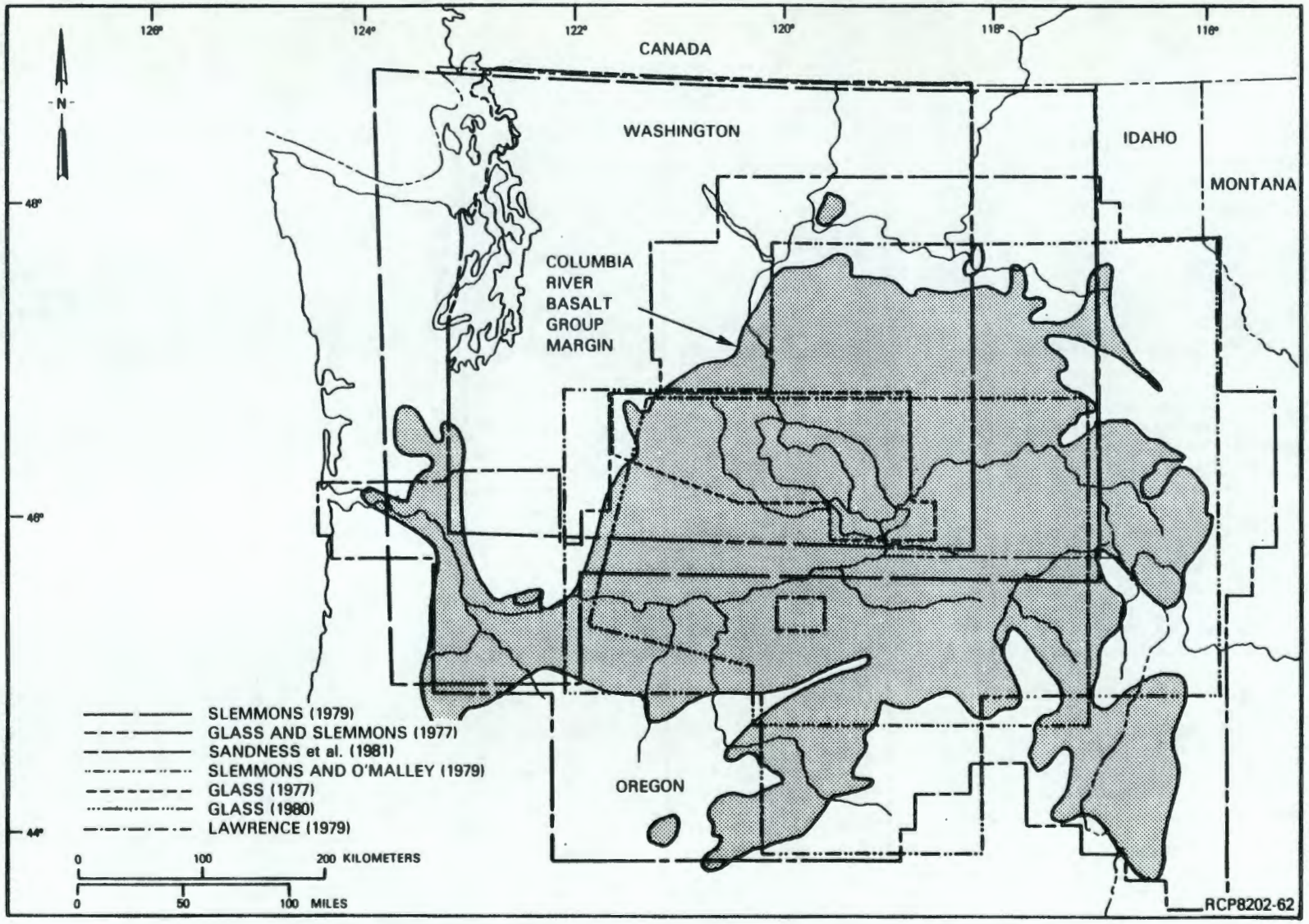

FIGURE 3-42. Remote-Sensing Studies Conducted Within the Columbia Plateau.

The work by Sandness et al. (1981) was conducted for the BWIP and is the most aerially comprehensive of these studies. The results are shown on 20 photolineament maps (scale 1:250,000) covering the plateau and bordering area. Photolineaments were interpreted from an analysis of Landsat imagery and Skylab and U-2 photography and are annotated based on a classification system designating image or data type and lineament source (e.g., cultural feature, probable joint, stream alignment, etc.). Regionally, the lineaments exhibit a predominant northwest-southeast trend with a secondary northeast-southwest trend. The uniformity of these trends over such a broad area conforms with known regional structural patterns. Most lineaments were expressed as erosional or drainage features such as straight-stream segments or alignments of stream segments.

A comparison of the lineament maps by Sandness et al. (1981) with geologic maps for Washington (Swanson et al., 1979b), Oregon (Wells and Peck, 1961; Walker, 1977), and Idaho (Bond et al., 1978b) showed that approximately 70 percent of the faults and 30 percent of the fold axes shown on the geologic maps were mapped as lineaments. The ratio of observed lineaments to mapped faults was found to generally vary between 5 to 1 and 50 to 1, but may be as high as 500 to 1.

Within the Pasco Basin, lineaments categorized by Sandness et al. (1981) as structural are related to mapped folds and faults. They observed that lineament density in the Pasco Basin is less than in surrounding areas, possibly due to sediment cover and to active eolian processes.

3.6.7 Borehole Geophysical Logging

Borehole geophysical logging on the Hanford Site has been conducted mainly to support geologic and hydrologic characterization. A discussion of its geologic application is contained in Myers/Price et al. (1979) and Moak (1981a; 1981b). Borehole geophysical logs run in support of geologic and hydrologic studies are maintained by Rockwell. Other geophysical logs, principally for the unconfined-groundwater system, are available through reports released by Washington State University, College of Engineering Research (Crosby, 1972; Summers et al., 1975; Jackson et al., 1976).

The application of geophysical logs to hydrologic work is discussed in Chapter 5. The most useful logs for stratigraphic studies have been the sonic, density, porosity, and natural gamma logs. The first three log types reflect variations in the characteristics of intraflow structures such as rubble zones, shears, faults, or vesicular zones; the fourth type is sensitive to chemical composition (e.g., potassium content). Because log responses are not unique, a combination of logs has generally been used in interpretations.

Borehole logs and interpretations for a section of Grande Ronde Basalt penetrated by borehole DC-1 are shown in Figure 3-43. The stratigraphic interpretation of the basalt is based on the similarity of the

9 2 1 2 4 9 5 0 7 2 0

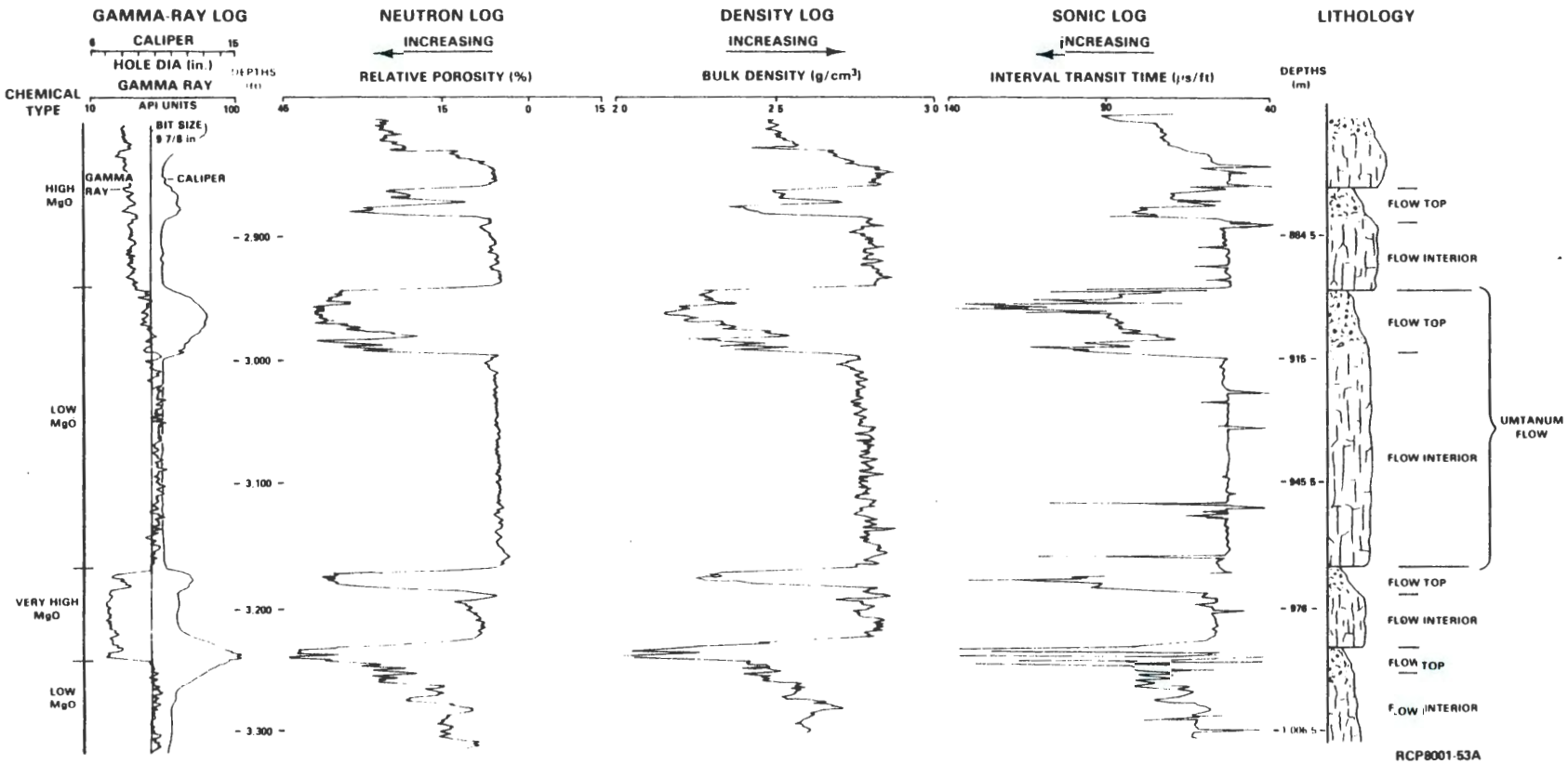

FIGURE 3-43. Illustrative Borehole Geophysical Log Response in Columbia River Basalt. Flow tops have higher porosity, lower density, and higher interval transit time than flow interiors. Gamma-ray log is sensitive to chemical types with different potassium content.

sonic, density, and neutron logs. Note that flow tops have a higher porosity, lower density, and higher interval-transmit time than the dense flow interiors. A shift in the gamma-ray log, at a depth of approximately 900 meters, is indicative of the high-potassium, low-magnesium oxide content of the Umtanum flow, which is overlain and underlain by basalt flows with lower potassium, higher magnesium oxide contents.

An example of the use of logs to establish stratigraphic correlations between four boreholes on the Hanford Site, separated by a total distance of 26 kilometers, is shown in Figure 3-44. Density logs from the Sentinel Bluffs sequence of Grande Ronde Basalt show decreasing bulk density in the rubble and vesicular zones and dense competent rock in the flow interiors. Note the strong correlation between the log characters of the uppermost breccia zones. The correlations suggested by these logs have been confirmed by chemical analysis of core and rotary chips and by remanent paleomagnetic analysis of core.

Use of borehole logs, other than for routine geologic work, has been limited, principally due to the variability in equipment types, logging methods, and reporting formats. In addition, most of the rock-mass properties have been derived from laboratory measurements of core, rather than from analyses of borehole logs. Direct calculations of porosities cannot be done as there is no calibration for basalt available.

At present, boreholes are regularly logged on an as-needed basis by a small unit operated by Pacific Northwest Laboratory. Such work is carried out in support of the BWIP drilling and hydrologic testing program. Only after completion of several boreholes is it deemed economically feasible to run a complete suite of logs using an oil-field-type service contractor.

Nonroutine borehole geophysical work has included the acquisition of vertical seismic-profile data in the reference repository location boreholes (Fig. 3-3) and downhole-gravity data in selected reference repository location boreholes and DC-3, -5, and -7. These data were collected to aid in the interpretation of ground-geophysical data sets.

3.6.8 Status

Geophysical work conducted in support of the BWIP has included (1) 195 kilometers of seismic-reflection profiling, (2) 109 magnetotelluric stations, (3) single-level and multilevel aeromagnetic surveys, and (4) localized ground-magnetic and ground-gravity surveys. This work, and geophysical work conducted by others, has been used in conjunction with available surface mapping, remote sensing, and borehole data to interpret the subsurface geology of the Pasco Basin. This interpretation indicates that, overall, the reference repository location appears to be free of potentially adverse bedrock structures (Myers and Price, 1981). Given existing data, there is also little reason to suspect the presence of localized heat sources within, or in the vicinity of, the reference repository location or to believe that the area is characterized by heat flow greater than the average heat flow for the Earth's crust.

9 2 1 2 4 9 5 0 7 2 2

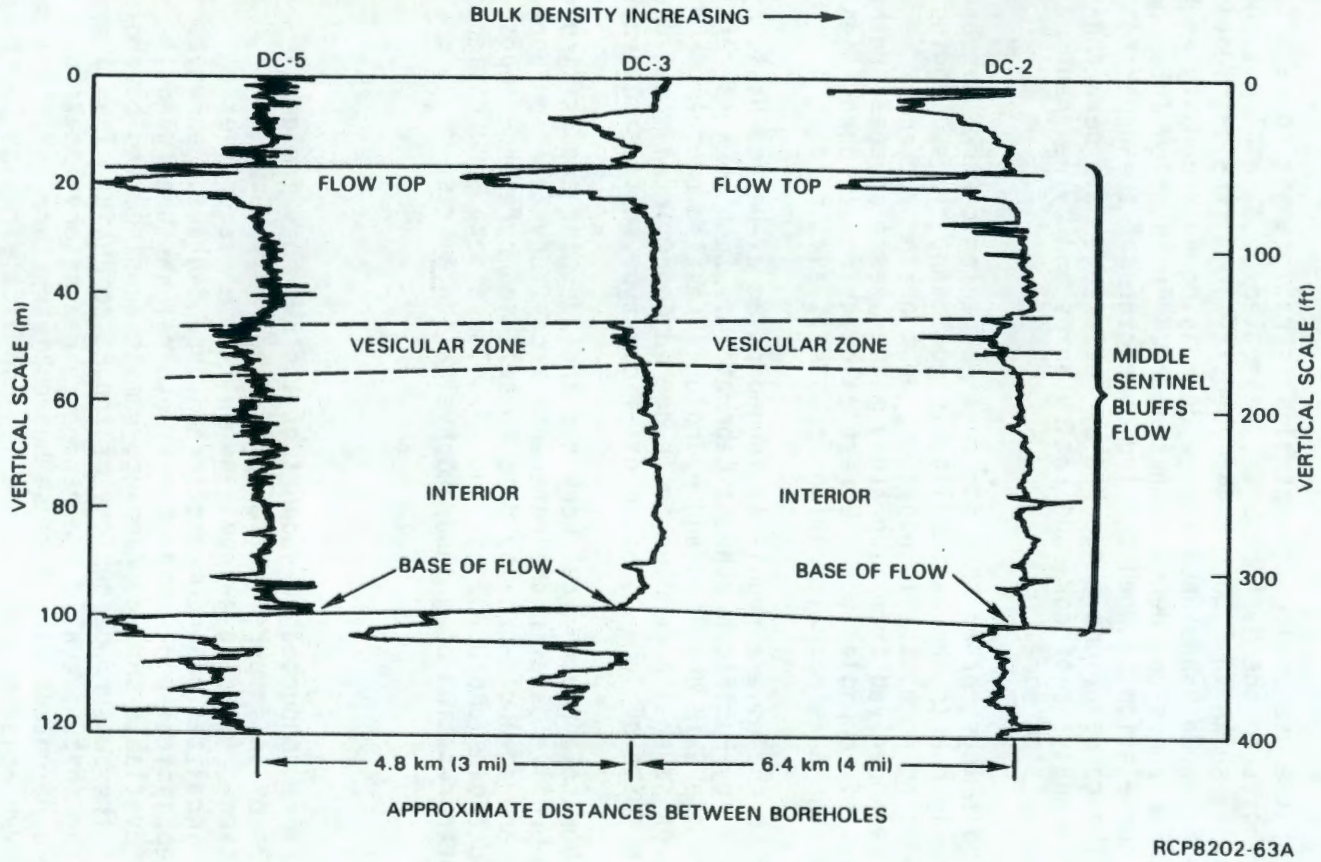

FIGURE 3-44. Gamma-Gamma-Log Response, Grande Ronde Basalt, Sentinel Bluffs Sequence. (See Fig. 3-17 for location.)

3.7 STRUCTURAL GEOLOGY AND TECTONICS

Structural and tectonic studies provide data and observations that can be integrated into a coherent conceptual tectonic model. Such a model will serve as the basis for a tectonic-stability assessment of the Pasco Basin (see Section 3.8). Work relating to the structural and tectonic setting of the Columbia Plateau is contained in Myers/Price et al. (1979), Myers and Price (1981), WPPSS (1981), and PSPL (1982); the content of this section is largely a summary of information contained in these publications.

3.7.1 Tectonic Framework

The topography of the Columbia Basin and Central Highlands physiographic subprovinces (Fig. 3-7) generally reflects geologic structure and provides a basis for defining three informal structural subprovinces: the Yakima Fold Belt subprovince, the Blue Mountains subprovince, and the Palouse subprovince (Fig. 3-45). The Yakima Fold Belt subprovince is characterized by generally east-trending, linear, anticlinal, topographic highs separated by broad synclinal valleys. The Blue Mountains subprovince represents a broad anticlinal arch extended northeastward from the Oregon Cascade Range to the Snake River. The Palouse subprovince is distinguished by its relative lack of deformation; landforms are predominantly geomorphic rather than structural in origin.

3.7.2 Tectonic History

Deformation of the Columbia Plateau began as early as late Grande Ronde Basalt.time. The stress regime that existed in the Columbia Plateau prior to the onset of Columbia River basalt volcanism must be inferred from the geologic history of older rocks which, in the central Columbia Plateau (i.e., the Pasco Basin area), are deeply buried. Rocks exposed along the margins of the Columbia Plateau (see Section 3.5.1) indicate a varied geologic history that can only suggest the structures and stresses that might be present in the rocks beneath the central Columbia Plateau and their possible effect on basalt deformation. A summary of information relating to the tectonic history of the Pasco Basin, from both the Columbia Plateau and surrounding provinces, follows.

3.7.2.1 Volcanic History. The chronology of volcanic events in the Pacific Northwest is summarized in Figure 3-46. In the volcanic terranes of the Pacific Northwest, volcanism has peaked approximately every 5 million years since Eocene time (McBirney et al., 1974; McBirney, 1978), and Holocene volcanism of the Cascade Range is well established. The candidate area is underlain by the Columbia River Basalt Group, which is discussed in Section 3.5. Magma origins, eruptive histories, and the neotectonic regime can be evaluated to determine the potential for future igneous activity in the Pacific Northwest and provide a basis for the following discussion.

9 2 1 2 4 9 5 0 7 2 4

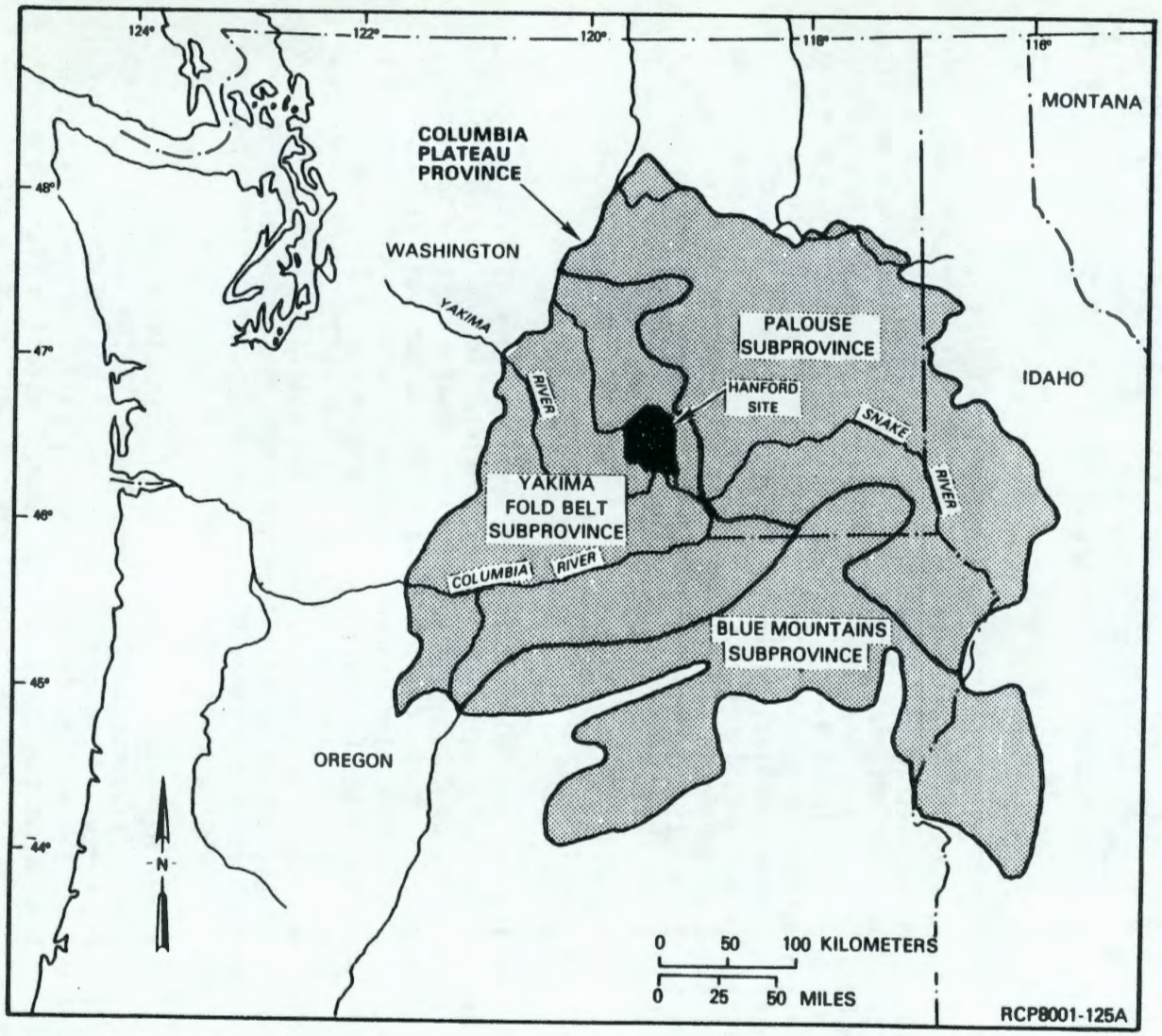

FIGURE 3-45. Informal Structural Subdivisions of the Columbia Plateau.

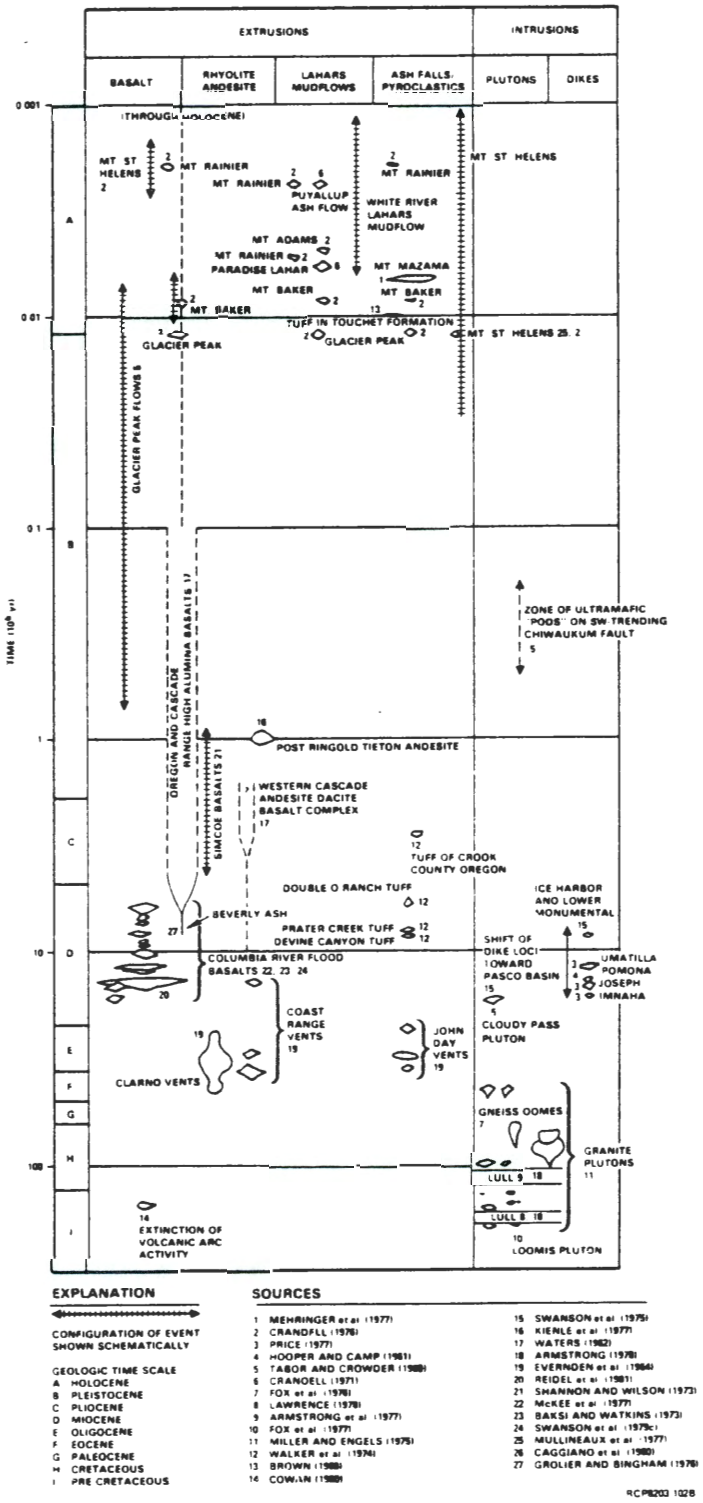

FIGURE 3-46. Chronology of Igneous Activity in the Pacific Northwest (modified after Johnpeer et al., 1981).

An event network analysis was utilized by Johnpeer et al. (1981) to evaluate relative probability of occurrence of future volcanic events and their consequences. The following discussion is taken from their work. Unlikely consequences of Cascade Range volcanism, such as flooding of the Pasco Basin or effects on the Pasco Basin resulting from Basin and Range volcanism, were considered in establishing a conservative bias to the risk-probability analysis. Waters (1973) reported that lava dams from Cascade volcanism have temporarily dammed the Columbia River in the past, although no geologic evidence has been found to suggest that such flooding was sufficiently extensive to affect the Pasco Basin. Volumes of pyroclastic materials in excess of 150 cubic kilometers have been produced by single eruptive events in the northern Basin and Range province during late Miocene and Pliocene time within the drainage basin of the Snake River.

The assessment of potential effects of renewed volcanism on a waste repository within the Hanford Site is a function of recurrence rates of volcanism from the Cascade Range, the Columbia Plateau, and the Basin and Range, and geologic conditional probabilities of a complex network of possible consequences. Of many possible-consequent events, relatively few were considered to be significant (e.g., volcanically induced flooding or covering of the site-area surface with thick air-fall tephra, ash flows, or lava flows). Still fewer consequent events were considered to represent hazards that are important to maintaining repository integrity (e.g., breach of the repository by a dike or fissure, or disturbance of the near-field groundwater flow system by a dike or fissure). Calculated probabilities of important consequent events are summarized in Table 3-7. Based on this assessment of consequent-event probabilities, the Pasco Basin may experience effects resulting from distant volcanic activity during the next 10,000 years, but probability of breach of a repository or of thermally induced disturbance of a repository resulting from volcanic activity is exceedingly low. Data supporting this conclusion are detailed in Johnpeer et al. (1981).

3.7.2.2 Faulting History. Folds and faults in Columbia River basalt appear to have developed contemporaneously during nearly north-south compression in Miocene and later time. Because fold and fault development appears to be related, the chronology and mechanics of deformation are primarily discussed in the section on folding (Section 3.7.2.3). A generalized tectonic map (Fig. 3-47) shows major folds and faults within and marginal to the Columbia Plateau. A discussion of the faulting history of the plateau is included in Myers/Price et al. (1979).

The extent to which faults may act as pathways to the accessible environment from the conceptual design repository has yet to be evaluated. The following discussion enumerates known faults in the repository area and presents some evidence supporting relatively less faulting in the Cold Creek syncline compared to the adjacent anticlines. However, the future impact of faulting is not known. Planned studies (Chapter 13) will determine the hydrologic and geologic parameters of faults zones or tectonic breccias in basalt. These data will be used to model the effects of known or potential faults on groundwater flow.

9 2 1 2 4 9 5 0 7 2 7

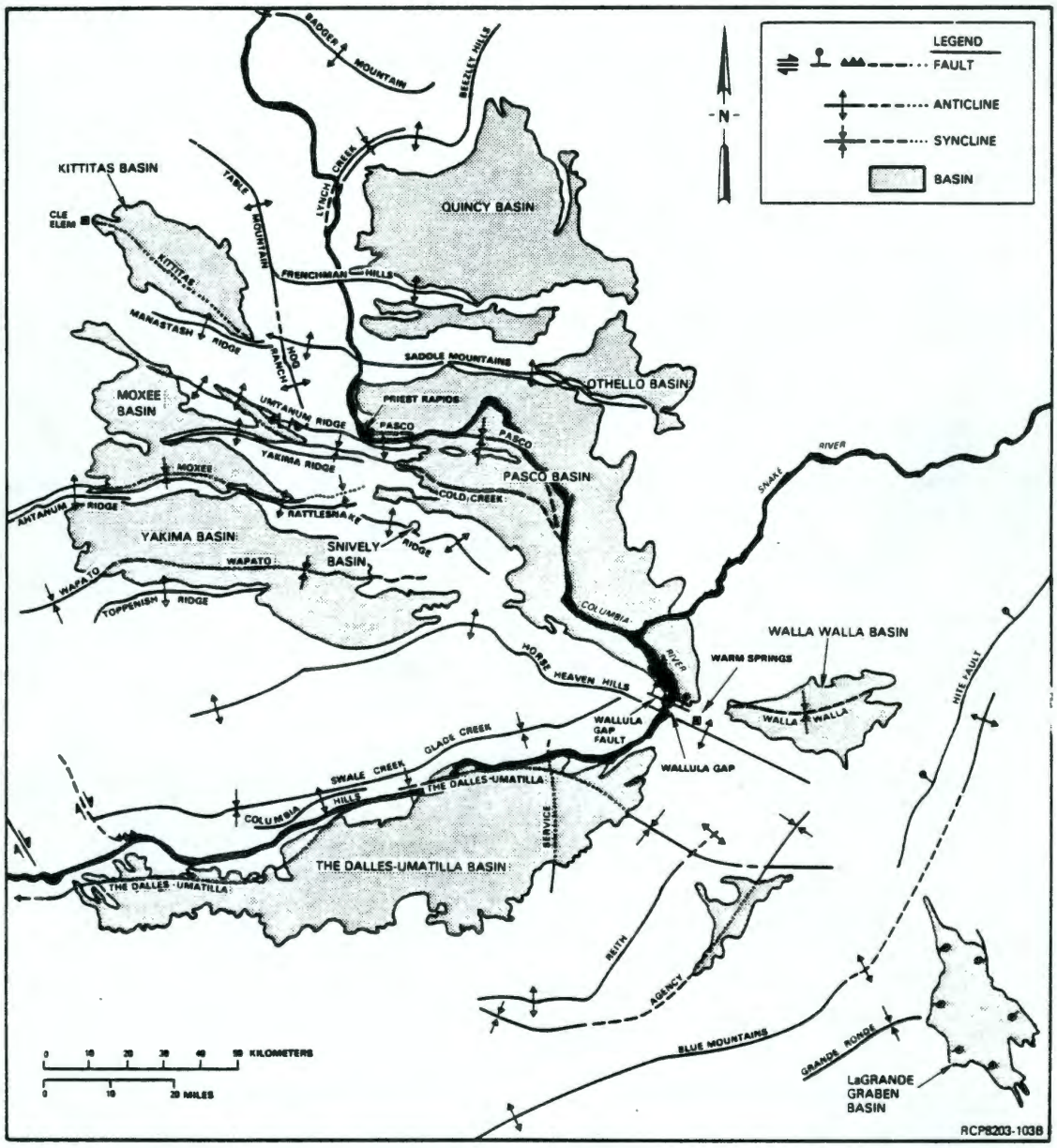

FIGURE 3-47. Generalized Tectonic Map of Part of the Columbia Plateau. Faults in the Pasco Basin are shown in Figure 3-48.

9 2 1 2 4 9 5 0 7 2 8

TABLE 3-7. Calculated Long-Term Probability of Consequent Volcanic Events (after Johnpeer et al., 1981).

Consequent event	Calculated probability (%) per 10^4 yr
Flooding of Hanford Site area surface with water due to disturbance of drainage due to volcanism	6.2
Covering of Hanford Site area surface with thick (>0.5 m) air-fall tephra layers	53.0
Ash flows affecting Hanford Site area surface	0.42
Lava flows affecting Hanford Site area surface	0.081
Breach or hydrologic effect on repository by dike or fissure	0.00053

3.7.2.2.1 Columbia Plateau. This section includes a brief discussion of faulting within each of the three structural subprovinces of the Columbia Plateau (Fig. 3-45). Emphasis is placed on the Yakima Fold Belt subprovince, where the site is located.

Blue Mountains Subprovince. The Blue Mountains subprovince of the Columbia Plateau (Fig. 3-45) is a broad faulted anticlinorium that was growing at least by early Miocene time. The general northeast trend of this province is cut by a series of north and northwest-trending, near-vertical faults, similar to faults in the High Lava Plains province to the south. Strike-slip movement has been documented on many faults. The last movement appears to have been dip-slip (Ross, 1978). Many faults terminate along the northern boundary of the subprovince where it abuts the Palouse subprovince. Specific faults within the subprovince are located in Figure 3-47.

Palouse Subprovince. The Palouse subprovince (Fig. 3-45) is underlain by basalt flows with a regional dip of about 1° to the southwest. In general, the area is structurally simple, with the most prominent structures consisting of broad folds with tens of meters of amplitude (Swanson and Wright, 1978). In the Spokane area a prominent regional

9 2 1 2 4 9 5 0 7 2 9

joint system, the Cheney fracture zone, is located along the projection of major structures in older rocks in northern Idaho (Griggs, 1976). Griggs (1976) and Swanson et al. (1979b) have suggested, therefore, that the fractures might reflect slight post-Priest Rapids adjustment of basalt strata to a structurally controlled topography in underlying rocks.

Yakima Fold Belt Subprovince. The Yakima Fold Belt subprovince covers the central and western parts of the Columbia Plateau (Fig. 3-45). The western half of the Pasco Basin, including the reference repository location, lies within this subprovince. The subprovince is characterized by long, narrow anticlines and broad synclines extending generally eastward from the Cascade Range to the approximate center of the plateau, where they generally die out (Fig. 3-47). Most known faults within the subprovince are associated with anticlinal fold axes, are thrust or reverse (although normal faults are also present), and probably developed at the same time as the folding. Northwest to north-south-trending shear zones and minor folds commonly transect these structures (Reidel, 1978a; Swanson et al., 1979b; Newcomb, 1970; Lawrence, 1976; Bentley et al., 1980). There is substantial evidence of dextral faulting along northwest trends, particularly in the southwest plateau. Some of the faults are interpreted to separate the plateau from the Basin and Range to the south (Lawrence, 1976); others are interpreted to offset the Yakima ridges and effect a net regional dextral shear. These faults are consistent with a regional tectonic regime of north-south compression and dextral plate transform along the western North American continental margin. Most faults within the subprovince do not disrupt overlying late Cenozoic sediments or post-Columbia River basalt volcanic rocks. Faults at Toppenish Ridge, Wallula Gap, and Finley Quarry that may exhibit Quaternary displacement are briefly described below. Other faults within the subprovince are discussed in Myers/Price et al. (1979).

Scarps that cut Miocene and Quaternary units occur near the crest and toe of Toppenish Ridge, the topographic expression of the Toppenish anticline that is about 40 kilometers long and about 75 kilometers west of the Hanford Site (Fig. 3-47) (Campbell and Bentley, 1981; Bentley et al., 1980; Rigby and Othberg, 1979; Myers/Price et al., 1979). Scarps near the crest and midslope on the north side of the ridge are nearly straight, dip nearly vertically, have relief of up to 2 meters, and are discontinuous, with individual scarp lengths of up to 3 kilometers. The scarp at the toe of the ridge has a relief of up to 2 meters, is continuous for several kilometers, cuts Quaternary alluvial fan and landslide units, sinuously follows topography, and approximates the trace of the 15° south dipping, largely concealed Mill Creek thrust fault (Bentley et al., 1980). A tectonic interpretation is favored for these features (Campbell and Bentley, 1981; WCC, 1981b), but a nontectonic interpretation has not been ruled out. Since the scarps cut deposits physically similar to those containing 13,200-year-old Mount St. Helens set S ash, they are assumed to be late Quaternary in age.

9 2 1 2 4 9 5 0 7 3 0

The Wallula fault is exposed intermittently from the west side of the Columbia River at Wallula Gap southeastward for approximately 50 kilometers along the north-facing slope of the Horse Heaven Hills (Fig. 3-48, no. 53). Quaternary faulting along the Wallula fault was suggested by Farooqui (1979). He found colluvium of undetermined age in fault contact with tectonic breccia, mantled by loess and Touchet beds. Trenching investigations (WCC, 1981c) support an interpretation that the faulting is probably Quaternary but older than the glaciofluvial Touchet beds. Trenching of the Wallula Gap fault, a branch of the Wallula fault located on the west side of the Columbia River, was carried out by Gardner et al. (1981). They found that faulted Ice Harbor Basalt is overlain only by undisturbed glaciofluvial gravels and Touchet beds. Gardner et al. (1981) concluded, therefore, that the last fault movement took place between Ice Harbor time (8.5 million years) and 13,000 to 22,000 years ago.

Quaternary faulting was suggested by Farooqui and Thoms (1980) along the Finley Quarry fault, a splay of the Wallula fault (Fig. 3-48, no. 51). The fault lies within one of the doubly plunging anticlines of the Rattlesnake Mountain-Wallula Gap trend (Fig. 3-48) known as The Butte. The fault juxtaposes an older colluvium against tectonic breccia along a high-angle reverse fault. Younger colluvium and loess units overlying the fault are not displaced. The younger sediments are overlain by two caliche soil horizons; the upper horizon was dated (WCC, 1981c) to be at least 70,000 years old, indicating displacement is greater than 70,000 years old. Woodward-Clyde Consultants (WCC, 1981c) concluded that the lower caliche might be equivalent in age to the pre-Quaternary Ringold Formation. Extension of this fault 3 kilometers to the northwest of the Finley Quarry exposure is suggested by a ground-magnetic survey (Cochran, 1981b).

3.7.2.2.2 Pasco Basin. Faults mapped in the Pasco Basin are associated with anticlines of the Yakima Fold Belt. Discussions of these faults are presented in Myers/Price et al. (1979, Plate III-1), WPPSS (1981), PSPL (1982), and Price (1982). The mapped faults (numbers are keyed to Fig. 3-48) closest to the reference repository location are the Umtanum fault at Priest Rapids (no. 8), faults on Gable Mountain (no. 1-4), the Silver Dollar fault on the south limb of the Umtanum Ridge structure (no. 16), two faults on the eastern end of Yakima Ridge (no. 30 and 31), thrust faults in the Snively Basin area of Rattlesnake Mountain (no. 39 and 40), and the Rattlesnake Mountain fault (no. 41). These and other faults within the Pasco Basin are located on Figure 3-48 and described in Table 3-8.

Umtanum Ridge-Gable Mountain. The Umtanum fault (Mackin, 1955) is a buried reverse fault along the base of Umtanum Ridge at Priest Rapids (Table 3-8 and Fig. 3-48, no. 8). The fault juxtaposes the vertical Frenchman Springs Member in the Umtanum Ridge anticline against the horizontal Priest Rapids Member of the Wahluke syncline. Results from drilling suggest that this fault dips southward under the ridge at approximately 30 to 40° (PSPL, 1982). Continuity of the Umtanum fault eastward toward Gable Mountain cannot be established by exposure; however, interpretations of ground-magnetic profiles suggest that Umtanum Ridge and Gable Butte could be one continuous structure (Cochran, 1981b).

9 2 1 2 4 9 5 0 7 3 1

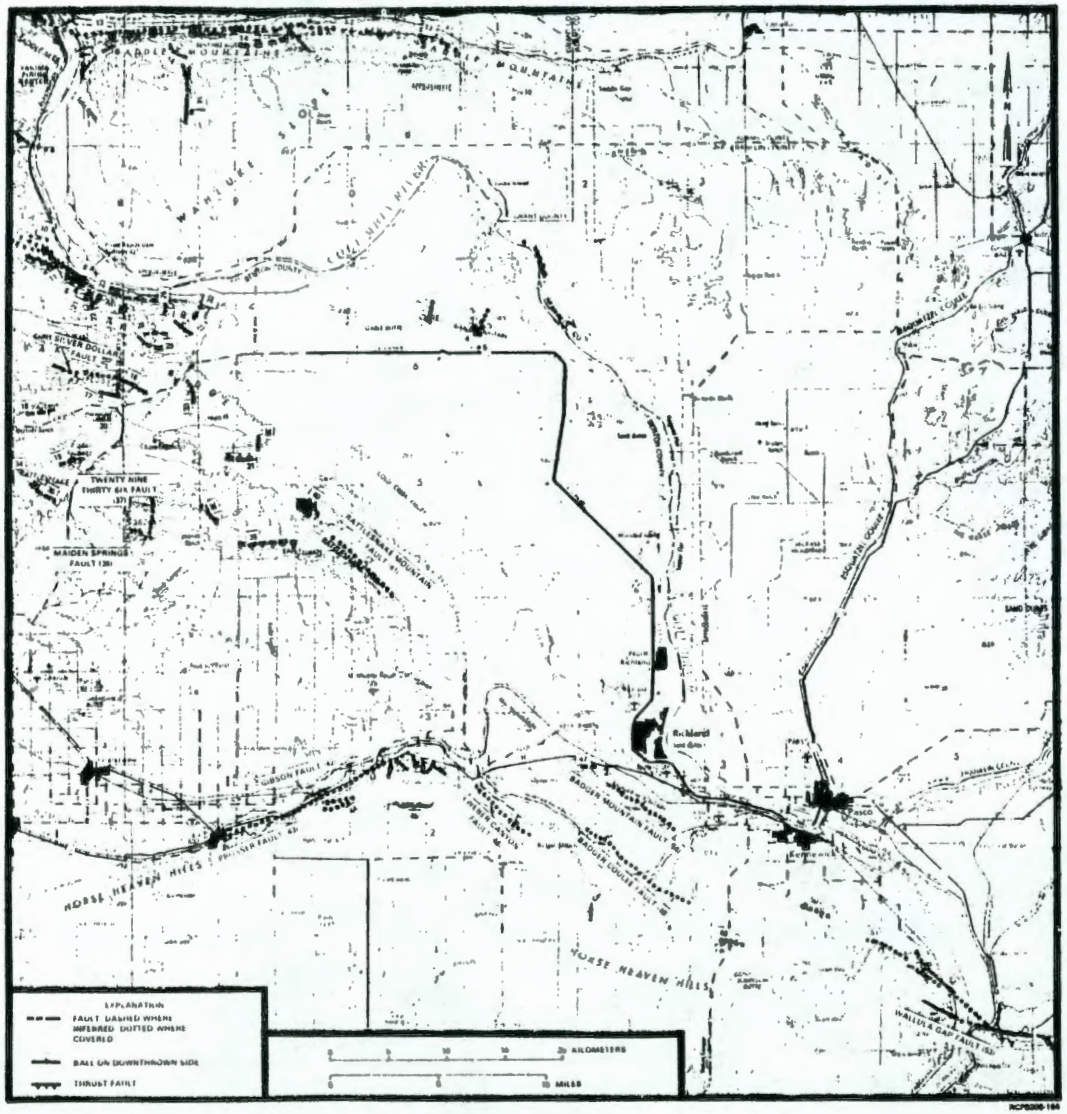

FIGURE 3-48. Faults of the Pasco Basin.

TABLE 3-8. Faults Within the Pasco Basin. (Sheet 1 of 6)

Fault* no.	Name	Length (km)	Strike/ dip	Characteristics	Age of latest displacement	References
1	West fault, Gable Mountain	∿0.8	N. 34° E./ steeply west	Normal, stratigraphic throw <5 m	Unknown	Golder (1981); Fecht (1978)
2	Central fault, Gable Mountain	<3.2	N. 55° E./ 30° S.	Reverse, 50-m dip-slip displacement, variable displacement with depth	13,000 yr	Golder (1981); Fecht (1978)
3	South fault Gable Mountain	≤1.2	E.-W./ 35° to 40° S.	Reverse, displacement 12 m	Unknown	Golder (1981)
4	North-dipping fault, Gable Mountain	Unknown	N. 65° W./ 13° N.	Reverse, 9.1 to 15.2 m wide in drill holes, stratigraphic throw 98 m	Unknown	Golder (1981)
5	DB-10 (upper) fault	0.8	Due S./ 25° to 45° W.	Reverse, dip-slip, ∿55 m displacement	Unknown	Myers/Price et al. (1979); Golder (1981)
6	Buck thrust	2.6	N. 50°- N. 80° W./ gently NE.	Thrust, zone 9 to 15 m thick, dies out in Umtanum anticline, 250 m displacement	Unknown	Price (1982)
7	Upper reverse	∿2.4	N. 60° E./ S.	Thrust, similar to Buck thrust	Unknown	Golder (1981)

TABLE 3-8. Faults Within the Pasco Basin. (Sheet 2 of 6)

Fault* no.	Name	Length (km)	Strike/ dip	Characteristics	Age of latest displacement	References
8	Umtanum fault	>12	N. 60° W./ 30° to 40° S.	Reverse, dip-slip, displacement on order of 150 m vertical and 300 m horizontal	Pre-glacio-fluvial	Goff and Myers (1978); Price (1982); Golder (1981)
9	Possible reverse fault	Unknown	Unknown	Reverse, inferred	Unknown	Golder (1981)
10	North reverse fault, Umtanum Ridge	1.5	NW./ inferred toward S.	Reverse, inferred	Post-Wanapum Basalt/-pre-Ellensburg growth	Golder (1981)
11	Twin fault	> 0.6	NE./unknown	Interpreted to be tear fault within Umtanum anticline	Unknown	Myers/Price et al. (1979); Golder (1981)
12	Smyrna fault	2	NW./vertical	Separates Smyrna Bench and Sentinel Gap segments of Saddle Mountains	Unknown	Reidel (1978a);
13	Saddle Mountains fault	>40	E.-W./less than 45° west side Sentinel Gap	Inferred reverse fault at base of the Saddle Mountains structure. Maximum stratigraphic displacement 600 m	Unknown	Reidel (1978a); Grolier and Bingham (1978)

TABLE 3-8. Faults Within the Pasco Basin. (Sheet 3 of 6)

Fault* no.	Name	Length (km)	Strike/ dip	Characteristics	Age of latest displacement	References
14	Hansen Creek fault	~5	E.-W./S.	Interpreted to be a high-angle reverse fault, displaces Priest Rapids against Frenchman Springs flows	Unknown	Bentley (1977); Myers/Price et al. (1979)
15	Secondary, unnamed faults of the Saddle Mountains structure	4 and 5	E.-W./ unknown and N.-S./ unknown	See Grolier and Bingham (1971) for alternative mapping	Unknown	Myers/Price et al. (1979)
16	Silver Dollar fault	~7	W.-NW./ unknown	Interpreted to be high angle-reverse fault (or normal), zone width 50 to 70 m, displaces Frenchman Springs Member against Umatilla and Pomona Members	Unknown	Goff (1981); Myers/Price et al. (1979)
17-20	Faults of Rattlesnake Hills-Yakima Ridge structures	1	Variable	Small fault associated with larger folds	Unknown	Myers/Price et al. (1979)
21-29	Faults of Umtanum Ridge structure	<1	NW.-SE. and N.-S./ unknown	All normal cross faults of the Umtanum anticline, displacements of a few meters	Unknown	Goff (1981)

TABLE 3-8. Faults Within the Pasco Basin. (Sheet 4 of 6)

Fault* no.	Name	Length (km)	Strike/ dip	Characteristics	Age of latest displacement	References
30	Rattlesnake Springs	~1.5	N.-NE./ unknown	Inferred fault to account for geometry change of Yakima Ridge strike-slip	Unknown	Myers/Price et al. (1979) (see text)
31	Unnamed	1.5	E.-W./N.	Inferred reverse fault under S. limb of Yakima Ridge	Unknown	Myers/Price et al. (1979) (see text)
14 32	Minor fault of Umtanum Ridge structure	Unknown	Unknown	Inferred normal fault	Unknown	Goff (1981)
33	Minor fault of Yakima Ridge structure	Unknown	Unknown	Inferred fault	Unknown	Myers/Price et al. (1979)
34-35	Faults of western Rattlesnake Hills	<2	N.-S. and NW.-SE./ unknown	Minor dip-slip cross faults associated with larger anticlines. Displacements in tens of meters	Unknown	Myers/Price et al. (1979)
36	Maiden Springs fault	~2.5	Unknown	Inferred, high angle-reverse fault with 45 to 60 m displacement.	Unknown	Bond et al. (1978a)
37	Twenty-Nine-Thirty-Six fault	4	N.-S./ vertical	Scissor fault, W. side up, 90 m displacement	Unknown	Bond et al. (1978a)

TABLE 3-8. Faults Within the Pasco Basin. (Sheet 5 of 6)

Fault* no.	Name	Length (km)	Strike/ dip	Characteristics	Age of latest displacement	References
38	Fault of central Rattlesnake Hills	1.5	NW./unknown	Vertically juxtaposes Priest Rapids basalts and Pomona basalts	Unknown	Bond et al. (1978a)
39-40	Thrust faults of Snively Basin area	>1	NW.-SE./ moderate	Not exposed, but Saddle Mountains Basalts section is repeated three times vertically with angular discordance at lower fault	Unknown	Myers/Price et al. (1979) (see text)
41	Rattlesnake Mountain fault	8	N. 50° W./ steep	Probably reverse, 400 m vertical displacement, zone 100 m wide, dies out into Rattlesnake Mountain anticline to SE.	Unknown	Bond et al. (1978a); Myers (1981) (cross section)
42	Gibbon fault	~1	NE./vertical	Juxtaposes Selah interbed against Levey interbed, 70 m vertical displacement.	Unknown	Bond et al. (1978a)
43	Prosser fault	~11	NE./unknown	Interpreted fault to account for topographic relief along Horse Heaven Hills	Unknown	Bond et al. (1978a)
44-45	Faults of Heaven Horse Hills structure	Variable	Variable	Small faults on N. slope of Horse Heaven Hills, partly owing to landsliding	Unknown	Bond et al. (1978a)

TABLE 3-8. Faults Within the Pasco Basin. (Sheet 6 of 6)

Fault* no.	Name	Length (km)	Strike/ dip	Characteristics	Age of latest displacement	References
46-48	Weber Canyon fault, Badger Coulee fault	5, 9	NW./vertical	Faults of the Badger Canyon monocline. Maximum vertical displacement 80 m down to NE.	Unknown	Myers/Price et al. (1979)
49	Minor fault associated with Horse Heaven Hills	Unknown	NW./unknown	Uncertain	Unknown	Myers/Price et al. (1979)
47, 50-52, 54	Faults associated with Rattlesnake Ridge-Badger Mountain structure. Includes Finley Quarry fault (no. 5)	Variable up to 8	Generally NW. to W.-NW./ unknown	Related to doubly plunging anticlines, dip-slip movements to 50 m	At least 70,000 yr at Finley Quarry	Jones and Landon (1978); Bond et al. (1978a); see text Section 3.7.2.2.1
53	Wallula Gap fault	50	NW./believed steep	Maximum vertical offset 330 m, scissor-type displacement, but last movement horizontal. Fault zone ~330 m wide	Undisturbed Hanford formation overlies fault. See text	Gardner (1977); Gardner et al. (1981)

*See Figure 3-48 for location of faults.

Faulting on Gable Mountain has most recently been investigated by Golder Associates (PSPL, 1982) using an extensive trenching and drilling program. These studies examined three previously mapped faults, termed the central, south, and west tear faults (Table 3-8, no. 1-3) (Bingham et al., 1970; Fecht, 1978) and discovered a fourth, buried fault (Table 3-8 and Fig. 3-48, no. 4). All faults on Gable Mountain, except for the west tear fault, are reverse faults that dip toward the north or south with displacements of approximately 12, 50, and 98 meters for the south, central, and buried reverse faults, respectively.

Golder's (1981) reexamination of trenches excavated in the late 1960s across the central Gable Mountain fault resulted in the detection of features suggestive of Quaternary movement. These features included slickensides in clastic dikes in the hanging wall, clastic dikes intruded along the fault plane, and apparent fractures in glaciofluvial deposits overlying the bedrock fault. New trenches exposed offsets of up to 6.5 centimeters along narrow fractures in glaciofluvial sediments that are continuous with a reverse fault in the basalt. These offset sediments are correlated with other glaciofluvial sediments that contain Mount St. Helens set S ash. Drilling shows that the fault has much greater displacement in the basalt at depth (the top of the Esquatzel flow is offset approximately 50 meters). The displacement in the glaciofluvial sediments is interpreted (PSPL, 1982) to be the latest movement on an older fault of greater displacement at depth. Long-term average displacement rates on the fault were calculated to be very low (approximately 5.08×10^{-6} meters per year), but this is not likely to represent the actual rate of slip during periods of quiescence or faulting.

Borehole DB-10 was cored through a structure thought to be a tight second-order fold associated with Gable Mountain (Myers/Price et al., 1979). Core from DB-10 revealed two fault zones characterized by slickensides and by tectonic breccia (Table 3-8 and Fig. 48, no. 5); one at about 130 meters depth and the other at about 192 meters depth. The stratigraphic section is repeated across the two faults in DB-10, which indicates that the two DB-10 faults are reverse faults with about 55 meters of combined displacement. Two boreholes were drilled adjacent to DB-10, and it was determined that the upper fault in DB-10 strikes north-south, dips 25° to 45° west, and is approximately 0.8 kilometer long (PSPL, 1982). Because the Gable Mountain faults are spatially and geometrically related to individual folds that make up Gable Mountain, Golder Associates concluded that all Gable Mountain faults are related to folding in a north-south to northeast-southwest compressional stress regime.

Yakima Ridge. The Silver Dollar fault (Table 3-8 and Fig. 3-48, no. 16) offsets the Frenchman Springs Member of the Wanapum Basalt against Umatilla and Pomona Members of the Saddle Mountains Basalt across a fault zone 50 to 70 meters wide (Goff and Myers, 1978; Goff, 1981). The mapped length of the fault is about 7 kilometers. Because exposures of the fault zone are poor, the inclination of the fault has not been determined. The Silver Dollar fault was interpreted by Goff and Myers (1978) and Goff (1981) as a high-angle, reverse fault, but by Bond et al. (1978a) as a possible normal fault.

9 2 1 2 4 9 5 0 7 3 9

A north-dipping, east-west trending, reverse fault and an associated fault with an interpreted strike-slip component along the southeastern end of Yakima Ridge are associated with the extension of one of the parasitic anticlines along the ridge (Table 3-8 and Fig. 3-40, no. 30 and 31). The fault with a strike-slip component is of limited extent and is interpreted to be a tear fault separating folds of different folding intensity in the anticline. The reverse fault parallels the southern limb of the anticline, but its eastern extent into the subsurface of the Hanford Site is not known. The extent of this fault is currently being investigated by a ground geophysical survey. A third fault was proposed by Kienle (in WPPSS, 1977) and by Bond et al. (1978a) to account for a linear escarpment and apparent structural displacement on the extreme eastern and southern ends of Yakima Ridge. The existence and nature of such a fault have not been confirmed because of the limited exposure in that area.

Rattlesnake Mountain. Imbricate faulting is associated with Rattlesnake Mountain, including the Rattlesnake Mountain fault and faults in the Snively Basin area (Table 3-8 and Fig. 3-48, no. 39-41). The Snively Basin area of Rattlesnake Mountain is the most structurally complex area near the reference respository location, containing at least three imbricate thrust faults involving the Saddle Mountains Basalts. Structural relations are obscured by loess and extensive landslides.

The Rattlesnake Mountain fault is a reverse fault within and parallel to the hinge area of the Rattlesnake Mountain anticline. The most recent mapping (Myers, 1981) shows that there is also a reverse fault to the northeast parallel to the Rattlesnake Mountain fault. Because of poor exposure, the relationship between the Rattlesnake Mountain faults and the thrust faults in the Snively Basin area has not yet been established.

Cold Creek Syncline. Most core holes within the Pasco Basin are located within synclines. Small fault zones a few centimeters to 1 meter in apparent width have been observed in cores taken from many core holes (Moak, 1981a). Gouge and fractures associated with these small faults physically resemble those observed within anticlines (Goff, 1981; Price, 1982). Based on the folding strain features (shear zones, shatter breccias, and anastomosing breccias) in Yakima folds (Price, 1982), any moderately dipping basalt may contain similar, small, disseminated low-dip faults. Because the Cold Creek syncline is a Yakima fold, small faults in moderately dipping basalt are probably related to folding strain. The structure of the Cold Creek syncline underlying the reference repository location is presently interpreted to be the result of folding and is discussed in greater detail in Section 3.7.2.3. However, it is possible that any dipping basalt within the reference repository location might contain at least small faults of very limited extent and displacement.

3.7.2.3 Folding History.

3.7.2.3.1 Columbia Plateau. Folding within the Columbia Plateau is discussed under the three structural subprovinces outlined in Figure 3-45: the Blue Mountains, the Palouse, and the Yakima Fold Belt. Emphasis is placed on the Yakima Fold Belt subprovince, the location of the reference repository location.

Blue Mountains Subprovince. The most prominent folding in the Blue Mountains subprovince is the Blue Mountains anticlinorium (Fig. 3-47). This uplift extends from between Clarno and Prineville, Oregon, northeast 330 kilometers to the Snake River near the Oregon-Washington border (Newcomb, 1970). The northeastern segment of the Blue Mountains anticlinorium is composed of a first-order anticline-syncline pair with narrow hinge zones and broad, flat limbs. Monoclinal axes and second-order folds steepen the otherwise gently-dipping fold limbs, primarily to the south of the fold crest (Ross, 1978; Swanson et al., 1980). In places, the oversteepened south limb is breached by a reverse fault related to the concentric nature of the folding. Folding began at least as early as late Grande Ronde time as most of the younger flows are confined to localized basins.

North of the Blue Mountains uplift near Clarkston, Washington is a complex series of folds and faults known as the Lewiston structure. The primary structure is a sharply asymmetrical, plunging, fault-bounded, anticlinal wedge; secondary folding and faulting is associated with the major structures (Camp, 1976). Formation of the Lewiston structure began as early as Wanapum time but was accelerated in Saddle Mountains time (Hooper and Camp, 1981).

Palouse Subprovince. Within the Palouse subprovince, basalts dip slightly to the southwest across the Palouse Slope. A series of long (on the order of 50 kilometers), northwest-trending, low-amplitude anticlines and synclines has developed on this slope (Fig. 3-39) (Swanson et al., 1980). Trough-to-crest distances average about 10 kilometers and axes plunge both to the northwest and southeast. Age of these structures is unknown, although Wanapum and upper Grande Ronde Basalts are involved in the folding.

Yakima Fold Belt Subprovince. The Yakima Fold Belt subprovince (Fig. 3-45) is characterized by long, narrow, anticlinal ridges and broad, sediment-filled synclinal valleys (Fig. 3-47). Deformation within this subprovince is most intense along a 40-kilometer-wide zone between Cle Elum and Wallula, Washington, a distance of approximately 200 kilometers (Fig. 3-47). This zone is referred to as the Cle Elum-Wallula lineament (Kienle et al., 1977) or deformed belt. In the Yakima area, structures within the Cle Elum-Wallula deformed belt are oblique to the northwest-southeast trend of the belt; those near Cle Elum and Wallula are more parallel to it (Laubscher, 1981). Structures outside this zone (i.e., Ahtanum and Toppenish Ridges and Horse Heaven Hills, Fig. 3-47) change trend from east-west and northeast-southwest to northwest-southeast, where they merge with the Cle Elum-Wallula deformed belt (Kienle et al., 1977). Both thin-skinned and thick-skinned tectonic models have been proposed for the origin of the Yakima folds and the deformed belt. A discussion of these models is included in Section 3.8.

West of the Pasco Basin, in the southwestern part of the Yakima Fold Belt subprovince, a system of northwest-trending, strike-slip faults is developed and displaces the Yakima folds in a clockwise sense (Swanson et al., 1979b). Northwest-trending minor folds are associated with these faults. These structures have been interpreted as part of a wrench-fault system.

9 2 1 2 4 9 5 0 7 4 1

One major cross structure is present in the Yakima Fold Belt subprovince. The north-trending Hog Ranch anticline to the west of the Columbia River (Mackin, 1961) is represented by culminations in five anticlines from the Frenchman Hills in the north to Yakima Ridge in the south (Tabor et al., 1977). Based on the distribution of basalt flows and sediments of the Ellensburg Formation, the age of the Hog Ranch structure is estimated to be at least as old as late Grande Ronde time (Reidel and Fecht, 1981) and has had a substantial influence on the evolution of the course of the Columbia River (Fecht et al., 1982).

Major anticlinal folds within the Yakima Fold Belt subprovince are long, sometimes extending 180 kilometers from the eastern edge of the subprovince to the Cascades. Fold wavelengths vary from 5 to 20 kilometers and amplitudes range up to 640 meters; structural relief is often increased by thrusting and reverse faulting along the tighter anticlines. The folds terminate eastward from the Cascades in the central Columbia Plateau as the amplitude slowly decreases to negligible levels. In some cases, a major anticline changes into a series of parallel or en echelon anticlines and synclines that plunge eastward under sediments. To the west, the folds merge with or terminate in the Cascade structures or are covered by younger rock units.

The anticlines typically are concentric, gentle to tight, and upright to inclined. The gentle, upright folds are generally symmetric, whereas the tighter, inclined folds are asymmetric, with the steeper limb sometimes vertical to overturned (Price, 1982). Asymmetric folds are generally steeper to the north. Strain is often concentrated in narrow hinges, as is common in flexural-flow folding, with a box-shaped fold profile often resulting. Monoclinal axes typically parallel major anticlinal crests throughout the Yakima Fold Belt. In the tighter folds, the concentric geometry causes a volume problem in the fold cores, necessitating the formation of thrust and reverse faults. Thus, the steep fold limbs are usually associated with faults dipping toward the anticlinal axis. Second-order folds of about 5 kilometers of wavelength, and third-order folds of less than 1 kilometer of wavelength are related to the major folds. Minor layer internal faults and cross faults are common on the fold limbs.

Structural analyses at five localities within three Yakima-fold-system anticlines (Fig. 3-47) have been conducted by Price (1982). His findings suggest that the strain geometries and distributions are consistent along any one anticline and between different anticlines. Because the distribution of strain elements (faults and other shear zones, shatter breccias, and tectonic joints) is systematically related to their position within the fold, the strain is interpreted to be related to the folding process.

The Umtanum Ridge structure, well exposed at Priest Rapids (Fig. 3-47), is believed by Price (1982) to be typical of the style of folding in the Yakima fold system. The mechanical model proposed for this fold is that of buckling of the basalt flows accompanied by reverse slip parallel to flow contacts and by internal shear and bending strain within individual basalt flows. The strain distribution and geometry are illustrated in a reconstructed cross section of the Umtanum anticline after the mechanism of flexural-flow buckling (Ramsay, 1967). This cross section is shown in Figure 3-49. Overall, the fold geometry and strain distribution are in remarkable accord with that predicted in the mechanical model. The Umtanum Ridge structure and internal layer strain geometry suggest that displacement along the Umtanum reverse fault grew from the fold core to the surface because of mass balance problems inherent in concentric folding. Therefore, faulting along the Umtanum fault below the level of the fold core is not required.

3.7.2.3.2 Reference Repository Location. The reference repository location is situated within the Cold Creek syncline of the Pasco Basin. Folding within the basin and syncline is discussed in Myers/Price et al. (1979) and Myers and Price (1981).

Pasco Basin. The Pasco Basin spans the area of transition between the Yakima Fold Belt subprovince and the Palouse subprovince. Anticlinal folds bound the basin on the north and south and plunge eastward into the Pasco Basin from the west (Fig. 3-47). Synclines between the anticlines are generally broad, open folds that are sediment-filled. The characteristics of folds within the Pasco Basin are summarized in Table 3-9; locations of these folds are shown in Figure 3-50. Most of the anticlines are asymmetric and have second-order folds in their hinge zones. Their style of deformation changes along strike and their steep flanks are commonly faulted where structural relief is high. Most subsurface structures in the central Pasco Basin appear to be extensions of the anticlinal folds and their associated second-order structures; however, a few subsurface structures might be related to north-west-trending structures that appear to crosscut the east-west-trending folds (Myers/Price et al., 1979; Myers, 1981).

The distribution of flows in the subsurface suggests that initial folding and uplift along anticlinal ridges in the Pasco Basin occurred during Grande Ronde time; however, the large volume and rapid outpouring of Grande Ronde Basalt may have obscured slow, ongoing deformation. Earliest deformation detected in the Pasco Basin is along an east-west and northwest-southeast-trending fold in the Saddle Mountains during Grande Ronde time (Reidel, 1978a; Reidel et al., 1980). The greatest amount of relief on most structures took place after Elephant Mountain time (Kienle et al., 1978; Bentley, 1977; Bond et al., 1978a; Brown and McConiga, 1960; WPPSS, 1977; Reidel, 1978a; Reidel et al., 1980). Maximum relief on anticlines of the southern part of the Pasco Basin, such as the Horse Heaven Hills and the Rattlesnake Mountain-Wallula trend of ridges, took place after eruption of the Ice Harbor Member (Bond et al., 1978a), 8.5 million

9 2 1 2 4 9 5 0 7 4 3

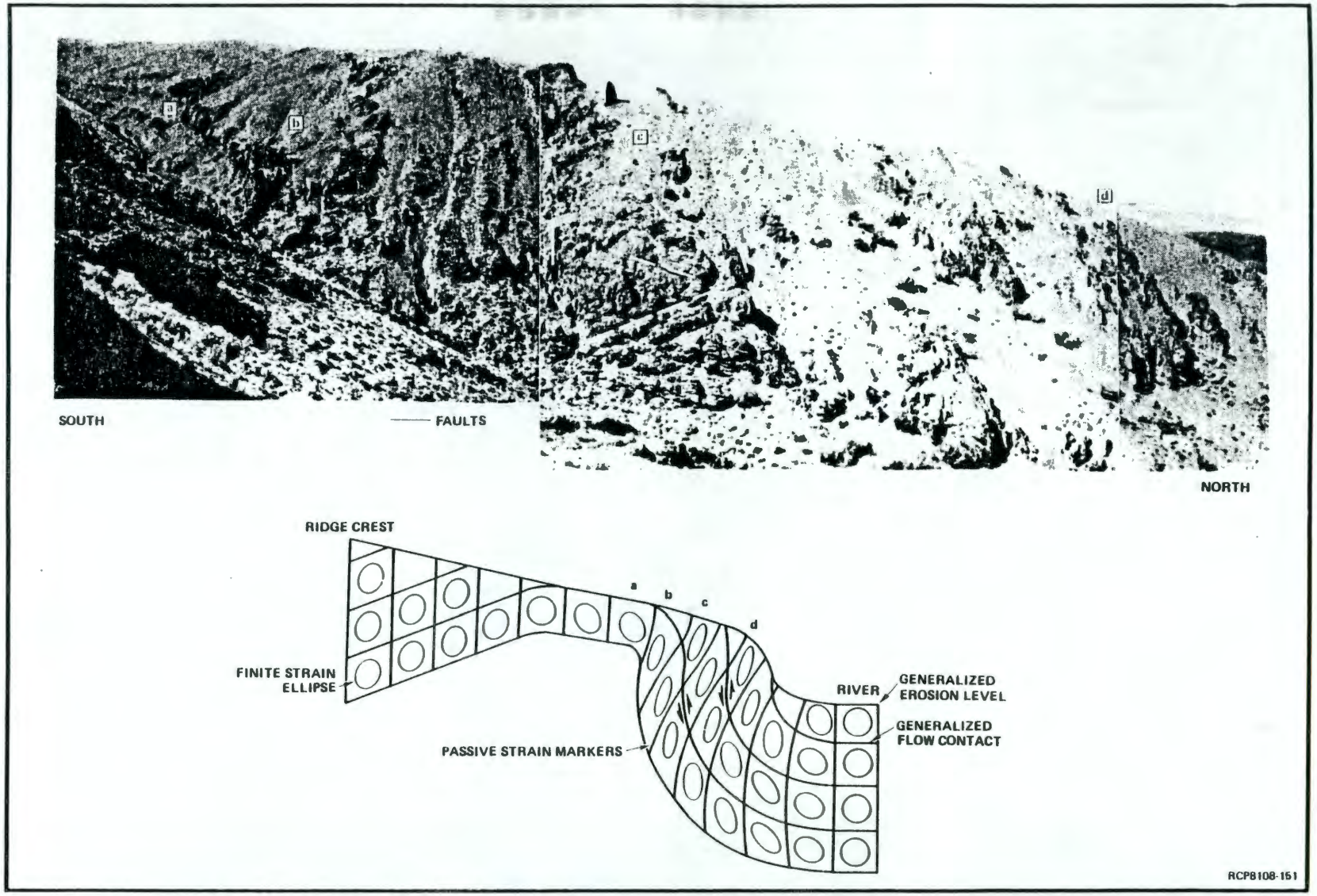

FIGURE 3-49. Comparison of the Interpreted Strain Geometry of the Umtanum Anticline with a Photomosaic of a Canyon in the Priest Rapids Area (SE¼ of NE¼, sec. 4, T. 1.3 N., R. 23 E.). Strain geometry interpretation for the Umtanum anticline includes a generalization of the present erosional topography. Regions designated a, b, c, and d are interpreted to correspond with areas noted in the photomosaic by like symbols. No vertical exaggeration. Note shrubs for scale.

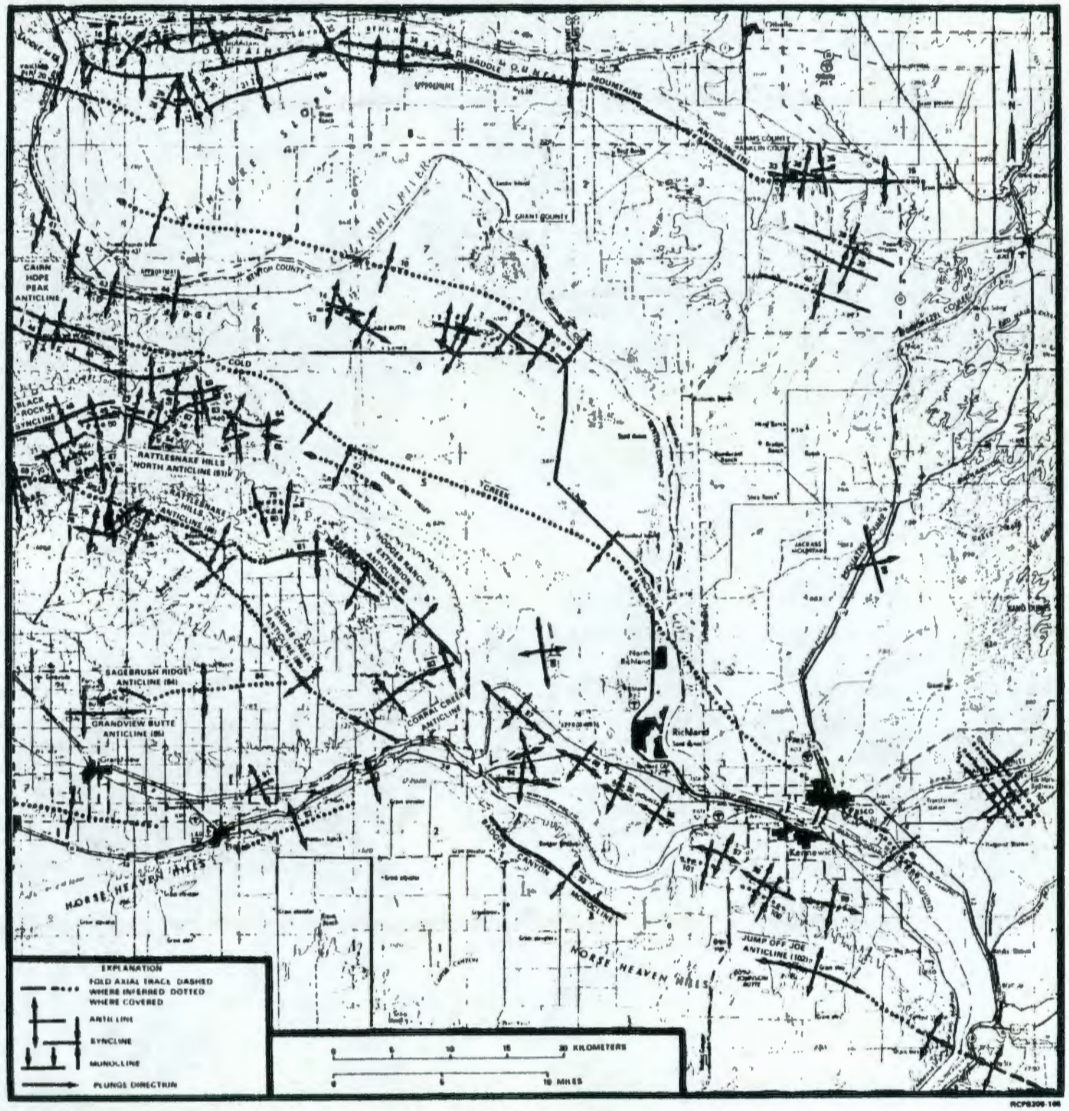

FIGURE 3-50. Folds of the Pasco Basin.

TABLE 3-9. Characteristics of Folds Within the Pasco Basin. (Sheet 1 of 3)

Fold* no.	Name	Length (km)	Geometry	References
1-9	Folds associated with Gable Mountain structure	Up to 13	Asymmetric to symmetric, amplitude to 300 m, most plunge to SE., W.-NW.-E.-SE. to NW.-SE. trend, open to tight, rounded to angular hinges, eastern segment of Umtanum Ridge structure	Fecht (1978); Golder (1981)
10	Wahluke syncline	∿40	Asymmetric, plunges to SE., not exposed	Myers/Price et al. (1979)
11-14	Folds associated with Gable Butte structure	Up to 3	Symmetric, amplitude to 300 m, generally plunge to SE., W.-NW.-E.-SE. to E.-NE.-W.-SW. trend, open, rounded hinges, part of Umtanum Ridge structure	Fecht (1978); Golder (1981)
15-37	Saddle Mountains anticline and related folds	110 primary, 3 to 11 secondary	Asymmetric, amplitude to 600 m, plunges to E., E.-SE. trend, gentle to open, box fold in part, faulted on N. side, second-order folds trend E.-W. to NW.-SE.	Myers/Price et al. (1979); Price (1982); Reidel (1978a)
38-40, 89,103	Folds of eastern Pasco Basin	3 to 6.5	Low-amplitude folds on larger homocline, W.-NW.-E.-SE. and N.-NW.-S.-SE. trends	Myers/Price et al. (1979)
41-44	Folds of the Umtanum Ridge structure	110	Asymmetric, amplitude to 1,500 m, variable plunge, E.-W. to W.-NW.-E.-SE. trend, open to tight, box fold in parts, fault on N. side (Umtanum), axial line not continuously mapped	Goff (1981); Myers/Price et al. (1979); Price (1982)

TABLE 3-9. Characteristics of Folds Within the Pasco Basin. (Sheet 2 of 3)

Fold* no.	Name	Length (km)	Geometry	References
45	Cold Creek syncline	60	Asymmetric, low-amplitude, 3° to 5° SE. plunge, W.-NW.-E.-SE. trend, gentle, two depressions along trough	Myers/Price et al. (1979); Myers and Price (1981)
46-50, 52-66	Yakima Ridge and associated folds	75	Asymmetric, SE. plunge, W.-NW.-E.-SE. trend. E. end buried by sediments, eastern exposed part is series of en echelon, doubly plunging, asymmetric folds	Bond et al. (1978a); Goff (1981); Myers/Price et al. (1979)
51, 67-81	Rattlesnake anticline, western segment	56	Asymmetric, E.-W. trend, tight, rounded hinge, numerous second-order folds on hinge and crest	Bond et al. (1978a); Myers/Price et al. (1979)
82,87, 88, 95-101	Rattlesnake anticline, eastern segment	70	Asymmetric, NW.-trending series of doubly plunging, slightly en echelon, locally faulted folds. No. 82 is asymmetric, amplitude to 640 m, NW. trend, and faulted on N. side	Bond et al. (1978a); Jones and Landon, (1978); Myers/Price et al. (1979)
83-86, 91	Rattlesnake anticline, second-order folds on S. limb	5 to 16	Variable plunge and trend	Bond et al. (1978a); Myers/Price et al. (1979)

TABLE 3-9. Characteristics of Folds Within the Pasco Basin. (Sheet 3 of 3)

Fold* no.	Name	Length (km)	Geometry	References
92	Horse Heaven Hills anticline, western segment	>80	Asymmetric, ∿70 m amplitude, NE.-SW. trend, open, monoclinal northern hinge.	Bond et al. (1978a); Myers/Price et al. (1979)
93, 102	Horse Heaven Hills anticline, eastern segment	70	Asymmetric, doubly plunging, NW.-SE. to W.-NW.-E.-SE. trend, gentle to open. No. 102 is asymmetric, second-order fold	Bond et al. (1978a); Jones and Landon (1978); Myers/Price et al. (1979)
90	Folds of the Horn Rapids lineament	>1	Poorly exposed, aligned basalt knolls interpreted to be plunging, open anticlines	Bond et al. (1978a)
94	Goose Hill anticline	∿3	Symmetrical, 150 m amplitude, doubly plunging, curvilinear axis of E.-W. trend	Bond et al. (1978a)

*See Figure 3-50 for location of folds.

years before present. The Ringold Formation (3.7 to 8.5 million years before present) overlying the basalt of the central Pasco Basin is slightly folded; the strata dip concordantly with the basalt in the Yakima fold system (Grolier and Bingham, 1978; Routson and Fecht, 1979; Tallman et al., 1979; PSPL, 1982). Current data and interpretations suggest that deformation of the Pasco Basin began in the Miocene at a low rate of strain and has continued at such a rate into the present.

Major synclines within the Pasco Basin include the Wahluke and Cold Creek synclines. The Wahluke syncline lies between the Saddle Mountains and Umtanum Ridge-Gable Mountain anticlinal structures (Fig. 3-50). The Cold Creek syncline is the relatively low-relief, sediment-filled trough that is bounded by the Umtanum Ridge-Gable Mountain anticlinal structures and the Yakima Ridge and Rattlesnake Mountain anticlinal structures (Fig. 3-50).

Cold Creek Syncline. The reference repository location is located within the Cold Creek syncline, the southernmost of two major synclines within the Pasco Basin. The structure of the Cold Creek syncline area is characterized by (1) areas of nearly flat-lying basalt; (2) three east-southeast-plunging, first-order anticlines (Umtanum Ridge, Yakima Ridge, and Rattlesnake Mountain structures); (3) two southeast-plunging, second-order anticlines (Gable Butte and Gable Mountain); (4) third-order folds within the hinge zones of the second-order anticlines and on the limbs of the first-order anticlines; and (5) northwest- and possible northeast-trending cross structures. The dominant structural trend in the Cold Creek syncline area is east-west to northwest-southeast. Structural relief is approximately 300 meters in the western part of the Cold Creek syncline area and decreases to the east.

The structure of the Cold Creek syncline has been interpreted by Myers (1981) utilizing available borehole, seismic reflection, multilevel aeromagnetic, ground-magnetic, and gravity data. Because of the large number of boreholes to the top of basalt, Myers (1981) used this surface as a datum for interpretation of the general structure of deeper horizons, which have been penetrated with only a few boreholes. Although the top-of-basalt map (Fig. 3-51) is not a structure contour map in the strictest sense, it is believed to depict the general deformation of the syncline (Myers, 1981). The use of this structure contour for extrapolating deep horizons is limited because of ongoing deformation throughout the Miocene, which resulted in thickness variation in deeper basalt flow.

The Cold Creek syncline is an asymmetric, open, broad, and relatively flat-bottomed fold (Fig. 3-51) with a steeper south limb. Two depressions occur along the trough line of the Cold Creek syncline: the Cold Creek Valley depression and the Wye Barricade depression. The top of basalt in the center of the Cold Creek Valley depression is nearly flat, except perhaps for small flexures. The Wye Barricade depression, a large, irregular-shaped area, appears to be divided into northern and southern subdepressions separated by a buried ridge. The Cold Creek syncline plunges and dies out to the east in the vicinity of the Wye Barricade depression. The reference repository location is located in the Cold Creek Valley depression.

9 2 1 2 4 9 5 0 7 4 9

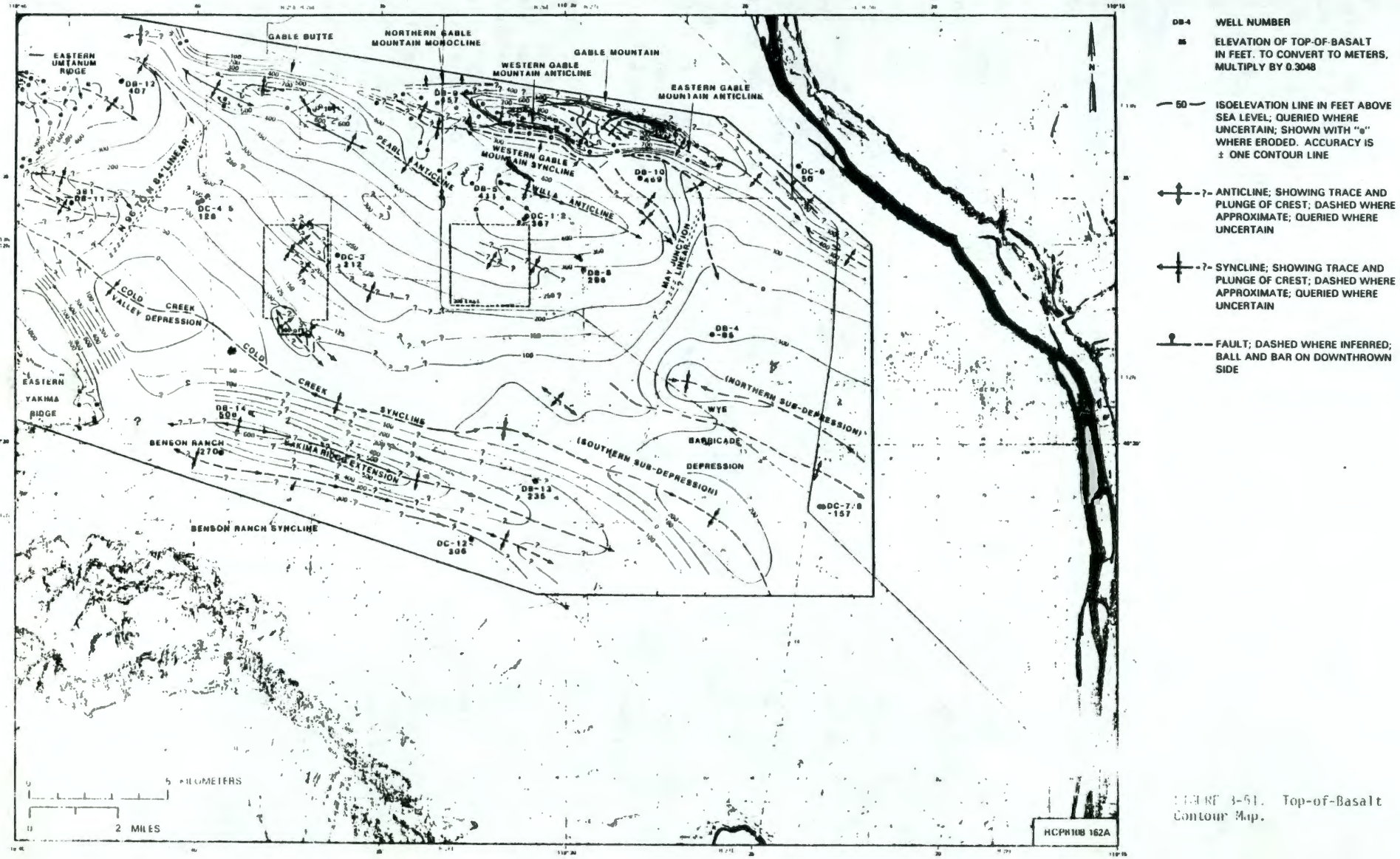

DB-4 WELL NUMBER

85 ELEVATION OF TOP-OF-BASALT IN FEET. TO CONVERT TO METERS, MULTIPLY BY 0.3048

50 ISOELEVATION LINE IN FEET ABOVE SEA LEVEL; QUERIED WHERE UNCERTAIN; SHOWN WITH "e" WHERE ERODED. ACCURACY IS ± ONE CONTOUR LINE

?- ANTICLINE; SHOWING TRACE AND PLUNGE OF CREST; DASHED WHERE APPROXIMATE; QUERIED WHERE UNCERTAIN

?- SYNCLINE; SHOWING TRACE AND PLUNGE OF CREST; DASHED WHERE APPROXIMATE; QUERIED WHERE UNCERTAIN

FAULT; DASHED WHERE INFERRED; BALL AND BAR ON DOWNTHROWN SIDE

FIGURE 3-51. Top-of-Basalt Contour Map.

Based on data that was used to compile the top-of-basalt map, Myers (1981) divided the western Cold Creek syncline (i.e., the area of the reference repository location), into five (I through V) large, relatively intact volumes of bedrock whose boundaries are defined by the known or potential structures identified in Figure 3-52.

The reference repository location lies within intact bedrock volume I (Fig. 3-52), in which six aeromagnetic anomalies have been identified by Werner deconvolution solutions (Holmes and Mitchell, 1981, Fig. B-11 and B-12). Because these solutions might correspond to bedrock structures, they were conservatively interpreted as such and used to further subdivide intact bedrock volume I into smaller volumes designated Ia through Ig. The reference repository location is almost entirely within Ia, Ib, and Id; the Cold Creek Valley depression is almost entirely within Ia and Ib. Overall, the central and eastern parts of the Cold Creek Valley depression appear to be free of bedrock structures compared with other parts of the Cold Creek syncline and the Hanford Site. Geologic structure of the basalt within this area is interpreted as being nearly flat lying with very gentle dips toward the trough of the Cold Creek syncline and with a slight westward component of dip toward the deepest point of the Cold Creek Valley depression.

Structural analysis of the Yakima fold structures (Price, 1982) shows that any dipping basalt might be expected to contain small breccia zones or faults. Within the Cold Creek syncline, discrete shear zones or faults a few centimeters to 1 meter wide may be present (Fig. 3-53). Brecciation is a dilational process that would locally increase the permeability and porosity until the breccia is sealed with a precipitated cement. Although most individual fault breccias noted in boreholes within the Pasco Basin have not been tested hydrologically, some hydrologic test intervals have included some small faults as part of a large composite test (Moak, 1981a). Recently, a tectonic breccia in the Frenchman Springs Member in RRL-6 was tested. The results of these tests are discussed in Section 5.1.3.3. Future studies will include the determination of the properties of breccia zones for input to hydrological models (Chapter 13).

3.7.2.4 Jointing History. Major joints in the Columbia Plateau have been analyzed using U-2 high-altitude photographs (Sandness et al., 1981; Section 3.6.6). Linear features in basalt are identified only as "probable" joints, as image analysis could not be used to distinguish between tectonic and primary joints. Northwest- and northeast-trending joints were observed to occur principally in the eastern portion of the plateau in areas where loess has been stripped by catastrophic floods. The loess-covered parts of the Columbia Plateau have few lineaments classified as joints, but this was attributed more to the result of cover than to their absence (Sandness et al., 1981). The age and major characteristics other than orientation are not generally known for the areally identified joints.

9 2 1 2 4 9 5 0 7 5 2

DRAFT

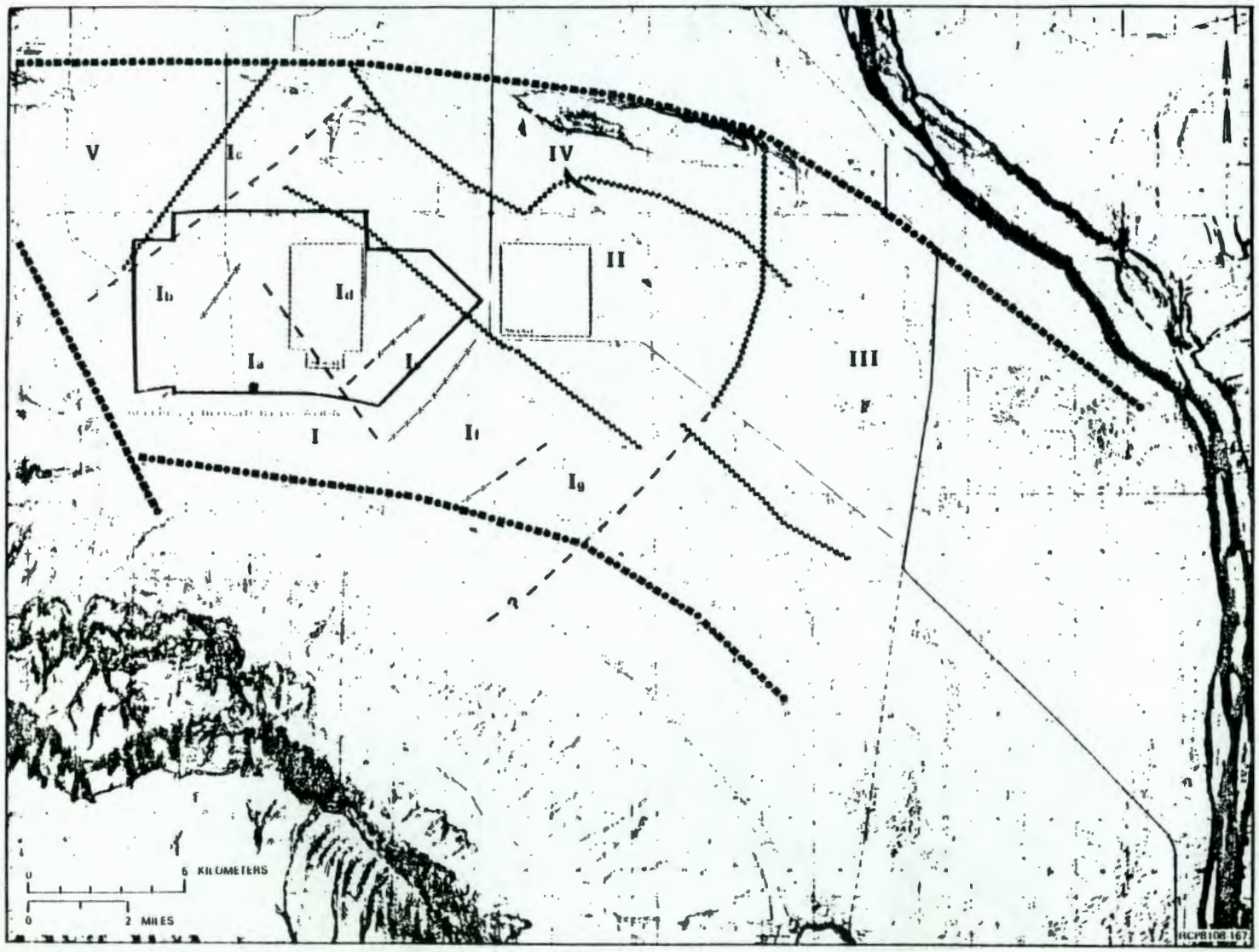

KNOWN AND INFERRED STRUCTURE

- MAJOR
- INTERMEDIATE
- SMALL
- DEEP (MAY NOT AFFECT SADDLE MOUNTAINS GROUNDWATER FLOW)

FIGURE 3-52. Interpretive Bedrock-Structure Map. Areas I through V are plan views of large, relatively intact volumes of bedrock with boundaries defined by known and inferred structures as shown. Areas Ia through Ig are subdivisions of Area I, also based on known and inferred structures.

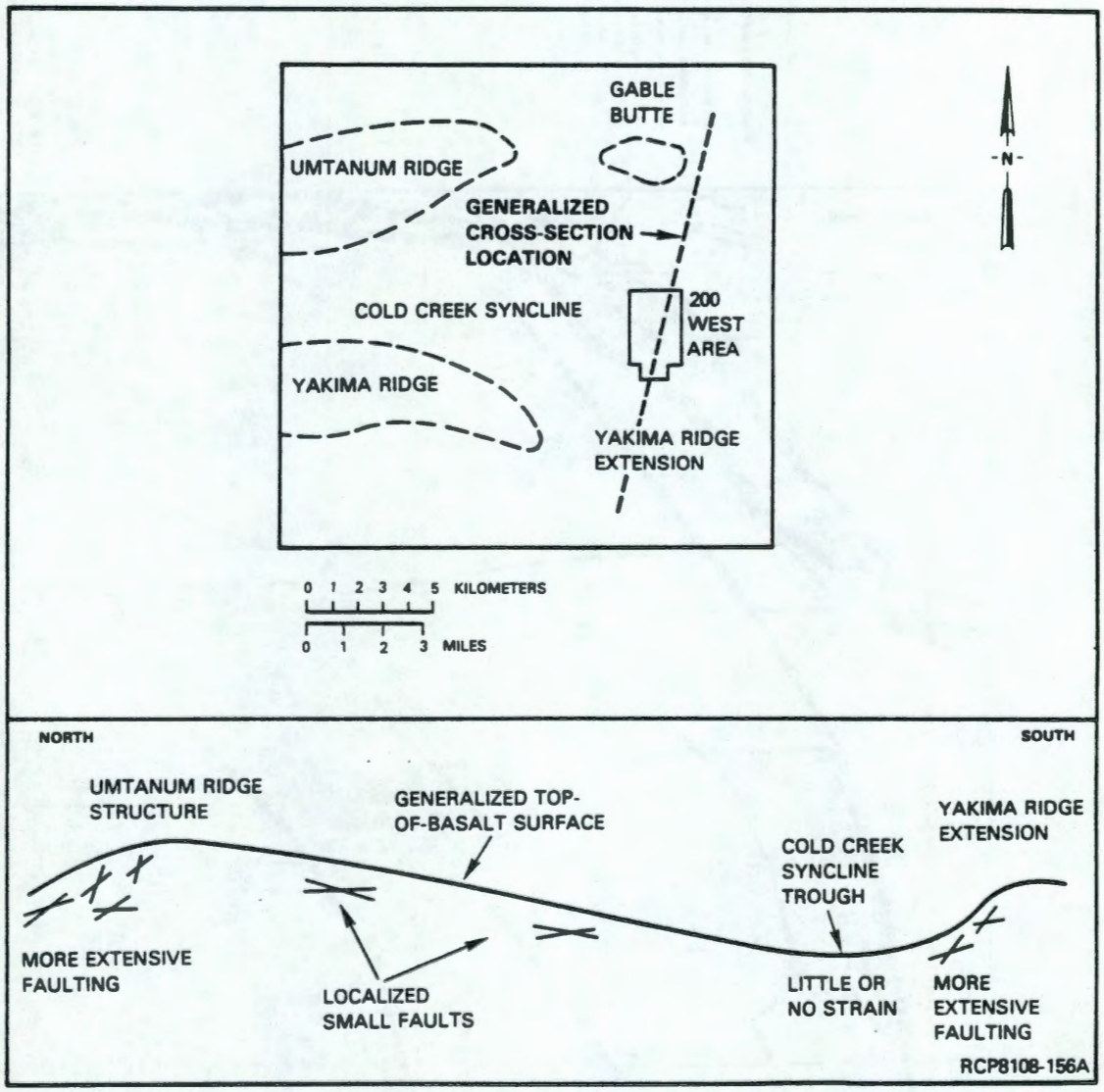

FIGURE 3-53. Schematic Cross Section, Cold Creek Syncline (illustrating predicted distribution of faults with respect to folds).

Joints within the Umtanum Ridge anticline in the Yakima River Canyon at Baldy were examined by Price (1982) in order to compare the joint densities and orientations between the anticline and the syncline to the south (Price, 1982). That syncline, the Burbank Creek syncline, is analogous to the Cold Creek syncline in the Pasco Basin, in that it is located south of the Umtanum anticline. Price found that the number of tectonic joints decreases and the distance between joints increases from the anticlinal hinge toward the synclinal trough. Examination of excellent exposures within the trough of the Burbank Creek syncline revealed no joints that are clearly tectonic (Price, 1982).

A study by Price (1982) on Umtanum Ridge at Priest Rapids revealed that four tectonic joint sets are dominant. Two sets strike perpendicular to and parallel to the fold axis, respectively, and have vertical dips. The other two sets strike perpendicular to the fold axis but are conjugate sets with inclined dips. These sets represent extension parallel to the fold axis and extension perpendicular to the fold axis during folding. The most pronounced joints occur in the core of the fold, and joints decrease upward in the structure to where they are not recognized above the Vantage horizon. Because jointing is systematically related to folding, the joints are interpreted to be the same age as the folds (Price, 1982).

Price (1982) also examined outcrops of Pomona and Elephant Mountain basalt at Gable Mountain and Gable Butte within the Hanford Site. In spite of excellent exposure, no conclusively tectonic joints were recognized in outcrops using criteria established for joint recognition on Umtanum Ridge. However, studies of the Near-Surface Test Facility (Moak and Wintczak, 1980) suggest that tectonic jointing might be more pronounced within the cores of the Gable Mountain fold. Observations on Gable Butte-Gable Mountain seem consistent with the distribution of joints on Umtanum Ridge.

The pattern of joints described above suggests that relatively few tectonic joints should be found in the Cold Creek syncline. Those present should strike either perpendicular to or parallel to the fold axis, have near vertical dip, and cross flow contacts at a high angle (Price, 1982). The effect of tectonic joints on groundwater flow depends on their frequency, spacing, extent of filling, aperture, and the hydraulic head (Arnett et al., 1980). Minerals filling tectonic fractures have not been identified, but presumably are similar to those that fill cooling joints and vesicles (i.e., smectites, zeolites (clinoptilolite) and various silica polymorphs (see Section 6.15)). The age of mineral fillings has not been determined.

3.7.2.5 Uplift, Tilting, and Subsidence. The lateral extent of basalt flows suggests that a westward dipping regional slope of 1 to 2 meters per kilometer was present in Grande Ronde time (Hooper and Camp, 1981; Reidel, 1981). The persistence of the gradient of the Snake River suggests that this slope has remained relatively constant from Saddle Mountains time to today (Swanson and Wright, 1976).

9 2 1 2 4 9 5 0 7 5 4

Long-term rates of uplift and subsidence for the Pasco Basin have been calculated (Reidel et al., 1980; Reidel and Fecht, 1981) by extrapolating the regional paleoslope into the Pasco Basin and determining those areas that have either raised or subsided relative to this datum. It is not possible to separate the roles of uplift and subsidence. From isopach maps of the Wanapum and Saddle Mountains Basalts, Reidel et al. (1980) found that the anticlinal ridges were developing in the Miocene, perhaps earlier than late Grande Ronde time (about 14.5 million years ago). The thickness of noneroded basalt flows essentially forms a cast of the topography of the area during an instant of Miocene time. The difference in thickness of noneroded flows is a measure of the topographic relief during the time of solidification of these flows. The thinnest portions of flows occur in areas that are currently anticlines, suggesting that these ridges had already begun development in the Miocene. When this difference in thickness is plotted against the radiometrically determined ages of the flows, it indicates a nearly uniform average rate of uplift. Plots of such data from the Saddle Mountains and from Rattlesnake Mountain (using some borehole data) indicate long-term average rates of uplift of 40 meters per million years (Reidel et al., 1980).

This relatively low rate of long-term uplift and subsidence has apparently persisted into recent times (Caggiano et al., 1980). Recent geodetic surveys (Savage et al., 1981) of a 19-station trilateration array within the Pasco Basin indicate that the present rate of crustal shortening is less than 1.0 millimeter per year. Sediments overlying the basalt show cumulative deformation, suggesting ongoing deformation through their deposition. Extrapolating this rate of subsidence and uplift from the Miocene until the present places various basalt members at an elevation that corresponds to their present elevation (Reidel and Fecht, 1981).

Estimating short-term deformation rates is constrained by the data available. The lack of continuous basalt and sediment deposition allows only long-term rates to be calculated and thus the periodicity and magnitude of short-term activity can only be estimated. Several lines of evidence, however, constrain the maximum short-term rates. The presence of folded Miocene basalt, rather than fault scarps with measurable offset preserved beneath younger flows, suggests that deformation occurred at a rate slow enough to permit ductile deformation. This is also consistent with a short periodicity, rather than brief periods of significant activity separated by long periods of inactivity. The lack of Quaternary faults with considerable offset suggests that deformation during this period has been of low magnitude. The present seismic record and trilateration surveys suggest that stress that is now being released is also of low magnitude and short periodicity. Recorded activity in the Miocene to present suggests that the long-term rate provides a reasonable estimate of past short-term rates.

3.7.2.6 Active Stress Field. Using published geologic and tectonic studies, in situ test data, and focal mechanism solutions, Zoback and Zoback (1980) divided the United States into stress provinces. The Pacific Northwest stress province is characterized by nearly horizontal, nearly north-south compression, which seems incompatible with eastward subduction of the Juan de Fuca Plate (see Section 3.8.2). Although few studies have been performed, changes in line lengths of trilateration surveys in the Puget Sound region and the Hanford area (Savage et al., 1981), along with changes in level lines (Ando and Balazs, 1979) suggest that subduction may be continuing relatively aseismically at a relatively low rate of 3 to 4 centimeters per year (Riddihough and Hyndman, 1976). Earthquakes have been recorded to a depth of 90 kilometers in the Puget Sound area (Crosson, 1972) and their distribution suggests a northeastward gently dipping zone of seismicity (Crosson, 1980). Residuals from long refraction surveys suggest the presence of steeply dipping slabs of high-velocity material beneath the Cascades (Rohay, 1982), but clear evidence of a Benioff zone, as is common along a consumptive plate boundary, is absent.

The extant stress field for the Pasco Basin has been assessed through the orientation of geologic structures, geodetic surveys, and focal-mechanism solutions. The nearly east-west trend of Umtanum Ridge-Gable Mountain, Yakima Ridge, and the Saddle Mountains suggests compression along a generally north-south axis to develop these anticlines. Northwest-trending, steeply dipping faults with inferred oblique slip along Rattlesnake Mountain and in the Cle Elum-Wallula zone of deformation similarly suggest compression along a near north-south axis. Thrust faults of east-west trend on the east-west anticlinal ridges similarly indicate north-south compression. Changes in line length of the Hanford trilateration array suggest that nonuniform compression is occurring in the Pasco Basin (Savage et al., 1981). While the data are barely beyond the limits of the technique, a low rate of strain of about 0.04 millimeter per kilometer per year along a northeast axis and 0.02 millimeter per kilometer per year along a northwest trend is indicated. The contemporary rate of strain determined geodetically approximately agrees with that determined geologically during the period 10 to 14 million years ago. Focal mechanism solutions for individual shallow and deep events, as well as composite solutions for shallow swarm events, indicate that slip occurs on different planes oriented approximately east-west and dipping steeply to the north or south (see Section 3.7.3). Thus, contemporary seismicity similarly indicates north-south compression at a relatively low rate of strain, as judged by the size and distribution of earthquakes.

In situ testing, using hydrofracturing (Haimson, 1978) and overcoring (Kim, 1980) techniques, has been performed at shallow depths in the Near-Surface Test Facility at Gable Mountain and hydrofracturing tests have been conducted in boreholes DB-15 and DC-12. Preliminary analysis of the Umtanum level of DC-12 and the Roza level of DB-15 indicate that the average ratio of maximum horizontal to vertical stress is approximately 2. A more detailed discussion of in situ stress studies is presented in Section 4.6.

3.7.2.7 Vertical Crustal Movement. Average rates of net uplift and subsidence of Rattlesnake Mountain and the Saddle Mountains were calculated for the period 14 to 10 million years ago and found to be less than 80 meters per million years (Reidel et al., 1980). Details of this analysis are discussed in Section 3.7.2.5.

Analysis of data from four leveling surveys was conducted by Tillson (1970). These surveys were run from four distant points to Pasco, Washington from different azimuths at different times. The subsidence determined was relative to a Seattle to Pasco line that was arbitrarily taken as fixed (i.e., no change in elevation); thus, the estimated rate of approximately 1 millimeter per year is relative. No accelerated rate of crustal change was seen in the vicinity of mapped faults. Tillson (1970) concluded that average subsidence of the area had been continuous at a very low rate since the early Cenozoic. Subsidence and uplift rates are too low to be demonstrated with gravity over the past few years.

Nonuniform shortening of lines of the Hanford trilateration array suggests that elevation changes may be occurring at a very slow rate (Savage et al., 1981). From such data, it is possible to determine that some crustal shortening is occurring, but it is not possible to determine whether the deformation is producing uplift or subsidence, or whether it is localized along specific structures. To answer the question of possible localized shortening, several small trilateration surveys have been recently established across mapped or inferred geologic structures (i.e., Horse Heaven Hills, Snively Basin, Warm Springs (Fig. 3-47 and 3-50)). These arrays have been surveyed once and will be resurveyed at periodic intervals to see if there is localized crustal shortening and at what rate the shortening is occurring.

3.7.3 Seismicity of the Columbia Plateau

Records of earthquakes in the Pacific Northwest go back to about 1850, but early records are very qualitative and permit only general indications of stress release in the Columbia Plateau and region. A network of seismographs that locates earthquakes with reasonable precision appeared only in the last two decades. A review of historical seismicity before and after installation of this network, now operated by the University of Washington, is contained in Myers/Price et al. (1979), Weston (1977), WPPSS (1981), and WCC (1979).

3.7.3.1 Regional Seismicity. Prior to 1960, instrumental detection and location of earthquakes were limited to the few events that were sufficiently large (generally greater than 4.0 magnitude) to have been recorded by the sparse network of stations. Most events were located from felt reports, with resultant uncertainty as to epicentral (latitude and longitude) and hypocentral (depth) location. With 112 stations now operating in Washington and northern Oregon, the regional monitoring network in Washington is sufficiently dense to detect and locate all earthquakes of 1.8 or greater magnitude. Details of the operation of the regional network are contained in Malone (1976) and UWGP (1977; 1978; 1979; 1980; 1981).

9 2 1 2 4 9 5 0 7 5 7

Epicenter maps for earthquakes through the end of 1979 were prepared by WCC (1979) in the region 44° to 49° north, 115° to 125° west at a scale of 1:2,000,000. Epicenter maps of historic earthquakes in the catalog with a focal depth of less than 10 kilometers and events with hypocenters of 10 kilometers or more are plotted in Myers/Price et al. (1979, Fig. IV-1 and IV-2, respectively). Epicenter maps for the period 1965 to 1979 with hypocenters less than 10 kilometers and with hypocenters greater than 10 kilometers are plotted in Myers/Price et al. (1979, Fig. IV-3 and IV-4, respectively) for shallow (less than 10-kilometer) and deep (greater than or equal to 10-kilometer) events. Cross sections at a scale of 1:2,000,000 along the 47.5° north parallel show events projected from within the area 45.5° to 49.5° north for events greater than 3.0 magnitude and greater than 2.0 magnitude (Myers/Price et al., 1979, Fig. IV-5 and IV-6, respectively).

Although data presented in figures referred to above vary in quality, these figures illustrate patterns of activity and the contrast in stress release over the region shown. Clearly, the Puget Sound lowland is an area of much greater earthquake activity than the Columbia Plateau in terms of total number of earthquakes reported, greater size and frequency of events, and greater focal depth of events. Events throughout Washington State are generally shallow (less than 70 kilometers). Known events in eastern Washington are confined to the crust (depths less than 30 kilometers), while events in the Puget Sound lowland have occurred to depths of about 70 kilometers. Activity in eastern Washington is mostly restricted to swarms of very shallow (less than 3 kilometers) focal depth.

Activity in the region since 1979 has occurred mostly in the Cascade Range. Most of this activity occurred in the vicinity of Mount St. Helens and probably was related to eruptive activity.

However, two Cascade earthquakes greater than 5.0 magnitude and apparently unrelated to eruptive activity were recorded in early 1981: (1) the 5.5 magnitude Elk Lake earthquake of February 14, which occurred at a depth of about 7 kilometers about 15 kilometers north of Mount St. Helens; and (2) the 5.0 magnitude earthquake of May 18, which occurred at a depth of about 3 kilometers in the Goat Rocks Wilderness Area, north of Mount St. Helens. Both of these events were followed by hundreds of aftershocks. Seismicity associated with Mount St. Helens and the Elk Lake and Goat Rocks event is discussed in detail in UWGP (1981).

3.7.3.2 Seismicity of the Columbia Plateau. The Columbia Plateau is an area of low seismicity (Berg and Baker, 1963; Couch and Lowell, 1971; Rasmussen, 1967). Historic earthquakes have been felt in only a few areas and have been small (Fig. 3-54), except for two moderate-sized events in 1893 and 1936. The 1893 event occurred near Umatilla, Oregon; based on a probable limit of the felt area and the maximum intensity, it has been considered to be a modified Mercalli intensity VI (WPPSS, 1974). The 1936 event is the largest known earthquake in the Columbia Plateau (5.75 magnitude) and occurred in the Milton-Freewater area. This earthquake was felt over much of eastern Washington and northeastern Oregon and was accompanied by a number of foreshocks and aftershocks (Rasmussen, 1967;

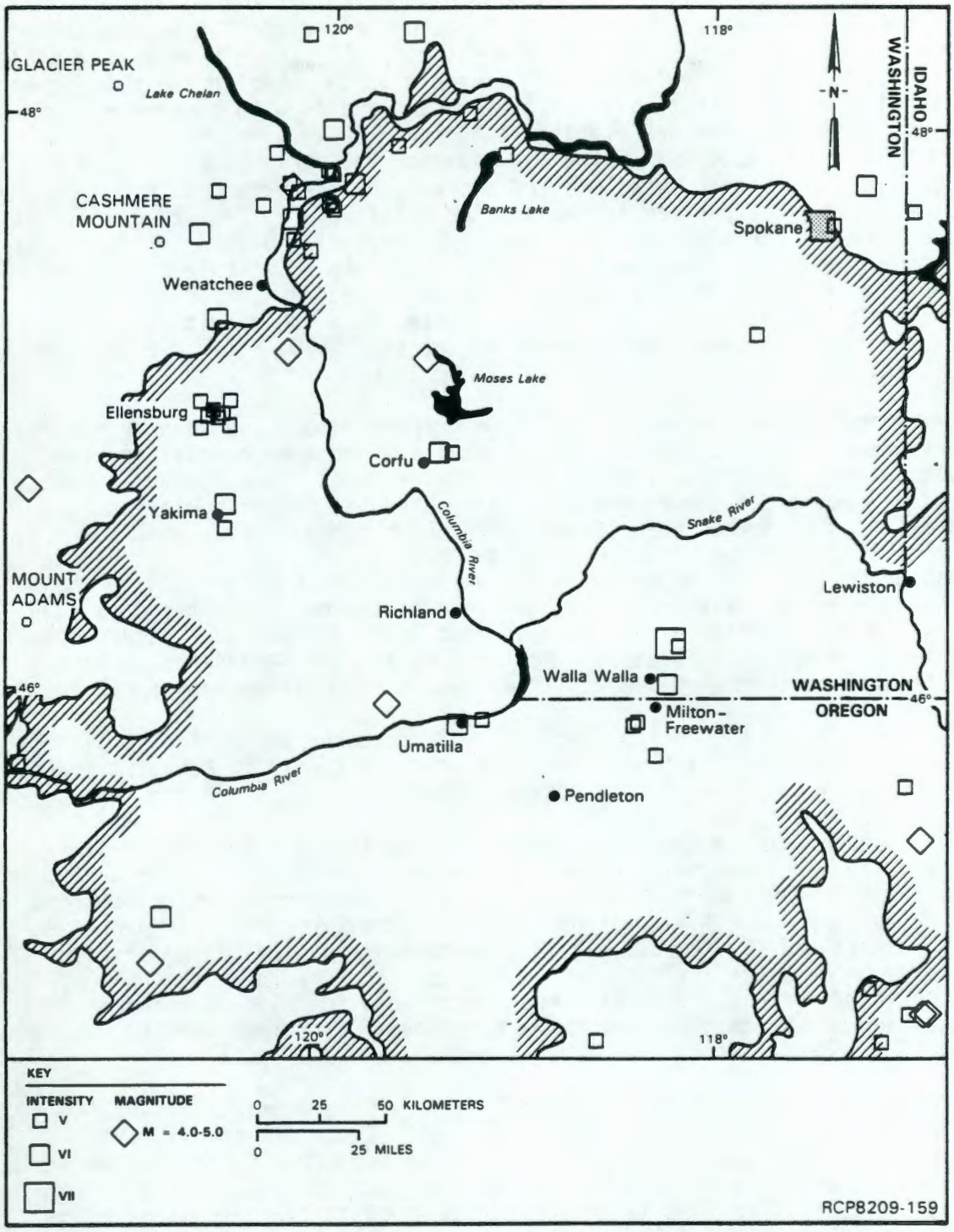

FIGURE 3-54. Historical Seismicity of the Columbia Plateau Tectonic Province. All earthquakes with modified Mercalli intensity greater than IV are shown (Table 3-10). Instrumental magnitudes are shown for some events above magnitude 4.0.

Coffman and von Hake, 1973). Based on effects discussed by Brown (1937), the maximum intensity of this earthquake has been considered to be of a large modified Mercalli intensity VII. Since 1936, a number of small earthquakes (less than modified Mercalli intensity V) have occurred in the area around Milton-Freewater, Oregon and Walla Walla, Washington, but most have not been instrumentally recorded. The largest event recorded in the Milton-Freewater area since the deployment of the eastern Washington State seismic recording network occurred in 1979 (UWGP, 1979). This event was shallow, 3 to 6 kilometers in depth, with a magnitude of 4.1.

Jones and Deacon (1966) postulated that the 5.75 magnitude July 15, 1936 Milton-Freewater earthquake was associated with the Rattlesnake Mountain-Wallula-Milton-Freewater fault system. In the absence of definitive geologic evidence to the contrary, the Rattlesnake Mountain-Wallula alignment was postulated to be a capable structure for the purpose of developing seismic design criteria for nuclear generating plants at Hanford (Blume, 1971). The northeast trend of isoseismals and the aftershock zone of the 1936 event were cited as evidence for association of this earthquake with the Blue Mountain uplift or the Hite fault by WPPSS (1974), but they nevertheless also postulated this feature as capable in the absence of clear evidence to the contrary. Recently, this earthquake has been relocated using the few distant available instrumental records and was found to have occurred near Waitsburg, Washington, some 25 to 30 kilometers northeast of the epicenter located from felt reports. This recent instrumental location is considered accurate to 11 to 16 kilometers (90 percent confidence ellipse) and is unchanged from the original instrumental location determined by the International Seismological Center. In addition, the new location is consistent with the seismograph records obtained at Spokane, Washington through comparison with current velocity models and recent well-located earthquakes near the epicenter (WCC, 1980b).

Hypocenter and epicenter plots of Washington State earthquakes (Myers/Price et al., 1979, Fig. IV-1 through IV-4) reveal no clear alignment of epicenters along the Rattlesnake Mountain-Wallula alignment, or along the entire Olympic-Wallowa lineament. Events have occurred along the lineament, but in no greater numbers or concentrations than elsewhere in the vicinity. Epicenters (Myers/Price et al., 1979, Fig. IV-3 and IV-4) do not suggest the presence of the feature either in shallow (less than 10 kilometers) or deep events (greater than 10 kilometers).

An earthquake occurred in the vicinity of the Saddle Mountains near Corfu on November 1, 1918. The epicenter of this earthquake is reported as 46.7° north, 119.50° west (Coffman and von Hake, 1973), which is on the south flank of the Saddle Mountains near the northern margin of the Hanford Site. However, the original felt reports of this event suggest a location on the north side of the Saddle Mountains near Corfu (46.8° north, 119.5° west) (WCC, 1981a). Because this event was not instrumentally located, the compiler of an earthquake catalog probably intended the town nearest the point of maximum effects to be the epicenter, but a typographical error occurred somewhere in the process of compiling a

3 2 1 2 4 9 5 0 7 6 0

catalog (Fifer, 1966). In addition, the seismograph records of this event recorded at Spokane, Washington indicate through comparison with recent well-located earthquakes (WPPSS, 1981) that the location is on the north flank of the Saddle Mountains. According to Fifer (1966), the original report classified this event as a Rossi-Forel intensity IV, which would be equivalent to a modified Mercalli intensity IV. The currently listed intensity of V to VI could also be a typographical error (Fifer, 1966). Jones and Deacon (1966) hypothesized that active faulting and formation of a graben occurred on the north flank of the Saddle Mountains during this event, a hypothesis rejected by Jahns (1967) and Bingham et al. (1970).

A number of other small, felt earthquakes (less than modified Mercalli intensity V) have occurred in or along the margins of the Columbia Plateau (WPPSS, 1974). A catalog of felt earthquakes for the Pacific Northwest through December 1979 is included in WCC (1979). Table 3-10 lists all felt earthquakes with modified Mercalli intensity greater than V and instrumental earthquakes with magnitude greater than 4.0 for the Columbia Plateau tectonic province. The location for post-1969 instrumentally located earthquakes above magnitude 3.0 is shown in Figure 3-55.

Earthquakes located by the regional network from 1969 to 1979 in the immediate Hanford area are summarized in UWGP (1979) (Fig. 3-56). Both compression and shear-wave arrival times are used with a velocity model derived by UWGP (1977) in locating eastern Washington earthquakes. Epicenters are usually accurately located to better than 2 kilometers (Weston, 1981). Focal depths are generally within 2 to 4 kilometers of actual depth as a result of the general shallow depth and station spacing. Coda length magnitudes developed for this region (UWGP, 1979) have been calibrated with Wood-Anderson magnitudes. Prior to 1971, Richter magnitudes were determined from trace amplitudes (Pitt, 1971) and may be different from coda length magnitudes (UWGP, 1979). Earthquakes greater than 4.0 magnitude that have been located by this network are listed with felt earthquakes in Table 3-10. The most seismically active area in the region since 1969 has been the Chelan area, where several felt earthquakes have been located.

Shallow, spatially and temporally restricted swarms of low-magnitude earthquakes are characteristic of the Columbia Plateau (Malone et al., 1975; Bingham et al., 1970; Rothe, 1978). These earthquakes range in magnitude from less than 0 to about 3.5, but most are less than 2.0 magnitude. The focal depth of most events is less than 3 kilometers. However, the focal depths of these shallow earthquakes, located by the regional network stations, are likely to be in error by 2 to 4 kilometers due to the spacing of stations (20 kilometers or more). Earthquake swarms may consist of several, to several hundred, to over 1,000 events (one-half to two-thirds of which are too small to locate) that occur in a restricted volume of generally less than 50 cubic kilometers within a period of a few days to several months. Within any one swarm, there is no major event preceded by foreshocks and followed by a series of aftershocks that decrease in size and frequency. Plots of epicenters and hypocenters are not aligned along a plane or planar zone.

TABLE 3-10. Felt[a] and Recorded[b] Earthquakes Within the Columbia Plateau and Surrounding Area Through 1980. (Sheet 1 of 3)

Date	Year	Time	Intensity/ magnitude	Coordinates		Location/ remarks
05 Mar.	1892	l.t.	VI	46.6° N.	120.5° W.	North Yakima, Washington
05 Mar.	1893	l.t.	VI	45.9° N.	119.3° W.	Umatilla, Oregon
15 Dec.	1897	l.t.	V	47.8° N.	120.0° W.	Lakeside, Washington
18 Oct.	1905	23:l.t.	V	47.8° N.	120.0° W.	Chelan, Washington
18 Feb.	1907	12:20l.t.	V	47.84° N.	120.02° W.	Chelan, Washington
12 Jun.	1908	Unknown	V	45.0° N.	117.25° W.	Cornucopia, Oregon
24 May	1909	22:l.t.	V	47.73° N.	120.36° W.	Chelan-Leavenworth, Washington
05 Jul.	1911	08:00	V	47.00° N.	120.54° W.	Ellensburg, Washington
14 Oct.	1913	23:00	V	45.7° N.	117.1° W.	Seven Devils, Idaho
28 Feb.	1918	23:15	V	46.5° N.	120.5° W.	Yakima, Washington
12 Mar.	1918	03:26	V	47.7° N.	117.0° W.	Spokane, Washington
01 Nov.	1918	17:20	VI	46.8° N.	119.5° W.	Corfu, Washington
07 Oct.	1920	02:l.t.	V	47.6° N.	120.1° W.	Waterville, Washington
28 Nov.	1920	Unknown	IV-V	45.7° N.	121.5° W.	Hood River, Oregon
14 Sep.	1921	11:00	VI	46.1° N.	118.25° W.	Dixie-Walla Walla, Washington
06 Jan.	1924	23:10	V	45.8° N.	118.3° W.	Milton and Weston, Oregon
17 Oct.	1926	02:45	V	45.73° N.	121.48° W.	White Salmon, Washington
30 Dec.	1926	17:57	VI	47.7° N.	120.2° W.	Chelan, Washington
03 Jan.	1927	04:58	VI	47.59° N.	120.66° W.	Leavenworth, Washington
09 Apr.	1927	05:00	V	44.8° N.	117.2° W.	Richland, Oregon
03 Sep.	1930	13:00	V	47.3° N.	117.8° W.	Lamont, Washington
18 Sep.	1934	24:l.t.	V	47.0° N.	120.54° W.	Ellensburg, Washington
26 Sep.	1934	16:15l.t.	V	47.0° N.	120.54° W.	Ellensburg, Washington
26 Sep.	1934	16:45	V	47.0° N.	120.54° W.	Ellensburg, Washington

TABLE 3-10. Felt[a] and Recorded[b] Earthquakes Within the Columbia Plateau and Surrounding Area Through 1980. (Sheet 2 of 3)

Date	Year	Time	Intensity/ magnitude	Coordinates		Location/ remarks
26 Sep.	1934	21:15	V	47.0° N.	120.54° W.	Ellensburg, Washington
19 Oct.	1934	23:31l.t.	V	47.0° N.	120.54° W.	Ellensburg, Washington
01 Nov.	1934	07:28	V	47.0° N.	120.54° W.	Ellensburg, Washington
02 Nov.	1934	15:17l.t.	V	47.0° N.	120.54° W.	Ellensburg, Washington
09 Jul.	1935	22:45	V	47.7° N.	120.0° W.	Chelan Falls, Washington
12 Oct.	1935	01:03	V	47.66° N.	120.22° W.	Entiat, Washington
16 Jul.	1936	07:07:49:0	VII 6.1M_L	46.21° N.	118.23° W.	Milton-Freewater, Oregon (WCC Relocated)
18 Jul.	1936	16:30	V	45.93° N.	118.38° W.	Milton-Freewater, Oregon
04 Aug.	1936	09:19	V	44.8° N.	118.6° W.	Helix, Oregon
28 Aug.	1936	04:39	V	45.93° N.	118.38° W.	Milton-Freewater, Oregon
29 Nov.	1939	09:15	V	47.7° N.	120.0° W.	Chelan Falls, Washington
07 Apr.	1941	09:25	VI 4.5M_L	48.3° N.	119.6° W.	Mazama, Washington (Okanogan)
23 Feb.	1942	14:03	V	47.6° N.	120.2° W.	Wenatchee-Chelan Falls, Washington
12 Jun.	1942	09:30	V	44.9° N.	117.1° W.	Halfway and Pine, Oregon
24 Apr.	1943	00:10:46.0	VI	47.3° N.	120.6° W.	Leavenworth, Washington
31 Oct.	1944	11.34:28.7	V	47.8° N.	120.6° W.	Entiat, Washington
04 Jan.	1945	02:34:48.7	V	47.7° N.	120.2° W.	Entiat, Washingston
13 Jan.	1948	06:55:00.0	V	47.9° N.	120.3° W.	Lucerne, Waterville, Washington
28 Aug.	1948	22:25	VI-V	47.8° N.	117.25° W.	Deer Park, Denison, Washington
15 Mar.	1949	20:53:11.0	4.8M_L	45.5° N.	117.0° W.	Joseph, Oregon
04 Jan.	1951	13:45.00.0	V	47.7° N.	120.0° W.	Chelan-Waterville, Washington
07 Jan.	1951	22:45:00.0	V	45.9° N.	119.2° W.	McNary, Oregon
04 Mar.	1952	19:42:00.0	V	47.67° N.	117.40° W.	Spokane, Washington
23 May	1954	13:41:42.0	V	48.34° N.	120.14° W.	Twisp, Winthrop, Washington

TABLE 3-10. Felt[a] and Recorded[b] Earthquakes Within the Columbia Plateau and Surrounding Area Through 1980. (Sheet 3 of 3)

Date	Year	Time	Intensity/ magnitude	Coordinates		Location/ remarks
24 Feb.	1956	22:00:00.0	V	47.9° N.	119.1° W.	Electric City, Washington
01 Nov.	1957	10:12:02.0	$4.2M_L$	46.7° N.	121.5° W.	Mount Rainier, Washington
12 Apr.	1958	22:37:11.0	VI $4.1M_L$	48.0° N.	120.0° W.	Chelan, Washington
20 Jan.	1959		V	46.2° N.	118.2° W.	Milton-Freewater, Oregon
06 Aug.	1959	03:44:32:0	VI $4.4M_L$	47.8° N.	119.9° N.	Chelan, Washington
15 Jan.	1962	05:29.00.0	$4.3M_L$	47.8° N.	120.2° W.	Chelan, Washington
22 Dec.	1963	02:54:	V $4.4M_B$	48.0° N.	119.3° W.	Discrepancy in location
07 Nov.	1965	16:41:47.4	$4.3M_B$	44.9° N.	117.0° W.	5-km depth
23 Jul.	1966	01:47:08.8	$4.3M_B$	47.2° N.	119.5° W.	Ephrata, Washington
30 Dec.	1966	03:51:40.3	$4.2M_B$	44.9° N.	117.0° W.	10-km depth
20 Dec.	1973	01:08:28.2	V $4.4M_C$	46.87° N.	119.35° W.	2.4-km depth Corfu, Washington (UW)
13 Apr.	1976	00:47:17.1	VI $4.8M_L$ $4.5M_B$	45.22° N.	120.77° W.	15-km depth constrained (NOAA)
17 Apr.	1976	02:11:44.4	$4.2M_L$	45.08° N.	120.80° W.	15-km depth constrained (NOAA)
19 Jan.	1979	14:55:15.4	V $3.6M_C$	47.92° N.	119.68° W.	Chief Joseph, Washington (UW)
08 Apr.	1979	07:29:37.8	$4.15M_C$	45.99° N.	118.45° W.	Walla Walla, Washington (UW)
18 Feb.	1980	06:00	$4.1M_C$	47.25° N.	120.22° W.	Cle Elum, Washington (UW)

l.t. = Local time.

M_B = body-wave magnitude.

M_C = coda-length magnitude.

M_L = local magnitude.

NOAA = National Oceanic and Atmospheric Administration.

UW = University of Washington.

WCC = Woodward-Clyde Consultants.

[a]Greater than IV intensity.

[b]Greater than 4.0 magnitude.

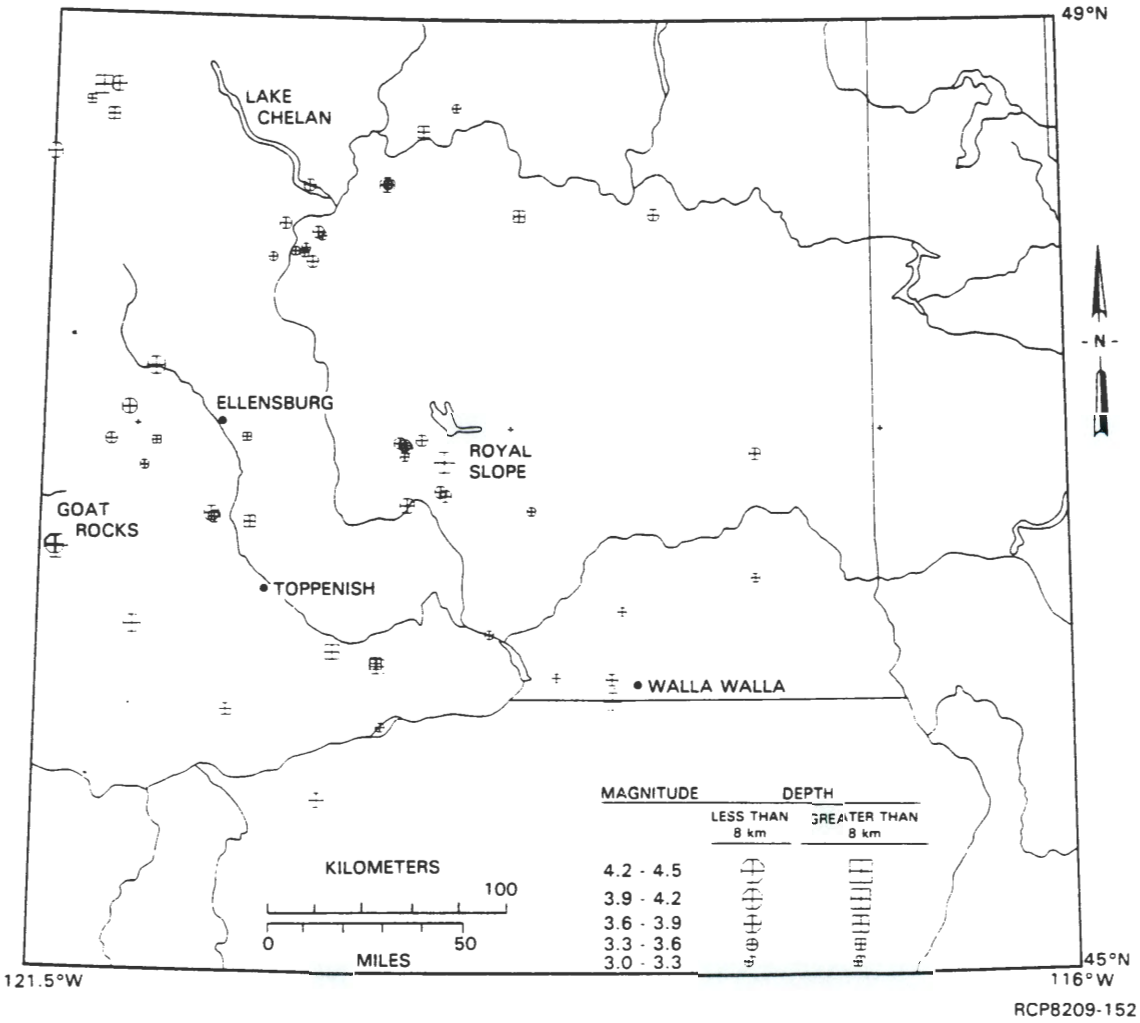

FIGURE 3-55. Instrumental Seismicity (post-1969) above Magnitude 3.0, Columbia Plateau Tectonic Province. Activity not interpreted to be affected by the changing location threshold due to gradual network development.

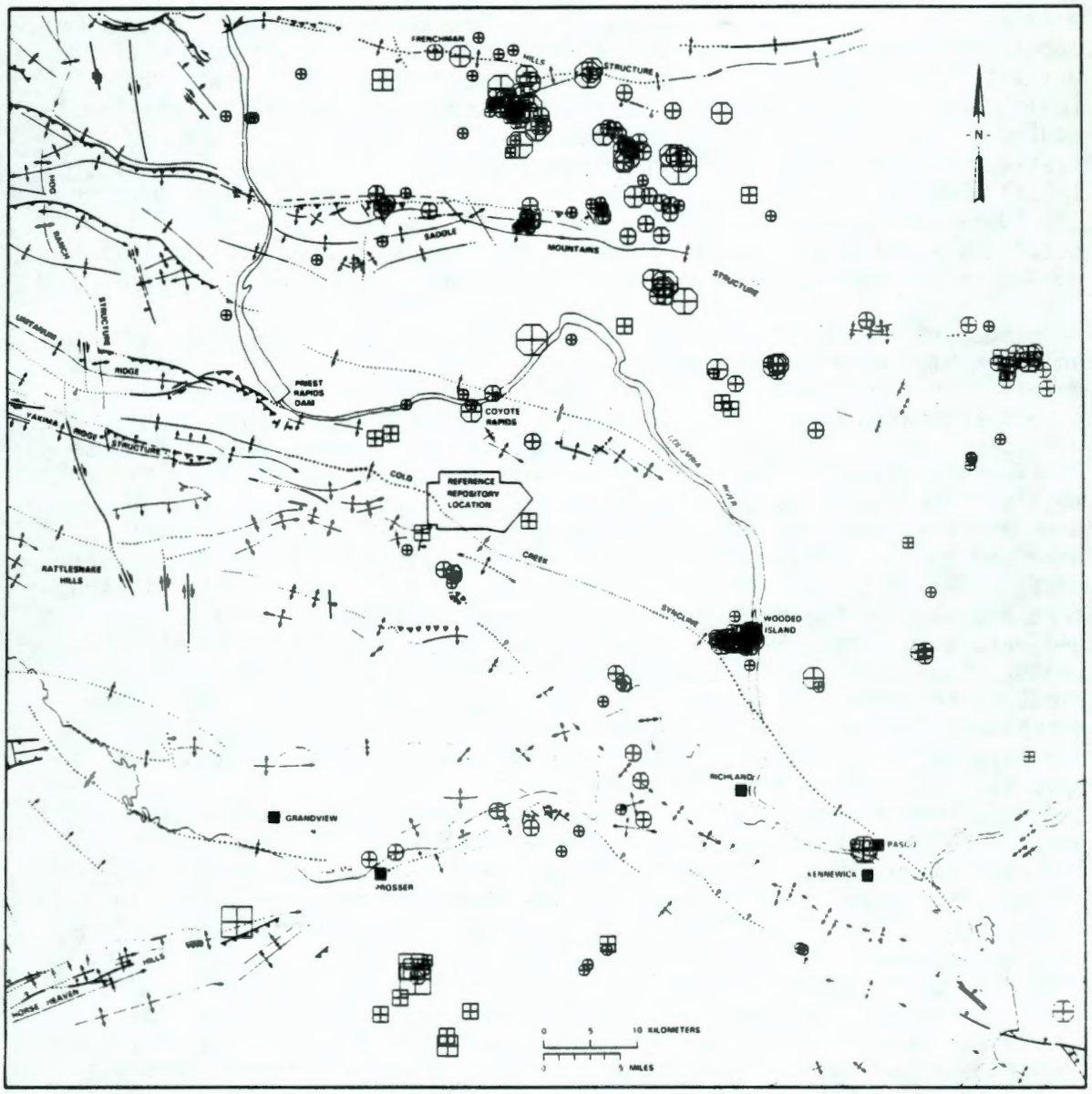

MAGNITUDE	DEPTH: LESS THAN 8 km	DEPTH: GREATER THAN 8 km
4.0 4.5		
3.5 4.0		
3.0 3.5		
2.5 3.0		
2.0 2.5		
1.5 2.0		

LEGEND

FOLDS DASHED WHERE INFERRED DOTTED WHERE COVERED

- ANTICLINE
- SYNCLINE
- MONOCLINE
- PLUNGE DIRECTION

FAULTS DASHED WHERE INFERRED. DOTTED WHERE COVERED

- BALL ON DOWNTHROWN SIDE
- THRUST FAULT

RCP8209-153

FIGURE 3-56. Instrumental Seismicity of the Pasco Basin. The largest events are concentrated near the Saddle Mountains and Frenchman Hills.

9 2 1 2 4 9 5 0 7 6 6

The pattern of occurrence of successive swarms in the same geologic area is variable. In a few cases, successive swarms have been centered in about the same location, but the general tendency is for migration of the activity, in most cases in a particular direction. Some linear trends (using regional network locations) have emerged and include the northwest-southeast trend of the November-December 1972 Eltopia (ET) swarm and the east-west trends of the 1970-1971 Scooteney Reservoir (SR) swarms (WCC, 1981a) (Fig. 3-57), but relatively short east-west trends are evident in the 1969-1970 Wooded Island (WI) swarm (Pitt, 1971). Rothe (1978) also noted east-west trends in the better-determined epicenters of the 1975 Wooded Island swarm, using a dense local network of stations.

Most of the swarm activity has occurred between the Saddle Mountains and Frenchman Hills anticlines (Fig. 3-47 and 3-57). In this region most events larger than 3.0 coda length magnitude have occurred several kilometers from axes of geologic structures and from mapped faults associated with these folds. Epicenters of some smaller earthquakes have a diffuse east-west trend along the Saddle Mountains structure for about 30 kilometers. The larger earthquakes (greater than magnitude 3.0), however, have occurred north of the Saddle Mountains in the Royal Slope swarm area and in the poorly defined north-south-oriented Frenchman Hills swarm area. Swarm activity in other areas (south of the Saddle Mountains structure and east of the Hanford Site) has no clear association with any known geologic structure. Swarms in these areas are widely separated by quiet areas. None of the earthquake swarms detected since 1969 have had an event larger than 3.5 coda length magnitude, except the 4.4 Royal Slope earthquake and the 3.8 Coyote Rapids event. The December 20, 1973, 4.4 Royal Slope earthquake is the largest instrumentally located event to have occurred in the central Columbia Plateau region, and its epicenter and magnitude are comparable to those found for the 1918 Corfu earthquake. This 2.4-kilometer-deep event was immediately followed by 22 shallow earthquakes that decreased in frequency with time, but not in magnitude, thus exhibiting a mixture of the characteristics of swarms and aftershocks. The spatial distribution of epicenters for the Royal Slope events, determined by Malone et al. (1975) using a dense local network, shows an apparent 2-kilometer alignment of epicenters near the location of the main shock. The October 25, 1971, 3.8-coda-length magnitude Coyote Rapids earthquake (less than 1 kilometer deep) was associated with three magnitude less than 1.0 earthquakes, not appreciably different from the continuous but unclustered low rate of earthquake occurrence in this area.

3.7.3.2.1 Recurrence Relations. Recurrence relationships for shallow earthquakes (less than 6 kilometers) and deep earthquakes (greater than 6 kilometers) are different (UWGP, 1979). Over a long enough period of time, approximately ten times more earthquakes of a given magnitude occur than earthquakes one magnitude unit larger. This corresponds to a "log-normal distribution" or a b-value of 1.0. The deep earthquakes in the central Columbia Plateau have a b-value (slope of a recurrence curve) of about 0.80 (Fig. 3-58). The shallow events have b-values higher than 1.0, suggesting that stress or strain rates are different, or that the layered basalts react differently to deformation than does the basement. Lower b-values are characteristic of tectonic earthquakes in the Cordillera, while higher b-values are characteristic of regions that exhibit swarm activity (UWGP, 1979).

9 2 1 2 4 9 5 0 7 6 7

9 2 1 2 4 9 5 0 7 6 8

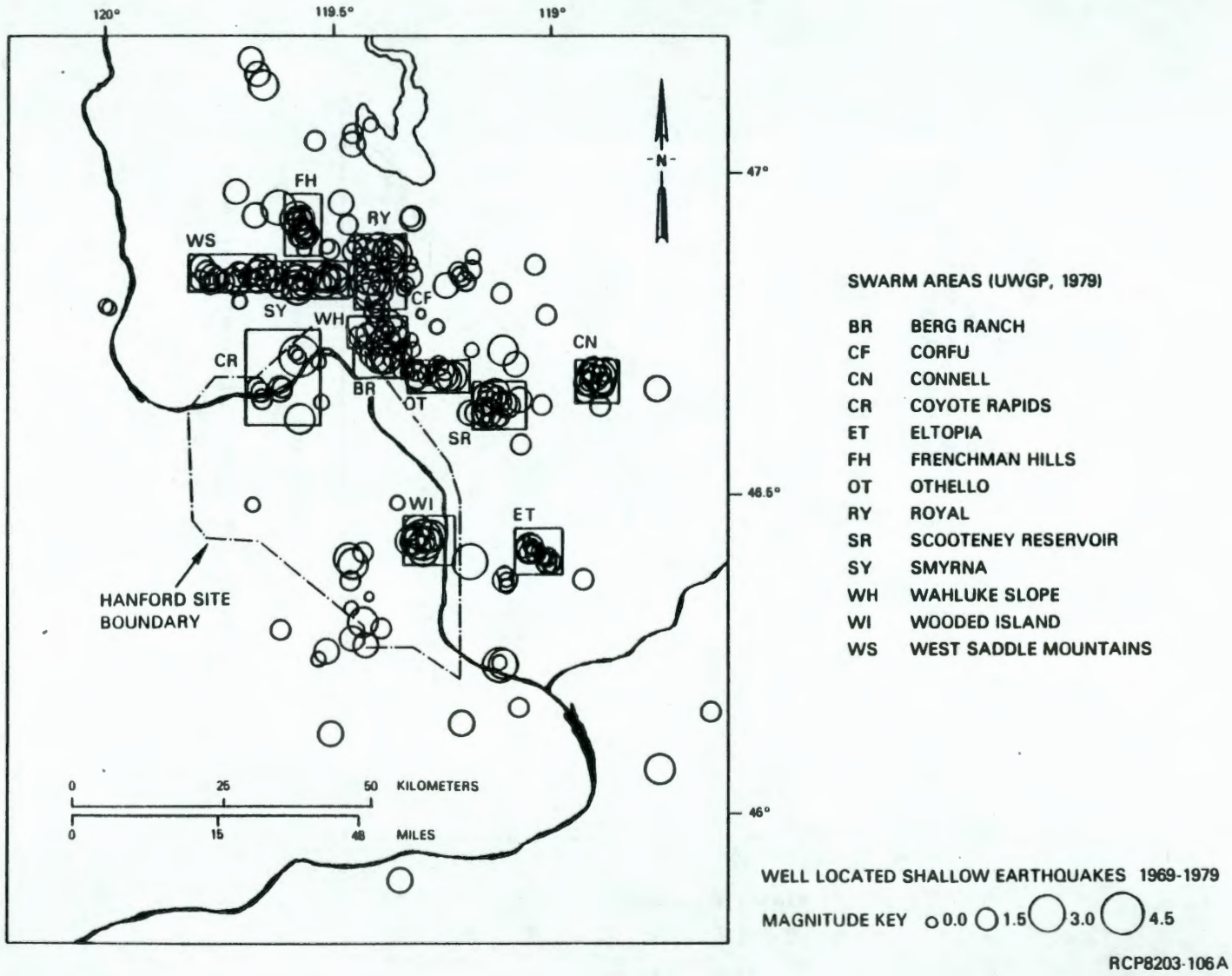

FIGURE 3-57. Well-Located Shallow Earthquakes, Pasco Basin and Surrounding Area, 1969-1979.

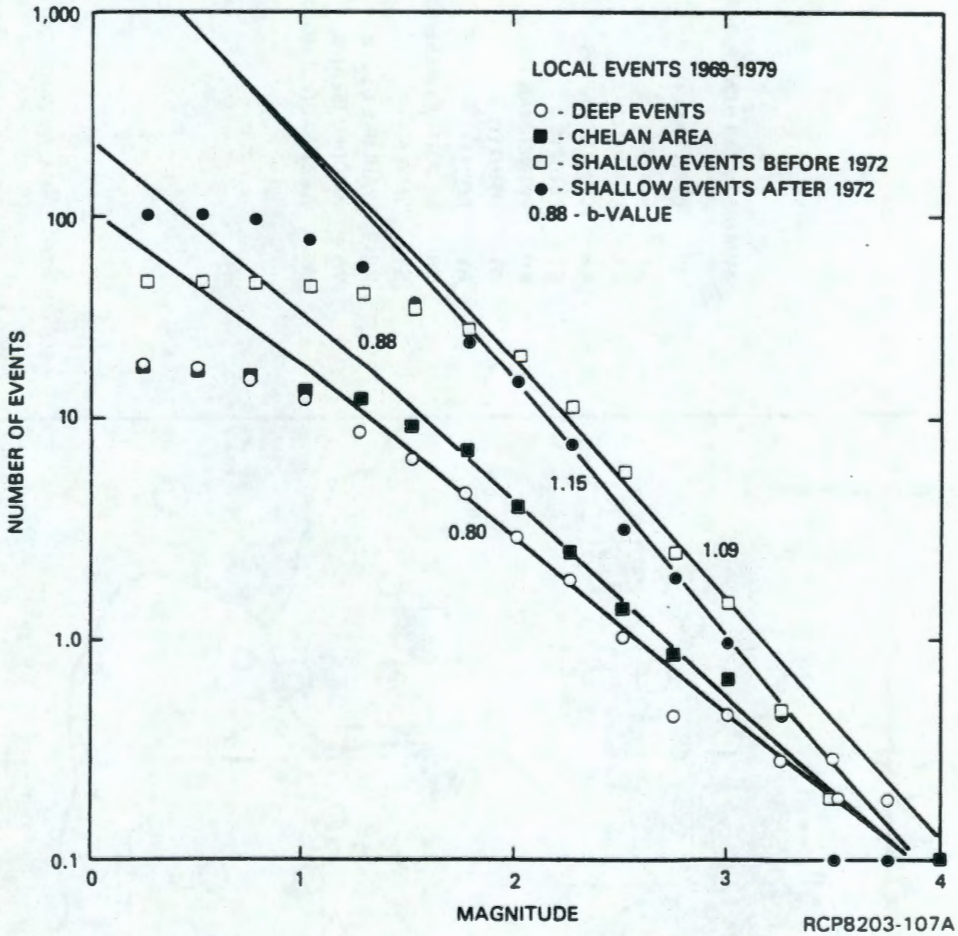

FIGURE 3-58. Cumulative Number of Events per Year Versus Magnitude for Entire Region.

3.7.3.2.2 Focal Mechanisms. The small size of swarm earthquakes usually precludes the determination of a focal mechanism for individual events, but composite focal-mechanism solutions have been performed on groups of similar data from a single swarm. Inconsistent focal planes frequently emerged from these analyses. The focal mechanism solutions (Table 3-11) indicate that earthquakes in the Columbia Plateau are a response to approximately north-south, nearly horizontal maximum compression (Fig. 3-59). Tension axes are commonly near vertical (Table 3-11). Thrust and reverse faulting on east-west planes is indicated by focal-mechanism solutions. Thrust and reverse faults are common in anticlinal ridges. Variable focal mechanisms indicate that earthquakes occur on numerous planes with different orientations. Stress concentrations on existing weak zones or planes may locally reorient the stress field, but there is no surface displacement or indication of youthful offset to allow association of earthquakes and mapped geologic structures.

Both single-event and composite focal-mechanism solutions are listed for the deep events and regional events on the northern, western, and southern margin of the plateau (Table 3-11). With some variation, these events indicate principally north-south compression, except for events in the Walla Walla-Milton-Freewater region on the southeast margin of the plateau (WCC, 1980b). The April 1979 and July 1936 events have horizontal-compression axes oriented nearly east-west and nonvertical-tension axes indicating mixed thrusting and strike-slip faulting. East-west compression for these events is anomalous to the region. Other than these two events in the Walla Walla-Milton-Freewater area, there is no apparent difference in the focal mechanisms of shallow and deep earthquakes in the Pasco Basin. Events on the eastern margin of the Cascade Range do have a tendency to have east-west rather than vertical extension, implying strike-slip faulting (UWGP, 1981).

3.7.3.2.3 Mainshock-Aftershock Sequences. Events deeper than 6 kilometers in the central Columbia Plateau, or otherwise located as occurring below the Columbia River basalts, are more frequently associated with classical aftershock distributions. Aftershocks associated with the larger events (equal to or greater than 3.5 coda length magnitude) and the numerous Chelan area events (less than 3.5 coda length magnitude) occurred within areas of historical seismicity, but are not associated with mapped geologic structures.

Three deep events have occurred in the central Columbia Plateau region with magnitudes greater than 3.5; two occurred south of the reference repository location in the Horse Heaven Hills near Prosser (June 28, 1975, 3.8 coda length magnitude, 10 kilometers deep; February 17, 1979, 3.6 coda length magnitude, 10 kilometers deep) (Fig. 3-56) and one west of the reference repository location near Yakima (September 11, 1970, 3.5 coda length magnitude, 10 kilometers deep). An extensive series of foreshocks and aftershocks accompanied the 1975 event (all 8 to 11 kilometers deep). The 3.5- and 3.6-magnitude events were not accompanied by either foreshocks or aftershocks.

9 2 1 2 4 9 5 0 7 7 0

TABLE 3-11. Eastern Washington Focal Mechanism Solutions. (Sheet 1 of 2)

Location	Compression		Tension		Remarks	Source
	Azim.	Dip	Azim.	Dip		
Central Columbia Plateau Deep Events						
Prosser/Horse Heaven Hills	180°	01°	082°	86°	Composite	WCC (1980a)
Rattlesnake Mountain	174	24	295	51	Composite	WCC (1980a)
Yakima/Umtanum/Gable Ridges	160	16	292	66	Composite	WCC (1980a)
Eltopia north	293	43	032	09	Composite, poorly constrained	WCC (1980a)
Corfu/Royal/Othello	172	05	058	78	Composite	WCC (1980a)
NW. Hanford/Midway	218	04	097	74	Two event composite	Weston (1977)
NW. Hanford/Midway	032	04	292	54	Alternative	Weston (1977)
Horse Heaven Hills (06/28/75)	326	00	235	74	M=3.8, z=10.2 km	Weston (1977)
Regional Events						
Walla Walla (04/08/79)	269	11	166	48	M=4.1	WCC (1980a)
Milton-Freewater (1936)	056	22	161	32	M=6.1, historical	WCC (1980a)
Cle Elum mainshock (06/26/78)	334	23	223	52	M=3.7	UWGP (1978)
Cle Elum aftershocks (6 months)	344	19	119	64	Composite	WCC (1978)
Lake Chelan	321	03	058	58	Composite, 0/9 km	UWGP (1978)
Chief Joseph Dam (01/19/79)	129	03	024	68	M=3.9, z=7 km	UWGP (1979)
Toppenish (02/02/81)	196	04	100	60	M=3.9, z=5 km	UWGP (1981)

TABLE 3-11. Eastern Washington Focal Mechanism Solutions. (Sheet 2 of 2)

Location	Compression		Tension		Remarks	Source
	Azim.	Dip	Azim.	Dip		
Central Columbia Plateau Shallow Events						
Eltopia swarm (1)	346	17	244	34	Composite	Malone et al. (1975)
Eltopia swarm (2)	333	30	189	54	Composite	Malone et al. (1975)
Eltopia swarm (3)	358	05	136	81	Composite	Malone et al. (1975)
Royal mainshock (12/20/73)	201	09	310	61	M=4.4	WPPSS (1981)
Royal sequence	001	04	198	85	Week after mainshock, composite	Malone et al. (1975)
Royal sequence	172	34	326	63	Week after mainshock, composite	Malone et al. (1975)
Royal (09/04/74)	184	23	000	67	M=2.8, swarm event	WPPSS (1981)
Smyrna (09/22/72)	072	05	334	62	M=2.5, swarm event	WPPSS (1981)
Scooteney Reservoir (02/15/73)	100	10	320	77	M=1.4, swarm event	WPPSS (1981)
Wahluke Slope (10/18/72)	182	05	340	85	M=1.7, swarm event	WPPSS (1981)
Wahluke Slope (10/19/72)	286	13	106	77	M=1.4, swarm event	WPPSS (1981)
Wahluke Slope (11/30/72)	343	04	069	57	M=2.0, swarm event	WPPSS (1981)
Wahluke Slope (12/03/72)	356	05	135	84	M=1.4, swarm event	WPPSS (1981)
Wahluke Slope (12/15/72)	278	04	037	80	M=1.0, swarm event	WPPSS (1981)
Coyote Rapids (10/25/71)	340	03	200	84	M=3.8, swarm event	Rasmussen and Rohay (1982)

M = magnitude.

z = depth.

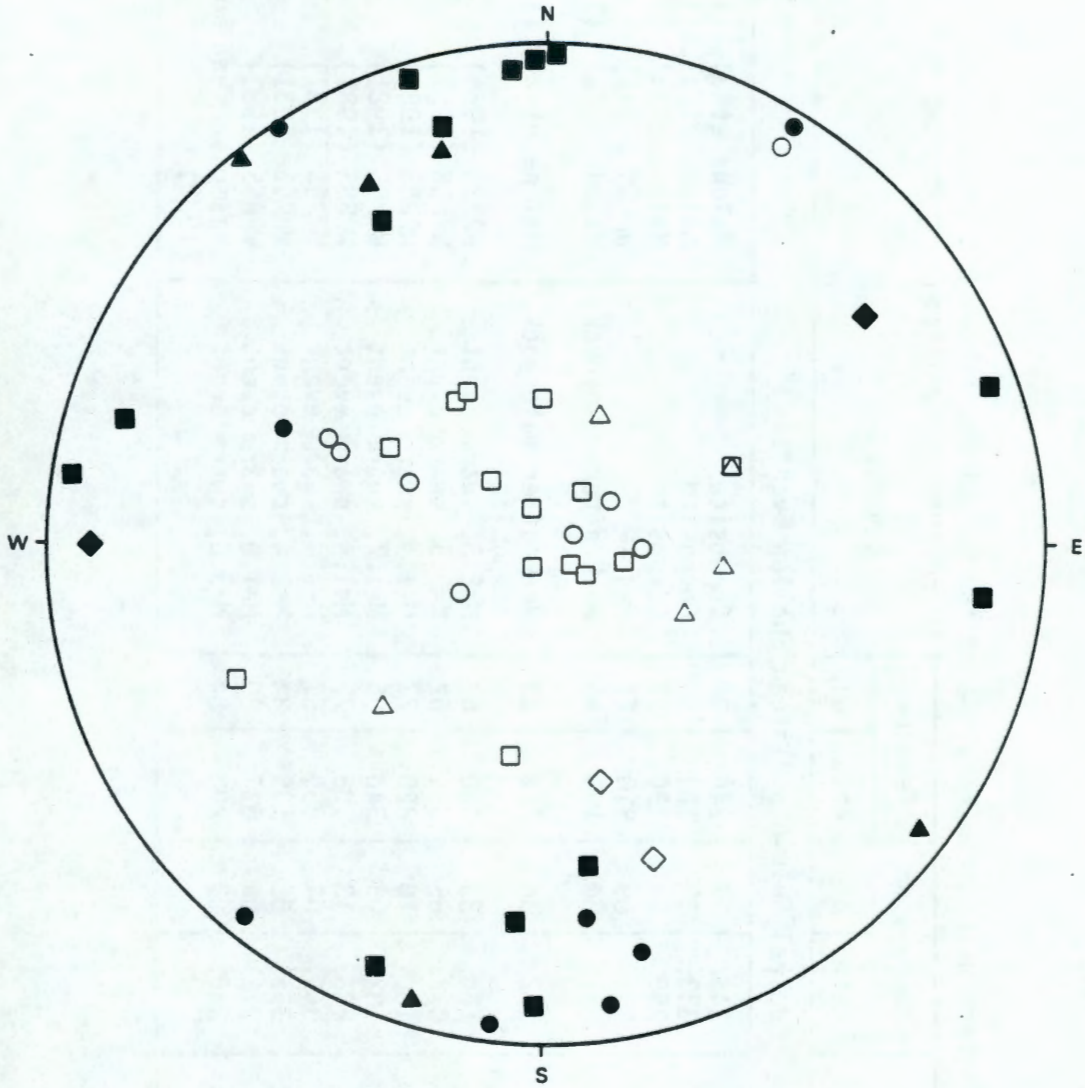

RCP8203-108

FIGURE 3-59. Columbia Plateau Earthquakes Focal-Mechanism Summary. Lower hemisphere equal area projection of inferred principal stress axes as listed in Table 3-11.

In the Ellensburg-Cle Elum area, events above 3.5 coda length magnitude occurred on July 13, 1977 (3.8), July 28, 1979 (3.7), and February 17, 1981 (4.1) all of which were followed by aftershocks. To the south of these, an event occurred near Toppenish on February 2, 1981 (3.8). Two events greater than 3.5 coda length magnitude occurred in northern Oregon (July 1, 1975, (3.6) and December 18, 1980, (3.5)). A 4.1 magnitude earthquake that occurred on April 8, 1979 near Walla Walla, Washington nearly coincided with the felt epicenter of the 1936 Milton-Freewater, Oregon historical earthquake. The 1979 event was not followed by any aftershocks, which is unusual for an event of this size. While some concentration of activity has occurred in the central Columbia Plateau region above 2.5 coda length magnitude (associated with swarms), the level of activity above 3.5 is concentrated around the northern, western, and southern borders of the Columbia Plateau. However, there are no geologic or topographic features suggesting through-going faults that could be associated with these larger events.

3.7.3.2.4 Magnitude/Fault-Length Relationship. There are no known instances of surface-fault rupture accompanying earthquakes in the Columbia Plateau on which to base a magnitude/fault-length relationship. Fissures and cracks probably related to landslides were noted by Brown (1937) after the July 15, 1936 earthquake near Walla Walla, but these are atypical and probably not tectonic in origin. In the absence of such data, and considering that the Pasco Basin area of the Columbia Plateau appears to be one of low strain rate (Caggiano et al., 1980), there are no data on which to base a local magnitude/fault-length relationship. Some displacements in Quaternary sediments in or near fault zones have recently been noted (Campbell and Bentley, 1981; Farooqui, 1979; Farooqui and Thoms, 1980), but the age of displacement and whether it is tectonic are still being evaluated. In addition, the earthquakes in the region are not clearly related to mapped geologic structures. In the absence of proven active faults and the association of such faults with moderate to large earthquakes, no such data are available on which to base source parameter-magnitude relationships specific for the Columbia Plateau.

3.7.3.2.5 Repository Design. Subsurface facilities of a repository may respond to earthquake ground motion differently than surface facilities. Damage to surface and underground equipment could be important during construction and emplacement of wastes in a nuclear waste repository. Damage to borehole seals or the host rock in the postclosure period could result in permeability enhancement.

Little or no damage to deep mines has been reported during large earthquakes that caused considerable damage to surface facilities (Pratt et al., 1978). Relatively high accelerations well in excess of 1.0 g have been recorded in deep mines with no corresponding damage.

9 2 1 2 4 9 5 0 7 7 4

Pratt et al. (1978) surveyed available reports of earthquake damage to underground openings and found that damage is significantly less in the subsurface (below a few hundred meters) than it is at the surface. No damage of underground openings was associated with events having either a surface intensity less than VIII or 0.2-g peak surface acceleration. Only minor damage was observed from ground accelerations up to 0.5 g, and this was limited to portals, openings, and preexisting fractures.

McGarr et al. (1981) reports no damage occurred when a peak acceleration as high as 12 g was measured in a deep South African gold mine and suggests that peak velocities may better reflect the damaging effects of near-field earthquakes on underground facilities.

Owen and Scholl (1981) summarized damage criteria on underground openings for earthquakes and explosions based on ground velocity. No damage was reported at peak velocities less than about 24 centimeters per second, and no damage to lined tunnels occurred below 90 to 120 centimeters per second. A study by Rozen (1976) reported in Pratt et al. (1978) estimated that a magnitude 6.0 event at a distance of 5 kilometers would produce a peak velocity (underground) of 100 centimeters per second, and that peak velocities of 100 centimeters per second did not cause damage to openings in intact rock.

For a nuclear waste repository, damage must be considered in the repository host rock on which long-term isolation is dependent. A fault occurring through or close to a repository could provide a near vertical groundwater pathway that may have a greater hydraulic conductivity than the competent basalt (Arnett et al., 1980). This scenario is described in a preliminary way by assuming a fault that produces an earthquake of magnitude 6.5 passes through or close to the repository. In addition, a microearthquake swarm scenario was also considered, but the permeability effects of swarms are considered to be much less than those due to a single large magnitude earthquake.

9 2 1 2 4 9 5 0 7 7 5

Surface Facilities

Surface facilities will be needed to support an underground repository, but the procedure for determination of seismic design for such structures may be different than that in use for surface reactors shielded by heavy concrete containment vessels. Design for some level of vibratory ground must be included, but the design will vary with the function of the building.

The design of Washington Public Power Supply System, Inc. Unit 2 (WNP-2) has been recently evaluated by the U.S. Nuclear Regulatory Commission (NRC, 1982). The design of WNP-2 was based on a zero period ground acceleration of 0.25 g, originally by assigning a modified Mercalli intensity VIII event to the Rattlesnake-Wallula topographic alignment. The 1936 modified Mercalli intensity VII Milton-Freewater earthquake was

assumed to occur at the point of closest approach of this alignment to the site, and for conservatism, was assigned a maximum modified Mercalli intensity of VIII. The recent evaluation used several methods in selecting design basis events. The three most significant to the design evaluation were (1) a magnitude 6.0 to 6.5 earthquake on the (presumed capable) Rattlesnake-Wallula alignment, 19.5 kilometers from WNP-2; (2) a magnitude 5.7 to 5.8 earthquake, equivalent to the 1936 Milton-Freewater earthquake, in the site vicinity (in this case, at a 15 kilometer hypocentral distance); and (3) a magnitude 4.0 swarm earthquake at a distance of 3 kilometers (NRC, 1982). These three events are discribed in more detail below.

The Rattlesnake-Wallula alignment was assumed to have a capable length of 120 kilometers. Using estimates of total fault length, fractional fault length, and slip rate, a maximum surface wave magnitude of 6.5 was determined. This magnitude estimate for an event on this alignment is consistent with a modified Mercalli intensity VIII maximum epicentral intensity, as used in the original design of this and other surface facilities at Hanford.

An earthquake equivalent to the 1936 Milton-Freewater earthquake was postulated to occur on an unknown or buried fault in the vicinity of the site because of a lack of conclusive association of the 1936 event on a specific geologic structure. The maximum surface wave magnitude of this event has recently been estimated to be 5.7 to 5.8, in agreement with the original magnitude of 5-3/4 (Gutenberg and Richter, 1954). The location, focal mechanism, and after-shock pattern suggest an association of this earthquake with the Hite fault, but the location is sufficiently uncertain at present to preclude assigning this event to a specified structure. There was no apparent surface faulting associated with this earthquake, and geologic mapping in the epicentral area has failed to locate any source structure with very recent offset.

The maximum swarm earthquake in the Columbia Plateau region was the coda-length-magnitude 4.4 Royal Slope earthquake north of the Saddle Mountains structure. An event of this size was assumed to be possible to occur anywhere, in the absence of conclusive association of swarm earthquakes with known geological structures and the lack of convincing alignments of swarm epicenters indicative of buried or unmapped faults. The coda-length-magnitude scale may be higher than local magnitude by 0.3 units, and local magnitude of 4.0 was assumed to occur near Wooded Island, where recurrent swarms have been located.

Other sources considered were found to be of less significance than the three above sources. Other sources considered were capable faults on Gable Mountain, postulated capable faults on Toppenish Ridge, and the 1872 earthquake in the North Cascades tectonic province. None of the above six sources was found to significantly exceed the 0.25 g design spectrum for the plant.

9 2 1 2 4 9 5 0 7 7 6

3.7.3.3 Summary of Columbia Plateau Seismicity. Historically, the Columbia Plateau has been an area of relatively low seismicity. The largest historically reported events had epicentral intensities of modified Mercalli intensity VII or less and occurred beyond the Pasco Basin; none of these has been associated with a particular geologic structure. The largest instrumentally recorded event was a 4.4 magnitude event that occurred on the Royal Slope, the limb of a Yakima fold north of the Pasco Basin.

Instrumental monitoring since 1969 reveals continuing microearthquake activity, which indicates that stress is continually being relieved; however, the nature of the stress and the mechanism responsible for shallow swarm activity is not well understood. The steep dip of focal planes and the limited vertical distribution of swarm events at Wooded Island led Rothe (1978) to hypothesize that slip was occurring on columnar joints in thick, competent basalt flows, perhaps due to strain relaxation along folds.

Most earthquakes detected and located by the eastern Washington array have been shallow; however, activity does occur at focal depths of 6 to 30 kilometers. Hypocenters of deeper earthquakes below basalt in the Columbia Plateau occur in a different pattern from that of shallow events. Swarms apparently do not occur below the basalt, or at least not in the same spatial and temporal pattern. Whether deeper earthquakes are related to geologic structure is unknown, since the structure and rock types beneath the basalt are largely unknown. The deep events (greater than 6 kilometers) are small (less than 4.5 magnitude) and are apparently randomly distributed in time and space. Some deep events occur in areas experiencing swarms, but most deep events show no correlation with shallow activity.

3.7.4 Seismicity of the Reference Repository Location

No earthquakes were instrumentally located near the reference repository location before the U.S. Geological Survey installed a six-station network in the central Columbia Plateau in 1969. In 1970, the U.S. Geological Survey network increased to 16 stations, and by 1971 it included 24 stations. Since installation of the initial regional network, all earthquakes above 1.8 magnitude have been consistently located with a 1- to 2-kilometer accuracy; depths are accurate to plus or minus 3 kilometers and somewhat greater for shallow events.

Detailed monitoring of the reference repository location was initiated by the BWIP in 1980 with the installation of a permanent four-station network and a temporary five-station portable network of three-component short-period instruments (Fig. 3-50). The four vertical-component stations are expected to improve location accuracy to better than 1 kilometer and to reduce the threshold for location of all events near the site to less than 1.0 magnitude.

The operation of a deep-borehole (1,100 meters) seismic station was also initiated in 1980. This instrument operated successfully in borehole DC-3 (Fig. 3-60) during March, April, and May 1980 before its failure. Recordings of microearthquakes (less than 1.0) were obtained in addition to numerous regional earthquakes near Mount St. Helens. The microearthquakes recorded by this instrument could not be detected nor located using the surface networks.

The seismicity of the reference repository location is relatively low in comparison to the seismicity of the central Columbia Plateau region. No shallow earthquake swarms have actually occurred within the boundaries of the reference repository location, although three earthquake sequences (described below) have occurred nearby. Deeper earthquakes, greater than 6 kilometers deep have occurred within the reference repository location, but at a rate comparable to the average rate of occurrence over the central Columbia Plateau region.

A sequence of four events in the depth range of 10 to 3 kilometers with maximum magnitude (Richter) of 2.2 occurred from November 10 to 26, 1969 (WCC, 1981c). A second earthquake swarm of 12 events less than 5 kilometers deep and with a maximum magnitude of 2.4 occurred between July 8 and November 4, 1979, with seven of these events occurring on September 8, 1979. A swarm of three small events of a maximum magnitude 1.4 and depths less than 2 kilometers was recorded during August 24 and 25, 1981. The deep sequence of events occurred at the southern border of the site; the more recent (1981) shallow activity is concentrated 5 to 8 kilometers south of the site, close to the north flank of Rattlesnake Mountain. A composite focal mechanism of the 1979 swarm events indicated north-south compression and vertical tension, consistent with other focal mechanisms in eastern Washington.

The closest area of more intense swarm activity is located 10 kilometers north of the site, near Coyote Rapids (Fig. 3-57). The Coyote Rapids swarm area has had relatively continuous low-level activity throughout the instrumental monitoring period, totaling 63 events by 1979 (UWGP, 1979). The largest event in this swarm area (and the second largest in the central Columbia Plateau region) was a 3.8-magnitude event on October 25, 1971. This event was located at a depth of 0.07 kilometer, but could be as deep as 1 to 2 kilometers in view of poor depth control for shallow events. This event has a focal mechanism with nearly north-south, horizontal compression, and near-vertical tension, typical of other eastern Washington microearthquakes (see Section 3.7.3). This event occurred to the north of the Umtanum Ridge-Gable Mountain structure.

3.7.5 Status

The Columbia Plateau is located approximately 200 kilometers east of the consumptive border of the Juan de Fuca and North American plates. Miocene Columbia River basalt borders a Tertiary volcanic arc, the Cascades, and older Tertiary, Mesozoic, and Paleozoic terrain to the south, east, and north. The Columbia River basalt was deforming along east-west, northwest, and northeast trends at an apparently low rate of

3 2 1 2 4 9 5 0 7 7 8

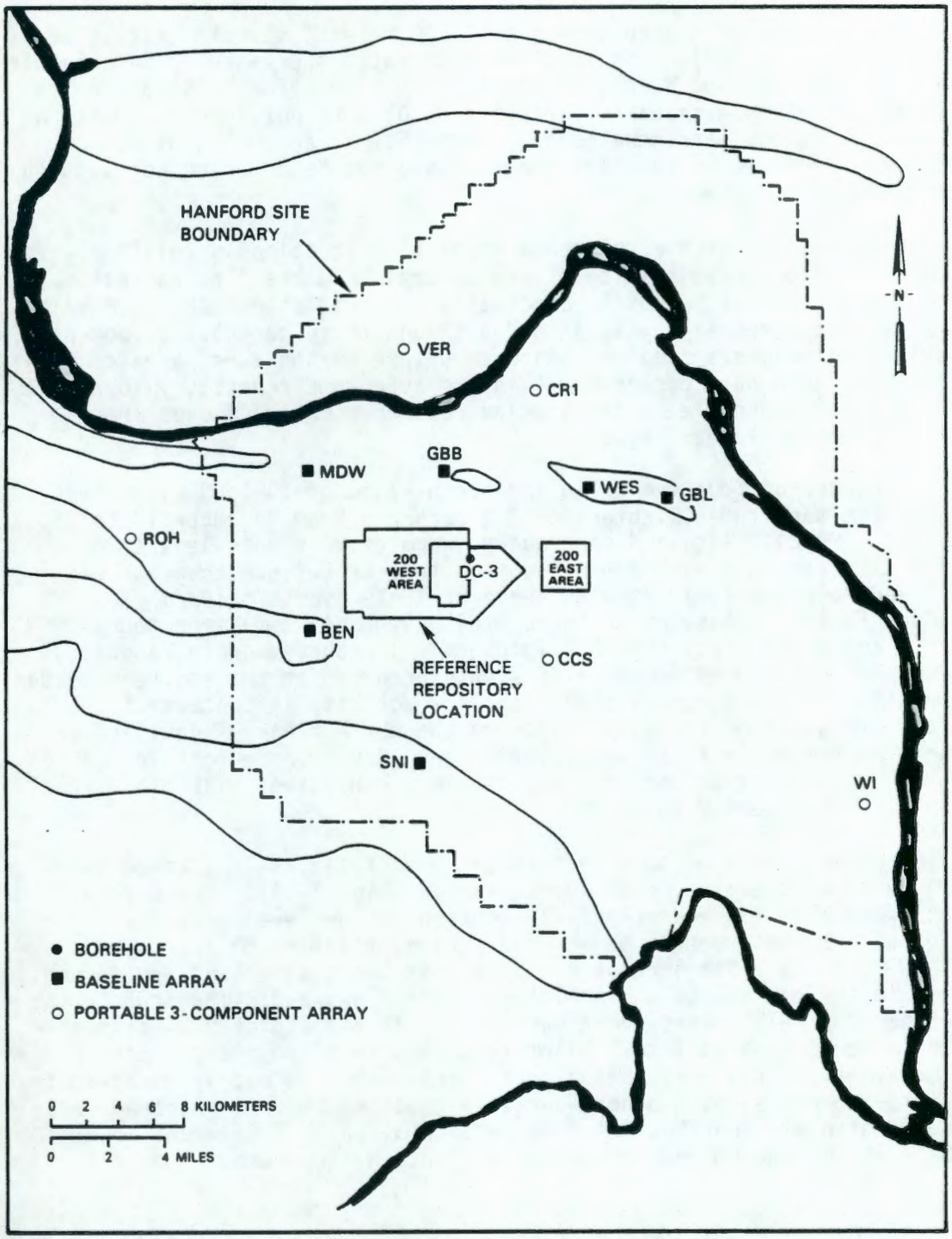

BEN	BENSON RANCH	GBL	GABLE MOUNTAIN	VER	VERNITA
CCS	COLD CREEK SYNCLINE	MDW	MIDWAY	WES	WEST POND
CR1	COYOTE RAPIDS #1	ROH	ROHAY	WI	WOODED ISLAND
GBB	GABLE BUTTE	SNI	SNIVELY BASIN		

RCP8203-110B

FIGURE 3-60. Hanford Seismic Array.

3 2 1 2 4 9 5 0 7 7 9

strain in the Miocene, penecontemporaneously with extrusion of basalt from essentially north-south linear vent systems in the eastern plateau. Once established, deformation at a low rate of strain appears to have continued under nearly north-south, nearly horizontal compression along folds and faults developed early in the deformation process. The rate and chronology of deformation remain to be confirmed, but preliminary interpretations indicate that the site meets the criteria for tectonic stability.

Historical data indicate that the reference repository location is an area of relatively low seismicity. Microearthquake activity is largely shallow, confined to a crust of 30-kilometer thickness, and is characterized by swarms of low-magnitude earthquakes that occur in and below basalt. Focal mechanisms of individual and composite shallow and deep events indicate reverse faulting along nearly east-west planes under nearly horizontal, nearly north-south compression.

The potential for renewal of basaltic volcanism similar to the Columbia River basalt fissure eruptions is extremely low. Effects of volcanism from sources in the Cascades and the Northern Basin and Range are minimal and of very low probability.

THIS PAGE INTENTIONALLY
LEFT BLANK

92124950781

3.8 LONG-TERM REGIONAL STABILITY

A tectonically stable area is one in which the present and projected rates of late Cenozoic tectonic processes are considered not to pose a hazard to repository construction and operation or to the long-term isolation of radioactive waste. The BWIP has been assessing the tectonic stability of the Pasco Basin by integrating geologic, geophysical, geodetic, and seismologic data. Geologic data provide information on the chronological development of geologic structures and the stresses responsible for their development. Geophysical data provide information on gross crustal properties and structures. Seismologic and geodetic data provide information on currently operating processes. The ultimate objective of this assessment is the development of a conceptual tectonic model that (1) satisfactorily explains the tectonic evolution of the region in the recent geologic past and (2) predicts the potential effects of tectonic processes. Of particular concern are tectonic effects that could alter the rate or route of groundwater movement.

3.8.1 Preliminary Deformation Rate

A preliminary assessment of geologic, geodetic, and seismologic data discussed in Section 3.7 suggests that the Pasco Basin was deforming at a low rate of strain in the Miocene and has continued deforming at such a rate throughout the late Cenozoic. The basis for this conclusion is summarized as follows:

(1) Uplift rates (vertical-strain rates) for the Pasco Basin (Section 3.7.2.5) were approximately 40 meters per thousand years on bounding anticlinal folds from 10 to 14 million years ago, assuming an average rate of uplift. Actual uplift may have occurred as the cumulative effect of episodic pulses or at varying rates that average to this preliminary rate. The magnitude and periodicity of short-term rates are constrained by the style of deformation. Once initiated, deformation appears to have continued along the same anticlinal structures that formed in the Miocene.

(2) Six trilateration surveys across the Pasco Basin indicate that nonuniform compression at a rate of less than 0.1 millimeter per kilometer per year is occurring along northeast and northwest axes, respectively.

(3) Instrumental earthquake data for eastern Washington (UWGP, 1979) indicate minor stress release as microearthquakes. The frequency, areal distribution, and mechanisms indicate that stress does not appear to be relieved as earthquakes along geologically mapped faults. Therefore, stress may be relieved in part aseismically. The east-west to northwest trend of folds and faults and the north-south trend of dikes in the basalt suggest north-south compression; such compression agrees with the stress field determined from focal-mechanism solutions.

9212495078 2

These results indicate that deformation of the Pasco Basin has occurred very slowly and may be expected to continue at a very slow rate. Deformation can be expected to proceed seismically or aseismically. Therefore, the future style of deformation must be predicted from observation of past deformations and kinematic analysis; the future nature of seismicity can be predicted empirically from historical seismicity. As such, the reference repository location meets the criteria for tectonic stability.

3.8.2 Synopsis of Current Tectonic Models

Adequate definition of tectonic processes and their rates of operation requires development of a conceptual tectonic model. A tectonic model is a non-numerical descriptive theory that incorporates geologic, geophysical, seismologic, and geodetic data into a satisfactory explanation of the chronological and kinematic development of geologic structures. The plate-tectonic setting of the Pacific Northwest is dominated by the Juan de Fuca-North American plate boundary. Some evidence suggests that the Juan de Fuca plate is presently consumed, but the data are permissive of the hypothesis that subduction has ceased. Alternative explanations for plate-boundary mechanics include oblique subduction, distributed transform shear, partial plate coupling, oblique rifting, and transition between transform and subduction. Whereas the exact plate boundary mechanism may not be well understood, it is still possible to examine the effects of plate interactions east of the Cascades in the past and predict future effects. For the purposes of evaluating tectonic stability, the plate-tectonic regime of the Pacific Northwest is not likely to change appreciably in the next 100,000 years. Tectonic models proposed for the Pacific Northwest, with specific application to the Pasco Basin and reference repository location, are summarized below.

Tectonic models for the Columbia Plateau must explain the synchroneity of north-south shortening of the Yakima folds and extension leading to the development of north-south linear vent systems in the Palouse Slope. The Palouse Slope is defined as the generally undeformed, southwest tilting dip slope of the Palouse subprovince. The synchronous extensional and compressional regime existed from at least 14.5 to 6 million years ago and may have been operating earlier. The style of deformation and the structural trends have recently been interpreted as the product of wrench tectonics under nearly north-south compression by Laubscher (1981) and Davis (1981). However, their interpretations of the mechanics of deformation differ.

Laubscher in WPPSS (1981) recognized the existence of two strain fields in the Columbia Plateau compatible with a nearly north-south, horizontal axis of maximum compression: (1) the eastern Palouse Slope, characterized by east-northeast extension; and (2) the western Yakima fold system, characterized by generally north-south compression. The north-south-trending border between the Yakima folds and Palouse fields was

labeled as a zone of north-south dextral shear and named the Wallula Gap-Moses Lake Belt (Laubscher, 1981). The Cle Elum-Wallula lineament was viewed by Laubscher (1981) as a zone of more intense deformation, in which the trend of some anticlines of the Yakima fold system changes from east-west to northwest with corresponding changes in the strike of faults.

From an analysis of the two-dimensional geometry of structures in the Yakima fold system, Laubscher (1981) has proposed that folds in Columbia River basalt resulted from décollement slip within or at the base of the basalt. The folds form where thrust faults ramp upward from this décollement. Laubscher envisioned a south-to-north progressive development of Yakima folds that resulted from the major process of slip along the décollement. This deformation is driven by a large shear couple with near-parallel arms in the Cascades and the eastern margin of the Pasco Basin (Fig. 3-61). North-south compression resulted in approximately 3 kilometers of crustal shortening and led to the development of east-west as well as northwest-trending wrench structures, most notable of which are those in the Cle Elum-Wallula lineament.

Laubscher (1981) envisioned the crust of the Columbia Plateau to be a mosaic of relatively rigid blocks with deformation concentrated along the margins. These blocks are then translated as well as rotated to account for the geometry of folds and faults that bound the blocks. In this model, the Cle Elum-Wallula lineament is a major crustal discontinuity, where about 10 blocks terminate. Deformation is concentrated between blocks and is taking place under north-south compression driven by a northwest-trending buried wrench system that is rooted in the Blue Mountains of Oregon.

Davis (1981) postulated that the basalts folded under north-south compression and, in contrast to Laubscher (1981), that the faults developed relatively late in the deformation as the folds began to lock up. In the latter stages of folding under nonuniform compression, the folds steepen differentially, leading to overturning of part(s) of the structure and the development of tear faults at high oblique angles to the structure (with strike-slip sense of displacement) and thrust or reverse faults when flows (layers) are no longer able to slip relative to one another in flexural slip folding. Driven by a northwest-trending right-lateral wrench system of unspecified dimensions in the basement, folding and faulting are a thin-skinned response to deeper wrenching below the basalt in the area of the Cle Elum-Wallula lineament. Similar to Laubscher (1981), the postulation of deep basement structure is based on the geometry and orientation of shallow structures in basalt.

The Cle Elum-Wallula lineament is considered to be mostly of Neogene and Quaternary age (Laubscher, 1981; Farooqui, 1979; Farooqui and Thoms, 1980). However, Davis (1981) has suggested that deformation along the lineament waned during the late Quaternary and may have ceased. Also, Laubscher (1981) hypothesized that movement ceased on the lineament early in the deformational sequence. Control by older structures of similar trend is suggested by exposures along the plateau margin. However, the

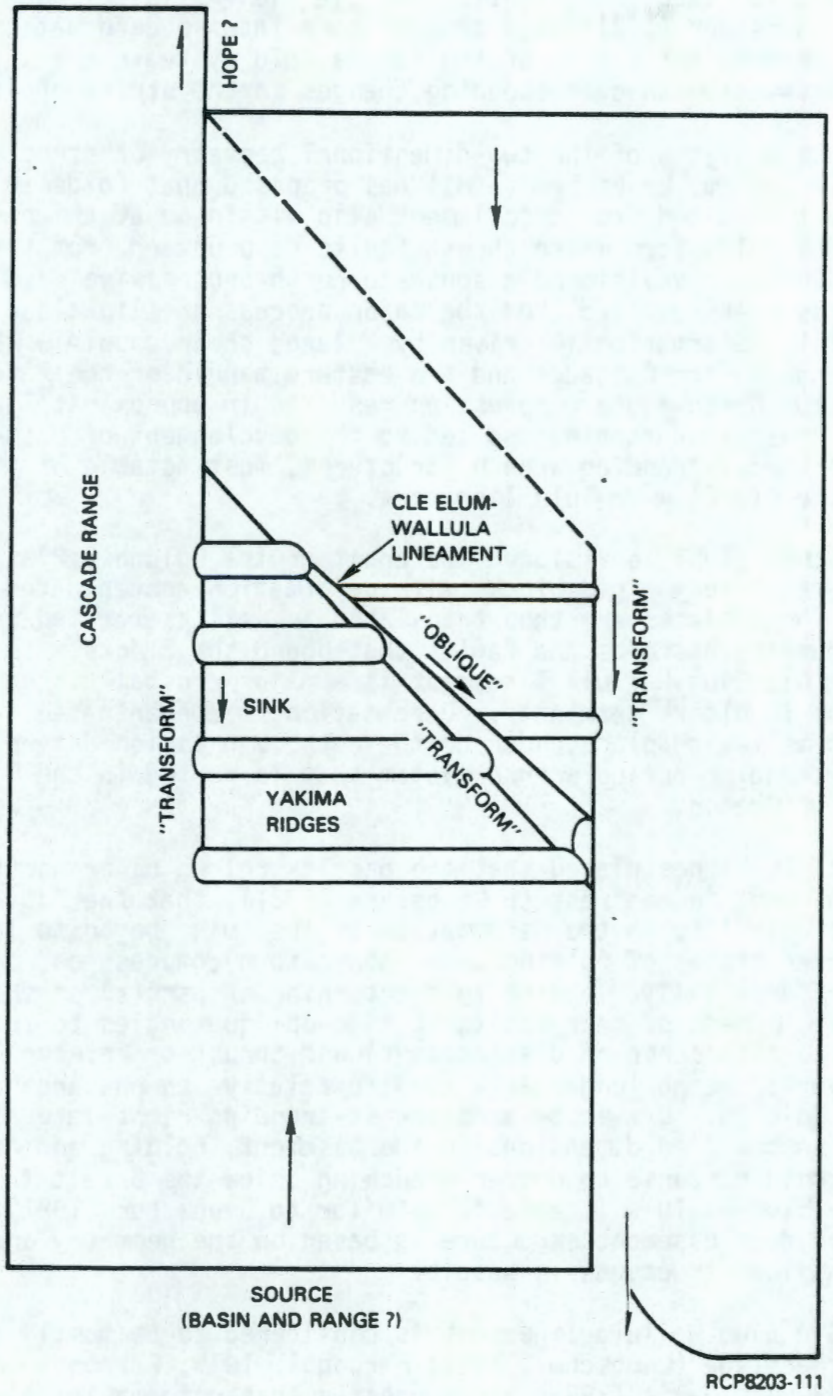

FIGURE 3-61. Simple Translation Model of Oblique-Transform Faulting and Compressional Folding.

presence of deeply buried structures (e.g., a major crustal discontinuity or a zone of major right-lateral offset) within or below Columbia River basalt as hypothesized by Davis (1981) and Laubscher (1981) is not supported by available geophysical investigations (WPPSS, 1977; Myers/Price et al., 1979; and UWGP, 1979).

From analysis of imagery of the southeastern Columbia Plateau, Glass (1980) hypothesized that the east-west trending folds, along with steeply dipping northwest and northeast-trending faults, result from nearly horizontal, nearly north-south compression. He attributed the westward increase in amplitude of Yakima folds to rotation about a point in the vicinity of Wallula Gap.

Bentley (1977) proposed that Yakima folds were drape structures developed where steeply dipping dip-slip faults that bound blocks in pre-Columbia River basalt basement extend nearly to the surface. More recently, he considered the faults associated with Yakima folds to be shallow dipping thrust faults that accommodate north-south compression between a system of relatively closely spaced, northwest-trending right-lateral strike-slip faults (Bentley, 1980).

Price (1982) (see Section 3.7.2.3.1) showed that the basalts have been very sensitive to folding strain with brittle failure along shear zones in any dipping basalt. He concluded that a lack of extensional features in the folded basalts precluded a reverse-fault, drape-fold origin. Similarly, he concluded that if basalt in the crestal area of a box fold in the Yakima fold system had migrated into the position through one or two fold hinges, the basalt of the crest areas should show extensive brecciation. On the contrary, the crestal areas are the least deformed parts of the anticlines. Thus, Price (1982) did not believe that thrust ramps associated with a regional décollement underlie individual anticlines. He considered thick-skinned tectonics involving sinusoidal folding or layer-parallel shortening at depth, coupled with local, shallow detachments under the anticlines, to be the most reasonable for the Yakima fold system.

Price (1982) further concluded that the change in orientation of the Rattlesnake and Horse Heaven Hills, along with the change in amplitude and orientation of the fold axes of the Umtanum Ridge-Gable Mountain structure, suggest that rotation and dextral shear were involved in the formation of these ridges. The movement of basalt into the folds perpendicular to the fold axis and the apparent rigidity of Columbia River basalt in the Palouse Slope indicate that clockwise rotation has occurred, accompanied by limited dextral shear along the eastern termini of the folds. According to this model, rotation occurs around a diamond-shaped rigidly behaving buttress in the sub-basalt basement. Clay modeling in a squeeze box has been able to reproduce the Yakima folds under north-south horizontal compression. However, the nature of the basement beneath the basalt of the Pasco Basin and its rigid behavior remain to be confirmed.

In summary, hypotheses have been proposed to account for the deformation in the Cle Elum-Wallula lineament and the Yakima folds. Differences in interpretations reflect, in part, a deficiency of data, especially with regard to basement lithology and structure. Nevertheless, these models adequately explain many of the major strain features and serve as hypotheses that can guide further tectonic studies.

3.8.3 Status

Detailed studies required to confirm a tectonic model remain to be performed. However, a preliminary quantitative assessment indicates that the tectonic processes within the Pasco Basin do not pose a hazard to repository construction and operation or to long-term isolation of radioactive waste. Specific details of the mechanics and timing of deformation remain to be confirmed, but investigations to date have not discovered any major tectonic structures that would appear to preclude development of a repository beneath the Hanford Site. While the mechanical details of deformation are uncertain, deformation under nearly north-south, nearly horizontal compression seems to be following a well-recognized pattern. Deformation, once initiated, appears to have continued along the same structures that were developing in the Miocene. Strain appears to be concentrated in steeply dipping limbs of anticlines, suggesting that broad open synclines such as the Cold Creek syncline, where very gently dipping basalt is relatively undeformed, appear suitable for development of the tunnels required for a repository. Deformation either appears to be continuing at a very slow rate similar to that which was effective in the Miocene or is on the wane. Since the pattern of deformation summarized above appears to have been in operation for the past 14 million years, it seems reasonable to conclude that this pattern will continue over the next 10,000 or more years. Under such an environment, major displacement, even along the Cle Elum-Wallula lineament, would not be anticipated.

3.9 MINERAL RESOURCES

This section contains (1) an inventory and description of subsurface mining and drilling for resource exploration and development in the reference repository location and vicinity (100-kilometer radius); (2) economic analysis of known and potential resources of the reference repository location and vicinity; (3) economic analysis of known and potential resources of the remainder of the Columbia Plateau for comparison with the reference repository location; and (4) geologic and economic analysis of attractiveness of the reference repository location compared to other areas of the Columbia Plateau and western United States, because of its known or potential mineral resources (mineral resources are defined in an economic sense, groundwater resources are discussed in Sections 5.1.9 and 7.3). The data and analysis upon which this section is based are detailed in GG/GLA (1981).

Areas of study utilized in this section are shown in Figure 3-62. The reference repository location vicinity study area is the area within 100 kilometers of the reference repository location. The adjacent-counties study area is defined by the county lines that most closely approximate the reference repository location vicinity study area. The Columbia Plateau study area, defined by county lines, encompasses the approximate outcrop area of the Columbia River Basalt Group.

3.9.1 Subsurface Mining

Wells drilled for the purpose of oil and gas exploration and development in the vicinity of the reference repository location were discussed in Section 3.2 and are detailed in GG/GLA (1981). Within 100 kilometers of the reference repository location, only one subsurface excavation, about 5 kilometers east of Prosser, Washington, for the purpose of mineral exploration (gold) is recorded; no production has been reported from this prospect.

3.9.2 Mineral-Resource Values--Reference Repository Location and Vicinity

Available information was utilized to determine current and past mineral-resource production within 100 kilometers of the reference repository location and in the remainder of the Columbia Plateau, and to project gross values of potential production from 1981 to 2005. The 25-year projection is considered to be the maximum foreseeable forecast period for the economic data analyzed (GG/GLA, 1981). The 100-kilometer study area was chosen to provide a better, more representative basis for analysis of known and undiscovered potential resources than is provided by the Hanford Site; the Hanford Site has been closed to mineral exploration and development for more than 40 years. An additional means of economic analysis of mineral resources was to estimate, on the basis of available geologic data, production that could reasonably be expected from presently undiscovered resources in the vicinity of the reference repository location and elsewhere in the Columbia Plateau.

9 2 1 2 4 9 5 0 7 8 8

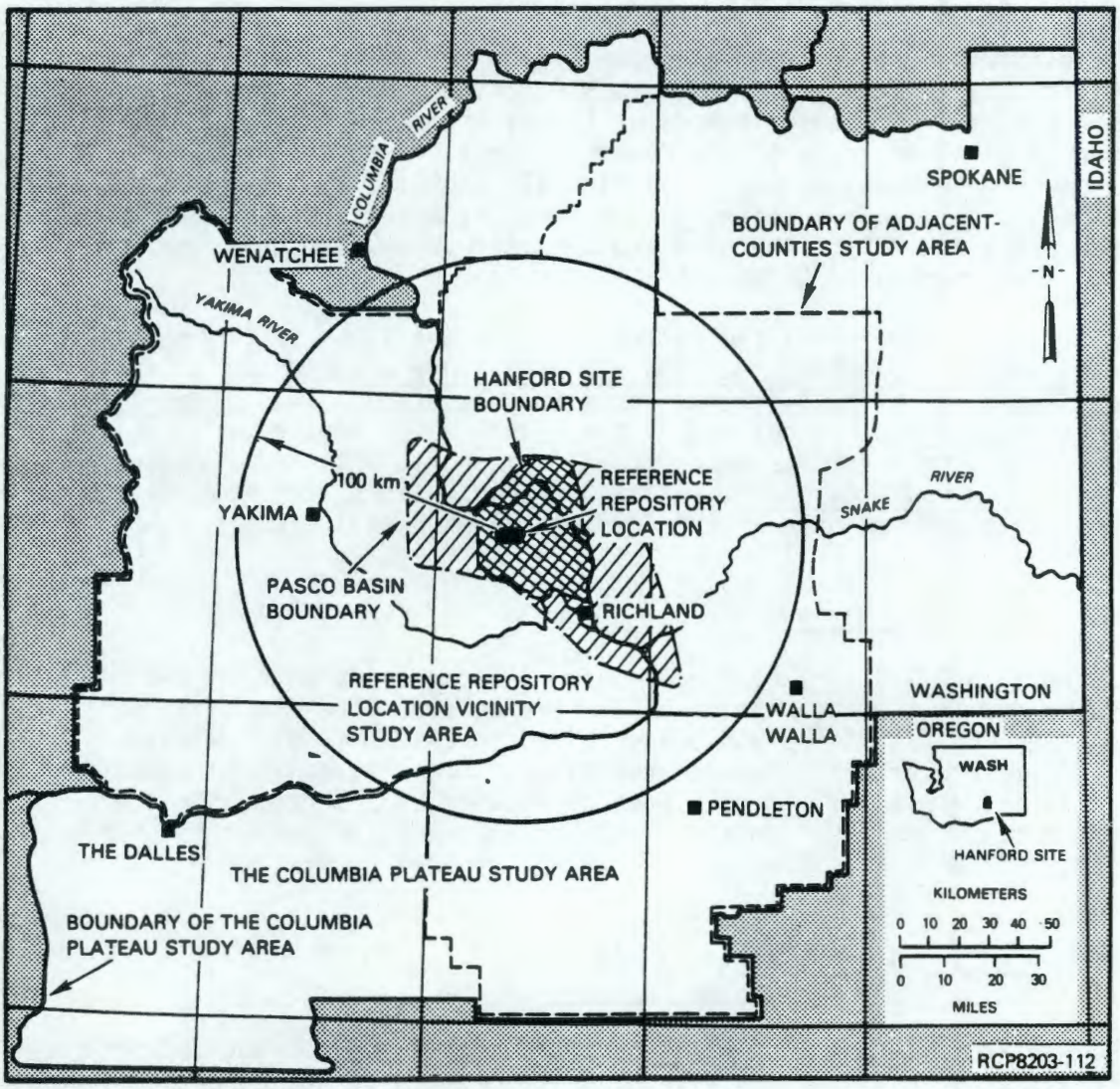

FIGURE 3-62. Locations of the Reference Repository Location Vicinity, Pasco Basin, Adjacent-Counties, and Columbia Plateau Study Areas.

Economic evaluation of mineral resources within the reference repository location and vicinity was confined to minerals known to exist, or which could feasibly exist, in commercial or potentially commercial quantities. These minerals are oil, peat, natural gas, gold, clay, diatomaceous earth, perlite, pumice, stone, saline compounds, sand and gravel, and geothermal water (GG/GLA, 1981, Fig. I-16, I-20, and I-21, and II-5). Minerals that might occur below the Columbia Plateau basalts in the Pasco Basin were not considered because the thick basalt cover is considered too costly to remove.

Active producers of geologic resources within 100 kilometers of the site, and known geologic resources within the same area, are listed in GG/GLA (1981, Tables II-1 and II-2). The projected gross and net values and estimated present values of mineral resources are given in Table 3-12.

Development, production, and marketing costs of known or undiscovered geologic resources of the adjacent-counties study area (Fig. 3-62) are given in Table 3-13. The costs given are based on historical costs of exploration, development, distribution, and marketing for each commodity (GG/GLA, 1981).

Net values (gross value minus costs of exploration, development, production, and marketing) of geologic resources that might be found and produced in the adjacent-counties study area over the next 25 years are given in Table 3-12. For purposes of calculating present net value (value at the beginning of a series of periodic payments) of potential undiscovered resources of natural gas within the Columbia River Basalt Group, it is assumed that the $3.4 million net value will be distributed evenly during the forecast period. This, in effect, maximizes present value by assuming that currently undiscovered resources will be discovered in 1981 and will be produced at a uniform rate over the next 25 years. In reality, such resources may be discovered after 1981 and may be produced for less than 25 years. In calculating present value of a series of 25 equal net-value payments, two interest rates have been used. Twelve percent is the approximate interest rate that could be received from a safe alternate investment (e.g., tax-free municipal bonds or certificates of deposit in insured financial institutions). Eighteen percent is the approximate rate to borrow money to invest in mineral-resource development in the study area.

For potential natural gas resources within the reference repository location vicinity, the present net value of $3.4 million over 25 years is an estimated $1.1 million (at a 12 percent discount rate) or $0.7 million (at an 18 percent discount rate). These estimates have a subjective probability of realization of 0.37 (Table 3-12). These estimates do not include natural gas, if any exists, beneath the Columbia River Basalt Group.

The same assumptions, methods, and discount rates utilized to calculate present net value of undiscovered natural gas have been used to calculate present net value for known deposits of peat, placer gold, diatomaceous earth, and sand, gravel, and stone (Table 3-12).

0 7 9 5 0 9 4 2 1

TABLE 3-12. Projected Gross and Net Values and Estimated Present Values of Mineral Resources in the Adjacent Counties Study Area,[a] 1981-2005 (GG/GLA, 1981).

Mineral commodity	Gross value[b]	Production cost[b]	Net value[b]	Present net value[b]	
				At 12%	At 18%
Mineral Fuels					
Natural gas[c]	$19,500,000	$16,100,000	$3,400,000	$1,070,000	$740,000
Peat	800,000	600,000	200,000	60,000	40,000
Metallic Minerals					
Gold (placer)	11,100,000	8,700,000	2,400,000	750,000	520,000
Nonmetallic Minerals					
Diatomaceous earth	185,200,000	172,600,000	12,600,000	3,950,000	2,760,000
Sand, gravel, and stone	253,900,000	239,200,000	14,700,000	4,610,000	3,210,000
Totals			$33,300,000	$10,440,000	$7,270,000

[a]Values calculated for the adjacent counties study area in approximation of the immediate vicinity study area because of the availability of economic data only on a county basis.

[b]Values are expressed in 1980 dollars. Present value at the beginning of 1981 of a stream of 25 annual payments equal to 1/25th of the total net value.

[c]Natural gas values expected from presently undiscovered deposits within the Columbia River Basalt Group. The subjective probability of realization is estimated at 0.37. All other values are for currently known deposits rounded to the nearest hundred thousand.

TABLE 3-13. Development, Production, and Marketing Costs of Known or Potential Geologic Resources of the Reference Repository Location Vicinity Study Area and the Remainder of the Columbia Plateau. Costs are estimated in terms of costs per dollar of gross value, 1980 (GG/GLA, 1981).

Mineral commodity	Estimated cost					
	Per unit of output			Per dollar of gross unit value		
	Development/ production	Wholesale marketing	Total	Development/ production	Wholesale marketing	Total
Fuel minerals						
Natural gas	$3.26/10^3 ft^3$	$0.86/10^3 ft^3$	$4.12/10^3 ft^3$	$0.652	$0.172	$0.824
Peat[a]	6.22/ton	4.36/ton	10.58/ton	0.454	0.318	0.772
Metallic minerals						
Gold (placer)[b,c]	390/oz	-0-	390/oz	0.785	-0-	0.785
Industrial minerals						
Diatomaceous earth[c]	145/ton	-0-	145/ton	0.932	-0-	0.932
Sand, gravel, stone[d,c]	2.40/ton	-0-	2.40/ton	0.942	-0-	0.942

NOTE: All estimates exclude federal and state income taxes.

[a]Estimates assume commercial production. Current total costs are apparently estimated by prospective investors at more than $13.70/ton, the current market price, making the deposits economically unviabale at current market prices.

[b]Estimates assume production of gold as a by-product or co-product of sand and gravel production. Assumes 1/600 oz/yd^3 gold content and a processing cost of 65¢/yd^3 for silver.

[c]Current approximate production cost. Transportation and marketing costs are considered to be negligible relative to production cost.

[d]Based on recent U.S. Department of Commerce and U.S. Bureau of Mines data.

3.9.3 Assessment of Comparison Area - Columbia Plateau Region

Projected (25-year basis) gross and net values and estimated present values of mineral resources for the Columbia Plateau (as defined by county-line boundaries) are summarized in Table 3-14. Costs utilized to compute net values from gross values are the costs reported in Table 3-14 for the reference repository location vicinity study area. Discount rates utilized for computation of present values are the rates used in Table 3-13.

3.9.4 Analysis of Resources - Relative Attractiveness of the Reference Repository Location for Mineral-Resource Exploration and Development

Projected net value of mineral resources with potential for production in the adjacent-counties study area over the next 25 years is $33.3 million (Table 3-15), or 41 percent of net value of such mineral resources in the Columbia Plateau study area. Estimates of net mineral-resource value per unit area and per inhabitant indicate that mineral resources are much more important in the portion of the Columbia Plateau outside of the adjacent-counties study area than would be indicated by the 59 to 41 ratio of net-resource values. For the entire state of Washington, net value of sand, gravel, and crushed stone alone is approximately $700 per square kilometer and net value of all the state's mineral resources is estimated at over $1,700 per square kilometer, or more than three times the ratio in the vicinity of the reference repository location. For a mineral-rich state such as New Mexico, the comparable figure is $17,600 per square kilometer, or over 30 times the ratio for counties adjacent to, and including, the reference repository location.

Personal income, employment, and tax revenue comparisons for the vicinity of the reference repository location (100-kilometer radius from reference repository location) and the remainder of the Columbia Plateau are shown in Table 3-15.

3.9.5 Status

Current mineral-industry activity within 100 kilometers of the reference repository location is limited to surface-mined diatomaceous earth, sand and gravel, and stone. Occurrences of relatively low-unit-value minerals (mineral is here defined to include fossil beds, sand and gravel, and diatomite) within 100 kilometers of the site consist of peat, diatomaceous earth, pumicite, quarry rock, and sand and gravel. Such resources are surficial in occurrence and are not concentrated within the Pasco Basin relative to the remainder of the Columbia Plateau. A small, depleted, low-pressure natural gas field in production from 1929 to 1941 is present at the southern edge of the Hanford Site. No other current or

2124950793

) 2 1 2 4 9 5 0 7 9 4

TABLE 3-14. Projected Gross and Net Values and Estimated Present Values of Mineral Resources in the Columbia Plateau Study Area,[a] 1981-2005 (GG/GLA, 1981).

Mineral commodity	Gross value[b]	Production cost[b]	Net value[b]	Present net value[b]	
				At 12%	At 18%
Mineral Fuels					
Natural gas[c]	$19,500,000	$16,100,000	$3,400,000	$1,070,000	$740,000
Peat	1,500,000	1,200,000	300,000	90,000	70,000
Metallic Minerals					
Gold (placer)	19,400,000	15,200,000	4,200,000	1,320,000	920,000
Nonmetallic Minerals					
Diatomaceous earth	185,200,000	172,600,000	12,600,000	3,950,000	2,760,000
Sand, gravel, and stone	457,000,000	430,500,000	26,500,000	8,310,000	5,790,000
Totals	$682,600,000		$47,000,000	$14,740,000	$10,280,000

[a]As defined on a county-line boundary basis.

[b]Values are expressed in 1980 dollars. Present net value is at the beginning of 1981 of a stream of 25 annual payments equal to 1/25th of the total net value.

[c]Natural gas values expected from presently undiscovered deposits within the Columbia River Basalt Group. The subjective probability of realization is estimated at 0.37. All other values are for currently known deposits rounded to the nearest hundred thousand.

TABLE 3-15. Economic Comparisons of Mineral-Resource Values--the Reference Repository Location Vicinity Versus the Remainder of the Columbia Plateau (GG/GLA, 1981).

Variable factor	Reference repository location vicinity study area[a]	Remainder of Columbia Plateau[b]
Net resource value[c]	$33,300,000	$47,000,000
Area (square kilometers)	58,500	97,830
Population (1980)	533,241	478,793
Total employment (1980)	231,050	189,180
Net resource value[c]	$33,300,000	$47,000,000
Per square kilometer	$569	1,195
Per inhabitant	$62	98
Mining personal income[d]	$4,479,000	$4,945,000
Per square kilometer	$77	$126
Per inhabitant	$8.40	$10.33
Jobs in mining (1980)	280	340
Per thousand square kilometers	4.8	8.6
Per thousand inhabitants	0.5	0.7
Government revenues[e]	$192,400	$77,000
Per square kilometer	$3.29	$1.96
Per inhabitant	$0.36	$0.16

[a]Closest approximation of a 100-km radius from the reference repository location achievable using county boundaries.

[b]Closest approximation of main area of Columbia River Basalt Group outcrop less the reference repository location vicinity study area using county boundaries.

[c]Net resource value is the projected value, in 1980 dollars, of minerals that could be produced from 1981 to 2005. In each of the two areas considered, net values are only for those minerals found within 100 km of the potential site and exclude values for other minerals, even though they may be found and produced elsewhere on the Columbia Plateau.

[d]Mining personal income is personal income derived directly from mining in 1978 as reported by the U.S. Department of Commerce, Bureau of Economic Analysis.

[e]Government revenues are defined as state and local taxes contributed by mining enterprises. Relative values reflect the fact that the state of Washington taxes natural gas production at a higher rate than other minerals.

past commercial production of mineral fuels has been recorded in the area. Lignitic zones in sediments interbedded with basalt flows of the Columbia River Basalt Group in the Pasco Basin are too thin, too impure, and of too low rank to be attractive for exploration and development in the foreseeable future. With the exception of small gold placers along the Columbia River, no high-unit-value mineral resources with significant commercial potential are known to occur within 100 kilometers of the site.

Economic analysis of the area within 100 kilometers of the site indicates that gross value of known resources and probable gross value of potential remaining undiscovered natural gas within the Columbia River Basalt Group is $470.4 million dollars. Subtracting estimated costs of exploration, development, production, and wholesale marketing from gross value leaves a net value of $33.3 million, with a present net value over the next 25 years of $7.3 million calculated at an 18 percent discount rate. Projected net value for the area within 100 kilometers of the reference repository location averages $569 per square kilometer or $62 per current inhabitant. For the remainder of the Columbia Plateau, the respective value is $1,195 per square kilometer or $98 per inhabitant. For a mineral-rich state such as New Mexico, comparable net value per area is $17,600 per square kilometer.

It is concluded that the mineral industry of the reference repository location, based on geologic environment and mineral production, is a relatively insignificant component of employment, personal income, and tax revenues derived from all sources and is likely to remain so. The area is relatively unattractive for future subsurface mineral exploration and development within the Columbia River Basalt Group compared to other areas of the Columbia Plateau and United States.

9 6 0 7 5 0 9 4 2 1

THIS PAGE INTENTIONALLY
LEFT BLANK

0 2 1 2 4 9 5 0 7 9 7

3.10 SUMMARY OF UNRESOLVED ISSUES

Issues regarding the geology of the reference repository location and vicinity are discussed in Chapter 13.

1 2 1 2 4 9 5 0 7 9 8

THIS PAGE INTENTIONALLY
LEFT BLANK

3.11 REFERENCES

Ando, M. and Balazs, E. I., 1979, "Geodetic Evidence for Aseismic Subduction of the Juan de Fuca Plate," Journal of Geophysical Research, Vol. 84. pp. 3023-3028.

ARHCO, 1976, Preliminary Feasibility Study on Storage of Radioactive Waste in Columbia River Basalts, ARH-ST-137, Atlantic Richfield Hanford Company, Richland, Washington.

Armstrong, R. L., 1978, Cenozoic Igneous History of the U.S. Cordillera from Latitude 42° to 49° North, Memoir 152, Geological Society of America, pp. 265-282.

Armstrong, R. L., Taubeneck, W. H., and Hales, P. O., 1977, "Rb-Sr and K-Ar Geochronometry of Mesozoic Granitic Rocks and Their Sr Isotropic Composition, Oregon, Washington, and Idaho," Geological Society of America Bulletin, Vol. 88, pp. 397-411.

Arnett, R. C., Baca, R. G., Caggiano, J. A., Price, S. M., Gephart, R. E., and Logan, S. E., 1980, Preliminary Hydrologic Release Scenarios for a Candidate Repository Site in the Columbia River Basalts, RHO-BWI-ST-12, Rockwell Hanford Operations, Richland, Washington, November 1980.

Ault, T. D., 1981, "Geophysical Investigations of the Gable Mountain-Gable Butte Area," in Myers, C. W. and Price, S. M., eds., Subsurface Geology of the Cold Creek Syncline, RHO-BWI-ST-14, Rockwell Hanford Operations, Richland, Washington, July 1981.

Baksi, A. K. and Watkins, N. D., 1973, "Volcanic Production Rates: Comparison of Oceanic Ridges, Islands, and the Columbia Plateau Basalts," Science, Vol. 180, No. 4085, pp. 493-496.

Beck, M. E., Engebretson, D. C., and Plumley, P. W., 1978, Magnetostratigraphy of the Grande Ronde Sequence, RHO-BWI-C-18, Western Washington University for Rockwell Hanford Operations, Richland, Washington.

Bentley, R. D., 1977, "Stratigraphy of the Yakima Basalts and Structural Evolution of the Yakima Ridges in the Western Columbia Plateau," in Geology Excursions in the Pacific Northwest, Brown, E. H. and Ellis, R. C., eds., Western Washington University, Bellingham, Washington, pp. 339-389.

Bentley, R. D., 1980, "Angular Unconformity and Thrust Fault in the Umtanum Anticlinal Uplift Near Priest Rapids Dam, Central Washington," EOS, Transactions of the American Geophysical Union, Vol. 61, No. 46, p. 1108.

Bentley, R. D., Anderson, J. L., Campbell, N. P., and Swanson, D. A., 1980, Stratigraphy and Structure of the Yakima Reservation, with Emphasis on the Columbia River Basalt Group," Open-File Report 80-200, U.S. Geological Survey, Reston, Virginia.

Berg, J. W. and Baker, C. D., 1963, "Oregon Earthquakes, 1841 through 1958," Bulletin of the Seismological Society of America, Vol. 53, No. 1, p. 65.

Bingham, J. W., Londquist, C. J., and Baltz, E. H., 1970, Geologic Investigation of Faulting in the Hanford Region, Washington, Open-File Report, U.S. Geological Survey, Washington, D.C.

Blackwell, D. D., 1978, "Heat Flow and Energy Loss in the Western United States," in Cenozoic Tectonics and Regional Geophysics of the Western Cordillera, Smith, R. B. and Eaton, G. P., eds., Memoir 152, Geological Society of America.

Blackwell, D. D., 1980, "Heat Flow and Geothermal Gradient Measurements in Washington through 1979," in The 1978-1980 Geothermal Resource Assessment Program in Washington, by Korosec, M. A. and Schuster, J. E., Open-File Report 81-3, Washington State Department of Natural Resources, Division of Geology and Earth Resources, Olympia, Washington.

Blackwell, D. D., 1981, "Heat Flow of the Cascade Range," in Symposium on the Geothermal Potential of the Cascade Mountain Range, Geothermal Resource Council, Program with Abstracts.

Blume, J. A., 1971, Subsurface Geologic Investigations for the FFTF Project in Pasco Basin, JABE-WADCO-07, J. A. Blume and Associates, San Francisco, California.

Bond, J. G., Kauffman, J. D., Miller, D. A., and Barrash, W., 1978a, Geology of the Southwest Pasco Basin, RHO-BWI-C-25, Geoscience Research Consultants for Rockwell Hanford Operations, Richland, Washington.

Bond, J. G., Kauffman, J. D., Miller, D. A., and Venkatakrishnam, R., 1978b, Geologic Map of Idaho, 1:5000,000, Idaho Bureau of Mines and Geology, Moscow, Idaho.

Bonini, W. E., Hughes, D. W., and Danes, Z. F., 1974, Complete Bouguer Gravity Anomaly Map of Washington, Washington State Department of Natural Resources, Division of Geology and Earth Resources, Olympia, Washington.

Bretz, J H., 1959, "Washington's Channeled Scabland," Washington Division of Mines and Geology Bulletin, No. 45, Olympia, Washington.

Brewer, W. A., 1977, Lineament Map of the State of Washington; Overlay to Landsat Space Imagery, 1:500,000, Open-File Map, Washington State Department of Natural Resources, Division of Geology and Earth Resources, Olympia, Washington.

Brown, B. H., 1937, "The State-Line Earthquake at Milton and Walla Walla," Seismological Society of America Bulletin, Vol. 27, p. 205.

Brown, J. C., 1978, Discussion of Geology and Ground-Water Hydrology of the Columbia Plateau, With Specific Analysis of the Horse Heaven, Sagebrush Flats, and Odessa-Lind Areas, Washington, Research Report 78/15-23, Research Division, College of Engineering, Washington State University, Pullman, Washington.

Brown, R. E., 1968, A Study of Reported Faulting in the Pasco Basin, PNL-SA-1704, Pacific Northwest Laboratory, Richland, Washington.

Brown, R. E. and McConiga, M. W., 1960, "Some Contributions to the Stratigraphy and Indicated Deformation of the Ringold Formation," Northwest Science, Vol. 34, No. 2, p. 43.

Caggiano, J. A. Fecht, K. R., Price, S. M., Reidel, S. P., and Tallman, A. M., 1980, "A Preliminary Assessment of the Relative Rate of Deformation in the Pasco Basin, South-Central Washington," Geological Society of America Abstracts with Programs, Vol. 12, No. 7, p. 297.

Camp, V. E., 1976, Petrochemical Stratigraphy and Structure of the Columbia River Basalt, Lewiston Basin Area, Idaho-Washington, Ph. D. Dissertation, Washington State University, Pullman, Washington.

Camp, V. E., 1981, "Geologic Studies of the Columbia Plateau Part II, Upper Miocene Basalt Distribution Reflecting Source Locations, Tectonism and Drainage History in the Clearwater Embayment, Idaho," Geological Society of America Bulletin, Part I, Vol. 92, pp. 669-678.

Campbell, N. P. and Bentley, R. D., 1981, "Late Quaternary Deformation of the Toppenish Ridge Uplift in South-Central Washington," Geology, Vol. 9, pp. 519-524.

Cochran, M. P., 1981a, "Geophysical Investigations in the West Gable Butte Area," in Myers, C. W. and Price, S. M., eds., Subsurface Geology of the Cold Creek Syncline, RHO-BWI-ST-14, Rockwell Hanford Operations, Richland, Washington, July 1981.

Cochran, M. P., 1981b, Ground Geophysical Investigations of a Segment of the Rattlesnake Hills Lineament, RHO-BWI-SA-155A, Rockwell Hanford Operations, Richland, Washington.

COE, 1959, "Lower Monumental Lock and Dam, Snake River, Washington, Oregon and Idaho," General Design Memorandum, Vol. 2, No. 1, Appendix D - Geology, U.S. Army Corps of Engineers, Walla Walla, Washington.

Coe, R. S., Bogue, S., and Myers, C. W., 1978, Paleomagnetism of the Grande Ronde (Lower Yakima) Basalt Exposed at Sentinel Gap; Potential Use for Stratigraphic Correlation, RHO-BWI-ST-2, Rockwell Hanford Operations, Richland, Washington.

Coffman, J. L. and von Hake, C. A., 1973, Earthquake History of the United States, Publication 41-1 (revised edition), U.S. Department of Commerce, Washington, D.C.

Couch, R. W. and Lowell, R. P., 1971, "Earthquakes and Seismic Energy Release in Oregon," Ore Bin, Vol. 33, No. 4, pp. 61-84.

Cowan, D. S., 1980, "Late Mesozoic Tectonic Events in the Pacific Northwest," Geological Society of America Abstracts With Programs, Vol. 12, p. 102.

Crandell, D. R., 1971, Postglacial Lahars from Mount Rainier Volcano, Washington, Professional Paper 677, U.S. Geological Survey, Washington, D.C.

Crandell, D. R., 1976, Preliminary Assessment of Potential Hazards from Future Volcanic Eruptions in Washington, Miscellaneous Field Studies Map MF-774, U.S. Geological Survey, Denver, Colorado.

Crosby, J. W., 1972, Borehole Geophysical Investigation of the Area Surrounding the Hanford Atomic Energy Works, Quarterly Report, Research Division, College of Engineering, Washington State University, Pullman, Washington.

Crosson, R. S., 1972, "Small Earthquakes, Structure, and Tectonics of the Puget Sound Region," Seismological Society of America Bulletin, Vol. 62, p. 1133.

Crosson, R. S., 1980, "Seismicity and Tectonics of the Puget Sound Region, Results from the Regional Seismograph Network," Earthquake Notes, Vol. 50, No. 4, p. 58.

Davis, G. A., 1981, "Late Cenozoic Tectonics of the Pacific Northwest with Special Reference to the Columbia Plateau," in Final Safety Analysis Report, Appendix 2.5 N, Washington Public Power Supply System, Inc., Richland, Washington.

Day, N. F. and Hall, W. B., 1973, "Tectonic Map of Idaho From ERTS Imagery," Geological Society of America Abstracts With Programs, Vol. 5, No. 7, p. 594.

Deju, R. A. and Richard, B. H., 1975, A Regional Gravity Investigation of the Hanford Reservation, ARH-C-8, Atlantic Richfield Hanford Company, Richland, Washington.

Eaton, J. P., Wahl, R. R., Prostka, H. J., Mabey, D. R., and Kleinkopf, D. R., 1978, "Regional Gravity and Tectonic Patterns, their Relation to Late Cenozoic Epeirogeny and Lateral Spreading in the Western Cordillera," in Cenozoic Tectonics and Regional Geophysics of the Western Cordillera, Smith, R. B. and Eaton, G. P., eds., Memoir 152, Geological Society of America, Boulder, Colorado, pp. 51-91.

Edwards, R. C., 1978, "Magnetotelluric Surveying on the Hanford Site, Washington," in Basalt Waste Isolation Program Annual Report - Fiscal Year 1978, RHO-BWI-78-100, Rockwell Hanford Operations, Richland, Washington.

Evernden, J. F., Savage, D. E., Curtis, G. H., and James, G. T., 1964, "Potassium-Argon Dates and the Cenozoic Mammalian Chronology of North America," American Journal of Science, Vol. 262, pp. 145-198.

Farooqui, S. M., 1979, Evaluation of Faulting in the Warm Springs Canyon Area, Southeast Washington, Shannon and Wilson, Inc., Portland Oregon.

Farooqui, S. M. and Thoms, R. E., 1980, Geologic Evaluation of Selected Faults and Lineaments, Pasco and Walla Walla Basins, Washington, Shannon Wilson, Inc. for Washington Public Power Supply System, Inc., Richland, Washington.

Farooqui, S. M., Beaulieu, J. D., Bunker, R. C., Stensland, D. E., and Thoms, R. E., 1981a, "Dalles Group Neogene Formations Overlying the Columbia River Basalt Group in North-Central Oregon," Oregon Geology, Vol. 43, p. 131-140.

Farooqui, S. M., Bunker, R. C., Thoms, R. E., Clayton, D. C., and Bela, J. L., 1981b, Post-Columbia River Basalt Group Stratigraphy and Map Compilation of the Columbia Plateau, Open-File Report 0-81-10, State of Oregon Department of Geology and Mineral Industries, Portland, Oregon.

Fecht, K. R., 1978, Geology of Gable Mountain-Gable Butte Area, RHO-BWI-LD-5, Rockwell Hanford Operations, Richland, Washington.

Fecht, K. R. and Lillie, J. T., 1981, A Catalog of Borehole Lithologic Logs From the 600 Area, Hanford Site, RHO-LD-158, Rockwell Hanford Operations, Richland, Washington.

Fecht, K. R., Reidel, S. P., and Tallman, A. M., 1982, "Evolution of the Columbia River System in the Central Columbia Plateau of Washington from Miocene to the Present," Geological Society of America Abstracts With Programs, Vol. 14, No. 4, p. 163.

Fifer, N. F., 1966, 1918 Corfu Earthquake, DUN-1524, Douglas United Nuclear, Inc., Richland, Washington.

Fifer, N. F., 1968, Earthquake Studies of the Hanford Area, DUN-3625 Douglas United Nuclear, Inc., Richland, Washington.

Fox, K. F., Jr., Rinehart, C. D., Engels, J. C., and Stern, T. W., 1976, "Age of Emplacement of the Okanogan Gneiss Domes," Geological Society of America Bulletin, Vol. 87, pp. 1217-1224.

Fox, K. F., Jr., Rinehart, C. D., Engels, J. C., and Stern, T. W., 1977, Plutonism and Orogeny in North-Central Washington - Timing and Regional Context, Professional Paper 989, U.S. Geological Survey, Washington, D.C.

Freeman, O. W., Forrester, J. D., and Lupher, R. L., 1945, "Physiographic Divisions of the Columbia Intermontane Province," Association of American Geographers, Annuals, Vol. 35, 53-75.

Fruchter, J. S. and Baldwin, S. F., 1975, "Correlations Between Dikes of the Monument Swarm, Central Oregon, and Picture Gorge Basalt Flows," Geological Society of America Bulletin, Vol. 86, p. 514.

Gardner, J. N., 1977, "Stratigraphy and Faulting of Columbia River Basalt in Wallula Gap, Washington," EOS, American Geophysical Union Abstracts, Vol. 58, p. 1247.

Gardner, J. N., Snow, M. G., and Fecht, K. R., 1981, Geology of the Wallula Gap Area, Washington, RHO-BWI-LD-9, Rockwell Hanford Operations, Richland, Washington.

GG/GLA, 1981, Economic Geology of the Pasco Basin, Washington and Vicinity, RHO-BWI-C-109, Geosciences Group and George Leaming Associates for Rockwell Hanford Operations, Richland, Washington, July 1981.

Glass, C. E., 1977, "Remote Sensing Analysis of the Columbia Plateau," in Preliminary Safety Analysis Report, Amendment 23, Appendix 2RK, Washington Public Power Supply System, Inc., Richland, Washington.

Glass, C. E., 1980, Analysis and Interpretation of Remote Sensing Data Applied to the Columbia Plateau, Washington and Oregon, C. E. Glass, Consulting Engineer for Washington Public Power Supply System, Inc., Richland, Washington.

Glass, C. E. and Slemmons, D. B., 1977, "Imagery and Topographic Interpretation of Geologic Structures in Central Washington," in Preliminary Safety Analysis Report, Amendment 23, Appendix 2RF, Washington Public Power Supply System, Inc., Richland, Washington.

Godfrey, W. L., Brown, D. J., and Veatch, M. D., 1972, Remote Sensing of Southeastern Washington, Part I, Infrared Scanning Imagery, ARH-2251, Atlantic Richfield Hanford Company, Richland, Washington.

Goff, F. E., 1981, Preliminary Geology of Eastern Umtanum Ridge, South-Central Washington, RHO-BWI-C-21, F. E. Goff, Consulting Engineer, for Rockwell Hanford Operations, Richland, Washington.

Goff, F. E. and Myers, C. W., 1978, "Structural Evolution of East Umtanum and Yakima Ridges, South-Central Washington," Geological Society of America Abstracts with Programs, Vol. 10, No. 7, p. 408.

Golder, 1981, Gable Mountain, Structural Investigations and Analyses, Golder Associates, Inc., Kirkland, Washington.

Griggs, A. B., 1976, The Columbia River Basalt Group in the Spokane Quadrangle, Washington, Idaho, and Montana, Bulletin 1413, U.S. Geological Survey, Washington, D.C.

Grolier, M. J. and Bingham, J. W., 1971, Geologic Map and Sections of Parts of Grant, Adams, and Franklin Counties, Washington, Miscellaneous Geologic Investigations Map I-589, U.S. Geological Survey, Washington, D.C.

Grolier, M. J. and Bingham, J. W., 1978, Geology of Parts of Grant, Adams, and Franklin Counties, East-Central Washington, Bulletin 71, Washington State Department of Natural Resources, Division of Geology and Earth Resources, Olympia, Washington.

Gutenberg, B. and Richter, C. F., 1954, Seismicity of the Earth, 2nd Edition, Princeton University Press, Princeton, New Jersey.

Haimson, B. C., 1978, "Report on Hydrofracturing Tests for In Situ Stress Measurement, Near-Surface Test Facility, Hole DC-11, Hanford Reservation," in DuBois, A., Binnall, E., Chan, T., McEvoy, M., Nelson, P., and Remer, H., 1979, Heater Test Planning for the Near-Surface Test Facility at Hanford Reservation, LBL-8730, Lawrence Berkeley Laboratory, Berkeley, California, Vol. 2, pp. 10-1 and 10-19.

Haman, P. J., 1975, "A Lineament Analysis of the United States," West Canadian Research Publications of Geology and Related Sciences Series, Vol. 4, No. 1.

Hammer, A. A., 1934, "Rattlesnake Hills Gas Field, Benton County, Washington," Bulletin of the American Association of Petroleum Geologists, Vol. 18, No. 7, p. 847.

Heineck, R. L. and Beggs, H. G., 1978, Evaluation of Seismic Reflection Surveying in the Hanford Site, Benton County, Washington, RHO-BWI-C-20, Seismograph Service Corporation for Rockwell Hanford Operations, Richland, Washington.

Hill, D. B., 1972, "Crustal and Upper Mantle Structure of the Columbia Plateau from Long-Range Seismic-Refraction Measurements," Geological Society of America Bulletin, Vol. 83, p. 1639-1648.

Hill, D. B., 1978, "Seismic Evidence for the Structure and Cenozoic Tectonics of the Pacific Coast States," in Cenozoic Tectonics and Regional Geophysics of the Western Cordillera, Smith, R. B. and Eaton, G. P., eds., Memoir 152, Geological Society of America, Boulder, Colorado, pp. 145-174.

Holden G. S. and Hooper, P. R., 1976, "Petrology and Chemistry of a Columbia River Basalt Section, Rocky Canyon, West-Central Idaho," Geological Society of America Bulletin, Vol. 87, pp. 215-225.

Holmes, G. E. and Mitchell, T. H., 1981, "Seismic Reflection and Multilevel Aeromagnetic Surveys in Cold Creek Syncline Area," in Myers, C. W. and Price, S. M., eds., Subsurface Geology of the Cold Creek Syncline, RHO-BWI-ST-14, Rockwell Hanford Operations, Richland, Washington, July 1981.

Hooper, P. R. and Camp, V. E., 1981, "Deformation of the Southeast Part of the Columbia Plateau," Geology, Vol. 9, p. 323-328.

Jackson, E. D., Robinette, M. J., and Crosby, J. W., III, 1976, Geophysical Logging of the Hanford Reservation, Research Report 76/15/39, College of Engineering, Washington State University, Pullman, Washington.

Jaeger, J. C., 1961, "The Cooling of Irregularly Shaped Igneous Bodies," American Journal of Science, Vol. 259, pp. 721-734.

Jahns, R. H., 1967, Geologic Factors Relating to Engineering Seismology in the Hanford Area, Washington, DUN-3100, Douglas United Nuclear, Inc., Richland, Washington.

Jenkins, O. P., 1922, Underground Water Supply of the Region About White Bluffs and Hanford, Washington, Bulletin No. 26, Washington State Department of Conservation and Development, Division of Geology, Olympia, Washington.

Johnpeer, G. D., Miller, D., and Goles, G., 1981, Assessment of Potential Volcanic Hazards, Pasco Basin, Washington, RHO-BW-CR-130 P, Ertec Western, Inc. for Rockwell Hanford Operations, Richland, Washington, pp. 3-1-3-44, August 1981.

Jones, F. O. and Deacon, R. J., 1966, Geology and Tectonic History of the Hanford Area and its Relation to the Geology and Tectonic History of the State of Washington and the Active Seismic Zones of Western Washington and Western Montana, DUN-1410, Douglas United Nuclear, Inc., Richland, Washington, p. 21.

Jones, M. G. and Landon, R. D., 1978, Geology of the Nine Canyon Map Area, RHO-BWI-LD-6, Rockwell Hanford Operations, Richland, Washington.

Kienle, C. F., Jr., Bentley, R. D., and Anderson, J. L., 1977, "Geologic Reconnaissance of the Cle Elum-Wallula Lineament and Related Structures," in Preliminary Safety Analysis Report, Amendment 23, Vol. 2A, Subappendix 2R D, Shannon and Wilson, Inc. for Washington Public Power Supply System, Inc., Richland, Washington.

Kienle, C. F., Jr., Bentley, R. D., Farooqui, S. M., Anderson, J. L., Thoms, R. E., and Couch, R. C., 1978, "The Yakima Ridges - An Indication of an Anomalous Plio-Pleistocene Stress Field," Geological Society of America Abstracts With Programs, Vol. 10, No. 3, p. 111.

Kim, K., 1980, "Rock Mechanics Field Test Results to Date," in Basalt Waste Isolation Project Annual Report - Fiscal Year 1980, RHO-BWI-80-100, Rockwell Hanford Operations, Richland, Washington, November 1980, pp. V-26-V-34.

Kleck, W. D., 1976, Chemistry, Petrography, and Stratigraphy of the Columbia River Basalt Group in the Imnaha River Valley Region, Eastern Oregon and Western Idaho, Ph. D. Dissertation, Washington State University, Pullman, Washington.

Klosterman, K. E., 1974, An Evaluation of the ERTS-I System Imagery in a Structural Study and a Map Application, ERTS-I Imagery in Southeastern Washington, Northeastern Oregon, and Parts of Western Idaho, M.S. Thesis, University of Washington, Seattle, Washington.

Koniček, D. L., 1975, "Geophysical Survey in South-Central Washington," Northwest Science, Vol. 49, No. 2, pp. 106-117.

Korosec, M. A. and Schuster, J., 1980, The 1978-1980 Geothermal Resource Assessment Program in Washington, Open-File Report 81-3, Division of Geology and Earth Resources, Washington State Department of Natural Resources, Olympia, Washington, July 1981.

Kunk, J. R., 1981, "Geophysical Investigations in the Southwestern Cold Creek Syncline," in Myers, C. W. and Price, S. M., eds., Subsurface Geology of the Cold Creek Syncline, RHO-BWI-ST-14, Rockwell Hanford Operations, Richland, Washington, July 1981.

Laubscher, H. P., 1981, "Models of the Development of Yakima Deformation," in Final Safety Analysis Report, Amendment No. 18, Appendix 2.5 O, Washington Public Power Supply System, Inc., Richland, Washington.

Lawrence, R. D., 1976, "Strike-slip Faulting Terminates the Basin and Range Province in Oregon" Geological Society of America Bulletin, Vol. 87, pp. 846-850.

Lawrence, R. D., 1978, "Tectonic Significance of Petrofabric Studies Along the Chewack-Pasayten Fault, North-Central Washington," Geological Society of America Bulletin, Vol. 89, No. 5, pp. 731-743.

Lawrence, R. D., 1979, "Tectonic Significance of Regional Jointing in Columbia River Basalt, North-Central Oregon," Northwest Science, Vol. 53, No. 1, pp. 33-42.

Lawrence, R. D. and Carter, J., 1974, Preliminary Lineament Map of Oregon from ERTS Imagery at 1:1,000,000, Oregon Nuclear and Thermal Energy Council and Department of Geology and Mineral Industries, Portland, Oregon.

Lillie, J. T. and Richard, B. H., 1977, An Analysis of Selected Gravity Profiles on the Hanford Reservation, Richland, Washington, RHO-BWI-C-6, Rockwell Hanford Operations, Richland, Washington.

Lillie, J. T., Tallman, A. M., and Caggiano, J. A., 1978, Preliminary Geologic Map of Late Cenozoic Sediments of the Western Half of the Pasco Basin, RHO-BWI-LD-8, Rockwell Hanford Operations, Richland, Washington.

Long, P. E., 1978, Characterization and Recognition of Intraflow Structures, Grande Ronde Basalt, RHO-BWI-LD-10, Rockwell Hanford Operations, Richland, Washington.

Long, P. E. and Davidson, N. J., 1981, "Lithology of the Grande Ronde Basalt With Emphasis on the Umtanum and McCoy Canyon Flows," in Myers, C. W. and Price, S. M., eds., Subsurface Geology of the Cold Creek Syncline, RHO-BWI-ST-14, Rockwell Hanford Operations, Richland, Washington, July 1981.

Long, P. E. and Landon, R. D., 1981, "Stratigraphy of the Grande Ronde Basalt," in Myers, C. W. and Price, S. M., eds., Subsurface Geology of the Cold Creek Syncline, RHO-BWI-ST-14, Rockwell Hanford Operations, Richland, Washington, July 1981.

Long, P. E., Ledgerwood, R. K., Myers, C. W., Reidel, S. P., Landon, R. D., and Hooper, P. R., 1980, Chemical Stratigraphy of Grande Ronde Basalt, Pasco Basin, South-Central Washington, RHO-BWI-SA-32, Rockwell Hanford Operations, Richland, Washington; also in Geological Society of America Abstracts with Programs, Vol. 12, No. 12.

Long, P. E., Landon, R. D., Reidel, S. P., and Goles, G. G., 1981, "Trace Element Composition of Grande Ronde Basalt, Pasco Basin, South-Central Washington," EOS, Transactions of the American Geophysical Union, Vol. 62, No. 6.

Mackin, J. H., 1955, Geology of the Priest Rapids Development, Priest Rapids Hyroelectric Project, Columbia River, Washington, Grant County Public Utility District, Ephrata, Washington.

Mackin, J. H., 1961, A Stratigraphic Section in the Yakima Basalt and the Ellensburg Formation in South-Central Washington, Report of Investigations No. 19, Washington Division of Mines and Geology, Olympia, Washington.

Malone, S. D., 1976, Annual Report on Earthquake Monitoring of Eastern Washington, University of Washington, Seattle, Washington.

Malone, S. D., Rothe, G. H., and Smith, S. W., 1975, "Details of Micro-earthquake Swarms in the Columbia Basin, Washington," Seismological Society of America Bulletin, Vol. 65, No. 4, pp. 855-864.

McBirney, A. R., 1978, "Volcanic Evolution of the Cascade Range," Annual Review of Earth and Planetary Science Letters, Vol. 6, pp. 437-456.

McBirney, A. R., Sutter, J. F., Naslund, H. R., Sutton, K. G., and White, C. M., 1974, "Episodic Volcanism in the Central Oregon Cascade Range," Geology, Vol. 2, No. 12, pp. 585-589.

McFarland, C. R., 1979, Oil and Gas Exploration in Washington 1900-1978, Information Circular 67, Washington State Department of Natural Resources, Olympia, Washington.

McGarr, A., Green, R. W. E., and Spottiswoode, S. M., 1981, "Strong Ground Motion of Mine Tremors: Some Implications for Near-Surface Ground Motion Parameters," Seismological Society of America Bulletin, Vol. 71, No. 1, pp. 295-319.

McGhan, V. L. and Damschen, D. W., 1979, Hanford Wells, PNL-2894, Pacific Northwest Laboratory, Richland, Washington.

McKee, E. H., Swanson, D. A., and Wright, T. L., 1977, "Duration and Volume of Columbia River Basalt Volcanism; Washington, Oregon and Idaho," Geological Society of America Abstracts with Programs, Vol. 9, No. 4, pp. 463-464.

Mehringer, P. J., Blinmae, E., and Peterson, K. L., 1977, "Pollen Influx and Volcanic Ash," Science, Vol. 1, No. 198, pp. 267-291.

Merriam, J. C., 1901, A Contribution to the Geology of the John Day Basin, Department of Geologic Sciences Bulletin, Vol. 2, University of California, pp. 269-314.

Miller, F. K. and Engels, J. C., 1975, "Distribution and Trends of Discordant Ages of the Plutonic Rocks of Northeastern Washington and Northern Idaho," Geological Society of America Bulletin, Vol. 86, pp. 517-528.

Moak, D. J., 1981a, "Borehole Geologic Studies," in Myers, C. W. and Price, S. M., eds., Subsurface Geology of the Cold Creek Syncline, RHO-BWI-ST-14, Rockwell Hanford Operations, Richland, Washington, July 1981.

Moak, D. J., 1981b, "Summary of Borehole Locations and Geologic Activities at Borehole Sites," in Myers, C. W., and Price, S. M., eds., Subsurface Geology of the Cold Creek Syncline, RHO-BWI-ST-14, Rockwell Hanford Operations, Richland, Washington, July 1981.

Moak, D. J. and Wintczak, T. M., 1980, Near-Surface Test Facility Phase I Geologic Site Characterization Report, RHO-BWI-ST-8, Rockwell Hanford Operations, Richland, Washington.

Mullineaux, D. R., Hyde, J. H., and Rubin, M., 1975, "Widespread Late Glacial and Post-Glacial Tephra Deposits From Mount St. Helens Volcano, Washington," Journal of Research of the U.S. Geological Survey, Vol. 3, pp. 329-225.

Mullineaux, D. R., Wilcox, R. E., Ebaugh, W. F., Fryxell, R., and Rubin, M., 1977, "Age of the Last Major Scabland Flood of Eastern Washington, as Inferred From Associated Ash Beds of Mount St. Helens Set S," Geological Society of America, Abstracts with Program, Vol. 9, No. 7, p. 1105.

Murphy, P. J. and Johnpeer, G. D., 1981, An Assessment of Geothermal Resource Potential, Pasco Basin and Vicinity, Washington, RHO-BW-CR-128 P, Ertec Western, Inc. for Rockwell Hanford Operations, Richland, Washington.

Myers, C. W., 1973, Yakima Basalt Flows near Vantage, and From Core Holes in the Pasco Basin, Washington, Ph. D. Dissertation, University of California at Santa Cruz, Santa Cruz, California.

Myers, C. W., 1981, "Bedrock Structure of the Cold Creek Syncline Area," in Myers, C. W. and Price, S. M., eds., Subsurface Geology of the Cold Creek Syncline, RHO-BWI-ST-14, Rockwell Hanford Operations, Richland, Washington, July 1981.

Myers, C. W. and Brown, D. J., 1973, "Stratigraphy of the Yakima Basalt in the Pasco Basin, Washington," Geological Society of America, Abstracts with Program (Cordilleran Section), Vol. 5, No. 1, p. 80.

Myers, C. W./Price, S. M., and Caggiano, J. A., Cochran, M. P., Czimer, W. J., Davidson, N. J., Edwards, R. C., Fecht, K. R., Holmes, G. E., Jones, M. G., Kunk, J. R., Landon, R. D., Ledgerwood, R. K., Lillie, J. T., Long, P. E., Mitchell, T. H., Price, E. H., Reidel, S. P., and Tallman, A. M., 1979, Geologic Studies of the Columbia Plateau: A Status Report, RHO-BWI-ST-4, Rockwell Hanford Operations, Richland, Washington, October 1979.

Myers, C. W. and Price, S. M., eds., 1981, Subsurface Geology of the Cold Creek Syncline, RHO-BWI-ST-14, Rockwell Hanford Operations, Richland, Washington, July 1981.

Newcomb, R. C., 1970, Tectonic Structure of the Main Part of the Basalt of the Columbia River Group, Washington, Oregon, and Idaho, Miscellaneous Geologic Investigations Map I-587, U.S. Geological Survey, Washington, D.C.

Newcomb, R. C., Strand, J. R., and Frank, F. J., 1972, Geology and Groundwater Characteristics of the Hanford Reservation of the U.S. Atomic Energy Commission, Washington, Professional Paper 717, U.S. Geological Survey, Washington, D.C.

NRC, 1982, Safety Evaluation Report, Washington Plant No. 2, NUREG-0892 Supplement #1, U.S. Nuclear Regulatory Commission, Washington, D.C.

Owen, G. N. and Scholl, R. E., 1981, Earthquake Engineering of Large Underground Structures, FHWA/RD-80/195, Federal Highway Administration and Department of Transportation, Washington, D. C.

Packer, D. R. and Petty, M. H., 1979, Magnetostratigraphy of the Grande Ronde Basalt, Pasco Basin, Washington, RHO-BWI-C-46, Woodward-Clyde Consultants for Rockwell Hanford Operations, Richland, Washington.

Peterson, D. E., 1965, Variations in the Earth's Gravity Field at Hanford, BNWL-235, Battelle, Pacific Northwest Laboratories, Richland, Washington.

Peterson, D. E., 1966, Bouguer Gravity Anomalies on the Hanford Reservation, BNWL-481, Battelle, Pacific Northwest Laboratories, Richland, Washington.

Pitt, A. M., 1971, Microearthquake Activity in the Vicinity of Wooded Island, Hanford Region, Washington, Open-File Report, U.S. Geological Survey, Washington, D.C.

Porter, S. C., 1978, "Glacier Peak Tephra in the North Cascade Range, Washington, Stratigraphy, Distribution and Relationship to Late-Glacial Events," Quaternary Research, Vol. 10, pp. 30-41.

Pratt, H. R., Hustralid, W. A., and Stephenson, D. E., 1978, Earthquake Damage to Underground Facilities, USDOE Document DP-1513, E. I. du Pont de Nemours & Co., Savannah River Laboratory, Aiken, South Carolina.

Prentice, V. L., 1972, Multispectral Remote Sensing Techniques Applied to Salinity and Drainage Problems in the Columbia Basin, Washington, Ph. D. Thesis, University of Michigan, Ann Arbor, Michigan.

Price, E. H., 1982, Structural Geometry, Strain Distribution, and Tectonic Evolution of Umtanum Ridge at Priest Rapids, and a Comparison with Other Selected Localities Within Yakima Fold Structures, South-Central Washington, Ph. D. Dissertation, Washington State University, Pullman, Washington; also RHO-BWI-SA-138, Rockwell Hanford Operations, Richland, Washington.

Price, S. M., 1977, An Evaluation of Dike-Flow Correlations Indicated by Geochemistry, Chief Joseph Swarm, Columbia River Basalt, Ph. D. Dissertation, University of Idaho, Moscow, Idaho.

PSPL, 1982, Skagit-Hanford Nuclear Project, Preliminary Safety Analysis Report, Puget Sound Power and Light Company, Bellevue, Washington.

Ramsay, J. G., 1967, Folding and Fracturing of Rocks, McGraw-Hill, New York, New York.

Rasmussen, N. H., 1967, "Washington State Earthquakes 1840 through 1965," Bulletin of the Seismological Society of America, Vol. 57, No. 3, p. 463.

Rasmussen, N. H. and Rohay, A. C., 1982, Seismic Monitoring at a Potential Deep Nuclear Waste Repository Site Within the Columbia River Basalt Group, Pasco Basin, RHO-BWI-SA-178A, Rockwell Hanford Operations, Richland, Washington.

Raymond, J. R. and McGhan, V. L., 1963, Results of an Airborne Magnetometer Survey of the Hanford Project, HW-78924, General Electric Company, Richland, Washington, p. 15.

Raymond, J. R. and Tillson, D. D., 1968, Evaluation of a Thick Basalt Sequence in South-Central Washington, Geophysical and Hydrological Exploration of the Rattlesnake Hills Deep Stratigraphic Test Well, BNWL-776, Battelle, Pacific Northwest Laboratories, Richland, Washington.

Reidel, S. P., 1978a, Geology of the Saddle Mountains between Sentinel Gap and 119° 31' Longitude, RHO-BWI-LD-4, Rockwell Hanford Operations, Richland, Washington.

Reidel, S. P., 1978b, Stratigraphy and Petrogenesis of the Grande Ronde Basalt in the Lower Salmon and Adjacent Snake River Canyons, RHO-SA-62, Rockwell Hanford Operations, Richland, Washington.

Reidel, S. P., 1981, Stratigraphy and Petrogenesis of the Grande Ronde Basalt from the Deep Canyon Country of Washington, Oregon, and Idaho, A Summary, RHO-BWI-SA-114, Rockwell Hanford Operations, Richland, Washington.

Reidel, S. P. and Fecht, K. R., 1981, "Wanapum and Saddle Mountains Basalts of the Cold Creek Syncline Area," in Myers, C. W. and Price, S. M., eds., Subsurface Geology of the Cold Creek Syncline, RHO-BWI-ST-14, Rockwell Hanford Operations, Richland, Washington, July 1981.

Reidel, S. P., Ledgerwood, R. K., Myers, C. W., Jones, M. G., and Landon, R. D., 1980, "Rate of Deformation in the Pasco Basin During the Miocene as Determined by Distribution of Columbia River Basalt Flows," Geological Society of America, Abstracts with Program, Vol. 12, No. 3, p. 149; also, RHO-BWI-SA-29, Rockwell Hanford Operations, Richland, Washington.

Reidel, S. P., Long, P. E., Myers, C. W., and Mase, J., 1981, New Evidence for Greater Than 3.2 Kilometers of Columbia River Basalt Beneath the Central Columbia Plateau, RHO-BWI-SA-162A, Rockwell Hanford Operations, Richland, Washington.

Richard, B. H., 1976, Residual Gravity Analysis of Selected Cross Sections of the Hanford Reservation, ARH-C-23, Atlantic Richfield Hanford Company, Richland, Washington.

Richard, B. H. and Deju, R. A., 1977, Three-Dimensional Gravity Investigation of the Hanford Reservation, RHO-BWI-C-5, Rockwell Hanford Operations, Richland, Washington.

Richmond, G. M., Fryxell, R., Neff, G. E., and Weis, P. L., 1965, "The Cordilleran Icesheet of the Northern Rocky Mountains and Related Quaternary History of the Columbia Plateau," in The Quaternary of the United States, Wright, H. E. and Frey, D. G., eds., Princeton University Press, Princeton, New Jersey, pp. 231-242.

Riddihough, R. P. and Hyndman, R. D., 1976, "Canada's Active Western Margin--the Case for Subduction," Geoscience/Canada, Vol. 3, p. 269.

Rigby, J. G. and Othberg, K., 1979, Reconnaissance Surficial Geologic Mapping of the Late Cenozoic Sediments of the Columbia Basin, Washington, Open-File Report 79-3, Washington State Department of Natural Resources, Division of Geology and Earth Resources, Olympia, Washington.

Robbins, S. L., Burt, R. J., and Gregg, D. O., 1975, Gravity and Aeromagnetic Study of Part of the Yakima River Basin, Washington, Professional Paper 726-E, U.S. Geological Survey, Washington, D.C.

Rohay, A. C., 1982, Seismic Velocity Structure of the Crust and Upper Mantle in the North Cascade Range, Washington, Ph. D. Dissertation, Department of Geology, University of Washington, Seattle, Washington.

Ross, M. E., 1978, Stratigraphy, Structure, and Petrology of the Columbia River Basalt in a Portion of the Grande Ronde-Blue Mountains Area of Oregon and Washington, RHO-SA-58, Rockwell Hanford Operations, Richland, Washington.

Rothe, G. H., 1978, "Earthquake Swarms in the Columbia River Basalts," Ph. D. Thesis, University of Washington, Addendum to Annual Technical Report 1978, Earthquake Monitoring of the Hanford Region, University of Washington, Seattle, Washington.

Routson, R. C. and Fecht, K. R., 1979, Soil (Sediment) Properties of Twelve Hanford Wells, RHO-LD-82, Rockwell Hanford Operations, Richland, Washington.

Rozen, A., 1976, Response of Rock Tunnels in Earthquake Shaking, M.S. Thesis, Massachusetts Institute of Technology, Cambridge, Massachusetts.

Russell, I. G., 1893, Geologic Reconnaissance in Central Washington, Bulletin, U.S. Geological Survey, Washington, D.C.

Sandness, G. A., Kimball, C. S., Schmierer, K. E., Lindberg, J. W., Gibson, D., Kerbs, R., Scott, B. L., and Stephan, J. G., 1981, Geologic Remote Sensing of the Columbia Plateau, PNL-3140, Pacific Northwest Laboratory, Richland, Washington.

Sass, J. H. and Lachenbruch, A. H., 1979, "Heat Flow and Conduction-Dominated Thermal Regimes," in Muffler, L. J., Assessment of Geothermal Resources of the United States - 1978, Circular 790, U.S. Geological Survey, Washington, D.C., pp. 8-11.

Savage, J. C., Lisowski, M., and Prescott, W. H., 1981, "Geodetic Strain Measurements in Washington," Journal of Geophysical Research, Vol. 86, No. 136, pp. 4929-4940.

Shannon and Wilson, 1973, Geologic Studies of Columbia River Basalt Structures and Age of Deformation, The Dalles-Umatilla Region, Washington and Oregon, Boardman Nuclear Project, Shannon and Wilson, Inc. for the Portland General Electric Company, Portland, Oregon.

Slemmons, D. B., 1979, Remote Sensing Analysis of Geologic Structures, United Engineers and Constructors, Inc., Richland, Washington.

Slemmons, D. B. and O'Malley, P., 1979, Fault and Earthquake Hazard Evaluation of Five U.S. Corps of Engineers Dams in Southeastern Washington, U.S. Army Corps of Engineers, Seattle, Washington.

Slemmons, D. B., Carver, G., and Trexler, D. T., 1977, "Remote Sensing Analysis of the 1872 Earthquake Epicentral Region," in Preliminary Safety Analysis Report, Amendment 23, Appendix 2RG, Washington Public Power Supply System, Inc., Richland, Washington.

Smith, H. W., Okazaki, R., and Knowles, C. L., 1977, "Electron Microprobe Data for Tephra Attributed to Glacier Peak, Washington," Quaternary Research, Vol. 7, No. 2, pp. 197-206.

Spry, A., 1962, "The Origin of Columnar Jointing Particularly in Basalt Flows," Geological Society of Australia Journal, Vol. 8, pp. 191-216.

Summers, K. V., Crosby, J. W., III, Robinette, M. S., Strait, S. R., and Weber, T. L., 1975, Borehole Geophysical Investigation of the Hanford Reservation, Research Report 75/15-25, College of Engineering Research, Washington State University, Pullman, Washington.

Swanson, D. A., 1967, "Yakima Basalt of the Tieton River Area, South-Central Washington," Geological Society of America Bulletin, Vol. 78, pp. 1077-1110.

Swanson, D. A., 1979, "Source Areas and Distribution of Major Units in the Columbia River Basalt Group," Geological Society of America Abstracts with Programs, Vol. 11, No. 3, p. 131.

Swanson, D. A. and Wright, T. L., 1976, "Guide to Field Trip Between Pasco And Pullman, Washington Emphasizing Stratigraphy, Vent Areas, and Intercanyon Flows of Yakima Basalt," Geological Society of America (Cordilleran Section) 72nd Annual Meeting, Field Guide No. 1, Pullman, Washington.

Swanson, D. A. and Wright. T. L., 1978, "Bedrock Geology of the Northern Columbia Plateau and Adjacaent Areas," in Baker, V. R. and Nummedal, D., eds., The Channeled Scabland: A Guide to the Geomorphology of the Columbia Basin, Washington, Planetary Geology Program, Office of Space Science, National Aeronautics and Space Administration, Washington, D.C., pp. 37-57.

Swanson, D. A., Wright, T. L., and Helz, R. T., 1975, "Linear Vent Systems and Estimated Rates of Magma Production and Eruption for the Yakima Basalt on the Columbia Plateau," American Journal of Science, Vol. 275, No. 8, pp. 877-905.

Swanson, D. A., Wright, T. L., and Zietz, I., 1976, Geologic Interpretation of an Aeromagnetic Map of West-Central Columbia Plateau, Washington and Oregon, Open-File Report 76-51, U.S. Geological Survey, Denver, Colorado.

Swanson, D. A., Wright, T. L., and Zietz, I., 1979a, Aeromagnetic Map and Geologic Interpretation of the West-Central Columbia Plateau, Washington, and Adjacent Idaho, Geophysical Investigations Map GP-917, 1:250,000, U.S. Geological Survey, Denver, Colorado.

Swanson, D. A., Anderson, J. L., Bentley, R. D., Camp, V. W., Gardner, J. N., and Wright, T. L., 1979b, Reconnaissance Geologic Map of the Columbia River Basalt Group in Eastern Washington and Northern Idaho, Open-File Report 79-1363, U.S. Geological Survey, Washington, D.C.

Swanson, D. A., Wright, T. L., Hooper, P. R., and Bentley, R. D., 1979c, Revisions in Stratigraphic Nomenclature of the Columbia River Basalt Group, Bulletin 1457-H, U.S. Geological Survey, Washington, D.C.

Swanson, D. A., Wright, T. L., Camp, V. E., Gardner, J. N., Helz, R. T., Price, S. M., Reidel, S. P., and Ross, M. E., 1980, Reconnaissance Geologic Map of the Columbia River Basalt Group, Pullman and Walla Walla Quadrangles, Southeast Washington and Adjacent Idaho, Miscellaneous Investigations Series Map I-1139, U.S. Geological Survey, Denver, Colorado.

Swanson, D. A., Anderson, J. L., Camp, V. E., Hooper, P. R., Taubeneck, W. H., and Wright, T. L., 1981, Reconnaissance Geologic Map of the Columbia River Basalt Group, Northern Oregon and Western Idaho, Open-File Report 81-0797, U.S. Geological Survey, Washington, D.C.

Tabor, R. W. and Crowder, D. F., 1969, Ore Batholiths and Volcanoes Intrusion and Eruption of Late Cenozoic Magmas in the Glacier Peak Area, North Cascades, Washington, Professional Paper 604, U.S. Geological Survey, Washington, D.C.

Tabor, R. W., Waitt, R. B., Frizzell, V. A., Jr., Swanson, D. A., and Byerly, G. R., 1977, Preliminary Map of the Wenatchee 1:100,000 Quadrangle, Washington, Open-File Report 77-531, U.S. Geological Survey, Washington, D.C.

Tallman, A. M., Fecht, K. R., Marratt, M. C., and Last, G. V., 1979, Geology of the Separations Areas, Hanford Site, South-Central Washington, RHO-ST-23, Rockwell Hanford Operations, Richland, Washington.

Tallman, A. M., Lillie, J. T., and Fecht, K. R., 1981, "Suprabasalt Sediments of the Cold Creek Syncline Area," in Myers, C. W., and Price, S. M., eds., Subsurface Geology of the Cold Creek Syncline, RHO-BWI-ST-14, Rockwell Hanford Operations, Richland, Washington, July 1981.

Taubeneck, W. H., 1970, "Dikes of Columbia River Basalt in North-Eastern Oregon, Western Idaho, and Southeastern Washington," in Proceedings of the Second Columbia River Basalt Symposium, Cheney, Washington, March 1969, Gilmour, E. H. and Stradling, D., eds., Eastern Washington State College Press, Cheney, Washington, pp. 73-96.

Thayer, T. P. and Brown, C. E., 1966, "Columbia River Group," in Changes in Stratigraphic Nomenclature by the U.S. Geological Survey 1965, Bulletin 1,244-A, U.S. Geological Survey, Washington, D.C., pp. A23-A25.

Thiruvathukal, J. V., 1968, Regional Gravity of Oregon, Ph. D. Dissertation, Oregon State University, Corvallis, Oregon.

Tillson, D. D., 1970, Analysis of Crustal Changes in the Columbia Plateau Area From Contemporary Triangulation and Leveling Measurements, BNWL-CC-2174, Battelle, Pacific Northwest Laboratories, Richland, Washington.

Tomkeieff, S. I., 1940, "Basalt Lavas of the Giants Causeway," Bulletin of Vulcanology, Vol. 2, pp. 89-146.

USGS, 1974, Aeromagnetic Map of Parts of the Okanogan, Sandpoint, Ritzville, and Spokane 1° by 2° Quadrangles, Northeastern Washington, Open-File Report 74-1105, U.S. Geological Survey, Denver, Colorado.

USGS, 1978, Aeromagnetic Map of Idaho, Map GP-919, U.S. Geological Survey, Denver, Colorado.

USGS, 1979, Aeromagnetic Map of Pendleton and Vicinity, Oregon and Washington, Open-File Report 79-278, U.S. Geological Survey, Denver, Colorado.

UWGP, 1977, Annual Report on Earthquake Monitoring of Eastern Washington, Geophysics Program, University of Washington, Seattle, Washington.

UWGP, 1978, Annual Report on Earthquake Monitoring of Eastern Washington, Geophysics Program, University of Washington, Seattle, Washington.

UWGP, 1979, Annual Report on Earthquake Monitoring of Eastern Washington, Geophysics Program, University of Washington, Seattle, Washington.

UWGP, 1980, Annual Report on Earthquake Monitoring of Eastern Washington, Geophysics Program, University of Washington, Seattle, Washington.

UWGP, 1981, Annual Report on Earthquake Monitoring of Eastern Washington, Geophysics Program, University of Washington, Seattle, Washington.

Van Alstine, D. R. and Gillett, S. L., 1981, Magnetostratigraphy of the Columbia River Basalt, Pasco Basin and Vicinity, Washington, RHO-BWI-C-110, Sierra Geophysics for Rockwell Hanford Operations, Richland, Washington.

Waitt, R. B., 1979, Late Cenozoic Deposits, Landforms, Stratigraphy, and Tectonism in Kittitas Valley, Washington, Professional Paper 1127, U.S. Geological Survey, Washington, D.C.

Walker, G. W., 1977, Geologic Map of Oregon East of the 121st Meridian, U.S. Geological Survey, Denver, Colorado.

Walker, G. W., Dalrymple, G. B., and Lanphere, M. A., 1974, Index to Potassium-Argon Ages of Cenozoic Volcanic Rocks of Oregon, Field Study Map No. MF-569, U.S. Geological Survey, Denver, Colorado.

Walters, K. L. and Grolier, M. J., 1960, Geology and Groundwater Resources of the Columbia Basin Project Area, Washington, Water-Supply Bulletin 8, Washington State Division of Water Resources, Olympia, Washington.

Waters, A. C., 1961, "Stratigraphic and Lithologic Variations in the Columbia River Basalt," American Journal of Science, Vol. 259, pp. 581-611.

Waters, A. C., 1962, Basalt Magma Types and Their Tectonic Associations: Pacific Northwest of the United States, Monograph 6, American Geophysical Union, pp. 158-170.

Waters, A. C., 1973, "Columbia River Gorge - Basalt Stratigraphy, Ancient Lava Dams, and Landslide Dams," in Geologic Field Trips in Northern Oregon and Southern Washington, Beaulieu, J. D., Chairman, Oregon State Department of Geology and Mineral Industries Bulletin 77, Portland, Oregon, p. 133-162.

Watkins, N. D. and Baksi, A. K., 1974, "Magnetostratigraphy and Oroclinal Folding of the Columbia River, Steens and Owyhee Basalts in Oregon, Washington and Idaho," American Journal of Science, Vol. 274, p. 148.

WCC, 1978, Microearthquake Studies, 1872 Earthquake Studies, WPPSS Nuclear Project No's 1 and 4, Woodward-Clyde Consultants for Washington Public Power Supply System, Inc., Richland, Washington.

WCC, 1979, Factors Influencing Seismic Exposure of the Southeast Washington Region, Woodward-Clyde Consultants for Washington Public Power Supply System, Inc., Richland, Washington.

WCC, 1980a, Recent Seismicity of the Hanford Region, Woodward-Clyde Consultants for Washington Public Power Supply System, Inc., Richland, Washington.

WCC, 1980b, Seismological Review of the July 16, 1936 Milton-Freewater Earthquake Source Region, Woodward-Clyde Consultants for Washington Public Power Supply System, Inc., Richland, Washington.

WCC, 1980c, Assessment of the Effects of Surficial Geologic Processes in the Pasco Basin, Final Report, RHO-BW-CR-129 P, Woodward-Clyde Consultants for Rockwell Hanford Operations, Richland, Washington.

WCC, 1981a, Analysis of Columbia Plateau Seismicity, Woodward-Clyde Consultants for Washington Public Power Supply System, Inc., Richland, Washington.

WCC, 1981b, Task D5, Toppenish Ridge Study, Woodward-Clyde Consultants for Washington Public Power Supply System, Inc., Richland, Washington.

WCC, 1981c, Task D3, Quaternary Sediments Study of the Pasco Basin and Adjacent Areas, Woodward-Clyde Consultants for Washington Public Power Supply System, Inc., Richland, Washington.

Wells, F. G. and Peck, D. L., 1961, Geologic Map of Oregon West of 121st Meridian, Miscellaneous Investigations Map I-325, U.S. Geological Survey, Denver, Colorado.

Westgate, J. A. and Evans, M. E., 1978, "Compositional Variability of Glacier Peak Tephra and its Stratigraphic Significance," Canadian Journal of Earth Sciences, Vol. 15, No. 10, pp. 1554-1567.

Weston, 1977, "Evaluation of Microearthquake Activity in Eastern Washington," in Preliminary Safety Analysis Report, Amendment 23, Appendix 2RJ, Weston Geophysical Research for Washington Public Power Supply System, Inc., Richland, Washington.

Weston, 1978a, Ground Geophysical Studies, Columbia Plateau and Adjacent Cascade Mountains, Weston Geophysical Research for Washington Public Power Supply System, Inc., Richland, Washington.

Weston, 1978b, Magnetic Modeling, Columbia Plateau Area, Weston Geophysical Research for Washington Public Power Supply System, Inc., Richland, Washington.

Weston, 1978c Qualitative Aeromagnetic Evaluation of Structures in the Columbia Plateau and Adjacent Cascade Mountain Area, Weston Geophysical Research for Washington Public Power Supply System, Inc., Richland, Washington.

Weston, 1979, Magnetic Modeling in the Vicinity of Walla Walla, Washington and Elgin, Oregon, Weston Geophysical Research for Washington Public Power Supply System, Inc., Richland, Washington.

Weston, 1981, Evaluation of Explosion Data as a Source of Local Crustal Information within the Central Columbia Plateau, Weston Geophysical Research for Washington Public Power Supply System, Inc., Richland, Washington.

Wilcox, R. E., 1965, "Volcanic-Ash Chronology," in The Quaternary of the United States, Wright, H. E. and Frey, D. G., eds., Princeton University Press, Princeton, New Jersey, pp. 807-816.

Williams, J. F., 1961, Well Report, Basalt Explorer Number 1, N/2 NE/4 NW/4 SW/4 Section 10, Township 21 North, Range 31 East, Lincoln County, Washington, Development Associates, Inc., Spokane, Washington.

Wood, B. J. and Long, P. E., 1981, "Structures, Textures and Cooling Histories of Columbia River Basalts," Geological Society of America Abstracts with Programs, Vol. 13, No. 7, p. 584.

WPPSS, 1974, Preliminary Safety Analysis Report, Amendment 9, Washington Public Power Supply System, Inc., Richland, Washington.

WPPSS, 1977, Preliminary Safety Analysis Report, Amendment 23, Vol. 1 and 2, Washington Public Power Supply System, Inc., Richland, Washington.

9 2 1 2 4 9 5 0 8 1 9

WPPSS, 1980, Final Safety Analysis Report, Amendment 10, Washington Public Power Supply System, Inc., Richland, Washington.

WPPSS, 1981, Final Safety Analysis Report, Washington Public Power Supply System, Inc., Richland, Washington.

Zietz, I., Hearn, B. C., Jr., Higgins, M. W., Robinson, G. D., and Swanson, D.A., 1971, "Interpretation of an Aeromagnetic Strip Across the Northwestern United States," Geological Society America of Bulletin, Vol. 82, No. 12, p. 3347-3372.

Zoback, M. L. and Zoback, M., 1980, "State of Stress in the Conterminous United States," Journal of Geophysical Research, Vol. 85, pp. 6113-6156.

9212495082 0

THIS PAGE INTENTIONALLY
LEFT BLANK

9 2 1 2 4 9 5 0 8 2 1

4. GEOENGINEERING

The nature of geologic materials is such that the design process for subsurface structures is a continuing one, with more and better quality data, more experience, and more confidence being gained as time progresses. Initial data generally come from projects of a similar nature. Additional data and experience are gained from laboratory tests on samples obtained from exploratory boreholes. Eventually, direct access to the site is needed for site-specific bench-scale and field testing and verification of conditions anticipated. New information that may influence design and performance assessment is developed and incorporated on a continuous basis during project construction and operation.

The introduction of nuclear waste into an underground geologic structure adds three complicating factors to the analysis discussed above. First, the addition of a thermal load to the system is unique, and there is no parallel or related project from which to gain experience. Second, the time frame of concern is now measured in thousands of years as opposed to the shorter period of 100 years or less for typical geotechnical projects. Third, the need to understand and predict performance in advance of construction and operation for licensing purposes requires that more data and analysis be available in the early stages of the project than for nonnuclear projects.

The basalt program has progressed from laboratory testing of cores to field tests in an operating facility including tunnels to access a near-surface basalt flow. The next step is to extend this work to testing from an exploratory shaft at candidate repository depths. Initially, the Umtanum flow of the Grande Ronde Basalt was considered the primary candidate horizon and the testing program was designed to emphasize the acquisition of data from this flow. The program has since been modified to include the middle Sentinel Bluffs flow as a candidate horizon. Testing of samples from this flow is in progress and very little data are currently available.

There is a limit to the applicability of the near-surface data for specific repository design parameters because of site-specific differences such as stress levels. The near surface, however, provides a useful field laboratory for developing instrumentation and techniques in advance of testing at depth and for obtaining much valuable data for preliminary assessment.

The geoengineering work discussed in this chapter relates not only to availability of the geotechnical data, but also to the availability and adequacy of techniques of measurement and analysis. A detailed evaluation of the limitations and the sources of potential error intrinsic to these techniques will be reported in separate Basalt Waste Isolation Project publications on each phase of testing. The plans for further geoengineering studies are discussed in Chapter 14 of this report.

9212495082 2

THIS PAGE INTENTIONALLY
LEFT BLANK

9 2 1 2 4 9 5 0 8 2 3

4.1 MECHANICAL PROPERTIES OF ROCK UNITS - CONTINUA

4.1.1 General

Laboratory testing of rock core samples is an integral part of the investigation for designing large structures in rock. Tests listed in this section provide characteristics of the rock fabric that are both directly and indirectly applicable to the performance of the structure during excavation and operation. Although discontinuities are present in most rock masses and can have a very significant influence on rock behavior, a laboratory study of intact rock properties can contribute to the understanding of observed in situ rock-mass behavior and can provide an initial data base for modeling studies that are carried out in conjunction with the mechanical property testing and field tests.

Strength properties are necessary to determine the stability of localized zones of high stress and the strength of intact pillars. Modulus of rupture and deformation modulus values can be related to the deformation and stability of the roof and walls of underground openings. Uniaxial compressive strength, point-load strength, and hardness have been related to drillability and ease of excavation by blasting or tunnel boring machine methods. Even simple characteristics such as density and porosity can be used to help explain discrepancies in strength or elastic modulus test results in different regions of the structure.

A clear understanding of the mechanical and thermal properties of the host rock is essential to the design of a nuclear waste repository. A comprehensive program of testing was undertaken to provide as much design information as possible and to generate a means of relating:

- Laboratory properties to in situ characteristics of basalt at both ambient and elevated temperatures and pressures
- Comparative characterizations of the Umtanum and middle Sentinel Bluffs flows as well as other Hanford basalt flows.

4.1.2 Test Methods and Results

The material properties used in the conceptual design (see Chapter 10) of a nuclear waste repository in basalt were based on laboratory properties selected from a literature survey. The survey (Agapito et al., 1977) was conducted prior to the initiation of Basalt Waste Isolation Project laboratory testing program. Estimated physical and mechanical property data selected from the survey are presented in Table 4-1.

9 2 1 2 4 9 5 0 8 2 4

TABLE 4-1. Mechanical Characteristics of Basalts Used for Conceptual Design (BWIP and KE/PB, 1982).

Property	Estimated value
Density, g/cm^3 (lb/ft^3)	2.8 (175)
Deformation modulus, MPa (lb/in^2)	67,800 (9,830,000)
Poisson's ratio	0.26
Cohesion, MPa (lb/in^2)	32 (4,640)
Uniaxial compressive strength, MPa (lb/in^2)	200 (29,000)
Angle of internal friction, deg	55
Tensile strength, MPa (lb/in^2)	14 (2,030)

Laboratory tests have since been conducted on core from the Hanford Site basalts, primarily from the Umtanum flow and the middle Sentinel Bluffs flow of the Grande Ronde Basalt and the Pomona Member of the Saddle Mountains Basalt (CSM, 1978; Duvall et al., 1978; Erikson and Krupka, 1980; FSI, 1980a; 1980b; 1980c; 1981a; Martinez-Baez and Amick, 1978; Miller and Bishop, 1979; Miller, 1979a; 1979b). The results of these investigations are summarized (Schmidt et al., 1980; FSI, 1981a) in Table 4-2 (a, b, and c). The data presented in this table are a compilation of the results for intact samples from the aforementioned references and on-going studies.

The data presented in Table 4-2 are representative of the the results acquired from the three major structural units found in each flow. In general, the basalt intraflow structures consist of upper and lower zones of relatively massive, irregular columns, termed colonnade zones, which surround a zone consisting of relatively small, regular columns termed the entablature zone. The interflow includes the flow top and contact zones above and below the colonnade zones.

The Grande Ronde Basalt consists of many flows (Swanson and Wright, 1978), including the candidate repository horizons:

- The Umtanum flow
- The middle Sentinel Bluffs flow.

9 2 1 2 4 9 5 0 8 2 5

TABLE 4-2(a). Physical and Mechanical Properties of Hanford Site Basalt Entablature Samples.

Property	Unit	Umtanum flow	Number of samples tested	Middle Sentinel Bluffs flow	Number of samples tested	Pomona Member of Saddle Mountains Basalt	Number of samples tested
Bulk density	g/cm^3 (lb/ft^3)	2.77±0.06 (173±4)	248	2.84±0.03 (177±2)	23	2.85±0.03 (178±2)	327
Grain density	g/cm^3 (lb/ft^3)	2.90±0.08 (181±5)	31	2.90±0.03 (181±2)	4	3.00±0.08 (187±5)	246
Apparent porosity	%	1.1±0.4	42	1.1±0.4	23	0.7±0.4	43
Total porosity	%	3.6±2.4	31	1.8±0.4	3	4.8±2.0	246
Deformation modulus (static)	MPa (E+06 lb/in^2)	65,500±26,600[b] (9.50±3.86)	13	75,000±5,000 (10.9±0.7)	7	85,600±9,400[b] (12.4±1.36)	29
Poisson's ratio (static)	Unitless	0.26±0.05[b]	9	0.27±0.02	7	0.27±0.03[b]	29
Deformation modulus (dynamic)	MPa (E+06 lb/in^2)	80,000±7,700 (11.6±1.12)	32	74,000±6,000 (10.7±0.9)	23	82,500±4,200 (12.0±0.609)	164
Poisson's ratio (dynamic)	Unitless	0.24±0.04	32	0.24±0.06	23	0.26±0.02	164
Compressional wave velocity	m/s (ft/s)	5,860±310 (19,200±1,000)	66	5,500±300 (18,000±980)	23	5,930±160 (19,500±500)	164
Shear wave velocity	m/s (ft/s)	3,420±180 (11,200±600)	48	3,300±200 (10,800±660)	23	3,390±90 (11,100±300)	164
Brazilian tensile strength	MPa (lb/in^2)	11.9±6.9 (1,730±1,000)	15	13.6±3.8 (1,970±550)	10	19.4±3.8 (2,810±550)	38
Modulus of rupture	MPa (lb/in^2)	a		42.1 (6,100)	1	a	
Uniaxial compressive strength	MPa (lb/in^2)	212±106 (30,700±15,400)	9	255±21 (37,000±3,000)	7	356±42 (51,600±6,100)	20
Angle of internal friction	deg	44	17	a		53	38
Cohesion (inherent shear strength)	MPa (lb/in^2)	45.0 (6,530)	17	a		59.0 (8.560)	38

[a]Measurements not made or not available.

[b]Average value includes all uniaxial and triaxial test results.

TABLE 4-2(b). Physical and Mechanical Properties of Hanford Site Basalt Colonnade Samples.

Property	Unit	Umtanum flow	Number of samples tested	Middle Sentinel Bluffs flow	Number of samples tested	Pomona Member of Saddle Mountains Basalt	Number of samples tested
Bulk density	g/cm^3 (lb/ft^3)	2.71±0.11 (169.8±6.9)	91	2.85±0.03 (178±2)	10	2.832±0.04 (176.9±2.5)	34
Grain density	g/cm^3 (lb/ft^3)	a		2.92±0.07 (182±4)	3	a	
Apparent porosity	%	a		1.0±0.8	9	3.007±0.76	4
Total porosity	%	a		2.4±1.2	3	7.83±1.04	4
Deformation modulus (static)	MPa (E+06 lb/in^2)	47,803±20,800 (6.93±3.02)	14	80,000±6,000 (11.6±0.9)	4	72,400±10,100 (10.50±1.46)	6
Poisson's ratio (static)	Unitless	0.24±0.06[b]	2	0.26±0.07	3	0.25±0.01	6
Deformation modulus (dynamic)	MPa (E+06 lb/in^2)	62,500± a (9.06± a)	45	77,000±7,000 (11.2±1.0)	8	a	
Poisson's ratio (dynamic)	Unitless	0.176± a		0.27±0.19	8	a	
Compressional wave velocity	m/s (ft/s)	4,986±1,017 (16,400±3,345)	45	5,800±240 (19,300±790)	8	a	
Shear wave velocity	m/s (ft/s)	3,131±754 (10,300±2,480)	46	3,300±160 (10,800±525)	8	a	
Brazilian tensile strength	MPa (lb/in^2)	8.34±3.7 (1,210±540)	3	13.6±2.2 (1,970±320)	2	17.56±3.0 (2,550±440)	6
Modulus of rupture	MPa (lb/in^2)	20±5 (2,900±700)	3	39.4±4.5 (5,700±65)	2	415±5.03 (6,000±700)	6
Uniaxial compressive strength	MPa (lb/in^2)	230±111 (33,300±16,100)	4	285±32 (41,000±4,600)	4	290±13.72 (42,000±2,000)	6
Angle of internal friction	deg	a		a		a	
Cohesion (inherent shear strength)	MPa (lb/in^2)	a		a		a	

[a]Measurements not made or not available.

[b]Average value includes all uniaxial and triaxial test results.

TABLE 4-2(c). Physical and Mechanical Properties of Hanford Site Basalt Interflow Zone Samples.

Property	Unit	Umtanum flow	Number of samples tested	Middle Sentinel Bluffs flow	Number of samples tested	Pomona Member of Saddle Mountains Basalt	Number of samples tested
Bulk density	g/cm^3 (lb/ft^3)	2.412±0.08 (150.7±5.0)	101	2.29±0.10 (143±6)	14	a	
Grain density	g/cm^3 (lb/ft^3)	a		2.88±0.01 (180±37)	3	a	
Apparent porosity	%	a		12.6±2.4	14	a	
Total porosity	%	a		23.0±5.0	3	a	
Deformation modulus (static)	MPa (E+06 lb/in^2)	24,500±19,400 (3.55±2.81)	2	a		a	
Poisson's ratio (static)	Unitless	0.247±0.5[b]	19	a		a	
Deformation modulus (dynamic)	MPa (E+06 lb/in^2)	38,000± a (5.51± a)	77	54,000±4,500 (7.8±0.7)	2	a	
Poisson's ratio (dynamic)	Unitless	0.168± a	77	0.24±0.01	2	a	
Compressional wave velocity	m/s (ft/s)	4,110±998 (13,484±3,274)	77	5,200±94 (17,000±300)	2	a	
Shear wave velocity	m/s (ft/s)	2,595±567 (8,514±1,860)	78	3,000±89 (9,800±290)	2	a	
Brazilian tensile strength	MPa (lb/in^2)	a		8.0±2.0 (1,160±300)	9	17.5 (2,540)	1
Modulus of rupture	MPa (lb/in^2)	a		a		a	
Uniaxial compressive strength	MPa (lb/in^2)	29.6±4.0 (4,290±580)	2	70±20 (10,000±3,000)	5	a	
Angle of internal friction	deg	a		a		a	
Cohesion (inherent shear strength)	MPa (lb/in2)	a		a		a	

[a]Measurements not made or not available.

[b]Average value includes all uniaxial and triaxial test results.

The data presented for these basalts represent a compendium of results from numerous boreholes located on the Hanford Site. For comparative purposes, data for the Pomona flow have been included in Table 4-2, since the Pomona was extensively characterized as the host rock for the Near-Surface Test Facility. Pomona samples were obtained from shallow boreholes in the floor of one of these tunnels. A site map showing the location of Gable Mountain and boreholes in the Hanford area is presented in Chapter 5.

The physical and mechanical property tests conducted on basalt core samples are listed in Table 4-3. As indicated, these tests were conducted by following either American Society for Testing and Materials test procedures, those procedures established in current literature, or those procedures specifically adapted for the current testing program. Further details of the testing techniques and experimental apparatus are fully described in the references (ASTM, 1977; 1976a; 1974; 1969; 1971; 1972; Lama and Vutukuri, 1978; FSI; 1981b).

TABLE 4-3. Physical and Mechanical Property Tests.

Test	Procedure
Physical Properties	
Bulk density	ASTM-C-97 (ASTM, 1977)
Grain density	Lama and Vutukuri (1978)
Apparent porosity	FSI (1981b)
Mechanical Properties	
Uniaxial compressive strength	ASTM-D-2938 (ASTM, 1971)
Triaxial compressive strength	ASTM-D-2664 (ASTM, 1974)
Brazilian tensile strength	ASTM-in draft
Modulus of rupture (bending strength)	ASTM-C-99 (ASTM, 1976a)
Static elastic properties	ASTM-D-3148 (ASTM, 1972)
Dynamic elastic properties	ASTM-D-2845 (ASTM, 1969)

9 2 1 2 4 9 5 0 8 2 9

4.1.3 Discussion of Results

A comparison of the basalt characteristics used in the repository conceptual design (see Table 4-1) with the laboratory results listed for the Umtanum flow in Table 4-2 shows agreement within 15 percent, except for the shear strength parameters (i.e., cohesion and angle of internal friction, ϕ). The laboratory-determined ϕ value, an important parameter indicating how the shear strength of a rock increases with confinement, was found to be 20 percent lower than estimated earlier. On the other hand, the experimentally determined cohesion was 40% higher than estimated. Of significance is the considerable scatter of laboratory data for compressive strength, both uniaxial and triaxial. Very high standard deviations observed for uniaxial strengths diminished only slightly with the addition of confining pressure. Sample identification, preparation, and testing techniques contributed significantly to this scatter. Such a wide variation of test results was also observed for porosity and tensile strength values.

Tests completed so far indicate that the uniaxial compressive strength of intact (unfractured) Umtanum entablature samples decreases as temperature increases. For intact samples at room temperature, the compressive strength increases with confining pressure, as expected and predicted by the Mohr-Coulomb failure criterion (Fig. 4-1). Firm conclusions about the magnitude of strength reduction at higher temperatures must be withheld at this time due to the small number of heated samples tested (five in uniaxial compression; one in triaxial compression) and the large standard deviations observed (39 to 50 percent of the mean value). Furthermore, there is, in some cases, insufficient information from the testing contractor to determine with absolute certainty that the samples were intact and unfractured. The lack of sample availability was the result of a large number of near-vertical joints, core discing, handling disturbances, program constraints, and other variables. It should also be noted that the remaining undisced portions used to obtain the data base in Table 4-2 may be somewhat stronger than those sections that experienced discing.

A laboratory testing program has recently been initiated by Rockwell Hanford Operations to provide additional information on the strength of the Umtanum and middle Sentinel Bluffs flows. Preliminary results from uniaxial compression tests on three samples of Umtanum entablature show substantially higher values than have been previously reported. Expanded and finalized results will be included in future reports.

The effects of elevated temperature and confining pressure on the static moduli indicate that the deformation modulus is relatively constant up to 300°C and 0.69 megapascal (100 pounds per square inch) confining stress (Fig. 4-2). However, except for work conducted on samples of the Pomona Member, determinations on other basalt samples such as the Umtanum flow have been limited in number, as indicated in Figure 4-2. Poisson's ratio for Umtanum samples also remained fairly constant with temperature.

9 2 1 2 4 9 5 0 8 3 0

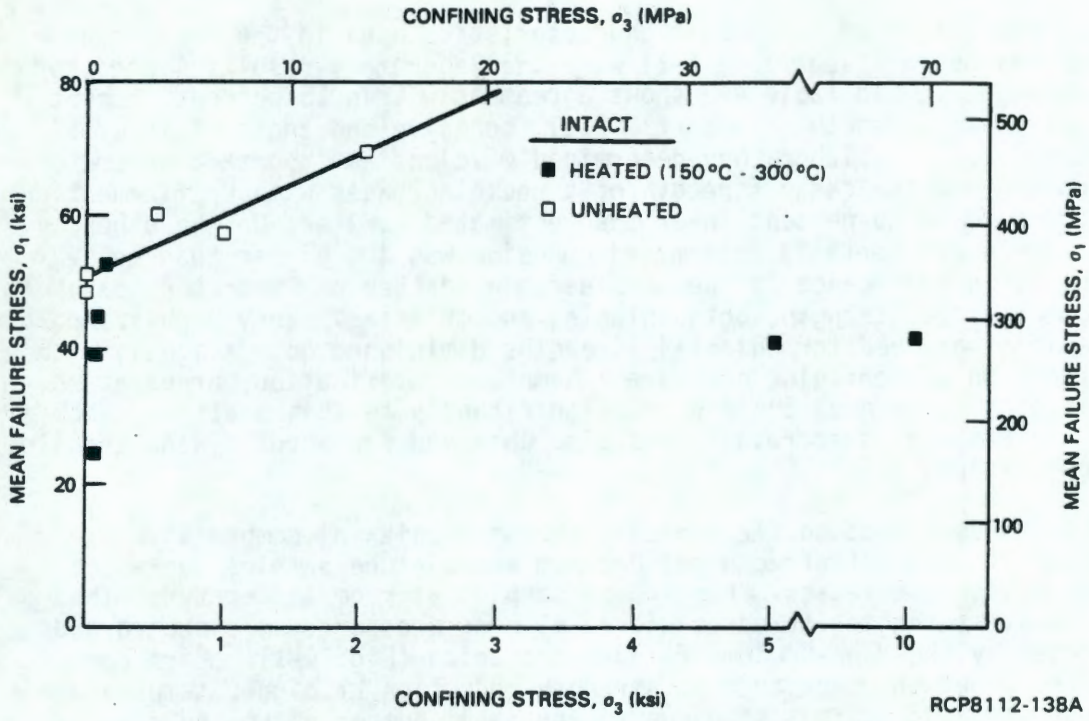

FIGURE 4-1. Strength Versus Confining Stress for Pomona Basalt (FSI, 1980c).

A comparison of the characteristics of the entablature zone of the Umtanum flow with those of the Pomona flow indicates that there are recognizable differences between basalt flows within the same stratigraphic section. The properties of the Pomona flow show it to be a denser and stronger rock than the Umtanum flow. A comparison between the characteristics of the three flow units (colonnade, entablature, and interflow) indicates that the physical and mechanical property values are generally similar between the entablature and colonnade within a respective flow, while the results determined from interflow samples indicate a significantly less competent material.

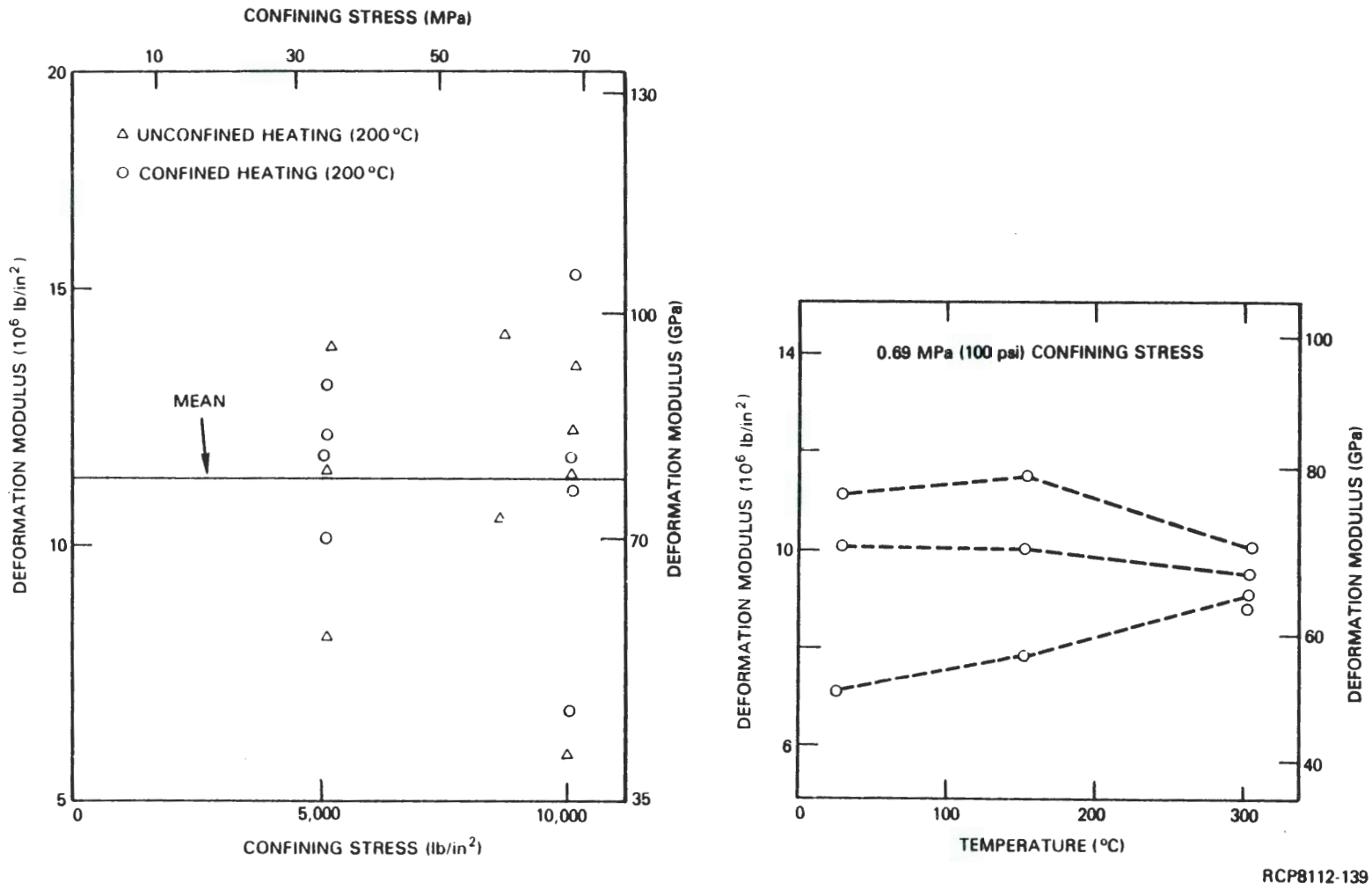

FIGURE 4-2. Effects of Confining Stress and Temperature on the Deformation Modulus for Umtanum Basalt Specimens (FSI, 1980c; 1981a).

4.1.4 Summary

A review of the available laboratory data on the mechanical properties of basalt as presented in this section leads to the following conclusions:

(1) Basalt is a strong, brittle rock that may exhibit substantial variation in mechanical properties within a particular flow zone.

(2) Recognizable differences exist between physical and mechanical properties of the same zone of different flows (e.g., Pomona entablature versus Umtanum entablature). Little difference in those properties exists between the entablature and the colonnade zone of a single flow. However, the interflow zone is much less competent.

(3) Preliminary indications are that some decrease in compressive strength, but little change in deformation characteristics, occurs as temperature is increased. These observations must be considered tentative in view of the very small sample population. Because of the thermal loading that will be imposed on the rock during operation of the repository, it is of critical importance to clearly assess the effect of temperature on rock properties.

(4) Physical and mechanical property data are currently being obtained for one of the candidate horizons, the middle Sentinel Bluffs flow. Additional strength tests on samples from the other candidate horizon, the Umtanum flow, are needed to gain confidence in the data base. Testing of intact samples from both candidate horizons is in progress.

9 2 1 2 4 9 5 0 8 3 3

4.2 MECHANICAL PROPERTIES OF ROCK UNITS - LARGE SCALE

4.2.1 General

The comprehensive design of large structures in rock requires knowledge of the engineering properties and behavior of the rock on the laboratory, large, and in situ scales. The direct and indirect application of laboratory test data has been reviewed in Section 4.1. Large-scale tests to obtain behavioral characteristics of rock on a scale equivalent to the size of the proposed structure are even more critical, and should govern design considerations. At such a scale it is the network of discontinuities encompassing the intact rock matrix that controls the rock-mass response, not the rock fabric itself. The physical characteristics of the discontinuities (joints, fractures, bedding and foliation planes, shear zones, etc.) and their orientation and spacing all contribute to the manner in which the rock mass will perform during the construction and operation of the repository.

The parameters that describe the mechanical response of the rock mass are:

- Strength - specifically the tensile strength, T_0, and values for the cohesion, τ_0, and angle of internal friction, ϕ, which are used to describe the shear strength through empirical expressions such as the Mohr-Coulomb failure equation:

  Limiting shear stress, τ, = $\tau_0 + \sigma \tan\phi$

  where σ = compressive stress normal to plane of failure.

- Deformability - as represented by the modulus of deformation, E, and Poisson's ratio, ν.

The strength parameters are necessary to determine whether stress conditions introduced by excavation and operation of the repository will cause instability in the rock mass, which could reduce its ability to isolate the waste materials. Difficulty in obtaining these parameters on a large scale arises from the need for very large-capacity load-application devices and complicated and expensive specimen-preparation measures. Large-scale strength tests have not yet been conducted in this investigation.

Deformation parameters are needed to predict how the rock surrounding the repository tunnels and storage boreholes will deform following excavation and waste emplacement. Excessive deformation could result in damage to waste package, isolation, and support systems and should therefore be considered in the design process to establish that the magnitude of the movements can be controlled within acceptable levels.

The large-scale tests conducted to evaluate methods to obtain the strength and deformability parameters of jointed basalt are described below. These tests were conducted in Pomona basalt at the Near-Surface

9 2 1 2 4 9 5 0 8 3 4

Test Facility. Although the mechanical strength of the Pomona flow is somewhat higher than that of the candidate repository horizons, these measurements allow the development of testing and analysis techniques to be used at depth and the data generated may be useful in guiding the selection of the parameter value used in the design process up to the point when access is available to the repository horizon.

4.2.2 Borehole Jacking Tests

Tests available to determine the modulus of elasticity of rock masses on a large scale are, in order of increasing size, borehole jacking, flat jack and plate bearing, pressure chamber, tunnel relaxation, and field seismic tests. The tests selected were conducted in the shallow Pomona flow at the Near-Surface Test Facility to obtain data for use in predictive modeling, to gain experience in the use of the techniques in jointed basalt, and to perfect the use and interpretation of the tests prior to their application at depth. As a result, some data were obtained that can be used in preliminary design and assessment of repository performance. These tests included Goodman jack, modified Goodman jack (jack-fracturing), and flat jack tests.

The Goodman jack applies radial stresses to opposite walls of a borehole through semicircular steel platens approximately 20 centimeters (8 inches) in length. Radial displacement of the borehole wall is measured with linearvariable differential transducers mounted on the jack as pressure is applied hydraulically. Deformation-modulus values thus obtained are then corrected by the method of Heuzé and Salem (1976) to account for the effect of bending of the steel platens. The effect of borehole/platen radius mismatch could not be corrected for by the usual method (Hustrulid, 1976) because most boreholes were slightly undersize.

A total of 75 Goodman-jack tests were conducted in six boreholes at depths ranging from 1.5 to 7.6 meters (5 to 25 feet) in the walls or floor of the Near-Surface Test Facility tunnel and with varying platen orientations. The results are tabulated in Table 4-4.

The stress-strain behavior showed upward concavity below 21 megapascals (3,000 pounds per square inch) of jacking pressure, with accordingly lower modulus values in that region. This inelastic behavior is presumably related to joint closure, platen seating and/or crushing of rock asperities at the rock/platen interface during initial stages of pressurization. It should also be noted that modulus values below 3 meters (10 feet) of depth are significantly higher than those above that depth, a possible indication of deeper excavation-induced disturbance than could be discerned visually (approximately 1.5 meters (5 feet) were disturbed as determined by core inspection).

The effect of platen orientation is not entirely clear. Modulus values seemed to be highest in a direction parallel to the Near-Surface Test Facility (and therefore to the Gable Mountain anticline) axis, but only for the 1.5- to 4.5-meter (5- to 15-foot) depths.

9 2 1 2 4 9 5 0 8 3 5

TABLE 4-4. Goodman Jack Test: Modulus Values in the Entablature Zone of the Pomona Flow at the Near-Surface Test Facility (Shuri et al., 1980).

Borehole orientation	Depth, m (ft)	Pressure range, MPa (lb/in^2)	Average modulus, GPa (lb/in^2 E+06)	Range, GPa (lb/in^2 E+06)
Horizontal	1.5 - 13.7 (5 - 45)	>20.7 (3,000)	18.75±1.87 (2.72±0.27)	6.0 - 60.6 (0.87 - 8.79)
	1.5 - 13.7 (5 - 45)	6.9 - 20.7 (1,000 - 3,000)	8.55±1.24 (1.24±0.18)	3.45 - 19.79 (0.50 - 2.87)
	1.5 - 13.7 (5 - 45)	<6.9 (1,000)	2.55±0.41 (0.37±0.06)	0.97 - 6.83 (0.14 - 0.99)
Vertical	1.5 - 3 (5 - 10)	>20.7 (3,000)	6.9±0.69 (1.0±0.1)	3.65 - 13.93 (0.53 - 2.02)
	6.1 - 7.6 (20 - 25)	>20.7 (3,000)	13.1±1.93 (1.9±0.2)	5.72 - 40.2 (0.83 - 5.83)
	1.5 - 7.6 (5 - 25)	<20.7 (3,000)	0.62±0.12 (0.09±0.017)	0.19 - 2.14 (0.028 - 0.31)

Note: All tests conducted at the ambient rock mass temperature.

An additional 50 tests were conducted by the modified Goodman jack (jack-fracturing) method, primarily in the colonnade zone of the Pomona flow at the Near-Surface Test Facility, using vertical boreholes in the floor of the tunnel. Test depths ranged from 2.4 to 9.1 meters (8 to 30 feet) and measurements were made at stress levels from 6.9 to 41 megapascals (1,000 to 5,900 pounds per square inch). The results are given in Figure 4-3. The modified Goodman jack tests were run as a supplement to the other borehole jacking data with the intent of evaluating the modified jack method and confirming results from the conventional technique.

The modified test procedure employs a Goodman borehole jack with shorter platens and is used to cause fracturing in the borehole wall. To ensure that fracture would take place in the intact rock, a borescope was used to examine the condition of the borehole and select an unjointed location for platen placement. Modulus values may therefore tend to be higher than if random platen locations were used. Some variation in modulus values with orientation is shown in Figure 4-3, but numerical differences are not significant. The colonnade could then be described as isotropic in the horizontal plane perpendicular to the columns.

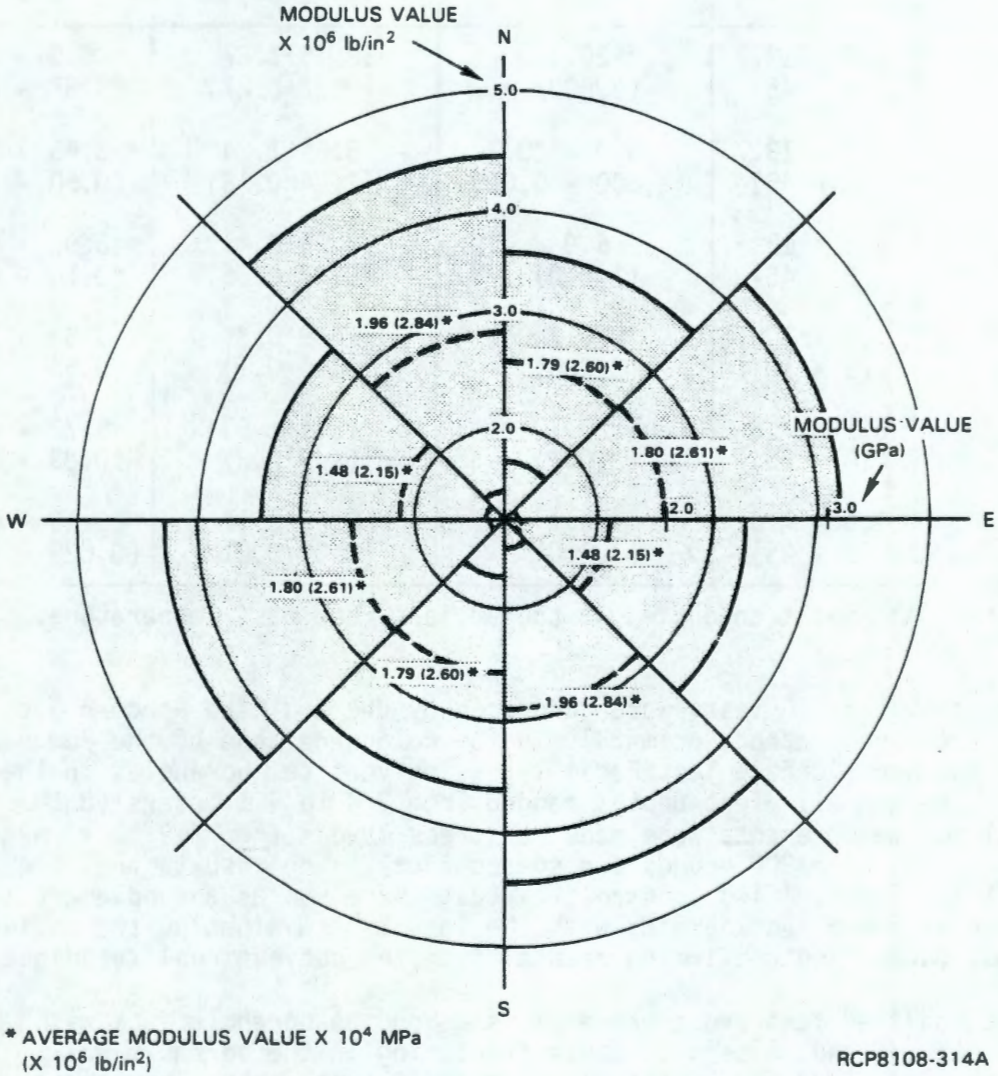

FIGURE 4-3. Average Modulus Value (uncorrected) Versus Orientation, from Modified Goodman Jack Tests in the Colonnade Zone of Pomona Flow at the Near-Surface Test Facility Site.

There are inherent weaknesses in the borehole jacking tests employed at the Near-Surface Test Facility. The volume of rock being stressed is rather small and does not include a sufficient number of discontinuities to truly represent the rock-mass characteristics. The results could likewise be adversely affected by one or two discontinuities in the immediate vicinity of the platen, causing irregular displacements. Results are also affected by the in situ stress field, with higher and perhaps more uniform modulus values associated with higher stresses and tighter joints. This influence of the in situ stress and the distribution of this stress field around the tunnel opening is probably the major reason for the variance in the results as a function of depth and jack pressure.

4.2.3 Jointed Block Test

A two-step flat jack test was conceived for in situ determination of mechanical and thermomechanical behavior in the Pomona flow. This test, hereafter referred to as the "jointed block test," will provide for temperature and stress control on a block of entablature basalt 2 meters (6.5 feet) on each side, located 1.5 to 3.5 meters (5 to 11.5 feet) horizontally into the tunnel wall (Fig. 4-4). A system of flat jacks on the top and sides of the block, combined with stabilizing tendons extending from the tunnel face inward, will create a large-scale triaxial test. A series of differential loading cycles will be applied at ambient and then successively higher temperature levels as instrumentation within the block measures the actual distribution of stresses and displacements. Deformation modulus, Poisson's ratio and thermal expansion coefficient values can then be calculated as a function of stress levels up to 20 MPa (2,900 pounds per square inch) and temperatures up to 200°C.

Step 1 of the test (which has been completed) consisted of a single horizontal slot with the instrumentation and heaters as shown in Figure 4-5. The purpose of Step 1 was to evaluate the slot-cutting techniques and the instrumentation prior to their use in the full test, as well as to provide preliminary deformation modulus measurements. Step 2 of the test will consist of isolating the remainder of the basalt block, completing installation of the triaxial loading apparatus, and conducting tests to measure the rock-mass deformation characteristics for a controlled range of temperatures and multiaxial state of stress.

The single slot of Step 1 was drilled by successive boring of alternate 14-centimeter (5.5-inch) diameter holes and removal of the intervening web. During the drilling operation, vibrating wire stressmeters, installed in holes 5U03 and 5U04 (see Fig. 4-5), monitored the relaxation experienced by the rock mass. After installation of the flat jacks in the slot, the jacks were pressurized until the output from the vibrating wire stressmeter gauges returned to the pre-slot level. The pressure in the flat jacks, when each individual vibrating wire stressmeter gauge returned to its initial value, indicates the pattern of stress distribution (Fig. 4-6) from the tunnel wall into the rock perpendicular to the tunnel. This stress distribution, when compared to the theoretical stress concentration around an intact circular tunnel, also gives a qualitative indication of the depth of penetration of the blast-damage zone around the opening.

9 2 1 2 4 9 5 0 8 3 8

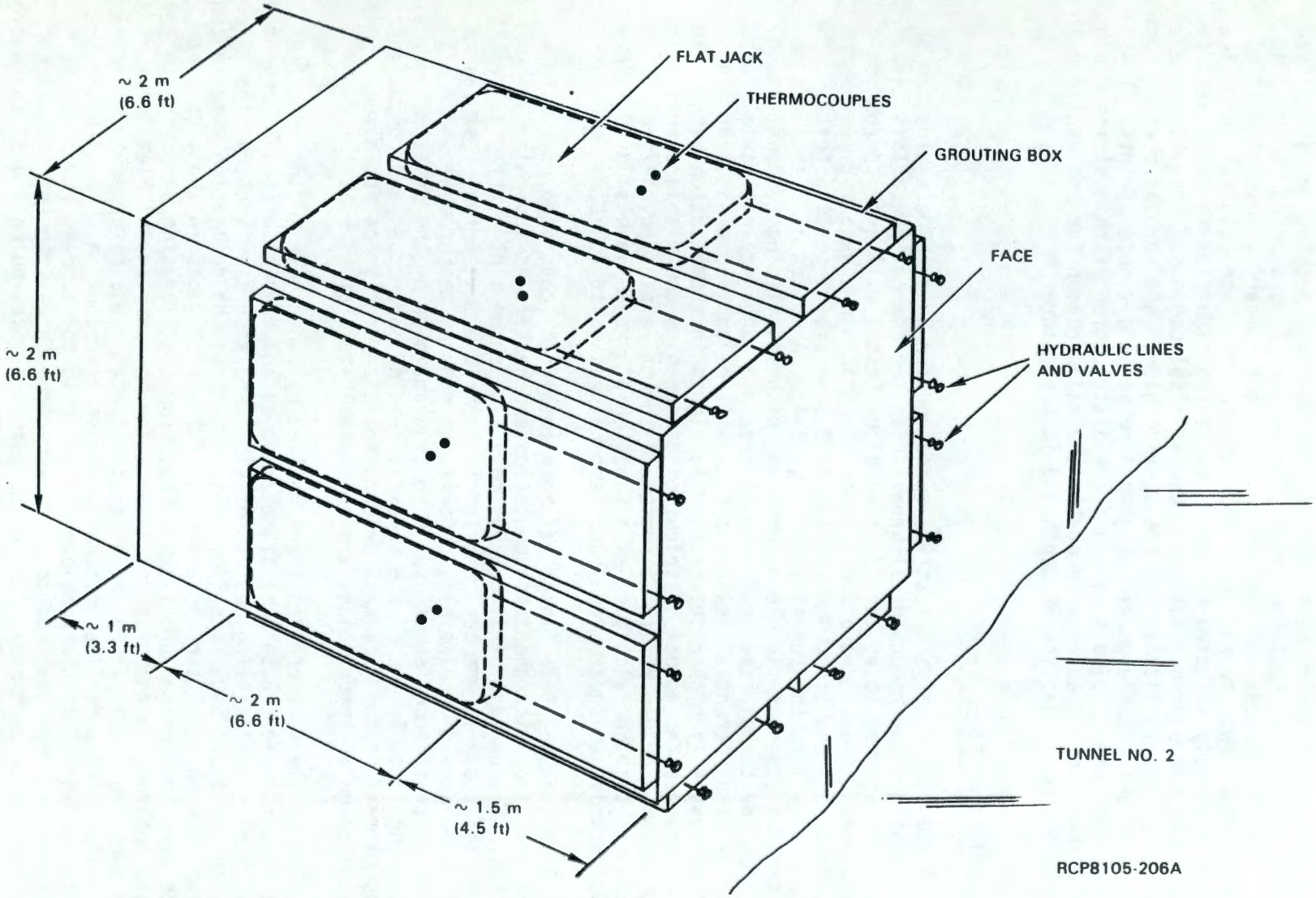

FIGURE 4-4. Block Test Number 1 Flat Jack and Grouting Boxes.

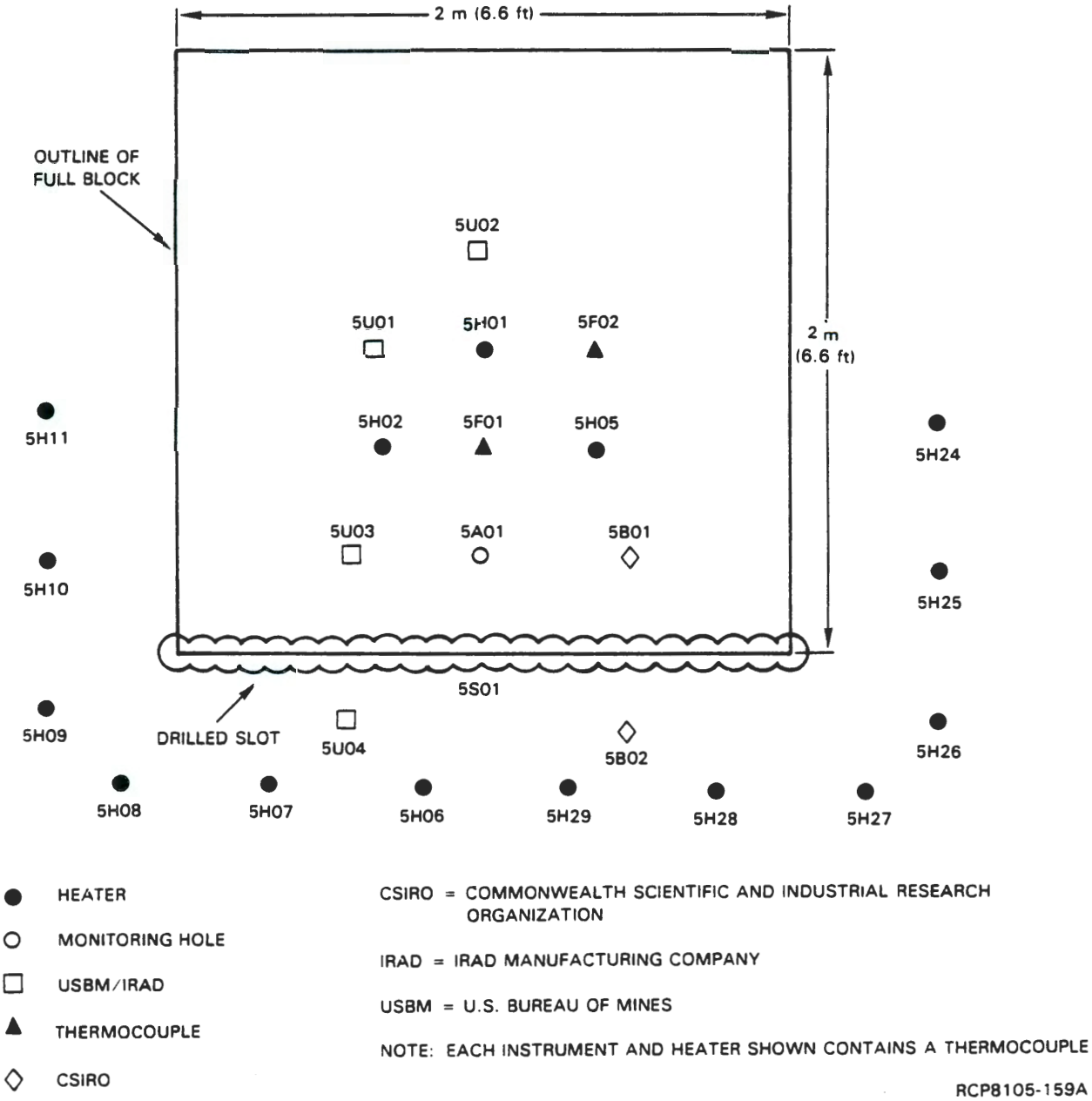

FIGURE 4-5. Heater and Instrumentation Holes - Block Test Step 1.

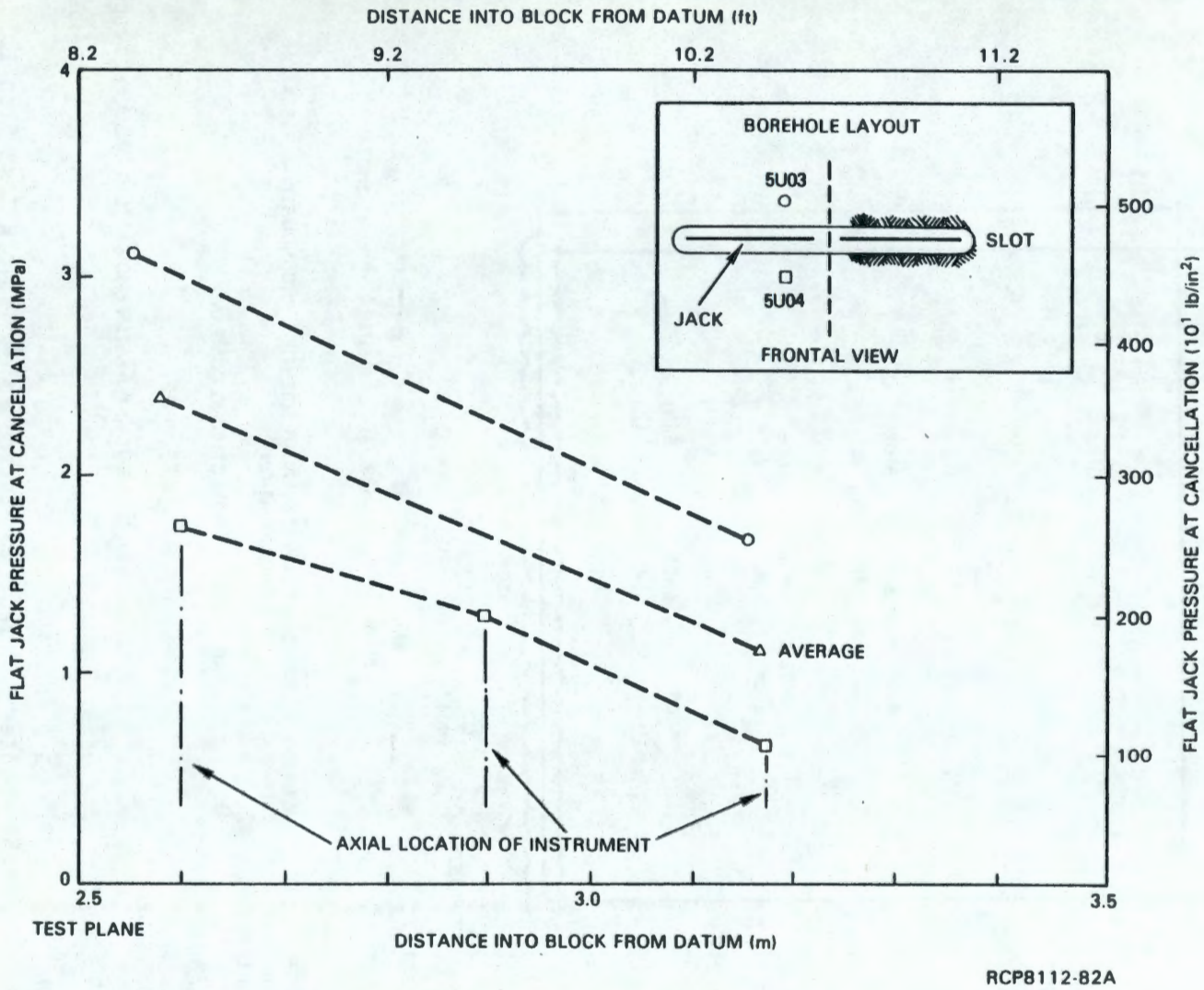

FIGURE 4-6. Individual Stress Cancellation Values for Vibrating Wire Stressmeters in Step 1 of the Block Test.

The flat jack stress measurement method does not require knowledge of the elastic properties of the rock and, thus, is considered to be a true stress measuring method. For the same reason, this method is better adapted to measurement in inelastic rock. Also, because of the averaging effect due to the comparatively large area of the flat jack, it is less sensitive to local variations in the rock stress, which is a problem associated with most borehole stress measurement techniques. Although the relaxation technique is more cumbersome than most borehole stress measurement techniques, its reliability and direct measurement capability make it a desirable method of stress determination.

An important analytical result of Step 1 of the block test was the determination of a preliminary value for the modulus of elasticity for the rock mass. The Step 1 instrumentation allowed evaluation of the modulus of deformation by two independent techniques, utilizing U.S. Bureau of Mines borehole deformation gauges and deformeters installed within the flat jacks, coupled with analytical procedures. The modulus results for three identical pressure cycles at different temperatures of Step 1 (Fig. 4-7) are given in Table 4-5. With the redundancy afforded by using two independent techniques, the close agreement between values tends to confirm the validity of either method.

TABLE 4-5. Step 1 - Modulus of Deformation for Pomona Entablature at the Near-Surface Test Facility.

°C	Borehole deformation gauges				Flat jack deformeters
	5U01	5U03	5U04	Average	
	GPa (lb/in^2 E+06)				
17	46 (6.67)	42 (6.09)	44 (6.38)	44 (6.38)	40 (5.80)
50	--	37 (5.36)	48 (6.96)	43 (6.24)	--
100	--	34 (4.93)	--	34 (4.93)	--

While the deformation modulus seemed to be unaffected by increasing the rock temperature to 50°C, a further increase to 100°C produced the lowest value of the data set. As only one borehole deformation gauge survived at 100°C, a firm conclusion regarding the influence of temperature on rock mass deformation properties should be withheld until confirming tests can be conducted. Step 2 of the block test should provide that information, as well as any evidence of deformational anisotropy at ambient and elevated temperatures.

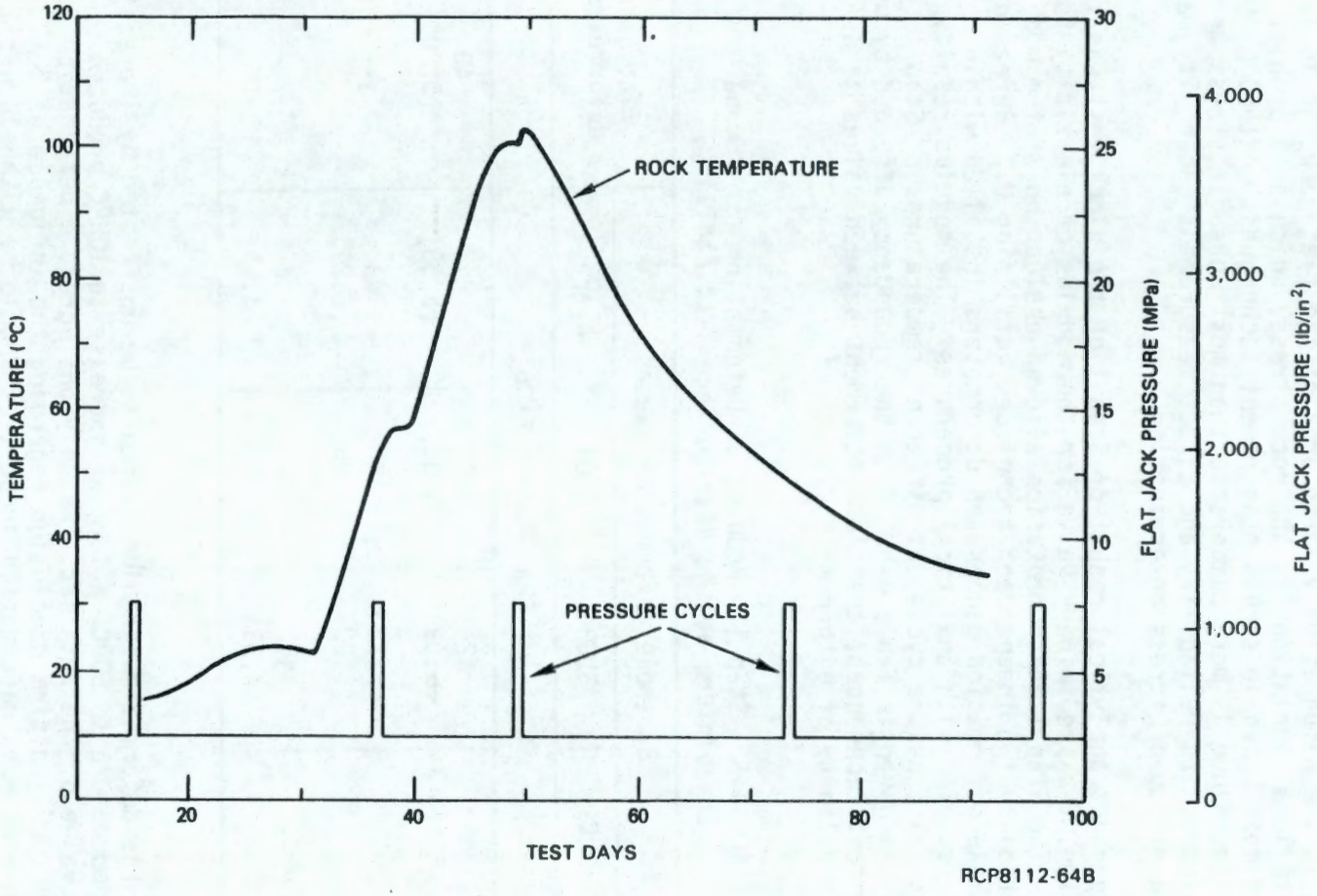

FIGURE 4-7. Temperature and Flat Jack Pressure Cycles During Step 1.

4.2.4 Discussion of Results

It should again be emphasized that deformation modulus values obtained in the above tests are for the shallow Pomona flow at the Near-Surface Test Facility, which was constructed using less-than-optimum drill and blast methods (see Section 4.8). The test results obtained by the borehole jacking methods yielded substantially lower modulus values than the block test results. This is attributed to the inherent shortcomings of the borehole jacking method; namely, the effects of the smaller volume of stressed rock, jack platen/borehole radius mismatch, longitudinal bending of the jack, and the deformation of joints adjacent to and in the test interval. Similar tests have not been conducted at depth in the Umtanum or middle Sentinel Bluffs flows because of lack of access. When access to the repository horizon becomes available, borehole tests and possibly one or more of the large-scale tests available (i.e., flat jack, plate bearing, hydrostatic pressure, radial jacking, and room convergence tests) are likely to be required in the reference repository horizon to establish values of the deformation modulus needed for design and modeling.

Based on experience gained in conducting early phases of the flat-jack test, the philosophy of first attempting large-scale tests in the Near-Surface Test Facility to perfect test systems and techniques appears sound.

4.2.5 Summary

Review of the available field data on the mechanical properties of basalt presented in this section leads to the following specific conclusions:

(1) Goodman (borehole) jack tests conducted in the Pomona entablature produced stress-strain curves exhibiting upward concavity at lower stresses. The effect of platen orientation (i.e., rock-mass anisotropy) is not clear from the data obtained. Lower modulus values at shallow depths is suspected to be related to blast damage.

(2) Modified Goodman jack tests conducted in the Pomona colonnade indicate isotropy of deformation characteristics in the plane perpendicular to the basalt columns.

(3) A single-slot flat jack test conducted in the Pomona entablature produced rock-mass deformation modulus values in the range of 34 to 48 GPa (4.93 to 6.96 x 10^6 pounds per square inch) for a direction parallel to the basalt columns. The average modulus value was generally two or more times that obtained from borehole jacking tests.

9 2 1 2 4 9 5 0 8 4 4

(4) Anisotropy of deformational characteristics of a basalt rock mass is anticipated based on the columnar structure of this material. Any such anisotropic effect is required for repository design and should be measured at ambient and elevated temperatures. These measurements are being made in Step 2 of the block test, currently in progress. Confirming measurements must also be made at the candidate repository horizon.

(5) Strength parameters for a jointed basalt rock mass as a function of temperature, moisture conditions, and direction are required for the assessment of site suitability. Appropriate tests to measure these parameters must be selected and conducted as required. Methods for estimating the parameters should be refined.

9 2 1 2 4 9 5 0 8 4 5

4.3 MECHANICAL PROPERTIES OF ROCK UNITS - DISCONTINUA

4.3.1 General

Rock-mass discontinuities are the weakest and most highly deformable elements of the rock-mass system. Inadequate frictional resistance along critically oriented joints and weakness planes is a major cause of instability in the roof, sidewalls, pillars, and benches of mines and tunnels. Such instabilities must be considered in the design of a repository facility. The contribution of joint deformation to deformability of the rock mass and the effect of joint characteristics such as aperture, infilling material, and roughness on that contribution are important to designers. Methods of quantitatively describing these properties have recently been standardized by the International Society of Rock Mechanics (Brown, 1981). With such information the designer can modify modeling parameters in accordance with conditions reported by the geologist during exploration or construction. Another particular concern is how joint strength and deformability change with temperature.

Accordingly, the purpose of this portion of the geoengineering investigation was to (1) identify and describe the physical appearance of the discontinuities as they exist in situ and (2) determine the properties and mechanical behavior of these discontinuities, separate and distinct from the entire rock mass itself, by means of appropriate laboratory and in situ tests.

4.3.2 Field Investigation

The physical nature of the discontinuities, primarily joints and large-scale structural heterogeneity, in the candidate repository horizons (i.e., Umtanum and middle Sentinel Bluffs flows) has been documented by both surface exposure and borehole-core studies.

The surface exposure investigation addressed the undifferentiated Grande Ronde Basalt and described a typical vertical intraflow structure as follows:

- A ropy-to-brecciated vesicular flow top
- Upper colonnade with relatively large (0.7 to 2.2 meters (2.3 to 7.2 feet) in diameter) irregular columns, with or without vesicles
- Entablature, consisting of relatively small (0.2 to 0.9 meter (0.6 to 3.0 feet) in diameter) columns
- Lower colonnade consisting of well-formed-to-wavy large (0.5 to 1.5 meters (1.6 to 4.9 feet) in diameter) columns
- A glassy basal zone that varies significantly in thickness and may be highly fractured, vesicular, or pillowed.

9 2 1 2 4 9 5 0 8 4 6

This description is somewhat idealized and generally applies to most of the flows, although the intensity and definition of the individual characteristics may vary significantly.

The entablature is presently the structural zone most likely to receive the repository. It consists of relatively small, hackly to regular columns (0.2 to 0.9 meter (0.6 to 3.0 feet) in diameter) most commonly occupying the middle portion of a flow. Entablature "columns" weather to hackly pieces characterized by fluted surfaces. Contacts with adjacent intraflow structures range from sharp to gradational over several meters. Orientation of columns varies significantly within most entablatures. In some places columns are vertical, but in other cases they form fanning arrays or are even horizontal.

Qualitatively, the dominant fractures range from those that define well-formed regular polygonal solids to those that define irregular elongate-to-equant blocks. There is nearly an entire spectrum from regular, well-formed columns to irregular (hackly) blocks. Both columns and blocks range widely in size; 0.20 to 2.3 meters (0.6 to 7.5 feet) for columns and 0.1 to 0.7 meter (0.3 to 2.3 feet) for the more equant blocks. In plan view the fractures are arranged as four-, five-, or six-sided polygons. Commonly, well-formed columns possess five or six sides, whereas less regular columns either possess three or four sides, or their sides are not well defined. The columnar character cannot readily be traced as single fractures through the entablature, but is instead commonly fractured into fluted, hackly blocks, 0.15 to 0.3 meter (0.5 to 1.0 foot) in maximum dimension. The blocks may be elongate, forming a crude columnar structure in some flows.

Virtually all columns or blocks are subdivided into smaller blocks by cross fractures. These cross fractures occur in a wide range of orientations, were formed mainly after the primary column-defining fractures, and typically are terminated by the primary fractures. In outcrops the secondary fractures rarely exhibit the rough surface that is common on column faces.

Borehole logging provided data on horizontal joint spacing and characteristics at depth in the Grande Ronde Basalt. Fractures logged in the drill core were defined as any subplanar or planar crack, filled or unfilled, that partially or fully transects the core. Most fractures had narrow apertures (less than 0.5 millimeter (0.02 inch)) and contained secondary minerals. Fractures with apertures on the order of several millimeters or larger are estimated to constitute less than 0.1 percent of all fractures and are typically associated with flow tops or flow bottoms that show relatively high permeabilities. They are not expected to be encountered in the entablature zones.

4.3.3 Laboratory and In Situ Testing

To develop a model that accurately reflects the behavior of a jointed rock mass on the scale of the proposed repository, the mechanical behavior of the discontinuities must be determined, and parameters representative

9 2 1 2 4 9 5 0 8 4 7

of the behavior must be defined. The most useful parameters are the peak and residual angles of joint friction, which describe the shear strength of the joint as a function of applied stresses, the cohesion, and the "stiffness" of the joint, or its stress-displacement characteristics. These parameters are obtained from direct shear or triaxial shear tests on jointed specimens. Some triaxial testing has been conducted on jointed samples of Umtanum basalt as a means of assessing the effect of jointing on a laboratory scale. Samples tested in this series often contained more than one joint or fracture. Results showed a substantially reduced coefficient of internal friction for the jointed samples, but the joints were randomly oriented and no clear inference can be made about characteristics of the joints themselves.

In another series of tests, Umtanum samples containing only one obvious joint were tested in triaxial compression to measure the frictional characteristics of the joints as a function of stress levels to 34.5 megapascals (5,000 pounds per square inch), temperatures to 500°C, and moisture conditions. Samples selected were those with critically oriented joints, such that failure would occur through the joint. One group of samples was tested at room temperature (20°C). The samples were initially subjected to a constant confining stress of 6.9 megapascals (1,000 pounds per square inch), then to an increasing axial load until the peak stress level was observed. The confining pressure was then increased to the next increment and the axial load resumed until a peak stress was again observed. This process was then repeated for the same sample at the remaining confining stress increments. At each value of peak stress, the actual shear and normal stress on the joint were calculated and used to obtain the coefficient of friction (i.e., shear stress divided by normal stress). The results of this test series are shown in Table 4-6.

A second group of single-jointed samples was tested at temperatures up to 500°C. Each sample was subjected to a low confining stress of 0.7 megapascal 100 pounds per square inch), then to an increasing axial load until the peak stress level was observed. The sample was then heated to progressively higher temperatures, with axial load again applied at the same confining stress for each temperature increment. The joint coefficient of friction was calculated, as indicated previously, and the results are presented in Table 4-7.

Results indicate that the friction angle for the joints is in the same range as the angle of internal friction determined from triaxial tests on intact samples (see Table 4-2). This trend seemed to be affected only slightly by higher temperatures and moisture conditions. However, the use of a single sample for multiple tests resulted in a polishing effect, and in many cases a corresponding reduction in friction coefficient with additional loading cycles. Distinction between the effects of polishing and those of stress level and temperature was therefore not entirely straightforward.

TABLE 4-6. Coefficient of Friction of Joints for Umtanum Entablature Samples Tested in Triaxial Compression at 20°C (from Miller, 1979a; 1979b; Miller and Bishop, 1979).

Hole	Depth, m (ft)	Flow zone*	Moisture conditions	Density, g/cm^3 (lb/ft^3)	Confining stress, MPa (lb/in^2)			
					6.9 (1,000)	13.8 (2,000)	20.7 (3,000)	34.5 (5,000)
					Joint coefficient of friction			
DC-4	1,114.4 (3,656.0)	I	Saturated	2.52 (157)	1.337	Sample failed completely		
DC-4	1,119.5 (3,673.0)	C	Dry	2.69 (168)	1.080	1.046	1.012	Failed
DC-4	1,123.3 (3,685.3)	E	Saturated	2.65 (166)	1.076	0.947	0.776	0.560
DC-4	1,139.3 (3,737.9)	E	Dry	2.81 (176)	1.583	1.494	1.347	1.140
DC-4	1,153.1 (3,783.1)	E	Dry	2.77 (173)	1.012	1.020	0.995	0.945
DC-6	932.2 (3,058.5)	I	Dry	2.44 (152)	0.821	--	--	--
DC-6	970.1 (3,182.6)	E	Saturated	2.74 (171)	3.029	2.152	1.934	1.617
DC-6	990.9 (3,251.1)	C	Saturated	2.83 (177)	0.685	0.630	0.633	0.627
DC-6	991.0 (3,251.3)	C	Dry	2.84 (177)	0.966	0.929	0.867	--
DC-6	992.7 (3,257.0)	C	Dry	2.68 (167)	0.937	0.834	0.817	0.781
DC-8	1,101.8 (3,614.9)	I	Dry	2.41 (151)	1.205	1.210	1.031	0.678
DC-8	1,112.1 (3,648.5)	C	Dry	2.67 (167)	1.263	1.638	0.901	0.851
DC-8	1,113.0 (3,651.4)	C	Dry	2.76 (172)	1.186	0.921	0.799	0.818
DC-8	1,115.9 (3,661.1)	C	Saturated	2.71 (169)	1.203	1.132	1.031	0.898

*I = interflow zone; C = colonnade zone; E = entablature zone.

TABLE 4-7. Coefficient of Friction of Joints for Umtanum Entablature Samples Tested in Triaxial Compression at Elevated Temperatures (Miller 1979a; 1979b; Miller and Bishop, 1979).

Hole	Depth, m (ft)	Flow zone*	Initial moisture	Density, g/cm^3 (lb/ft^3)	Confining stress, MPa (lb/in^2)	Temperature (°C)			
						20	150	300	500
						Joint coefficient of friction			
DC-4	1,111.9 (3,648.0)	I	Dry	2.59 (162)	0.7 (100)	0	0.262	0.794	0.722
DC-4	1,115.9 (3,661.2)	C	Dry	2.67 (167)	0.7 (100)	1.263	0.950	0.794	0.794
DC-4	1,123.2 (3,685.0)	E	Dry	2.74 (171)	0.7 (100)	1.767	0.169	0.169	0.175
DC-4	1,124.6 (3,689.7)	E	Dry	2.70 (169)	0.7 (100)	1.152	1.133	1.122	1.121
DC-4	1,144.8 (3,755.9)	E	Dry	2.8 (175)	0.7 (100)	0.981	0.984	0.979	0.966
DC-6	953.7 (3,128.9)	E	Dry	2.75 (172)	0.7 (100)	0.674	0.678	0.689	0.688
DC-6	957.6 (3,141.8)	E	Dry	2.51 (157)	0.7 (100)	2.102	2.062	1.815	1.307
DC-6	969.3 (3,180.1)	E	Dry	2.69 (168)	0.7 (100)	1.690	Complete failure of sample		
DC-8	1,100.2 (3,609.6)	I	Dry	2.48 (155)	0.7 (100)	3.185	1.519	0.921	1.391
DC-8	1,109.8 (3,640.9)	I	Dry	2.49 (156)	0.7 (100)	1.160	1.138	1.133	1.145
DC-8	1,109.9 (3,641.2)	I	Dry	2.48 (155)	0.7 (100)	1.200	1.215	1.193	1.135
DC-8	1,113.8 (3,654.3)	C	Dry	2.78 (174)	0.7 (100)	0.960	0.994	0.992	0.953
DC-8	1,114.3 (3,655.9)	C	Saturated	2.8 (175)	0.7 (100)	0.997	0.994	0.990	0.984

*I = interflow zone; C = colonnade zone; E = entablature zone.

Time effects (creep) on the behavior of joints could be extremely important, especially in the presence of high temperatures and significant infilling material. Creep tests on joints are currently being conducted to preview any tendency of jointed Pomona and Umtanum samples to undergo significant time-dependent deformation. Similar efforts to determine creep characteristics of a heated basalt rock mass must be made in situ (see Chapter 14).

Limited information on jointing in the Umtanum and middle Sentinel Bluffs flows has been obtained from studies of outcroppings and borehole samples. Additional information is needed on the nature of vertical joints within these candidate repository horizons.

A full complement of mechanical behavior tests must be undertaken in the laboratory and the field to provide joint strength and deformability parameters.

4.3.4 Summary

A review of the information presented in this section on the mechanical properties of the rock discontinuities leads to the following conclusions:

(1) Core logging and visual examination of outcrops have provided information on the nature of jointing in Grande Ronde Basalts in general. Site-specific information on the horizontal character of vertical joint systems and on the characteristics of the joints themselves (aperture, roughness, etc.) is required. Access to the candidate horizons from the exploratory shaft can provide this information.

(2) Results from a limited number of joint shear tests conducted on Umtanum samples from all flow zones under triaxial stress conditions indicate that joint peak friction angles are in the same range as friction angles obtained for intact samples. Preliminary indications are that the joint friction coefficients at low stress levels are not substantially affected by temperatures up to 500°C. These conclusions must be considered tentative in view of the small sample population and limitations of the test technique.

(3) A thorough knowledge of joint strength parameters (peak and residual friction angles, cohesion) and joint stiffness values as a function of temperature and moisture conditions must be obtained through laboratory and field testing. This information will be used in numerical models to examine the stability of repository tunnels.

(4) Time-dependent effects on joint strength and deformability must be determined, especially at elevated temperatures. Initial work in this area is now in progress.

4.4 THERMAL AND THERMOMECHANICAL PROPERTIES - LABORATORY RESULTS

4.4.1 General

The thermal and thermomechanical properties of basalt are required parameters that will be utilized in modeling and design of a nuclear waste repository. The effects of temperature, such as induced temperature gradients and thermal stress fields, must be adequately understood before waste canisters may be placed in a basalt medium. The conceptual design was based upon the thermal property values listed in Table 4-8. The information available for basalt resulting from a 1977 review of the literature on basalt properties is also summarized in Table 4-8.

TABLE 4-8. Thermal and Thermomechanical Characteristics of Basalts Used for Conceptual Design (BWIP and KE/PB, 1982).

Property	Estimated value	Range
Diffusivity (m^2/s)	6.5 E-07	5.2 - 8.0 E-07
Thermal conductivity (W/m^oK)	2.3	1.4 - 4.28
Specific heat (kJ/kg^oK)	0.95	0.95 - 1.05
Thermal expansion coefficient (cm/cm^oK)	7.45 E-06	2.9 - 11.8 E-06

Since 1977, additional thermal property tests have been conducted on basalt from a variety of flows and horizons within the Hanford Site and are reported in CSM (1978), Duvall et al. (1978), Erikson and Krupka (1980), FSI (1980a; 1980b; 1980c; 1981a; 1981b), Martinez-Baez and Amick (1978), Miller and Bishop (1979), Miller (1979a; 1979b), and a compendium of past test results assembled by Schmidt et al. (1980). The thermal properties of Hanford Site basalts as determined by these tests are presented in Table 4-9.

4.4.2 Results and Discussion

Thermal properties are those parameters that describe the effects of heat on a material. Specific heat is the ratio of the amount of energy required to heat a material (i.e., raise its temperature) to that required to heat an equal volume of water. The thermal expansion coefficient describes the amount of dimensional change experienced by a material that has been heated or cooled. Thermal conductivity measures the rate of heat conduction through a unit volume of material. Thermal diffusivity is a narrower expression of the rate of heat conduction through a material. The diffusivity simply equals the thermal conductivity divided by the product of the specific heat and the density of the material in question.

9 2 1 2 4 9 5 0 8 5 2

TABLE 4-9. Thermal Properties of Hanford Site Basalts.

Property	Grande Ronde Basalt				Pomona Member of the Saddle Mountains Basalt	
	Umtanum flow		Middle Sentinel Bluffs flow			
	Range	Mean	Range	Mean	Range	Mean
Thermal diffusivity (m^2/s) E-07	4.0 - 9.0	5.22		7.18 @ 50°C	4.5 - 8.0	6.1
Thermal conductivity (W/m°K)	1.25 - 2.50	2.16+(0.78 E-03)T*	1.34 - 1.86	1.60±0.21 @ 60°C	1.10 - 2.4	1.91+(1.56 E-03)T*
Specific heat (kJ/kg°K)	0.820 - 1.160	0.930+(234 E-03)T*	0.791 - 0.937	0.762+(0.81 E-03)T*	0.750 - 1.250	0.838+(0.513 E-03)T*
Thermal expansion coefficient (cm/cm°K) E-06	6.21 - 10.77	8.81±1.78	5.78 - 6.56	6.17±0.55	5.0 - 8.5	5.52±0.56

*T = Temperature (°C): 20° to 350°C

Thermomechanical properties are those parameters that describe the mechanical response produced by increasing temperature and are discussed in this section only. The coefficient of thermal expansion is a true thermomechanical property.

All the data presented in this section are from laboratory tests on core from the entablature portion of the respective flow or formation. As indicated in Table 4-10, these tests have been performed according to either American Society for Testing and Materials techniques or those generally accepted or referenced.

TABLE 4-10. Thermal Property Tests.

Test	Procedure
Thermal expansion	FSI (1981b)
Thermal conductivity	ASTM-C-518 (ASTM, 1976b)
Specific heat	ASTM-C-351 (ASTM, 1973)
Thermal diffusivity	Danielson and Sidles (1969)

A comparison of data in Tables 4-8 and 4-9 indicates that the current mean thermal property values are generally within the ranges established for the repository conceptual design. Thermal diffusivity and the coefficient of thermal expansion were found to be constant over the investigated temperature range of 20° to 300°C. The variability found in the range of values for thermal diffusivity is partially related to the method by which the value was derived. This value may be directly measured experimentally or it may be calculated using other measured parameters. Thus, any variability in the other measured parameters, such as thermal conductivity or specific heat, will lead to an even larger range of calculated values for thermal diffusivity. The statistical variations seen in both experimental and calculated values are weighted to arrive at the mean value listed in Table 4-9.

A conservative value for the coefficient of thermal expansion of 19 E-06 centimeters per centimeter degree kelvin was recommended for use by Schmidt et al. (1980). Comparison of the means of all the basalts tested indicates that probable textural or compositional differences between basalt samples do yield slightly differing results.

Thermal conductivity and specific heat were found to increase linearly with increasing temperature in the range of 20° to 300°C. Other workers have found that for many materials these thermal properties are related nonlinearly to temperature (Goldsmith et al., 1961). In the present work, however, measurements were made at only three or four temperatures, so use of a nonlinear curve fit was unjustified. Large-scale in situ heater tests have shown that the thermal conductivity of a basalt rock mass

behaves in a manner that can be adequately modeled using laboratory-determined values (see Section 4.5). Further measurements at varying temperatures are required to refine the relationships between thermal conductivity, specific heat, and temperature. Once this is completed, these relationships may be used to more accurately predict in situ behavior. For the present time, the relationships shown in Table 4-9 yield values that are comparable to those of Table 4-8. All of the thermal-property measurements made have been on small, intact laboratory specimens at ambient confining pressure conditions. The presence of joints in an in situ mass of basalt will affect the thermal properties to varying degrees. As the fracture density of a rock mass increases with an increase in the number of joint sets, jointing should have a tendency to decrease the thermal conductivity. This, in turn, should affect the thermal diffusivity. The coefficient of thermal expansion may also be affected in a similar fashion.

The influence of confining pressure on thermal properties has not yet been simulated in any of the laboratory measurements taken. The increase in confining pressure at depth may have a tendency to negate some of the effects due to the joint structure.

Further thermal property tests are required to assess the effects of jointing and confining pressure on these properties. By conducting the tests at a number of temperatures, relationships between jointing and thermal properties can be determined. Since a relatively small amount of data exists for the Grande Ronde Basalt and the candidate horizons, further tests must be conducted as core becomes available from the principal borehole at the reference repository location.

4.4.3 Summary

A review of the laboratory-determined thermal and thermomechanical properties of intact specimens of basalt presented in this section leads to the following conclusions:

(1) Limited data are available on the thermal and thermomechanical properties of intact specimens of basalt from the candidate repository horizons and overlying basalt flows. The variability and range of data indicate that site-specific data are needed for design and performance assessment. Additional laboratory tests will be conducted to build a statistically valid data base.

(2) Some experimenters have identified nonlinear responses of conductivity and specific heat with respect to temperature, but the available basalt data are too limited to do so, and additional tests need to be conducted to define this response.

(3) The influence of confining pressure and jointing on thermal properties is not well understood. Laboratory tests need to be conducted to investigate this relationship.

9 2 1 2 4 9 5 0 8 5 5

4.5 THERMAL AND THERMOMECHANICAL PROPERTIES - IN SITU

4.5.1 General

A unique feature of the design of a nuclear waste repository is that an additional design variable, heat, must be considered in all its aspects. Section 4.4 described the thermal properties of basalt in the laboratory. The logical next step is to consider the impact of heat on the more complicated rock mass at the scale of the proposed repository. The effect of discontinuities on the thermal properties (i.e., specific heat, conductivity, and diffusivity) must be established to define the temperature field surrounding the canister cavity and repository tunnel during the storage period. Furthermore, the changes in strength and deformability of the discontinuous rock mass due to elevated temperatures must be determined to assess whether the rock mass will be adversely affected, thereby compromising its isolating capability.

Several tests were therefore devised and conducted to physically measure the thermal and thermomechanical properties of the rock mass in situ. A large-scale in situ test was designed to examine mechanical and thermomechanical behavior of the heated rock mass. This test, designated the jointed block test, was described in Section 4.2. Additionally, the response of basalt to thermal loading at the Near-Surface Test Facility was examined using electric heater tests, designated Full-Scale Heater Tests No. 1 and 2.

The process of conducting the tests and interpreting the results for use in design was complicated by several factors:

- Empirical relationships between laboratory and field behavior at elevated temperatures have not been established as have similar relationships at ambient temperatures (e.g., expressions relating compressive strength to sample size and relating smaller-scale modulus test values to large-scale values).

- The relative importance of the system of discontinuities to the thermal behavior of a rock mass has not been established for rocks in general.

- Very few monitoring instruments now exist that are capable of extended operation at elevated temperatures. This consideration is further complicated by the fractured nature of the basalt and the potential for localized aberrations in stress and displacement fields.

- As with the case for purely mechanical behavior testing, the candidate repository horizons were not available for in situ testing. Only results for the Pomona flow were obtained.

9 2 1 2 4 9 5 0 8 5 6

4.5.2 Full-Scale Heater Tests

Two full-scale electric heater tests are currently under way in the Pomona basalt (Hocking et al., 1980) at the Near-Surface Test Facility. Heater Test No. 1 consists of a central full-size canister of electric heaters surrounded by eight peripheral electric heaters (not in canisters). Heater Test No. 2 consists of a single full-size canister of electric heaters. These tests have been operated at various power levels representing the range of expected and extreme (not expected) repository conditions. Plan views of Heater Tests No. 1 and 2, including heater and instrumentation locations, are shown in Figures 4-8 and 4-9, respectively. The canister-heating schedules are presented in Figures 4-10 and 4-11.

These full-scale heater tests were designed to provide a data base of temperature, displacement, and stress information for basalt under thermally loaded conditions. They also provide the opportunity to model the rock response and compare actual and predictive results. Evaluation of the tests, which were started in July 1980, is currently under way and final analysis is not yet available.

A preliminary analysis, based on 270 days of operating data, allows some conclusions to be drawn as to the homogeneity, variability with direction, and relative magnitudes of the thermal properties of the basalt. An evaluation of temperatures, taken in horizontal planes through the test area, shows that the thermal properties are isotropic in a horizontal plane. Temperatures are similar at instruments located at approximately the same radius. A typical radial distribution of both predicted and measured temperatures is shown in Figure 4-12.

It is more difficult to determine from the test data whether the thermal properties for heat conduction in a vertical direction are the same as those in a horizontal direction, because the shape of the heater and the boundary conditions destroy the symmetry required for a simple comparison. Predictive modeling was done, assuming that thermal properties were isotropic. The actual test data followed the general shape of the predicted thermal contours, which indicates that the thermal properties of basalt are not greatly different in the vertical and horizontal directions. More specific information about this question will be acquired during the jointed block test.

The predicted temperatures, as originally modeled, consistently overestimated by 20 percent the actual rock temperature at the various instrument locations. Updated laboratory tests have shown that a value for thermal conductivity of 1.9 watts per meter degree kelvin may be more appropriate than the original value of 1.4 watts per meter degree centigrade. Additionally, heat energy was lost from the rock, since some water in the test area escaped as vapor and steam. When these two factors were considered in an upgraded model (Fig. 4-13 and 4-14), agreement between actual and predicted thermal response was within approximately 10 percent.

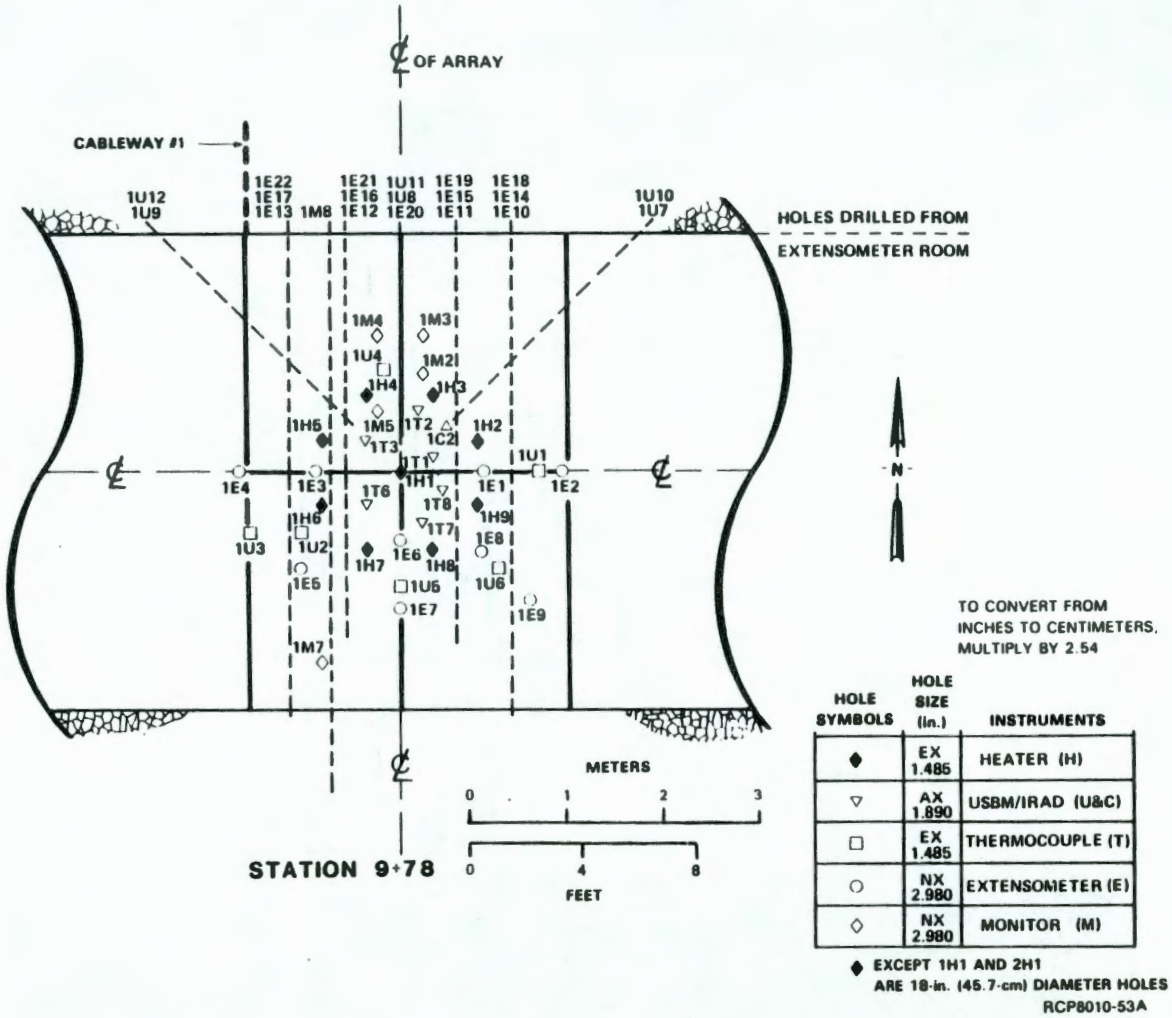

FIGURE 4-8. Plan View of Boreholes Drilled for Full-Scale Heater Test No. 1.

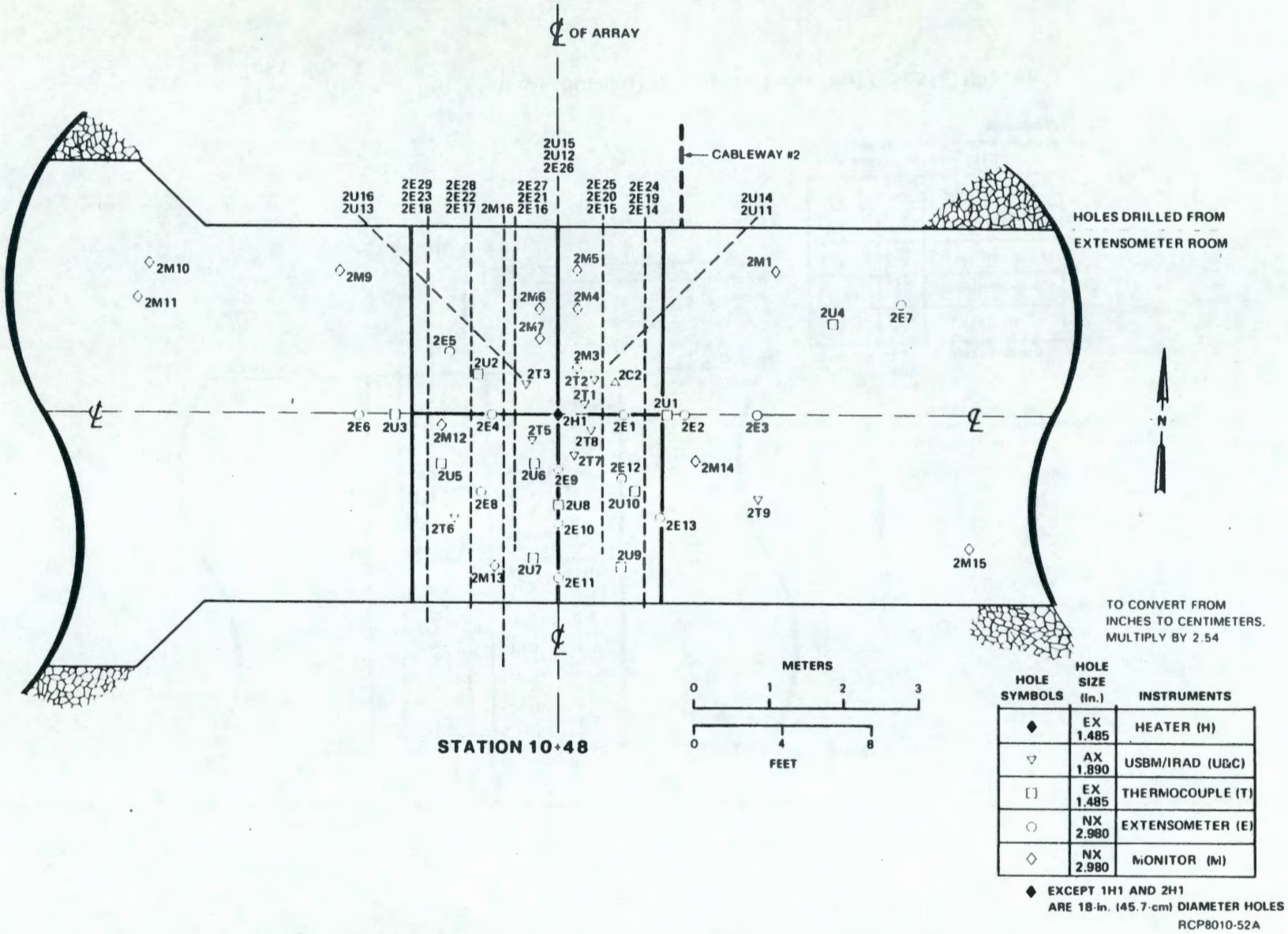

FIGURE 4-9. Plan View of Boreholes Drilled for Full-Scale Heater Test No. 2.

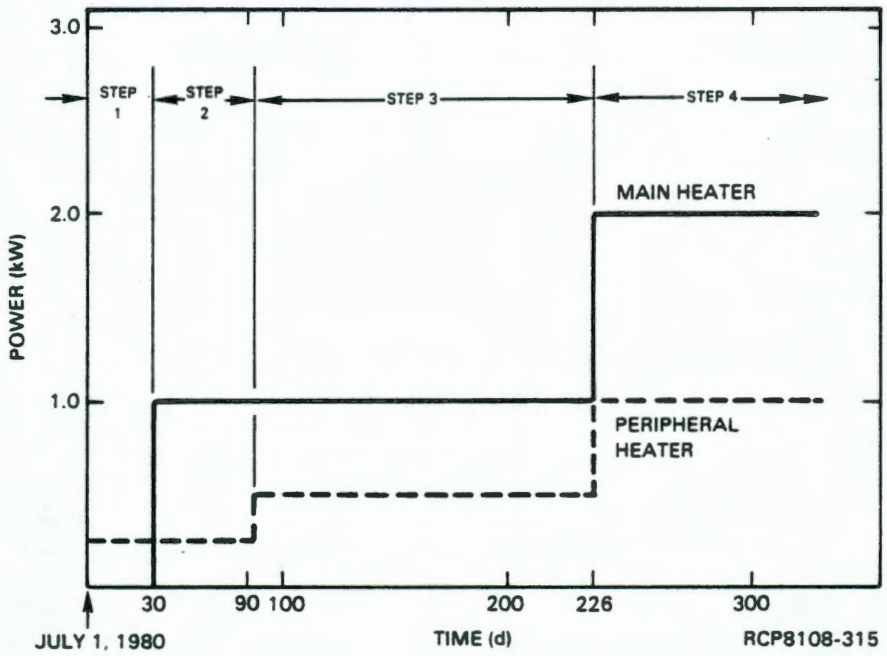

FIGURE 4-10. Heater Power Levels for Full-Scale Heater Test No. 1.

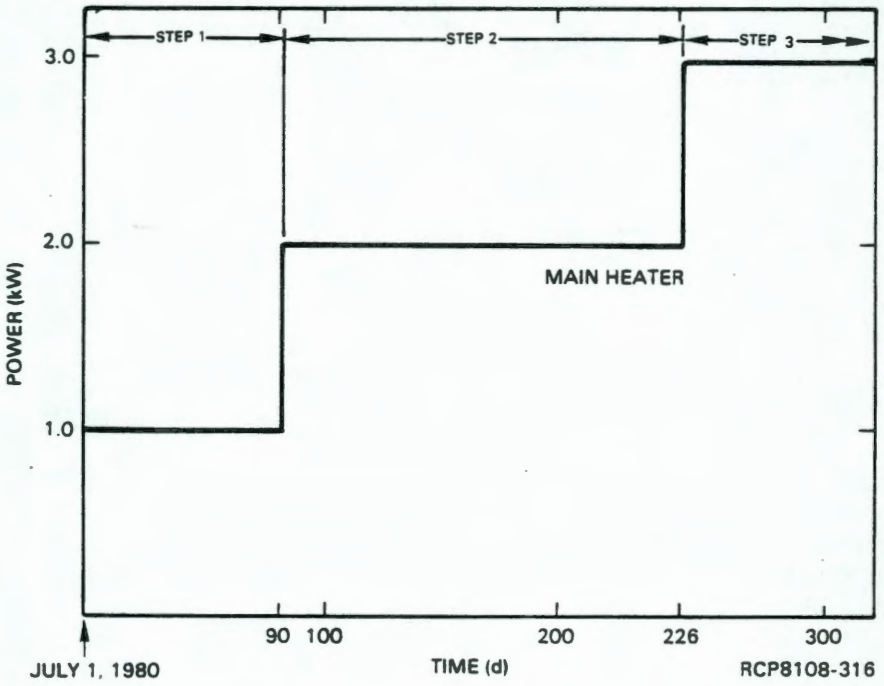

FIGURE 4-11. Heater Power Levels for Full-Scale Heater Test No. 2.

9 2 1 2 4 9 5 0 8 6 0

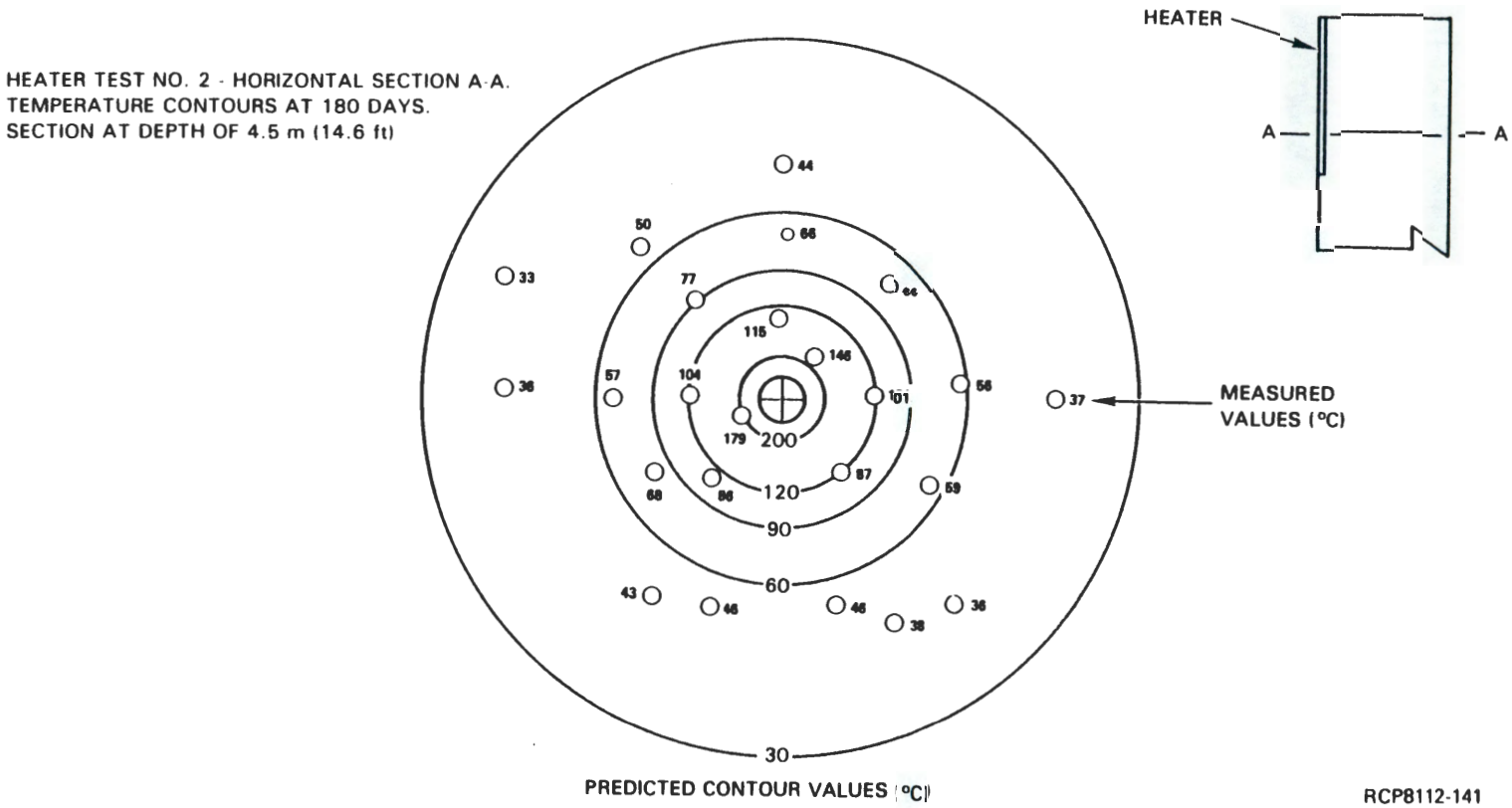

FIGURE 4-12. Comparison of Full-Scale Heater Test No. 2 Actual Data with Predictive Analysis Value.

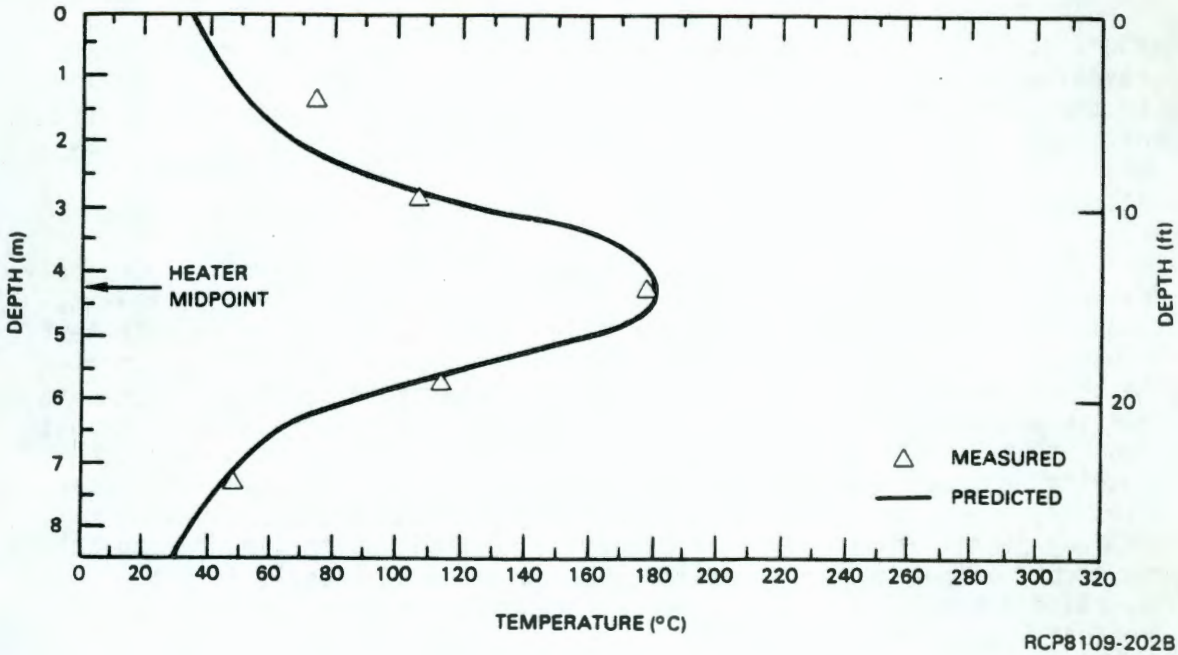

FIGURE 4-13. Axial Temperature Profile in Basalt at 0.71 Meter (2.3 Feet) from Heater-Hole Axis on Test Day 259 for Full-Scale Heater Test No. 1.

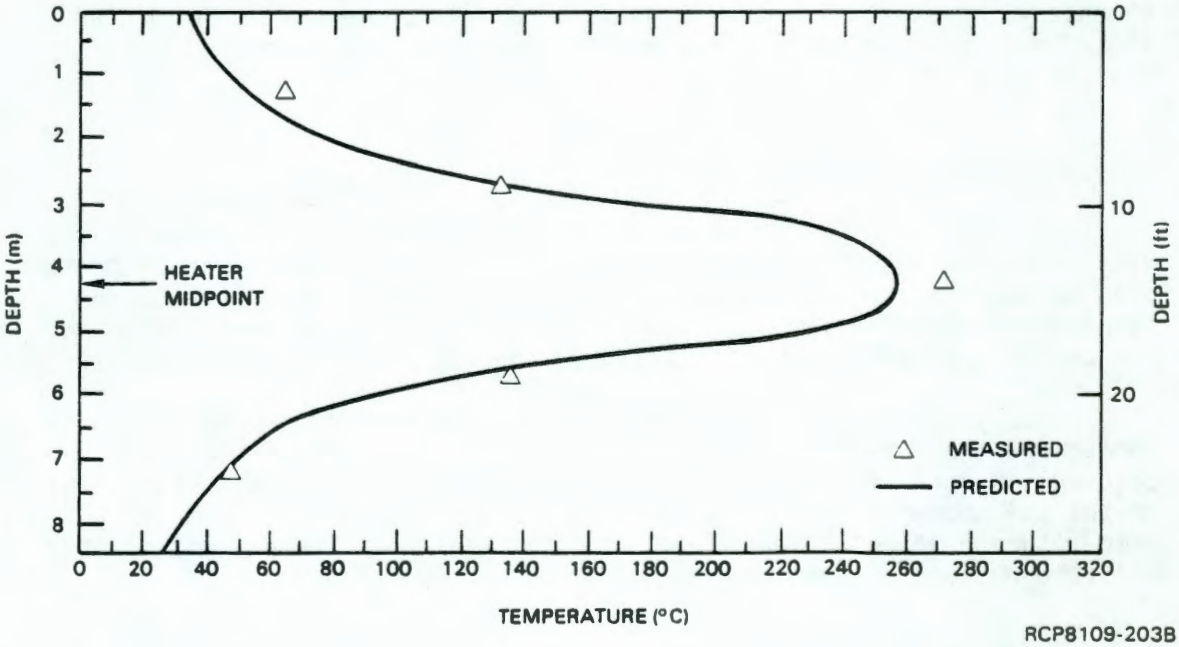

FIGURE 4-14. Axial Temperature Profile in Basalt at 0.40 Meter (1.3 Feet) from Heater-Hole Axis on Test Day 259 for Full-Scale Heater Test No. 1.

9 2 1 2 4 9 5 0 8 6 2

Rock-mass displacements have been measured in Heater Tests No. 1 and 2 using multipoint borehole extensometers. The displacements are revealed in the observation of anchor movements within the rock relative to the extensometer head. The movement data are corrected for the effect of temperature changes on the measurement system (Super Invar rods) by means of thermocouple data incorporated into specially developed algorithms. Analysis of extensometer data is an ongoing activity.

A qualitative comparison of the predicted and experimental vertical-extensometer readings indicates that in most boreholes there is fair-to-good correlation between the observed and predicted results in both tests. A high degree of symmetry exists in the experimental data from Heater Tests No. 1 and 2. A similar evaluation of horizontal extensometer data was less conclusive and is under further evaluation. Preliminary results indicate that horizontal displacements correlate poorly with predicted results and that symmetry is also poor. The reason for these discrepancies may lie in the columnar structure of the Pomona entablature, with primary joints in the vertical direction possibly distorting horizontal movement, although more specific information on the basalt in situ mechanical properties is required before definite conclusions can be reached.

The full-scale electric heater tests were not designed to determine the mechanical properties of in situ basalt. Rather, they provide a data base of actual data against which hypotheses of rock response can be evaluated. To a limited extent, some estimate of in situ rock property values can be made by back analysis. A test under controlled conditions is necessary, however, in order to measure in situ properties. A jointed block test is proposed for this and is currently in progress at the Near-Surface Test Facility.

4.5.3 Instrumentation Performance

The rock instrumentation in Full-Scale Heater Tests No. 1 and 2 met with varied success. Generally speaking, the performance of instruments used to monitor stress change was fair to poor, while displacement and temperature-measuring devices performed well. All gauge types did have periods of good performance, usually in the beginning of the heater tests.

Rock, instrument, and heater thermocouples performed extremely well throughout the entire test period. Occasionally, anomalous behavior occurred in rock and instrument thermocouples due to moisture intrusion on the thermocouple-measuring junction. This resulted in fluctuating temperature readings below actual rock temperature. The net effect of this phenomenon, however, is negligible.

Multiple-position borehole extensometers produced displacement data judged to be generally reliable. The downhole anchor hydraulic system did experience many pressure losses for undetermined reasons. It appears, however, that no inconsistencies in extensometer data were induced by such pressure losses and that anchorage was maintained.

9 2 1 2 4 9 5 0 8 6 3

Borehole deformation gauges performed reasonably well in both tests until heater power reached 5 kilowatts. At that time many gauges in vertical boreholes began producing very erratic readings, while most horizontally oriented gauges continued producing reliable data. Several gauges removed from the boreholes for calibration testing during the heater test displayed significant permanent zero offset changes. These changes are observable in the instrument data and have been noted to precede erratic readings. An attempt will be made to retrofit the borehole deformation gauge data after further calibration studies are complete.

Vibrating wire stressmeters in both Full-Scale Heater Tests No. 1 and 2 exhibited sporadic performance due to moisture infiltration. When readings were not obtained for a given scan, this was due to a default system in the scanner responding to erroneous data. Several of the vibrating wire stressmeters yielded data after an apparent "dead period," probably due to drying effects in a higher temperature field. When this occurred, much of the data appear to be valid based on continuation of the same trend as before the dead period. However, further investigation is required for data verification.

The present vibrating wire stressmeter conversion algorithm is not adequate for test analysis and will be revised based on the results from the Phase II scoping investigations, calibration test, and analytical studies.

4.5.4 Summary

A review of the results of in situ thermal and mechanical property tests conducted in Pomona basalt at the Near-Surface Test Facility leads to the following conclusions:

(1) Preliminary results from the full-scale heater tests suggest that Pomona basalt responds to thermal loading in a predictable fashion in the vertical direction. Numerical models of the experiments produce vertical displacements that agree reasonably well with measured values. Measured horizontal displacements do not correlate well with prediction, possibly because of the columnar structure of the basalt. A different instrument arrangement or additional tests may be necessary to clarify this structural effect. The specific nature of the basalt structure at depth is not currently known, including the spacing between columnar joints and joint conditions. The corresponding effect on thermomechanical response will be determined as access to the candidate horizons is obtained.

(2) In situ thermal properties determined in the full-scale heater tests compare well with those obtained in the laboratory, implying that these properties are not significantly sensitive to rock-mass discontinuities of the type and condition encountered in the Pomona entablature. Numerical models of the experiment produce temperature profiles that agree well with measured values.

9 2 1 2 4 9 5 0 8 6 4

(3) Thermocouples and extensometers have functioned well at all temperatures in full-scale tests conducted to date. Borehole deformation gauges (U.S. Bureau of Mines type) and vibrating-wire stressmeters generally performed well at room temperatures, but became erratic or failed completely at high temperatures. Efforts to improve the reliability of instrumentation must continue.

4.6 STRESS FIELD

4.6.1 General

Knowledge of the state of in situ stress is of fundamental importance in the design of a stable underground opening and the prediction of rock-mass movement in static and dynamic loading conditions. The ambient state of stress in the underground increases in general with depth. The rate of change (or stress gradient) varies, depending on the tectonic history of the region and the geologic factors in the location of concern. The principal stresses forming the axes of the stress ellipsoid are essential engineering parameters required for the design of a repository. These values are used in various stages of the design processes for evaluation of constructibility and of opening stability, and for calculations of tunnel-support requirements. An immediate need exists for in situ stress data for the design of the exploratory shaft facilities and the conceptual design of the repository.

The in situ stress data are also among the most sensitive and critical input parameters required for numerical models used in various design processes and in interpretation of results obtained from in situ tests. Measurements of in situ stress prior to excavation have gained more acceptance recently as a standard procedure for major underground civil structures. It has been recognized that earlier knowledge of the stress state can make a substantial cost savings in design and construction of a facility.

Several methods of in situ stress determination (Goodman, 1980) are available and have been used in various geotechnical projects around the world. The methods are grouped in the following manner:

- Complete strain relief by overcoring, including the use of soft gauges or inclusions in a borehole
- Partial strain relief, including the use of rigid elements such as flat jacks, photoelastic inclusions, etc.
- Rock flow or fracture, including hydraulic fracturing, jack fracturing, core discing, etc.
- Correlations between rock properties and stress, and miscellaneous techniques including resistivity, rock noise, and X-ray techniques, etc.

The applicability of any of these methods for stress determination in a jointed/fractured rock such as basalt has not been clearly established and needs to be addressed in additional field tests.

In the absence of site-specific stress measurements, the available geologic data base must be used to obtain an insight into possible stress levels and orientations. The regional tectonic setting sometimes provides the basis for satisfactory determination of stress orientation, but may

9 2 1 2 4 9 5 0 8 6 6

contribute little to an understanding of the stress magnitudes. Core discing, if present, is considered indicative of a horizontal-to-vertical stress ratio greater than 1, but does not provide a quantitative measure of stress.

4.6.2 Stress Measurements by Hydraulic Fracturing

Hydraulic fracturing tests have been conducted to assess the in situ stress state in two boreholes (DB-15 and DC-12 (Fig. 4-15) located approximately 8 to 9.6 kilometers (5 to 6 miles) away from the reference repository location.

The method consists of sealing off a segment of a borehole using a straddle packer and pressurizing the sealed-off segment with water until the borehole ruptures. The pressures obtained at the moment of borehole rupture and in the subsequent pressurization cycles and shut-in operations can be related to the maximum and minimum horizontal stress magnitudes as delineated in the following equations:

$$P_{C1} = 3\sigma_{Hmin} - \sigma_{Hmax} + T - P_o \qquad (4\text{-}1)$$

$$P_s = \sigma_{Hmin} \qquad (4\text{-}2)$$

where

P_{C1} = fracture initiation pressure
P_s = shut-in pressure
T = borehole rupture strength
P_o = pore pressure
σ_{Hmax} = maximum horizontal stress
σ_{Hmin} = minimum horizontal stress.

The minimum horizontal stress is directly measured in shut-in operations. The maximum horizontal stress is determined by rearranging Equation 4-1 after substituting σ_{Hmin} for P_s.

$$\sigma_{Hmax} = 3\,P_s - P_{C1} + T - P_o \qquad (4\text{-}3)$$

Borehole rupture strength (T) is estimated by laboratory test of the cores obtained from the test intervals. Alternately, the differential pressure between the fracture initiation pressure (P_{C1}) and the fracture reopening pressure (P_{C2}) can be used for borehole rupture strength. In our current analysis, the latter method was used.

The directions of the principal stresses are determined by the fracture orientation operation, which employs methods such as impression packer or borehole televiewer. In our tests, the impression packer method was used with a gyroscopic orientation device.

9 2 1 2 4 9 5 0 8 6 7

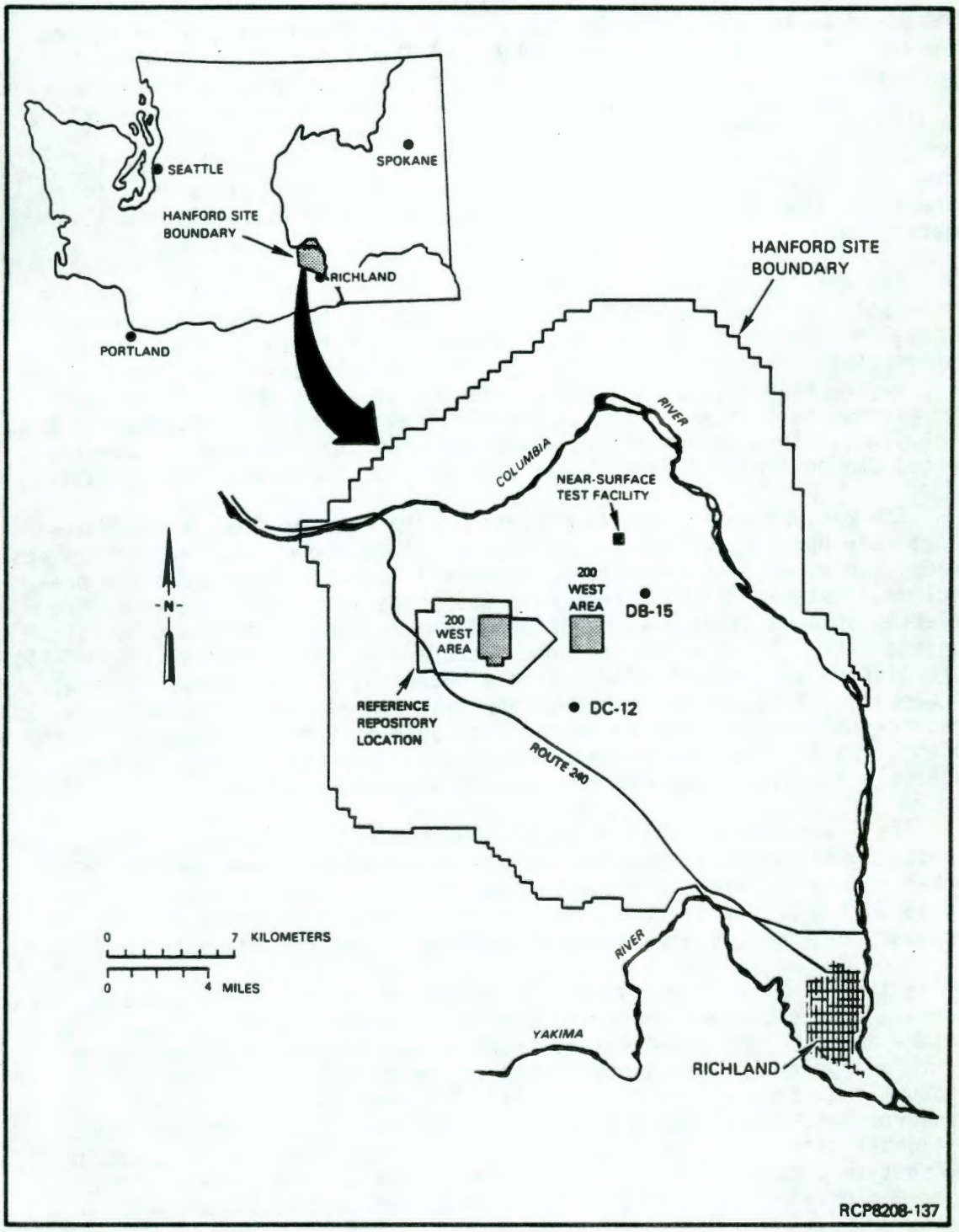

FIGURE 4-15. Map of the Hanford Site Showing Location of Drill Hole DB-15 and DC-12.

The tests in borehole DB-15 (see Fig. 4-15), carried out prior to the DC-12 tests, were intended to evaluate the feasibility of using the hydraulic fracturing method in closely jointed basalt. Tests were conducted 340 meters (1,105 feet) down in the Roza Member. Fracture impressions obtained from two intervals exhibited relatively well-defined vertical fractures orienting generally in a northeast direction. It should be noted that hydrofractures are induced in an axial direction usually regardless of the orientation of the principal stresses. It is understood that the influence of packer pressure is attributed to this phenomenon.

The results obtained from this test show that the least (smallest) principal stress is the vertical stress, and the two horizontal stresses, acting in a northeast and northwest direction, form the maximum and intermediate stresses, respectively. Their magnitudes range from 8.3 to 16.6 megapascals (1,200 to 2,400 pounds per square inch), and the ratio of the maximum horizontal stress to the vertical stress is approximately 2 at that depth. This series of tests demonstrated that the hydrofracturing method can be employed in a basalt rock despite the presence of joints.

The measurement of in situ stress in the Umtanum flow, a candidate repository horizon, was of great interest since the stress information was needed for an ongoing repository conceptual design. Based upon the preliminary tests in DB-15, a test plan was prepared. Test intervals were selected after a careful examination of the core pictures and geophysical logging data. As shown in the core picture of a test interval (Fig. 4-16) core discing was present, indicating a potentially high stress ratio at that depth. Borehole wall impressions taken in an interval with a similar frequency of core discing showed no traceable mechanical fractures on the borehole wall. A permeability test conducted over the entire six test intervals also indicated extremely tight borehole conditions.

The fracturing operations were conducted from the deepest interval to the shallowest without removing the packer assembly to the surface. The packer pressure, borehole pressure, and flow rate were monitored continuously during pressurization. Adjustment of packer pressure became necessary at times to ensure proper sealing of the straddled interval.

A typical plot of pressure-time curves is given in Figure 4-17. The curve indicates a sharp decrease in pressure after the initial borehole rupture and a slightly decreasing trend in shut-in pressure during the first few cycles (probably attributed to the propagation of the hydrofracture away from the borehole wall). The break-down and shut-in pressures were determined and used to calculate the greatest and least horizontal stresses. The shut-in pressures were determined by plotting the shut-in portion of the pressure-time curves on a semi-logarithmic paper and drawing two straight lines, as illustrated in Figure 4-18.

Figure 4-19 presents an impression of a typical hydraulically induced fracture, exhibiting two vertical fractures approximately 180 degrees apart. The causes of the branch fractures shown in the figure have not been established. The test results are summarized in Table 4-11.

9 2 1 2 4 9 5 0 8 6 9

8100459-187cn

FIGURE 4-16. Basalt Core Recovered from Borehole DC-12 at Test Depth Between 1,011 and 1,014 Meters (3,317 and 3,325 feet).

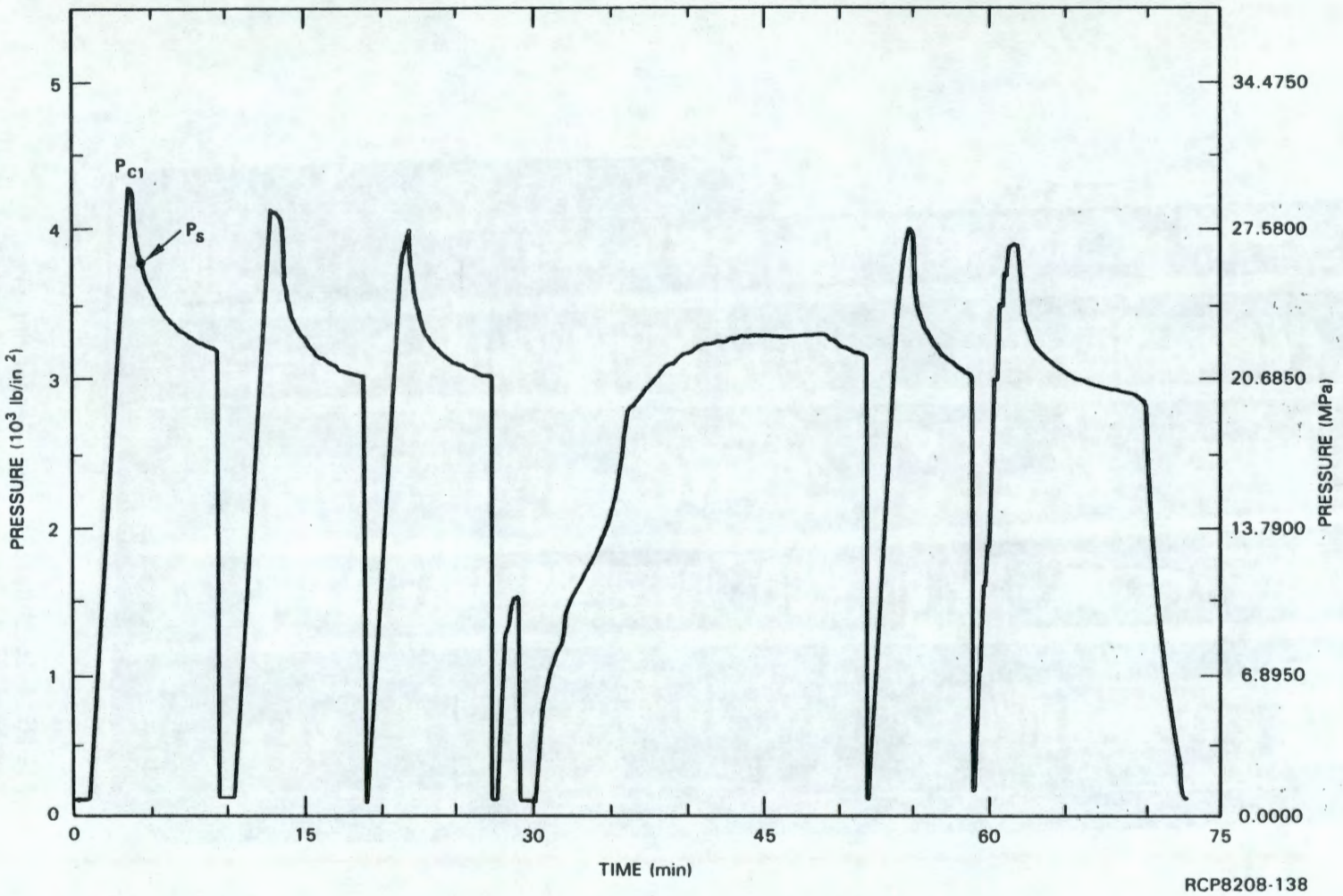

FIGURE 4-17. Typical Pressure-Time Curve Obtained in Borehole DC-12 at Test Depth of 1,013 Meters (3,323 feet).

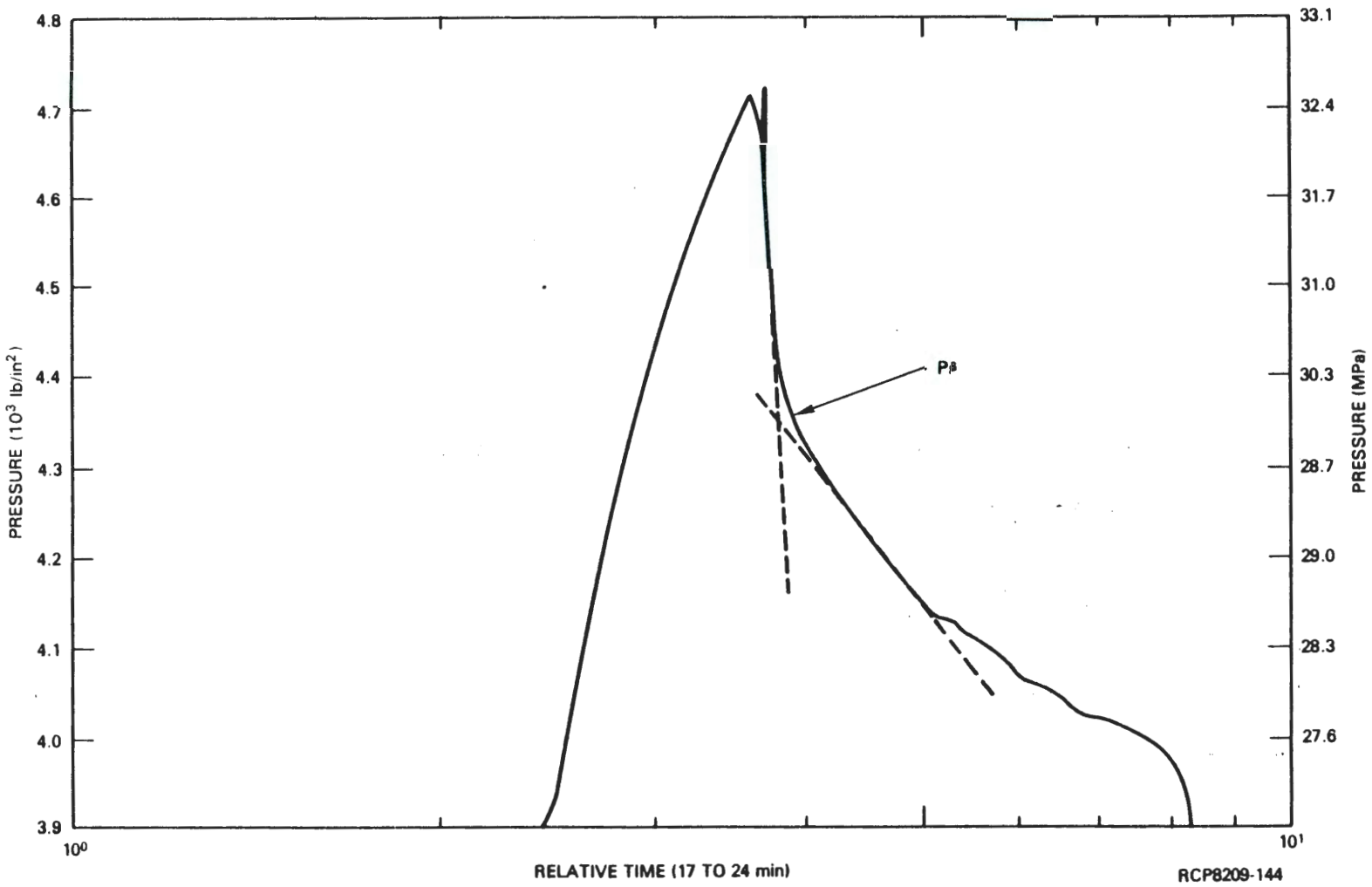

FIGURE 4-18. Pressure-Time Curve Plotted on a Semi-Logarithmic Paper to Determine the Shut-In Pressure at Test Depth of 1,036 Meters (3,400 Feet).

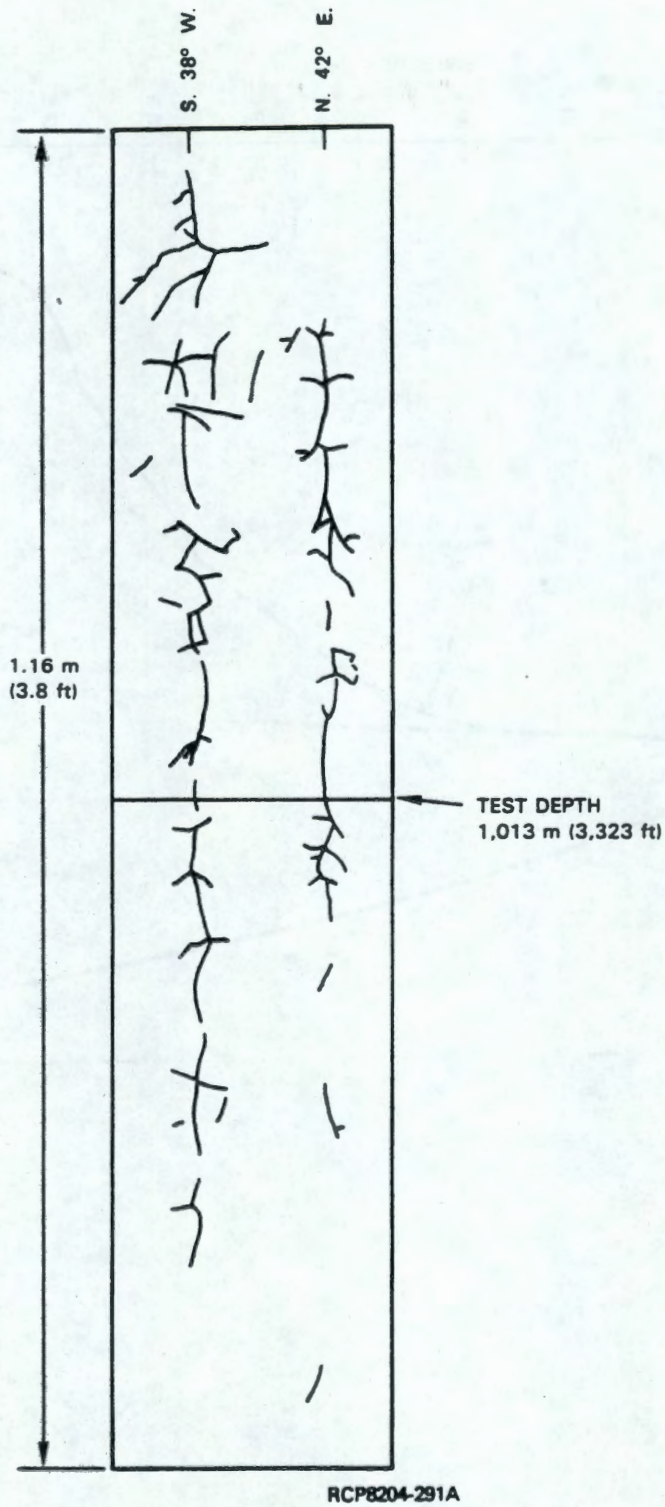

FIGURE 4-19. A Typical Fracture Impression Obtained at Test Depth (1,013 meters (3,323 feet)), Exhibiting Two Vertical Fractures Approximately 180 Degrees Apart.

9 2 1 2 4 9 5 0 8 7 3

TABLE 4-11. Summary of In Situ Stress Data Obtained by the Hydrofracturing Method (Kim and Haimson, 1982).

Borehole number	Test depth, m (ft)	σ_V, MPa (E+03 lb/in^2)	σ_{Hmin}, MPa (E+03 lb/in^2)	σ_{Hmax}, MPa (E+03 lb/in^2)	Fracture orientation	$\frac{\sigma_{Hmax}}{\sigma_{Hmin}}$	$\frac{\sigma_{Hmax}}{\sigma_V}$
DB-15 (Roza)	344 (1,128)	8.3 (1.2)	11.7 (1.7)	16.6 (2.4)	N. 20° E.	1.4	2.0
DC-12 (Umtanum)	1,002 (3,287)	25.6 (3.7)	33.3 (4.8)	55.3 (7.8)	--	1.66	2.15
	1,013 (3,323)	25.9 (3.6)	34.4 (5.0)	63.0 (9.1)	N. 40° E.	1.83	2.43
	1,021 (3,349)	26.1 (3.8)	31.4 (4.6)	53.8 (7.8)	N. 09° E.	1.71	2.06
	1,031 (3,382)	26.4 (3.8)	34.2 (5.0)	58.2 (8.4)	N. 01° E.	1.70	2.21
	1,036 (3,399)	26.5 (3.8)	39.5 (5.7)	71.5 (10.4)	N. 42° E.	1.81	2.70
	1,042 (3,418)	26.7 (3.9)	35.7 (5.2)	65.7 (9.5)	--	1.85	2.47
Mean values	1,024 (3,360)	26.2 (3.8)	34.7 (5.0)	61.2 (8.9)	N. 23° E.	1.76	2.33

The greatest horizontal stresses range from 53.8 to 71.5 megapascals and the least horizontal stresses from 31.4 to 39.5 megapascals (4,550 to 5,730 pounds per square inch). The vertical stresses calculated from the weight of the overburden (gravity logs) range from 25.6 to 26.7 megapascals (3,710 to 3,870 pounds per square inch). These data yield the average ratio of the maximum horizontal to vertical stress of 2.3. The maximum horizontal stress is acting N. 23° E., which is approximately perpendicular to the axis of the Cold Creek syncline at the test location.

Continuing efforts are being made to obtain more representative and statistically meaningful data. Additional tests are to be conducted to define the stress regime quantitatively in the reference repository location prior to the excavation of the exploratory shaft. It is necessary to ascertain the accuracy of the hydrofracturing data by conducting overcoring tests underground when the access tunnel becomes available in the reference repository location.

9 2 1 2 4 9 5 0 8 7 4

As part of the Near-Surface Test Facility site characterization effort, in situ stress measurements were made at the 50-meter (164-foot) level in the Pomona basalt flow. After completion of the facility (Kim, 1980), hydraulic fracturing tests were conducted prior to excavation (Haimson, 1979) and overcoring. Overcoring techniques involve the measurement of deformations experienced by a cylinder or annulus of rock at the bottom of a borehole, as it is detached from the surrounding rock mass (i.e., stress relieved) by drilling. The magnitude of the deformations in various directions can then be related to the in situ stress field through the elastic constants of the rock and elastic theory. The high fracture frequency (12 to 18 fractures per meter (3.6 to 5.5 fractures per foot) caused serious difficulties in conducting the tests and in interpreting the results. The data presented in Table 4-12 illustrate, in part, the difficulty in interpreting in situ stress-measurement data. In these tests there was general agreement on stress orientations. The orientations also agreed with those expected from the geologic structure. Stress magnitudes varied widely enough to be of little value in defining the exact state of stress at the Near-Surface Test Facility.

TABLE 4-12. Comparison of the Three Principal Stresses Measured by Overcoring and Hydrofracturing Methods in Pomona Basalt at the Near-Surface Test Facility Level (Kim, 1980).

	Overcoring method U.S. Bureau of Mines		Hydrofracturing method	
	Magnitudes, MPa (lb/in^2)	Orientations	Magnitudes, MPa (lb/in^2)	Orientations
σ_{Max}	6.9 (1,000)	N. 81° W. (11 degrees up)	13.6 (2,000)	N. 70° W
σ_{Min}	2.1 (300)	N. 8° E. (5 degrees up)	1.0 (150)	N. 20° E.
σ_{Int}	2.1 (300)	S. 65° W. (77 degrees up)	1.4 (200)	Vertical

σ_{Max} = Maximum principal stress.
σ_{Min} = Minimum principal stress.
σ_{Int} = Intermediate principal stress.

The only measurement technique that can presently be utilized in deep boreholes is hydraulic fracturing. This method assumes that the borehole direction is one of the principal stress directions.

Hydraulic fracturing in in situ stress measurements should be coupled with measurements made by an alternate method. The alternate methods also have limitations that may affect their applicability to basalt. As a minimum, it will require considerable judgment and experience in interpreting and applying the results of these tests, as indicated in Table 4-12.

Methods of measurement that rely upon overcoring to obtain the stress are affected by the relatively high joint/fracture frequency in basalt. These and other methods, such as flat jack tests, are limited in that they may be affected by the induced stresses around the opening. Additional work may be needed in modifying and/or developing in situ stressmeasurement techniques for use in basalt. Validation tests and comparisons between several methods are required before confidence can be placed in the quantitative aspects of in situ stress measurements.

4.6.3 Geologic Evidence

Information on past and current tectonic influences in the region and at the repository site was presented in Chapter 3. It indicates that the repository site has experienced a general north-south compression. The magnitude of the stresses cannot be assessed from the geologic evidence, although the presence of core discing (Myers/Price, 1979; Myers and Price, 1981) at various depths and at different drill holes in the Grande Ronde Basalt is taken as indicative of a likely horizontal-to-vertical stress ratio greater than 1. Efforts made to elucidate this phenomenon by core analysis and numerical modeling studies have enhanced the understanding of the rock failure mechanism and served to delineate approximate conditions for which discing might occur (Lenhoff et al., 1982).

Experiences at other underground locations (not in basalt) provide an indication of the range of stress ratios that have been observed in practice. As shown in Figure 4-20, ratios near the 1,000-meter (3,300-foot) level have ranged from about 0.4 to 2.0. Should a high ratio be found at the repository site, it could influence the design, including the shape, size, and orientation of the opening and the cost of constructing the repository, and the near-field sealing requirements. It should be realized, of course, that there is a still-undefined upper limit to the ratio, for which the repository could not be safely constructed and operated.

4.6.4 Summary

Knowledge of the state of stress surrounding the excavations in an underground waste repository in basalt is essential for design and performance assessment. The stress levels have a direct effect on determining the optimum size and shape of the tunnel opening as well as on groundwater flow. The data obtained to date indicate that both the stress magnitudes and orientations are within reasonable ranges expected from the ancillary information, including core discing, geomorphology, and tectonics. Although the stress data obtained at a candidate repository horizon are some 8 kilometers (5 miles) away from the reference repository location, it is reasonable to assume that the stress ratio at the reference repository location is approximately equal to that at the test location.

9 2 1 2 4 9 5 0 8 7 6

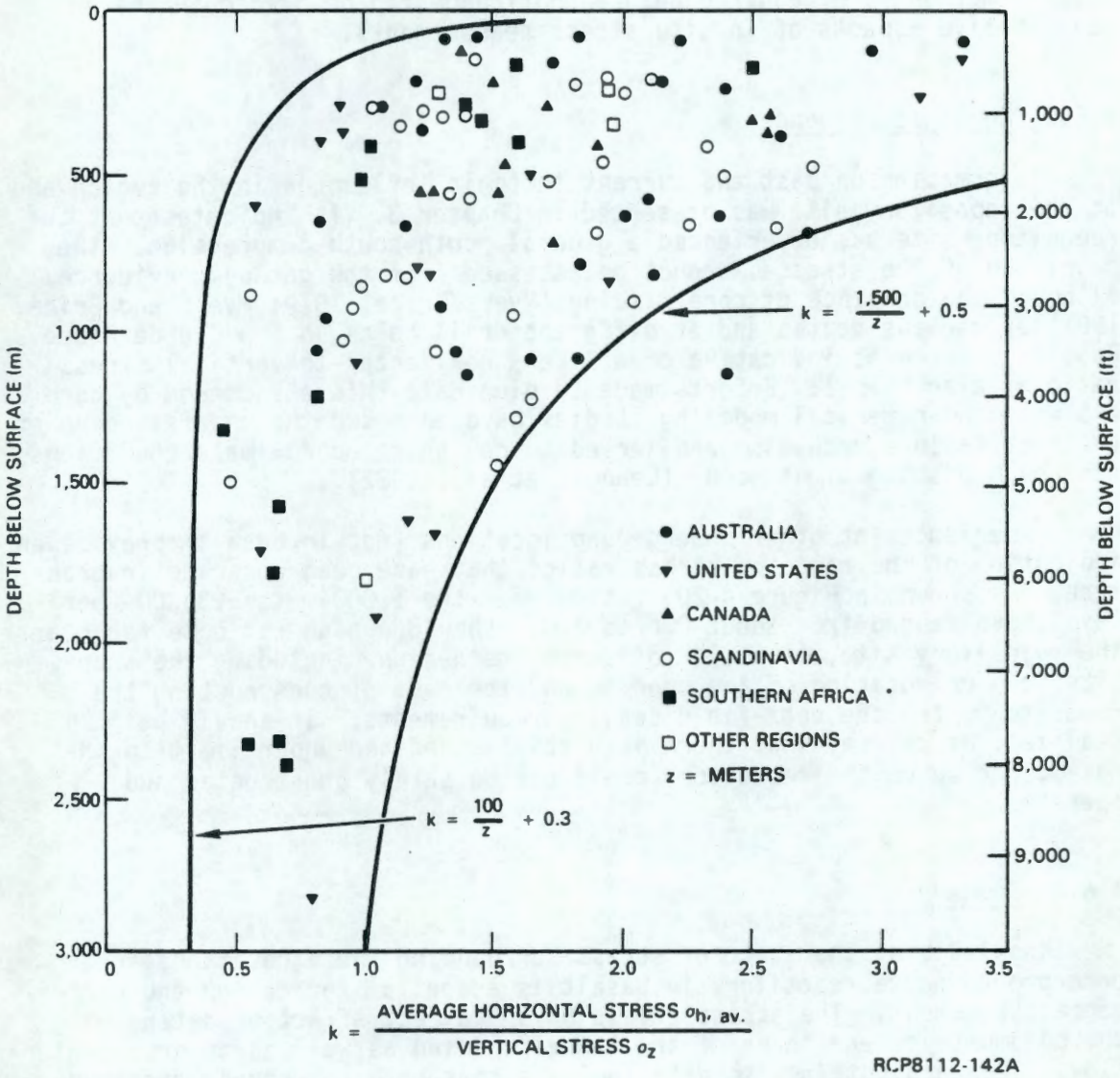

FIGURE 4-20. Variation of Ratio of Average Horizontal Stress to Vertical Stress with Depth Below Surface (Hoek and Brown, 1981).

9 2 1 2 4 9 5 0 8 7 7

As a result of the stress measurement in borehole DC-12, the functional design criteria (BWIP and KE/PB, 1982) were changed from a 1:1 to a 2:1 stress ratio. Additionally, consideration was given to changing the shape of the tunnel to that of a horizontally elongated horseshoe.

Scoping calculations based on empirical methods and two- and three-dimensional numerical modeling studies indicate that the in situ stress and the rock mass strength at the candidate repository horizons will not pose a major problem to repository contribution.

The Basalt Waste Isolation Project is continuing its efforts to establish a more extensive and reliable data base for repository design.

THIS PAGE INTENTIONALLY
LEFT BLANK

4.7 SPECIAL GEOENGINEERING PROPERTIES

No special geoengineering properties of the basalt rock units were considered in the conceptual design of the repository. The following sections address areas that must be studied to successfully design the repository.

4.7.1 Potential for Rock Bursts and Sudden Collapse of Mined Openings

Rock bursts are a coupled effect of the material property (brittle failure characteristics) that permits accumulation of strain energy, structural properties including geologic discontinuities that can permit release of the stored strain energy, and the state of in situ and induced stresses around the mined opening. It is understood that rock burst occurrences decrease rapidly with a decrease in extraction ratio. The conceptual repository design currently requires an extraction ratio of 6 percent. This value is substantially lower than that used in conventional mining where extraction ratios are often 50 percent or higher.

There seems to be no consensus on the mechanism by which such events occur. However, it is clear that bursting as well as smaller scale dynamic failure (e.g., slabbing and spalling) are related to high concentrations of stress in the vicinity of the opening. A room-scale finite-element stress analysis, conducted for the repository conceptual design using the hydrofracturing in situ stress data obtained at the Umtanum horizon and laboratory mechanical property data, has produced no indication of unusual stress conditions. In view of the results of that analysis, the very low extraction ratios, the generally uncomplicated geologic conditions, and the closely jointed nature of the basalt, the possibility for rock bursting would seem remote. This possibility will continue to be examined through activities outlined in Chapter 14.

4.7.2 Potential for Thermal Degradation and Slabbing

Thermal spalling and slabbing is commonly observed when rock material is subjected to heating and thermal shock. In general, rocks with a high quartz content, like quartzite and granite, are more susceptible to thermal fracture and fragmentation than rocks like basalt that have a high glass content. The potential for rock materials, including basalt, to degrade by thermal fracture, spalling, and slabbing has been tested (Thirumalai, 1975; Thirumalai and Demon, 1970). The results show a low potential for basalt thermal degradation in the laboratory. The slabbing phenomenon at depth is a coupled effect of material weakening by heating and prevailing stresses around the opening. While field data on thermal spalling and slabbing of the Umtanum and middle Sentinel Bluffs flows have not yet been obtained, such information for the Pomona flow has been

9 2 1 2 4 9 5 0 8 8 0

generated during tests at the Near-Surface Test Facility. Full-Scale Heater Test No. 2, which was described in Section 4.5, subjected the Pomona basalt to temperatures up to 490°C at the borehole wall. No spalling or slabbing was observed in the before-heating and after-heating photographs. However, several instances of opening of existing small fractures and creation of new small fractures were observed. Analysis of the probable cause and extent of these features is ongoing. Although this information is of a somewhat qualitative nature with regard to predicting the response of the basalt under actual repository conditions where some openings will be larger and stresses higher, the indication is that basalt has a stronger resistance to thermal degradation than do most other rock types.

9 2 1 2 4 9 5 0 3 8 1

4.8 EXCAVATION CHARACTERISTICS OF THE ROCK MASS

4.8.1 General

The selection of an excavation method for repository construction requires careful consideration from several aspects. First, the construction activity can alter the permeability of the rock mass in the vicinity of the excavation by opening preexisting fractures or by creating new ones, thus affecting the radionuclide migration characteristics of the repository. Second, the choice of excavation method will have an influence on the size, shape, and stability of the excavation. Third, the choice of excavation method may influence the rock support requirements during the construction and operation phases.

Two basic methods of excavation (drill-and-blast and tunnel boring) are available and applicable for repository construction. In all probability, some portions of the repository will be excavated using drill-and-blast techniques, regardless of a decision to use the tunnel boring method. Construction experience in near-surface basalt suggests that both approaches are feasible.

4.8.2 Existing Basalt Construction Experience

Universal experience with both the drill-and-blast and the tunnel boring methods in the construction industry and in a limited number of research projects has indicated the potential for significant differences in rock-mass disturbance, resultant near-field stress-field characteristics, and support requirements, depending on the excavation method used. Existing excavations in basalt have only a limited potential for contributing to an understanding of the effect of the excavation method on the rock mass, for several reasons. First, a suitable technology for evaluating construction-induced rock-mass changes has not been developed and validated that can be applied at the construction site in a meaningful way. Second, no deep excavations exist in basalt that are similar to expected repository conditions. Third, there is no experience with roof support or rock response on the room scale at expected repository mechanical stress and thermal loads.

In a survey of known basalt excavation projects, 19 structures were identified, including tunnels for rail and vehicular transportation and hydroelectric power facilities. A list of the projects and their locations is given in Table 4-13. The tunnel depths ranged from 20 to approximately 80 meters (65 to 260 feet). Tunnel widths varied from 2.5 to 15 meters (8 to 49 feet). Even with the widely varying types and conditions of basalt flows encountered in these projects, a general summary of the construction experiences was possible.

9 2 1 2 4 9 5 0 8 3 2

TABLE 4-13. Construction Projects Completed in Basalt.

Structure	Location
Bacon Tunnel	Coulee City, Washington
Baltimore Tunnel	Dumbartonshire, Scotland
Black Butte Dam, diversion tunnel	Orland, California
Burlington Northern Railroad Tunnel	Pasco, Washington
Cougar Dam, diversion tunnel	Willamette Basin, Oregon
Foster Dam, diversion tunnel	South Santiam River, Oregon
Green Peter Dam, diversion tunnel	Middle Santiam River, Oregon
Highway No. 14 Tunnel	Vancouver, Washington
Krafla Geothermal Power Plant	Krafla, Iceland
Keweenawan Copper Mines	Keweenaw Peninsula, Michigan
Lost Creek Lake, outlet and diversion tunnel	Medford, Oregon
Lucky Peak Dam, outlet tunnel	Boise River, Idaho
Mahi Hydel Hydroelectric Power Plant	Deccan Basin, India
Park River Tunnel	Hartford, Connecticut
Poatina Underground Power Station	Central Tasmania
River Sog Hydroelectric Development	Reykjavic, Iceland
Snoqualmie Falls Hydroelectric Project (turbine chamber, headrace, and tailrace tunnels)	Snoqualmie, Washington
Vista Ridge Tunnel	Portland, Oregon
Amchitka Shaft	Amchitka, Alaska

For drill-and-blast construction, which encompasses all but two of the projects, excavation into columnar or entablature zones produces a generally stable cavity with minimal support requirements. Overbreak of up to 1 meter (3.3 feet) was observed on some of the projects, with overbreak morphology controlled by the joint system. Excavation into vesicular or flow-breccia zones will require greater, but not excessive, support requirements. These zones usually produce less overbreak.

The Baltimore Tunnel near Dumbartonshire, Scotland and the Park River Tunnel in Hartford, Connecticut were driven using a tunnel boring machine. The machine performed satisfactorily in competent basalt, but had to be withdrawn when weathered zones of flow breccia were encountered in the Baltimore Tunnel.

The basalt excavations identified in the survey (including the Near-Surface Test Facility) were not constructed as controlled research projects allowing for assessment of rock damage as a function of the excavation method. This, plus the lack of technology available at the time of construction to assess changes, and the different stress conditions between the near-surface facility and the repository horizon, make an evaluation of the existing basalt excavations of little quantitative value. Controlled excavation methods need to be utilized during the early stages of underground development to provide this data base. A study prepared for the exploratory shaft architect-engineer has evaluated the feasibility of using tunnel boring machine technology in the basalts at Hanford. This report concludes that current tunnel boring machine technology can be successfully applied in rocks with compressive strengths on the order of 276 to 414 megapascals (40,000 to 60,000 pounds per square inch) and under conditions similar to those anticipated in the candidate repository horizons. However, current technology must be extended for tunnel boring machine techniques to be applied to noncircular openings.

4.8.3 Excavation Effects on the Rock Mass

When an underground excavation is made in rock, stresses are redistributed around the opening. An understanding of this redistribution is helpful from a waste isolation performance assessment viewpoint because it affects: (1) the permeability of the rock mass adjacent to the opening, (2) the stability of the opening, and (3) the optimization of a rock support method.

From several standpoints, the selection and optimization of an excavation method is a significant factor in determining the stress distribution and ensuring the integrity of the openings. The excavation method may create additional fractured rock (e.g., by blasting) or may open and/or extend existing fractures. While it is generally considered that tunnel boring methods create less damage than conventional drill-and-blast techniques, this difference is not easily quantified. Additionally, careful use of controlled blasting, presplitting, and other techniques can reduce blast damage.

Future efforts to characterize the nature and extent of both stress redistribution and excavation-induced disturbance are addressed in Chapter 14.

The choice of excavation method can also limit the shape of the opening, which in turn affects the stress redistribution and stability. Tunnel boring methods produce circular openings, while drill-and-blast methods can produce a variety of shapes.

The choice of excavation method and the associated stress distribution about the opening can influence the choice and performance of the roof support system. The roof support system, in addition to providing for opening stability, can function to limit changes in the rock-mass

permeability in the vicinity of the excavation. There is no existing experience with which to evaluate the performance of the room-scale rock mass and rock supports under expected repository thermal loads. Test needs in this area will require further assessment.

4.8.4 Summary

A review of the excavation characteristics of basalt presented in this section leads to the conclusion that there is limited excavation experience in basalt of characteristics similar to the candidate horizons at the potential repository depths. An assessment of various excavation techniques will be completed prior to final design.

4.9 SUMMARY OF UNRESOLVED ISSUES

A comprehensive evaluation of the current geoengineering test program and results has identified issues related to site characterization, repository design and construction, and performance assessment, which need resolution in order to complete the development of a nuclear waste repository in basalt. These issues are identified in Chapter 14 together with the plans for their resolution.

THIS PAGE INTENTIONALLY
LEFT BLANK

4.10 REFERENCES

Agapito, J. F. T., Hardy, M. P., and St. Laurent, D. R., 1977, Geo-Engineering Review and Proposed, Program Outline for the Structural Design of a Radioactive Waste Repository in Columbia Plateau Basalts, RHO-ST-6, Rockwell Hanford Operations, Richland, Washington, September 1977.

ASTM, 1969, Standard Method for Laboratory Determination of Pulse Velocities and Ultrasonic Elastic Constants of Rock, D-2845, American Society for Testing and Materials, Philadelphia, Pennsylvania.

ASTM, 1971, Standard Test Methods for Unconfined Compressive Strength of Intact Rock Core Specimens, D-2938, American Society for Testing and Materials, Philadelphia, Pennsylvania.

ASTM, 1972, Standard Test Methods for Elastic Moduli of Rock Core Specimens in Uniaxial Compression, D-3148, American Society for Testing and Materials, Philadelphia, Pennsylvania.

ASTM, 1973, Standard Test Method for Mean Specific Heat of Thermal Insulation, C-351, American Society for Testing and Materials, Philadelphia, Pennsylvania.

ASTM, 1974, Standard Test Method for Triaxial Compressive Strength of Undrained Rock Core Specimens without Pore Pressure Measurements, D-2664, American Society for Testing and Materials, Philadelphia, Pennsylvania.

ASTM, 1976a, Standard Test Method for Modulus of Rupture of Natural Building Stone, C-99, American Society for Testing and Materials, Philadelphia, Pennsylvania.

ASTM, 1976b, Standard Method of Test for Thermal Conductivity of Materials by Means of the Heat Flow Meter, C-518, American Society for Testing and Materials, Philadelphia, Pennsylvania.

ASTM, 1977, Standard Test Methods for Absorption and Bulk Specific Gravity of Natural Building Stone, C-97, American Society for Testing and Materials, Philadelphia, Pennsylvania.

Brown, E. T., 1981, Rock Mass Characterization, Testing and Monitoring, ISRM Suggested Methods, Pergamon Press, New York, New York, pp. 3-52.

BWIP and KE/PB, 1982 Nuclear Waste Repository in Basalt, Project B-301, Functional Design Criteria, RHO-BW-DC-1 P, Staff, Basalt Waste Isolation Project and KE/PB, A Joint Venture of Kaiser Engineers, Inc. and Parsons Brinckerhoff Quade & Douglas, Inc., for Rockwell Hanford Operations, Richland, Washington, March 1982.

CSM, 1978, Final Report for Fiscal Year 1978 on the Physical and Thermal Properties of Basalt Cores, RHO-BWI-C-38, Colorado School of Mines for Rockwell Hanford Operations, Richland, Washington, December 1978.

Danielson, G. C. and Sidles, P. H., 1969, "Thermal Diffusivity and Other Non-Steady-State Methods," in Thermal Conductivity, Tye, R. P., ed., Academic Press, New York, New York, pp. 149-199.

Duvall, W. I., Miller, R. J., and Wang, F. D., 1978, Preliminary Report on Physical and Thermal Properties of Basalt, Drill Hole DC-10; Pomona Flow-Gable Mountain, RHO-BWI-C-11, Colorado School of Mines for Rockwell Hanford Operations, Richland, Washington, May 1978.

Erikson, R. L. and Krupka, K. M., 1980, Thermal Property Measurements of Pomona Member Basalt from Core Holes DB-5 and DB-15, Hanford Site, Southeastern Washngton, RHO-BWI-C-76, Pacific Northwest Laboratory for Rockwell Hanford Operations, Richland, Washington, May 1980.

FSI, 1980a, Thermal/Mechanical Properties of Pomona Member Basalt-Full-Scale Heater Test #1 (Area 1), RHO-BWI-C-77, Foundation Sciences, Inc. for Rockwell Hanford Operations, Richland, Washington, July 1980.

FSI, 1980b, Thermal/Mechanical Properties of Pomona Member Basalt-Full--Scale Heater Test #2 (Area 2), RHO-BWI-C-85, Foundation Sciences, Inc. for Rockwell Hanford Operations, Richland, Washington, November 1980.

FSI, 1980c, Thermal/Mechanical Properties of Pomona and Umtanum Basalts--Elevated Temperature Comparative Triaxial Test, RHO-BWI-C-91, Foundation Sciences, Inc. for Rockwell Hanford Operations, Richland, Washington, December 1980.

FSI, 1981a, Thermal/Mechanical Properties of Umtanum Basalt - Borehole DC-2, RHO-BWI-C-92, Foundation Sciences, Inc. for Rockwell Hanford Operations, Richland, Washington, January 1981.

FSI, 1981b, Thermal/Mechanical Properties of Pomona Member Basalt - Area 3 and Summary, RHO-BWI-C-100, Foundation Sciences, Inc. for Rockwell Hanford Operations, Richland, Washington, February 1981.

Goldsmith, A., Waterman, T. E., and Hirschborn, H. J., 1961, Handbook of Thermophysical Properties of Solid Materials, Vol. I Elements, pp. 247-260; Vol. III Ceramics, pp. 891-904, MacMillan Company, New York, New York.

Goodman, R. E., 1980, Introduction to Rock Mechanics, John Wiley & Sons, New York, New York.

Haimson, B. C., 1979, Hydraulic Fracturing Results at Gable Mountain, LBL-7061, Lawrence Berkeley Laboratory, Berkeley, California.

Heuzé, F. E. and Salem, A., 1976, "Plate Bearing and Borehole Jack Tests in Rock - A Finite Element Analysis," in Proceedings of the 17th Symposium on Rock Mechanics, Snowbird, Utah.

Hocking, G., Williams, J. R., Boonlualohr, P., Mathews, I. C., and Mustoe, G., 1980, Numerical Prediction of Basalt Response for Near-Surface Test Facility Heater Tests #1 and #2, RHO-BWI-C-86, Dames & Moore for Rockwell Hanford Operations, Richland, Washington, September 1980.

Hoek, E. and Brown, E. T., 1981, Underground Excavation in Rock, Institution of Mining and Metallurgy, London, England.

Hustrulid, W. A., 1976, "An Analysis of the Goodman Jack," in Proceedings of the 17th Symposium on Rock Mechanics, Snowbird, Utah.

Kim, K., 1980, "Rock Mechanics Field Test Results to Date," in Basalt Waste Isolation Project Annual Report - Fiscal Year 1980, RHO-BWI-80-100, Rockwell Hanford Operations, Richland, Washington, November 1980, pp. V-26-V-34.

Kim, K. and Haimson, B. C., 1982, In Situ Stress Measurement at a Candidate Repository Horizon, RHO-BW-SA-257 P, Rockwell Hanford Operations, Richland, Washington, September 1982.

Lama, R. D. and Vutukuri, V. S., 1978, Handbook on Mechanical Properties of Rocks, Volumes 1-4, TransTech Publications, Aedermannsdorf, Switzerland.

Lehnhoff, T. F., Stefansson, B., Thirumalai, K., and Wintczak, T. M., 1982, The Core Disking Phenomenon and its Relation to In Situ Stress at Hanford, RHO-BW-ST-41 P, University of Missouri-Rolla, Parsons Brinckerhoff Quade & Douglas, Inc. for Rockwell Hanford Operations, Richland, Washington, April 26, 1982.

Martinez-Baez, I. F. and Amick, C. H., 1978, Thermal Properties of Gable Mountain Basalt Cores, Hanford Nuclear Reservation, LBL-7038, Lawrence Berkeley Laboratory, Berkeley, California.

Miller, R. J., 1979a, Determination of Basalt Physical and Thermal Properties at Varying Temperatures, Pressures, and Moisture Contents, Second Progress Report, Fiscal Year 1979, RHO-BWI-C-54, Colorado School of Mines for Rockwell Hanford Operations, Richland, Washington, August 13, 1979.

Miller, R. J., 1979b, Determination of Basalt Physical and Thermal Properties at Varying Temperatures, Pressures, and Moisture Contents, Third Progress Report, Fiscal Year 1979, RHO-BWI-C-55, Colorado School of Mines for Rockwell Hanford Operations, Richland, Washington, August 13, 1979.

Miller, R. J. and Bishop, R. C., 1979, Determination of Basalt Physical and Thermal Properties at Varying Temperatures, Pressures, and Moisture Contents, First Progress Report, Fiscal Year 1979, RHO-BWI-C-50, Colorado School of Mines for Rockwell Hanford Operations, Richland, Washington, March 26, 1979.

Myers, C. W./Price, S. M., and Caggiano, J. A., Cochran, M. P., Czimer, W. J., Davidson, N. J., Edwards, R. C., Fecht, K. R., Holmes, G. E., Jones, M. G., Kunk, J. R., Landon, R. D., Ledgerwood, R. K., Lillie, J. T., Long, P. E., Mitchell, T. H., Price, E. H., Reidel, S. P., and Tallman, A. M., 1979, Geologic Studies of the Columbia Plateau: A Status Report, RHO-BWI-ST-4, Rockwell Hanford Operations, Richland, Washington, October 1979.

Myers, C. W. and Price, S. M. eds., 1981, Subsurface Geology of the Cold Creek Syncline, RHO-BWI-ST-14, Rockwell Hanford Operations, Richland, Washington, July 1981.

Schmidt, B., Daly, W. F., Bradley, S. W., Squire, P. R., and Hulstrom, L. C., 1980, Thermal and Mechanical Properties of Hanford Basalts; Compilation and Analyses, RHO-BWI-C-90, KE/PB, A Joint Venture of Kaiser Engineers, Inc./Parsons Brinckerhoff Quade & Douglas, Inc. for Rockwell Hanford Operations, Richland, Washington, October 1980.

Shuri, F. S., Dodds, D. J., and Kim, K., 1980, Measurement of Rock-Mass Deformation Properties by the Borehole Jacking Method at the Near-Surface Test Facility, RHO-BWI-C-89, Foundation Sciences, Inc. for Rockwell Hanford Operations, Richland, Washington, October 1980.

Swanson, D. A. and Wright, T. L., 1978, "Bedrock Geology of the Northern Columbia Plateau and Adjacent Areas," in Baker, V. R. and Nummedal, D., eds., The Channeled Scabland: Planetary Geology Program, A Guide to the Geomorphology of the Columbia Basin, Washington, Office of Space Science, National Aeronautics and Space Administration, Washington, D.C., pp. 37-57.

Thirumulai, K., 1975, "Rock Mechanics and Development of Advanced Hard Rock Breaking Methods," in Proceedings of Fifteenth Symposium on Rock Mechanics, Hoskins, E. R., ed., American Society of Civil Engineers, New York, New York, pp. 449-467.

Thirumalai, K. and Demon, S. V., 1970, "Thermal Expansion Behavior of Rock and its Significance to Removal Fragmentation," Journal of Applied Physics, Vol. 41, No. 13, pp. 5,147-5,151.

9 2 1 2 4 9 5 0 8 9 1

5. HYDROGEOLOGY

This chapter addresses the hydrogeology of the Columbia River basalts and overlying sediments found beneath or within the vicinity of the Hanford Site (Fig. 5-1). The chapter is divided into two major sections. Section 5.1 addresses the hydrogeologic conditions occurring both within and surrounding the reference repository location. Section 5.2 deals with those hydrologic characteristics expected to be found within the reference repository location during site characterization studies.

Hydrogeologic data are key inputs into the assessment of repository performance and the evaluation of the potential for nuclear waste isolation in basalt. The results of numerical analyses of postclosure groundwater travel times and waste transport are addressed in Chapter 12.

Chapter 13 summarizes the work activities planned to resolve specific technical questions regarding the nature and dynamics of the groundwater system significant in evaluating waste isolation in a basalt medium.

5.1 REGIONAL AND SITE HYDROGEOLOGIC INVESTIGATIONS

5.1.1 Introduction

One of the initial activities of the Basalt Waste Isolation Project (BWIP) involved a compilation and review of available literature, data, and other information pertaining to the hydrogeology of the Columbia Plateau, emphasizing the Pasco Basin. This effort culminated with two series of documents:

- A set of bibliographies, listing and describing available local, state, and federal governmental and university and private reports relating to the geology and hydrology within the Columbia Plateau region (Bela, 1979; Strowd, 1978; Summers and Schwab, 1978; Tanaka and Wildrick, 1978)

- A series of integration reports on the geology, hydrology, and geochemistry of the Columbia River basalt (Myers/Price et al., 1979; Gephart et al., 1979a; Smith et al., 1980; respectively).

Collectively, these documents constitute a summary of hydrogeologic information assembled to the referenced date and are, therefore, considered to be an important informational baseline upon which portions of this chapter are based.

With regard to specific information on the Columbia River basalt at the Hanford Site, the integration reports (Myers/Price et al., 1979; Gephart et al., 1979a; Smith et al., 1980) provide a comprehensive overview. Gephart et al. (1979a) contains a summary and evaluation of hydrologic test data gathered at the Hanford Site prior to 1979. A listing of

9 2 1 2 4 9 5 0 8 9 2

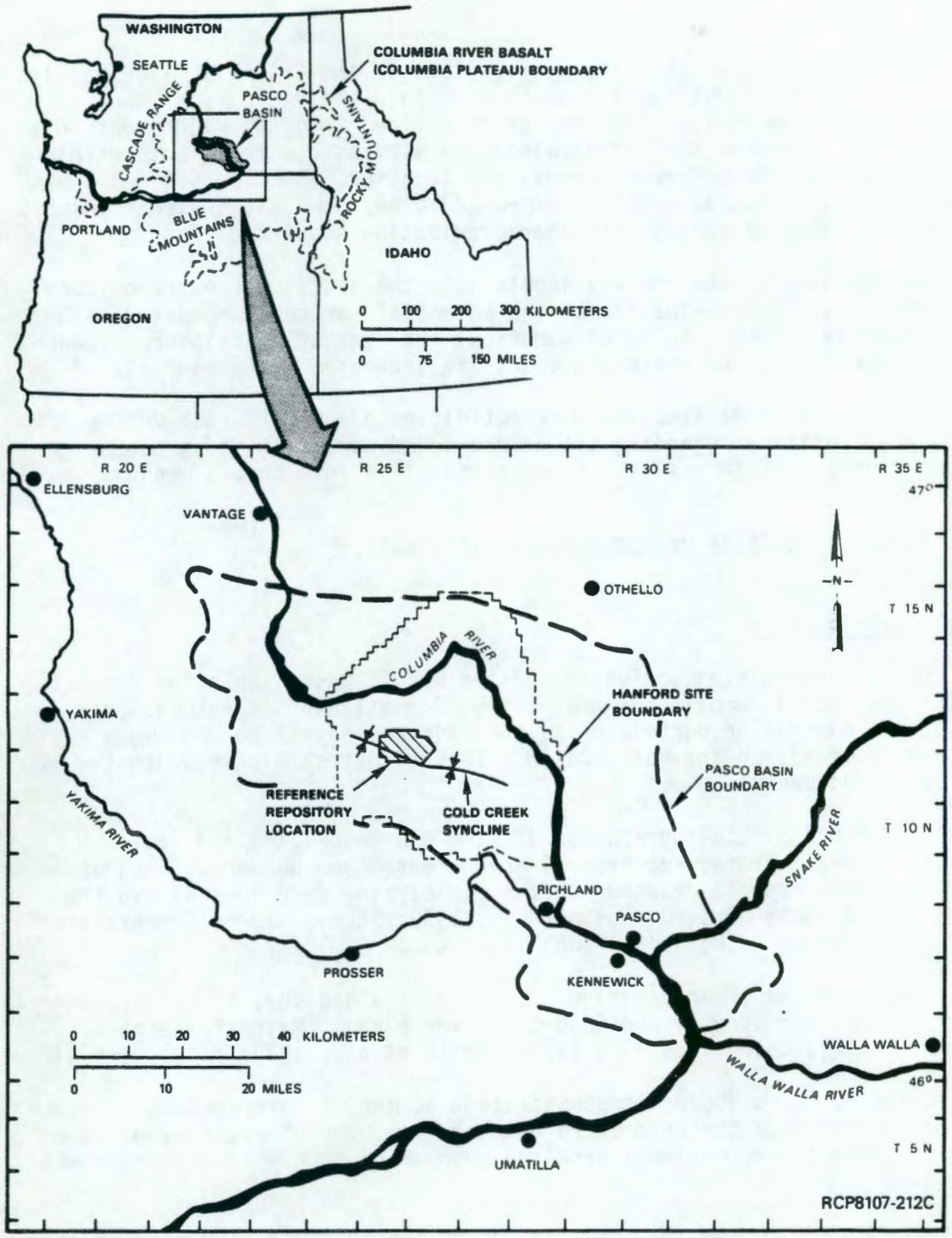

FIGURE 5-1. Geographic Setting of the Pasco Basin.

organizations that have been or are involved in the hydrologic testing effort are listed in Table 5-1 along with a brief identification of work accomplished and the boreholes and strata tested. In examining this table, it is seen that hydrologic characterization at the Hanford Site has intensified significantly since 1978. The locations and basalt horizons where this testing has taken place are shown in Figure 5-2 (a, b, c). Descriptions for most of these boreholes may be found within Myers/Price et al. (1979). Hydrologic tests are now (September 1982) being conducted in two new boreholes (RRL-6 and -14) sited in the reference repository location. Borehole RRL-14 is not located on Figure 5-2 because hydrologic data are yet unavailable for inclusion in this report. However, for general reference, borehole RRL-14 is located 3 kilometers northwest of borehole RRL-2.

5.1.2 Rock Units

Rock units that occur within the Columbia Plateau include the formations of the Columbia River Basalt Group and surficial sedimentary deposits. Within the Pasco Basin, the surficial deposits include sediments of the Hanford and Ringold Formations. Formations of the Columbia River Basalt Group that crop out in the Pasco Basin include the Saddle Mountains, Wanapum, and Grande Ronde Basalts. General information concerning the areal extent and thickness of these formations is presented in Table 5-2. The stratigraphy and lithology of these formation are discussed in Chapter 3. The following hydrogeologic descriptions of these units pertain primarily to the Pasco Basin.

5.1.2.1 Hanford and Ringold Formations. The Hanford and Ringold Formations are found extensively within the low-lying areas of the Pasco Basin. Groundwater within the Hanford and Ringold Formations exists under unconfined aquifer conditions, except where locally semiconfined in the lower portion of the Ringold Formation. The thickness of the unconfined aquifer at the Hanford Site ranges from 0 to over 60 meters. The base of this aquifer is defined by either the silt and clay sediment characteristic of the lower portion of the Ringold Formation or the upper surface of the underlying Columbia River basalt.

Hydrogeologically, the unconfined aquifer is strongly influenced by the presence of the middle portion of the Ringold Formation, which is composed of well-sorted sands and gravels under varying degrees of cementation (Gephart et al., 1979a). The degree of induration and thickness has a direct bearing on the hydraulic characteristics of this aquifer. The transmissivity and equivalent hydraulic conductivity of the unconfined aquifer range from 10^{-3} to 10^{0} meters squared per second and 10^{-5} to 10^{-2} meters per second, respectively. Storativity values of 10^{-2} to 10^{-1} fall within the range commonly cited for unconfined systems (Heath and Trainer, 1968).

TABLE 5-1. Principal Groups Involved in Basalt Hydrologic Testing.

Date	Group	Borehole*	Work accomplished	Basalt formation
1968	Raymond and Tillson (1968), Battelle, Pacific Northwest Laboratories	RSH-1	7 drill stem tests, 7 head measurements	Grande Ronde
1969	LaSala and Doty (1971), U.S. Geological Survey	DC-1	4 pumping tests, 11 fluid injection and withdrawal tests, 22 head measurements, water samples	Saddle Mountains, Wanapum, and Grande Ronde
1977	Gephart et al. (1979b), Rockwell Hanford Operations	RSH-1	7 withdrawal and injection tests, water samples	Grande Ronde
1978	SAI (1978), Science Applications, Inc.	DC-2	6 injection tests, 2 head measurements	Grande Ronde
1978	Apps et al. (1979), Lawrence Berkeley Laboratory	DC-2	6 head measurements, 1 water sample	Grande Ronde
		DC-6	15 head measurements, 12 flow tests, 1 water sample	Grande Ronde
		DC-8	4 head measurements	Wanapum
1978	W. K. Summers and Associates	8 springs	8 water samples	Saddle Mountains and Wanapum
1978-79	Rockwell Hanford Operations	DB-1, -2, -4, -5, -7, -9, -10, -11, -12, -13, -14; DH-8; and WPPSS-3	20 head measurements, 12 pump tests, 10 water samples	Saddle Mountains and Wanapum
		4 irrigation wells in Cold Creek Valley area	4 head measurements, 1 pump test, 4 water samples	Wanapum
1980-82	Rockwell Hanford Operations	DB-1, -2, -4, -5, -7, -9, -10, -11, -12, -13, -14, -15; DC-3, -6, -7, -8, -12, -14, -15, -16A; DH-8; 699-S11-E12A; BH-16; RRL-2, -6; 47-50, 50-45, 50-48, 51-46, 52-46, 52-48, 53-50; 4 irrigation wells; and 15 springs	Approximately 145 separate intervals in the noted boreholes have had constant discharge, constant drawdown, displacement, constant head injection tests, water samples, and/or head measurements made.	Saddle Mountains, Wanapum, and Grande Ronde

*Boreholes in which hydrologic tests have been conducted.

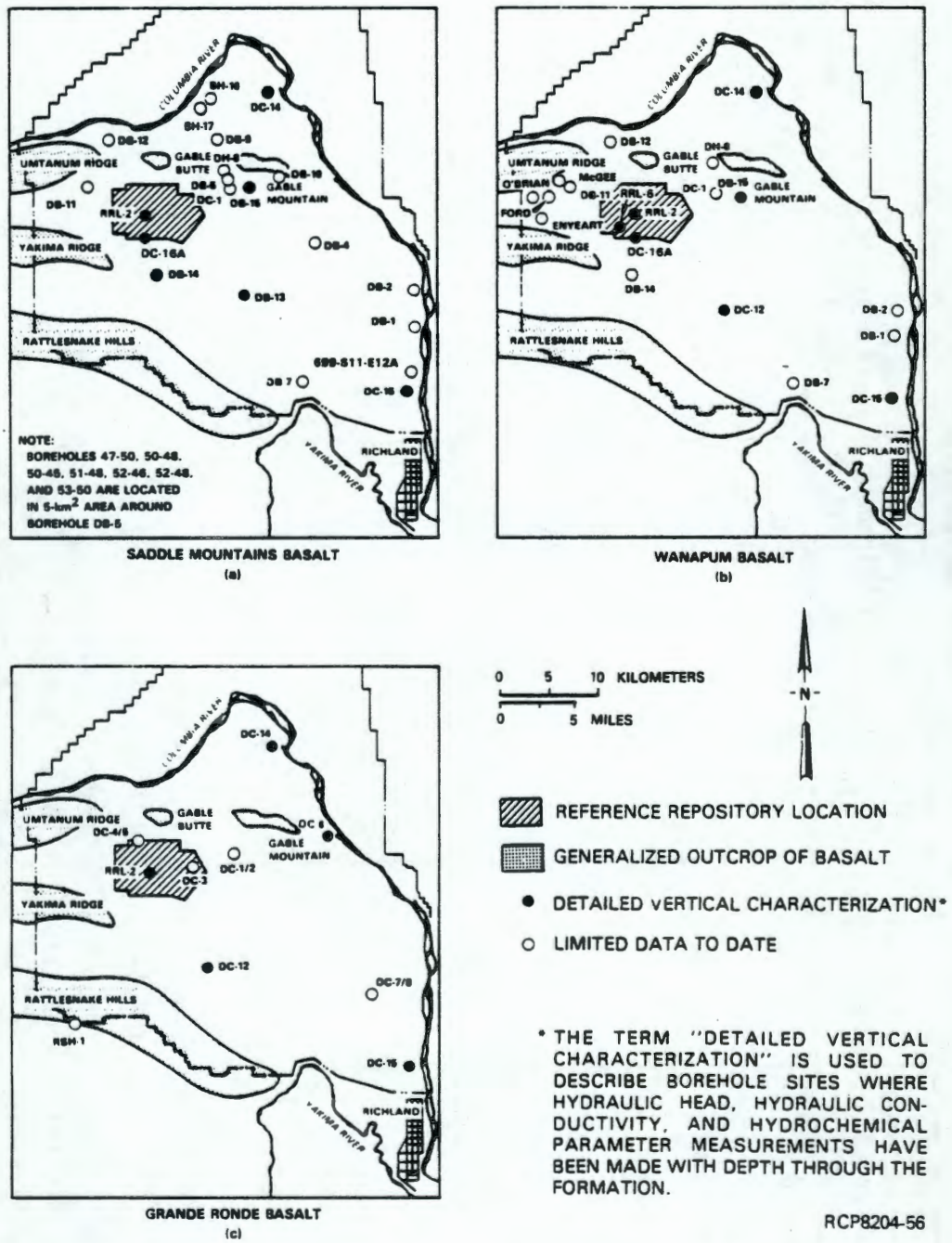

FIGURE 5-2. Hydrologic Test Sites for Individual Formations Within the Columbia River Basalt Group.

TABLE 5-2. Dimensional Statistics of the Principal Stratigraphic Units Within the Columbia Plateau.

Stratigraphic interval	Volume[a] ($km^3 \times 10^3$)	Columbia River basalt (vol%)	Maximum thickness (m)	Maximum areal extent[b] ($km^2 \times 10^3$)	Area of outcrop[c] ($km^2 \times 10^3$)
Ringold	ND	ND	ND	ND	8
Saddle Mountains	2.5	<1	290[d]	32	8
Wanapum	10	3.1	350[d]	83	31
Grande Ronde	275	85	2,750[a]	112	12
Picture Gorge	17.5	5.4	300[e]	9	ND
Imnaha	20	6.2	500[f]	21	0.05
Pre-basalt basement	ND	ND	ND	ND	0.5

NOTE: Statistics apply to the areas mapped and depicted on Figures 5-3 and 5-4.

ND = Not determined

[a]Estimated from Reidel et al. (1981)

[b]Estimated from Swanson and Wright (1978)

[c]Estimated from Myers/Price et al. (1979)

[d]Estimated from Reidel and Fecht (1981)

[e]Estimated from Swanson et al. (1979)

[f]Estimated from Kleck (1976).

5.1.2.2 Columbia River Basalt Group. The areal geometry of the principal formations within the Columbia River Basalt Group and the overlying sediment is shown in Figure 5-3. The occurrence and areal distribution of these different basalt formations are important in defining groundwater movement both within the Columbia Plateau and the Pasco Basin (Gephart et al., 1979a). Areas of groundwater recharge and discharge are addressed in Sections 5.1.4 and 5.1.10. The locations of outcrops of Saddle Mountains, Wanapum, and Grande Ronde Basalts are shown in Figure 5-4, along with post-basalt sediment outcrops. In examining Figures 5-3 and 5-4, the following observations are made:

- Although the Grande Ronde Basalt is the most areally extensive formation within the Columbia River Basalt Group, it has been successively covered by the Wanapum and Saddle Mountains Basalts. As a result, there are few outcrops of the Grande Ronde Basalt within the Pasco Basin. Hydrologically, this is believed to be an important consideration in regard to direct surface or near-surface recharge of the Grande Ronde Basalt.

- Outcrops of the Grande Ronde Basalt tend to be situated along the outer fringe of the Columbia Plateau and in the central portion of the Columbia Plateau (i.e., Pasco Basin) where surface erosion has exposed this formation. (Refer to Chapter 3 for details regarding the location of geologic structures.) Groundwater recharge of the Grande Ronde Basalt is believed to occur principally where the formation is at or near ground surface. Recharging may also take place as a result of leakage from overlying formations.

- The Saddle Mountains Basalt crops out along the edges of the Pasco Basin, but is mainly covered in the central portion of the Pasco Basin by post-basalt sediments. (Another major outcrop of Saddle Mountains Basalt is found along the Snake River near the Washington-Idaho border.) The Saddle Mountains Basalt is recharged within or near the Pasco Basin.

- For most regional hydrogeologic purposes, the Grande Ronde and Wanapum Basalts can be considered present and contiguous as units throughout the region, whereas basalt flows of the Saddle Mountains Basalt are generally discontinuous.

- Basalts older than the Grande Ronde (i.e., Imnaha and Picture Gorge Basalts) are probably of comparatively minor interest to the regional hydrology due to their limited locations, volumes, areal extent, and depth (Table 5-2).

The dimensional statistics of the principal stratigraphic units within the Columbia Plateau that support the above observations are summarized in Table 5-2. The Grande Ronde Basalt is regionally significant by virtue of its greater thickness and volume across the Columbia Plateau compared to the other basalt formations in the Columbia Plateau.

9 2 1 2 4 9 5 0 8 9 8

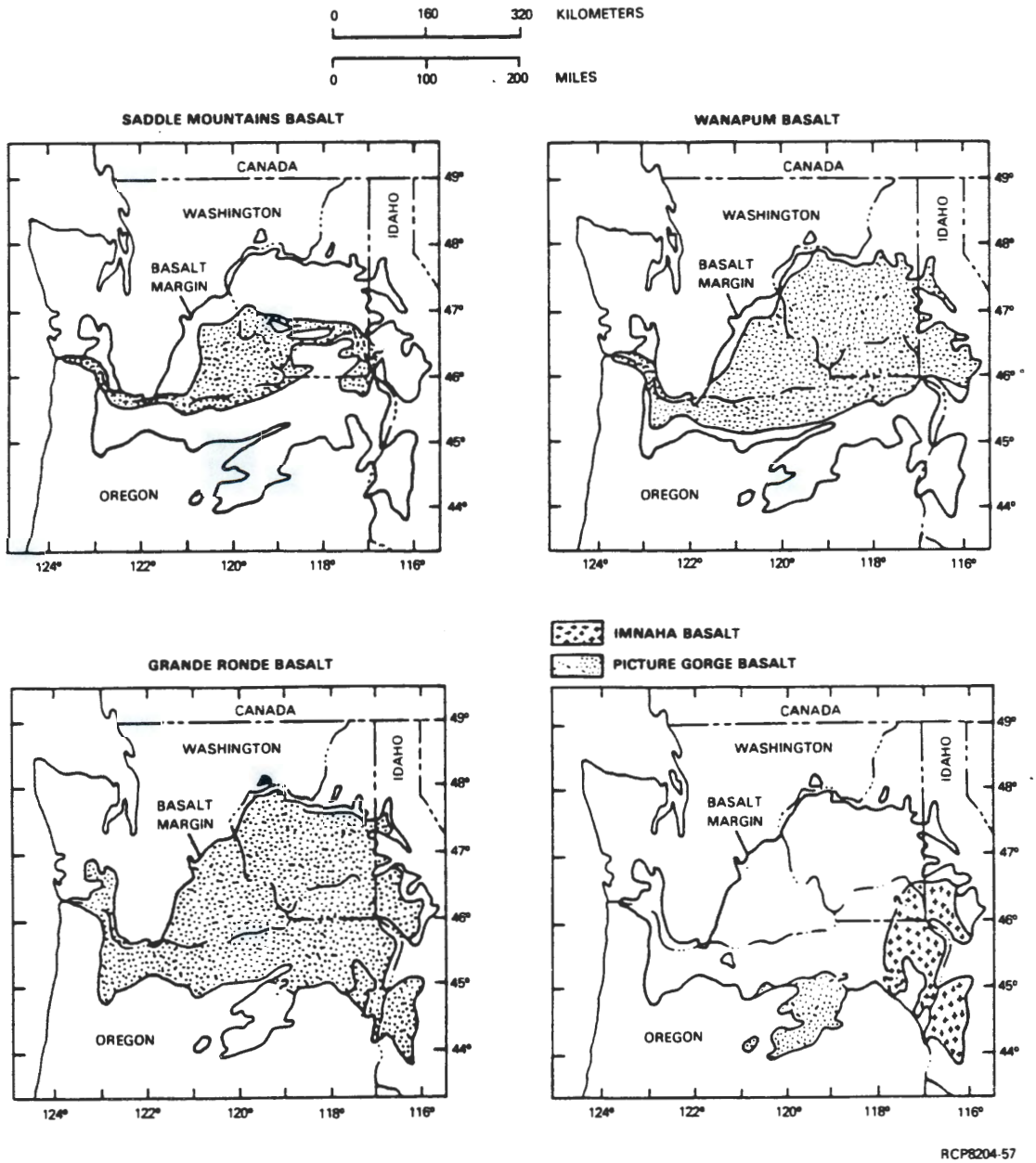

FIGURE 5-3. Areal Distribution of Formations Within the Columbia River Basalt Group (after Swanson and Wright, 1978).

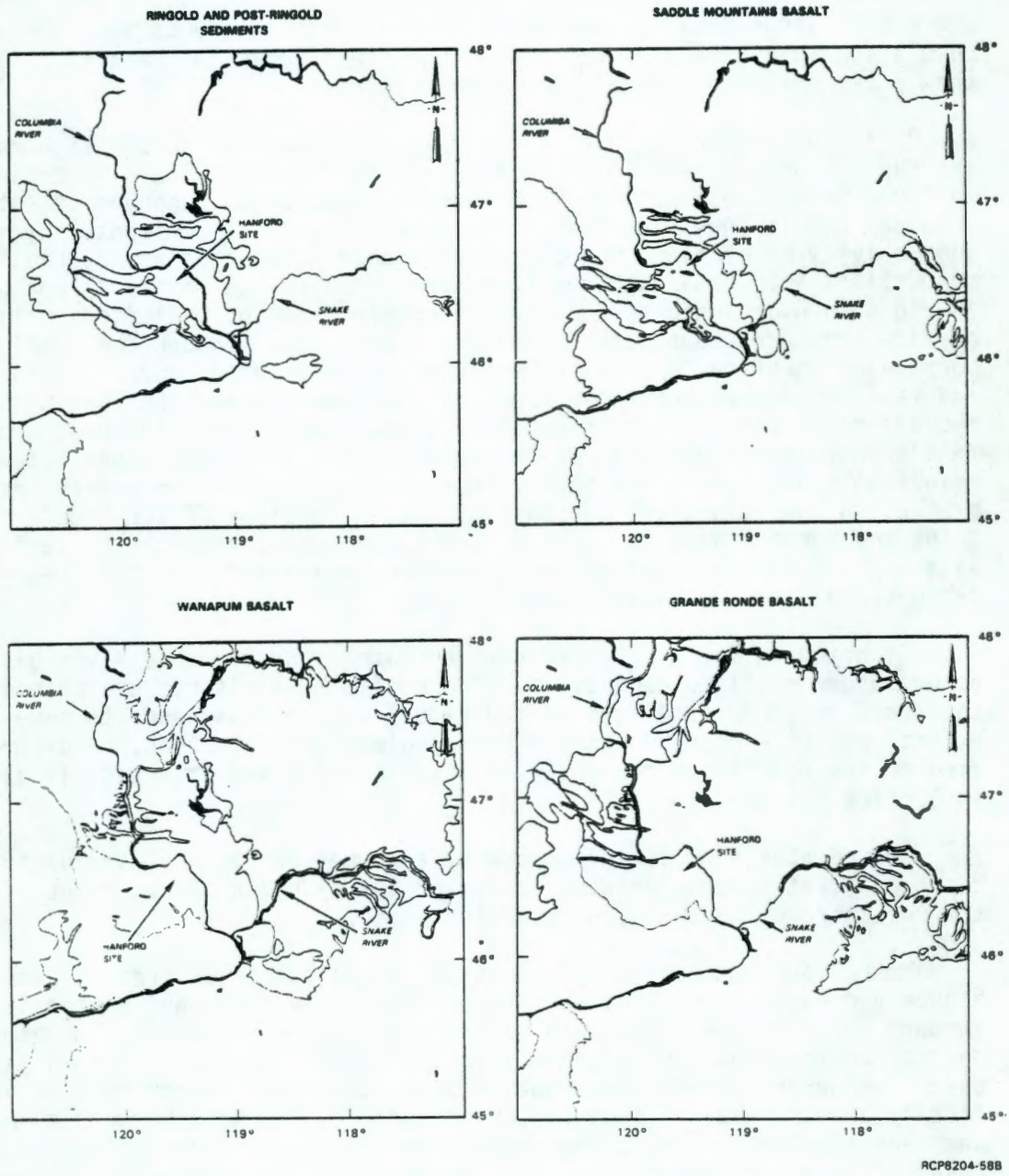

FIGURE 5-4. Outcrop Distributions of the Saddle Mountains, Wanapum, and Grande Ronde Basalts and Overburden Sediments.

Within the Pasco Basin, differences are also evident between the three basalt formations with respect to the presence and thickness of sedimentary interbeds, which are intercalated with basalt flows (see Fig. 3-16). The Saddle Mountains Basalt contains the most laterally extensive and greatest cumulative thickness of sedimentary interbeds of all Columbia River basalt formations within the Pasco Basin. Interbeds comprise up to 25 percent of the formation, with individual interbeds locally attaining thicknesses of 45 meters. Interbeds within the Wanapum and Grande Ronde Basalts, in comparison, are discontinuous and thin. The cumulative thickness of interbeds within these lower two basalts is less than 1 percent of the total formation thickness.

5.1.2.3 Groundwater Occurrence and Movement. General information regarding the subsurface hydrologic setting within the Pasco Basin is presented in Table 5-3. The majority of the basalt sequence is composed of either columnar basalt zones possessing low porosity and low horizontal hydraulic conductivity or of flow tops that have higher porosities and hydraulic conductivities. Data gathered from core sampling, geophysical logging, and in situ hydrologic testing have suggested that only limited portions of flow tops are groundwater producers (aquifers). Though the remaining portion of the flow top may be vesicular or brecciated, these fractures and vesicles appear not to be highly interconnected and the rock mass is hydraulically tight. Therefore, only a small percentage (perhaps approximately less than 5 percent) of the total basalt thickness constitutes principal groundwater flow paths. Most of the groundwater quantities present in the Columbia River basalts lie in portions of the Saddle Mountains and Wanapum Basalts. The Grande Ronde Basalt beneath the Hanford Site appears to have smaller groundwater quantities compared to the overlying sedimentary and basalt formations.

As noted in Table 5-3, groundwater within the Columbia River basalt occurs under confined conditions. The confining aquitards are principally the dense columnar interiors of individual basalt flows and, to some extent, possibly clay horizons within sedimentary interbeds. A description of the hydrologic properties for the basalts and interbeds is given in Section 5.1.3.

Groundwater flow is influenced by a number of factors, including topography, structure, stratigraphy, and the hydrologic properties of the rock through which the groundwater moves.

Most groundwater within the basalts moves laterally through zones of higher hydraulic conductivity (interbeds and flow tops) and vertically through the fractured basalt interiors (the degree of vertical movement depends on the flow's vertical transmissivity). In an undisturbed layered basalt sequence, minimal groundwater quantities are thought to move vertically across basalt flow interiors separating the more permeable interbeds and flow tops. Thus, the entablature and colonnade portions of a basalt flow are believed to act as low conductivity aquitards. Because of the greater-than-normal occurrence and length of fracturing in structurally disturbed areas (e.g., anticlines), water is considered to seep

TABLE 5-3. General Information Regarding Groundwater Hydrology

Formation and thickness (m)	Lithology	Thickness by rock type*	Aquifer type	Groundwater hydrochemistry	Groundwater recharge and discharge areas
Hanford and Ringold sediments 0 - 200	Unconsolidated to consolidated sediments	100% sediments	Unconfined	$Ca\text{-}HCO_3$	Recharge from precipitation, irrigation, and water disposal. Discharge to the major rivers.
Saddle Mountains ~300	10 basalt flows; 4 sedimentary interbeds	25% sedimentary interbeds; 10% flow tops, vesicular zones; 65% columnar basalt	Series of confined aquifers existing in interbeds and flow tops separated by low-hydraulic-conductivity aquitards (i.e., zones of columnar basalt). Groundwater production in individual flow tops and interbeds of the Saddle Mountains and Wanapum Basalts vary from <1 to hundreds of L/min (upper Wanapum may produce >4,000 L/min). Flow tops in Grande Ronde Basalt are overall hydraulically tighter than shallower basalt and produce <1 to several hundred L/min.	With increased depths in the basalts, the groundwaters are progressively older, isotopically heavier, and exhibit distinct hydrochemical breaks over short stratigraphic distances.	Shallow groundwaters within the Saddle Mountains and possible upper Wanapum Basalts are recharged from precipitation on basalt outcrops surrounding the Pasco Basin. Discharge is to the unconfined aquifer and/or Columbia River at locations where hydraulic interconnection exists.
Wanapum ~350	10 to 14 basalt flows; 1 sedimentary interbed	25% flow tops, vesicular zones; 75% columnar basalt			Deeper groundwaters within the Wanapum and Grande Ronde Basalts are believed recharged, to a small extent, locally, but are mostly recharged from groundwater inflow from outside the Pasco Basin where these basalts lie at or near ground surface. Discharge is thought to be to the Columbia River south of the Hanford Site, where the deep basalts are in direct contact with the river.
Grande Ronde ~2,000	>30 basalt flows	30% flow tops, vesicular zones; 70% columnar basalt			

*Percentages from core at borehole DC-4.

vertically along these zones to a larger extent than in geologically non-disturbed areas. Synclines are broad, open features having undergone little structural disturbance. Thus, they should contain less secondary fracturing and less vertical groundwater leakage compared to anticlines.

Overall, groundwater moves from areas of recharge to discharge. Recharge areas are usually basalt outcrops surrounding the Pasco Basin or in other basins of the Columbia Plateau where basalts lie at or near ground surface. Groundwater then moves down a hydraulic gradient to discharge into either an overlying aquifer or into a surface water body.

Along this flow path, confined groundwaters are under artesian heads. This means that water from a specific stratigraphic horizon will rise in a well to some given elevation above that horizon. If this water level is above the ground surface, the well is said to be under flowing artesian conditions. Artesian conditions exist in most of the confined aquifers beneath the Pasco Basin. Areas of artesian flowing wells are known to exist in the Cold Creek Valley (e.g., Ford, O'Brian, Enyeart, and McGee wells) and along the Columbia River (e.g., in borehole DC-6 and portions of DC-14 and -15).

5.1.3 Hydrologic Characteristics

Data available for the characterization of hydraulic properties for individual geologic formations are primarily limited to tests conducted within the Hanford Site. Most data available outside the Hanford Site are generally for specific capacity tests of short duration and for shallow irrigation wells (i.e., less than 300 meters deep) completed in multiple contributing zones (Gephart et al., 1979a; Tanaka et al., 1979).

Many of the values of hydrologic properties presented in this section are given to the nearest order of magnitude. More specific numbers will be written into the literature once peer review and full documentation of all test results are completed.

5.1.3.1 Hydrologic Test Methods. Several types of standard hydrologic tests are used for the in situ characterization of hydraulic properties on the Hanford Site. These include constant discharge, constant drawdown, displacement, constant-head injection, water potential, and tracer tests. Generally, these tests employ single- or straddle-packer systems and are used to obtain field estimates of transmissivity, equivalent hydraulic conductivity, storativity, effective porosity, and dispersivity.

The majority of the hydrologic property and hydrochemical data contained within this chapter has been collected since 1978 by the staff of the BWIP. A brief description is given below of the collection methodology and testing approach used.

The objective of the hydrologic field-testing program is to provide data for characterization of those groundwater systems within the Hanford Site and surrounding area significant to understanding waste isolation. This effort is directed toward characterizing the areal and vertical distributions of hydrauic head, hydraulic properties, and hydrochemistry. A preliminary understanding of these data is contained within this chapter. Data obtained from these studies provide input for numerical modeling of groundwater flow and solute transport as discussed in Chapter 12.

The program of data collection and analysis necessary to complete site characterization is specified in Chapter 13.

To date, hydrologic testing has concentrated on characterizing the more permeable interbeds and basalt flow tops to depths of about 1,500 meters. The diameter of test boreholes range from 8 to 10 centimeters for cored holes and up to 20 centimeters for rotary holes. Single and straddle packers are used to test selected rock intervals. The single-packer system is normally used in boreholes where testing is done on a progressive drill-and-test basis. This packer arrangement consists of a pneumatic or mechanical packer attached to steel tubing of sufficient diameter to install a small-diameter submersible pump or air line.

The surface recording equipment used to monitor fluid responses in the isolated interval as well as in the annulus includes surface quartz pressure transducers and surface data recording equipment capable of recording temperature and pressure measurements at intervals of more than one reading per second.

Other water-level-monitoring equipment that is used in conjunction with the electronic recording equipment includes electronic water-level indicators, chalked steel tape, and continuous float recorders.

A straddle-packer system has frequently been used to test anticipated high- and low-permeability zones across open intervals after completion of a borehole. This system consists of downhole probes capable of measuring temperatures and pressures above, in between, and below the straddled interval. These data are transmitted via a single-conductor cable to surface electronic equipment for printing and recording. The surface equipment is capable of monitoring downhole pressure responses every 0.5 second and at sample rates of 0.5 second to 1 hour. Major components of the downhole equipment are:

- Packers--The packers are water inflatable and about 1 meter long.
- Sensor carrier--The carrier is located above the top packer. It houses three quartz pressure transducers and thermistors. These probes are capable of measuring pressures and temperatures above, below, and within the straddled interval. Steel tape and electric water-level measurements are used to obtain hydrologic heads and to calibrate downhole pressure readings.

- The J-slot tool--Depending on the position of the J-slot, the tool is used to equalize pressures between the packer interval and the annulus, inflate the packer, and open the tool to the test interval.

- Shut-in tool--This tool serves to isolate the tubing above the upper packer from the overlying rock formation. The shut-in tool is useful for conducting slug and pulse tests, because water can be swabbed or the tubing filled without disturbing the formation head when the shut-in tool is closed.

The hydrologic test procedures relied on at the Hanford Site depend on the transmissive characteristics of the basalt zone under evaluation. The flow chart shown in Figure 5-5 illustrates the general procedures used to hydrologically test an interval.

Selection of the test interval is based on an examination of the rock core, as well as a suite of borehole geophysical logs (e.g., temperature, resistivity/spontaneous potential, natural gamma, gamma-gamma, sonic, caliper, and neutron logs). The core and geophysical logs are also useful for identifying intact rock needed for good packer seats.

After the packers are set, the tubing is swabbed or air lifted to determine if the packers are properly seated. The fluid response monitored during this activity also provides information of the test methods that will be subsequently used.

Next, air-lift pumping is initiated to remove drilling fluid from the tubing and formation prior to follow-up hydraulic testing and groundwater sampling.

In zones where the transmissivity is low, pulse and constant head-injection tests are generally conducted (Fig. 5-6). These tests normally require up to 6 weeks to be completed in low-transmissivity zones. In the high-transmissivity rocks, constant-discharge tests are the primary test method utilized. If flowing artesian conditions are encountered, constant-drawdown tests are conducted. Generally, water samples are obtained after testing, using a submersible pump. This is followed by slug withdrawal and injection tests after the head has reached equilibrium. In high-transmissivity rocks, hydrologic testing normally takes from 1 to 2 weeks to be completed. As can be noted from the above discussion, multiple tests are carried out so as to corroborate test data. Such multiple testing also allows for additional well development prior to groundwater sampling.

The hydraulic properties determined from aquifer testing are hydraulic head, transmissivity, hydraulic conductivity, storativity, dispersivity, and effective porosity.

9 2 1 2 4 9 5 0 9 0 5

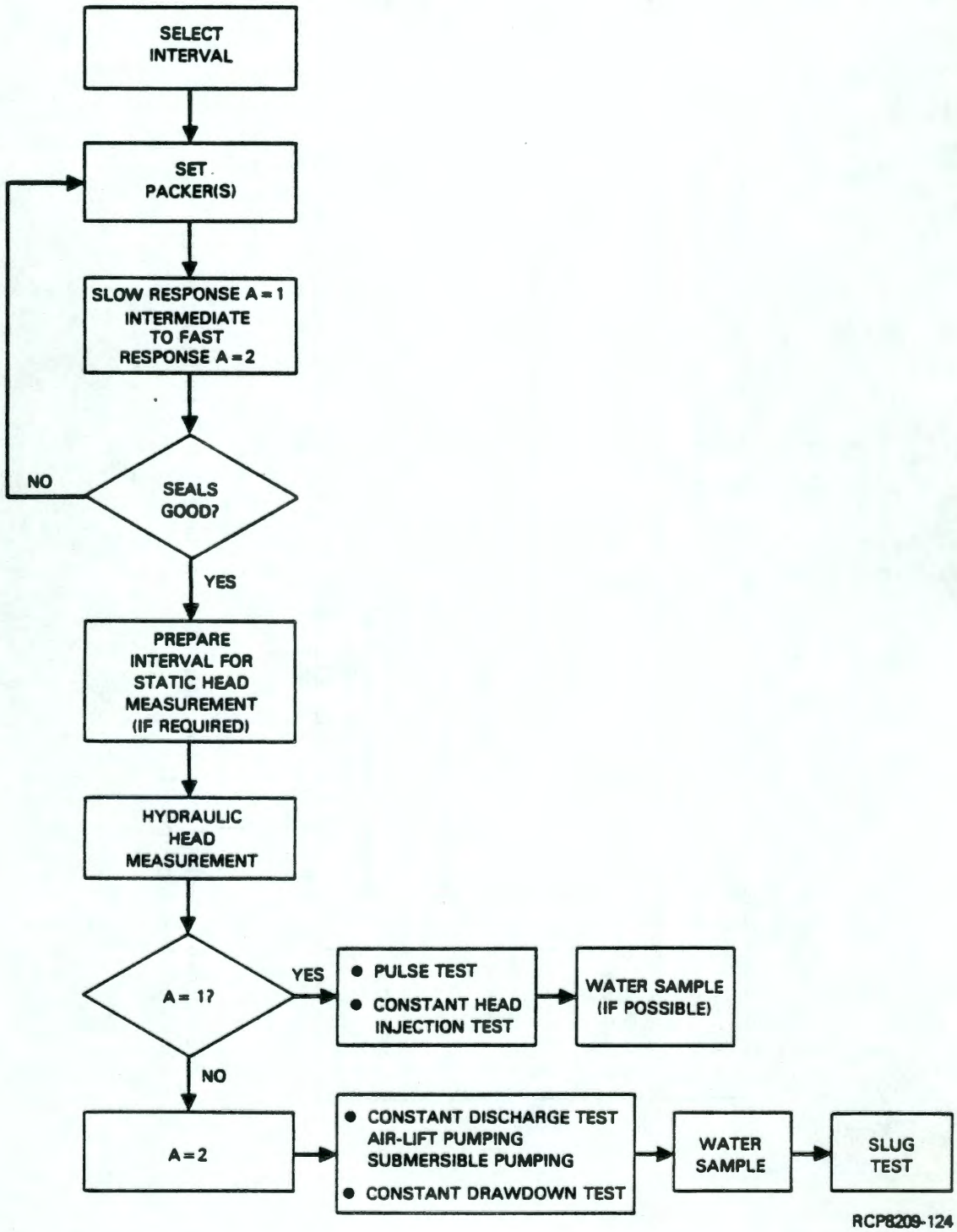

FIGURE 5-5. Flow Chart of General Procedures Used in Hydrologic Testing.

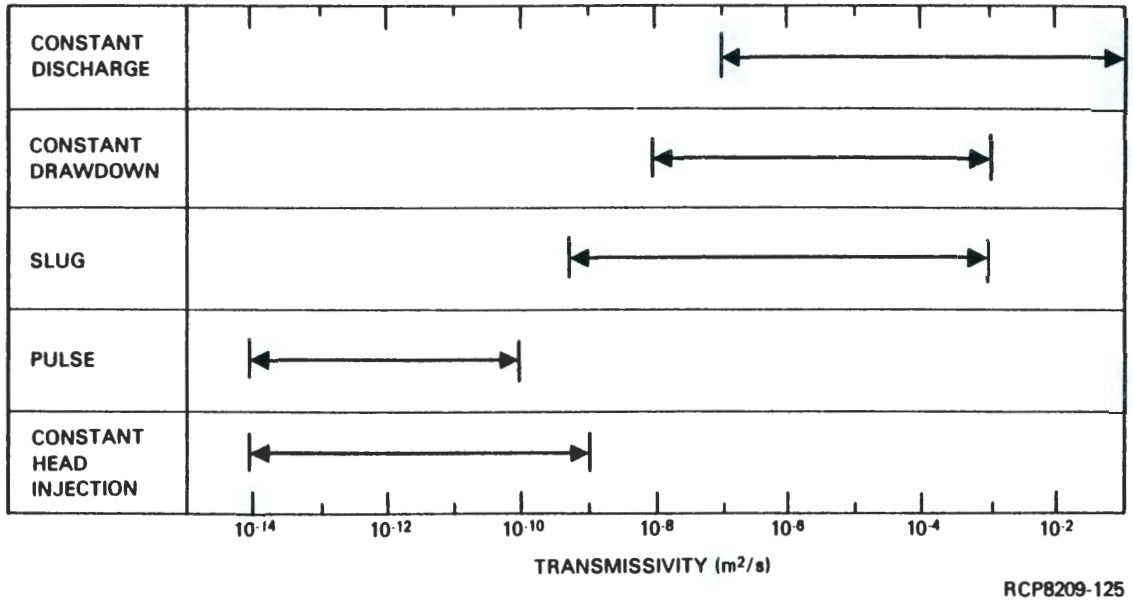

FIGURE 5-6. Guidelines for Application Range of Test Methods for Test Zones at the Hanford Site.

5.1.3.1.1 Neutron-Epithermal Neutron Geophysical Logs. In subsequent sections of this chapter numerous illustrations are based on data collected from boreholes DB-15, DC-6, -7, -12, -14, -15, -16A, and RRL-2. Figures 5-7 through 5-14 show the neutron-epithermal-neutron logs for these same boreholes. These logs were acquired as part of the routine downhole hydrologic testing program. Pertinent stratigraphy is noted along side the log responses. These logs are presented here so the reader may become more aware of the general stratigraphy and intraflow structural characteristics of the basalt before proceeding to the data sections of this chapter.

These logs record the epithermal neutrons produced when fast neutrons from an americium-beryllium source are reduced in energy by interactions with the surrounding rock. Since neutrons are moderated primarily by collisions with hydrogen atoms, the log is indicative of water content within the investigated zone. Water saturated rock of higher porosity exhibits lower backscattering radiation, thus the log shows a characteristic "kick" to lower counts per second (to left on figures). Rock intervals of lower porosity have high backscattering and, therefore, log "kicks" to the right. These log responses are of value in locating zones of high or low porosities that may identify aquifers or aquitards (final proof of the rock's transmissive nature comes from hydrologic testing) and aid in correlating stratigraphic units.

5.1.3.2 Unconfined Aquifer. The unconfined aquifer in the Pasco Basin consists of saturated sediments of the Hanford and Ringold Formations. The range and mean values for hydraulic properties within the unconfined aquifer were given in Gephart et al. (1979a) and represent the results from pumping tests conducted by several investigators. More recent information lists the range of hydraulic conductivity for the Hanford and Ringold Formations as 7×10^{-3} to 4×10^{-2} and 1×10^{-5} to 8×10^{-4} meters per second, respectively (Graham et al., 1981).

These data indicate that a wide range of hydraulic conductivities exists for formations within the unconfined aquifer. This range is reflective of the heterogeneity of the geologic formations. Zones of higher conductivity are attributable to paleostream deposits within the Hanford formation, while lower values commonly occur within the lower Ringold Formation. Reported storativity values, 10^{-2} to 10^{-1}, fall within the range commonly cited for unconfined aquifers (Heath and Trainer, 1968). No effective porosity values are reported for these formations.

The areal distribution of hydraulic conductivity, as averaged over the thickness of the unconfined aquifer, is shown in Figure 5-15 (Cearlock et al., 1975). Two features are noteworthy. The first is an area of lower hydraulic conductivity lying south of Gable Butte. This region consists of saturated Ringold sediments of relatively low hydraulic conductivity. The second feature is the area of high conductivity (more than 10^{-3} meters per second) extending southeast from between Gable Butte and Gable Mountain. This area consists of reworked Ringold and Hanford Formation sediments. These sediments of high hydraulic conductivity influence the movement and development of the nitrate, tritium, and gross beta plumes reported in Eddy and Wilbur (1981).

9 0 9 5 0 4 9 2 1

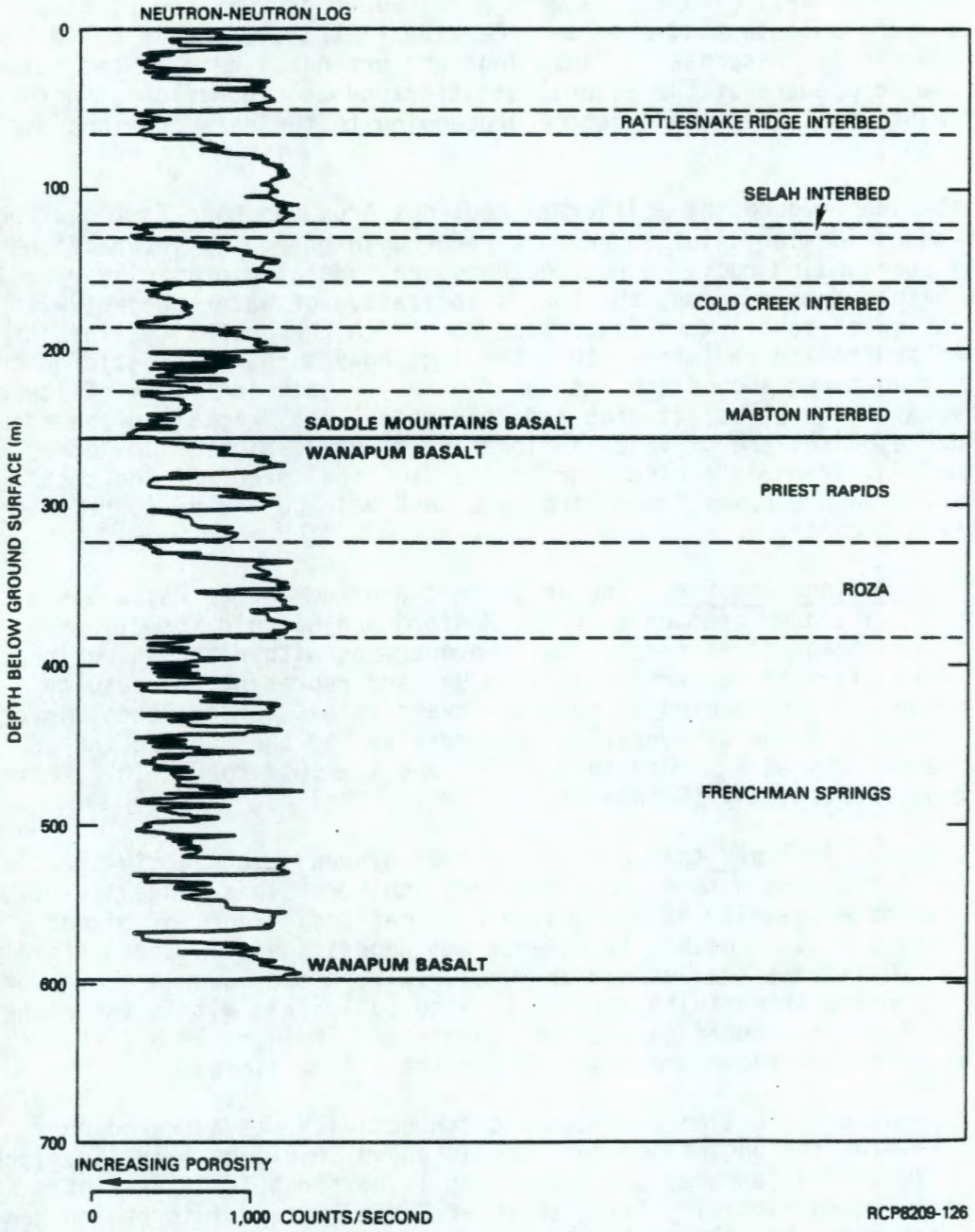

FIGURE 5-7. Borehole Geophysical Log for Borehole DB-15.

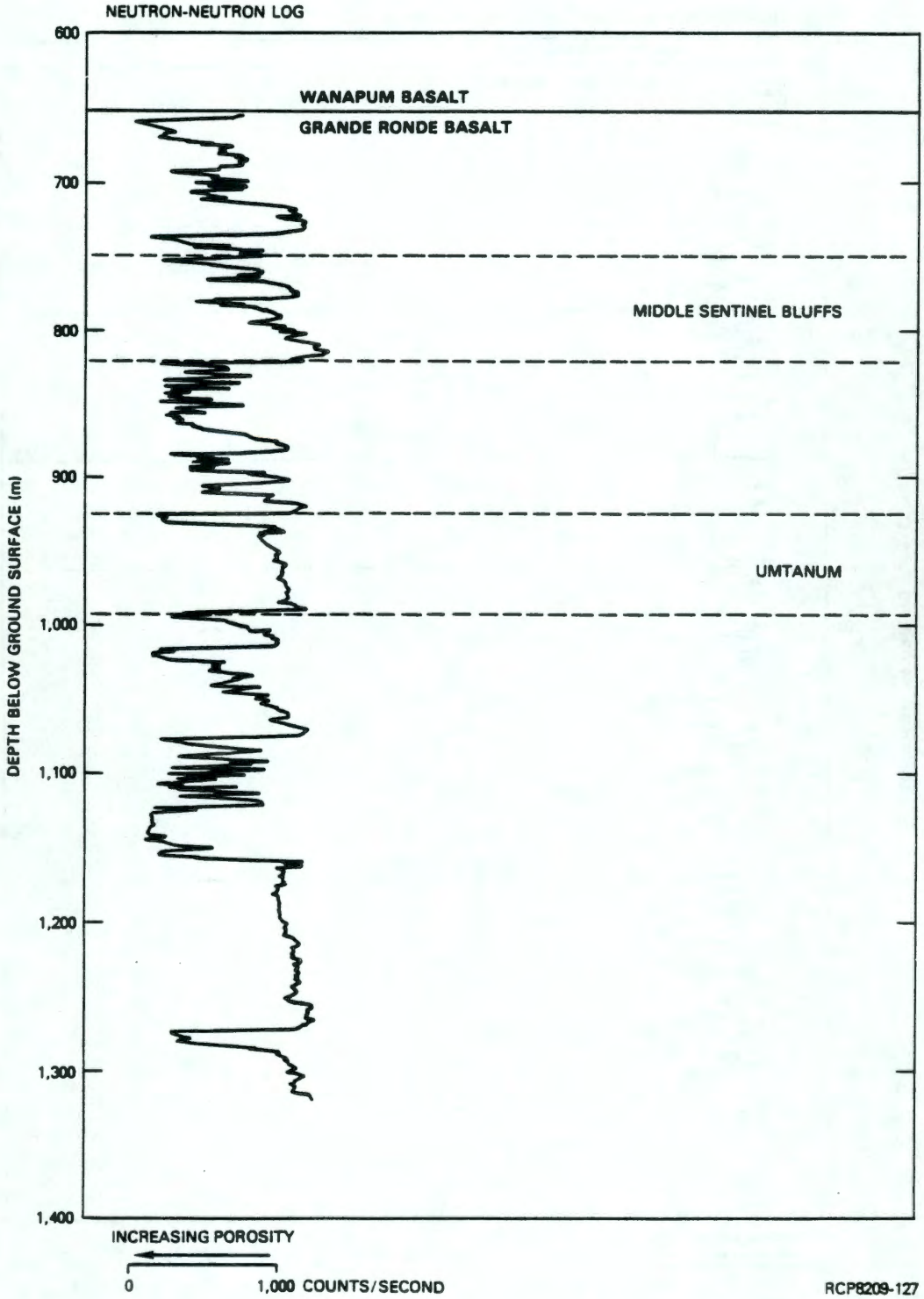

FIGURE 5-8. Borehole Geophysical Log for Borehole DC-6.

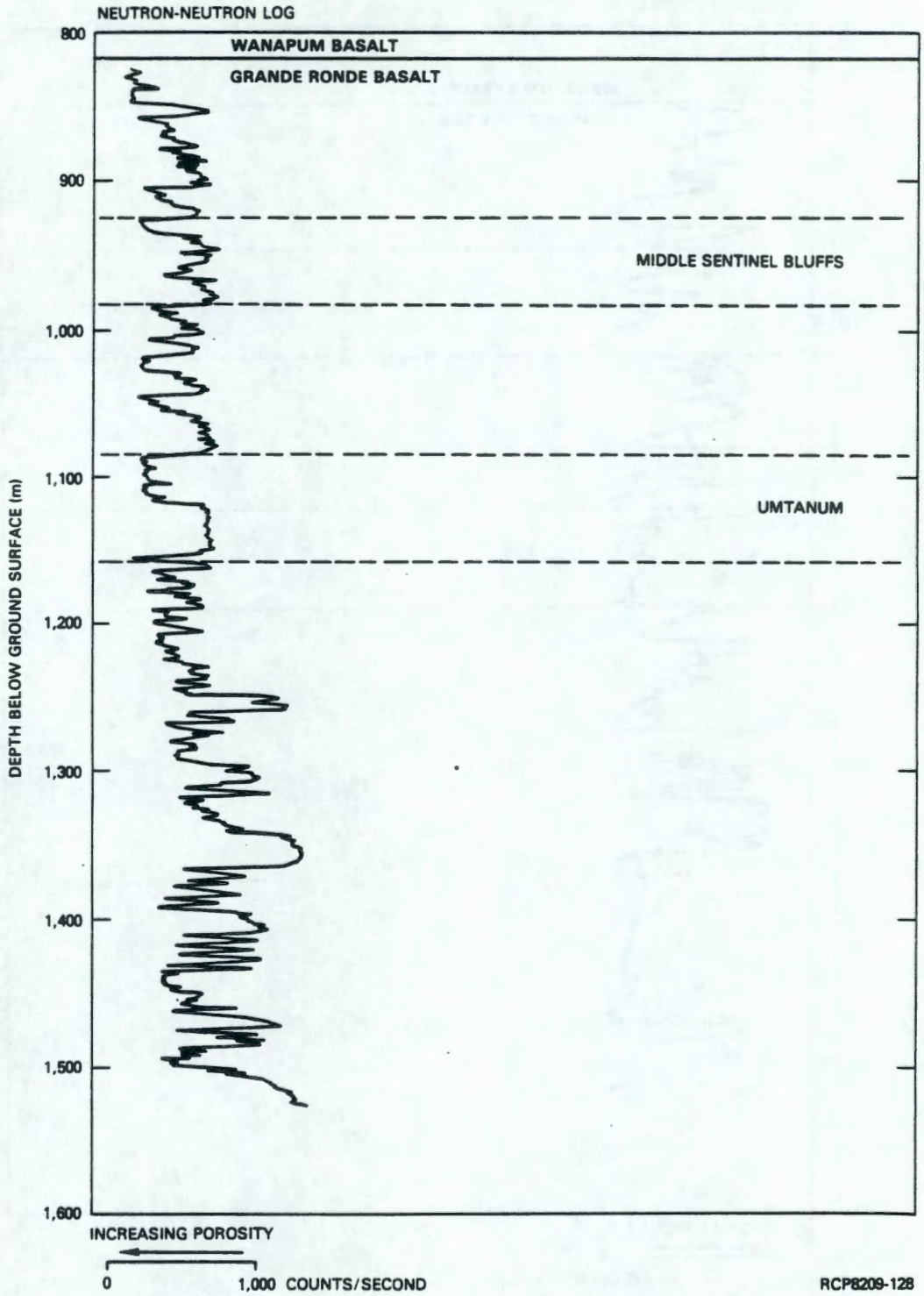

FIGURE 5-9. Borehole Geophysical Log for Borehole DC-7.

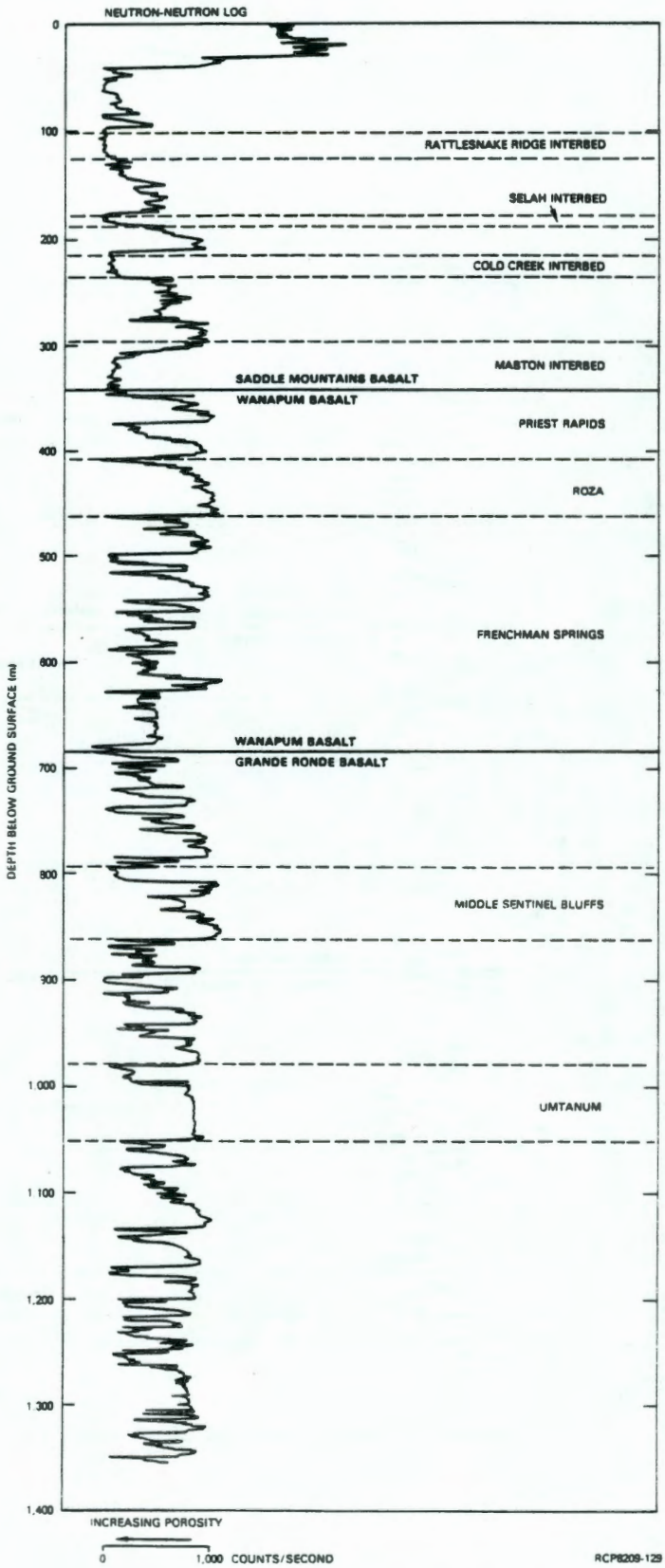

FIGURE 5-10. Borehole Geophysical Log for Borehole DC-12.

1-2-1 2 4 9 5 0 9 1 2

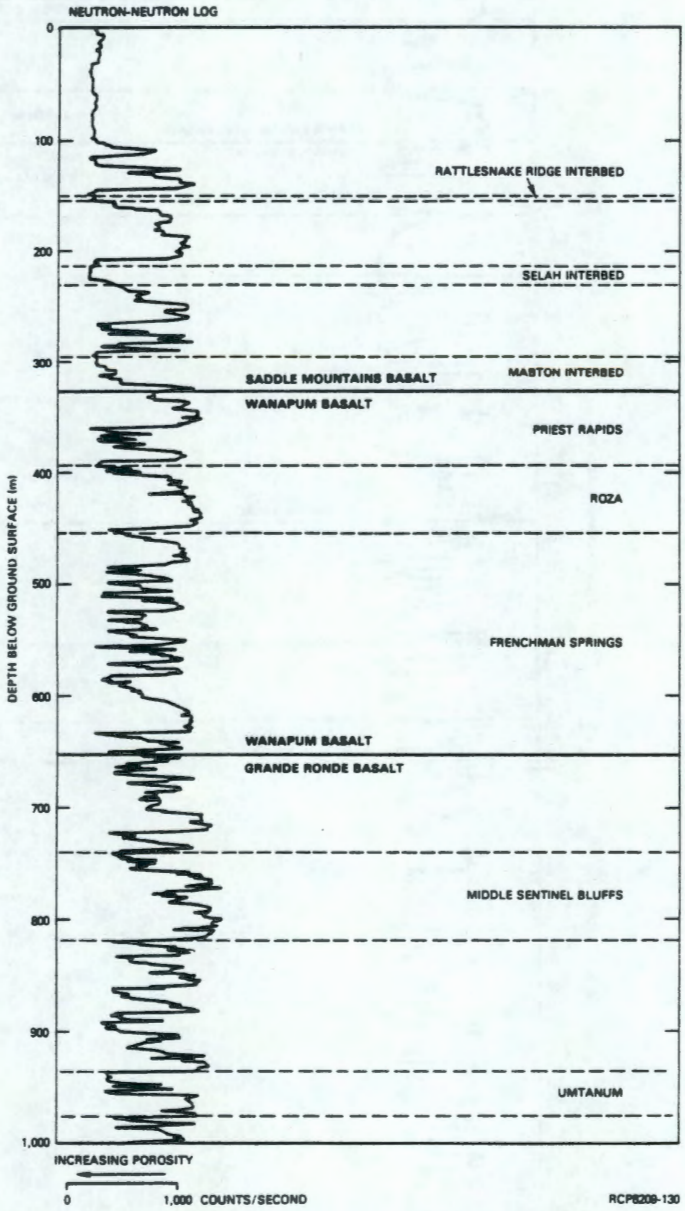

FIGURE 5-11. Borehole Geophysical Log for Borehole DC-14.

1 2 1 2 4 9 5 0 9 1 3

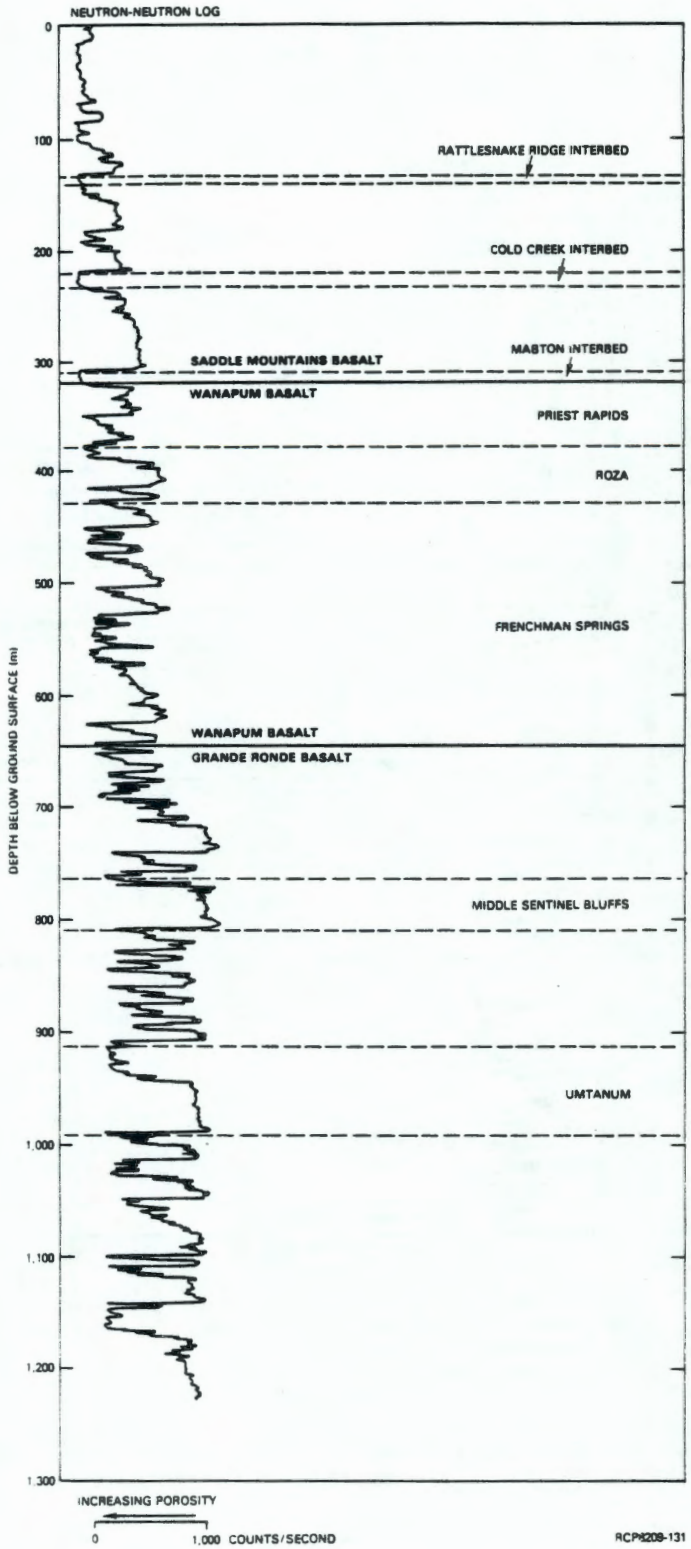

FIGURE 5-12. Borehole Geophysical Log for Borehole DC-15.

1 2 1 2 4 9 5 0 9 1 4

9212495091 5

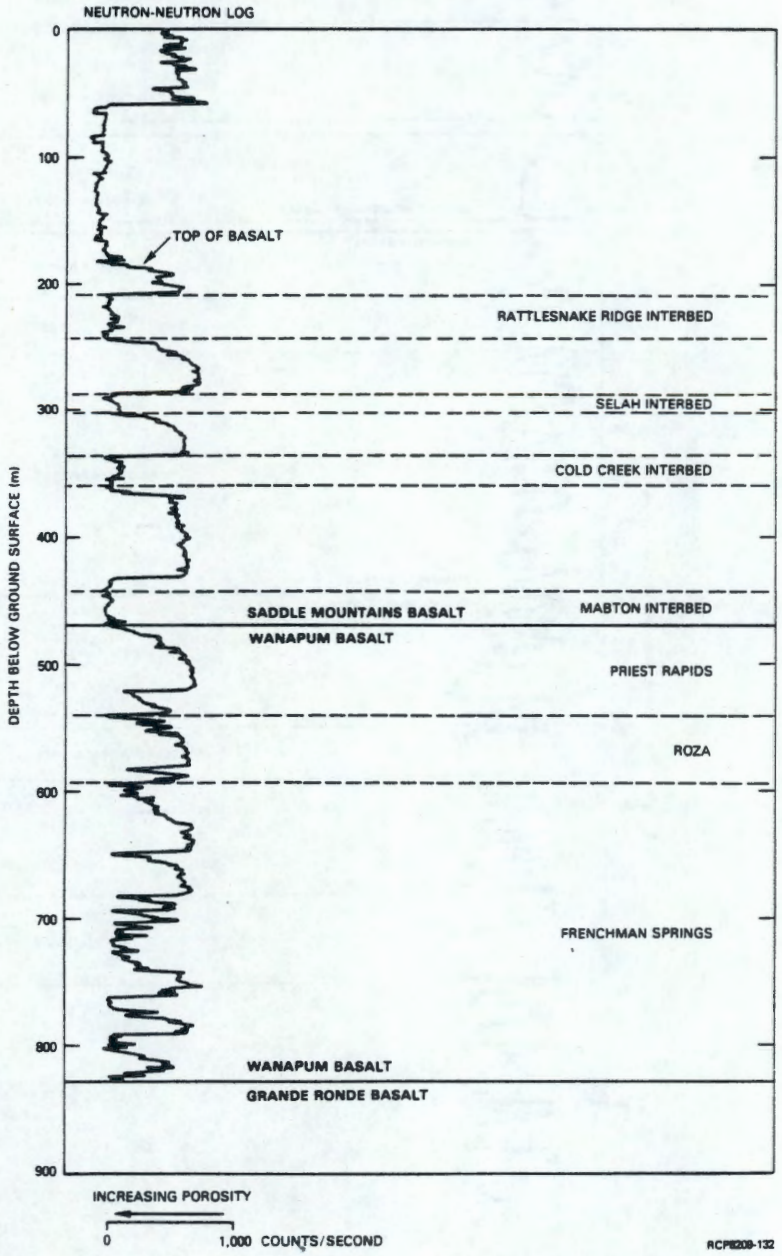

FIGURE 5-13. Borehole Geophysical Log for Borehole DC-16A.

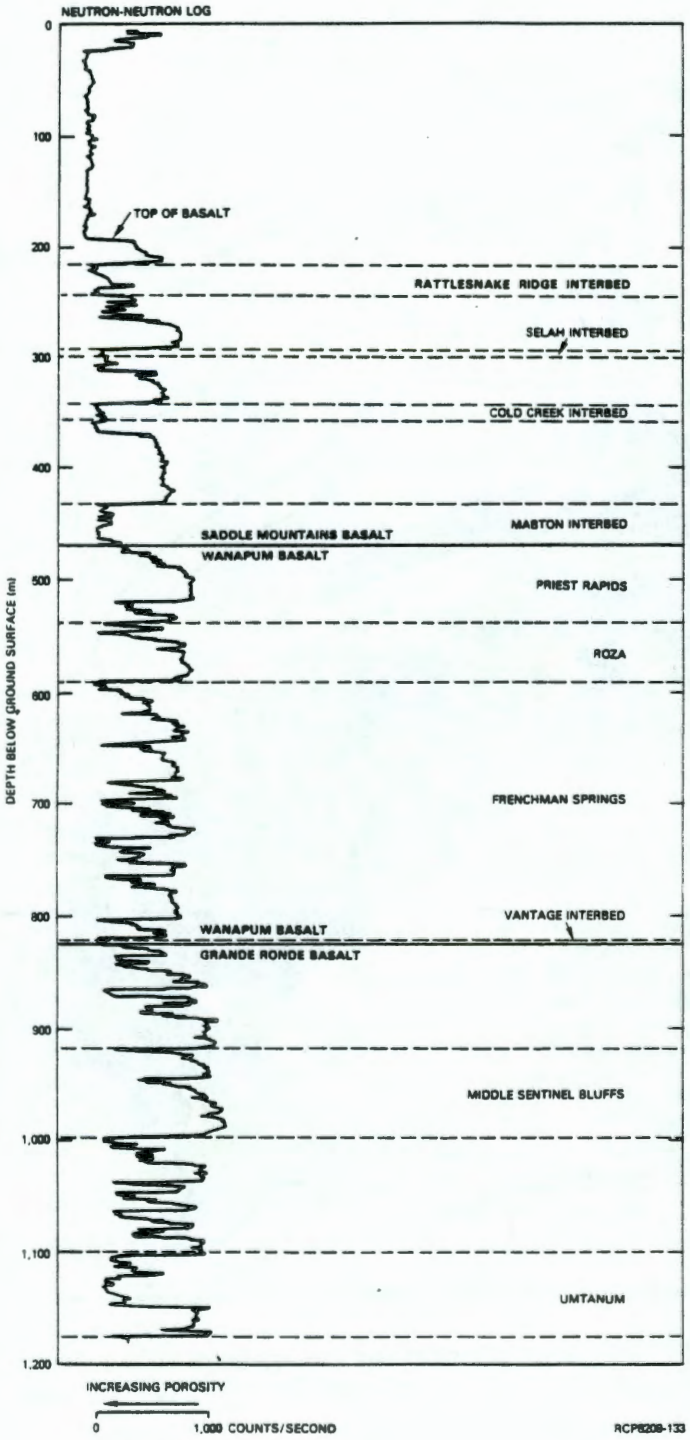

FIGURE 5-14. Borehole Geophysical Log for Borehole RRL-2.

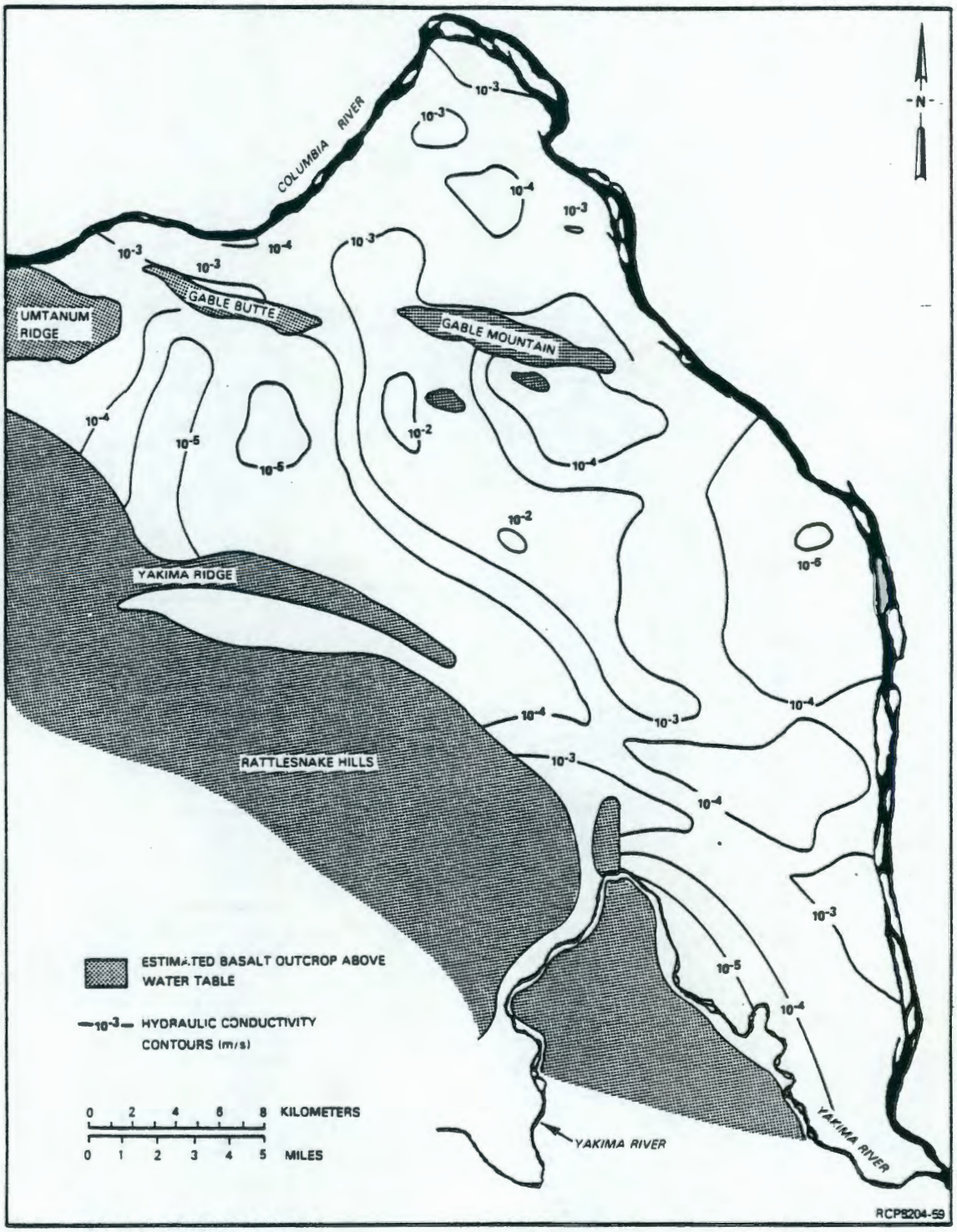

FIGURE 5-15. Areal Distribution of Hydraulic Conductivity Across the Hanford Site for the Unconfined Aquifer (after Cearlock et al., 1975).

5.1.3.3 Columbia River Basalt. The primary emphasis in hydraulic testing of new or existing boreholes has been across sedimentary interbeds and flow tops where hydraulic conductivities are highest. Each of these tests takes several days to complete. Testing of columnar basalt zones is more time consuming (weeks to months per test) and therefore, in the testing sequence, these tests are undertaken after the higher conductivity zones are evaluated.

The range and mean values of hydraulic properties for formations within the Columbia River Basalt Group in the Hanford Site are shown in Table 5-4. Values for equivalent hydraulic conductivity for the basalt formations were determined from approximately 145 tests conducted at about 35 borehole sites. About 95 percent of these tests have been conducted across flow tops and interbeds (i.e., across rock intervals containing zones of higher hydraulic conductivity). The distribution of equivalent hydraulic conductivity for these intervals is shown in Figure 5-16. (Equivalent hydraulic conductivity is determined by dividing transmissivity by the effective thickness of the zone tested. For example, if geophysical logs and core samples indicate that 2 meters of a 20-meter-long straddle interval is of high porosity and contributes fluid to the borehole, then that 2 meters is divided into the zone's transmissivity to obtain equivalent hydraulic conductivity.)

Histograms for the distribution of equivalent hydraulic-conductivity values for sedimentary interbeds and flow tops within the Columbia River basalts are shown in Figure 5-16. (Hydraulic conductivities across colonnade or entablature zones of basalt flows are not included in this figure, but are addressed later in this section.) Although these histograms result from data compilation from numerous boreholes, a large percentage of the data is derived from boreholes DB-13, -14, -15, DC-6, -7, -12, -14, -15, -16A, and RRL-2 (Fig. 5-2). The specific hydraulic conductivities for each borehole used as input to Figure 5-16 are either listed in Table 5-5 or are shown in figures later in this section. All values are from hydrologic testing on the Hanford Site since about 1978. The hydraulic-conductivity values for the Saddle Mountains Basalt are from testing flow tops and interbeds. Because no major interbeds exist in the Wanapum and Grande Ronde Basalts (except the Vantage), values reported for these formations are from flow tops.

Within the Saddle Mountains Basalt, most hydraulic conductivities for flow tops and interbeds range between 10^{-4} and 10^{-6} meters per second, with the mean value being 10^{-5} meters per second. The majority of hydraulic conductivity values for flow tops in the Wanapum Basalt range between 10^{-4} and 10^{-7} meters per second, with a mean value of 10^{-5} meters per second. Hydraulic conductivities for flow tops within the Grande Ronde Basalt generally range between 10^{-5} and 10^{-9} meters per second, with a mean value of about 10^{-7} meters per second. Thus, a 2-order-of magnitude decrease in the mean value of hydraulic conductivity in the flow tops of the Grande Ronde appears to exist as compared to the upper two basalt formations. This decrease is also noticed when hydraulic conductivities are plotted as a

TABLE 5-4. General Ranges and Values for Selected Hydrologic Properties.

Basalt formation	Rock type as percentage of formation thickness[a]	Equivalent horizontal hydraulic conductivity[b] (m/s)	Storativity (dimensionless)
Saddle Mountains			
Interbeds	24	10^{-9} to 10^{-4}	10^{-3} to 10^{-4}
Flow tops	9	10^{-7} to 10^{-3}	
Columnar zones	67	ND	
Wanapum			
Flow tops	25	10^{-10} to 10^{-2}	10^{-4} to 10^{-5}
Columnar zones	75	10^{-12} to 10^{-11}	
Grande Ronde			
Flow tops	29	10^{-10} to 10^{-3}	10^{-3} to 10^{-6}
Columnar zones	71	10^{-13} to 10^{-12}	
Basalt intrastructure			Effective porosity[c] (%)
Interbeds			<10.
Flow tops			<5
Columnar zones			<1

ND = Not determined

[a]Percentage based upon rock pentrated at borehole DC-4. Lithologic description determined by examining rock core.

[b]Approximately 145 tests have been conducted. The range of storativity is from about 30 individual tests.

[c]Values estimated from geophysical logs and core observation. These values are considered preliminary for quantitative values have not yet been fully field determined.

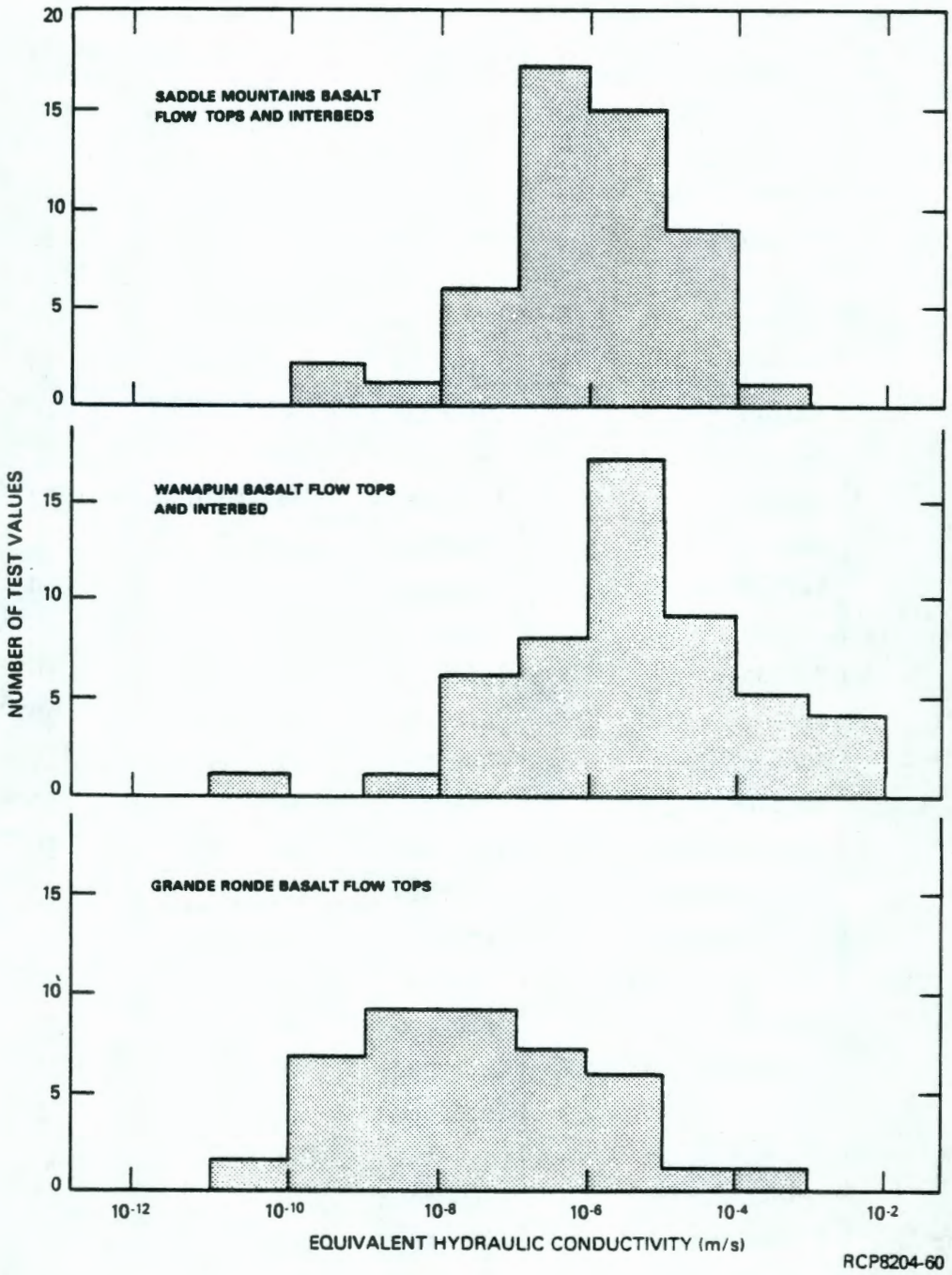

FIGURE 5-16. Comparison of Equivalent Hydraulic-Conductivity Values for all Flow Tops and Interbeds Tested Within the Columbia River Basalts.

TABLE 5-5. Equivalent Hydraulic Conductivity for Selected Stratigraphic Intervals.

Borehole	Stratigraphic interval	Lithology	Test interval (m below ground surface)	Equivalent hydraulic conductivity (m/s)
DB-1	Mabton	Interbed	297 - 302	10^{-4}
DB-2	Mabton	Interbed	274 - 282	10^{-4}
DB-4	Mabton	Interbed	416 - 428	10^{-4}
DB-5	Mabton	Interbed	254 - 277	10^{-6}
DB-7	Mabton	Interbed	237 - 247	10^{-4}
DB-9	Mabton	Interbed	153 - 180	10^{-6}
DB-10	Mabton	Interbed	259 - 272	10^{-8}
DB-11	Mabton	Interbed	266 - 310	10^{-9}
DB-12	Mabton	Interbed	115 - 156	10^{-5}
DB-14	Rattlesnake Ridge	Interbed	64 - 87	10^{-7}
	Cold Creek	Interbed	188 - 202	10^{-4}
	Mabton	Interbed	280 - 315	10^{-6}
BH-16	Selah	Interbed	265 - 281	10^{-6}
BH-17	Asotin	Flow top	312 - 334	10^{-7}
53-50	Rattlesnake Ridge	Interbed	44 - 59	10^{-5}
52-48	Rattlesnake Ridge	Interbed	44 - 59	10^{-6}
52-46	Rattlesnake Ridge	Interbed	52 - 69	10^{-6}
51-46	Rattlesnake Ridge	Interbed	36 - 50	10^{-6}
50-45	Rattlesnake Ridge	Interbed	40 - 54	10^{-5}
50-48	Rattlesnake Ridge	Interbed	65 - 76	10^{-5}
47-50	Rattlesnake Ridge	Interbed	79 - 90	10^{-5}
699-S11-E12A	Levey	Interbed	72 - 81	10^{-6}
O'Brian	Priest Rapids*	Flow top	209 - 212	10^{-2}
Ford	Priest Rapids*	Flow top	226 - 229	10^{-2}
Enyeart	Priest Rapids*	Flow top	328 - 332	10^{-2}
McGee	Upper Priest Rapids*	Flow top	247 - 250	10^{-3}
McGee	Lower Priest Rapids*	Flow top	282 - 285	10^{-3}

*Members of the Wanapum Basalt. All other intervals are within the Saddle Mountains Basalt.

function of depth at some individual borehole sites. Possible explanations for this decrease include a lowering of fracture conductivity due to greater lithostatic loading and/or increased secondary mineralization with depth. Future borehole testing and fracture studies of borehole core samples will address this possible phenomenon.

The decrease or depth dependence of hydraulic properties has been noted by others investigating intrusive crystalline rocks (e.g., Olsson (1979) and Carlsson and Olsson (1977a; 1977b)). Fractures within basalt may have a greater degree of secondary mineralization with depth. Although comparative studies of the degree of secondary mineralization have not been completed for the basalt formations, Long (1978) has reported that a high percentage (i.e., greater than 80 percent) of fractures within core from Grande Ronde Basalt boreholes are completely "rehealed" with secondary minerals. The remaining fractures are lined with secondary minerals. If it is assumed that fractures within the overlying basalt formations have less secondary mineralization (i.e., they are more open), then possible increased fracture mineralization in the Grande Ronde Basalt may be responsible for the observed decrease in hydraulic conductivity.

As shown in Table 5-4, the dense interior columnar (entablature and colonnade) sections of basalt flows possess significantly lower horizontal hydraulic conductivities than do sedimentary interbeds and flow tops. Mean hydraulic-conductivity values for columnar zones within the Wanapum and Grande Ronde Basalts range several orders of magnitude lower than their formational flow-top counterparts. The results of tests completed across basalt flow interiors are shown in Figure 5-17. The ranges shown for a given borehole result from the application of more than one hydrologic test technique and/or stress levels (see Section 5.1.3.1). Best estimates of hydraulic conductivity determined from these field tests are 10^{-12} meters per second for the Roza and middle Sentinel Bluffs flow interiors and 10^{-13} meters per second for the Umtanum flow interior.

The vertical distributions of equivalent hydraulic conductivities for interbeds and flow tops in boreholes DB-13, -15, DC-6, -7, -12, -14, -15, -16A, and RRL-2 are shown in Figures 5-18 through 5-26. Data from these and other boreholes were used to construct the histograms shown in Figure 5-16. Borehole DB-13 is shown because of its proximity (about 3 kilometers to the northwest) to DC-12. Data from DB-13 and DC-12, together, can be used to provide a vertical definition of hydraulic conductivity through the Saddle Mountains, Wanapum, and Grande Ronde Basalts in the vicinity of the Cold Creek syncline. The hydraulic-conductivity values shown are conservative estimates (i.e., if the results of a test analysis ranged over 1 order of magnitude, the largest hydraulic-conductivity value was plotted).

1 2 1 2 4 9 5 0 9 2 2

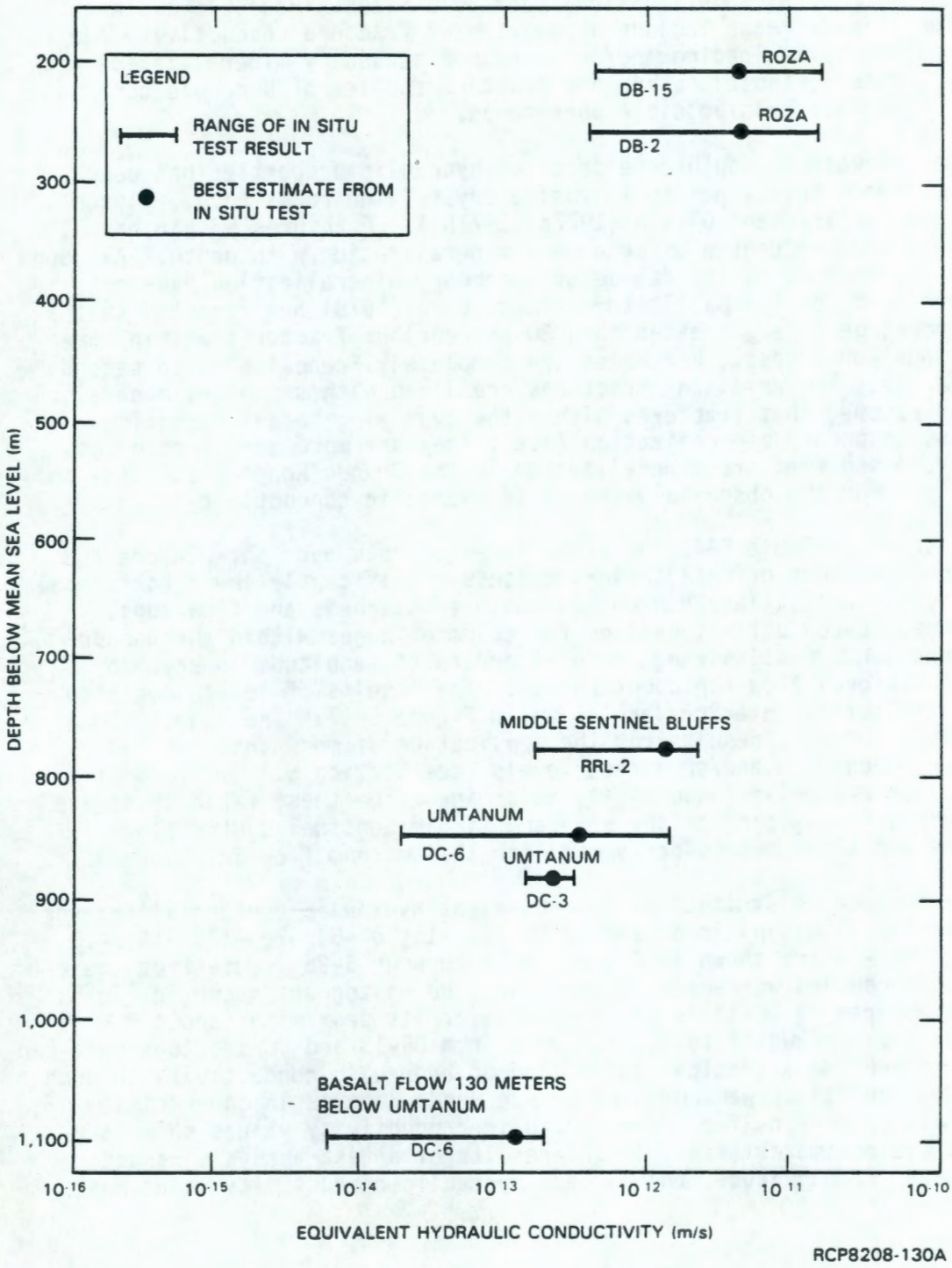

FIGURE 5-17. Comparison of Equivalent Hydraulic Conductivity Values Versus Depth for Flow Interiors (colonnade and entablature) of Selected Columbia River Basalts.

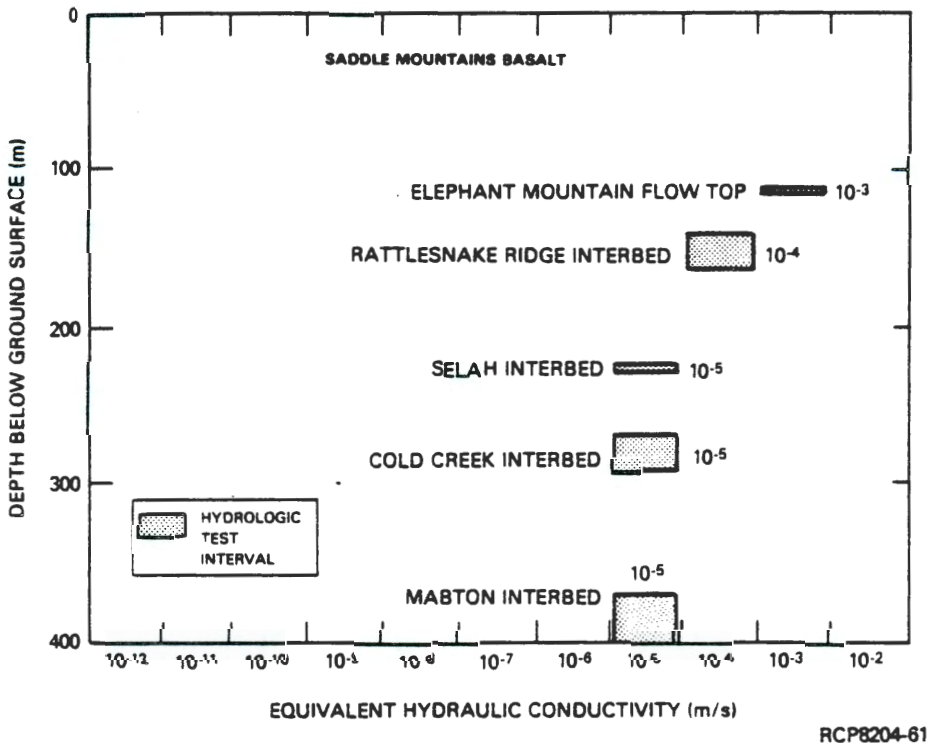

FIGURE 5-18. Equivalent Hydraulic Conductivity Values for Test Intervals Across Interbeds and Flow Tops in Borehole DB-13.

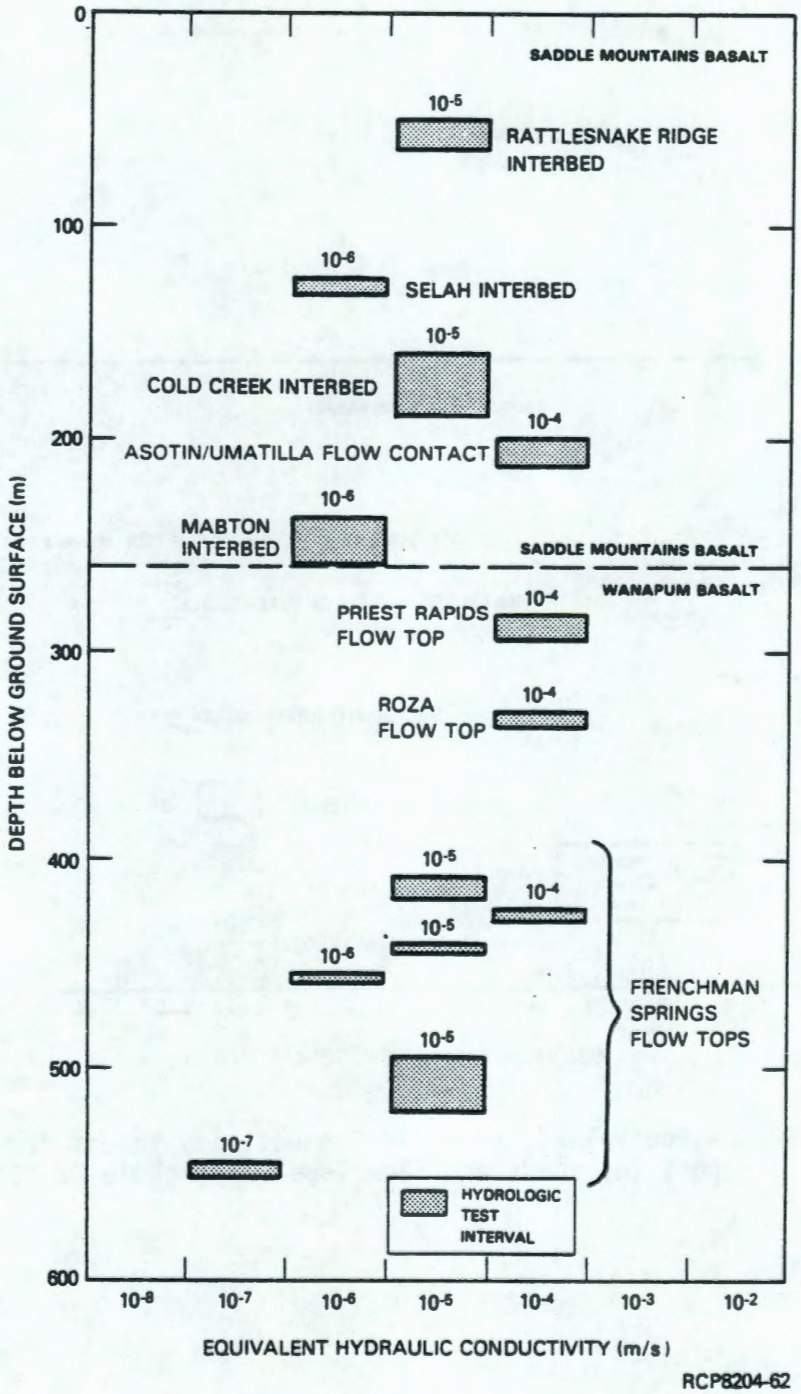

FIGURE 5-19. Equivalent Hydraulic Conductivity Values for Test Intervals Across Interbeds and Flow Tops in Borehole DB-15.

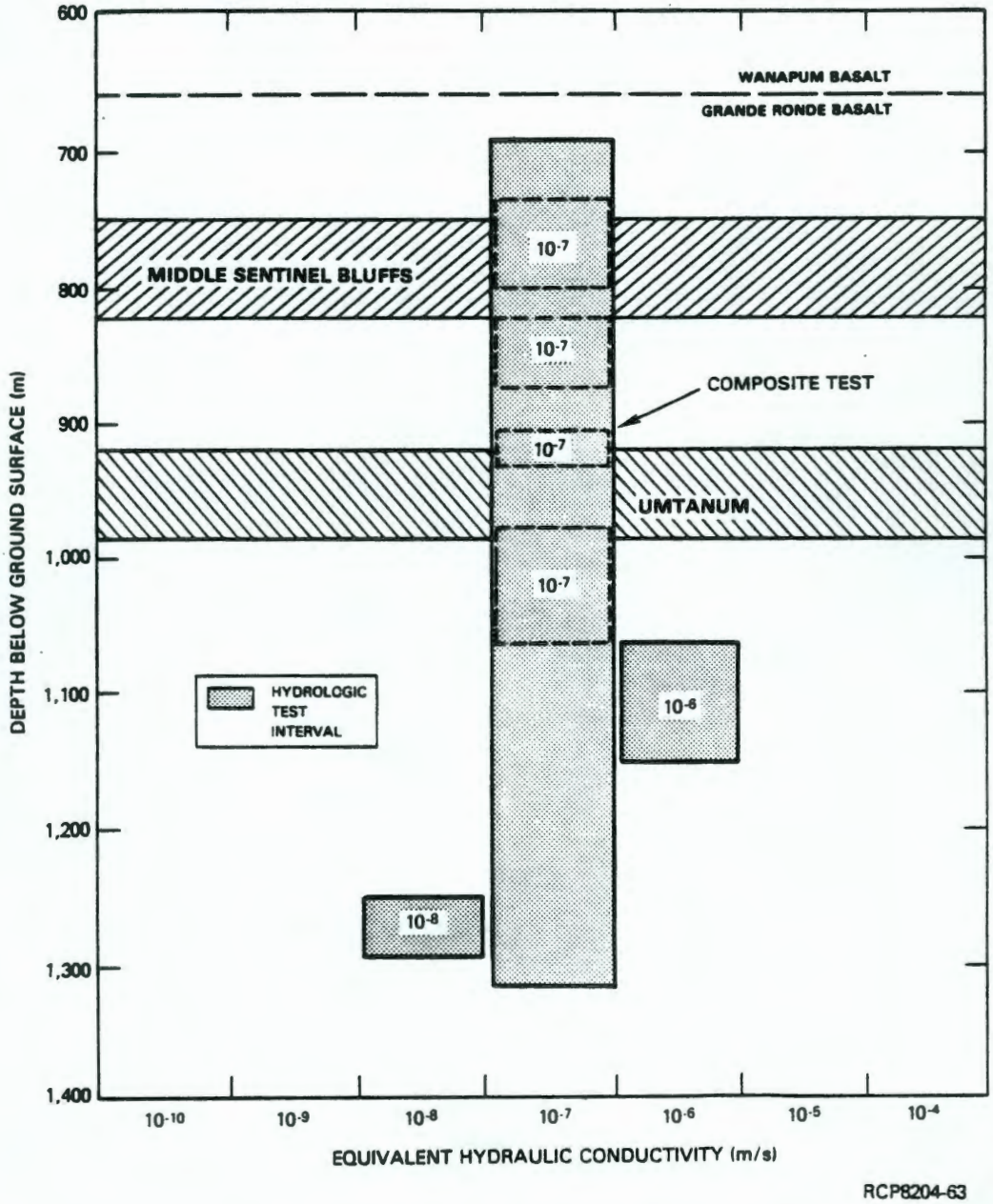

FIGURE 5-20. Equivalent Hydraulic Conductivity Values for Test Intervals Across Flow Tops in Borehole DC-6.

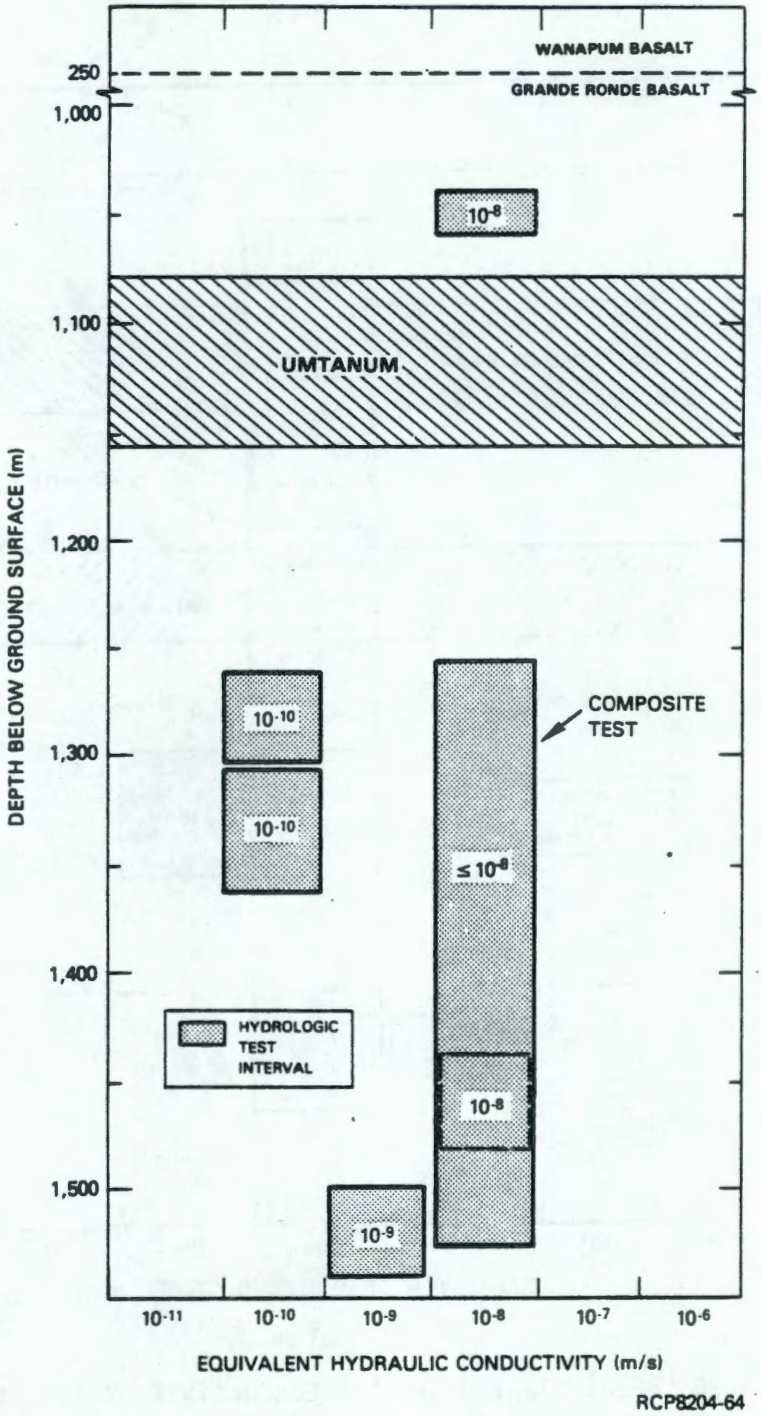

FIGURE 5-21. Equivalent Hydraulic Conductivity Values for Test Intervals Across Flow Tops in Borehole DC-7.

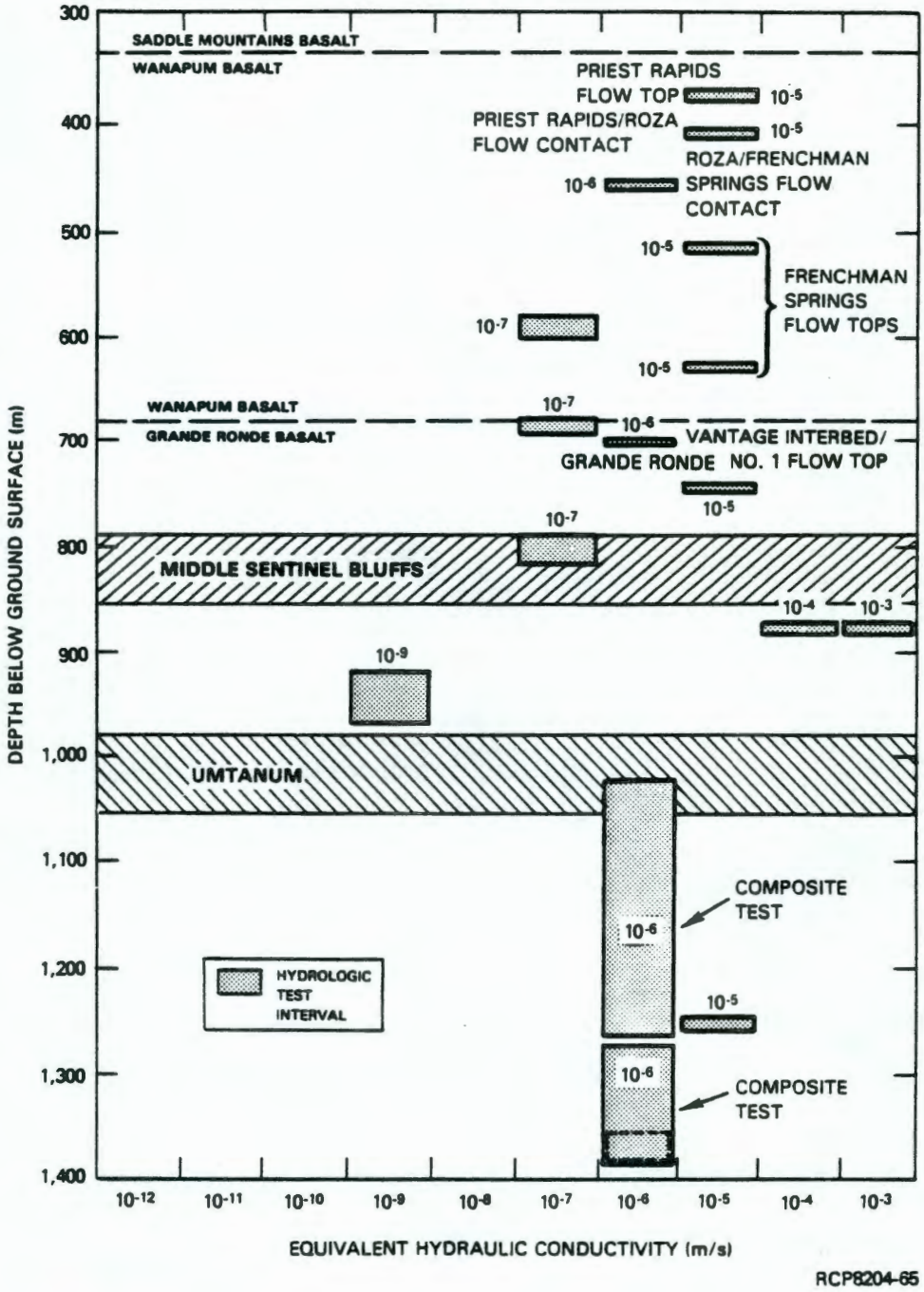

FIGURE 5-22. Equivalent Hydraulic Conductivity Values for Test Intervals Across Flow Tops and One Interbed in Borehole DC-12.

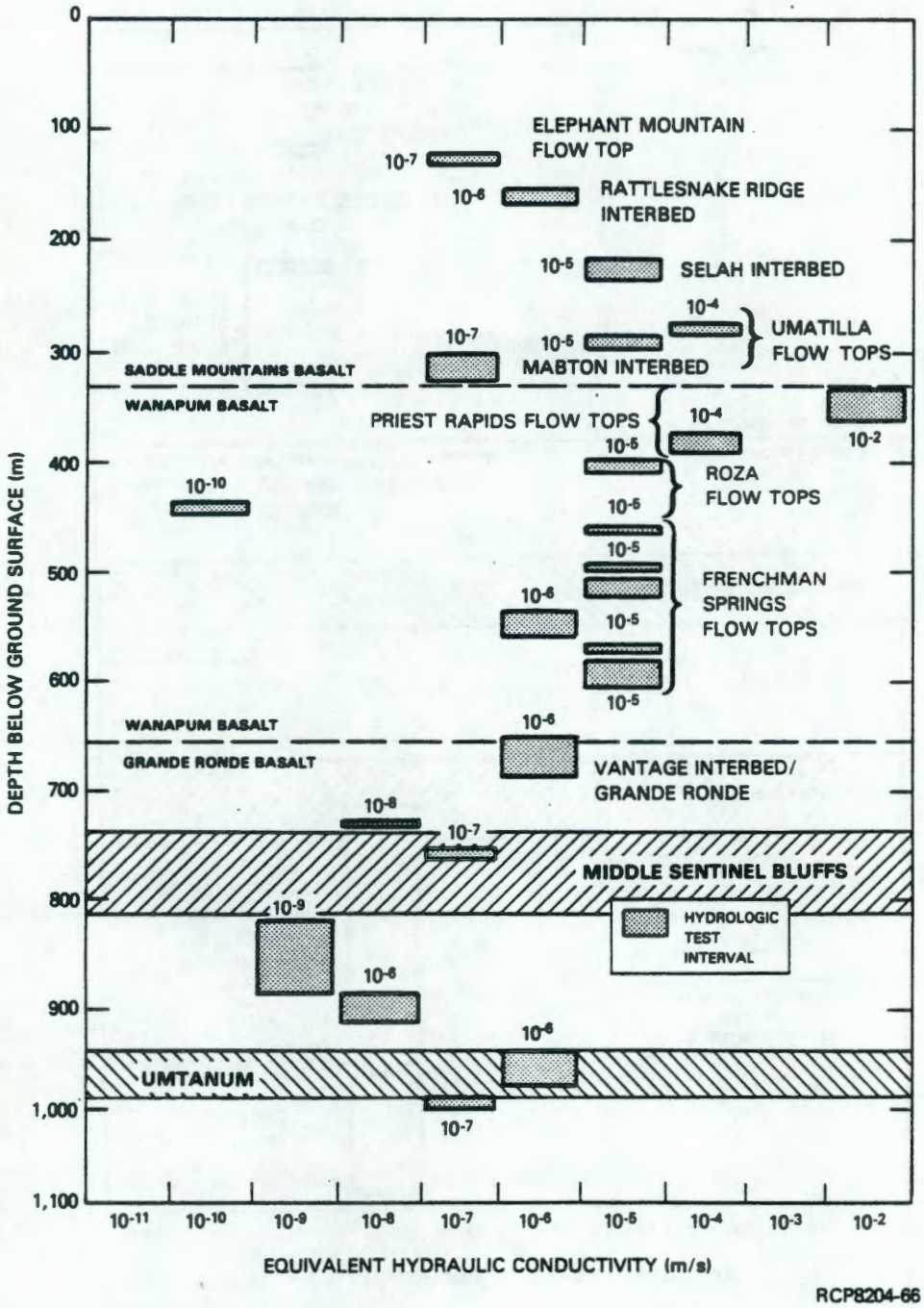

FIGURE 5-23. Equivalent Hydraulic Conductivity Values for Test Intervals Across Flow Tops and Interbeds in Borehole DC-14.

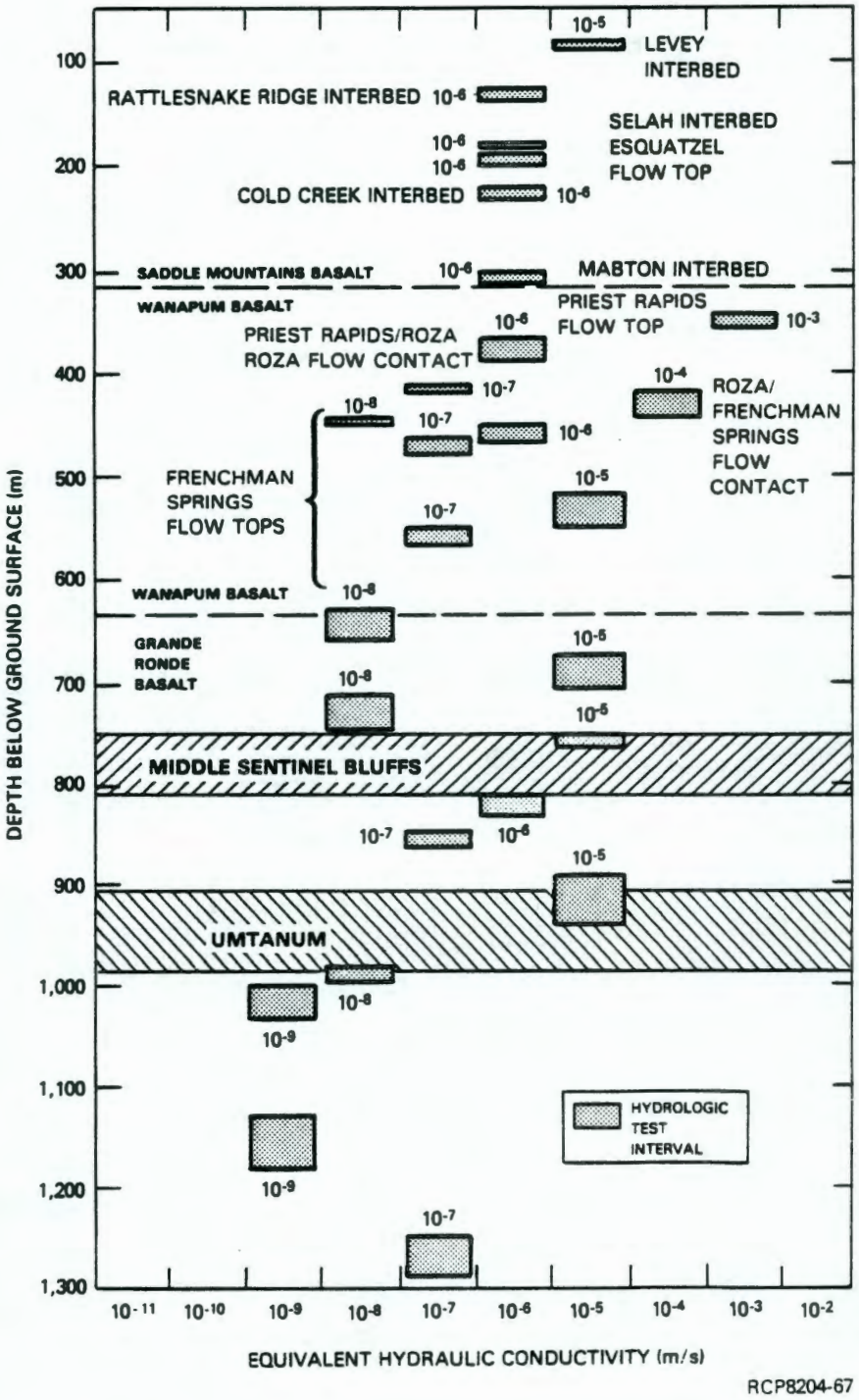

FIGURE 5-24. Equivalent Hydraulic Conductivity Values for Test Intervals Across Flow Tops and Interbeds in Borehole DC-15.

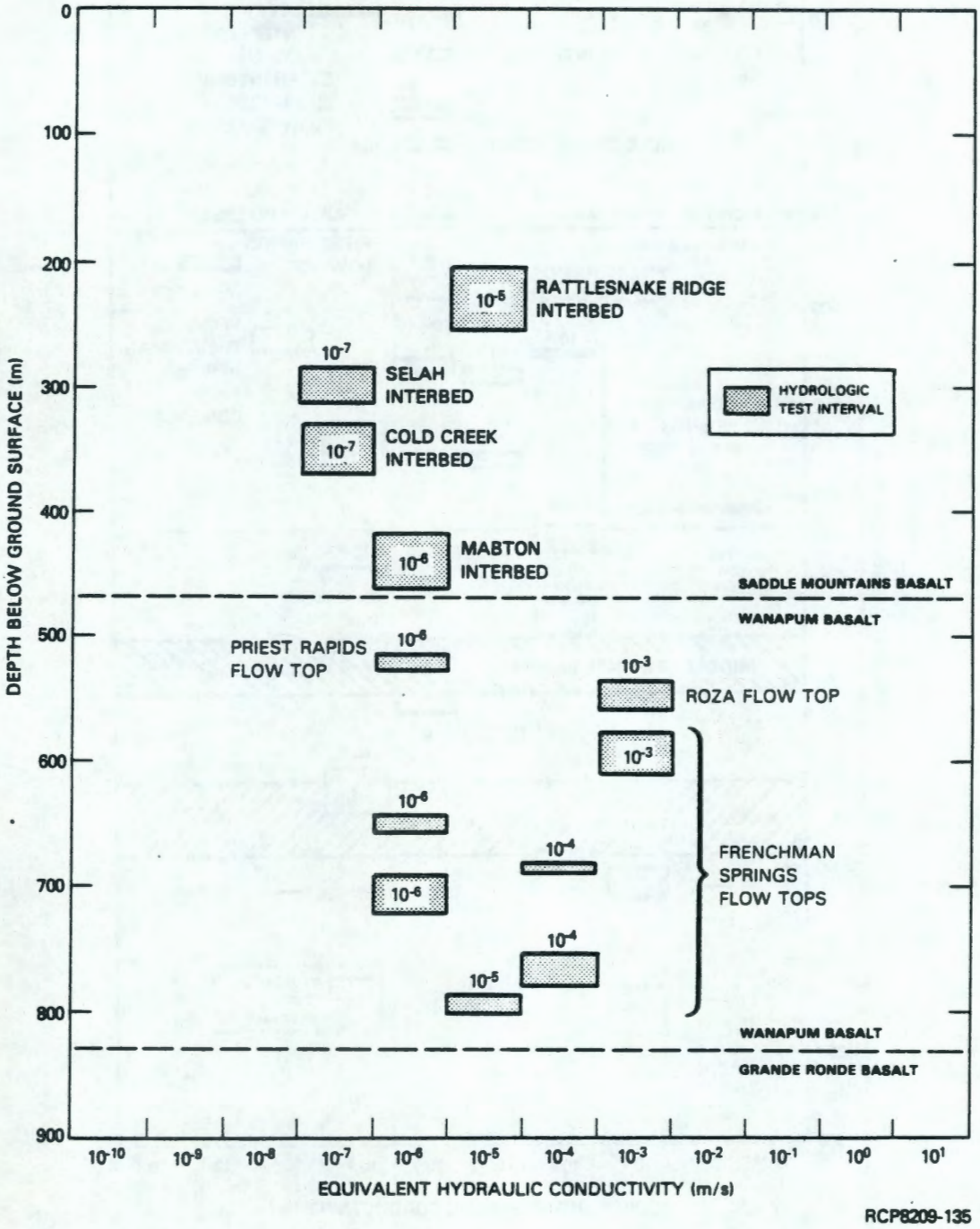

FIGURE 5-25. Equivalent Hydraulic Conductivity Values for Test Intervals Across Mostly Flow Tops and Interbeds in Borehole DC-16A.

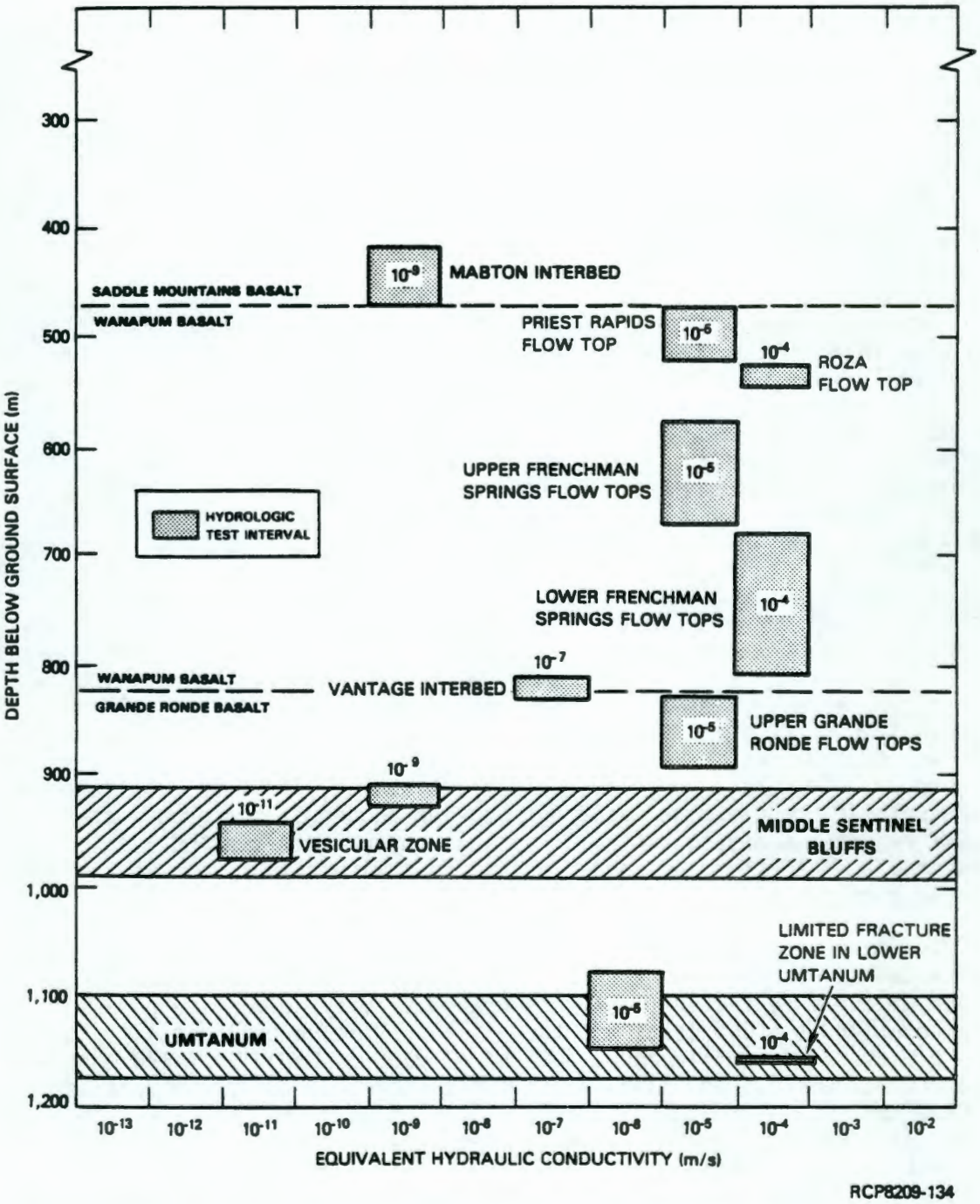

FIGURE 5-26. Equivalent Hydraulic Conductivity Values for Test Intervals Across Mostly Flow Tops and Interbeds in Borehole RRL-2.

Table 5-6 contains a data comparison between known hydrologic properties for the middle Sentinel Bluffs and Umtanum flows of the Grande Ronde Basalt. These two flows are the two candidates for future site characterization and possible repository development. Based on limited data, the equivalent hydraulic conductivity of the middle Sentinel Bluffs flow top varies between 10^{-5} and 10^{-9} meters per second. while that of the Umtanum flow ranges between 10^{-5} to 10^{-7} meters per second. Most of these values fall within the mean conductivities commonly reported for Grande Ronde flow tops (see Fig. 5-16). The variability in conductivity values is probably a function of spatial changes in fracture frequency and interconnection plus mineral infilling. These features are related to a flow's cooling and emplacement history in addition to any postemplacement disturbance.

Determinations of hydraulic conductivity have been conducted within the flow interiors of the middle Sentinel Bluffs and Umtanum flows. As noted in Table 5-6, data include a measurement across the vesicular intraflow zone of the middle Sentinel Bluffs flow. A best estimate of hydraulic conductivity within the interior of the Umtanum flow is 10^{-13} meters per second with the exception of a high-conductivity zone (10^{-4} meters per second) at the lowermost base of the Umtanum flow's entablature at borehole RRL-2. The areal extent and hydraulic continuity of this zone are presently unknown and will be studied during site characterization.

As mentioned in Section 3.7.2.3, tectonic breccias are sometimes encountered during borehole drilling. Pulse testing was conducted across a tectonic breccia zone lying at a depth of 647 to 651 meters in borehole RRL-6. This zone occurs in the lower portion of the Frenchman Springs #1 flow of the Wanapum Basalt. It consists of low to moderately inclined slickensided fractures. No drilling fluid loss was reported during penetration. The equivalent hydraulic conductivity estimated was 10^{-11} meters per second. This is a very low conductivity value, and thus this particular tectonic breccia zone would not provide a conduit for groundwater crossflow between basalt units. Additional hydrologic testing will be conducted across other tectonic breccia zones with results documented in future reports.

Groundwater production rates from individual interbeds and flow tops within the Columbia River basalts vary according to the hydrologic properties of the zone tested (e.g., its transmissivity, effective porosity, thickness, and areal extent) and the nature of the borehole itself (i.e., hole diameter, well efficiency, pump size, etc.). Based on field observations, groundwater production rates of less than 1 liter per minute to several hundred liters per minute have been found to be possible from individual interbeds and flow tops in the Saddle Mountains Basalt. Flow tops within the Wanapum Basalt may produce from a few liters to several thousand liters per minute. The highest production zones appear associated with the Priest Rapids Member of the Wanapum Basalt within and near the Cold Creek Valley. Some high-production zones may also exist in the flow tops of the Roza and Frenchman Springs Members of the Wanapum Basalt, though these rates appear not as high as those found in the Priest Rapids.

TABLE 5-6. Comparison of Equivalent Hydraulic Conductivity Values Between the Middle Sentinel Bluffs and Umtanum Flows.

Borehole	Stratigraphic interval	Lithology	Test interval (m below ground surface)	Equivalent hydraulic conductivity (m/s)[a]
DC-6	Middle Sentinel Bluffs	Flow top	730 - 822	10^{-7}
DC-12	Middle Sentinel Bluffs	Flow top	782 - 811	10^{-7}
DC-15	Middle Sentinel Bluffs	Flow top	760 - 777	10^{-5}
RRL-2	Middle Sentinel Bluffs	Flow top	909 - 921	10^{-9}
RRL-2	Middle Sentinel Bluffs	Vesicular intraflow zone	932 - 968	10^{-11}
RRL-2	Middle Sentinel Bluffs	Flow interior	968 - 990	10^{-12}
DC-6	Umtanum	Flow top	912 - 938	10^{-7}
DC-14	Umtanum	Flow top	933 - 958	10^{-6}
DC-15	Umtanum	Flow top	902 - 949	10^{-5}
RRL-2	Umtanum	Flow top	1,088 - 1,152	10^{-6}
DC-3	Umtanum	Flow interior	1,090 - 1,108	10^{-13}
DC-6	Umtanum	Flow interior	938 - 989	10^{-13}
RRL-2	Umtanum	Fracture zone at base of entablature	1,162 - 1,165[b]	10^{-4}

[a]Highest value reported given for flow tops and vesicular zone. Best estimate given for flow interiors (from Fig. 5-17).

[b]Zone of effective thickness.

Overall, flow tops within the Grande Ronde Basalt appear to have lower hydraulic conductivities than the overlying basalts. Groundwater productions of less than 1 liter per minute to several hundred liters per minute are likely from production wells. As outlined in Chapter 13, future hydrologic testing will identify the areal and stratigraphic extent of all aquifers required for site characterization.

Composite transmissivity tests are sometimes conducted in boreholes to obtain an upper limit on the hydraulic properties across an extended length of borehole. Results of several tests are noted below.

Borehole	Tested basalt formation	Depth across which test performed (m)	Equivalent hydraulic conductivity (m/s)
DC-4/5	Grande Ronde	804 - 1,218	10^{-9}
DC-6	Grande Ronde	689 - 1,321	10^{-7}
DC-7/8	Grande Ronde	1,254 - 1,526	$\leq 10^{-8}$
DC-12	Grande Ronde	1,018 - 1,241	10^{-6}

These composite test results indicate that the hydraulic conductivity across extensive sections of Grande Ronde Basalt is relatively low. It has been found that a few flow tops across several hundred meters of basalt are the controlling hydraulic influence in composite testing and are the principal contributors to the conductivity values shown above.

The only reported estimates of vertical conductivity for Columbia River basalt are from numerical model studies of Tanaka et al. (1974) in the Columbia Basin Irrigation Project and from MacNish and Barker (1976) for the Walla Walla River Basin. Tanaka et al. (1974) estimated the vertical hydraulic conductivity for the basalt sequence to be between 10^{-12} and 10^{-10} meters per second. MacNish and Barker (1976) stated that it may be as low as 10^{-8} meters per second within their area of study. These estimates were iteratively derived from a model that simulated an observed head distribution.

As addressed in Chapter 12, numerical model simulations for studies in the BWIP use the conservative value of 10^{-10} meters per second as the vertical hydraulic conductivity across basalt flows. This is about 2 orders of magnitude larger than the mean horizontal conductivity for the columnar sections of a basalt flow, as determined from downhole hydrologic testing.

Vertical hydraulic conductivity testing will be initiated by the BWIP during fiscal year 1983. Past efforts by the BWIP and supporting subcontractors have focused on reviewing published test methods and analytical

procedures for potential use in testing the vertical hydraulic conductivity of selected low-transmissivity horizons (i.e., the interiors of basalt flows). Test methods that have been reviewed which may have potential for testing applications at Hanford include:

Single borehole test methods	Multiple borehole test methods
Burns (1969)	Hantush (1960)
Prats (1970)	Neuman and Witherspoon (1972)
Hirasaki (1974)	
Raghaven and Clark (1975)	

Of the vertical hydraulic conductivity methods reviewed, the "ratio method" described by Neuman and Witherspoon (1972) appears to have the greatest potential. Performance of this testing method required either the construction of piezometers in the stressed aquifer and adjoining confining layers or the use of multiple packer systems. The BWIP has been involved during 1981 and 1982 in acquiring downhole packer systems which will facilitate the performance of ratio-type tests.

Due to construction constraints, equipment costs, and long test time requirements, vertical hydraulic conductivity tests have not been routinely performed. Initial model runs indicate that for some test arrangements 2 to 12 months per test may be required for pressure responses to be observed in adjoining confining layers at the multiple borehole sites. Efforts in early 1983 will be focused on selecting horizons in which discernible pressure responses in adjoining confining layers can be measured during short periods of time (less than 2 months). Chapter 13 outlines the site characterization approach to and identifies boreholes when such vertical conductivity testing will be attempted.

As noted in Table 5-4, storativity for interbeds and flow tops falls in the range typical of confined aquifer systems (10^{-3} to 10^{-6}).

5.1.3.3.1 Tracer Testing. Tracer testing is being used within the BWIP to obtain estimates of longitudinal dispersivity and effective porosity. These parameters are essential input to the contaminant transport modeling addressed in Chapter 12. A discussion of the testing techniques and available results is presented in Leonhart et al. (1982).

The tracer testing method and configuration utilized by the BWIP is known as the two-well recirculating (injection/withdrawal) test, which has been described by various researchers including Webster et al. (1970), Grove and Beetem (1971), Fried (1975), and Thompson (1980). Initial testing was carried out at boreholes DC-7 and -8 (see Fig. 5-2) within the McCoy Canyon flow top (this is the basalt flow which lies immediately

above the Umtanum flow at the DC-7/8 site). This test interval was situated between 1,038 and 1,062 meters below ground surface. Separation between boreholes DC-7 and -8 at the test depth is about 16.8 meters.

The tracer selected for the experiment was a 0.95 normal aqueous solution of potassium thiocyanate. This tracer was selected on the basis of the conservative behavior of the thiocyanate anion, its low background level, and detectability using ultraviolet absorption techniques.

The results of the testing along with certain pertinent physical data are summarized below:

Test results	
Imposed gradient	1.4 m/m
Groundwater flow rate	3.8 L/min
Formation residence time of average tracer molecule	170 min
Effective thickness estimate (nb)	2×10^{-3} m
Longitudinal dispersivity estimate (α)	0.8 m
Other physical data	
Transmissivity of test horizon	1×10^{-6} m^2/s
Storativity of test horizon	10^{-5}
Test interval width	16.8 m
Test interval thickness	~24 m

The respective estimates of dispersivity (α) and effective thickness (nb) were obtained by a type-curve matching methodology developed after the theoretical results of Gelhar and Collins (1971). A precise resolution of the effective porosity (n) was not obtained due to uncertainty as to the total thickness of the transmissive horizons within the test interval. However, based on the total thickness of the test interval (approximately 24 meters), the effective porosity would probably range between 10^{-2} and 10^{-4}. Future tests will employ techniques (such as tracejector logging or thermal profiling) to further refine this or other porosity estimates.

5.1.3.4 Data From Specific-Capacity Tests. Outside of the Hanford Site, most hydrologic-value determinations for the basalts are from specific-capacity tests routinely run during development of relatively shallow (less than approximately 300 meters) irrigation wells. Within the Pasco Basin, most of these well sites are located east of the Columbia River or in the Pasco-Kennewick area and are completed in the Saddle Mountains or upper Wanapum Basalts. Compilation of these test values are found in Tanaka et al. (1974), Summers et al. (1978), and Gephart et al. (1979a).

Because of the very nature of specific-capacity tests, hydraulic-conductivity values from these data are rough estimates at best. Nonetheless, these values range between 10^{-8} and 10^{-4} meters per second. This is within the range reported by Gephart et al. (1979a) for hydraulic conductivity values of interbeds and flow tops within the Saddle Mountains Basalt. Although these comparisons may be more apparent than real, data from the specific-capacity tests are in the same order of magnitude as those hydraulic conductivity values reported in the previous section for shallow interbeds and flow tops beneath the Hanford Site.

5.1.3.5 Comparison of Hydraulic Conductivity Values. Ranges of hydraulic conductivities for the Columbia River basalt formations are shown in Figure 5-27 plotted in comparison to in situ permeability values reported by Brace (1980) for crystalline and argillaceous rock types. As shown, basalt measurements for flow top (and interbed zones) plot within the range commonly sited for other rock types, while basalt flow interiors (colonnade and entablature zones), being considered as potential repository horizons, occur in the lower range of reported values.

5.1.4 Potentiometric Levels

Potentiometric data for various geologic formations are available from numerous irrigation and domestic wells located throughout the Columbia Plateau. Most of the available regional data, however, are either for wells of shallow depth (i.e., less than 300 meters) or completed in multiple, contributing zones.

Potentiometric data are limited primarily to two sources: the Washington State Department of Ecology regional piezometric network and Rockwell Hanford Operations (Rockwell) studies within the Pasco Basin.

Most potentiometric measurements are from within the Pasco Basin, specifically the Hanford Site. The following discussion on potentiometric measurements and groundwater-flow patterns pertains to the unconfined and confined aquifers within the Columbia River basalts beneath the Pasco Basin.

5.1.4.1 Unconfined Aquifer. The unconfined aquifer is the best understood of all groundwater-flow systems within the Pasco Basin. In general, it consists of unconsolidated sediments of the Hanford and Ringold Formations.

The lateral margins of the unconfined aquifer are bounded by basaltic anticlines that rim the Pasco Basin. These include the Saddle Mountains to the north, Umtanum and Yakima Ridges to the west, Rattlesnake and Horse Heaven Hills to the south, and a broad monocline to the east. The unconfined aquifer thins across local bedrock highs. The most notable of these locations is the Gable Mountain and Gable Butte area located on the Hanford Site.

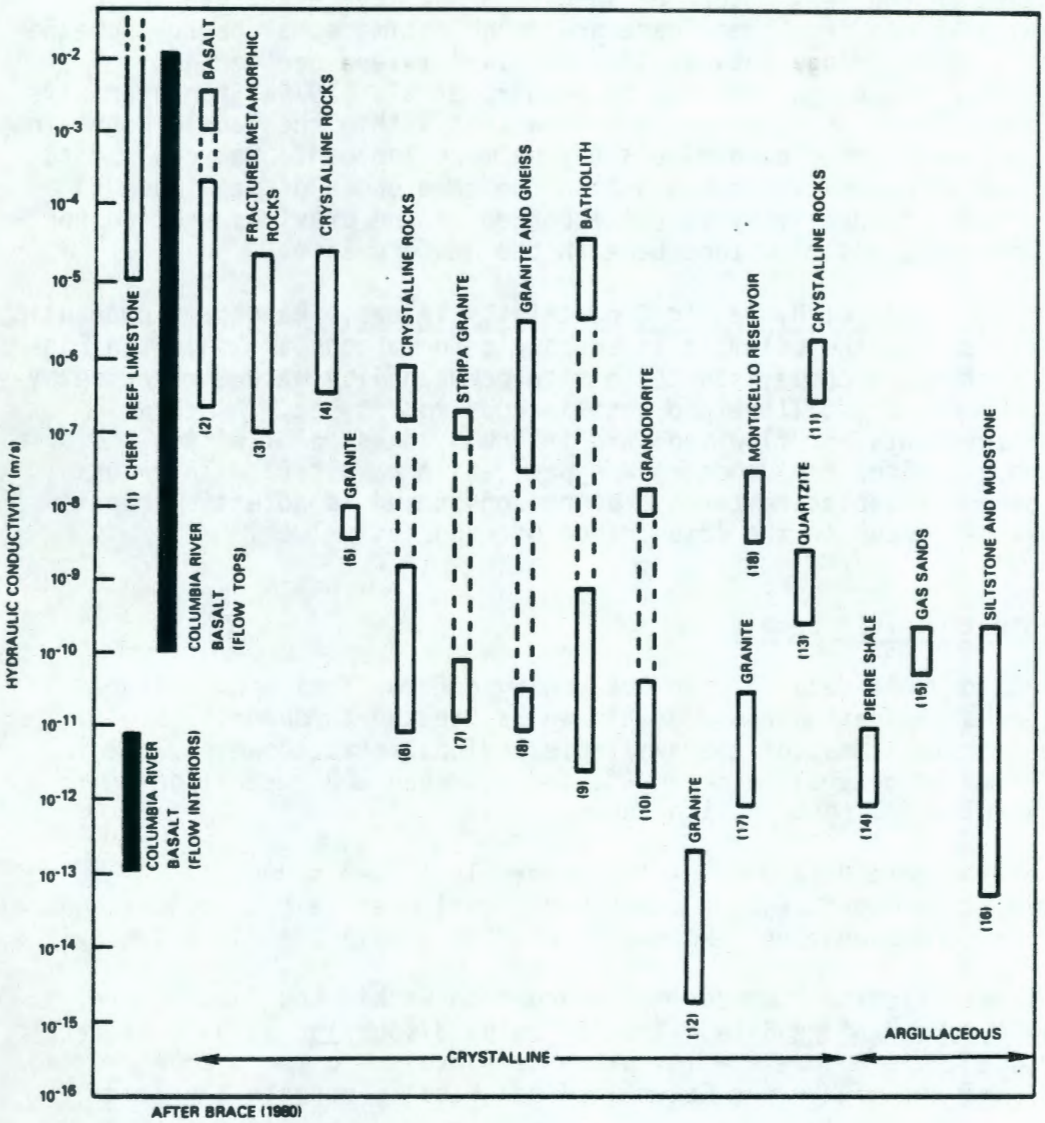

AFTER BRACE (1980)

NOTES:

(1) FRACTURED CHERT AND LIMESTONE; CORALLINE REEF LIMESTONE
(2) ALL BASALTS (ARMENIA, OAHU, IDAHO, AND NEVADA TEST SITE)
(3) DATA FROM WATER WELLS 60 METERS DEEP IN FRACTURED METAMORPHIC ROCKS IN COLORADO
(4) PUMPING TESTS AT 38 DAM SITES IN CRYSTALLINE ROCKS IN WESTERN UNITED STATES
(5) GRANITE NEAR LARAMIE, WYOMING
(6) CRYSTALLINE BASEMENT ROCKS IN SOUTH CAROLINA
(7) GRANITE AT STRIPA MINE, SWEDEN
(8) 500 PUMPING TESTS AT FIVE SITES IN GRANITES AND GNEISS, SWEDEN
(9) LAC du BONNET BATHOLITH, PINAWA, MANITOBA
(10) GRANODIORITE NEAR LOS ALAMOS, NEW MEXICO
(11) CRYSTALLINE ROCKS NEAR ROCKY MOUNTAIN ARSENAL NEAR DENVER, COLORADO
(12) CLIMAX GRANITIC STOCK
(13) BASED ON WATER INFLOW IN A TUNNEL IN QUARTZITE
(14) PIERRE SHALE
(15) GAS SANDS IN RULISON AND GASBUGGY SITES
(16) TRIASSIC SILTSTONE AND MUDSTONE, SOUTH CAROLINA
(17) CARNMENELLIS GRANITE, ENGLAND
(18) MONTICELLO RESERVOIR, SOUTH CAROLINA

RCP8208-136

FIGURE 5-27. Hydraulic Conductivity of Various Crystalline and Argillaceous Rocks.

The water-table contours in Figure 5-28 represent the upper surface of the unconfined aquifer in the Pasco Basin. Many of the water wells supporting Figure 5-28 are taken from the original driller's logs of wells, which span years of time (Gephart et al., 1979a). Where possible, most recent data were used. Contours are not shown in Figure 5-28 in areas where the aquifer is thin or nonexistent. Regionally, the map displays the general direction of lateral groundwater flow. Groundwater flows downgradient from natural recharge areas toward and into the Columbia River. The general pattern is locally interrupted by a major groundwater mound on the Hanford Site at the site of the reference repository location and one north of Pasco, Washington, where the water table has risen as a result of synthetic recharge. These mounds redirect groundwater flow around them, thereby locally influencing water levels and flow patterns.

A map of the 1944 (pre-Hanford) water table beneath the Hanford Site, projected backward from water-level data acquired between 1948 and 1952, is shown in Figure 5-29. The dramatic rise of the Hanford water table from synthetic recharge over the last 35 years is evident by comparing this figure to the Hanford Site portion of Figure 5-28.

Piezometers located near water-disposal ponds on the Hanford Site reveal higher hydraulic heads at the top of the unconfined aquifer than near the bottom. This head distribution is characteristic of groundwater-recharge areas. Piezometers near the Columbia River show increasing heads with depth during low river stages. This upward gradient identifies an area of groundwater discharge.

Recharge to the unconfined-aquifer system occurs from both natural and synthetic sources. Gephart et al. (1979a) reported that the principal sources of natural recharge to the unconfined aquifer occur along the periphery of the basin, where water from precipitation and ephemeral streams infiltrate. Several small ephemeral streams, such as Cold Creek and Dry Creek, located between Rattlesnake Hills and Umtanum Ridge, drain the western slopes of the basin, recharging water to the subsurface as they spread across the lower valley plains. Natural recharge also occurs along the Columbia River during high water levels (bank storage) and perennially along the Yakima River downstream from the Horn Rapids area (Raymond and Brown, 1963). Studies on the Hanford Site indicate that little, if any, recharge to the water table occurs directly from the precipitation on the broad desert plain covering most of the Hanford Site (Gutknecht et al., 1980).

Upward leakage from lower confined aquifers in basalt may also recharge the overlying unconfined aquifer, where favorable potentiometric conditions and hydraulic communication exist. The full extent and magnitude of hydraulic communication is currently unknown. However, an area where the hydraulic heads within the uppermost Saddle Mountains Basalt (specifically, the Rattlesnake Ridge interbed) exceed that for the overlying unconfined aquifer can be seen in Figure 5-30. Examination of this figure indicates that the northern and eastern sections of the Hanford Site have the required potentiometric conditions for upward leakage to occur.

9 2 1 2 4 9 5 0 9 4 0

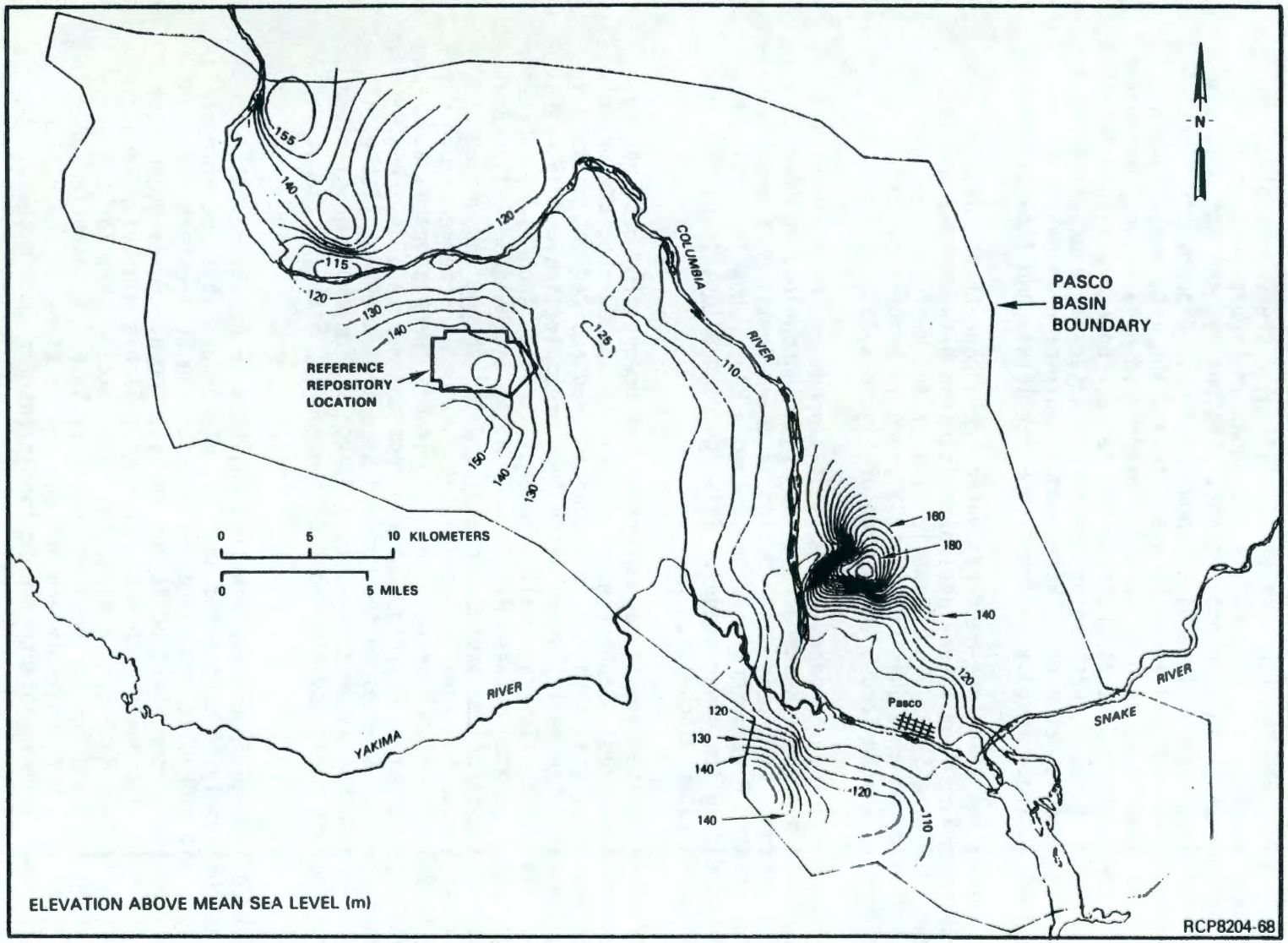

FIGURE 5-28. Elevation of the Groundwater Table Within the Pasco Basin.

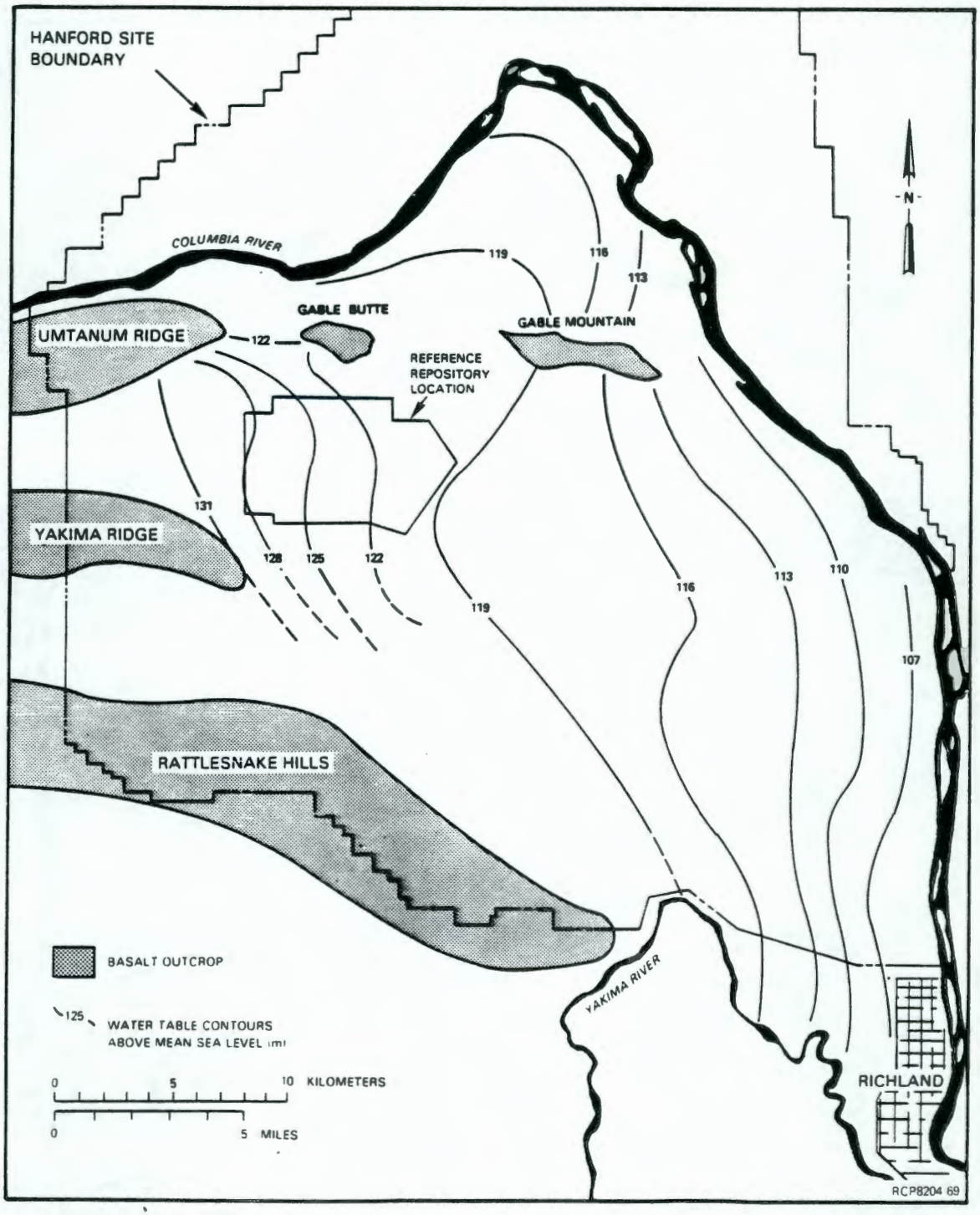

FIGURE 5-29. Estimated 1944 Water-Table Map for the Hanford Site.

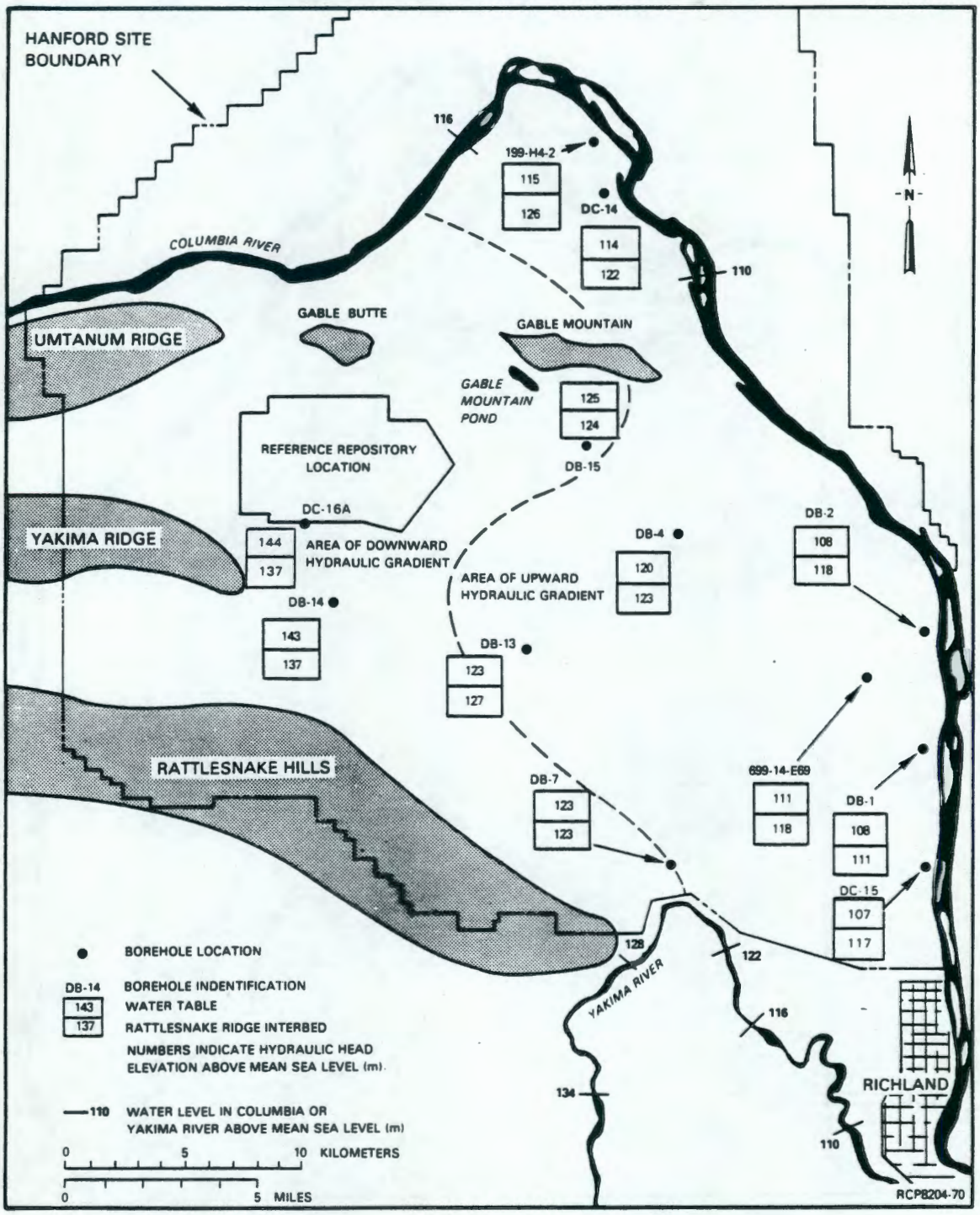

FIGURE 5-30. Comparison of Hydraulic Heads in the Rattlesnake Ridge Interbed to Water-Table Elevation.

Synthetic or artificial recharge to the unconfined aquifer occurs on the Hanford Site from waste-water disposal, primarily centered in the 200 Areas. Although these areas of synthetic recharge are limited in size, this recharge source has had a profound effect on the flow dynamics of the unconfined aquifer. These effects have been monitored and described previously by several investigators (e.g., Newcomb et al., 1972; Gephart et al., 1979a).

Additional sources of synthetic recharge to the unconfined aquifer in the Pasco Basin occur from infiltration of agricultural irrigation waters. The area of recharge from this source is considerably more extensive, occurring in the southeast section of the Pasco Basin within the Columbia Basin Irrigation Project and to a very limited extent west of the Hanford Site in the Cold Creek Valley.

Groundwater discharge from the unconfined aquifer is primarily to the Columbia River, with lesser amounts going to the Snake and Yakima Rivers. Discharge of unconfined groundwater from the Hanford Site is almost exclusively to the Columbia River north of Richland, Washington. In addition, minor groundwater discharge from the unconfined aquifer to the underlying uppermost confined-aquifer system may be occurring near Gable Mountain Pond located along the southwestern border of Gable Mountain (Gephart et al., 1976). In this case, hydraulic communication appears to be associated with paleostream channels cut into the basalt bedrock. Quantification of the amount of groundwater exchange between these flow systems is a topic of site characterization addressed in Chapter 13.

5.1.4.2 Columbia River Basalt Group. Groundwater within the Columbia River basalt occurs primarily under confined conditions in sedimentary interbeds and basalt flow tops. The following discussion pertains to potentiometric conditions for basalt formations within the Pasco Basin in general and the Hanford Site specifically.

5.1.4.2.1 Saddle Mountains Basalt. Confined aquifers within the Saddle Mountains Basalt are the best understood aquifers within the Columbia River basalt. Within the Saddle Mountains Basalt, four extensive interbeds (i.e., Rattlesnake Ridge, Selah, Cold Creek, and Mabton) have been identified as confined aquifers within the region. Flow tops within the Saddle Mountains Basalt, while often possessing higher hydraulic conductivities than interbeds, do not appear as laterally extensive as their sedimentary counterparts.

Sufficient head data are available for the Mabton interbed of the lower Saddle Mountains Basalt to construct a potentiometric surface. This surface is shown in Figure 5-31. The potentiometric map delineates the inferred groundwater-flow pattern. The pattern depicted is believed to be representative of groundwater flow within most of the Saddle Mountains Basalt, except the very uppermost horizons. Salient features shown in Figure 5-31 include:

- A prominent recharge mound extending eastward from Rattlesnake Hills

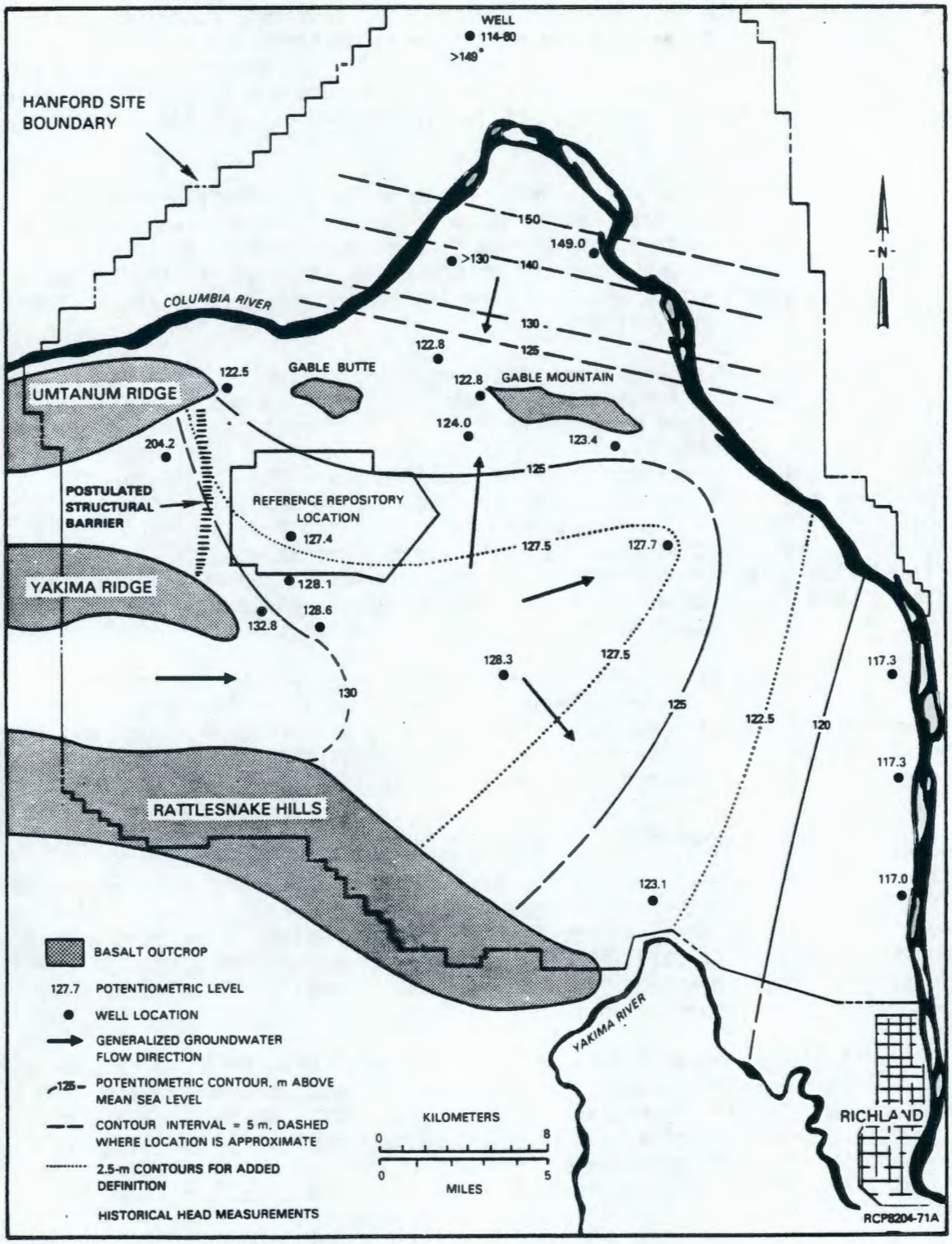

FIGURE 5-31. Potentiometric Map for and Inferred Flow Directions of Groundwater Within the Mabton Interbed Beneath the Hanford Site.

- The presence of a low hydraulic-head (potential-discharge) region in the Umtanum Ridge-Gable Mountain anticline area

- A postulated structural barrier at the mouth of the Cold Creek Valley across which heads drop approximately 70 meters within the Mabton interbed

- The lack of a dominant-line sink (potential-discharge) area along the Columbia River north of Gable Mountain.

As additional head data are collected and plotted on Figure 5-31, it is suspected that the 125- and 130-meter contours located north and south of the Umtanum Ridge-Gable Mountain anticline will join northwest of the reference repository location. Such a potentiometric distribution would continue to support the concept of a hydraulic low near Gable Butte and Gable Mountain. Groundwater in this area would then flow either vertically to shallower systems and/or move eastward toward the Columbia River.

Section 5.1.5.2 of this report contains hydrochemical data supporting the overall groundwater flow directions implied in Figure 5-31.

The hydraulic heads determined for selected boreholes within the Saddle Mountains Basalt are listed in Table 5-7. Dates of measurement indicate when the particular stratigraphic interval was penetrated prior to casing or cementing (refer to Fig. 5-2 for borehole locations). In Section 5.1.4.2.4, vertical-head profiles across the Saddle Mountains Basalt are given for boreholes DB-15, DC-14, -15, and -16A. Hydraulic heads in the boreholes listed in Table 5-7 and Section 5.1.4.2.4 rise to elevations above that of the test interval and therefore artesian conditions exist at these borehole sites.

Of the boreholes listed in Table 5-7, particular interest should be given to DB-13, -14, and DC-16A because these are sites where head measurements were determined in several intervals. The heads in DB-14 decrease with depth from an elevation of 136.8 meters in the Rattlesnake Ridge interbed to 128.6 meters in the Mabton interbed. This head gradient is characteristic of an area of potential groundwater recharge. The same gradient trend is true for borehole DC-16A, located 2.5 kilometers northwest of DB-14. Approximately 10 kilometers to the southeast is borehole DB-13, where a slight head increase with depth is indicated in Table 5-7. Because the head increase is so minor, this suggests an area of essentially lateral groundwater movement. No trend in hydraulic head with depth is indicated in the vicinity of DB-12. In borehole DC-1, the Mabton interbed head value is questioned. The remaining values for the Selah and Cold Creek interbeds suggest a generally uniform head.

Across the Cold Creek syncline, an average head gradient of 0.0003 meter per meter is determined for the Mabton interbed by comparing observed heads at boreholes RRL-2, 127.4 meters; and DC-15, 117.0 meters.

TABLE 5-7. Hydraulic Heads Within Selected Stratigraphic Intervals in the Saddle Mountains Basalt.

Borehole	Stratigraphic interval	Year of measurement	Hydraulic head (m above mean sea level)
DB-12	Selah interbed	1978	122.5
	Mabton interbed	1979	122.5
DB-13	Elephant Mountain flow top	1978	127.1
	Rattlesnake Ridge interbed	1978	127.4
	Cold Creek interbed	1978	128.0
	Mabton interbed	1979	128.3
DB-14	Rattlesnake Ridge interbed	1978	136.8
	Selah interbed	1978	129.2
	Cold Creek interbed	1978	128.9
	Mabton interbed	1979	128.6
DC-1	Selah interbed	1969	124.1
	Cold Creek interbed	1969	124.7
	Mabton interbed	1969	~122
DC-16A*	Rattlesnake Ridge interbed	1982	136.6
	Selah interbed	1982	133.7
	Cold Creek interbed	1982	127.5
	Mabton interbed	1982	128.1

*Drilling and testing in progress (September 1982).

From Section 5.1.4.2.4, it can be surmised that the hydraulic heads decrease with depth in borehole DC-16A, are uniform in borehole DB-15, increase with depth at borehole DC-14, and are variable in borehole DC-15. Thus, the overall vertical-head pattern for the Saddle Mountains Basalt appears to be one supporting recharge to the west, lateral groundwater movement beneath the Cold Creek syncline, and potential discharge toward the east.

Natural recharge to aquifers within the Saddle Mountains Basalt occurs from direct infiltration of precipitation and interbasin stream runoff within peripheral tributary areas (i.e., Rattlesnake Hills, Yakima Ridge, Umtanum Ridge, and the Saddle Mountains) of the Pasco Basin. Natural recharge to upper Saddle Mountains Basalt aquifers from the overlying unconfined aquifer has also been reported by Spane et al. (1980) and Gephart et al. (1976) to occur on the Hanford Site, where favorable potentiometric conditions and hydraulic communication exist. This is expected to take place in the Gable Mountain Pond area (see Fig. 5-30) or in any location where the overlying confining layers are absent and/or have been removed by erosion.

Synthetic recharge to aquifers within the Saddle Mountains Basalt also occurs from infiltration of irrigation waters within the Columbia Basin Irrigation Project. This occurs in the eastern and northeastern sections of the Pasco Basin, where this basalt formation crops out or lies close to ground surface. The influx of synthetic recharge can be distinguished by the presence of nitrate within shallow irrigation wells constructed in this area (Gephart et al., 1979a). For example, the association of nitrate levels for Saddle Mountains Basalt groundwater affected by irrigation water recharge within the Pasco Basin is shown in Figure 5-32. Most of the non-Hanford irrigation wells noted on this figure are within the Columbia Basin Irrigation Project. Additionally, a hydrograph of a well (10N/30E-19E) located to the north of Pasco, Washington is presented in Figure 5-33. The hydrograph illustrates a rise in the static water level, on the order of 0.75 meter per year. This phenomenon correlates largely with groundwater recharge resulting from irrigation practices.

The major discharge area for aquifers within the Saddle Mountains Basalt is believed to be the Columbia River, toward Wallula Gap and in the Priest Rapids Dam area. Along these river reaches, the Saddle Mountains are in direct contact and therefore in hydraulic communication with the Columbia River. Discharge also occurs to overlying or underlying aquifers where hydraulic communication and favorable potentiometric conditions exist. As suggested earlier, localized potential crossflow to adjacent aquifer systems may also occur in the area of the Umtanum Ridge-Gable Mountain anticline.

During site characterization, studies will be undertaken to quantify the amount of groundwater recharge and discharge occurring within the Saddle Mountains Basalt (see Chapter 13).

9 2 1 2 4 9 5 0 9 4 8

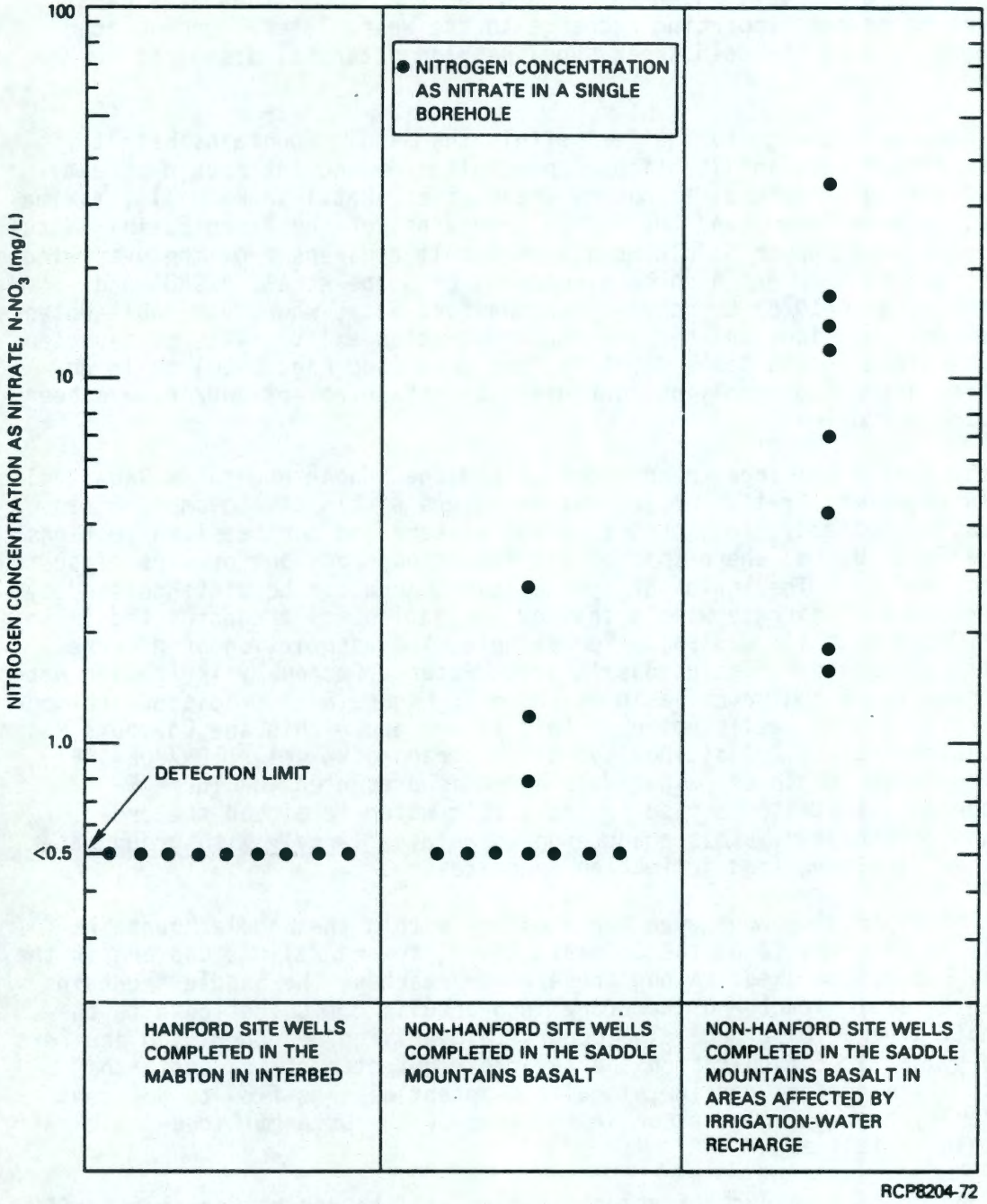

FIGURE 5-32. Total Nitrogen-Nitrate (N as NO_3) Concentration for Groundwater Within the Saddle Mountain Basalt in the Pasco Basin.

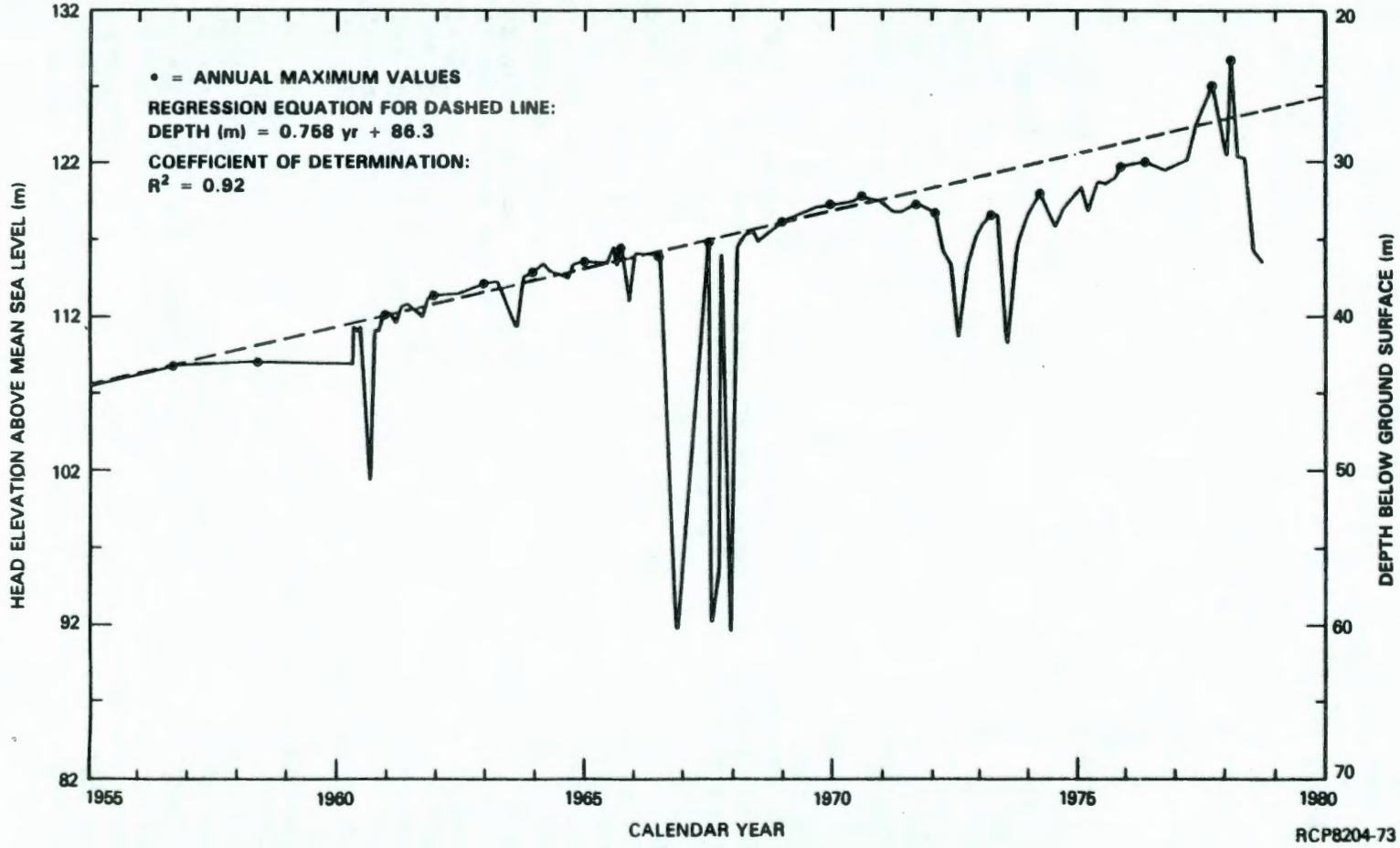

FIGURE 5-33. Hydrograph for Well 10N/30E-19E Located North of Pasco, Washington.

5.1.4.2.2 Wanapum Basalt. Confined aquifers within the Wanapum Basalt occur primarily within basalt flow tops and exist under artesian conditions. Extensive sedimentary interbeds, which characterize the overlying Saddle Mountains Basalt, are not present within the Wanapum Basalt. Only the Vantage interbed, which occurs stratigraphically between the Wanapum and Grande Ronde Basalts, can be locally identified. Regionally, the Squaw Creek and Quincy interbeds also occur. Within the Pasco Basin, however, the Vantage interbed is thin (i.e., less than 5 meters), discontinuous, and of no apparent hydrologic significance.

Principal aquifers within the Wanapum Basalt occur in the Priest Rapids Member (upper Wanapum) and Frenchman Springs Member (lower Wanapum) and appear to be laterally extensive within the Pasco Basin. These hydrogeologic units can be prolific groundwater producers and are reported to be major sources of groundwater supply in surrounding basins (Crosby et al., 1972; Strait, 1978). For example, the Priest Rapids Member beneath the Cold Creek Valley has the largest hydraulic conductivities (up to 10^{-2} meters/second) for a basalt unit reported within the Pasco Basin (Gephart et al., 1979a). Irrigation wells in that area typically produce 4,000 to 8,000 liters per minute from the upper portion of the Priest Rapids Member. These high withdrawals have over the last 50 years lowered the head in the Priest Rapids Member by some 60 meters (see Section 5.1.9.3). Within the Hanford Site south of the Umtanum Ridge-Gable Mountain anticline, hydraulic conductivities of 10^{-2} to 10^{-6} meters per second are reported for the Priest Rapids Member (Section 5.1.3.3). Therefore, large groundwater productions are possible from this same zone beneath portions of the Hanford Site.

Areal hydraulic head data for individual flow tops within the Wanapum Basalt are not as extensive as in the overlying Saddle Mountains Basalt. Currently, areal head coverage is insufficient for preparing detailed Wanapum potentiometric maps. However, general groundwater-flow patterns outside of the reference repository location can be deduced from the vertical-head profiles given in Section 5.1.4.2.4. Proceeding north to south across the Hanford Site, the average heads for the Wanapum Basalt in the four boreholes noted are DC-14, 150 meters; DB-15, 125 meters; DC-16A, 123 meters; and DC-15, 118 meters. These data suggest higher heads to the north and northwest and lower heads to the south across most of the Cold Creek syncline. Therefore, the general groundwater-flow direction in the Wanapum Basalt appears to be southward.

Within the central portion of the reference repository location at borehole RRL-2, the average hydraulic head elevation in the Wanapum Basalt is 122 meters (Section 5.1.4.2.4). At borehole DC-16A, located 2.5 kilometers south of RRL-2, the elevation of Wanapum Basalt heads is 122 to 123 meters. Therefore, even though the overall groundwater flow pattern in the Wanapum Basalt is southward in the Cold Creek syncline, some component of a more northern flow may exist near the reference repository location. The additional drilling and hydrologic testing outlined in Chapter 13 for site characterization studies will specifically address this question.

Table 5-8 gives the areal head gradients across a large section of the Cold Creek syncline for the members of the Wanapum Basalt. These gradients are determined between boreholes RRL-2/DC-15, DC-12/DC-15, and DB-15/DC-15. Gradients average between 0.0001 and 0.0003 meter per meter.

In Figure 5-31, it is seen that hydraulic heads within the Mabton interbed decrease nearly 80 meters between borehole DB-11 (head of 204.2 meters above mean sea level), which lies west of the Cold Creek structural barrier, compared to boreholes near the reference repository location. In comparison, the hydraulic head of the Priest Rapids Member of the Wanapum Basalt at DB-11 is 280 meters above mean sea level. This is 76 meters greater than that in the overlying Mabton interbed at that same borehole and some 160 meters larger than the Priest Rapids heads east of the structural barrier. Therefore, the confining nature of this barrier might increase with depth. Future drilling and testing will determine whether or not these head differences across the barrier continue into the lower Wanapum and Grande Ronde Basalts.

Recharge areas for aquifers within the Wanapum Basalt are more areally extensive than the overlying Saddle Mountains Basalt, as implied from outcrop areas shown in Figure 5-4. Intrabasin recharge occurs from direct infiltration of precipitation and stream runoff in the Saddle Mountains, Rattlesnake Hills, Umtanum Ridge, and Yakima Ridge areas. In addition to intrabasin recharge, regional interbasin recharge from surrounding areas is also thought to take place.

The major discharge area for aquifers within the Wanapum Basalt, like the overlying Saddle Mountains Basalt, is believed to be the Columbia River toward Wallula Gap and along the river's reach from Sentinel Gap to Priest Rapids Dam. The Wanapum Basalt is in direct hydraulic communication with the Columbia River in these areas. Other sources of discharge from the Wanapum Basalt is to adjoining basalt layers. The extent of such vertical leakage is a function of the basalt's vertical transmissivity characteristics. Major vertical leakage probably occurs in stratigraphically or structurally complex areas. As mentioned previously, one such area could be near Gable Mountain.

As noted above, the hydraulic heads in the Wanapum Basalts in boreholes DC-14 and -15 near the Columbia River adjacent to the Hanford Site are higher than the river's elevation (i.e., flowing artesian conditions exist). However, the vertical-head profiles in the Wanapum Basalt at these boreholes are relatively uniform, suggesting a rather flat vertical profile. In borehole DC-15, which lies on the eastern edge of the Cold Creek syncline, the vertical hydrochemical profile suggests that waters are isotopically heavier, older, and have distinct hydrochemical signatures with depth (Sections 5.1.5 and 5.1.6). Hydrochemical stratification is also evident at borehole DC-14 located adjacent to the Columbia River in the northern portion of the Hanford Site. Such hydrochemical stratification adjacent to the Columbia River suggests that no significant vertical groundwater mixing is taking place between deep and shallow basalt formations. As noted in Chapter 13, hydrochemical modeling is planned to examine this concept.

9212495095 2

TABLE 5-8. Areal Head Gradients in Selected Members of the Wanapum Basalt.

Stratigraphic interval	Comparison of hydraulic heads[a] (m above mean sea level)		Average gradient between boreholes[b] (m/m)
	Head in RRL-2	Head in DC-15	
Priest Rapids	122	118	0.0001
Roza	123	118	0.0001
Frenchman Springs	122	118	0.0001
	Head in DC-12	Head in DC-15	
Priest Rapids	124	118	0.0002
Roza	124	118	0.0002
Frenchman Springs	124	118	0.0002
	Head in DB-15	Head in DC-15	
Priest Rapids	125	118	0.0003
Roza	125	118	0.0003
Frenchman Springs	125	118	0.0003

[a]Observed head in flow tops to nearest meter; values taken from Section 5.1.4.2.4. Borehole elevations (m above mean sea level): RRL-2 = 194, DC-12 = 157, DC-15 = 122, DB-15 = 143. Borehole separation between RRL-2/DC-15, DC-12/DC-15, and DB-15/DC-15 are 34.5, 23.0, and 25.5 kilometers, respectively.

[b]Boreholes assumed located perpendicular to direction of groundwater flow.

9 2 1 2 4 9 5 0 9 5 3

5.1.4.2.3 Grande Ronde Basalt. Confined aquifers within the Grande Ronde Basalt are less understood than shallower groundwater systems. Groundwater within the Grande Ronde Basalt occurs primarily in basalt flow tops. No continuous significant sedimentary interbeds have been identified in the Grande Ronde Basalt within the Pasco Basin.

Areal hydraulic head data from individual flow tops within the Grande Ronde Basalt are limited. Development of potentiometric maps for separate flow tops is not currently possible. However, general groundwater-flow patterns can be deduced from vertical-head profiles (see Section 5.1.4.2.4). The average head gradients in several boreholes for the middle Sentinel Bluffs and Umtanum flows of the Grande Ronde Basalt are listed in Table 5-9. The predominant head pattern is that of decreasing head southward across the Hanford Site. An areal head gradient of 0.0002 and 0.0003 meter per meter appears to be most characteristic of the middle Sentinel Bluffs and Umtanum flow tops across the Cold Creek syncline.

TABLE 5-9. Areal Head Gradient in the Middle Sentinel Bluffs and Umtanum Flow Tops of the Grande Ronde Basalt.

Stratigraphic interval	Comparison of hydraulic heads[a] (m above mean sea level)		Average gradient between boreholes[b] (m/m)
	Head in RRL-2	Head in DC-15	
Middle Sentinel Bluffs	121	119	0.00005
Umtanum	124	117[c]	0.0002
	Head in DC-12	Head in DC-15	
Middle Sentinel Bluffs	124	119	0.0002
Umtanum	125	117[c]	0.0003

[a]Observed head in flow tops to nearest meter; values taken from Section 5.1.4.2.4. Borehole elevations (m above mean sea level): RRL-2 = 194, DC-12 = 157, DC-15 = 122. Borehole separation between RRL-2/DC-15 and DC-12/DC-15 are 34.5 and 23.0 kilometers, respectively.

[b]Boreholes assumed located perpendicular to direction of groundwater flow.

[c]Average value across Umtanum flow at borehole DC-15.

Recharge areas for the Grande Ronde Basalt are thought to be more widespread than those of the overlying Saddle Mountains and Wanapum Basalts (Fig. 5-4). Intrabasin recharge within the Pasco Basin from direct infiltration of precipitation and stream runoff in the Saddle Mountains, Rattlesnake Hills, Umtanum Ridge, and Yakima Ridge region is considered to be of only local significance in comparison to total recharge from regional systems within the Grande Ronde Basalt. Principal sources of recharge are believed to occur outside of the Pasco Basin in topographically high areas of the Columbia Plateau, where the Grande Ronde Basalt crops out. Of particular importance is interbasin recharge from the neighboring Big Bend and Palouse/Snake Basins located east-northeast of the Pasco Basin and the Yakima, Upper Yakima, and Kittitas Basins to the west (Gephart et al., 1979a).

Major discharge areas for groundwater within the Grande Ronde Basalt are believed to be similar to those cited for the Wanapum Basalt. These include the Columbia River toward Wallula Gap and along the Columbia River from Sentinel Gap to Priest Rapids Dam. In addition, significant regional discharge is expected to occur to the lower Snake River above its confluence with the Columbia River and to the Columbia River in the Columbia River Gorge region.

As will be noted in the following section (5.1.4.2.4), artesian or flowing artesian conditions exist in all Grande Ronde flow tops; therefore, some groundwater discharge to shallower stratigraphic horizons is possible throughout the Hanford Site. The amount of such discharge is influenced by the overall vertical hydraulic conductivity of the many individual basalt flows through which the groundwater would move to reach shallow flow systems.

5.1.4.2.4 Vertical-Head Profiles. The vertical distribution of known hydraulic heads in boreholes DB-15, DC-6, -7, -12, -14, -15, -16A, and RRL-2 are shown in Figures 5-34 through 5-41. (See Fig. 5-2 for borehole locations.) These data denote observed hydraulic heads. Heads were usually measured as the boreholes penetrated various interbeds and flow tops, the exception being borehole DC-6, which was an existing borehole open across the Grande Ronde Basalt originally drilled for stratigraphic data. Different abscissa scales are used in these figures. The scale selected was based on showing head variations, regardless of whether those variations were large or small. The heads in all of the boreholes shown in these figures exist under artesian conditions. In boreholes DC-6, -14, and -15, some zones of flowing artesian conditions also occur.

Borehole DB-15 is located just south of Gable Mountain, 8 kilometers east of the reference repository location. Head measurements were acquired across interbeds and flow tops of the Saddle Mountains and Wanapum Basalts as the borehole penetrated these horizons. Figure 5-34 displays the vertical distribution of these heads. The observed heads are very uniform across both the Saddle Mountains and Wanapum Basalts at 124 to 125 meters above mean sea level. The Rattlesnake Ridge interbed head of 124.6 meters is similar to the elevation of the local water table. This is expected since, as noted in Section 5.1.7.1, the unconfined and uppermost confined aquifers are in hydraulic communication near the Gable Mountain area.

9 2 1 2 4 9 5 0 9 5 5

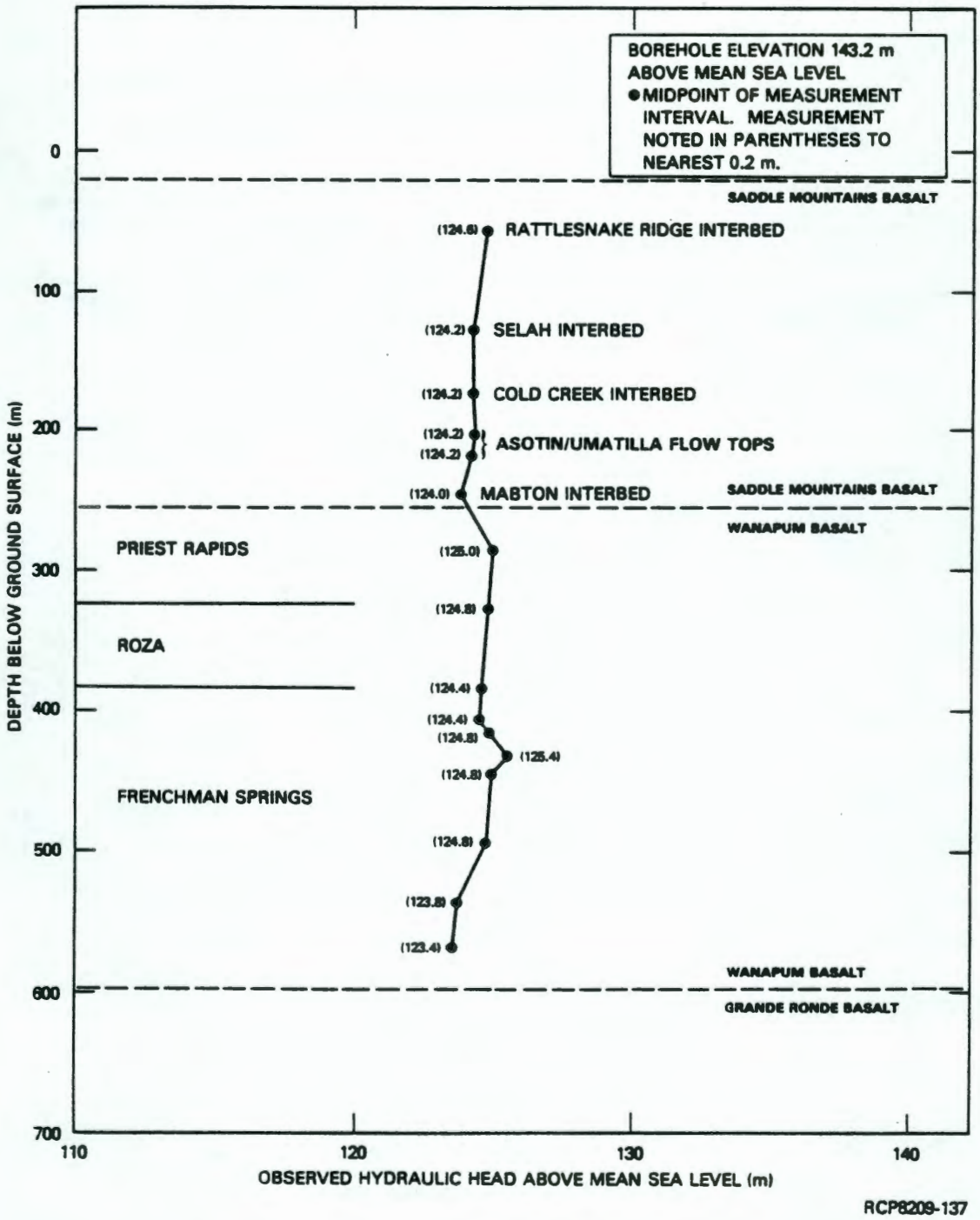

FIGURE 5-34. Hydraulic Head Measurements Within the Saddle Mountains and Wanapum Basalts at Borehole DB-15.

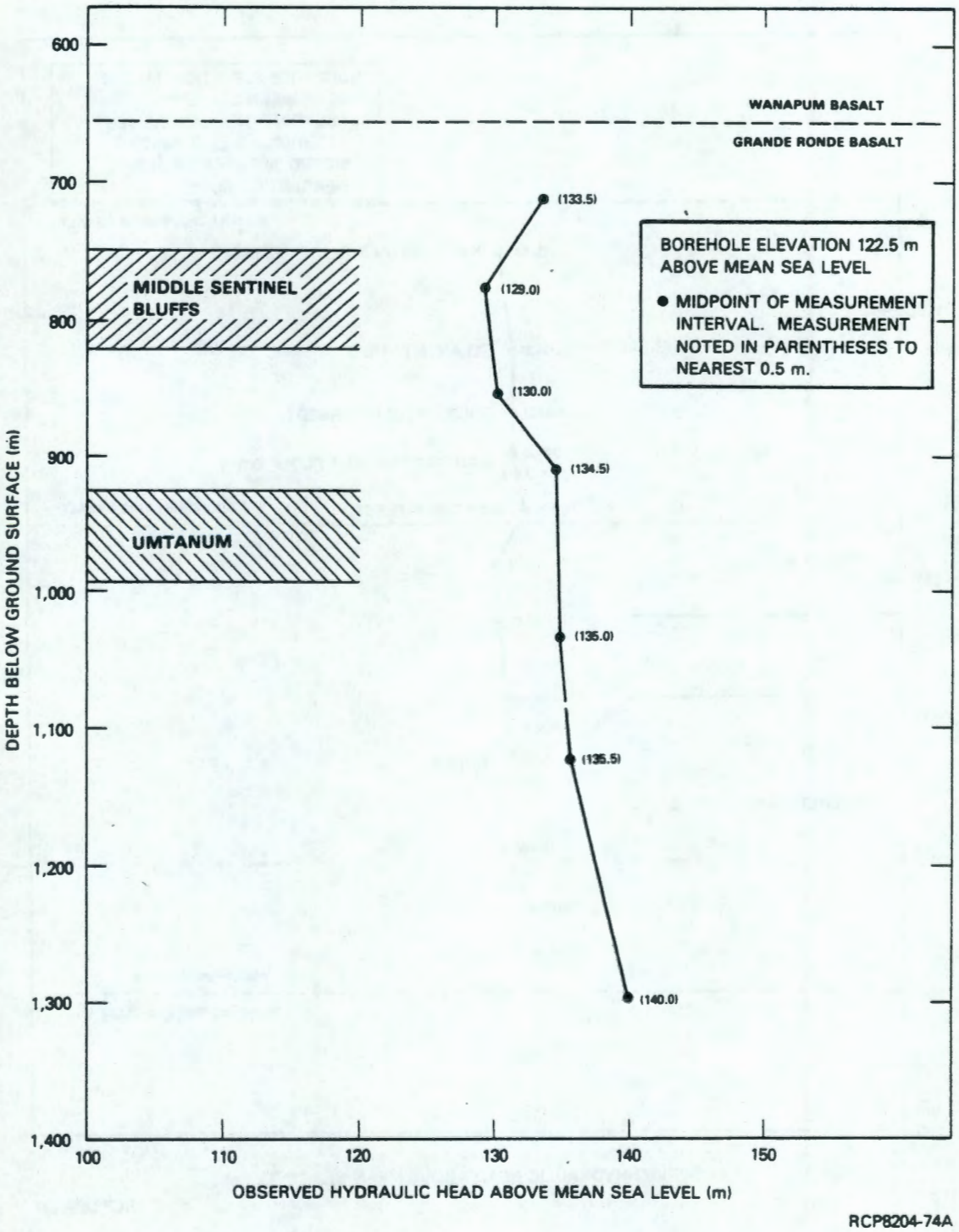

FIGURE 5-35. Hydraulic Head Measurements Within the Grande Ronde Basalt in Borehole DC-6.

9 2 1 2 4 9 5 0 9 5 7

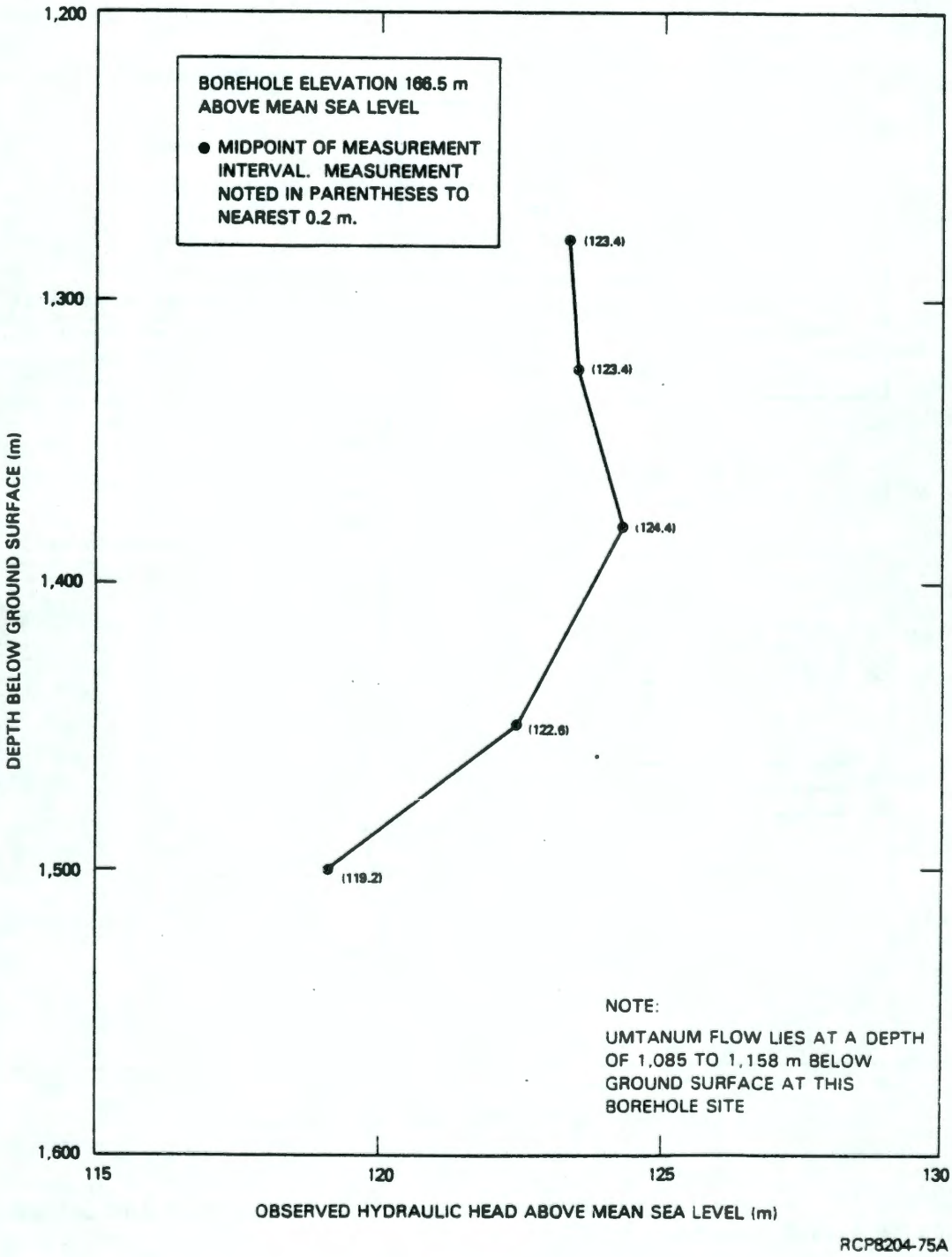

FIGURE 5-36. Hydraulic Head Measurements Within the Grande Ronde Basalt in Borehole DC-7.

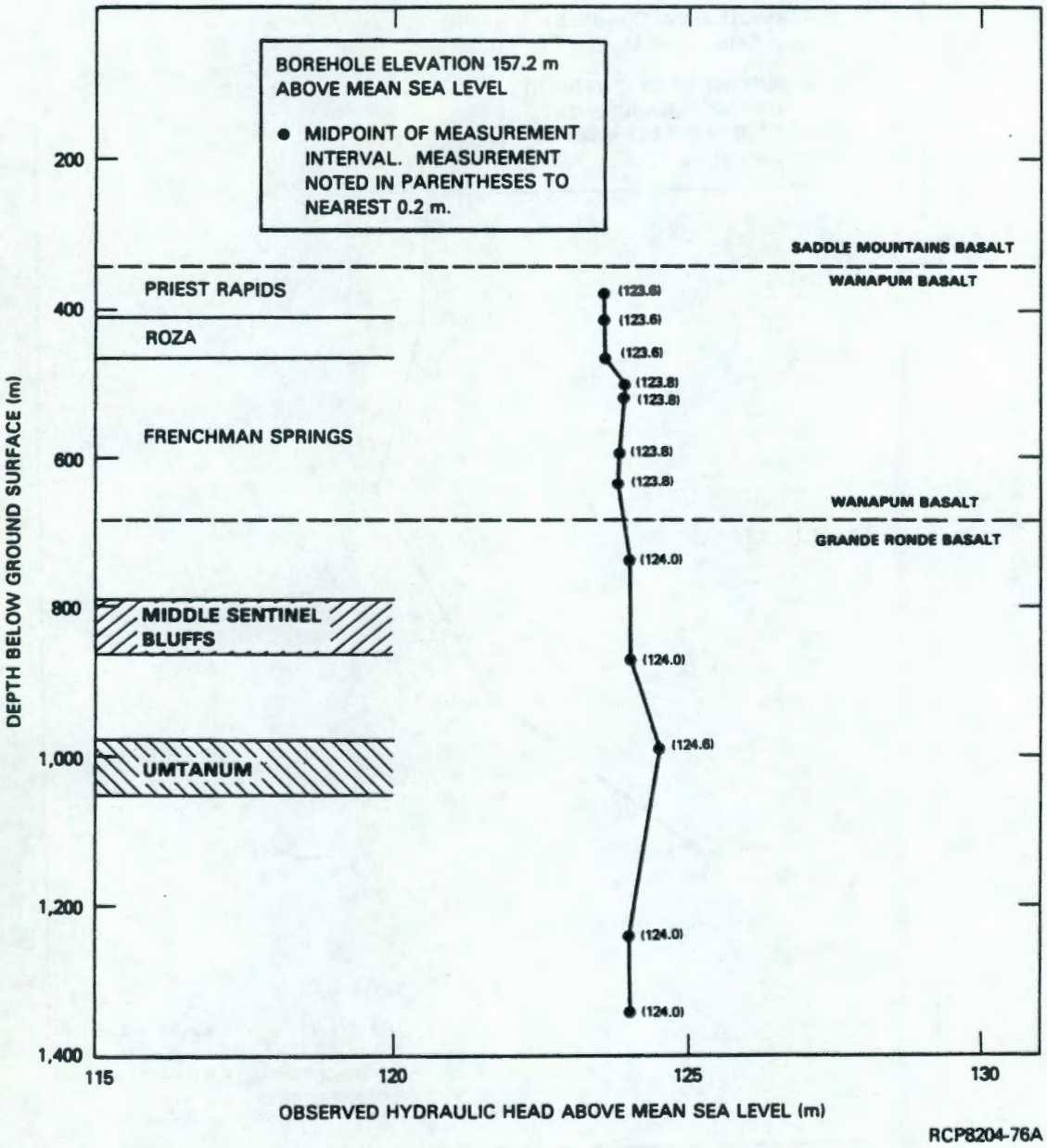

FIGURE 5-37. Hydraulic Head Measurements Within the Wanapum and Grande Ronde Basalts in Borehole DC-12.

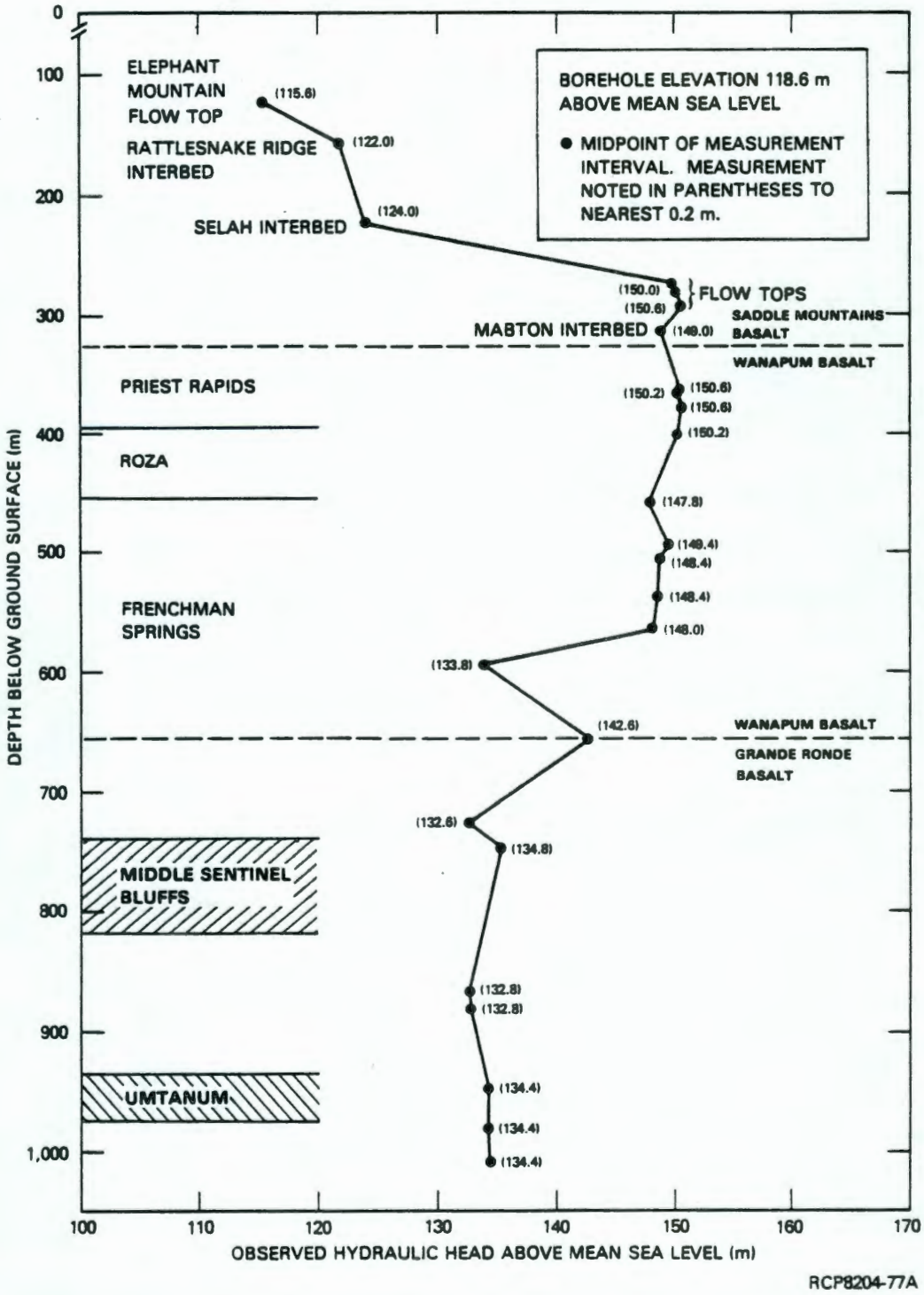

FIGURE 5-38. Hydraulic Head Measurements Within the Columbia River Basalts in Borehole DC-14.

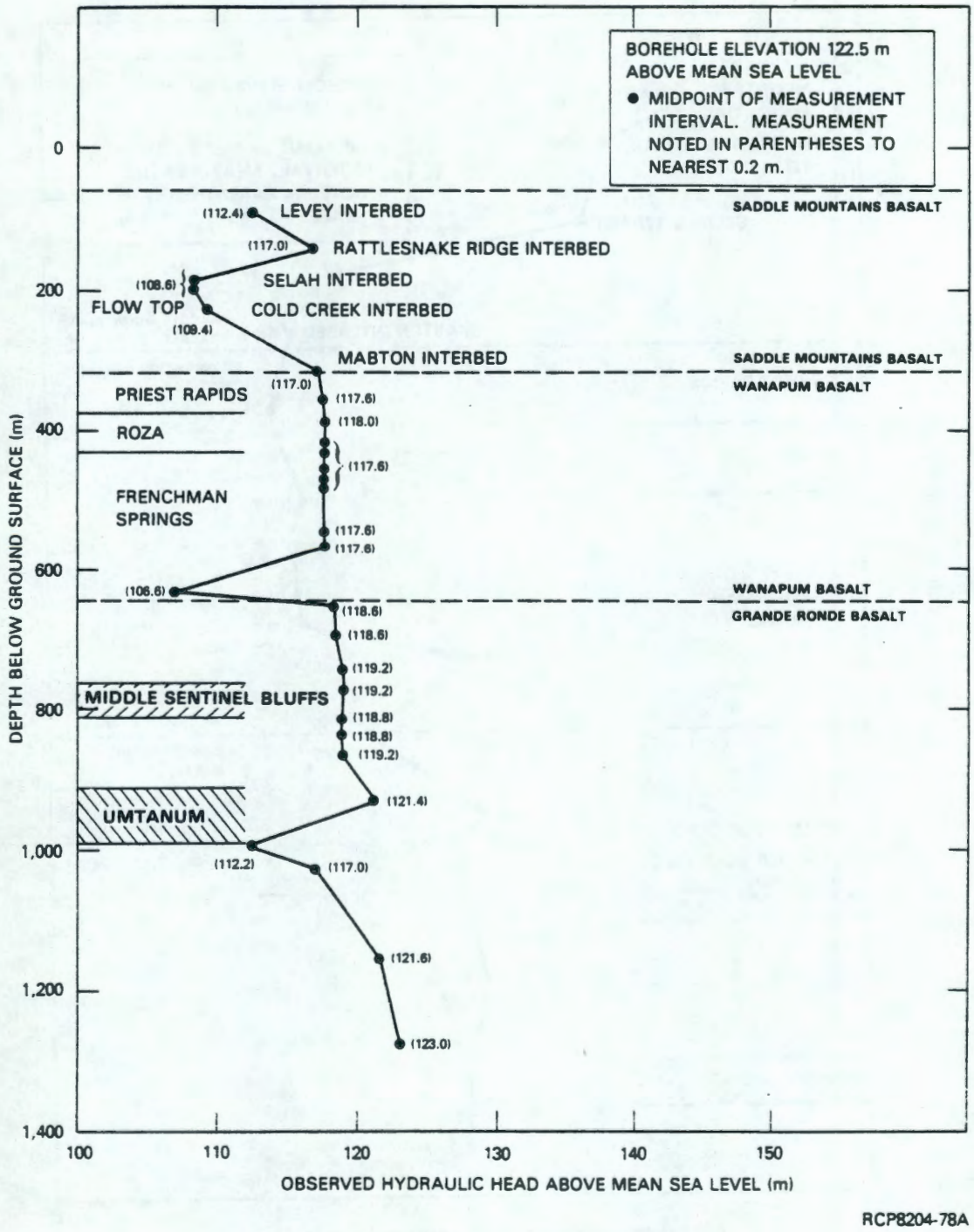

FIGURE 5-39. Hydraulic Head Measurements Within the Columbia River Basalts in Borehole DC-15.

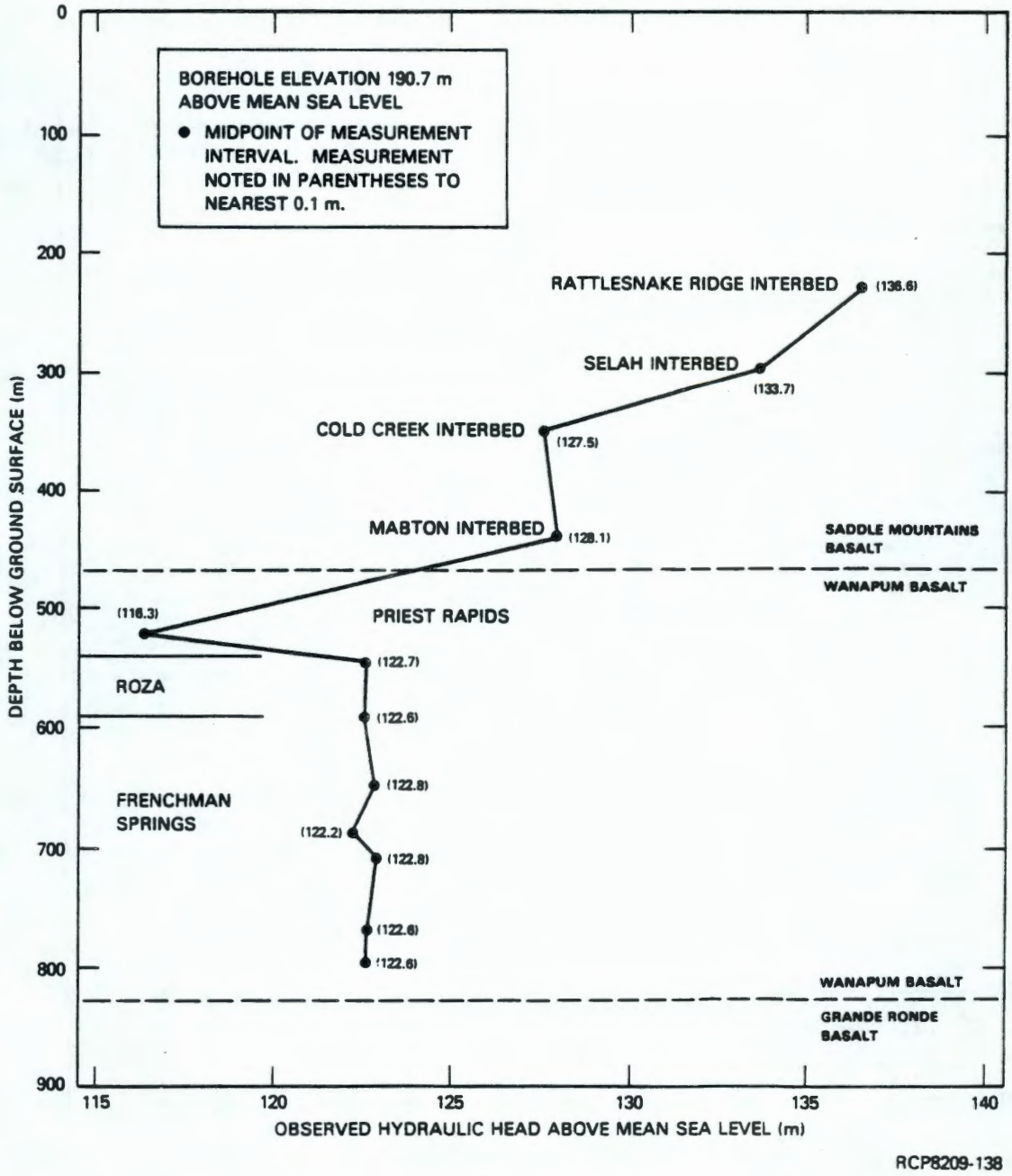

FIGURE 5-40. Hydraulic Head Measurements Within the Saddle Mountains and Wanapum Basalts at Borehole DC-16A.

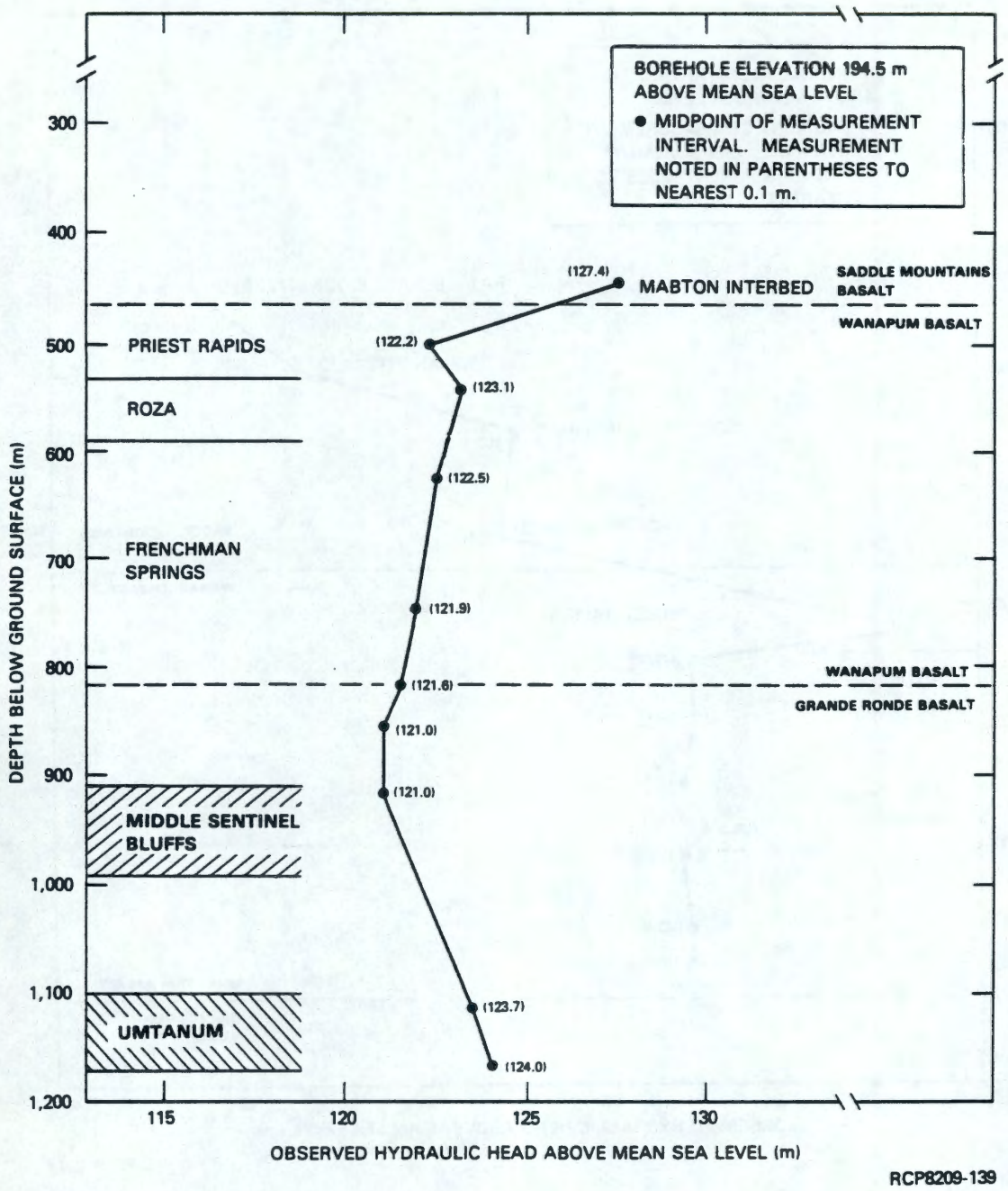

FIGURE 5-41. Hydraulic Head Measurements Within the Columbia River Basalts at Borehole RRL-2.

Borehole DC-6 is located near the axis of the Umtanum Ridge-Gable Mountain anticline, 19 kilometers east of the reference repository location. Hydraulic-head measurements were measured in the Grande Ronde Basalt after the hole had been completed to a depth of 1,322 meters and the upper two basalt formations had been cased and cemented off. An average head-gradient increase of 0.02 meter per meter is observed with increasing depth through the Grande Ronde Basalt (Fig. 5-35). As described in Section 5.1.7, increased groundwater movement may take place between the deep and shallow flow systems in this area, because of increased fracturing and faulting along the Umtanum Ridge-Gable Mountain anticline. The head increase noted in Figure 5-35 indicates the potential for such discharge.

Borehole DC-7 is located 20 kilometers southeast of the reference repository location. The borehole was originally drilled in 1977 to a depth of 1,249 meters. In 1980 this hole was deepened to 1,526 meters. Heads measured in the Grande Ronde Basalt during this additional deepening are shown in Figure 5-36. A head decrease averaging 0.02 meter per meter is evident between the depths of about 1,300 to 1,500 meters. Not enough data points are available below this depth to develop a trend.

Hydraulic heads are available from the Wanapum and Grande Ronde Basalts at borehole DC-12 (Fig. 5-37). This borehole is located 11 kilometers southeast of the reference repository location. The Wanapum heads are uniform at approximately 124 meters above mean sea level. Within the Grande Ronde Basalt, there is a slight head increase with depth averaging less than 1 meter greater compared to the Wanapum heads.

Borehole DC-14 is located north of the Umtanum Ridge-Gable Mountain anticline, 19 kilometers northeast of the reference repository location. This borehole was drilled adjacent to the Columbia River to examine the possible hydraulic interconnection between the confined aquifers and the river. At DC-14, an approximate 35-meter head increase is evident from top to bottom across the Saddle Mountains Basalt (Fig. 5-38). From the lower Saddle Mountains to the lower Wanapum Basalt, the heads have relatively uniform values (about 150 meters above mean sea level). The heads decrease in the lower Wanapum Basalt and average 133 to 135 meters above mean sea level through the Grande Ronde Basalt.

Borehole DC-15 is located approximately 32 kilometers southeast of the reference repository location and immediately adjacent to the Columbia River. A variable-head pattern is evident in the Saddle Mountains Basalt, varying between 109 and 117 meters above mean sea level (Fig. 5-39). Except for a low head value in the lower Wanapum Basalt, the heads across the Wanapum are uniform, averaging 118 meters. Heads are uniform in the upper Grande Ronde Basalt, averaging 119 meters. Below the Umtanum flow, heads increase with a gradient of 0.04 meter per meter.

Borehole DC-16A is located on the southern edge of the reference repository location. This borehole is presently (as of September 1982) located in the lower Frenchman Springs Member of the Wanapum Basalt. When the borehole is completed, its depth will be below the Umtanum flow of the Grande Ronde Basalt. As shown in Figure 5-40, there is an 8.5-meter head decrease between the Rattlesnake Ridge and Mabton interbeds. A hydraulic

9 2 1 2 4 9 5 0 9 6 4

head low of 116.3 meters above mean sea level exists in the Priest Rapids Member of the Wanapum Basalt. This is followed by rather uniform heads of 122 to 123 meters in the Roza and Frenchman Springs Members.

Borehole RRL-2 is located within the reference repository location. Hydraulic heads from the lower Saddle Mountains Basalt to below the Umtanum flow of the Grande Ronde Basalt are shown in Figure 5-41. Heads within the Wanapum Basalt average 122 to 123 meters above mean sea level. A 3-meter head increase (0.01 vertical gradient) occurs from the upper Grande Ronde Basalt to below the Umtanum flow.

One common explanation to the existence of high- or low-hydraulic head values along different stratigraphic intervals within a borehole is that the low-head zones coincide with high-transmissivity units. These high-transmissivity units act as "drains" to the system. Groundwater flow is supplied via vertical groundwater movement through lower transmissivity units.

As has been introduced in Section 5.1.2.3, the present concept of groundwater movement is that of predominantly lateral movement in interbeds and flow tops of high transmissivity with some degree of vertical movement through the interior portions of individual basalt flows. However, in comparing the hydraulic heads in Figures 5-34 through 5-41 to the hydraulic conductivity values for most of the same boreholes (Fig. 5-18 through 5-26), there does not appear to be a coincidence of high-conductivity zones to zones of lower head as proposed in the above paragraph. For example, zones of low head in the upper Saddle Mountains Basalt in borehole DC-14 (Fig. 5-38) correlate with interbeds of average (10^{-5} meters per second) to low hydraulic conductivity (10^{-6} to 10^{-7} meters per second) (see Fig. 5-23). In the same borehole, a zone of low head (133.8 meters) occurs in the lower Frenchman Springs Member of the Wanapum Basalt. That same zone has a hydraulic conductivity of 10^{-5} meters per second, which is basically the same value as compared to other Wanapum flows for which higher heads of 148 to 150 meters are recorded. In fact, in the Priest Rapids Member in borehole DC-14 where the largest hydraulic conductivity of 10^{-2} meters per second is measured, the hydraulic head value coincides with that of deeper and shallower stratigraphic horizons possessing conductivities orders of magnitude lower.

The same types of examples are also typical of other stratigraphic intervals in the other boreholes illustrated in this or previous sections. Thus, at the present time, there does not appear to be a correlation between high-transmissivity zones and low-hydraulic heads or vice versa. However, it is recognized that in the conceptual evaluation of the groundwater flow model:

- Lateral groundwater movement dominates the interbeds and flow tops

- Vertical groundwater movement occurs across flow interiors--the extent of which depends upon the vertical transmissivity and head differential across these flow interiors

9 2 1 2 4 9 5 0 9 6 5

- Zones of high transmissivity can behave as "drains" (i.e., the zones form lateral transmissive conduits through which larger volumes of groundwater move compared to zones of lower transmissivity).

5.1.4.2.5 Potentiometric Levels in the Columbia Plateau. Regionally, the discrete and composite potentials of the Saddle Mountains, Wanapum, and Grande Ronde Basalts have been mapped by Tanaka et al. (1979). The general accuracy and limitations of that mapping effort are discussed in Tanaka et al. (1979) and further detailed in Gephart et al. (1979a). These potentiometric data have been translated into digital format and reproduced as three-dimensional perspective views (Fig. 5-42 and 5-43). A comparison between these two figures and trend surface maps for corresponding stratigraphic units (Tanaka et al., 1979) reveals similarities in terms of surface morphologies, trends, and attitudes. Figures 5-42 and 5-43 also suggest that the Pasco Basin, in relation to the surrounding region, may be described as an area of groundwater-flow-system convergence.

In addition to these potentiometric maps, regional hydrostratigraphic relationships can be evaluated by means of the piezometric network established by the Washington State Department of Ecology. The locations of the wells which comprise this network are shown on Figure 5-44. A schematic representation of the vertical head distribution at these sites is also provided. It should be noted that these schematics are intended to represent only general relationships and vertical-head distributions for a fixed point in time. A summary of construction statistics with respect to these monitoring wells is given in Table 5-10, which also provides some general remarks regarding the head relationships and time-variant characteristics observed. This table is intended for use in conjunction with Figure 5-44. In examining these vertical-head data, the following generalizations have been noted:

- The data show a general trend of decreasing observed hydraulic heads with increasing depth from ground surface in most wells.

- At certain locations, head similarities are observed over tens to hundreds of meters of the vertical section. This phenomenon has not been actively evaluated but could possibly be attributed to any one (or combination) of the following factors:

  - High vertical communication

  - Relative vertical positioning of the open intervals of the piezometers

  - Failure of piezometer seals

  - Nearby groundwater-use patterns

  - Well positioned in area of lateral groundwater movement.

9 2 1 2 4 9 5 0 9 6 6

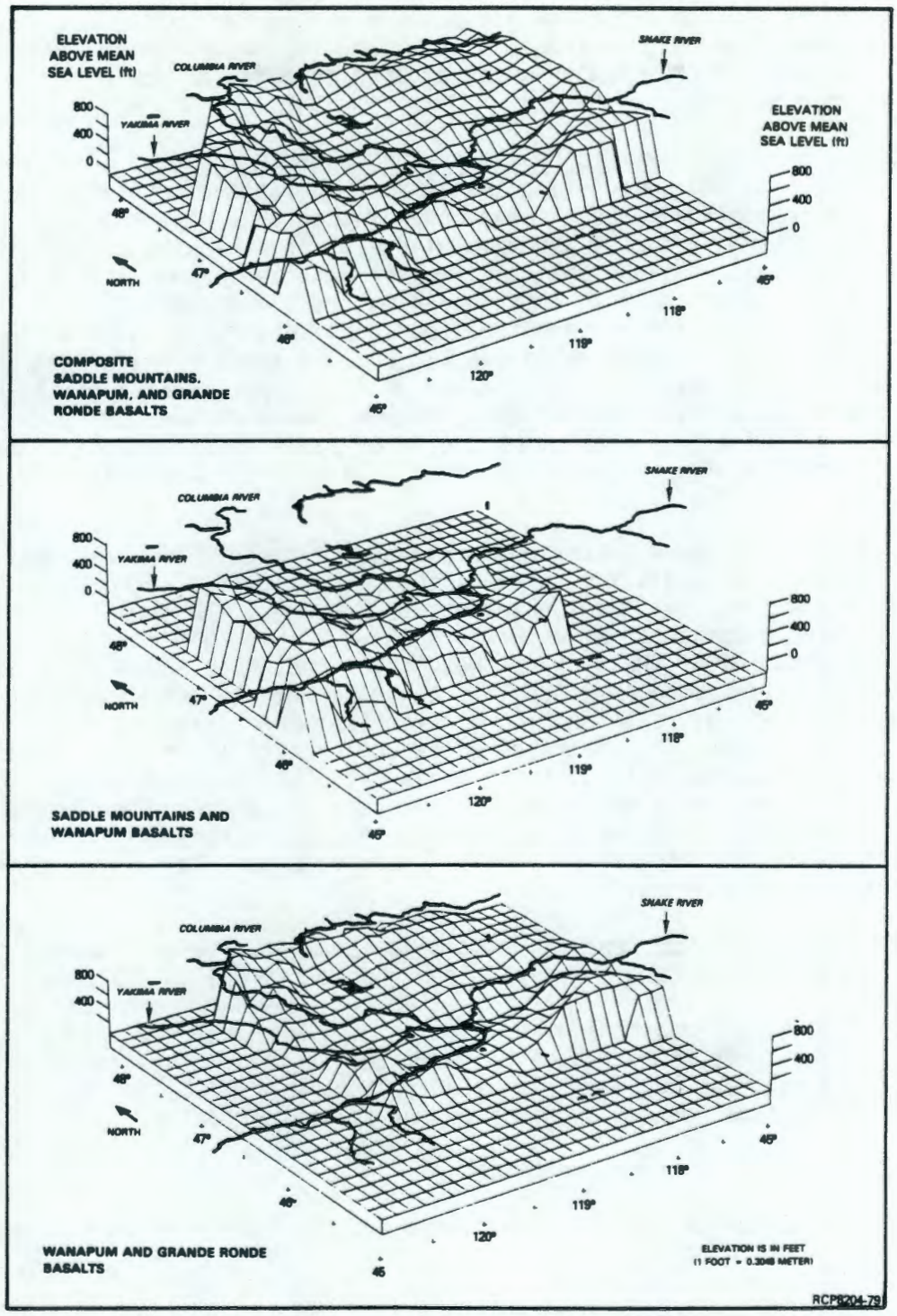

FIGURE 5-42. Three-Dimensional Perspective Views Showing Composite Potentiometric Surfaces for Various Strata Within the Columbia River Basalts.

9 2 1 2 4 9 5 0 9 6 7

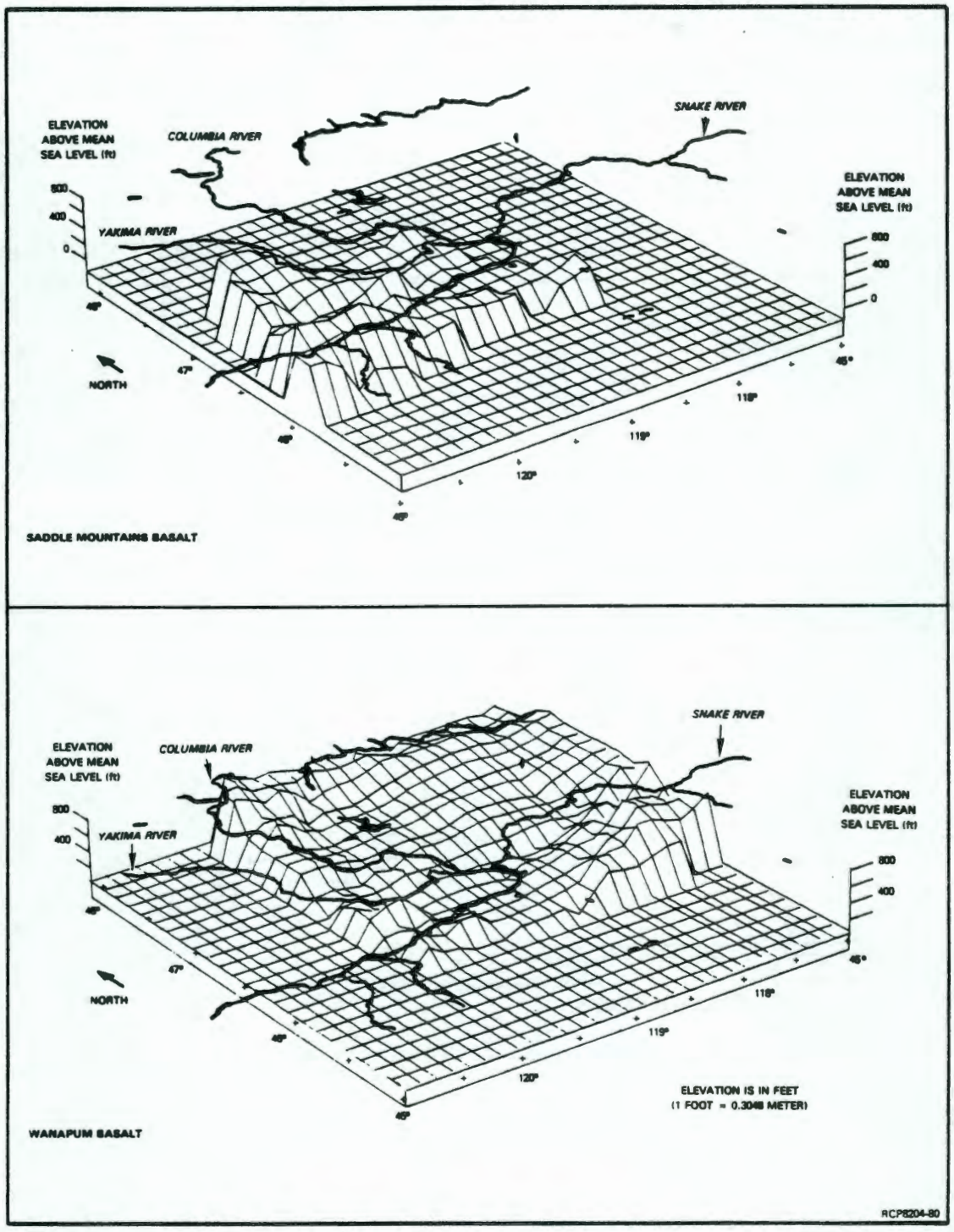

FIGURE 5-43. Three-Dimensional Perspective Views Showing the Potentiometric Surface Configuration of the Saddle Mountains and Wanapum Basalt.

9 2 1 2 4 9 5 0 9 6 8

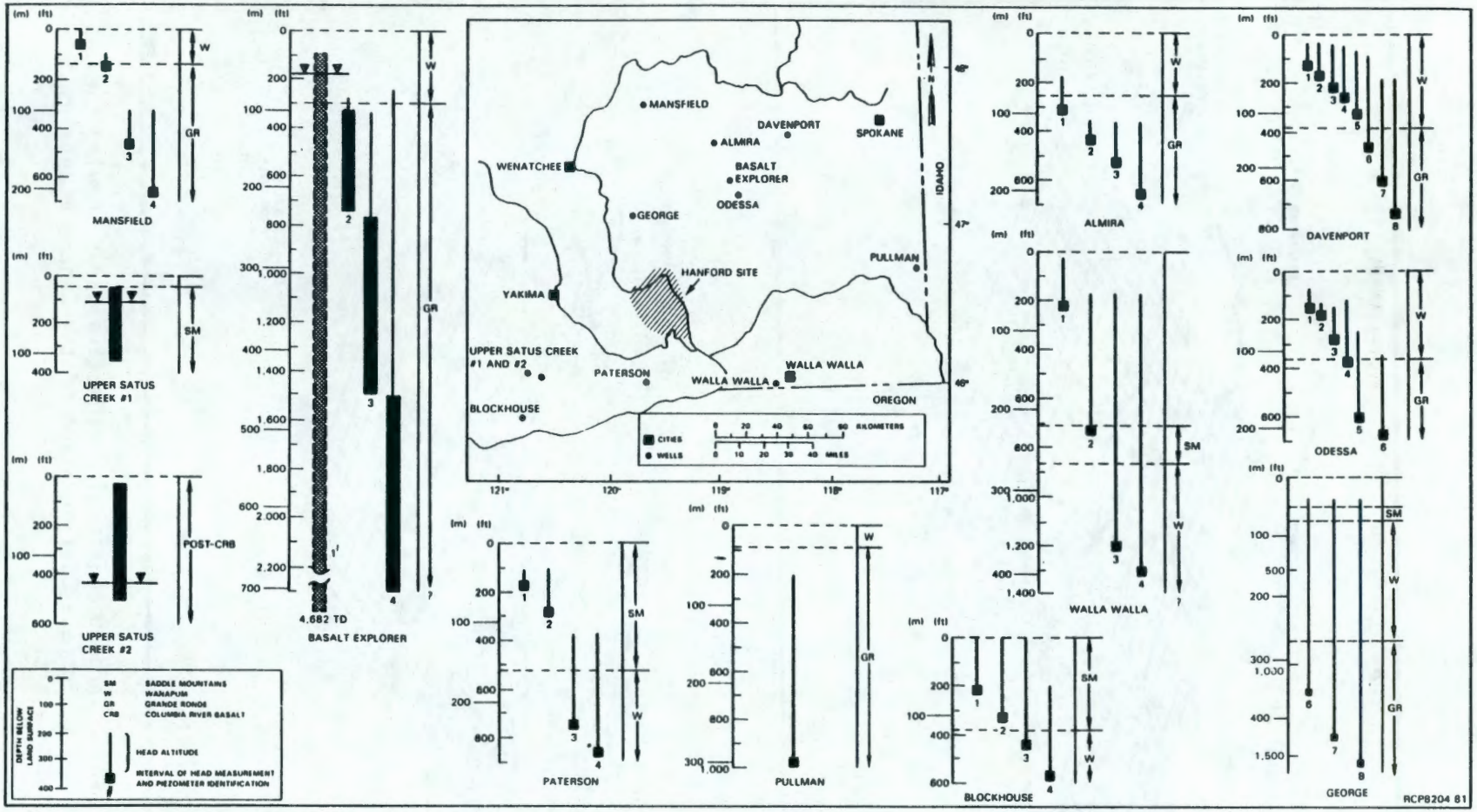

FIGURE 5-44. Locations and Vertical-Head Distributions of Washington State Department of Ecology Test/Observation Wells.

TABLE 5-10. Construction Data for Washington State Department of Ecology Test/Observation Wells in Eastern Washington.

Name of monitoring well	Piezometer no.	Location (township/range-section, tract, well serial identifier)	Surface elevation (m above mean sea level) (ft in parentheses)	Local stratigraphy depth in m (ft) below ground surface to top of flow: Pre-Columbia River basalts	Saddle Mountains Basalt	Wanapum Basalt	Grande Ronde Basalt	Post-Grande Ronde Basalt	Stratigraphic interval monitored	Open interval (depth below land surface): Top m	Top ft	Bottom m	Bottom ft	Thickness m	Thickness ft	Completion date	Remarks
Almira	1	24/31-16E01	562.5	0	--	2.4	76.2	?	Grande Ronde			96.6	317			01/01/71	Stratigraphy taken from Tanaka et al. (1979). Piezometers show significant difference in heads (~60 m (200 ft)) between shallowest and deeper portions of Grande Ronde. Piezometers in deeper Grande Ronde have similar heads.
	2	24/31-16E02	(1,845)	(0)		(8)	(250)		Grande Ronde	134.8	442	136.3	447	1.5	5	01/01/71	
	3	24/31-16E03							Grande Ronde	160.4	526	161.9	531	1.5	5	01/01/71	
	4	24/31-16E04							Grande Ronde			206.7	678			01/01/71	
Basalt explorer*	1	21/31-10M01	490.9	-	--	0	91.5	Pre-basalt granite basement 1,422.9 (4,667)	Composite	29.9	98	1,427.4	4,682	1,397.6	4,584	01/01/61	Stratigraphy taken from Tanaka et al. (1979). Initially, composite measurements were recorded over the entire borehole depth. Piezometers were installed in 1972. There are distinct differences in head between all zones monitored within the Grande Ronde. Heads in the deepest piezometer (#4) are distinctly higher than the upper two, and piezometer #2 has a higher head than #3. Cyclic trends are evident in all zones to some degree. The cyclic and long-term behavior of #2 most closely resembles that of the composite well.
	2	21/31-10M02	(1,610)			(0)	(300)		Grande Ronde	96.0	315	224.1	735	128.0	420	09/01/72	
	3	21/31-10M03							Grande Ronde	229.3	752	451.2	1,480	222.0	728	09/01/72	
	4	21/31-10M04							Grande Ronde	455.8	1,495	701.2	2,300	245.4	805	09/01/72	
Blockhouse	1	4/15-16F01	484.8	0	5.8	120.7	?	?	Saddle Mountains			64.0	210			01/01/70	Stratigraphy taken from Tanaka et al. (1979). Piezometers show head similarity throughout the Saddle Mountains and upper Wanapum. Lower portions of Wanapum show significantly lower heads (~50 m (175 ft)). Monitoring data suggest slight upward trend in heads in deeper zones.
	2	4/15-16F02	(1,590)	(0)	(19)	(396)			Saddle Mountains			100.6	330			01/01/70	
	3	4/15-16F03							Wanapum			134.1	440			01/01/70	
	4	4/15-16F04							Wanapum			176.8	580			01/01/70	
Davenport	1	24/36-16A01	723.2	0	--	2.1	119.5	?	Wanapum	22.9	75	35.7	117	12.8	42	01/01/70	Stratigraphy estimated from trend maps prepared by Tanaka et al. (1979). Piezometers show head similarities throughout the Wanapum and upper Grande Ronde with slight decrease in head with depth. Heads in deeper horizons of the Grande Ronde are significantly lower (~45 m (150 ft)). Strong cyclic variations are evident in deeper zones (#7 and #8). The same variations are probably present in the upper zones as well, but are more attenuated. Heads in the lower zones are probably decreasing slightly with time.
	2	24/36-16A02	(2,372)	(0)		(7)	(392)		Wanapum	43.3	142	48.8	160	5.5	18	01/01/70	
	3	24/36-16A03							Wanapum	65.5	215	67.1	220	1.5	5	01/01/70	
	4	24/36-16A04							Wanapum	77.4	254	79.0	259	1.5	5	01/01/70	
	5	24/36-16A05							Wanapum	103.4	339	104.9	344	1.5	5	01/01/70	
	6	24/36-16A06							Grande Ronde	142.7	468	144.2	473	1.5	5	01/01/70	
	7	24/36-16A07							Grande Ronde	186.3	611	186.9	613	0.6	2	01/01/70	
	8	24/36-16A08							Grande Ronde	225.3	739	226.8	744	1.5	5	01/01/70	
George	none	18/25-15E01	352.7	0	~57	~78	271.3	?	Wanapum/	354.6	1,163	356.1	1,168	1.5	5	03/14/79	The three piezometers measure heads within the Grande Ronde. Data show a distinct head similarity within the three zones. Cyclic fluctuations are also very similar with amplitudes on the order of 35 to 45 m.
			(1,157)	(0)	(~186)	(~257)	(890)		Grande Ronde	428.7	1,406	428.7	1,409	0.9	3	03/14/79	
										469.8	1,541	471.3	1,546	1.5	6	03/14/79	
Mansfield	1	27/26-25D01	675.3	0	--	1.5	41.2	?	Wanapum	11.6	38	18.3	60	6.7	22	01/01/72	Stratigraphy taken from Tanaka et al. (1979). Piezometers show that heads are significantly higher (~20 m (7 ft)) in the Wanapum than in the upper Grande Ronde and that the upper Grande Ronde head is significantly higher (~70 m (230 ft)) than the lower portions of the Grande Ronde. No cyclic patterns are apparent. The head in piezometer #4 declined between 1974 and 1976 and now exhibits definite similarity to that of piezometer #5.
	2	27/26-25D02	(2,215)	(0)		(5)	(135)		Grande Ronde	21.3	70	45.7	150	24.4	80	01/01/72	
	3	27/26-25D03							Grande Ronde							01/01/72	
	4	27/26-25D04							Grande Ronde	140.2	460	147.9	485	7.6	25	01/01/72	
	5	27/26-25D05							Grande Ronde	192.1	630	204.3	670	12.2	40	01/01/72	
Odessa	0	20/33-16E00	439.5	0	--	0.8	96.1	?	Composite	0	0	197.4	750	197.4	750	07/24/70	Stratigraphy taken from Tanaka et al. (1979). Piezometers show a general decrease in head with increasing depth with the exception of piezometer #4, which is situated at the Wanapum/Grande Ronde contact. No. 4 consistently exhibits heads slightly higher than #2 and #3, but on the order of 12 m (40 ft) lower than #1. Initially, #5 had head similarity to #2, #3, and #4, but an event in 1978 resulted in a permanent lowering of the head in #5 on the order of 30 m (100 ft). This lowering also resulted in a decrease in the amplitude of cyclic fluctuations within #2, #3, and #4. Cyclic fluctuations are most apparent within #5 and #6. No. 6 exhibits a trending decline.
	1	20/33-16E01	(1,670)	(0)		(3)	(365)		Wanapum	15.8	60	38.2	145	22.4	85	07/24/70	
	2	20/33-16E02							Wanapum	41.6	158	43.9	167	2.4	9	07/24/70	
	3	20/33-16E03							Wanapum	74.2	282	76.6	291	2.4	9	07/24/70	
	4	20/33-16E04							Wanapum	92.6	352	96.1	365	3.4	13	07/24/70	
	5	20/33-16E05							Grande Ronde	154.2	586	162.1	616	7.9	30	07/24/70	
	6	20/33-16E06							Grande Ronde	177.9	676	182.1	692	4.2	16	07/24/70	
Patterson	1	7/25-36N01	192.1	0	2.9	136.3	?	?	Saddle Mountains	27.6	105	48.7	185	21.1	80	01/01/72	Stratigraphy taken from Tanaka et al. (1979). Piezometers show significant head differences (~75 m (250 ft)) between the Saddle Mountains and Wanapum. No strong cyclic patterns or trends are evident.
	2	7/25-36N02	(730)	(0)	(11)	(518)			Saddle Mountains			76.3	290			01/01/72	
	3	7/25-36N03							Wanapum			198.7	755			01/01/72	
	4	7/25-36N04							Wanapum			226.3	860			01/01/72	
Pullman	1	14/45-01F01	651.3	0	--	3.2	25	?	Grande Ronde	257.9	980	258.4	982	0.5	2	07/18/75	Stratigraphy taken from Tanaka et al. (1979).
			(2,475)	(0)		(12)	(95)										
Upper Satus Creek #1	1	7/17-7M01	868.4	0	11.8	?	?	?	Composite	15.8	60	92.1	350	76.3	290	08/02/76	Stratigraphy taken from Tanaka et al. (1979), and geophysical logs.
			(3,300)	(0)	(45)												
Upper Satus Creek #2	1	8/16-28E01	921.1	131.6	?	?	?	?	Simcoe Mountains	4.7	18	131.6	500	126.8	482	08/16/76	Stratigraphy taken from geophysical logs.
			(3,500)	(500)													
Walla Walla	1	6/35-18A01	176.3	0	186.6	226.3	?	?	Saddle Mountains			60.5	230			01/01/73	Stratigraphy taken from Tanaka et al. (1979). Piezometers show that heads in the basalt overburden are significantly higher (~45 m (150 ft)) than in the basalts. Heads in the Saddle Mountains and Wanapum are similar. Strong cyclic patterns and a declining trend are apparent within the basalts. The shallower groundwater system may be rising slightly.
	2		(670)	(0)	(709)	(860)			Saddle Mountains			192.1	730			01/01/73	
	3								Wanapum			316.5	1,204			01/01/73	
	4								Wanapum			344.2	1,308			01/01/73	

*Alternate well name is "Krupp."

- At certain locations, a significant head drop across a threshold depth may be interpreted. While this may be a real phenomenon, several factors prevent its confirmation, based on the available data. These include:

  - Irregular intervals represented by piezometer placement over the vertical section

  - Groundwater use

  - Local hydrogeologic factors

  - Other factors as cited above.

- The distribution of wells across the region tends to provide data which evaluate vertical-head distributions of the Wanapum and Grande Ronde Basalts at locations where these units are nearest the surface and closer to their probable recharge source. The wells south of the Pasco Basin are designed to monitor conditions only within the Saddle Mountains and Wanapum Basalts. Vertical-head distributions of the Grande Ronde Basalt at these locations south of the Pasco Basin within the flow system are, therefore, unknown.

Because the piezometers shown in Figure 5-44 have been monitored by the U.S. Geological Survey on a periodic basis since installation, it is also possible to evaluate the time-variant bahavior of the potentiometric surfaces within the Columbia Plateau. Examples of the hydrographs recorded at selected wells are shown in Figure 5-45. A brief description of the dynamic behavior observed at each of the Washington State Department of Ecology test/observation wells can be found in Table 5-10.

5.1.5 Regional Hydrochemistry

Under certain conditions, the chemical character of groundwater, coupled with radioisotopic and/or chemical age determinations can be used to evaluate groundwater flow dynamics. Such interpretations are based on the assumption that the chemistry of groundwater is dependent on the following:

- Antecedent water chemistry

- Residence time

- Geochemistry of the groundwater flow continuum

- Temperature-pressure relationships in the groundwater flow continuum that control water-rock interactions.

9 2 1 2 4 9 5 0 9 7 1

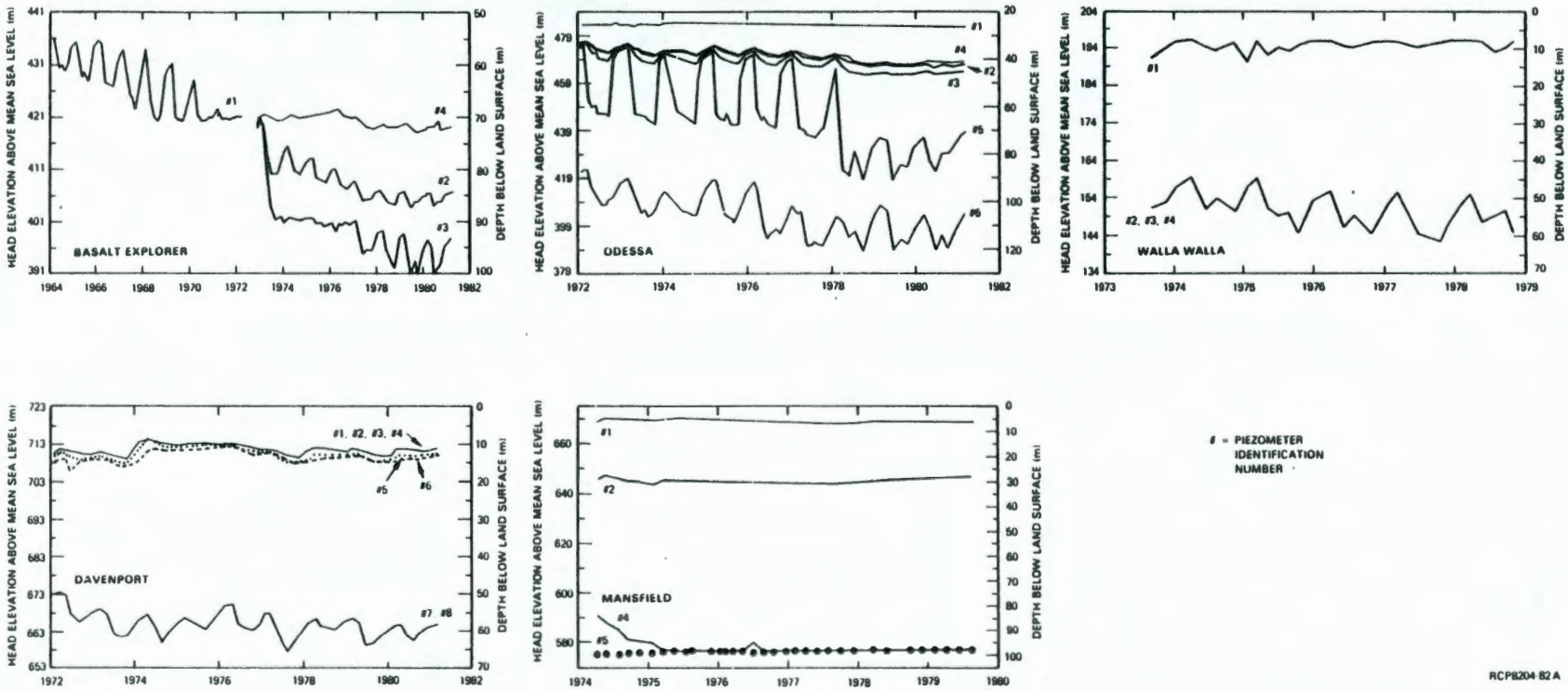

FIGURE 5-45. Selected Examples of Hydrographic Data for Wells Within the Columbia Plateau Region (after U.S. Geological Survey Groundwater Site Inventory Data Base).

While hydrochemical evaluations are largely interpretive and dependent upon local conditions, certain generalizations have been gleened from the experience of several researchers (Domenico, 1972):

- The concentration of total dissolved solids is generally proportional to the length of the flow path and residence time.
- Recharge areas are characterized by comparatively lower total dissolved solids.
- The upper limit of pH in a recharge area approaches that of rainwater in recharge areas where considerable leaching of soluble mineral matter has occurred.
- The ratio of sulfate to chloride often tends to decrease in the direction of flow.

The latter generalization stems from a theory by Chebotarev (1955) which, in essence, states that the chemistry of all groundwaters tends toward the composition of seawater. The anionic evolution postulated by Chebotarev is as follows:

$$\longrightarrow \text{Increasing distance of flow} \longrightarrow$$

$$HCO_3^- \quad HCO_3^- + SO_4^= \quad SO_4^= + HCO_3^- \quad SO_4^= + Cl \quad Cl + SO_4^= \quad Cl$$

$$\longrightarrow \text{Increasing Age} \longrightarrow$$

It should be noted, however, that this evolutionary cycle is highly subject to scale and to interruptions and, thus, the complete sequence is seldom observed within a single system.

The following discussion of hydrochemical data is organized according to hydrogeologic unit. For each unit, data relating to major inorganic composition, trace-element content, nonconservative hydrochemical parameters (i.e., those that must be measured in the field at or near the time of sampling because of their dynamic nature), and dissolved gas composition are discussed.

Hydrochemical data for groundwater within the Columbia River basalts are reported on a regional basis by Walters and Grolier (1959), Van Denburgh and Santos (1965), and Newcomb (1972). Chemical data for separate areas within the Columbia Plateau are available from a number of sources. These include Eakin (1946), Sceva et al. (1949), Foxworthy (1962), Foxworthy and Washburn (1963), and Newcomb (1965). Results from several of these studies are summarized in Gephart et al. (1979a).

9 2 1 2 4 9 5 0 9 7 3

Data presented in this section are based on analyses obtained from the groundwater-quality-data files of the U.S. Geological Survey for the Washington State portion of the Columbia Plateau exclusive of the Pasco Basin. Information for the Pasco Basin specifically will be presented in following sections. For most locations, available hydrochemical data consist of major inorganic constituents and selected trace elements.

Locations of regional sampling sites for which there appear to be reliable hydrochemical data from the basalt are shown in Figure 5-46.

Major Inorganic Composition. The range and mean composition of chemical constituents within the groundwater of the Columbia River basalts are presented in Table 5-11. These data are principally from wells penetrating the Saddle Mountains or upper Wanapum Basalts. Examination of these data indicate that, regionally, these groundwaters generally possess a low total-dissolved-solids content (i.e., less than approximately 350 milligrams per liter). Principal chemical constituents are present in the following dominance relationship (by weight): bicarbonate>silica>sodium >calcium = sulfate>magnesium.

The individual chemical compositions of groundwater samples listed in Table 5-11 are shown on the trilinear diagram in Figure 5-47. The scattered pattern of plotting points suggests a nonuniform chemical composition for groundwater over the Columbia Plateau. Chemical classifications range from calcium-magnesium bicarbonate to sodium bicarbonate-sulfate types. Regional dissimilarities in groundwater composition are ascribed to differences in aquifers sampled, groundwater mixing due to multiple aquifer completions, sources of recharge, and rock/groundwater reactions.

Trace-Element Content. The trace-element content for groundwater within the Columbia River basalt is shown in Table 5-12. Concentrations for reported trace elements are low and are commonly below detection levels of the analytical equipment used. The principal trace elements present are aluminum, boron, iron, manganese, strontium, and zinc. Ranges in trace elements listed in this table compare reasonably well with values reported by Newcomb (1972) for Columbia River basalt groundwater within the southeastern portion of the plateau. The higher concentration values listed in Table 5-12 for iron and manganese (i.e., 2.20 and 0.13 milligrams per liter, respectively), suggest that some analyses may exhibit the effects of poor sampling procedures and/or the corrosion of well casings.

As mentioned previously, chemical analyses available for the Columbia Plateau are usually composite and represent groundwater obtained from a number of hydrogeologic units penetrated at the sampled well site. Hydrochemical data for individual hydrogeologic units is primarily limited to data obtained at the Hanford Site. Hydrochemical data for individual geologic formations presented in the following sections pertains solely to data collected at the Hanford Site.

9 2 1 2 4 9 5 0 9 7 4

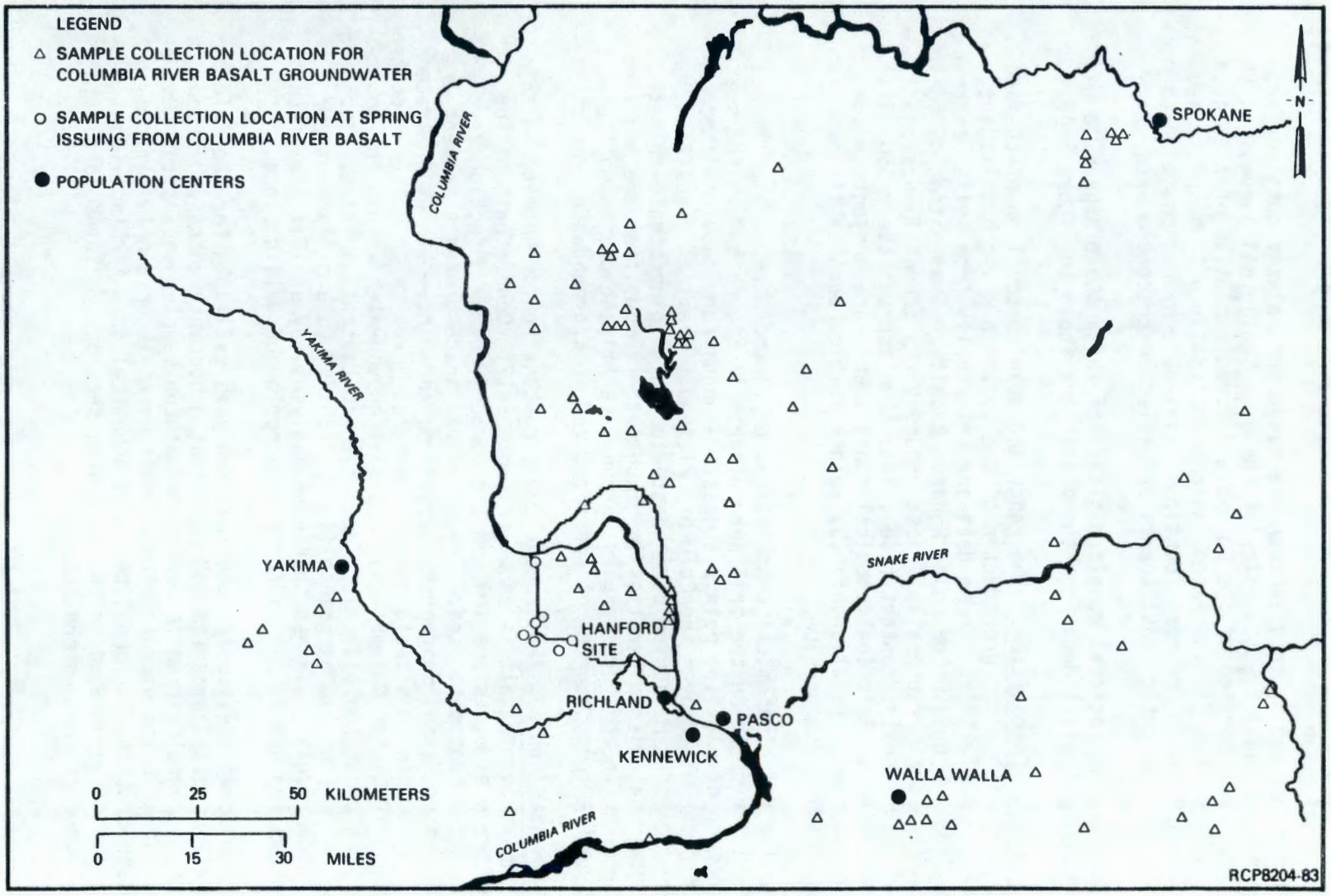

FIGURE 5-46. Sampling Sites for Groundwater Collected from Columbia River Basalt Zones.

TABLE 5-11. Range in Concentration and Mean Composition of Major Chemical Constituents Within Groundwater of the Columbia River Basalt Group.

Constituent	Range (mg/L)*	Mean (mg/L)*
Anions		
Alkalinity, as HCO_3^-	72 - 297	160
Cl^-	0.5 - 56	12
SO_4^{-2}	0.2 - 95	21
NO_3^-	0.01 - 18	2.3
F^-	0.1 - 3.9	0.76
Cations		
Na^+	7.8 - 80	34
K^+	0.1 - 38	6.5
Ca^{+2}	2.1 - 64	21
Mg^{+2}	0.2 - 24	10
SiO_2	30 - 83	55
Total dissolved solids	154 - 510	325

*Based on 83 hydrochemical analyses.

5.1.5.1 Unconfined Aquifer. Although numerous partial chemical analyses are available for groundwater within the unconfined aquifer, complete major inorganic determinations are limited to samples collected by the U.S. Geological Survey and the Pacific Northwest Laboratory at Hanford. Complete chemical analyses are available for 102 individual well samples collected at Hanford between the years 1974 and 1980. The analytical results are reported in annual documents by Pacific Northwest Laboratory: Raymond et al. (1976), Myers et al. (1976; 1977), Myers (1978), Eddy (1979), and Eddy and Wilbur (1980; 1981). Hydrochemical data presented in this section include only those chemical analyses which have an acceptable ionic balance (i.e., (Σ anions - Σ cations)/Σ cations $<\pm 5$ percent).

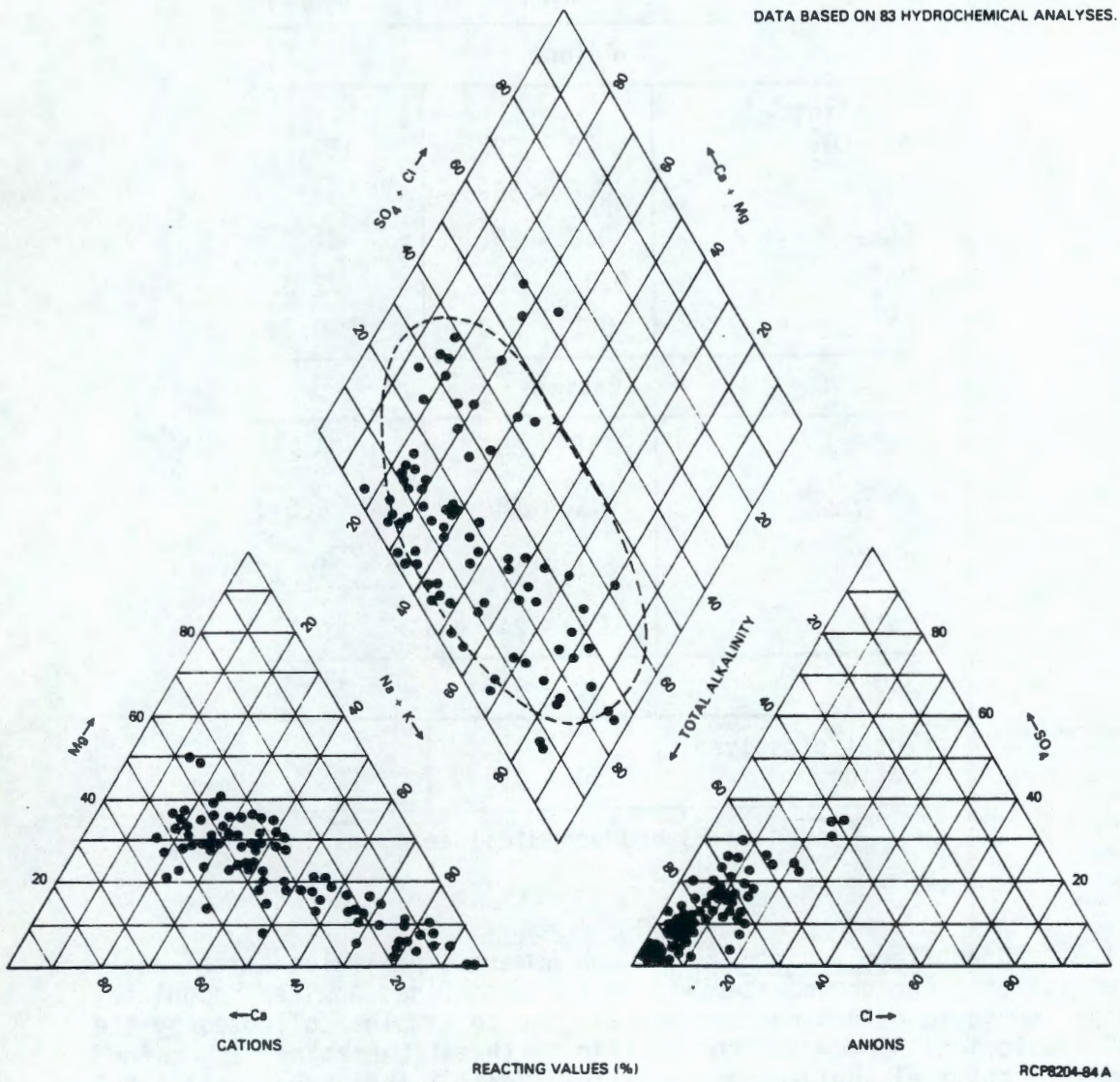

FIGURE 5-47. Chemical Composition of Groundwater Within the Columbia River Basalt Group.

TABLE 5-12. Range and Median Concentrations of Trace Elements for Groundwater Within Columbia River Basalt.

Trace element	Range (mg/L)	Median (mg/L)
Al	<0.010 - 0.010	<0.010
B	0.010 - 0.780	0.070
Cr	<0.030	<0.030
Cu	<0.001 - 0.050	<0.050
Fe	0.010 - 2.20	0.050
Mn	0.010 - 0.130	0.050
Pb	<0.100	<0.100
Sr	<0.050 - 0.330	0.060
Zn	<0.010 - 0.080	<0.010

5.1.5.1.1 Major Inorganic Composition. The range in concentration and mean composition for major chemical constituents within the unconfined aquifer at the Hanford Site are listed in Table 5-13. Examination of this table indicates that groundwaters of the unconfined aquifer generally possess a low total-dissolved-solids content (i.e., less than 350 milligrams per liter). Principal chemical constituents are present in the following dominance relationship (by weight): bicarbonate>sulfate≥calcium>silica >nitrate>sodium>chloride>magnesium>potassium>fluoride.

Although the average chemical composition of unconfined groundwater is of a calcium bicarbonate chemical type, considerable variability in chemical composition is evident for individual analyses. The wide range in concentration and variability evident for major ionic constituents shown in Table 5-13 is attributable primarily to waste-water disposal at the Hanford Site (Gephart et al., 1979a).

Of particular interest is the presence of elevated nitrate concentrations within the unconfined aquifer. As discussed previously, nitrate in the unconfined aquifer is the by-product of past water-disposal practices at the Hanford Site. Because of its mobility within aquifer systems, nitrate has been used previously to delineate the migration of waste plumes (Myers, 1978). The concentration of nitrate and the area within the unconfined aquifer affected by synthetic recharge at the Hanford Site is shown in Figure 5-48.

TABLE 5-13. Range in Concentration and Mean Composition for Major Chemical Constituents Within Groundwater in the Unconfined Aquifer at Hanford.

Constituent	Range (mg/L)	Mean (mg/L)
Anions		
Total alkalinity, as HCO_3^-	14 - 314	149
Cl^-	2.7 - 32	11
SO_4^{-2}	2.7 - 170	43
NO_3^-	0.1 - 270	27
F^-	0.1 - 1.3	0.5
Cations		
Na^+	2.9 - 69	23
K^+	2.4 - 13	6.2
Ca^{+2}	14 - 92	41
Mg^{+2}	0.4 - 30	11
SiO_2	8.8 - 50	35
Total dissolved solids	203 - 728	347
pH	7.5 - 10.7	7.9
Collection temperature (°C)	14 - 39	19

5.1.5.1.2 Trace-Element Content. Data concerning the trace-element content in unconfined groundwater at the Hanford Site are contained in reports previously cited for major inorganic composition. The range and median concentrations for selected trace elements are presented in Table 5-14. This table indicates that concentration levels for trace elements are low and commonly below the detection limit of the analytical equipment used. Principal detectable trace elements include aluminum, barium, boron, iron, manganese, and zinc.

9 2 1 2 4 9 5 0 9 7 9

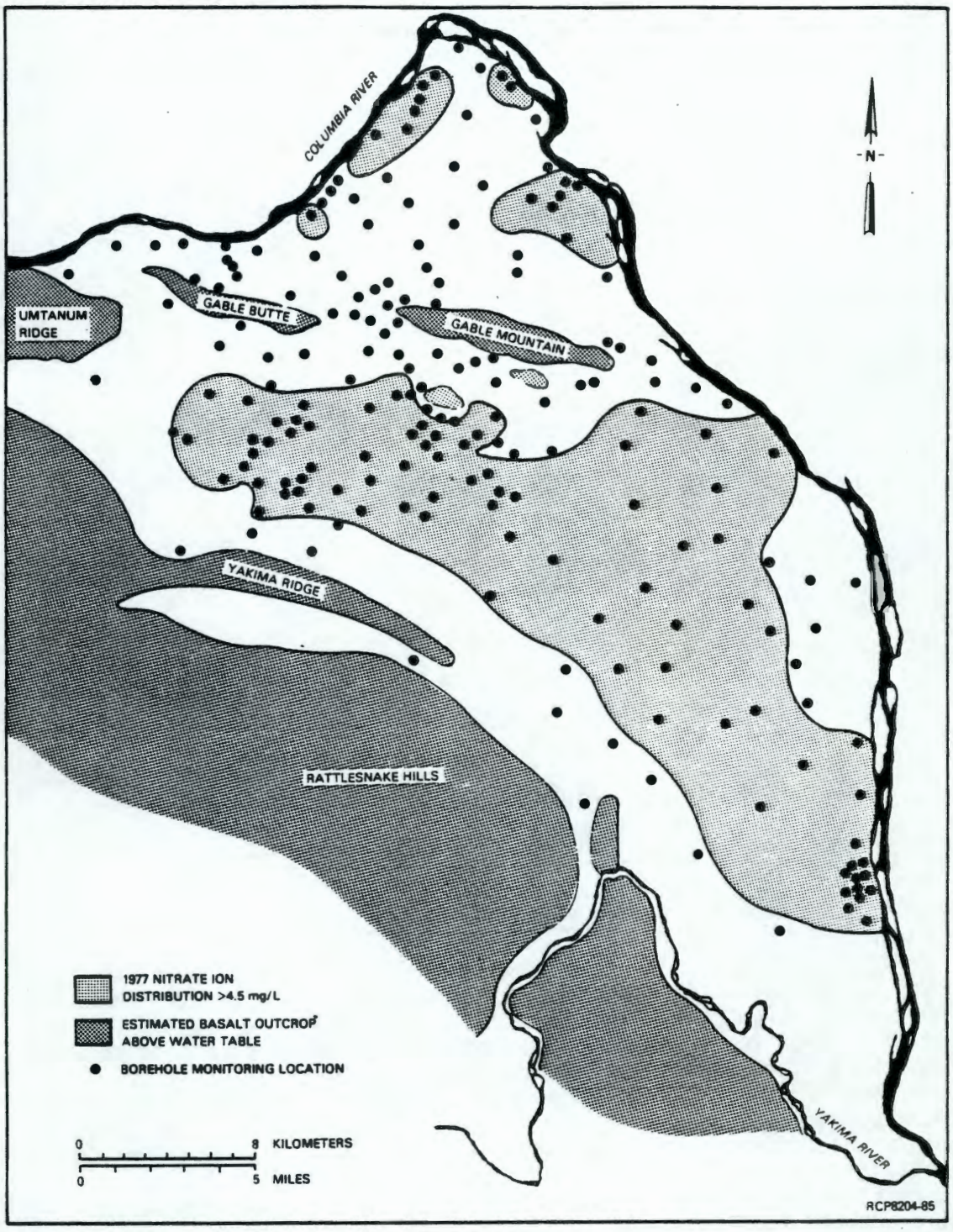

FIGURE 5-48. Nitrate-Ion Distribution in Unconfined Groundwater.

TABLE 5-14. Range and Median Concentrations of Trace Elements for Unconfined Groundwater at Hanford.

Trace element	Range (mg/L)	Median (mg/L)
Ag	<0.001 - 0.003	<0.001
Al	<0.050 - 0.470	<0.050
As	0.001 - 0.014	0.005
B	0.009 - 0.150	0.020
Ba	0.007 - 0.100	0.050
Cd	<0.003 - 0.140	<0.003
Co	<0.002 - 0.010	0.005
Cr	<0.050 - 0.100	0.007
Cu	<0.010 - 0.047	<0.010
Fe	<0.005 - 3.9	0.020
Mn	<0.001 - 0.480	0.010
Mo	<0.001 - 0.030	0.007
Pb	<0.002 - 0.017	0.006
Sb	<0.030	<0.030
Se	0.001 - 0.012	0.002
Sn	<0.010 - 0.120	0.010
Zn	<0.005 - 1.6	0.012

5.1.5.1.3 Nonconservative Hydrochemical Parameters.

Fluid Temperature. The range and mean of fluid temperatures measured at the ground surface at the time of sample collection were shown in Table 5-13. Groundwater temperature for shallow aquifer systems generally is reflective of the local mean annual air temperature. As shown in Table 5-13, the mean unconfined groundwater temperature is 19.0°C. This is considerably higher than the mean annual air temperature of 11.7°C reported by Stone et al. (1972) for the Hanford Site. The difference in unconfined groundwater and mean annual air temperature is principally attributable to the unconfined-aquifer depth (i.e., up to 200 meters) and warm water from synthetic recharge. Within the Gable Butte and Gable Mountain areas, some small temperature increases may be ascribed to natural groundwater discharge from deeper confined aquifers. However, such a cause would be very localized and is vastly overshadowed by major temperature variations resulting from synthetic-recharge in the

9 2 1 2 4 9 5 0 9 8 1

100, 200, and 300 Areas of the Hanford Site (ERDA, 1975). In localized areas, unconfined groundwater temperatures as high as 39°C have been measured. In these situations a direct association with synthetic recharge sources can be established.

pH. The pH within the unconfined aquifer ranges between 7.5 and 10.7, with a mean value of 7.9. Elevated pH values may be attributable to waste-water-disposal recharge to the unconfined aquifer near the 200 and 300 Areas. The pH in surface waters and shallow groundwater is often buffered by dissolved carbonate species (Stumm and Morgan, 1981). This appears to be the controlling factor in the unconfined aquifer at the Hanford Site.

Eh. The Eh is not currently measured on groundwater samples from the unconfined aquifer. A summary of numerous measurements compiled by Baas-Becking et al. (1960) indicates that the Eh values of Hanford unconfined groundwaters (for the pH range reported) are expected to be neutral to slightly reducing.

5.1.5.1.4 Dissolved-Gas Content. No dissolved-gas analyses are available for unconfined-aquifer groundwater at the Hanford Site. Based on results for the uppermost confined-aquifer system, dissolved gas within the unconfined aquifer is expected to be in extremely low concentrations and to be predominantly nitrogen.

5.1.5.2 Saddle Mountains Basalt. Available hydrochemical analyses for confined aquifers in the Saddle Mountains Basalt in the Pasco Basin were summarized by Gephart et al. (1979a). Hydrochemical data reported were primarily for groundwater samples collected from the Mabton interbed. Additional hydrochemical information has since been collected at a number of borehole sites including multiple sampling zones within the Saddle Mountains Basalt at four new boreholes (i.e., boreholes DB-15, DC-14, -15, and -16A.) (Refer to Fig. 5-49 for borehole locations). Groundwater samples from boreholes DC-16A and RRL-2, located adjacent to and within the reference repository location, are now being analyzed. All of these data will be documented in future reports.

Representative hydrochemical data from the Saddle Mountains Basalt are available for 21 boreholes on the Hanford Site (Table 5-15). To date 45 groundwater samples have been collected from these sites. Locations that have hydrochemical data for Saddle Mountains Basalt zones are shown in Figure 5-49. Boreholes for which data are available for multiple zones in the Saddle Mountains Basalt include DB-12, -13, -14, -15, DC-14, -15, and -16A. Boreholes DB-1, -2, -4, -5, -7, and -9 are completed solely in the Mabton interbed. In addition, seven boreholes are completed solely in the Rattlesnake Ridge interbed, within the upper Saddle Mountains Basalt in the vicinity of Gable Mountain Pond.

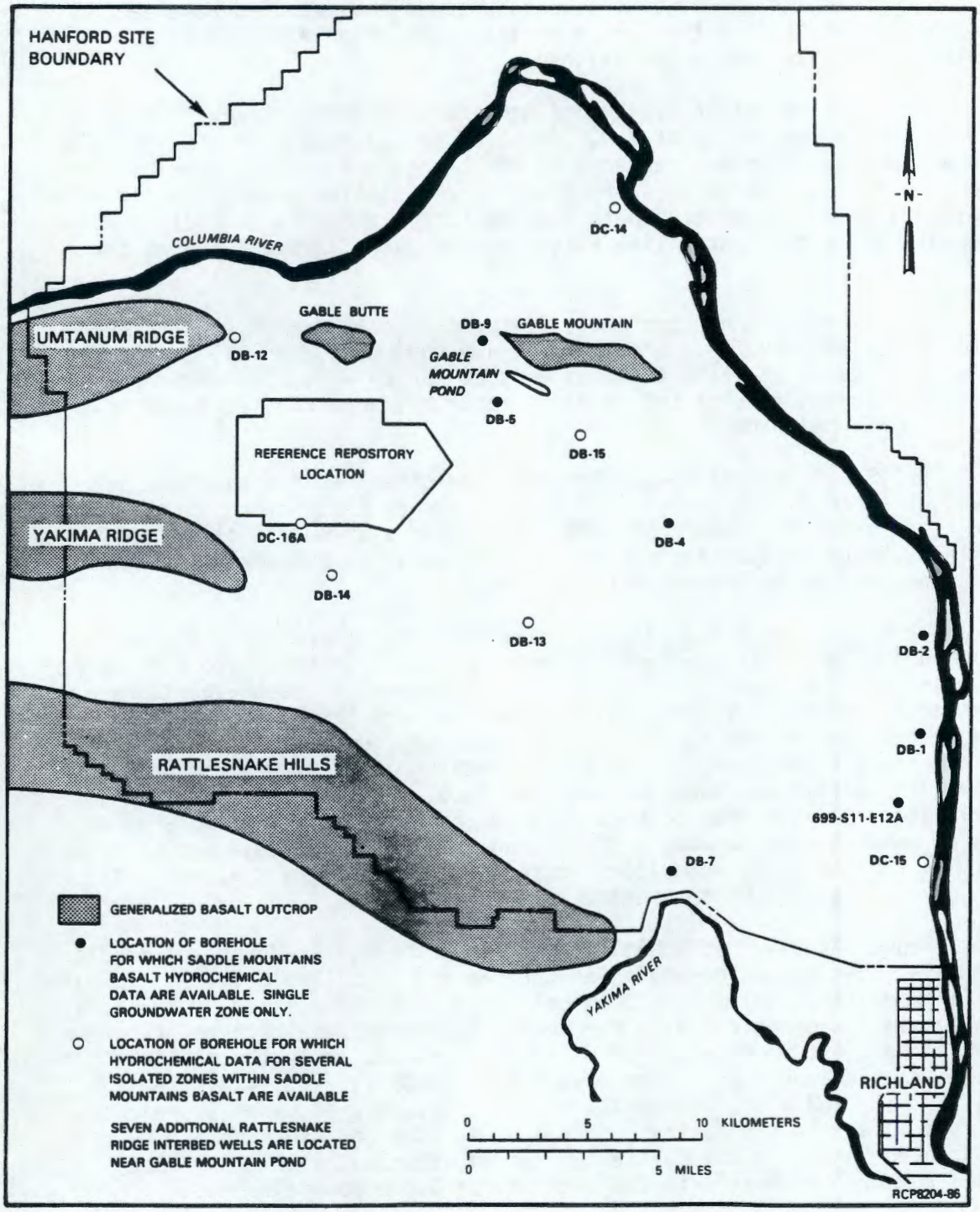

FIGURE 5-49. Location of Boreholes on the Hanford Site for Which Groundwater Hydrochemistry is Available from the Saddle Mountains Basalt.

TABLE 5-15. Location, Depth, and Date of Groundwater Sample Collection for Zones Within the Saddle Mountains Basalt. (Sheet 1 of 2)

Borehole	Stratigraphic interval	Depth below ground surface (m)	Date sampled
DB-1	Mabton interbed	297 - 302	07/20/78
			02/02/81
			11/10/81
DB-2	Mabton interbed	274 - 282	07/25/78
DB-4	Mabton interbed	416 - 428	07/25/78
DB-5	Mabton interbed	254 - 277	07/18/78
DB-7	Mabton interbed	237 - 248	07/24/78
DB-9	Mabton interbed	153 - 180	07/17/78
DB-12	Selah interbed	52 - 57	04/20/78
	Mabton interbed	114 - 156	05/11/78
DB-13	Elephant Mountain flow top	104 - 114	06/13/78
	Rattlesnake Ridge interbed	141 - 163	06/23/78
	Selah interbed	219 - 225	07/19/78
	Cold Creek interbed	264 - 287	08/05/78
	Mabton interbed	361 - 393	09/21/78
DB-14	Rattlesnake Ridge interbed	64 - 87	09/10/78
	Selah interbed	138 - 150	10/12/78
	Cold Creek interbed	188 - 202	10/30/78
	Mabton interbed	280 - 315	12/28/78
DB-15	Rattlesnake Ridge interbed	51 - 66	04/26/79
	Selah interbed	122 - 130	05/10/79
	Cold Creek interbed	158 - 187	05/24/79
	Upper Umatilla flow top	195 - 208	06/04/79
	Mabton interbed	227 - 256	07/03/79

9 2 1 2 4 9 5 0 9 8 4

TABLE 5-15. Location, Depth, and Date of Groundwater Sample Collection for Zones Within the Saddle Mountains Basalt. (Sheet 2 of 2)

Borehole	Stratigraphic interval	Depth below ground surface (m)	Date sampled
DC-14	Elephant Mountain flow top	120 - 127	01/22/80
	Rattlesnake Ridge interbed	150 - 162	01/18/80
	Selah interbed	214 - 231	02/05/80
	Asotin flow top	270 - 276	03/14/80
	Asotin intraflow	282 - 295	03/26/80
	Mabton interbed	296 - 327	04/07/80
DC-15	Levey interbed	87 - 95	01/04/80
	Rattlesnake Ridge interbed	127 - 151	01/23/80
	Cold Creek interbed	220 - 232	03/25/80
	Mabton interbed	310 - 324	04/14/80
DC-16A	Rattlesnake Ridge interbed	204 - 254	09/23/81
	Selah interbed	283 - 311	10/21/81
699-47-50	Rattlesnake Ridge interbed	79 - 90	06/25/80
699-50-45	Rattlesnake Ridge interbed	41 - 54	05/29/80
699-50-48	Rattlesnake Ridge interbed	65 - 76	06/10/80
699-51-46	Rattlesnake Ridge interbed	37 - 50	04/28/80
699-52-46	Rattlesnake Ridge interbed	52 - 69	05/09/80
699-52-48	Rattlesnake Ridge interbed	44 - 59	04/03/80
699-53-50	Rattlesnake Ridge interbed	44 - 59	04/15/80
699-S11-E12A	Levey interbed	73 - 81	03/20/80
			07/24/80

9 2 1 2 4 9 5 0 9 8 5

5.1.5.2.1 Major Inorganic Composition. The range in concentration and mean composition of major inorganic constituents for groundwater within the Saddle Mountains Basalt are listed in Table 5-16. For comparison purposes, results for the Mabton interbed groundwater are also included. Examination of the data indicates that Saddle Mountains Basalt groundwater generally possesses a relatively low total-dissolved-solids content (less than 500 milligrams per liter) and is of a sodium bicarbonate chemical type. Principal chemical constituents by weight occur in the following dominance relationship: total carbonate species>silica >sulfate≥calcium>chloride>potassium>magnesium>fluoride.

The mean values listed for major inorganic ion constituents in Mabton interbed groundwater are only slightly higher than mean concentrations for all Saddle Mountains Basalt groundwaters. Except for the uppermost confined zone, a similarity in major inorganic composition of Saddle Mountains Basalt groundwater is evident at most borehole sites (see Section 5.1.5.5). Boreholes where groundwaters exhibit differences in hydrochemical composition are normally limited to areas in which hydraulic communication between the unconfined and uppermost confined aquifer systems (e.g., Gable Mountain Pond area) is suspected.

Areal hydrochemical data for the Mabton interbed and composite confined aquifers within the lower Saddle Mountains Basalt are presented in a hydrochemical facies map shown in Figure 5-50. As previously mentioned, results obtained at the Hanford Site suggest that although apparent areal differences exist, groundwaters within the Saddle Mountains Basalt, at a given location, are similar in hydrochemical type. The use of multiple aquifer data sources outside the Hanford Site shown in Figure 5-50 is not valid for quantitative interpretation, but is considered acceptable for qualitative comparison of areal hydrochemical patterns.

Examination of Figure 5-50 indicates that areal hydrochemical changes are exhibited within the Mabton interbed and lower Saddle Mountains Basalt flow systems with increasing distance from areas of groundwater recharge. Hydrochemical changes include:

- A change in hydrochemical facies from a mixed cation (primarily calcium and magnesium) bicarbonate to a sodium bicarbonate chemical type
- Lower sulfate concentrations
- Greater total dissolved solids, sodium, and chloride concentrations.

Comparison of the Saddle Mountains Basalt potentiometric map (Fig. 5-31 and 5-43) and the hydrochemical facies map shown in Figure 5-50 indicates that, in natural recharge areas for the Saddle Mountains Basalt aquifers (i.e., Rattlesnake Hills, Yakima Ridge, Umtanum Ridge, and Saddle Mountains), groundwater is of a mixed cation (primarily calcium and magnesium) bicarbonate chemical type. The change in groundwater chemistry from a mixed cation bicarbonate to a sodium bicarbonate chemical type

9 2 1 2 4 9 5 0 9 8 6

TABLE 5-16. Range in Concentration and Mean Composition of Major Chemical Constituents for Groundwater Within the Mabton Interbed and Saddle Mountains Basalt.

Constituent	Saddle Mountains Basalt (mg/L)		Mabton interbed (mg/L)	
	Range	Mean	Range	Mean
	Anions			
HCO_3^-	104 - 298	180	164 - 275	202
CO_3^{-2}	0.8 - 23	4.2	1.3 - 22	4.7
Cl^-	3.4 - 63	12	4.6 - 63	20
SO_4^{-2}	<0.05 - 37	15	0.5 - 29	7.0
NO_3^-	<0.5 - 7.6	<0.5	<0.5	<0.5
F^-	0.03 - 8.0	1.3	0.1 - 8.0	2.0
$H_3SiO_4^-$*	0.5 - 22	4.0	0.7 - 21	5.5
OH^-	0.008 - 0.513	0.08	0.019 - 0.513	0.10
	Cations			
Na^+	17 - 122	58	36 - 122	85
K^+	6.2 - 15	11	7.7 - 14	12
Ca^{+2}	0.5 - 42	14	0.5 - 20	4.2
Mg^{+2}	0.1 - 16	4.2	0.1 - 12	1.5
H_4SiO_4*	50 - 140	97	50 - 140	103
Total dissolved solids	293 - 518	384	344 - 505	410
pH (field)	7.6 - 9.4	8.4	8.0 - 9.6	8.5
Eh (V) (field)	-0.09 - +0.06	-0.01	ND	ND

ND = Not determined.

*Total dissolved silica is shown in speciated forms due to elevated pH conditions in some zones. Total SiO_2 concentrations may be calculated by the relationships:

$$SiO_2 = 60\left[\frac{H_3SiO_4^-}{95} + \frac{H_4SiO_4}{96}\right]$$

9 2 1 2 4 9 5 0 9 8 7

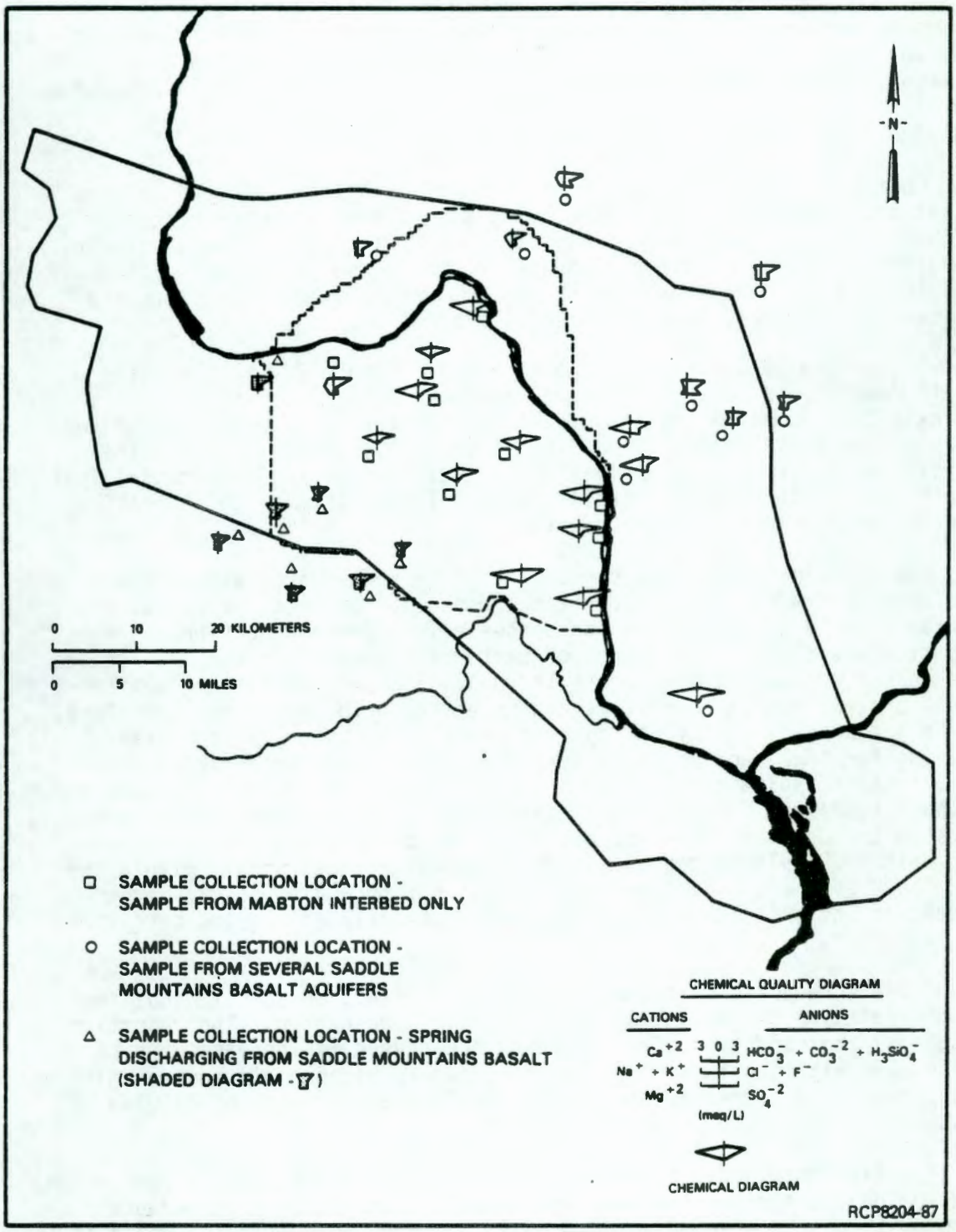

FIGURE 5-50. Hydrochemical Facies Map for Aquifers and Springs in the Saddle Mountains Basalt Within the Pasco Basin.

mentioned above is shown graphically by means of a trilinear diagram in Figure 5-51. This change is primarily attributable to cation-exchange processes and groundwater-mineral equilibria reactions. The presence of clay and tuffaceous units within sedimentary interbeds and the occurrence of secondary clay minerals and zeolites reported by Ames (1980) and Benson (1978) within basalt flows suggest that there is a significant cation-exchange capacity within the Saddle Mountains Basalt.

Chemical equilibria and mineral saturation within Saddle Mountains Basalt groundwater were evaluated using the WATEQ-F computer program. WATEQ-F calculates equilibrium distribution of inorganic aqueous species of major and important minor elements in aqueous solutions using chemical analyses and field measurements of temperature, pH, and redox potential (Truesdell and Jones, 1974; Plummer et al., 1976).

The saturation indices for calcite and cristobalite for selected Saddle Mountains Basalt groundwater are shown in Figure 5-52. Results indicate that Saddle Mountains Basalt groundwater is generally saturated with calcite and a silica mineral phase (probably cristobalite). The identification of calcite and various silica species in fracture fillings within the Saddle Mountains Basalt by Ames (1980) attests to the saturation of these minerals in groundwater.

The decrease in sulfate concentration in groundwater within the Saddle Mountains Basalt with distance from recharge areas is believed attributable to sulfate reduction processes. Sulfate reduction proceeds very slowly without the presence of bacteria. However, Hem (1970) states that, based on thermodynamic data in the literature, sulfate reduction should proceed spontaneously, releasing energy. The reaction, therefore, can be a source of energy for anaerobic bacteria, which can serve as a catalyst for the reaction. The presence of carbonaceous horizons which can assist the sulfate reduction process has been reported by Raymond and Tillson (1968) and identified in sedimentary interbeds and at flow contacts in the Columbia River basalt. The reduction of sulfate concentrations within Saddle Mountains Basalt groundwater appears only within the Cold Creek syncline. Outside this area (i.e., borehole DC-14), higher concentrations of sulfate, normally greater than 15 milligrams per liter, are exhibited.

Sulfate reduction also has a pronounced effect on calcite equilibria and the relative concentration of calcium in groundwater. The reduction of sulfate and oxidation of a carbon source causes an increase in bicarbonate concentration to occur. The increase in bicarbonate causes calcite precipitation to increase, thus causing a further decrease of calcium in solution.

The fact that total dissolved solids and individual mobile ions, such as chloride and sodium, increase in concentration within a groundwater system with distance from recharge areas is well known. The increase is due largely to the greater residence time for groundwater to react and dissolve minerals within the geologic framework and the higher solubility of salts that mobile ions (such as sodium and chloride) combine to form.

9 2 1 2 4 9 5 0 9 8 9

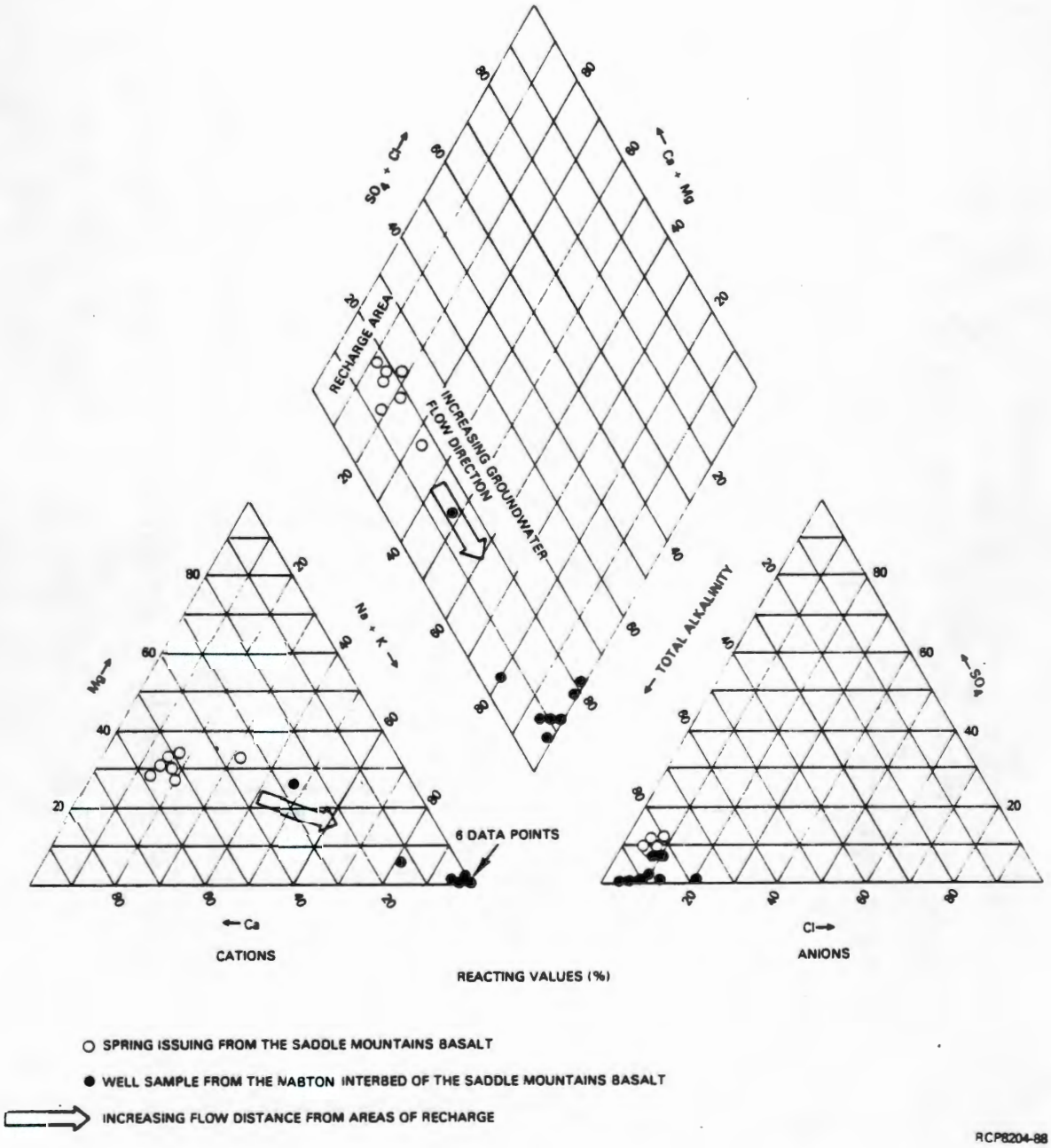

FIGURE 5-51. Chemical Composition of Springs and Groundwater Sampled from the Saddle Mountains Basalt.

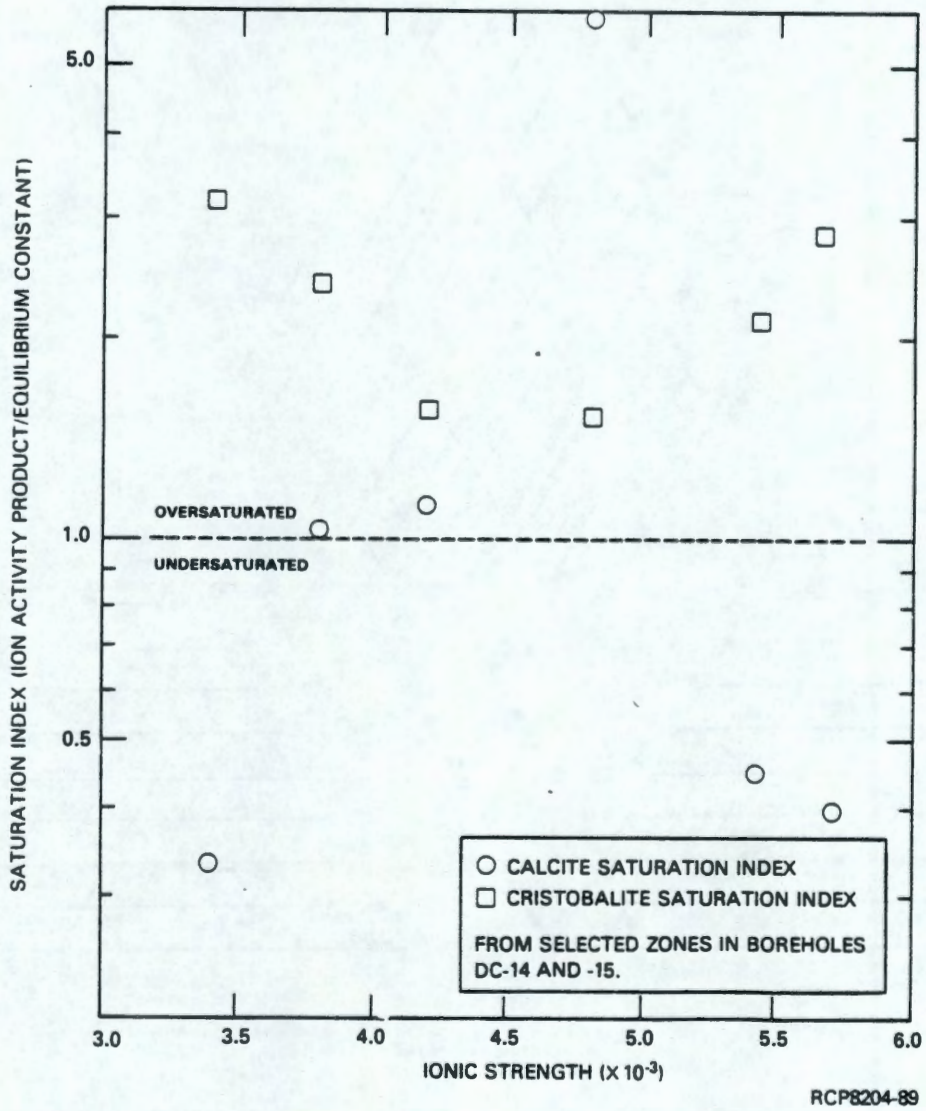

FIGURE 5-52. Saturation Index Data for Calcite and Cristobalite for Selected Saddle Mountains Basalt Groundwaters.

Maps that show the areal distribution of total dissolved solids or selected mobile ions can often be useful in the qualitative delineation of groundwater flow within individual aquifers. The distribution of total dissolved solids within the Mabton interbed is shown in Figure 5-53. The inferred direction of groundwater flow depicted compares favorably with the flow patterns determined from the potentiometric distribution previously shown in Figure 5-31.

The presence of nitrate in some uppermost confined Saddle Mountains Basalt groundwater is of hydraulic interest. As discussed previously, nitrate concentrations in regional groundwater are attributable to two sources: past water-disposal practices at the Hanford Site and irrigation within the Columbia Basin Irrigation Project. Elevated nitrate concentrations are common and characteristic of the unconfined groundwater at the Hanford Site. The presence of nitrate in confined groundwater is limited to the uppermost confined aquifer (i.e., the Rattlesnake Ridge interbed). Spane et al. (1980) have suggested that intercommunication between the unconfined zone and the upper Saddle Mountains Basalt zone may be indicated by the presence of nitrate in these waters. The degree and suspected area of intercommunication between unconfined and confined aquifers is described in Section 5.1.7.

Artificial recharge, induced by losses of irrigation water from the Columbia Basin Irrigation Project, also has a pronounced impact on the hydrochemical character of groundwater within the east-northeast part of the Pasco Basin. Selected water analyses which exhibit the effects of irrigation recharge in this area were previously shown in Figure 5-50. These water samples were collected from wells completed in more than one basalt flow top and/or interbed. Groundwater within this region generally has higher concentrations of nitrate, calcium, magnesium, sulfate, and chloride. Figure 5-32 compares nitrate concentrations for wells in this area with other wells in the Pasco Basin and illustrates the influence of irrigation recharge on Saddle Mountains Basalt aquifers.

5.1.5.2.2 Trace-Element Content. The range and median values of selected trace elements for groundwater sampled from Saddle Mountains Basalt at the Hanford Site are presented in Table 5-17. Data presented are only for samples collected using a turbine pump or air lift method, filtered through a 0.45-micron pressure filter, and stabilized with nitric acid. Values listed as less than (<) indicate a concentration below the analytical detection limit.

Examination of Table 5-17 indicates that the principal trace elements are aluminum, barium, boron, iron, and strontium. Ranges in trace elements listed compare reasonably well with values reported by Newcomb (1972) for Columbia River basalt aquifers within the Columbia Plateau.

Aluminum and iron exist as major components of Saddle Mountains Basalt flows (Myers/Price et al., 1979). Barium, boron, and strontium are most likely accessory components of basalt glass horizons. These trace elements are believed to enter the groundwater through groundwater/rock reactions that occur primarily within fractures and along flow contacts.

9 2 1 2 4 9 5 0 9 9 2

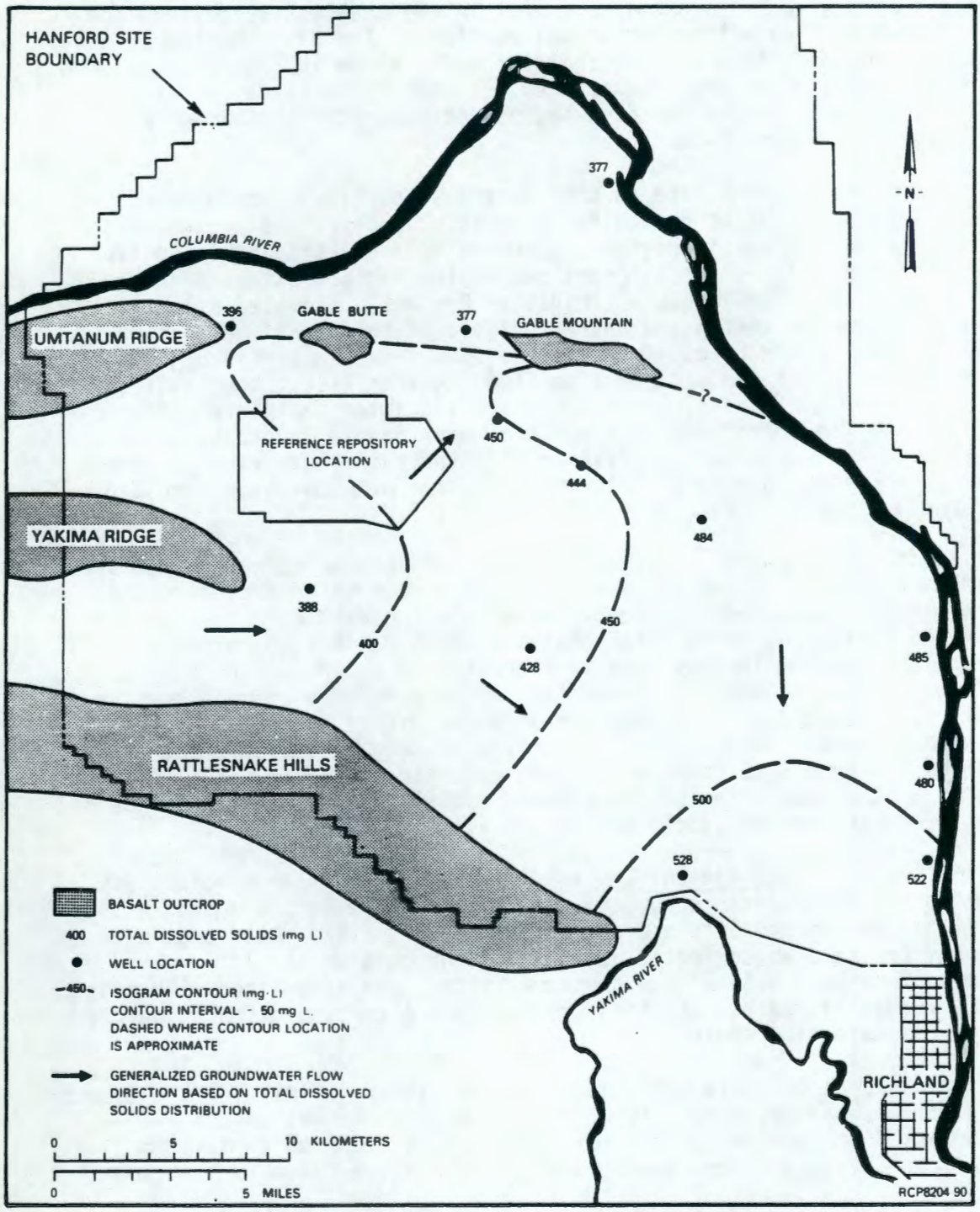

FIGURE 5-53. Distribution of Total Dissolved Solids and Inferred Flow Direction of Groundwater Within the Mabton Interbed.

TABLE 5-17. Range and Median Concentrations of Trace Elements for Groundwater Within Saddle Mountains Basalt at the Hanford Site.

Trace element	Saddle Mountains Basalt (mg/L)		Mabton interbed (mg/L)	
	Range	Median	Range	Median
Al	<0.02 - 2.17	0.14	<0.02 - 2.17	0.31
B	<0.005 - 0.539	0.04	<0.005 - 0.539	0.04
Ba	<0.005 - 0.265	0.03	<0.005 - 0.065	0.02
Cd	<0.005 - 0.007	<0.005	<0.005 - 0.007	<0.005
Co	<0.005 - 0.05	<0.005	<0.005 - 0.05	<0.005
Cr	<0.005 - 0.08	<0.005	<0.005 - 0.009	<0.005
Cu	<0.005 - 0.06	<0.005	<0.005	<0.005
Fe	<0.005 - 4.70	0.20	<0.005 - 4.70	0.27
Mn	<0.01 - 0.39	0.04	<0.01 - 0.39	<0.01
Mo	<0.01 - 0.31	<0.01	<0.01 - 0.11	<0.01
Ni	<0.005 - 0.04	<0.005	<0.005	<0.005
Pb	<0.005 - 0.34	<0.005	<0.005	<0.005
Sr	<0.005 - 0.115	0.06	<0.005 - 0.049	0.02
Zn	<0.005 - 0.11	0.02	<0.005 - 0.09	0.01

As was indicated previously for major inorganic compositions, no significant difference in median trace-element concentrations are evident between Mabton and other Saddle Mountains Basalt groundwater.

5.1.5.2.3 Nonconservative Hydrochemical Parameters.

Fluid Temperature. Fluid temperatures for Saddle Mountains Basalt groundwater measured at ground surface and downhole are listed in Table 5-18. Except at extremely shallow depths, surface-determined fluid temperatures are lower than their downhole counterparts. Downhole measurements are considered to be more representative of formation temperatures. Downhole measurements also allow groundwater pH measured at the ground surface to be corrected to formation conditions. Fluid temperature generally increases with depth and is reflective of the local geothermal gradient, which is about 3.8°C per 100 meters depth as based upon temperature measurements in several deep boreholes.

TABLE 5-18. Formation Fluid Temperature Within the Saddle Mountains Basalt in Selected Boreholes on the Hanford Site.

Borehole	Stratigraphic interval	Depth below ground surface (m)	Field temperature	
			Measured at ground surface (°C)	Measured at formation depth (°C)
DB-12	Selah interbed	55	15.8	16.3
	Mabton interbed	135	19.6	18.3
DB-14	Rattlesnake Ridge interbed	73	18.9	18.5
	Selah interbed	144	21.5	21.3
	Cold Creek interbed	195	23.4	23.3
	Mabton interbed	298	23.9	26.9
DB-15	Rattlesnake Ridge interbed	57	17.4	16.7
	Selah interbed	125	19.6	19.3
	Cold Creek interbed	172	21.2	21.4
	Upper Umatilla flow top	201	22.0	22.8
	Mabton interbed	244	22.8	24.9
DC-14	Elephant Mountain flow top	123	18.9	18.0
	Rattlesnake Ridge interbed	156	16.7	18.7
	Selah interbed	222	20.0	20.3
	Asotin flow top	273	19.3	24.8
	Mabton interbed	311	17.7	26.6
DC-15	Levey interbed	91	17.0	17.8
	Rattlesnake Ridge interbed	136	18.1	19.7
	Cold Creek interbed	226	20.6	23.1
	Mabton interbed	317	14.7	26.8
DC-16A	Rattlesnake Ridge interbed	229	21.0	22.2
	Selah interbed	297	24.1	24.6

9 2 1 2 4 9 5 0 9 9 5

Temperature is often used in groundwater systems to show mixing trends or groundwater flow direction (Domenico, 1972). Fluid temperature data for the Mabton interbed in boreholes on the Hanford Site are indicated in Figure 5-54. Measured fluid temperature within the Mabton interbed is given, as well as Mabton fluid temperature corrected to 300 meters of depth. Temperature corrections were made using the geothermal gradient in each borehole. Examination of Figure 5-54 indicates that areal temperature variation within the Mabton interbed is due to differences in depth below ground surface and so due to the geothermal gradient rather than groundwater-flow patterns.

pH. The pH measurements are routinely performed at the sample site at the time of collection. Several problems are associated with measurement of pH at the ground surface. Formation waters generally cool and may degas during transport from depth to the point of collection. Groundwater pH measured at the ground surface can be corrected to formation temperature; however, this does not take into account the effects of gas exchange. Future work will include in situ measurement of pH using a downhole probe to minimize temperature and gas effects. As indicated in Table 5-16 the mean pH values for groundwater within the Saddle Mountains Basalt at the Hanford Site is 8.4, with measured values ranging from 7.6 to 9.4.

The elevation of groundwater pH above 7 can generally be attributed to hydrolysis of silicate minerals. Silicate hydrolysis results in the release of hydroxide ions, leaving the resultant solution more basic (Krauskopf, 1979). Within the Saddle Mountains Basalt this trend is buffered by dissolved carbonate dissociation as indicated by the following reactions:

$$H_2CO_3 \rightleftharpoons H^+ + HCO_3^-$$

$$HCO_3^- \rightleftharpoons H^+ + CO_3^{-2}$$

Eh. While fluid temperatures and pH can be measured directly with reasonable accuracy, surface measurement of Eh is generally not suitable for quantitative interpretations (Stumm and Morgan, 1981; Langmuir, 1971); however, such measurements may be useful as a qualitative tool to indicate the general oxidizing or reducing conditions.

Potentiometric measurements of Eh on Saddle Mountains Basalt groundwater are limited to a few recent measurements made at boreholes DC-16A and 699-S11-E12A (see Fig. 5-49 for borehole locations). Measurements range from -0.09 to +0.06 volt (Table 5-16), indicating conditions may range from slightly oxidizing to slightly reducing. The presence of methane gas in some groundwater and pyrite in fracture filling at some borehole locations, however, suggest conditions may be more strongly reducing at depth than indicated by the surface potentiometric Eh measurements. Future work, including downhole electrode measurement of Eh and the measurement of redox pairs to calculate Eh (e.g., As^{+3}/As^{+5}) are planned to properly evaluate this parameter.

9 2 1 2 4 9 5 0 9 9 6

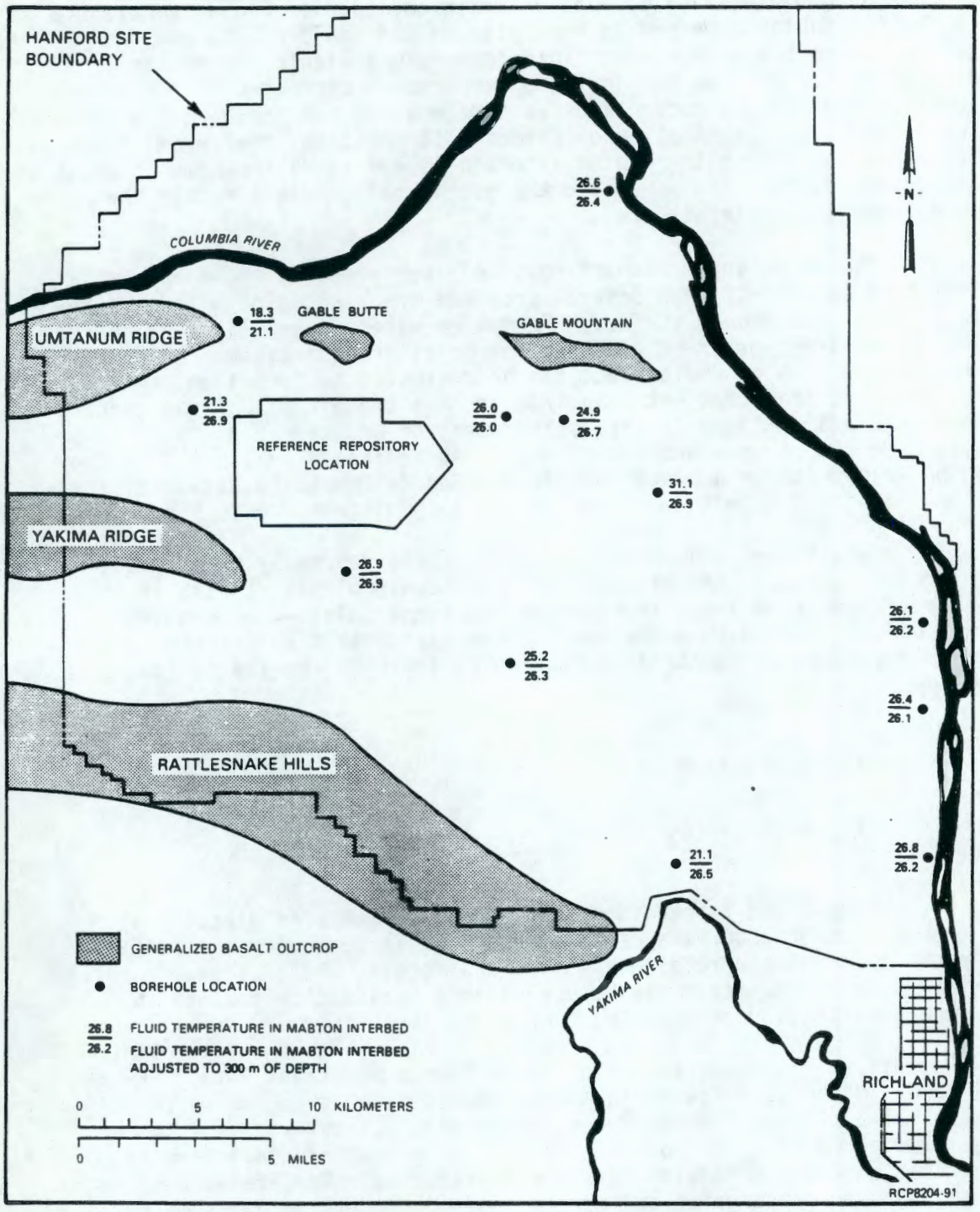

FIGURE 5-54. Mabton Interbed Groundwater Temperature in Boreholes on the Hanford Site.

9 2 1 2 4 9 5 0 9 9 7

5.1.5.2.4 Dissolved Gas. The presence of dissolved natural gas (principally methane and nitrogen) within the Saddle Mountains Basalt has been reported by several investigators. Glover (1936), for instance, reported the presence of methane in a geologic interval later identified as occurring in the lower Saddle Mountains and Wanapum Basalts. Several wells located along the northeastern flank of the Rattlesnake Hills produced natural gas during the 1930s for use in local communities. The quantity of natural gas developed, however, proved to be limited and was exhausted within a 12-year period.

Samples for dissolved-gas analysis have been collected in groundwater zones across the entire Saddle Mountains Basalt at two borehole sites, DC-14 and -15. Samples from two test intervals, the Mabton and Cold Creek interbeds in borehole DC-15, contain dissolved gas in detectable amounts. The percentages of gas present in the samples are listed in Table 5-19. As shown, methane (CH_4) makes up the major mole fraction by volume of the gas, with the remainder being mainly nitrogen. The source of the methane is not completely known. Isotopic and hydrochemical parameters, however, suggest a local biogenic origin.

TABLE 5-19. Dissolved Gas Content and Makeup for Groundwater Collected from the Saddle Mountains Basalt in Borehole DC-15.

Gas type	Cold Creek interbed[a] (mole %)	Mabton interbed[b] (mole %)
CO_2	0.51	0.07
Ar	0.25	0.08
O_2	<0.01	<0.01
N_2	11.1	3.18
CO	5.6	<0.10
He	<0.01	<0.01
H_2	0.06	<0.01
CH_4	82.5	96.7

[a]Yield: 3.68 mL gas per liter of water at standard temperature and pressure.

[b]Yield: 25 mL gas per liter of water at standard temperature and pressure.

9 2 1 2 4 9 5 0 9 9 8

Stahl (1980) reported that negative delta carbon-13 values for methane indicate that natural gas is produced through biogenic processes. As discussed in Section 5.1.6.2.1.2, delta carbon-13 values for methane from Cold Creek and Mabton interbed groundwaters are -63.57 and -46.46, respectively. A discussion of stable isotopic data that support a biogenic source of methane is also presented in that section.

Factors affecting the distribution of methane vertically in a borehole and areally in the region are not completely understood. The following conditions are generally required for methane occurrence in groundwater:

- A reducible carbon source
- An environment conducive to methane-producing bacteria.

Raymond and Tillson (1968) report the presence of carbonaceous horizons within sedimentary interbeds and in flow contacts of the Columbia River basalt in borehole RSH-1. Examination of core retrieved from other boreholes on the Hanford Site also confirms the existence of carbonaceous material within sedimentary interbeds and flow contacts of the Saddle Mountains Basalt. The occurrence of methane inside the Cold Creek syncline (i.e., borehole DC-15) and not apparently outside that structure (e.g., at borehole DC-14) may be due to variation in sulfate concentrations.

Methane-producing bacteria generally require a low sulfate environment to thrive. Sulfate-reducing bacteria compete more favorably for available hydrogen than do methanogens (Claypool and Kaplan, 1974). As discussed in Section 5.1.5.2.1, reduced sulfate concentrations (i.e., less than 2 milligrams per liter) occur within the lower Saddle Mountains Basalt inside the Cold Creek syncline. Outside this area (i.e., at borehole DC-14), sulfate concentrations are greater than 18 milligrams per liter. This concentration may be sufficient to prevent the carbonaceous reduction reactions from occurring and so explain the absence of methane in groundwater zones at borehole DC-14.

5.1.5.3 Wanapum Basalt. A summary of hydrologic data available for groundwater zones within the Wanapum Basalt was presented by Gephart et al. (1979a). Data noted were limited to analyses from 12 boreholes penetrating only the upper Priest Rapids member (upper Wanapum Basalt). Several of these boreholes were also open to zones within the lower Saddle Mountains Basalt. Since that report, additional hydrochemical information has been collected.

Analyses are available at four boreholes on the Hanford Site for multiple zones within the Wanapum Basalt (i.e., boreholes DB-11, -12, and 15, DC-12, -14, and -15) (Fig. 5-55). Refer to Section 5.1.5.5 for selected examples of vertical hydrochemical patterns evident from groundwater analyses. Groundwater samples from boreholes DC-16A and RRL-2, located adjacent to and within the reference repository location, are now being analyzed. These data will be reported in future reports.

9 2 1 2 4 9 5 0 9 9 9

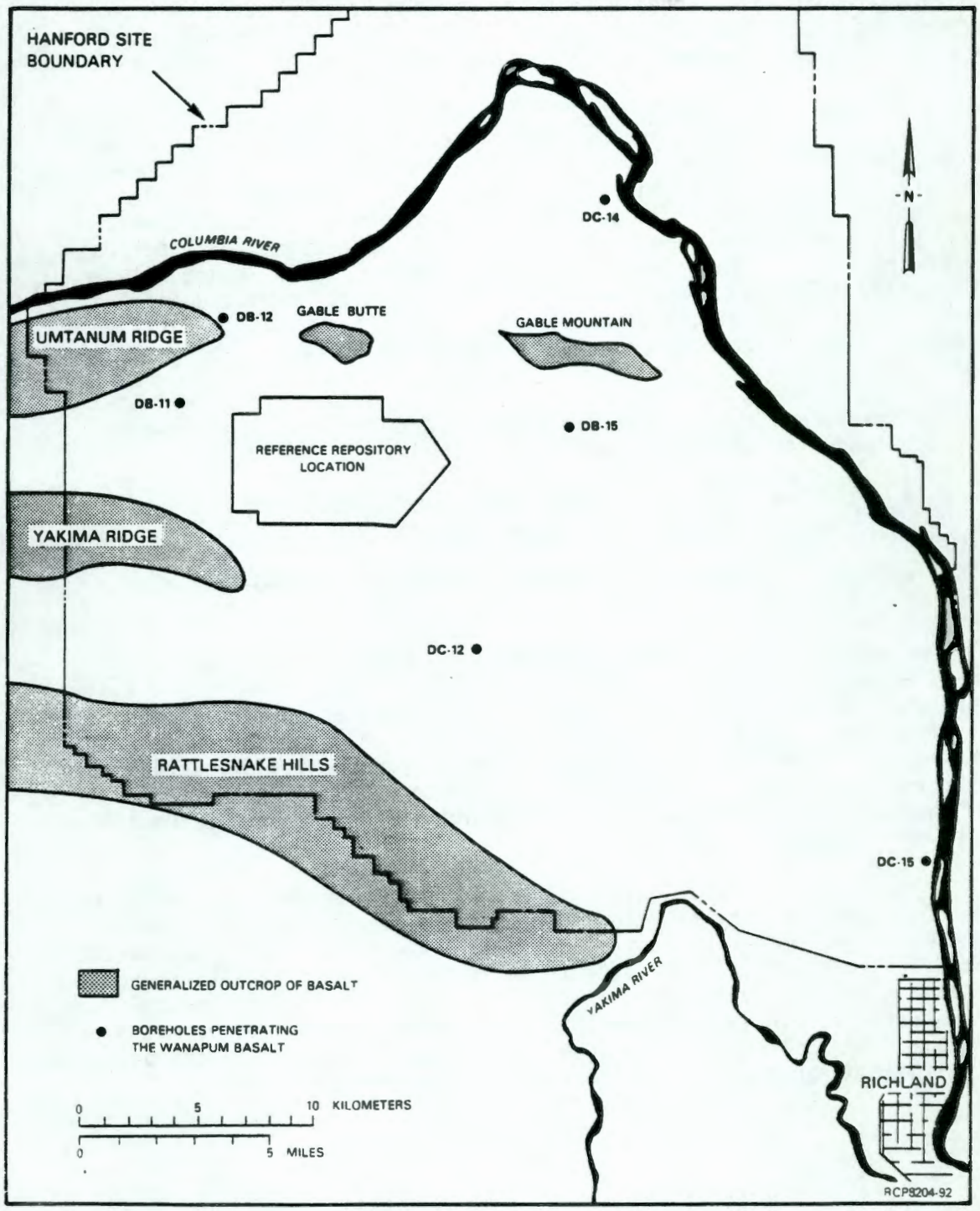

FIGURE 5-55. Boreholes with Hydrochemical Data from Groundwater Within the Wanapum Basalt on the Hanford Site.

Data presented in this report include only those recent analyses collected by the BWIP and earlier analyses that are representative of individual groundwater zones within the Wanapum Basalt. Boreholes and hydrogeologic units within the Wanapum Basalt for which hydrochemical data are available are summarized in Table 5-20.

5.1.5.3.1 Major Inorganic Composition. Analytical results for major inorganic constituents in groundwater collected from zones within the Wanapum Basalt are listed in Table 5-21. Considerable range in concentration of individual constituents is evident for Wanapum Basalt groundwater. Groundwater is generally of a sodium bicarbonate chemical type, although in some cases chloride contributes a significant percentage of the total anionic content. Total dissolved solids range between 300 and 700 milligrams per liter. Principal chemical constituents are present in the following dominance relationship (by weight): total carbonate>total silica≥sodium>chloride>potassium>sulfate>fluoride>calcium >magnesium.

Two discernible hydrochemical patterns are exhibited for Wanapum Basalt groundwater at the Hanford Site. They are as follows:

- Relatively uniform hydrochemistry with depth within the formation at individual locations
- Areal differences in chemical type and dissolved-solids concentrations.

The major inorganic composition for Wanapum Basalt groundwater in boreholes DC-14 and DB-15 is depicted in Figure 5-56. This figure indicates that, except for minor differences, groundwater chemical composition and hydrochemical type are relatively uniform within the Wanapum Basalt at a particular location. However considerable hydrochemical variation does occur areally within Wanapum Basalt groundwater. As discussed, these differences mainly take place between locations inside and outside the Cold Creek syncline.

As an example of areal variations, total-dissolved-solids and chloride concentrations in the Priest Rapids Member (upper Wanapum Basalt) groundwater for boreholes inside and outside the Cold Creek syncline are listed in Table 5-22. These data indicate that Wanapum Basalt groundwater within the syncline contains elevated total dissolved solids and chloride concentrations. These hydrochemical differences from inside versus outside the Cold Creek syncline are depicted graphically by data groupings on a trilinear diagram shown in Figure 5-57 (also see Fig. 5-90).

9 2 1 2 4 9 5 1 0 0 1

TABLE 5-20. Location, Depth, and Date of Groundwater-Sample Collection for Zones Within the Wanapum Basalt.

Borehole	Stratigraphic interval	Depth below ground surface (m)	Date sampled
DB-11	Priest Rapids	309 - 319	12/27/77
			04/13/78
			07/14/78
DB-12	Priest Rapids	156 - 196	05/23/79
DB-15	Priest Rapids	262 - 295	08/13/79
	Roza	319 - 337	08/27/79
	Frenchman Springs	398 - 410	09/27/79
	Frenchman Springs	425 - 440	10/18/79
	Frenchman Springs	443 - 466	10/15/79
	Frenchman Springs	481 - 506	11/09/79
DC-12	Priest Rapids	372 - 382	01/23/80
	Roza	405 - 416	02/07/80
	Frenchman Springs	460 - 468	02/25/80
	Frenchman Springs	625 - 634	05/08/80
DC-14	Priest Rapids	365 - 371	05/19/80
	Roza	394 - 409	06/11/80
	Squaw Creek interbed	451 - 462	06/23/80
	Frenchman Springs	480 - 497	07/07/80
	Frenchman Springs	500 - 521	07/14/80
	Frenchman Springs	524 - 555	07/29/80
	Frenchman Springs	664 - 681	09/09/80
DC-15	Roza	372 - 394	05/05/80
	Roza	414 - 424	06/12/80
	Frenchman Springs	451 - 459	06/30/80
	Frenchman Springs	469 - 485	07/15/80
	Frenchman Springs	529 - 559	08/04/80
	Frenchman Springs	559 - 575	08/12/80

9 2 1 2 4 9 5 1 0 0 2

TABLE 5-21. Range in Concentration and Mean Composition of Major Inorganic Constituents and Hydrochemical Parameters for Wanapum Basalt Groundwater on the Hanford Site.

Constituent	Range (mg/L)	Mean (mg/L)
Anions		
HCO_3^-	100 - 192	128
CO_3^{-2}	1.8 - 26	18
Cl^-	4.2 - 117	43
SO_4^{-2}	<0.05 - 26	11
NO_3^-	<0.5	<0.5
F^-	0.6 - 24	8.0
$H_3SiO_4^-$ [a]	1.7 - 55	28
OH^-	0.03 - 0.37	0.27
Cations		
Na^+	61 - 171	96
K^+	10 - 21	14
Ca^{+2}	1.0 - 18	3.4
Mg^{+2}	0.3 - 10	0.8
H_4SiO_4 [a]	6.2 - 152	71
Total dissolved solids	295 - 667	461
pH (field)	8.2 - 9.6	9.3
Eh (V) (field)	-0.18 - +0.12	+0.02[b]

[a]Total dissolved silica is shown in speciated forms due to elevated pH conditions in some zones. Total SiO_2 concentration may be calculated by the relationship:

$$SiO_2 = 60\left[\frac{H_3SiO_4^-}{95} + \frac{H_4SiO_4}{96}\right]$$

[b]Median value.

9 2 1 2 4 9 5 1 0 0 3

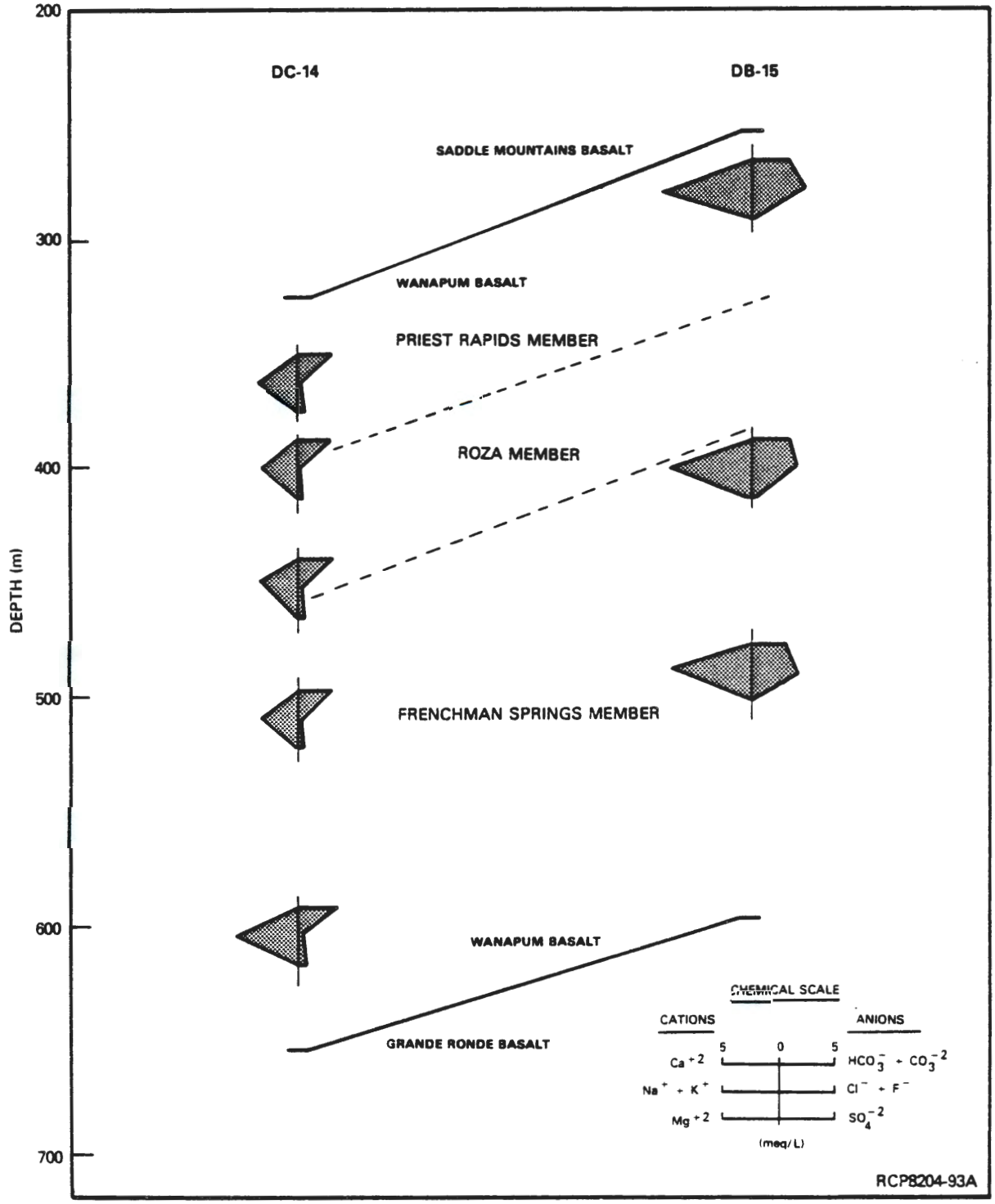

FIGURE 5-56. Major Inorganic Hydrochemistry for Groundwater Zones in Boreholes DC-14 and DB-15 Within the Wanapum Basalt.

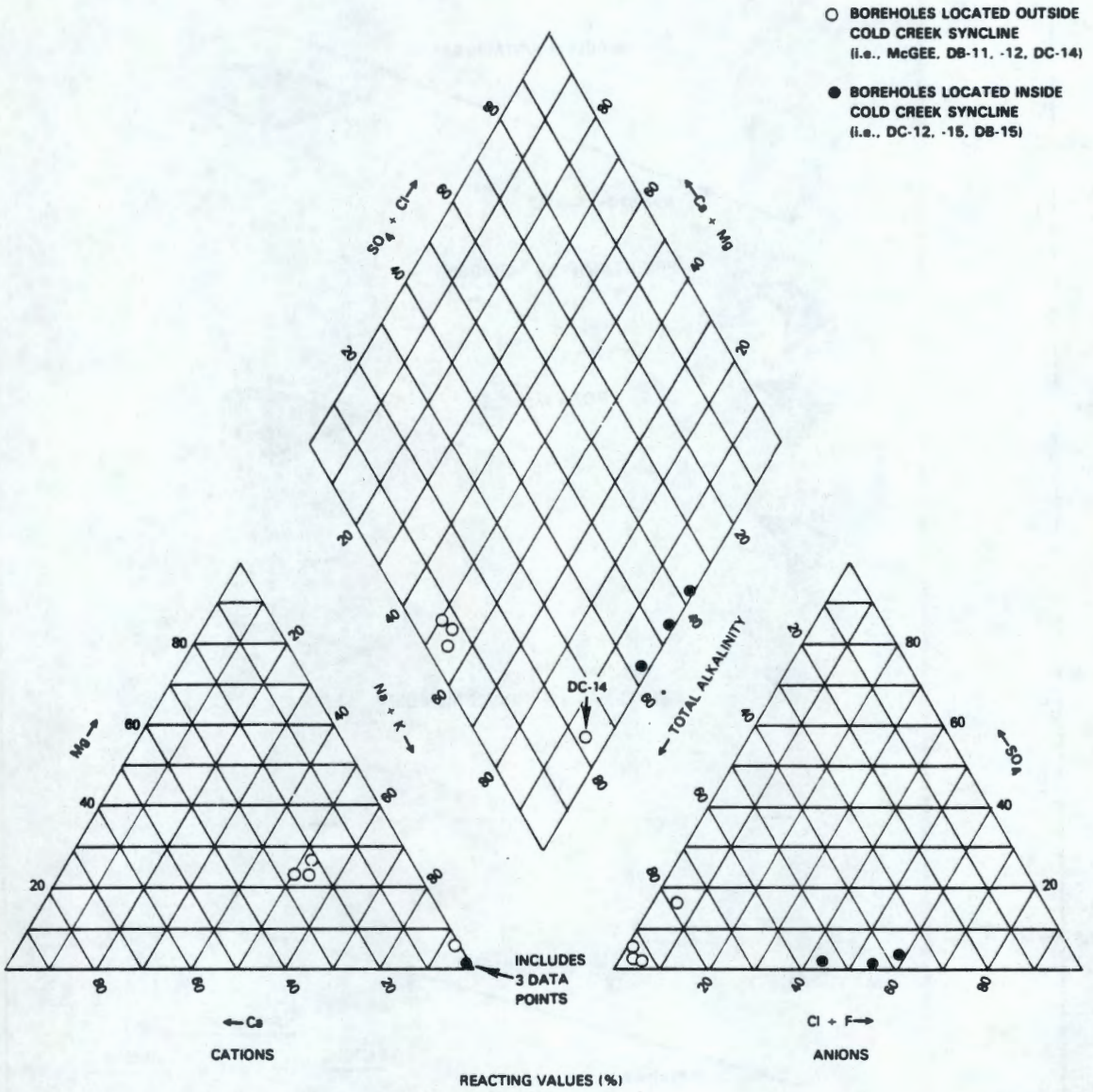

FIGURE 5-57. Major Inorganic Composition of Wanapum Groundwaters from Inside and Outside the Cold Creek Syncline.

TABLE 5-22. Total Dissolved Solids and Chloride Concentration in Priest Rapids Groundwater.

Location	Borehole	Total dissolved solids (mg/L)	Chloride (mg/L)
Outside Cold Creek syncline	DC-14	377	5.1
	DB-11	349	4.6
	DB-12	362	4.6
	McGee well (irrigation well)	295	4.2
Inside Cold Creek syncline	DC-12	400	104
	DB-15	654	117
	DC-15	390	47

The areal hydrochemical variation observed within Wanapum Basalt groundwater may be attributable to increased vertical permeability along the Umtanum Ridge-Gable Mountain anticline, as discussed in Section 5.1.7. This increased permeability may permit underlying Grande Ronde Basalt groundwater of higher total-dissolved-solids and chloride content to mix with shallower Wanapum Basalt groundwater inside the Cold Creek syncline, resulting in the areal variation observed. As previously discussed, this hydrochemical heterogeneity is also supported by areal variations in stable isotopic data.

Examination of Figure 5-57 indicates a close similarity in chemical-type compositions among samples of Wanapum Basalt groundwater inside (sodium chloride-bicarbonate) and outside (mixed cation predominantly sodium bicarbonate) the Cold Creek syncline area. It should be noted, however, that borehole DC-14 (located north of the Cold Creek syncline) exhibits a cationic content that appears transitional to the two chemical groupings. The difference in cation-plotting location from other "outside" groundwater may be attributable to different recharge sources and/or flow-system characteristics.

Chemical equilibria and mineral saturation within Wanapum Basalt groundwater were evaluated using the WATEQ-F computer program (Truesdell and Jones, 1974; Plummer et al., 1976).

The saturation indices for calcite and cristobalite for selected Wanapum Basalt groundwater are shown in Figure 5-58. Results indicate that, like the overlying basalt groundwater, the Wanapum Basalt groundwater is generally saturated with calcite and a silica mineral phase (probably cristobalite). The identification of calcite and various silica species in fracture fillings within Columbia River basalt by Ames (1980) attests to the saturation of these minerals in groundwater.

5.1.5.3.2 Trace-Element Content. The range in concentration and median composition of trace elements within the groundwater of the Wanapum Basalt are listed in Table 5-23. Aluminum, iron, and boron are consistently present in detectable trace concentrations. Aluminum is a major component of aluminosilicate minerals within basalts and may enter the solute phase through mineral/groundwater reactions. The presence of dissolved iron is primarily attributable to chemical reactions affecting ferromagnesian minerals. The source of boron is currently unknown. Hem (1970) reports, however, that boron commonly exists as an accessory constituent in biotite and amphiboles and as a component of basalt glass horizons. It is believed, therefore, to be released to groundwater through dissolution of ferromagnesian minerals and volcanic glass along basalt flow contacts.

TABLE 5-23. Range and Median Concentrations of Trace Elements for Groundwater Within the Wanapum Basalt.

Trace element	Range (mg/L)	Median (mg/L)
Al	<0.1 - 0.110	0.03
B	<0.013 - 0.940	0.23
Ba	<0.005 - 0.120	<0.005
Cd	<0.005	<0.005
Co	<0.005 - 0.010	<0.005
Cr	<0.005 - 0.010	<0.005
Cu	<0.005 - 0.010	<0.005
Fe	<0.005 - 0.228	<0.052
Mn	<0.10 - 0.044	<0.10
Mo	<0.10 - 0.260	<0.10
Ni	<0.005	<0.005
Pb	<0.10 - 0.180	<0.10
Zn	<0.005 - 0.015	<0.005

9 2 1 2 4 9 5 1 0 0 7

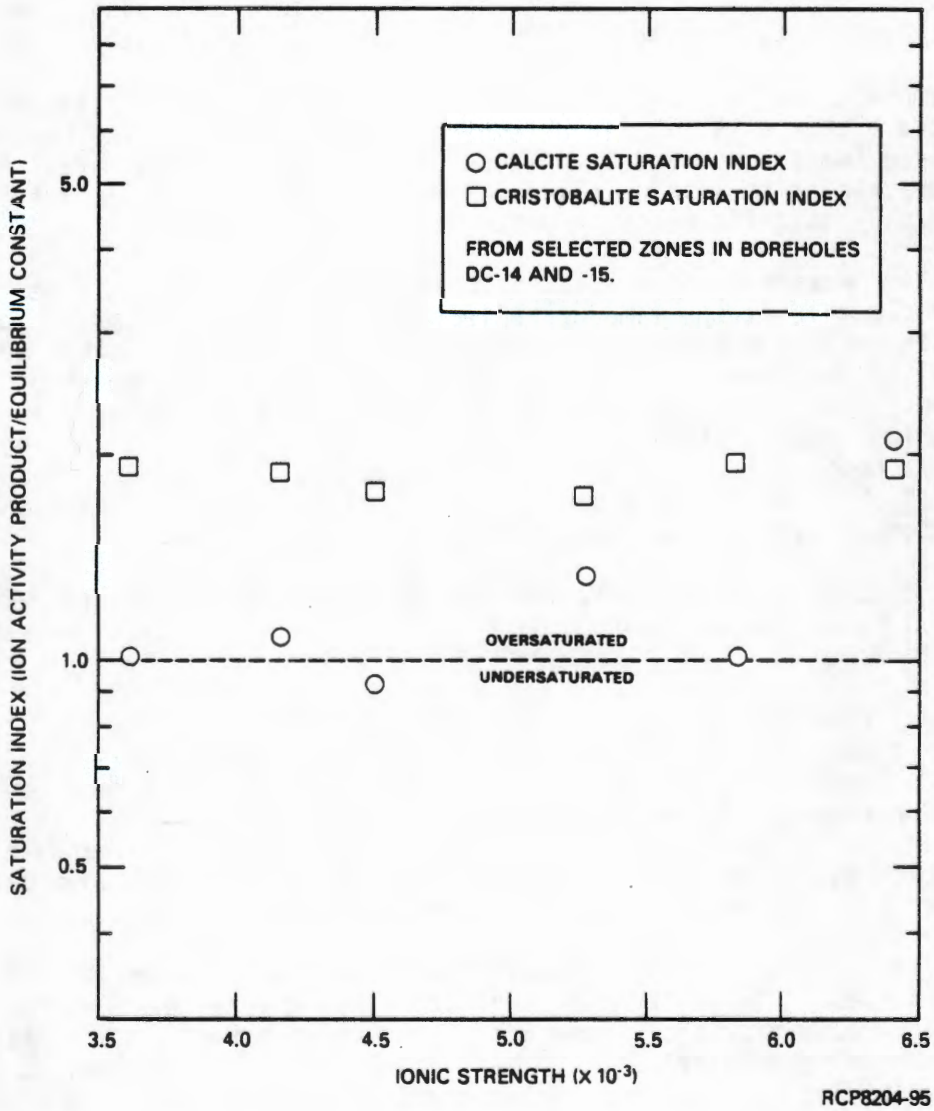

FIGURE 5-58. Calcite and Cristobalite Saturation Index for Selected Groundwaters Within the Wanapum Basalt.

5.1.5.3.3 Nonconservative Hydrochemical Parameters.

Fluid Temperature. Fluid temperatures for Wanapum Basalt groundwater measured at ground surface and downhole are listed in Table 5-24. Downhole temperatures, as expected, are higher than surface measurements and are considered more representative of formation conditions. Downhole measurements allow groundwater pH values measured at ground surface to be corrected to formation conditions. Fluid temperature generally increases with depth and is reflective of the local geothermal gradient.

Attempts to delineate mixing trends or groundwater flow patterns at the Hanford Site from areal fluid temperature data have not yet been successful (see Section 5.1.5.2.3). These studies indicate that areal fluid temperature variation within individual Wanapum Basalt flows is attributable primarily to differences in depth below ground surface.

pH. As previously discussed, pH measurements are routinely performed at the sample site at the time of collection. Several problems are associated with measurement of pH at ground surface. Formation waters generally cool and may de-gas during transport from depth to the point of collection. Groundwater pH measured at ground surface, however, can be corrected to formation-temperature conditions. However, this does not take into account the effects of gas exchange that might occur. Future work will include in situ measurement of pH using a downhole probe to minimize temperature and de-gassing effects.

As indicated in Table 5-21, the mean pH value for groundwater within the Wanapum Basalt at the Hanford Site is 9.3 with measured values ranging from 8.2 to 9.6.

Factors contributing to the elevation of groundwater pH above 7 were discussed in Section 5.1.5.2.3. Within the Wanapum Basalt this trend is primarily buffered by dissolved-carbonate dissociation. The range of pH measured for Wanapum Basalt groundwater is slightly higher than for groundwater of the Saddle Mountains Basalt. This may be attributable to lower concentrations of dissolved carbonate species within Wanapum Basalt groundwater, resulting in a reduced buffering capacity.

Eh. Limitations of potentiometric Eh measurement were mentioned in Section 5.1.5.2.3. In spite of the difficulties, Eh has been routinely measured on groundwater from zones within the Wanapum Basalt for qualitative geochemical characterization. Measured Eh values range from +0.12 to -0.18 volt (Table 5-25), indicating conditions range from slightly oxidizing to slightly reducing. Other qualitative Eh indicators (such as the presence of methane gas in groundwater, produced through biogenic reduction of carbon, and pyrite in fracture fillings) suggest that even stronger reducing conditions may exist. Additional work, including downhole potentiometric measurement of Eh and the measurement of redox pairs to allow calculation of Eh, is needed to adequately evaluate formation Eh conditions.

9 2 1 2 4 9 5 1 0 0 9

TABLE 5-24. Formation Temperature Within the Wanapum Basalt in Selected Boreholes on the Hanford Site.

Borehole	Stratigraphic interval	Depth below ground surface (m)	Collection temperature (°C)	Interval temperature (°C)
DB-11	Priest Rapids	310	26.7	27.0
DB-12	Priest Rapids	176		19.5
DB-15	Priest Rapids	279	21.4	26.9
	Middle Frenchman Springs	432	25.4	31.8
	Lower Frenchman Springs	445	23.10	32.2
DC-12	Priest Rapids	377	22.0	27.0
	Roza	464	22.6	29.8
	Frenchman Springs	629	24.1	33.3
DC-14	Priest Rapids	365	23.5	28.6
	Upper Frenchman Springs	489	30.7	34.0
	Lower Frenchman Springs	664	27.9	41.8
DC-15	Priest Rapids	385	24.7	29.5
	Upper Frenchman Springs	455	27.2	32.3
	Lower Frenchman Springs	544	27.0	33.4

TABLE 5-25. Potentiometric Measurement of Eh in Groundwaters Collected From Zones Within the Wanapum Basalt.

Borehole	Stratigraphic interval	Depth interval (m)	Eh (V)
DC-14	Roza flow top	394 - 409	+0.12
DC-14	Frenchman Springs	480 - 497	+0.02
DC-14	Frenchman Springs	500 - 521	+0.12
DC-14	Frenchman Springs	524 - 555	+0.03
DC-14	Frenchman Springs	664 - 681	-0.03
DC-15	Frenchman Springs	469 - 485	+0.10
DC-15	Frenchman Springs	529 - 559	-0.14
DC-15	Frenchman Springs	559 - 575	-0.18

5.1.5.3.4 Dissolved Gas. Historical reports concerning the presence of natural gas within the Wanapum Basalt were discussed in Section 5.1.5.2.4.

Samples for dissolved-gas analysis have been collected for individual groundwater zones within the Wanapum Basalt at four borehole sites: DC-12, -14, -15, and DB-15. The gas composition in volume percent is given in Table 5-26. As was evident for the overlying Saddle Mountains Basalt groundwater, dissolved-gas composition does not appear to be areally uniform. Outside the Cold Creek syncline (i.e., borehole DC-14), gas composition is dominated by nitrogen. Inside this syncline (i.e., boreholes DB-15, DC-12 and -15), gas composition is generally dominated by methane.

The source for methane within Wanapum Basalt groundwater is not completely known. Available hydrochemical and isotope data, however, suggests a biogenic origin. A discussion of geochemical and biological processes involved in the generation of methane within the Columbia River basalt was presented in Section 5.1.5.2.4.

5.1.5.4 Grande Ronde Basalt. A summary of pre-1979 hydrochemical information for confined aquifers within the Grande Ronde Basalt is discussed in Gephart et al. (1979a). That report presented data from three boreholes on the Hanford Site (DC-1, -2, and -6). More recent hydrochemical samples have been collected from numerous flow tops in the Grande Ronde Basalt zones in an additional three boreholes (i.e., DC-12, -14, and -15).

TABLE 5-26. Distribution of Dissolved Gas-Components in Wanapum Basalt Zones.

Borehole	Stratigraphic interval	Depth below ground surface (m)	Total dissolved gas (vol%)							
			Carbon dioxide	Argon	Oxygen	Nitrogen	Carbon monoxide	Helium	Hydrogen	Methane
DB-15	Frenchman Springs	398 - 410	0.22	0.18	0.18	8.34	<0.10	<0.01	1.28	89.80
	Frenchman Springs	425 - 440	0.01	0.11	<0.01	5.40	<0.10	0.01	0.09	94.40
	Frenchman Springs	443 - 466	<0.01	0.16	<0.01	8.02	<0.10	0.01	0.90	90.91
	Frenchman Springs	481 - 506	<0.01	0.15	<0.01	6.06	<0.10	<0.01	<0.01	93.80
DC-12	Priest Rapids	372 - 383	0.50	0.14	<0.01	3.42	<0.10	<0.01	<0.01	95.9
	Roza	405 - 416	<0.01	0.13	0.01	5.79	<0.10	<0.01	<0.01	94.1
	Frenchman Springs	460 - 468	0.06	0.12	0.11	5.20	1.80	<0.01	<0.01	92.7
	Frenchman Springs	625 - 634	0.04	0.14	<0.01	8.30	<0.10	<0.01	<0.01	91.5
DC-14	Priest Rapids	365 - 371	ND	ND	ND	ND	ND	ND	ND	ND
	Squaw Creek interbed	451 - 462	ND	ND	ND	ND	ND	ND	ND	ND
	Frenchman Springs	480 - 497	<0.01	0.97	<0.01	99.0	<0.10	<0.01	<0.01	<0.01
	Frenchman Springs	500 - 521	0.02	1.14	<0.01	98.8	<0.10	<0.01	<0.01	<0.01
	Frenchman Springs	527 - 555	ND	ND	ND	ND	ND	ND	ND	ND
	Frenchman Springs	664 - 681	ND	ND	ND	ND	ND	ND	ND	ND
DC-15	Roza	372 - 394	0.01	0.17	<0.01	11.90	<0.10	<0.01	<0.01	87.9
	Roza	414 - 424	<0.01	0.25	<0.01	19.70	<0.10	<0.01	<0.01	80.0
	Frenchman Springs	451 - 459	<0.01	0.32	<0.01	21.50	<0.10	<0.01	<0.01	78.2
	Frenchman Springs	469 - 485	0.01	0.41	0.01	33.80	<0.10	0.03	<0.01	65.7
	Frenchman Springs	529 - 559	0.01	1.14	0.05	98.50	<0.10	0.12	<0.01	0.14
	Frenchman Springs	559 - 575	<0.01	1.14	0.55	97.80	<0.10	0.11	<0.01	0.35

ND = No gas detected in groundwater sample.

The locations of boreholes from which hydrochemical data available are shown in Figure 5-59. The use of hydrochemical data previously presented in other reports, especially for boreholes RSH-1 (Raymond and Tillson, 1968) and DC-1 (LaSala and Doty, 1971) is generally unacceptable for quantitative interpretation, due to:

- Poor ionic balances (i.e., (Σ anions - Σ cations)/Σ cations $>\pm 5$ percent)
- Nonrepresentativeness of groundwater samples
- Composite zone sampling.

Boreholes and pertinent sample-collection-depth data for test intervals utilized in this report are listed in Table 5-27. See Section 5.1.5.5 for selected examples of vertical definition of hydrochemical types within the Grande Ronde Basalt.

Groundwater samples from the Grande Ronde Basalt in boreholes DC-16A and RRL-2 are now being analyzed. These data will be reported in future reports.

5.1.5.4.1 Major Inorganic Composition. The range in concentration and mean composition of major inorganic constituents for groundwater sampled from the Grande Ronde Basalt at the Hanford Site are listed in Table 5-28. Grande Ronde Basalt groundwater is considerably different in chemical composition from groundwater in the overlying Saddle Mountains and Wanapum Basalts. In general, Grande Ronde Basalt groundwaters are considerably more mineralized, are of a different chemical type, contain reduced levels of total carbonate, and possess elevated levels of fluoride.

Groundwater within the Grande Ronde Basalt is generally more mineralized than shallower groundwater, due to increased rock/water contact time. As discussed in Sections 5.1.3 and 5.1.4, Grande Ronde Basalts generally have lower transmissivities and more distant recharge areas than do shallower basalt systems. These characteristics result in longer residence times for dissolution and hydrolysis reactions to occur before reaching sampling locations at the Hanford Site.

The chemical composition of individual samples of Grande Ronde Basalt groundwater listed in Table 5-27 are shown on a trilinear diagram in Figure 5-60. The grouping of data points in this figure indicates that Grande Ronde groundwaters are predominantly a sodium chloride chemical type. In contrast, groundwater within the overlying Saddle Mountains and Wanapum Basalts are considerably less mineralized and of a sodium bicarbonate and a sodium bicarbonate-chloride chemical type, respectively. Principal chemical constituents are present in the following dominance relationship (by weight): sodium>total silica≥chloride>sulfate>total carbonate species>fluoride>potassium>calcium>magnesium.

9 2 1 2 4 9 5 1 0 1 3

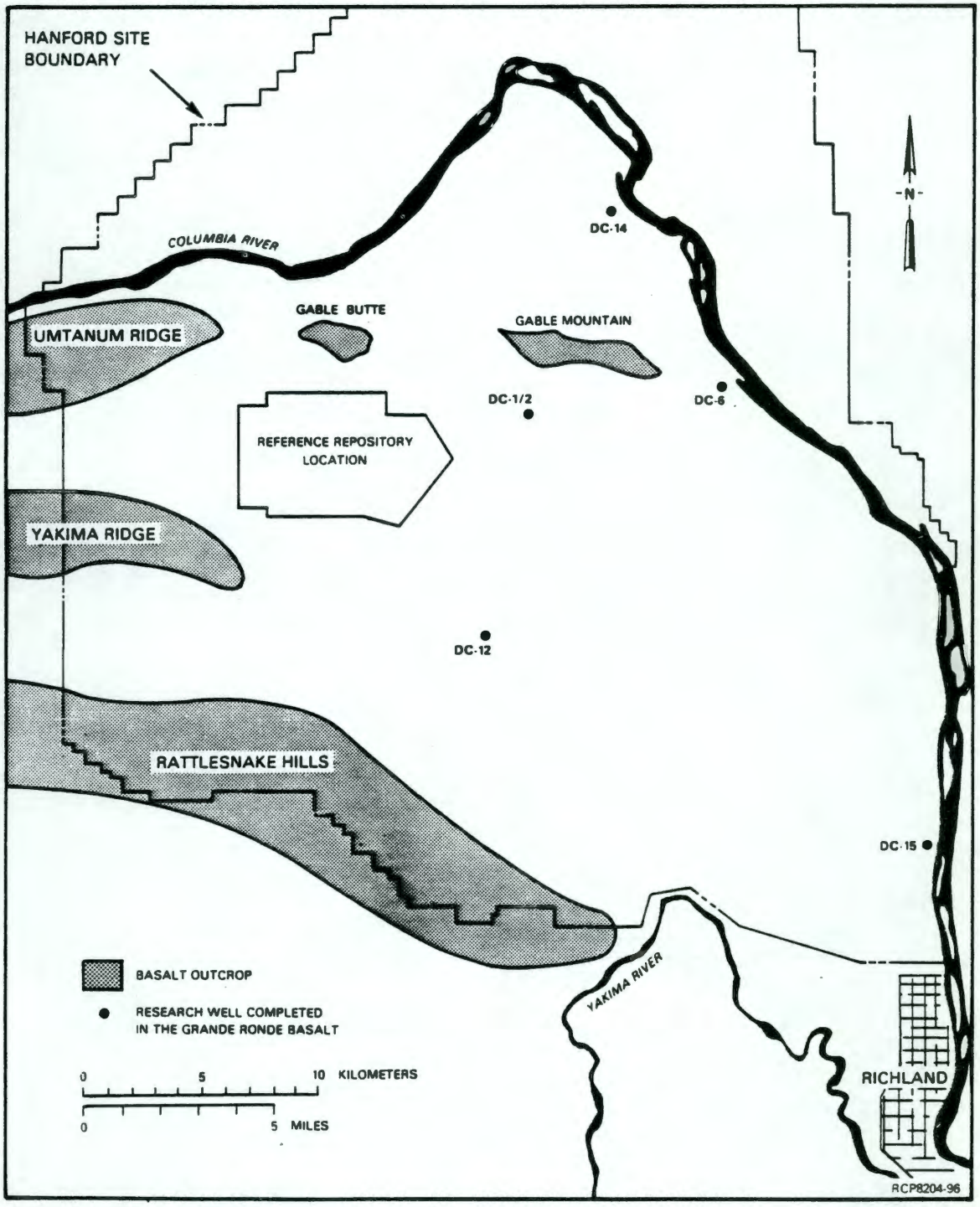

FIGURE 5-59. Borehole Locations Where Hydrochemical Data are Available from Within the Grande Ronde Basalt.

TABLE 5-27. Location, Depth, and Date of Groundwater Collection for Selected Zones Within the Grande Ronde Basalt.

Borehole	Depth below ground surface (m)	Date of collection
DC-6	720 - 822	08/14/80
	912 - 938	05/27/80
	988 - 1,076	02/24/81
	1,076 - 1,166	02/08/80
	1,124 - 1,134	08/02/79
	1,270 - 1,321	01/02/80
DC-12	734 - 746	07/14/80
	859 - 867	09/09/80
	935 - 961	04/20/81
	1,347 - 1,358	11/04/81
DC-14	936 - 958	12/23/8
	969 - 983	01/19/81
	1,000 - 1,017	02/11/81
DC-15	808 - 823	12/10/80
	820 - 842	01/08/81
	903 - 949	02/17/81
	1,006 - 1,040	04/10/81
	1,261 - 1,293	11/05/81

9 2 1 2 4 9 5 1 0 1 5

TABLE 5-28. Range of Concentration and Mean Composition of Major Inorganic Constituents and Hydrochemical Parameters Within the Groundwater of the Grande Ronde Basalt.

Constituent	Range (mg/L)	Mean (mg/L)
Anions		
HCO_3^-	16 - 102	57
CO_3^{-2}	3.8 - 55	21
Cl^-	96 - 297	169
SO_4^{-2}	4.2 - 199	125
NO_3^-	<0.5	0.5
F^-	13 - 42	30
$H_3SiO_4^-$ [a]	9.1 - 140	74
OH^-	0.12 - 7.4	0.98
Cations		
Na^+	161 - 360	257
K^+	0.34 - 24	6.5
Ca^{+2}	0.80 - 7.8	2.4
Mg^{+4}	<0.005 - 0.2	0.04
H_4SiO_4 [a]	39 - 132	101
Total dissolved solids	626 - 1,210	843
Eh (V) (field)	+0.21 to -0.22	-0.10[b]
pH (field)	8.8 - 10.6	9.7

[a]Total dissolved silica is shown in speciated forms due to elevated pH conditions in some zones. Total SiO_2 concentrations may be calculated by the relationship:

$$SiO_2 = 60 \left[\frac{H_3SiO_4^-}{95} + \frac{H_4SiO_4}{96} \right]$$

[b]Median value.

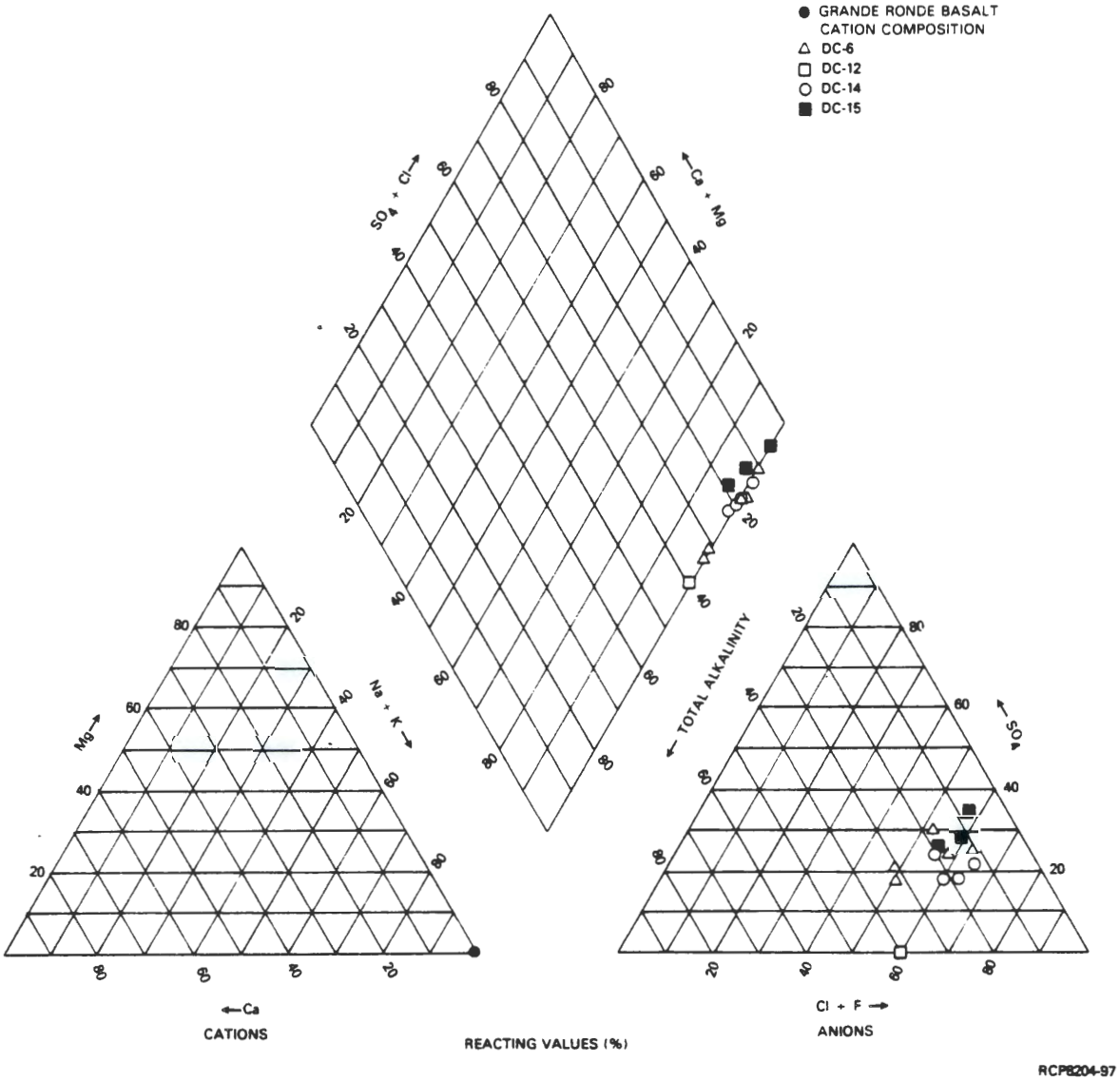

FIGURE 5-60. Chemical Composition of Groundwater Within the Grande Ronde Basalt Beneath the Hanford Site.

Carbonate species do not comprise a dominant portion of the anionic content in Grande Ronde Basalt groundwater, due to unfavorable geochemical conditions. Elevated pH values and reducing Eh conditions result in several geochemical processes removing bicarbonate and carbonate from the groundwater system. High pH levels are conducive to carbonate removal from groundwater through mineral precipitation. In addition, under reducing conditions, methanogenic processes may convert aqueous carbonate species to methane.

The source and processes responsible for elevated fluoride contents within Grande Ronde Basalt groundwater are not completely understood. Fluoride exists as a minor component of basalt flows, primarily within basaltic glass horizons. The accessory fluoride content within basalt flows is most likely concentrated in groundwater by selective leaching of volcanic glass during rock/water interactions along flow contacts. The anomalously higher concentrations within Grande Ronde Basalt groundwater may be attributable to greater rock/water reaction time and favorable hydrochemical factors which exist (e.g., high pH, low Eh, elevated temperature).

An insufficient quantity of hydrochemical data is currently available to evaluate areal hydrochemical patterns for individual aquifer systems. However, available data from the Grande Ronde Basalt with depth suggest a nonuniform vertical hydrochemical pattern (Section 5.1.5.5). The data show that although a similar hydrochemical type is maintained with depth, considerable variability in constituent concentration is evident.

Chemical equilibria and mineral saturation within Grande Ronde Basalt groundwater were evaluated using the WATEQ-F computer program (Truesdell and Jones, 1974; Plummer et al., 1976).

The saturation indices for calcite and cristobalite for selected Grande Ronde Basalt groundwaters are shown in Figure 5-61. Results indicate that Grande Ronde Basalt groundwater is generally saturated with calcite and a silica mineral phase (probably cristobalite). The identification of calcite and various silica species in fracture fillings within the Grande Ronde Basalt by Ames (1980) attests to the saturation of these minerals in groundwater.

5.1.5.4.2 Trace-Element Content. The range and median concentration of selected trace elements for groundwater sampled from Grande Ronde Basalt at the Hanford Site are presented in Table 5-29. Data shown are only for samples collected using a turbine pump or air lift method, filtered through a 0.45-micron pressure filter and preserved with nitric acid. Values listed as less than (<) indicate a concentration below the analytical detection limit.

9 2 1 2 4 9 5 1 0 1 8

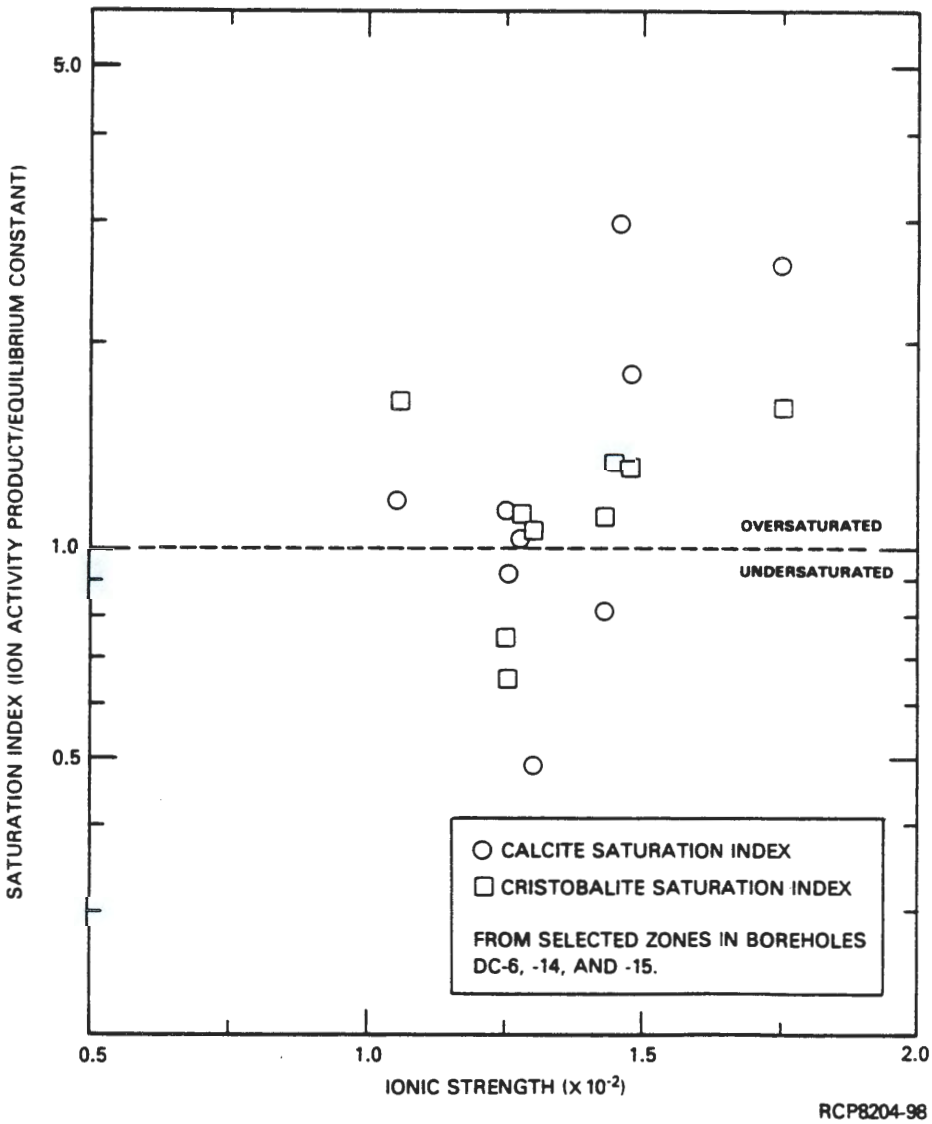

FIGURE 5-61. Saturation Index for Calcite and Cristobalite in Selected Groundwater Zones Within the Grande Ronde Basalt.

TABLE 5-29. Range and Median Concentrations of Trace Elements for Groundwater Within the Grande Ronde Basalt.

Trace element	Range (mg/L)	Median (mg/L)
Al	<0.02 - 0.180	0.090
B	<0.005 - 1.450	0.980
Ba	<0.005 - 0.080	0.005
Cd	<0.005	<0.005
Co	<0.005	<0.005
Cr	<0.005 - 0.010	<0.005
Cu	<0.005 - 0.009	<0.005
Fe	<0.005 - 2.0*	0.060
Mn	<0.010 - 0.470	<0.010
Mo	<0.010 - 0.99	0.440
Ni	<0.005	<0.005
Zn	<0.005 - 0.200	<0.005

*Maximum value is possible associated with nonrepresentative sample.

Examination of Table 5-29 indicates that the principal trace elements are aluminum, boron, iron, and molybdenum. Aluminum and iron exist as major components of Grande Ronde Basalt flows (Myers/Price et al., 1979; Myers and Price, 1981). Boron is most likely an accessory component in basalt glass horizons and is believed to enter the groundwater through groundwater/rock reactions that occur primarily within fractures and along flow contacts.

The presence of molybdenum in groundwater samples is probably attributable to minor contamination by molybdenum-based pipe-joint lubricant. Samples from the more productive flow-contact zones generally do not contain molybdenum in quantities above the detection limit. Analysis of the pipe-joint lubricant indicates it is not a source for other trace elements found in Grande Ronde Basalt groundwater.

5.1.5.4.3 Nonconservative Hydrochemical Parameters.

Fluid Temperature. Fluid temperatures for Grande Ronde Basalt groundwater measured at ground surface and downhole are listed in Table 5-30. Downhole measurements are considered to be more representative of formation temperatures. Downhole measurements also allow groundwater pH measured at ground surface to be corrected to formation conditions. Fluid temperature generally increases with depth and is reflective of the local geothermal gradient.

TABLE 5-30. Formation Fluid Temperatures for Groundwater Zones in the Grande Ronde Basalt in Selected Boreholes on the Hanford Site.

Borehole	Stratigraphic interval	Approximate depth below ground surface (m)	Collection temperature* (°C)	Formation temperature (°C)
DC-12	Umtanum flow top	950	41.7	46.2
DC-14	Umtanum flow top	945	19.8	54.9
DC-15	Upper Grande Ronde	830	24.1	48.2
	Umtanum flow top	925	37.5	52.0
RRL-2	Middle Sentinel Bluffs flow bottom	990	22.9	53.7
RRL-2	Umtanum flow top	1,100	29.4	56.6

*Collection temperature of groundwater sample dependent on ground-surface temperature on day of sampling and groundwater-sampling rate.

pH. The pH measurements are routinely performed at the sample site at the time of collection. As discussed in Section 5.1.5.2.3, several problems are associated with measurement of pH at ground surface. Formation waters generally cool and may de-gas during transport from depth to the point of collection. Groundwater pH measured at ground surface can be corrected to formation-temperature conditions. This, however, does not take into account the effect of gas exchange that probably occurs. Future work will include in situ measurement of pH using a downhole probe to minimize temperature and gas effects.

As indicated in Table 5-28, the mean pH value for Grande Ronde Basalt groundwater at the Hanford Site is 9.7, with values ranging from 8.8 to 10.6.

9 2 1 2 4 9 5 1 0 2 1

Factors contributing to the elevation of groundwater pH above 7 were discussed in Section 5.1.5.2.3. Due to low concentrations of dissolved carbonate species and elevated dissolved silica in Grande Ronde Basalt groundwaters, this above-noted trend is generally buffered by silica dissociation within these deep zones.

Eh. Limitations of potentiometric Eh measurement were mentioned in Section 5.1.5.2.3. Potentiometric measurements of Eh on Grande Ronde Basalt groundwater range from +0.21 to -0.22 volt, indicating that conditions may range from slightly oxidizing to slightly reducing (Table 5-31). Measurements made on groundwater from the Grande Ronde Basalt are generally more reducing than those for shallower basalts. The Eh values based on thermodynamic calculations for mineral assemblages assumed to be in equilibrium with groundwater at depth indicate that Eh conditions may range from -0.43 to -0.53 volt (see Chapter 11, Section 11.4). Based on Eh measurements and thermodynamic considerations, Eh within Grande Ronde Basalt groundwater most likely falls between -0.20 and -0.53 volt. Future studies will include downhole potentiometric measurement of Eh and measurement of redox couples (e.g., As^{+5}/As^{+3}).

TABLE 5-31. Measured Potentiometric Eh Values for Groundwater Collected from Zones Within the Grande Ronde Basalt.

Borehole	Depth below ground surface (m)	Eh (V)
DC-6	730 - 822	-0.14
DC-6	688 - 1,321	-0.10
DC-6	988 - 1,076	-0.22
DC-6	1,270 - 1,321	-0.12
DC-12	734 - 746	+0.03
DC-12	859 - 867	-0.01
DC-14	936 - 958	-0.04
DC-14	1,000 - 1,017	-0.15
DC-14	1,000 - 1,017	-0.20
DC-14	1,000 - 1,017	-0.14
DC-15	808 - 823	-0.06
DC-15	903 - 949	-0.09
DC-15	1,006 - 1,040	+0.21

9 2 1 2 4 9 5 1 0 2 2

5.1.5.4.4. Dissolved Gas. Table 5-32 presents dissolved-gas data from three boreholes within the Grande Ronde Basalt. An examination of the table indicates that nitrogen is the dominant gas component, making up 96 percent or more of the total dissolved gas for boreholes DC-6 and DC-14 located north of the Umtanum Ridge-Gable Mountain anticline. The remaining fraction is generally made up of argon and helium, with traces of various other gases. Small quantities of dissolved oxygen were detected in several samples, which may indicate atmospheric contamination of the gas sample since Eh values accepted for Grande Ronde Basalt groundwater preclude the presence of dissolved oxygen (see Section 5.1.5.4.3).

In borehole DC-15, located on the eastern side of the Cold Creek syncline, gas was not detected in the Grande Ronde Basalt. However, the negative carbon-13 values of dissolved inorganic carbon and high sulfate (100 to 200 milligrams per liter) concentrations found in the Grande Ronde Basalt water samples are characteristic of a non-methane gas environment. In borehole DC-12, located in southwest Hanford, no gas samples were collected. However, delta carbon-13 values are very positive, indicating that methane gas may be present in the Wanapum and Grande Ronde Basalts (see Section 5.1.6.2.1.2). Gas analyses from borehole RRL-2 identify methane as the principal gas present (Table 5-32). Therefore, the potential exists for groundwater from the western part of the Cold Creek syncline to contain greater quantities of methane gas than found farther east. Future site characterization activities will address this question.

5.1.5.5. Selected Stiff Diagrams. As addressed in detail in Sections 5.1.5.2.1, 5.1.5.3.1, and 5.1.5.4.1, distinct hydrochemical types exist in the Columbia River basalts. Changes from one type to another take place rapidly over a short stratigraphic interval. To illustrate these changes, Figures 5-62 through 5-66 have been drafted. These figures contain a selection of available Stiff diagrams (Stiff, 1951) for groundwater samples collected from sedimentary interbeds and basalt flow tops in five boreholes. The number of Stiff diagrams used was based upon illustrating the different groundwater chemical types present.

As seen in Figures 5-62 through 5-66, the chemistry of the groundwater in the Saddle Mountains Basalt is that of a sodium bicarbonate chemical type, in the Wanapum Basalt it is either a sodium chloride-bicarbonate or sodium bicarbonate-chloride chemical type, and in the Grande Ronde Basalt it is of a sodium chloride chemical type. As discussed by Chebeterov (1955), hydrochemical variations of this nature can be related to differences in host rock chemistry or groundwater residence time.

The stratigraphic locations where hydrochemical and isotopic shifts occur beneath the Hanford Site are illustrated in Table 5-33. North of the Umtanum Ridge-Gable Mountain anticline (at DC-14) and far south of the anticline (at DC-15), these shifts are located along the Wanapum and Grande Ronde Basalt contact. Closer to the southern flank of the anticline, the same chemical shifts occur along the Saddle Mountains and Wanapum Basalt contact. These changes suggest that vertical mixing of shallow groundwaters and deep groundwaters might be taking place along this structure. By the time these southward-moving groundwaters reach the

9 2 1 2 4 9 5 1 0 2 3

TABLE 5-32. Distribution of Dissolved Gas Components in Grande Ronde Basalt Zones.

Borehole	Stratigraphic interval	Depth below ground surface (m)	Total dissolved gas (vol%)							
			Carbon dioxide	Argon	Oxygen	Nitrogen	Carbon monoxide	Helium	Hydrogen	Methane
DB-6	Upper Grande Ronde	720 - 822	ND	ND	ND	ND	ND	ND	ND	ND
	Umtanum flow bottom	988 - 1,076	0.16	1.35	0.49	97.60	<0.10	0.39	<0.10	<0.10
	Lower Grande Ronde	1,076 - 1,166	0.04	1.16	<0.01	97.80	<0.10	0.31	0.17	0.48
	Lower Grande Ronde	1,270 - 1,321	<0.01	1.23	<0.01	96.0	<0.10	0.42	0.23	1.58
DC-14	Lower Grande Ronde	1,000 - 1,017	0.01	1.13	<0.01	98.4	<0.10	0.36	<0.01	0.14
RRL-2	Flow top immediately below Middle Sentinel Bluffs	829 - 889	0.04	0.04	<0.01	2.36	<0.1	<0.01	<0.01	97.6
RRL-2	Umtanum flow top	1,087 - 1,152	0.04	0.03	0.14	1.69	<0.1	<0.01	0.2	97.9

ND = Gas not detected in groundwater sample.

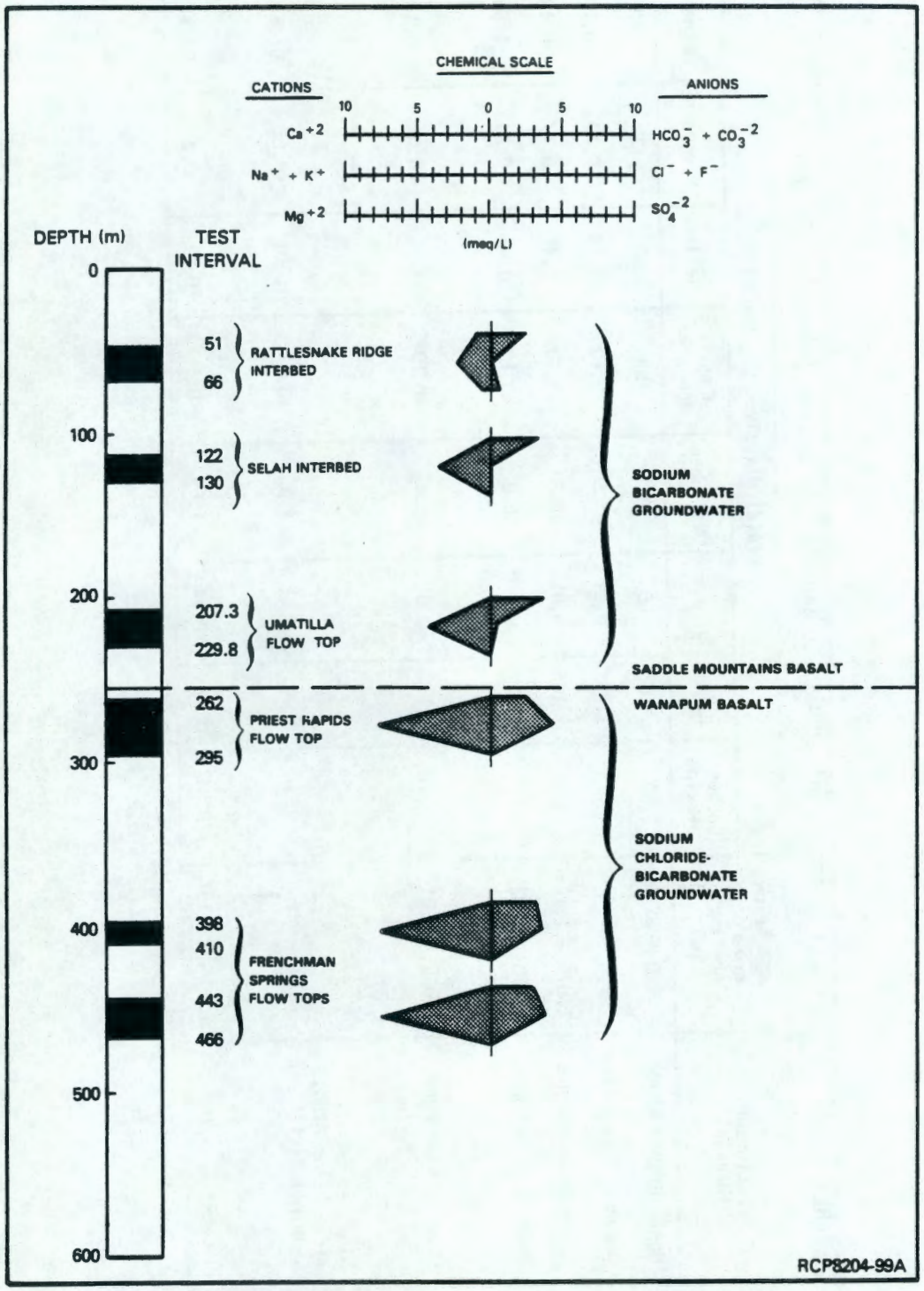

FIGURE 5-62. Stiff Diagrams for Selected Intervals in Borehole DB-15.

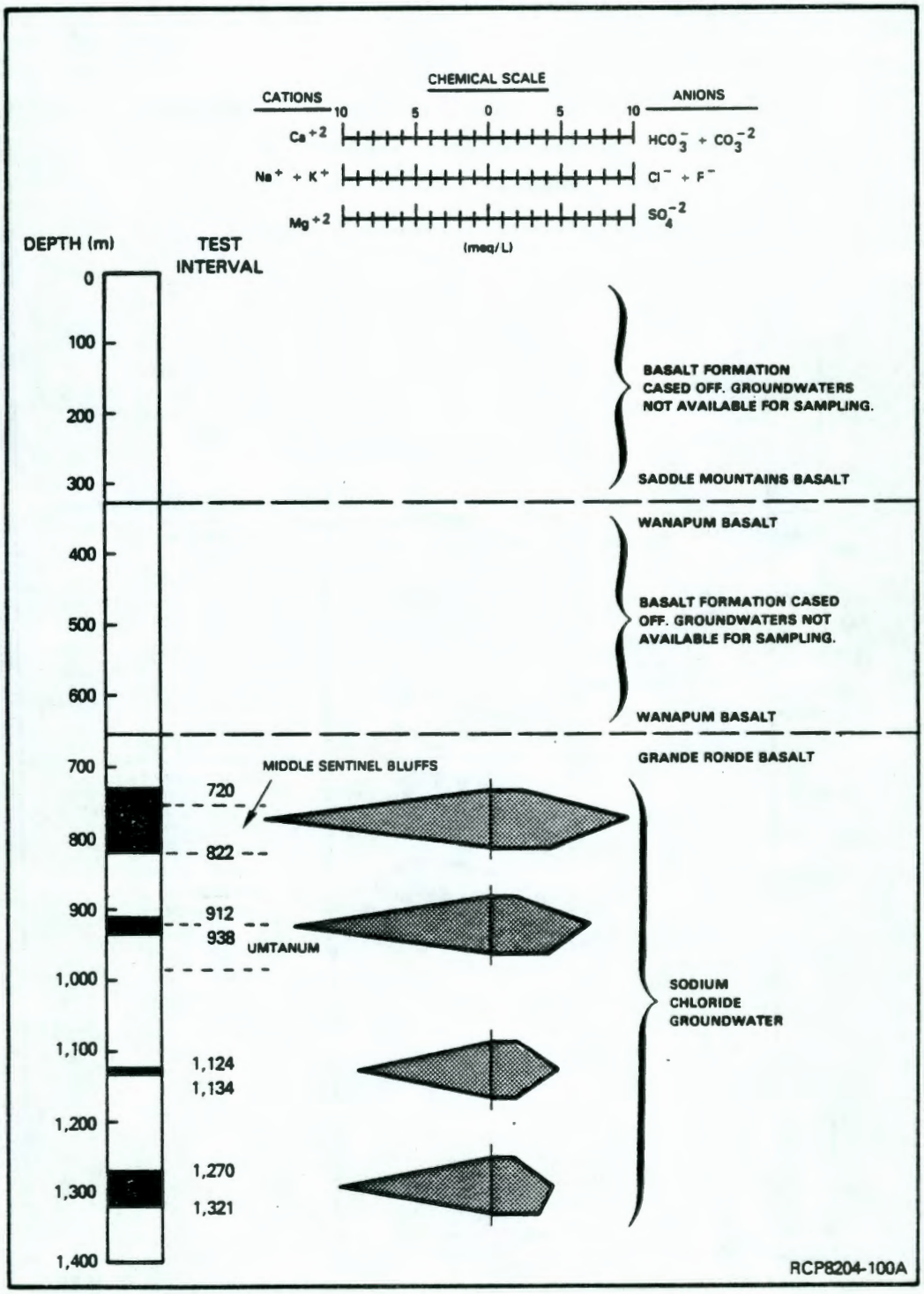

FIGURE 5-63. Stiff Diagrams for Selected Intervals in Borehole DC-6.

9 2 1 2 4 9 5 1 0 2 6

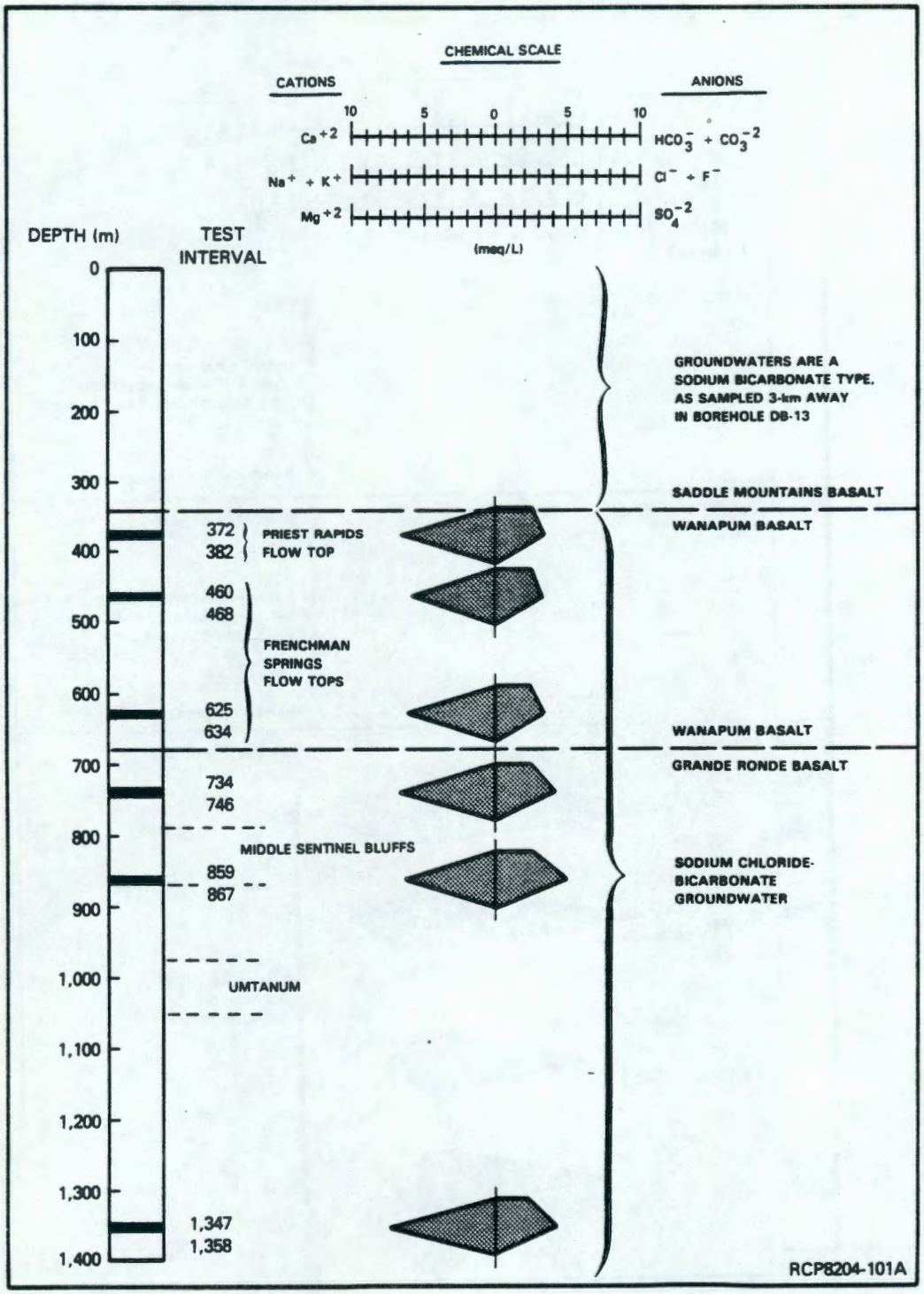

FIGURE 5-64. Stiff Diagrams for Selected Intervals in Borehole DC-12.

9 2 1 2 4 9 5 1 0 2 7

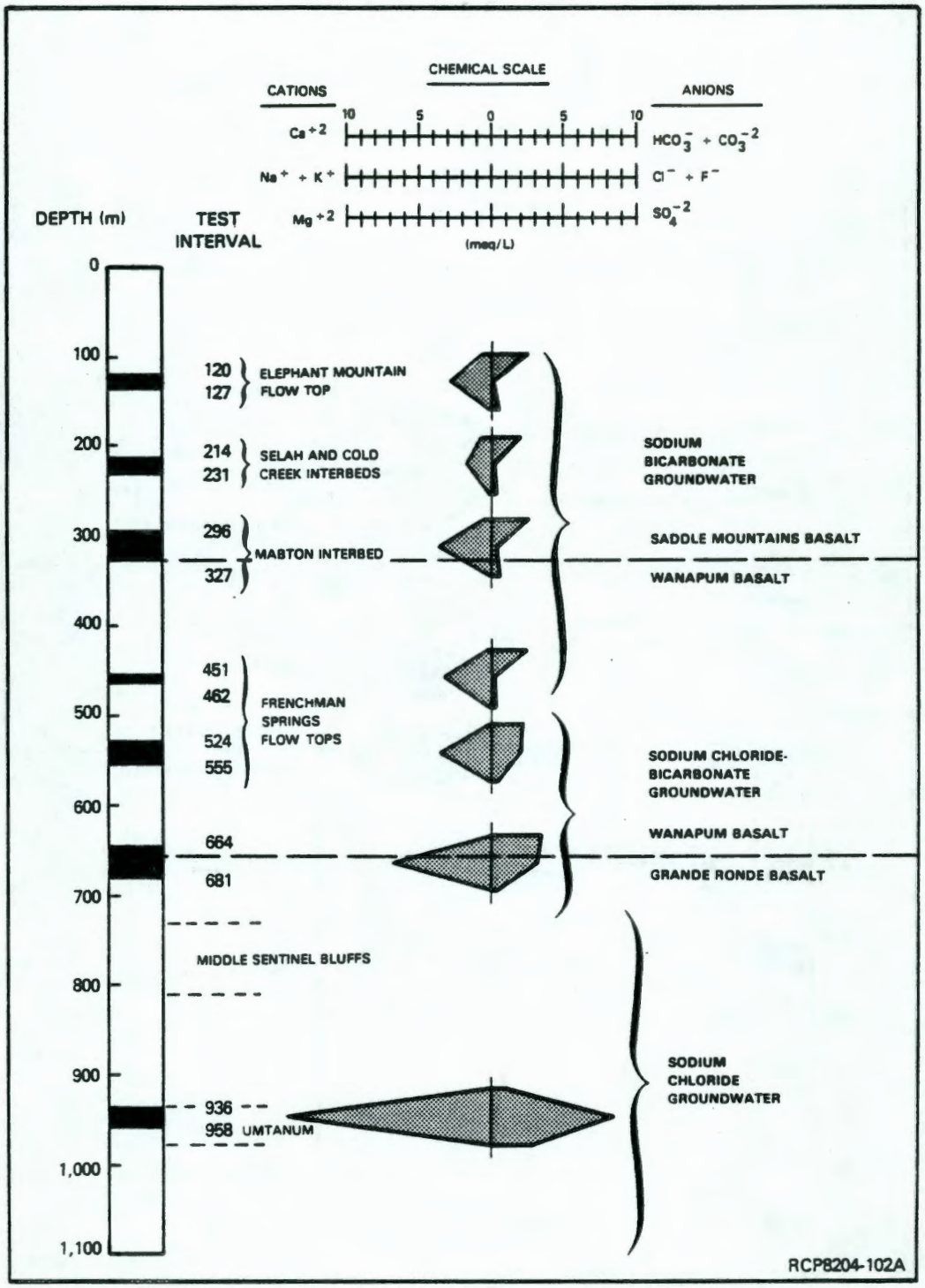

FIGURE 5-65. Stiff Diagrams for Selected Intervals in Borehole DC-14.

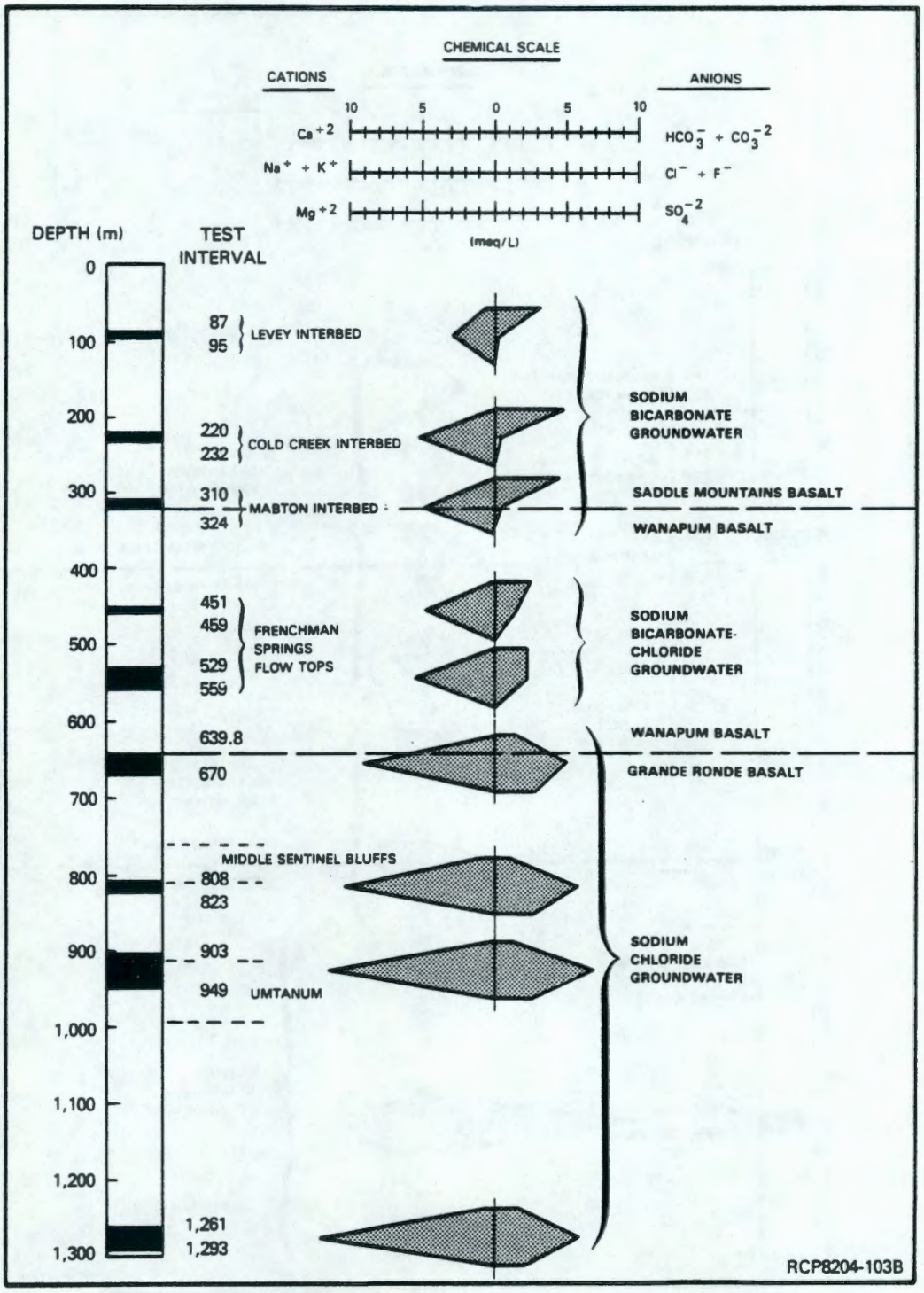

FIGURE 5-66. Stiff Diagrams for Selected Intervals in Borehole DC-15.

southeastern portion of the Cold Creek syncline (near DC-15), the original hydrochemical patterns, as found north of the anticline, are being reestablished. At borehole DC-15, the sodium bicarbonate-chloride chemical type of the Wanapum Basalt groundwater may result from earlier vertical mixing of shallow (sodium bicarbonate, low total dissolved solids and isotopically lighter) and deep (sodium chloride, high total dissolved solids and isotopically heavier) groundwaters.

TABLE 5-33. Stratigrahic Location of Hydrochemical and Isotopic Breaks Beneath the Hanford Site.

Borehole	Location of borehole	Basalt contact along which break occurs
DC-14	North of Umtanum Ridge-Gable Mountain anticline	Wanapum/Grande Ronde
DB-15	South of anticline	Saddle Mountains/Wanapum
RRL Area*	South of anticline	Saddle Mountains/Wanapum
DB-13/DC-12	South of anticline	Saddle Mountains/Wanapum
DC-15	Far south of anticline	Wanapum/Grande Ronde

*Preliminary data from boreholes RRL-2 and DC-16A.

Since these groundwater chemical shifts occur along different stratigraphic intervals, depending on areal location plus the fact that the overall mineralogy of the Columbia River basalt is similar, it appears that the observed hydrochemical variations cannot be explained by simply differences in rock chemistry.

Hydrochemical differences in Columbia River basalt groundwaters suggests increasing groundwater maturity (longer residence times) with depth (see Section 5.1.5). This is consistent with the current conceptual groundwater flow model for the Columbia River basalts (Section 5.1.10). That is, Saddle Mountains Basalt groundwaters are thought to be recharged at high elevations within the Pasco Basin (Section 5.1.4.2.1) and comprise a local groundwater flow system. Recharge areas for the Wanapum and Grande Ronde Basalts are more areally extensive and the associated flow systems are considered intermediate to regional (Sections 5.1.4.2.2 and 5.1.4.2.3).

The hydrochemical changes observed with increasing depth in the Pasco Basin generally occur abruptly and are also accompanied by major isotopic shifts (Section 5.1.6.2.1). These abrupt shifts in hydrochemistry may delineate flow system boundaries (i.e., local versus regional) and suggest a lack of significant vertical mixing in structurally nondeformed areas. Future hydrochemical modeling will examine this concept (Chapter 13).

9 2 1 2 4 9 5 1 0 4 3

The major inorganic chemistry for Grande Ronde Basalt groundwater in borehole DC-6 is shown in Figure 5-63. Examination of this figure indicates that the chemical composition of groundwater from the middle Sentinel Bluffs and the Umtanum flows are similar. Both are of a sodium chloride chemical type. The total dissolved solids content of the middle Sentinel Bluffs groundwater is elevated above that of Umtanum flow groundwater in borehole DC-6. This may be a local occurrence as it is not evident in borehole DC-15 (see Fig. 5-66). Detailed comparisons of the hydrochemical and isotopic compositions of middle Sentinel Bluffs and Umtanum flow groundwaters will be a focus of future hydrochemical studies.

5.1.6 Isotope Hydrochemistry

Stable and radioactive isotopes have been used extensively in groundwater hydrology. Useful isotopic applications include delineating groundwater movement, groundwater age, recharge-discharge relationships, and acting as environmental tracers. Numerous studies are available in the literature that cite the successful application of isotopes to hydrologic investigations (e.g., Craig, 1961; 1963; Kigoshi, 1971; Rightmire and Hanshaw, 1973; Pearson and White, 1967; Pearson and Hanshaw, 1970; Pearson and Rightmire, 1980; Fritz and Fontes, 1980; Barr et al., 1979; Osmond and Cowart, 1976).

The natural abundances by percent of some isotopes presently being used and/or under consideration for use in geohydrology are shown in Table 5-34. In most instances, an element will have more than one isotope. However, as shown in Table 5-34, there is usually one isotope that is significantly more abundant than the other naturally occurring isotopes. This dominant nuclide is referred to as the "normal" nuclide for that element.

A listing of the isotopes currently being used by the BWIP as part of the hydrologic characterization of the Columbia River Basalt Group is also noted in Table 5-34. In addition, future hydrologic studies will examine the applicability of the isotopes ^{15}N, ^{36}Ar, ^{40}Ar, ^{129}I, and ^{234}Th for age dating and flow-system characterization.

5.1.6.1 Unconfined Aquifer. Isotope data available for the unconfined aquifer at the Hanford Site are limited to selected radioisotopes. Radioisotopes are monitored in groundwater by Rockwell and Pacific Northwest Laboratory to trace contaminant migration within the unconfined aquifer related to past waste-disposal practices, which occurred primarily in the 200 West and 200 East Areas on the Hanford Site.

Due to its favorable tracer characteristics (e.g., mobility, nonreactiveness, low absorption, and/or ion-exchange capacity), tritium is routinely analyzed to monitor the migration of contamination in the unconfined aquifer. Because tritium is part of the water molecule, it is carried along with the groundwater flow and remains almost unaffected by

9 2 1 2 4 9 5 1 0 4 2

TABLE 5-34. Natural Abundance of Some Isotopes Presently Being Used and/or Considered for Use in Hydrologic Studies.

Element	Isotope	Natural abundance (%)[a]	Radionuclide half-life	Element	Isotope	Natural abundance (%)[a]	Radionuclide half-life
H	^{1}H	99.985		Ar	^{36}Ar[c]	0.34	
	^{2}H[b]	0.015			^{39}Ar	0	265 yr
	^{3}H[b]	0	12.26 yr		^{40}Ar[c]	99.59	
He	^{3}He	0.00013		Kr	^{83}Kr	11.5	
	^{4}He	99.99987			^{84}Kr	57.0	
					^{86}Kr	17.3	
C	^{12}C	98.89					
	^{13}C[b]	1.11		Sr	^{84}Sr	0.05	
	^{14}C[b]	0	5,730 yr		^{86}Sr	9.9	
					^{87}Sr	7.0	
N	^{14}N	99.64			^{88}Sr	82.6	
	^{15}N[c]	0.36					
				I	^{127}I	100.0	
O	^{16}O	97.76			^{129}I[c]	0	1.7 E+07 yr
	^{17}O	0.04					
	^{18}O[b]	0.20		Xe	^{131}Xe	21.2	
					^{132}Xe	26.9	
Ne	^{21}Ne	0.27			^{134}Xe	10.4	
	^{22}Ne	9.22			^{136}Xe	8.9	
S	^{32}S	95.0		Th	^{230}Th	0	8.0 E+04 yr
	^{33}S	0.76			^{234}Th[c]	0	24.1 d
	^{34}S[b]	4.22					
	^{36}S	0.02		U	^{234}U[b]	0.005	2.47 E+05 yr
					^{235}U	0.720	7.13 E+08 yr
Cl	^{35}Cl	75.77	3.1 E+05 yr		^{238}U[b]	99.275	4.51 E+09 yr
	^{36}Cl[b]	0					
	^{37}Cl	24.23					

NOTE: Radioactive isotopes are those for which half-life values are indicated. All others are considered to be stable.

[a]Percentages from Weast (1980).

[b]Presently utilized by the BWIP for hydrologic characterization.

[c]Being considered for use in future hydrologic characterization studies.

the geologic conditions that retard the mobility of other radionuclides. Tritium, therefore, serves as an effective indicator of the areal extent of groundwater contamination at the Hanford Site.

The concentration and distribution of tritium within the unconfined aquifer at Hanford is shown in Figure 5-67. This figure identifies well-defined contamination plumes originating from the 100 and 200 Areas. These plumes define areas of groundwater movement and contaminant transport in sediments of the unconfined aquifer formations having high hydraulic conductivities.

Other radionuclides monitored include gross alpha (α_t), gross beta (β_t), ^{90}Sr, ^{137}Cs, ^{60}Co, ^{129}I, and ^{99}Tc. Analytical results for the above radionuclides are contained in annual reports by Atlantic Richfield Hanford Company (ARHCO, 1977) and Pacific Northwest Laboratory (Eddy, 1979; Eddy and Wilbur, 1980).

5.1.6.2 Columbia River Basalt Group. Available isotopic data for the Columbia River basalts are primarily from sampling locations concentrated within the Pasco Basin. Isotopic data for most of the remaining portion of the Columbia Plateau are limited to carbon-14 analyses as, for example, reported by Crosby and Chatters (1965), Silar (1969), and Robinson (1971). These data are not distributed uniformly, but are confined primarily to two small areas within the southeastern portion of the plateau. In addition to previously cited problems of interpreting analyses for composite groundwater samples on a regional basis, the lack of carbon-13 data for groundwater and geologic materials precludes the use of carbon-dilution corrections for absolute age determinations. Due to the lack of carbon corrections, age dates cited in the discussion below are considered relative and can be compared only in a qualitative manner.

Crosby and Chatters (1965) determined age dates on 33 groundwater samples taken from the Columbia River basalt in the Pullman-Moscow area. The carbon-14 ages ranged from 1,685 to greater than 32,000 years. An evaluation of their data by Newcomb (1972) indicates that age generally increases with depth. Exceptions may be attributable to multiple aquifer completions at well sites and to substantial groundwater withdrawals in a given area.

Silar (1969), in examining 44 samples from a larger area in east-central Washington, concluded that age dates for groundwater in about the top 100 meters of basalt ranged from modern (approximately less than 30 years old) to 16,275 years. The age dates reported by Crosby and Chatters (1965) and Silar (1969) compare reasonably well with values determined by Robinson (1971) for groundwater in Columbia River basalts in the Hermiston area in Oregon. Age dates in this area ranged from modern to 27,250 years.

9 2 1 2 4 9 5 1 0 4 0

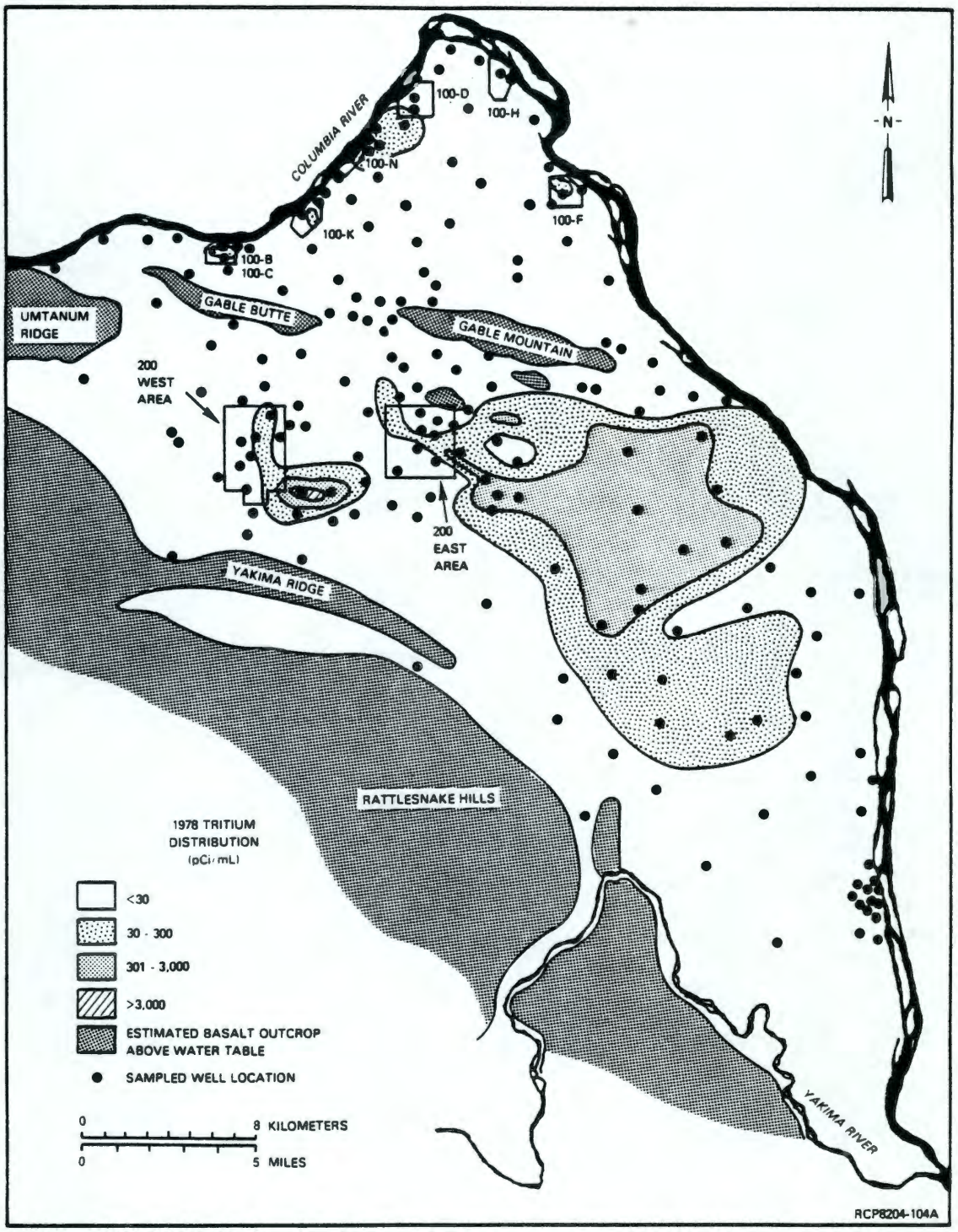

FIGURE 5-67. Tritium Distribution in the Unconfined Aquifer Beneath the Hanford Site.

Isotopic information and discussions in the following sections pertain to data collected for individual hydrogeologic units within basalt formations beneath the Hanford Site.

5.1.6.2.1. Stable Isotopes. Stable isotopes utilized in the hydrologic studies of the Columbia River basalts were listed in Table 5-34 Stable isotope concentrations listed in this report are reported as δ (delta) values. The units of delta values are parts per thousand (or per mill). These units give the amount of enrichment (positive value) or depletion (negative value) relative to a given standard. Delta values are calculated as follows:

$$\delta x = \frac{R_{sample} - R_{standard}}{R_{standard}} \qquad (5\text{-}1)$$

where

$R_{standard}$ = ratio of heavy to light isotopes in standard

and in per mill form as:

$$\delta x \ ^{o}/oo = \frac{R_{sample} - R_{standard}}{R_{standard}} \times 1{,}000 \qquad (5\text{-}2)$$

5.1.6.2.1.1. Deuterium and Oxygen-18. The principal stable molecular species in natural water are $H_2{}^{16}O$, $H_2{}^{18}O$, $H_2{}^{17}O$, and HDO. Craig (1963) reported the proportions of these species in ocean water to be 10^6, 2,000, 420, and 316, respectively. This composition is referred to as "standard mean ocean water." This standard agrees closely with the actual concentration of deep oceanic water. Deep oceanic waters are considered to be the source of oxygen-18 and deuterium (^2H) in the hydrologic cycle. Craig (1961) also demonstrated that there is a linear relationship between oxygen-18 and deuterium. This association was established based on meteoric water collected from approximately 400 stations around the world. By plotting ^2H versus ^{18}O, the "meteoric water line" was developed (Fig. 5-68). This relationship is described by the equation:

$$\delta^2H = 8\delta^{18}O + 10 \qquad (5\text{-}3)$$

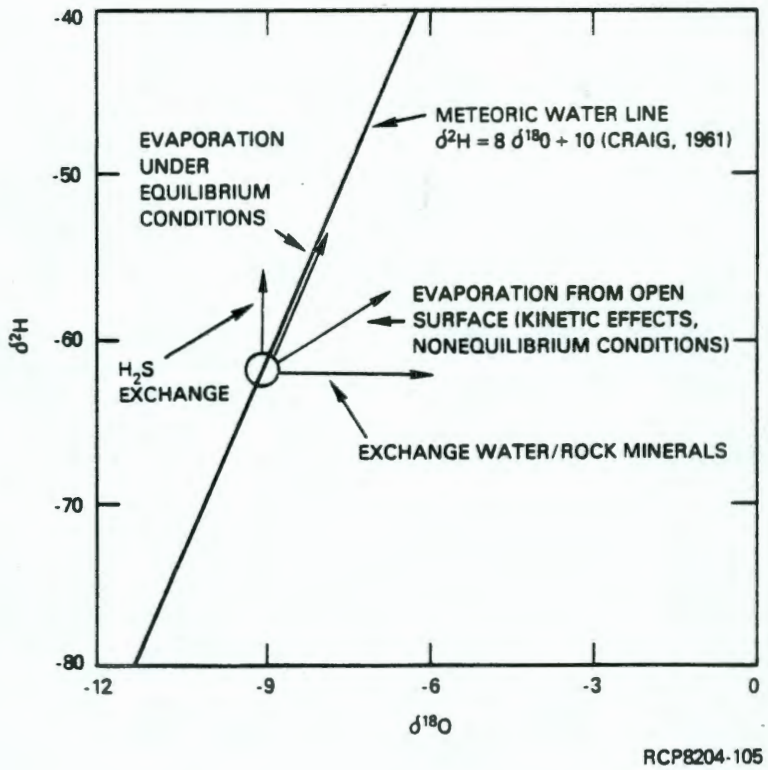

FIGURE 5-68. Generalized Plot of Delta Oxygen-18 Versus Delta Hydrogen-2, Showing the Meteoric Water Line and Possible Secondary Fractionation Processes.

The position of this line may vary locally in both intercept and slope. However, the slope is normally very close to eight. The linear relationship between deuterium and oxygen-18 arises from the fact that condensation from the Earth's atmosphere is essentially an equilibrium process. The fractionation of deuterium to hydrogen is proportional to that of oxygen-18 to oxygen-16. Deviations from the meteoric water line indicate that secondary fractionation processes are occurring. Some of these processes are illustrated in Figure 5-68. One of the more frequent and recognizable secondary fractionation processes is surface evaporation. When water evaporates from the ocean, the oxygen-18 and deuterium content is depleted relative to the original ocean water. This process is dominant over other reactions, and as a result, there is a net decrease in oxygen-18 and deuterium in precipitation as it moves from the ocean across a continental land mass. The oxygen-18 and deuterium content of precipitation is also affected by latitude, altitude, distance from the ocean, and amount of precipitation. These factors, and their effects, have been discussed in detail by Yurtsever (1975) and Siegenthaler and Deschger (1980). Yurtsever (1975) reports that the greatest effect on the fractionation of oxygen-18 and deuterium was due to temperature. The fractionation process is independent of pressure (Clayton et al., 1975).

Groundwater samples have been collected from all three formations of the Columbia River basalts beneath the Hanford Site and were analyzed for oxygen-18 and deuterium content. The relationship of deuterium and oxygen-18 for these samples is shown in Figure 5-69. The meteoric water line, as described by Craig (1961), is included for comparison.

All data fall below the meteoric water line. This is not unusual, since the meteoric water line was developed from surface-water and precipitation data, which are normally more enriched in both oxygen-18 and deuterium than average groundwaters. The slope of the line passing through the Hanford data is different than the slope of the meteoric water line (i.e., 6.2 versus 8). Gat (1980) has shown this to be common in arid and semiarid environments. Examination of Figure 5-69 indicates that considerable variation in isotopic content exists both between and within specific basalt formations. The range and distribution of isotopic values for the various basalt formations are presented in histograms shown in Figures 5-70 and 5-71. Values for all Columbia River basalts range from -20.4 to -12.7 per mill for oxygen-18 and -155 to -106 per mill for deuterium. Data in Figures 5-69, 5-70, and 5-71 indicate that the deepest formation groundwater (i.e., from the Grande Ronde Basalt) is more enriched in both oxygen-18 and deuterium than the two overlying basalt formations.

The differences in isotopic content between basalt formations is particularly pronounced at individual borehole sites. The significant isotopic shifts in deuterium and oxygen-18 values suggest the lack of major mixing of groundwater across these formational boundaries. Available data indicate that pronounced isotopic shifts occur at two different formational contacts beneath the Hanford Site. For locations inside the Cold Creek syncline, the shift occurs between the Saddle Mountains and Wanapum Basalts (e.g., Fig. 5-72). For locations north of the Umtanum Ridge-Gable Mountain anticline and far south in the Cold Creek syncline, this break occurs between the Wanapum and Grande Ronde Basalts (see Fig. 5-73 and 5-74). The position of the isotopic shifts is consistent with the location of major hydrochemical breaks previously discussed in Section 5.1.5.

Abrupt changes in delta oxygen-18 and delta hydrogen-2 are also observed when these parameters are plotted as a function of depth in a borehole (see Fig. 5-75 and 5-76). Changes such as these would not occur if significant vertical mixing were taking place near these borehole locations. Instead, a transitional trend would be evident.

The reason for differences in the stratigraphic location of isotopic shifts for areas inside and outside of the Cold Creek syncline is not fully understood. But as discussed in Section 5.1.5, the higher stratigraphic location of the isotopic shift for areas inside the Cold Creek syncline may be attributable to increased vertical hydraulic communication along the Umtanum Ridge-Gable Mountain anticline.

Several explanations for these differences in isotopic content for individual basalt formations are available. The most plausible include: (1) different recharge areas and conditions for the major basalt formations and (2) isotopic exchange due to increased temperatures within the deeper basalts.

9 2 1 2 4 9 5 1 0 3 6

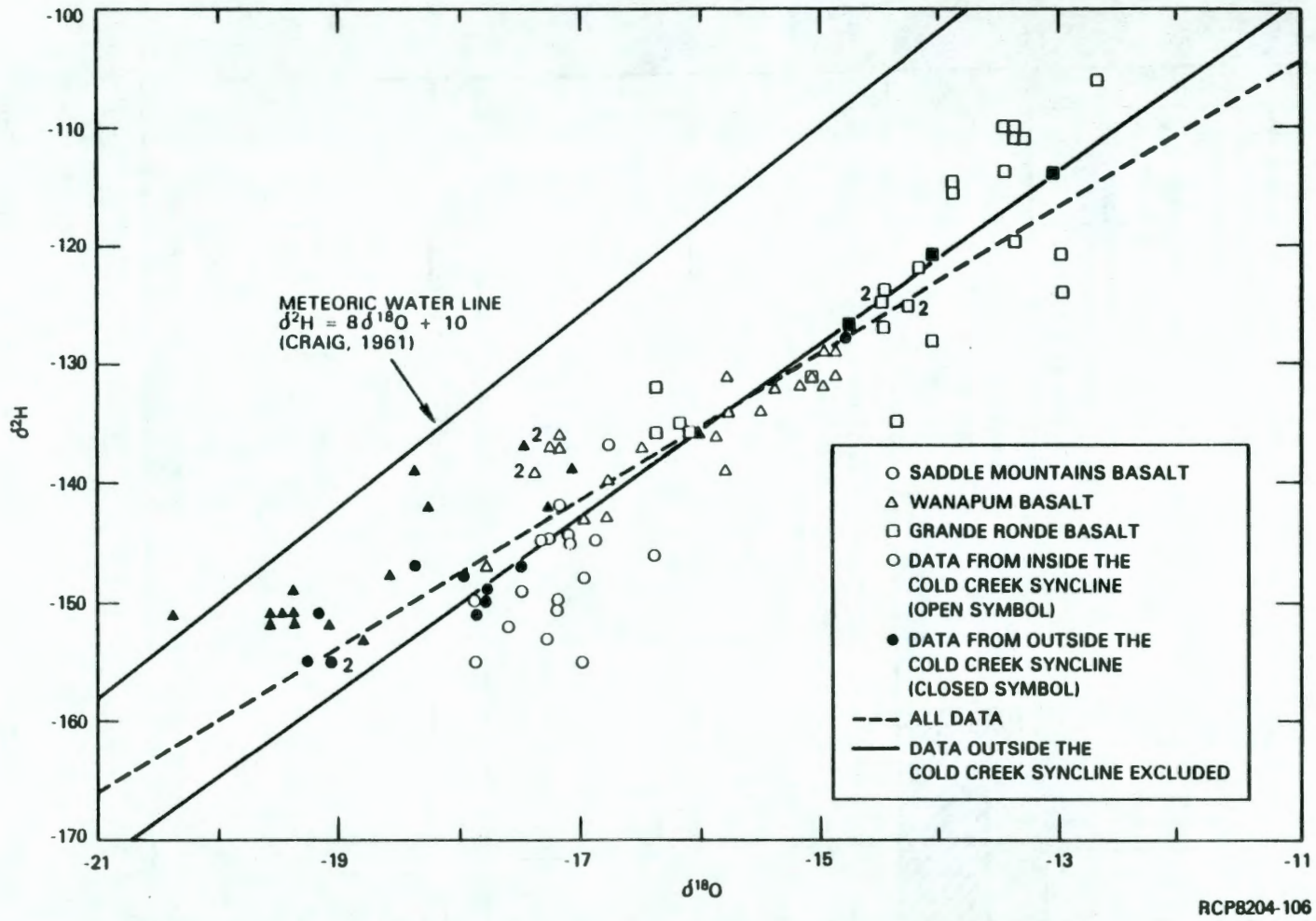

FIGURE 5-69. Plot of Delta Hydrogen-2 Versus Delta Oxygen-18 for the Deep Basalts Beneath the Hanford Site.

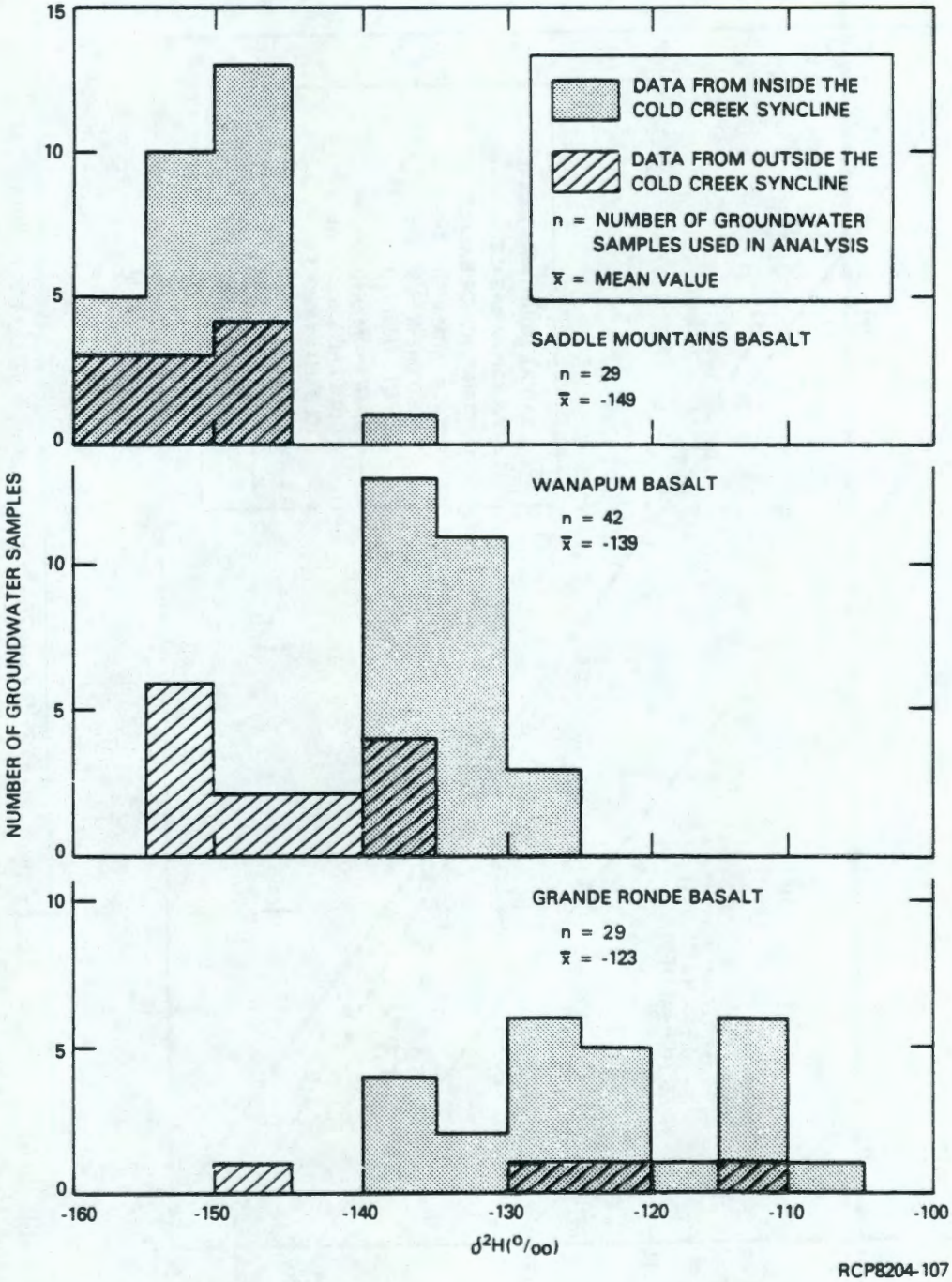

FIGURE 5-70. Distribution of Deuterium Within Three Formations of the Columbia River Basalt Group at the Hanford Site.

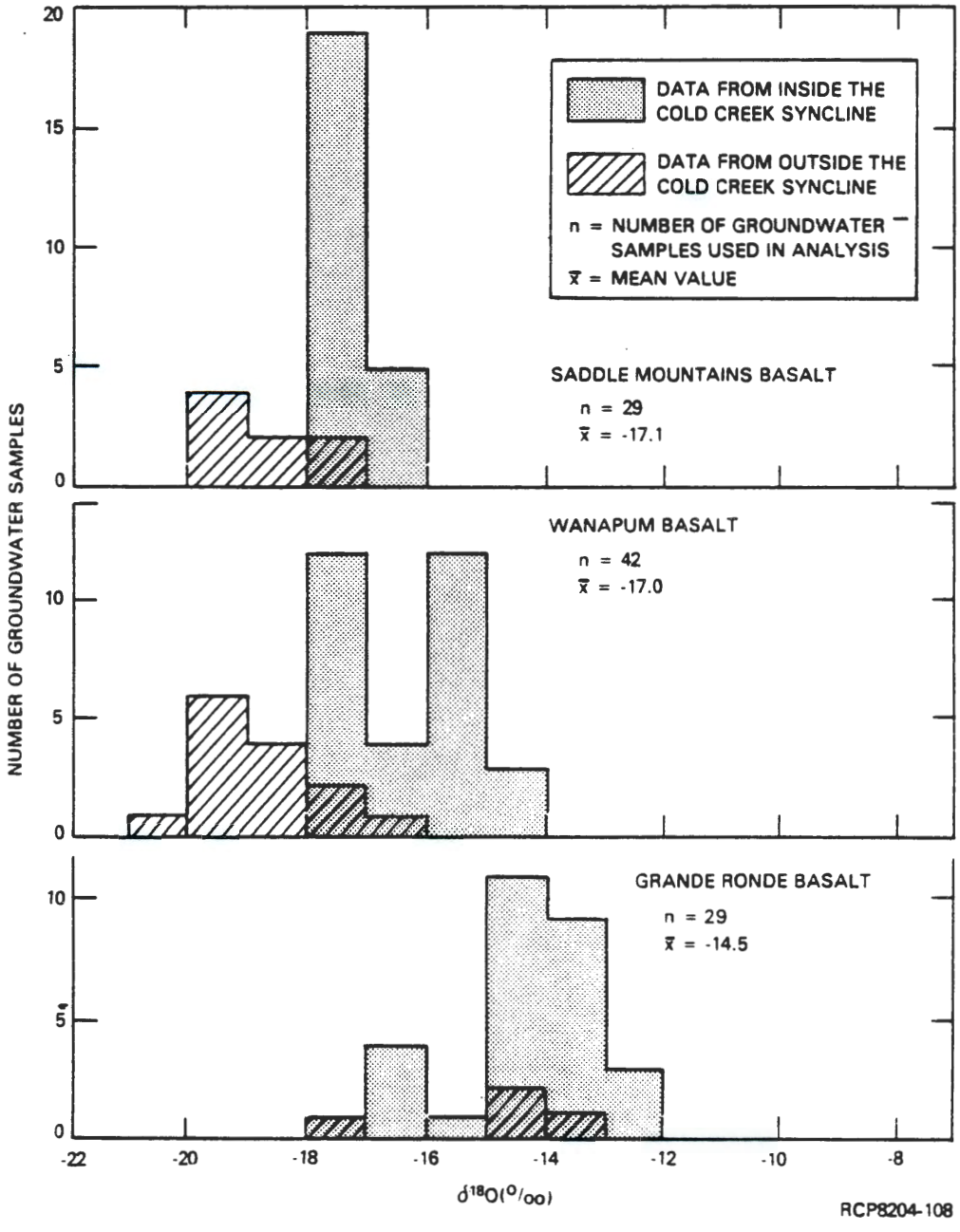

FIGURE 5-71. Distribution of Oxygen-18 Within Three Formations of the Columbia River Basalt Group at the Hanford Site.

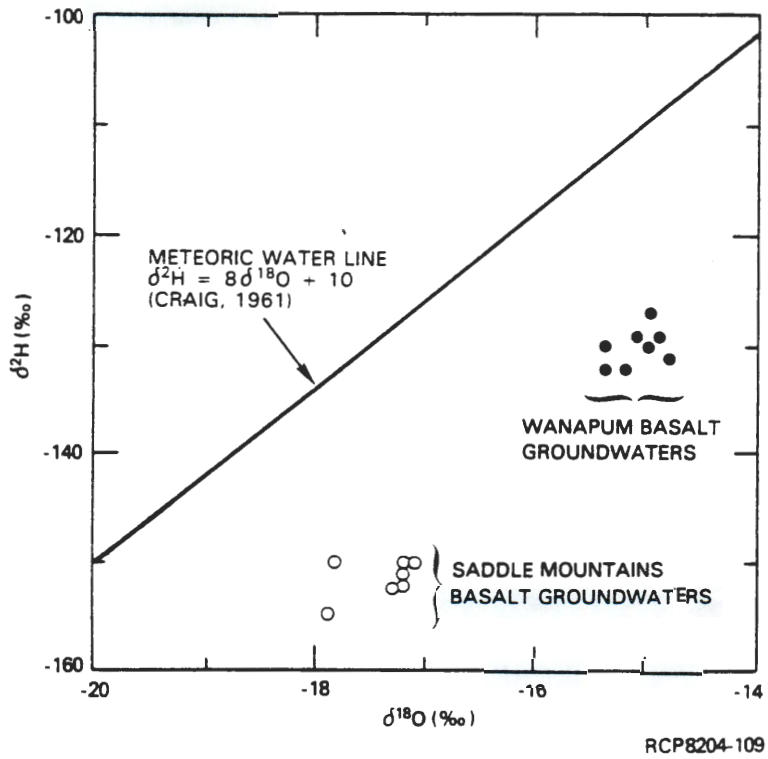

FIGURE 5-72. Deuterium and Oxygen-18 Relationship for Groundwater Within the Saddle Mountains and Wanapum Basalts at Borehole DB-15.

Variations in oxygen-18 and deuterium content between shallow versus deep basalt formations may also be explained by differences in recharge areas. As previously addressed, the regional outcrop areas of the major basalt formations widely differ in areal extent. This is particularly evident for the Saddle Mountains and Grande Ronde Basalts (see Section 5.1.2).

The Saddle Mountains Basalts are recharged locally from precipitation falling on the basalt ridges surrounding the Pasco Basin. The Wanapum Basalt also receives local recharge from precipitation falling on basalt ridges surrounding the Pasco Basin and from interbasin recharge. The Grande Ronde Basalt is thought to receive the majority of its recharge from outside the Pasco Basin. The differences in source areas for recharge, especially between the Saddle Mountains and Grande Ronde Basalts, should be reflected in the oxygen-18 and deuterium content of the groundwater. The fact that isotopic differences are, in fact, maintained along the flow system for long distances away from their recharge areas suggests that little groundwater mixing is occurring between basalt formations.

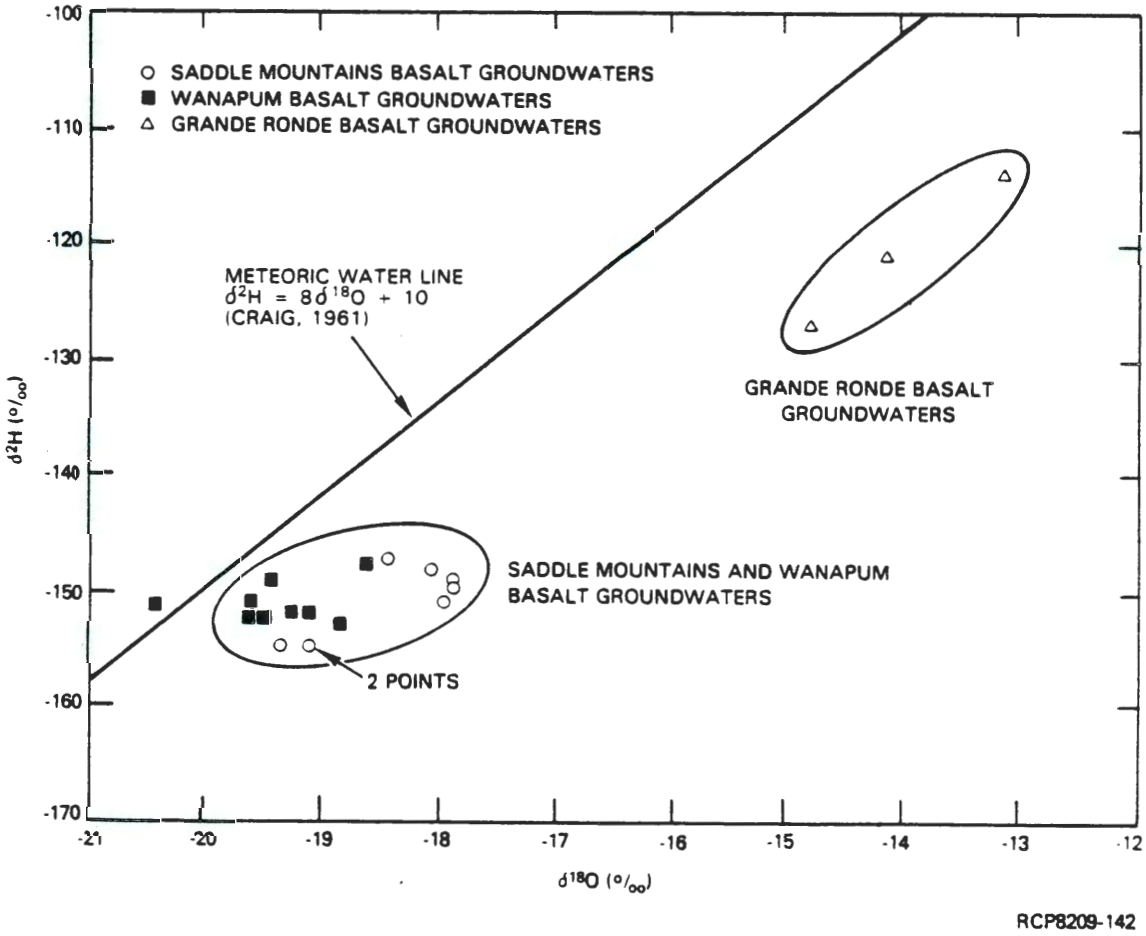

FIGURE 5-73. Deuterium and Oxygen-18 Relationship for Groundwaters Within the Columbia River Basalts at Borehole DC-14.

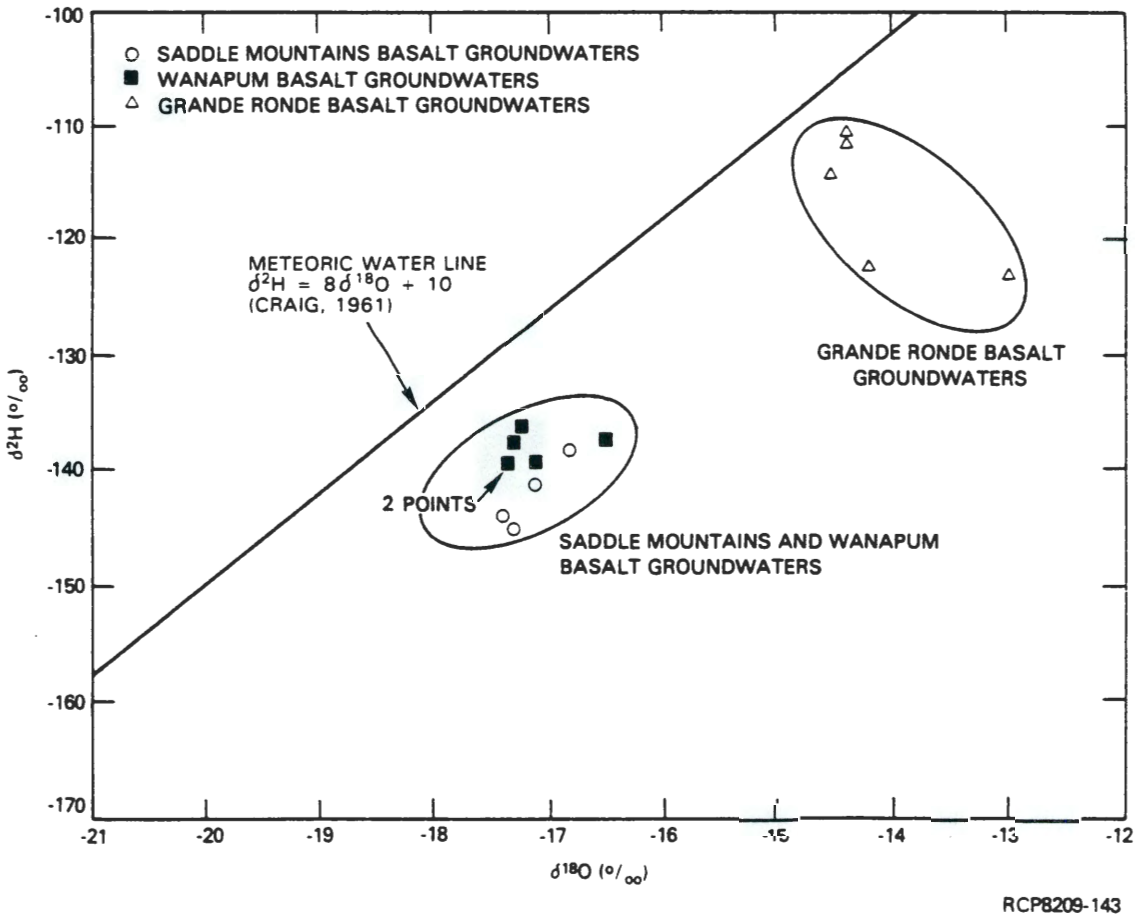

FIGURE 5-74. Deuterium and Oxygen-18 Relationships for Groundwaters Within the Columbia River Basalts at Borehole DC-15.

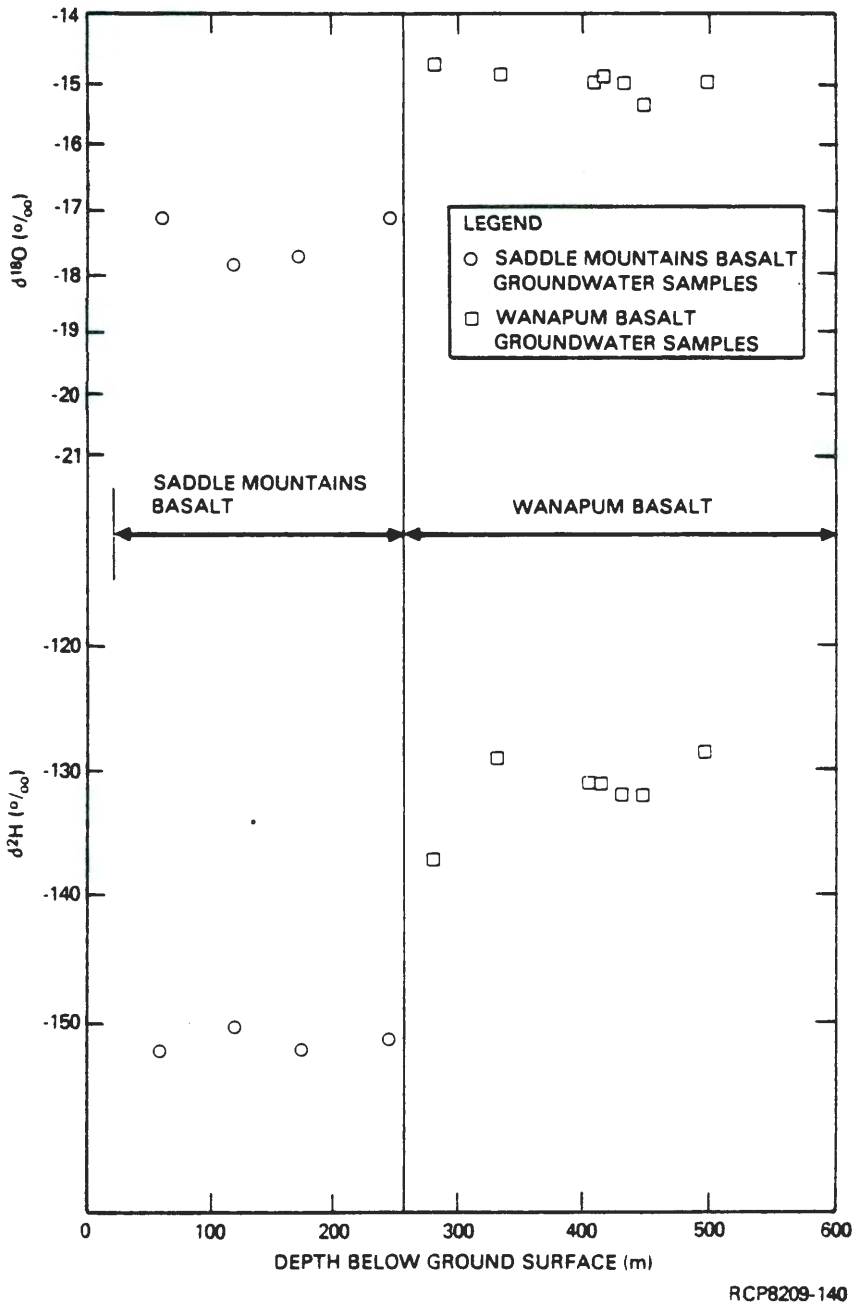

FIGURE 5-75. Variation of Delta Oxygen-18 and Delta Hydrogen-2 as a Function of Depth in Borehole DB-15.

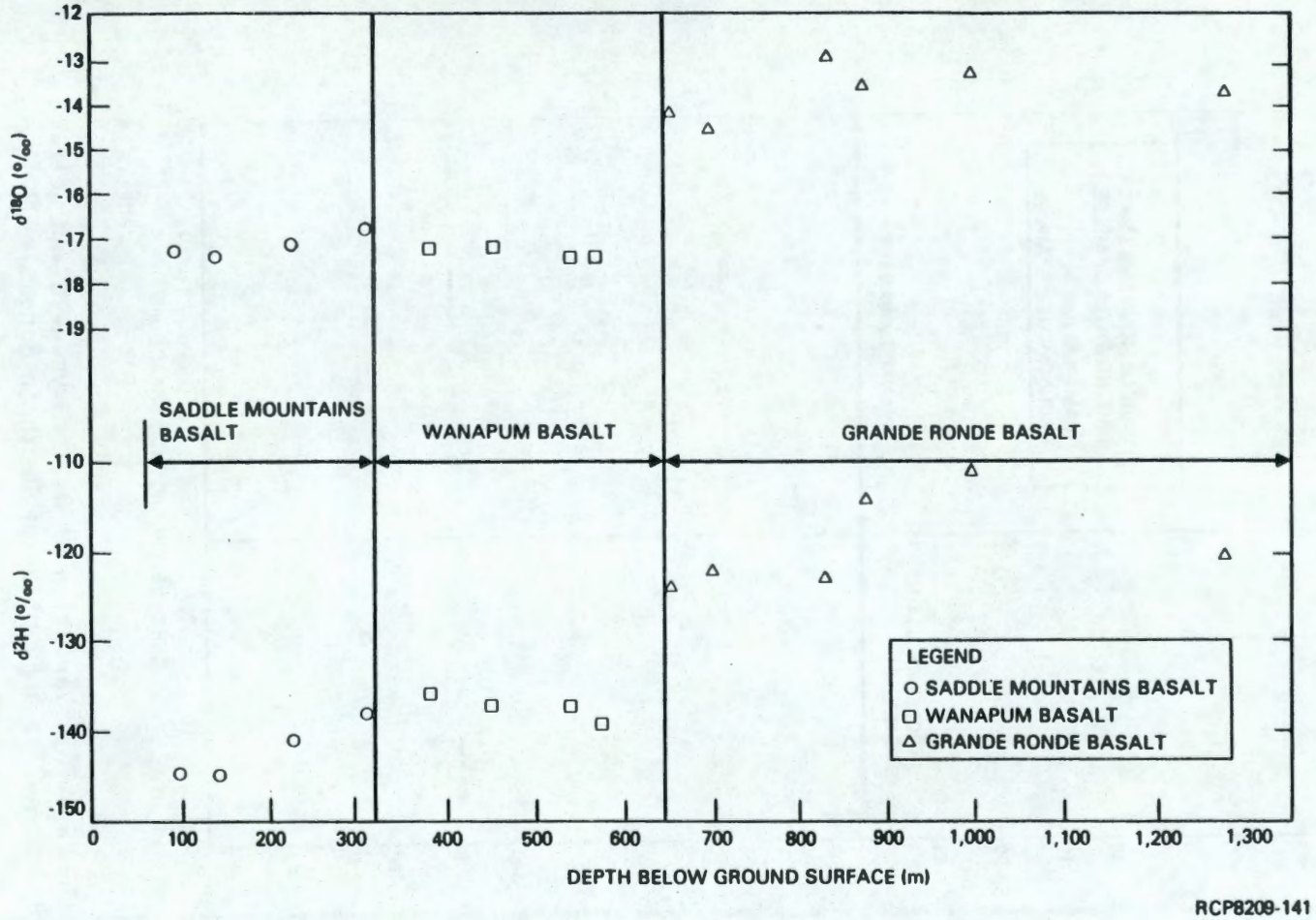

FIGURE 5-76. Variation of Delta Oxygen-18 and Delta Hydrogen-2 as a Function of Depth in Borehole DC-15.

Isotopic variations within an individual basalt formation can also be used to make inferences regarding the movement of groundwater through the formation. All formations show considerable isotopic variation (Table 5-35). This is due to the lack of major mixing within or across individual formations. Groundwater mixing tends to smooth out isotopic variability. When there is little mixing or dispersion, variations in precipitation events are preserved for long periods of time along a groundwater flow path.

TABLE 5-35. Ranges and Mean Values of Delta Oxygen-18 and Delta Hydrogen-2 for the Three Major Basalt Formations Beneath the Hanford Site.*

Basalt formation	^{18}O (°/oo)		^{2}H (°/oo)	
	Range $\delta^{18}O$	Mean $\delta^{18}O$	Range $\delta^{2}H$	Mean $\delta^{2}H$
Saddle Mountains	-19.3 to -16.4	-17.1	-155 to -138	-149
Wanapum	-20.4 to -14.8	-17.0	-153 to -129	-139
Grande Ronde	-17.7 to -12.7	-14.5	-145 to -106	-123

*Data from boreholes DB-1, -2, -4, -7, -9, -15, DC-6, -7, -12, -14, -15, 699-S11-E12A, and McGee.

Another possible explanation for isotopic differences between formations could be attributed to increased fractionation due to isotopic exchange between solid and liquid phases in the subsurface. This type of fractionation process is normally observed in subsurface environments where temperatures are in the range of approximately 50° to 100°C. Fractionation could be responsible for some of the isotopic differences in the lower flows of the Grande Ronde Basalt, where the temperatures are within the lower portion of this range. The degree of fractionation by isotopic exchange is enhanced in formations where groundwater movement is extremely slow. In environments where the rock-to-water ratio is relatively low (i.e., surface water or near-surface environments), the isotopic composition of the water is little affected by isotopic exchange. However, in groundwater regimes where the rock-to-water ratio is relatively high, the isotopic composition of the water may be substantially affected (Savin, 1980). It should be noted that this fractionation process would be expected to produce gradational changes in isotopic content with depth and/or with distance along a groundwater flow path. The data collected at the Hanford Site, however, shows very abrupt changes in isotopic content with depth at individual borehole sites.

9212495104 6

Besides isotopic differences in the groundwater between basalt formations, differences are evident between areas within the Pasco Basin. Figures 5-70 and 5-71 are histograms showing the distribution of oxygen-18 and deuterium for the various basalt formations. The hachured areas in these figures denote data from outside the Cold Creek syncline. Ranges and mean values for oxygen-18 and deuterium for groundwater inside and outside this syncline are shown in Table 5-36. The differences between the two data sets can also be seen in Figure 5-69.

Examination of these figures and table indicates discernible differences for Saddle Mountains and Wanapum Basalt groundwater for areas inside and outside the Cold Creek syncline. In contrast with this pattern, minimal differences are evident for Grande Ronde groundwater inside and outside the Cold Creek syncline. This suggests that isotopic differences may be attributable to either:

- Different sources of local recharge for Saddle Mountains and Wanapum Basalt groundwater within the Pasco Basin as compared to the Grande Ronde Basalt, or

- Possibility of mixing with deeper, isotopically heavier groundwater due to vertical hydraulic communication along the Umtanum Ridge-Gable Mountain anticline (see Section 5.1.7).

The deuterium and oxygen-18 data can also be used to reconstruct paleoclimatic conditions. Dansgaard (1964) derived equations that can estimate mean ground-surface temperatures from oxygen-18 and deuterium data. These equations were developed for work in glaciology and have some limiting assumptions. They do, however, provide an estimate of paleotemperatures at the time of recharge. The two equations developed are:

$$\delta^{18}O = (0.69\ t_a - 13.6)\ ^{o}/oo \qquad (5\text{-}4)$$

$$\delta^{2}H = (5.6\ t_a - 100)\ ^{o}/oo \qquad (5\text{-}5)$$

where

t_a = average annual ground surface temperature in degrees Celsius.

Using these equations and the average values in Table 5-35, the average annual surface temperature at the time of recharge for the basalt formations can be estimated. These results are listed in Table 5-37.

TABLE 5-36. Range and Mean Values of Delta Oxygen-18 and Delta Hydrogen-2 for the Three Major Basalt Formations Both Inside and Outside the Cold Creek Syncline Area, Hanford Site.

Basalt formation	Inside Cold Creek Syncline				Outside Cold Creek Syncline			
	$\delta^{18}O$ range (°/oo)	Mean	$\delta^{2}H$ range (°/oo)	Mean	$\delta^{18}O$ range (°/oo)	Mean	$\delta^{2}H$ range (°/oo)	Mean
Saddle Mountains	-17.9 to -16.4	-17.3	-155 to -138	-148	-19.3 to -17.5	-18.5	-155 to -147	-151
Wanapum	-17.4 to -14.8	-16.0	-143 to -129	-135	-20.4 to -16.0	-18.7	-153 to -136	-147
Grande Ronde	-16.2 to -12.7	-14.5	-136 to -106	-123	-17.7 to -13.1	-14.5	-145 to -114	-127

TABLE 5-37. Calculated Mean Surface Air Temperature from Delta Oxygen-18 and Delta Hydrogen-2 Values for Basalts Beneath the Hanford Site.

Basalt formation	Mean value (°/oo)		Mean air temperature (°C)	
	Mean $\delta^{18}O$	Mean $\delta^{2}H$	$\delta^{18}O$	$\delta^{2}H$
Saddle Mountains	-17.1	-149	-5.07	-8.75
Wanapum	-17.0	-139	-4.39	-6.96
Grande Ronde	-14.5	-123	-1.30	-4.11

Examination of these estimates suggests that the annual temperatures in the recharge areas were much colder than those occurring today. It should be noted, however, that these estimates can only be used for qualitative purposes. The use of Dansgaard's equations in such a simplified manner is not fully justified, because it is likely that climatic conditions in the past were considerably different than at present and that air masses responsible for past precipitation events would have been isotopically different from those observed today. This would have the tendency to shift both the slope and intercept of the oxygen-18- and deuterium-versus-temperature relationship (Fritz et al., 1979).

5.1.6.2.1.2. Carbon-13. In most natural materials, carbon consists of two stable isotopes, carbon-12 and carbon-I3. The abundance of these two isotopes was listed in Table 5-34. The ratio of carbon-13 to carbon-12 in nature is about 1 to 90. Fractionation processes result in a slight variation of this ratio in plants, atmospheric carbon dioxide, and marine carbonates. Typical delta carbon-13 values for some natural materials are listed in Table 5-38. The relative abundance of stable carbon isotopes is given in delta units as described in a previous section. The universally accepted carbon standard is PDB, which is a carbonate standard derived from the rostrum of *Belemnitella americana* from the Pee Dee Formation of South Carolina.

Carbon-13 is used in hydrologic isotope studies for: (1) correcting fractionation and dilution effects for carbon-14 dating, (2) determining sources of carbon species in groundwater, and (3) determining the origin of methane-gas generation.

TABLE 5-38. Values of Delta Carbon-13 for Various Natural Materials (after Hufen, 1974).

Material	Mean $\delta^{13}C$
Marine limestone	0
Oceanic CO_2	-2.2
Atmospheric CO_2	-7.0
Soil CO_2 (arid)	-17.5
Soil CO_2 (temperate)	-23.9
Terrestrial plants	-25.0

Sources of Carbon. Groundwater contains inorganic carbon in the form of dissolved carbon dioxide, bicarbonate, or carbonate. The relative proportions of these various species are dependent on the pH range of the groundwater. Most shallow groundwaters have a pH in the range of 7 to 9 (pH units). In this pH range the dominant carbonate species is bicarbonate. Sources of carbonate in groundwater include atmospheric carbon dioxide, carbon dioxide derived from plant respiration and decay, and carbonate minerals within the aquifer host rock.

Results and Discussion. Results for delta carbon-13 content within groundwater for 82 test intervals and 11 springs have been obtained in the last 2 years at the Hanford Site. The distributions of delta carbon-13 for springs and basalt formations are shown in Figures 5-77 and 5-78.

Several strong positive departures of the data are evident, however, in portions of the lower Saddle Mountains and upper Wanapum Basalts. These occurrences are coincident with methane concentrations at various borehole sites. The strong association of positive delta carbon-13 of dissolved carbon (HCO_3^-) in the groundwater with the occurrence of methane at borehole DC-15 is shown in Figure 5-79.

Methane can be produced in groundwater by microbial and thermocatalytic action on available organic material. Microbial degradation of organic matter under anaerobic conditions results in methane enriched in carbon-12 relative to methane produced by thermogenic action. Microbial processes are dominant in relatively shallow groundwater systems. With increased depth, processes such as hydrolysis, thermal cracking, and hydrogen disproportion can be of primary importance (Stahl, 1980). Reduction of carbon dioxide by methanogenic bacteria can probably best explain the relationship shown in Figure 5-79. Reduction of carbon dioxide produces methane according to the following reaction:

$$CO_2 + 4H_2 \longrightarrow CH_4 + 2H_2O. \qquad (5\text{-}6)$$

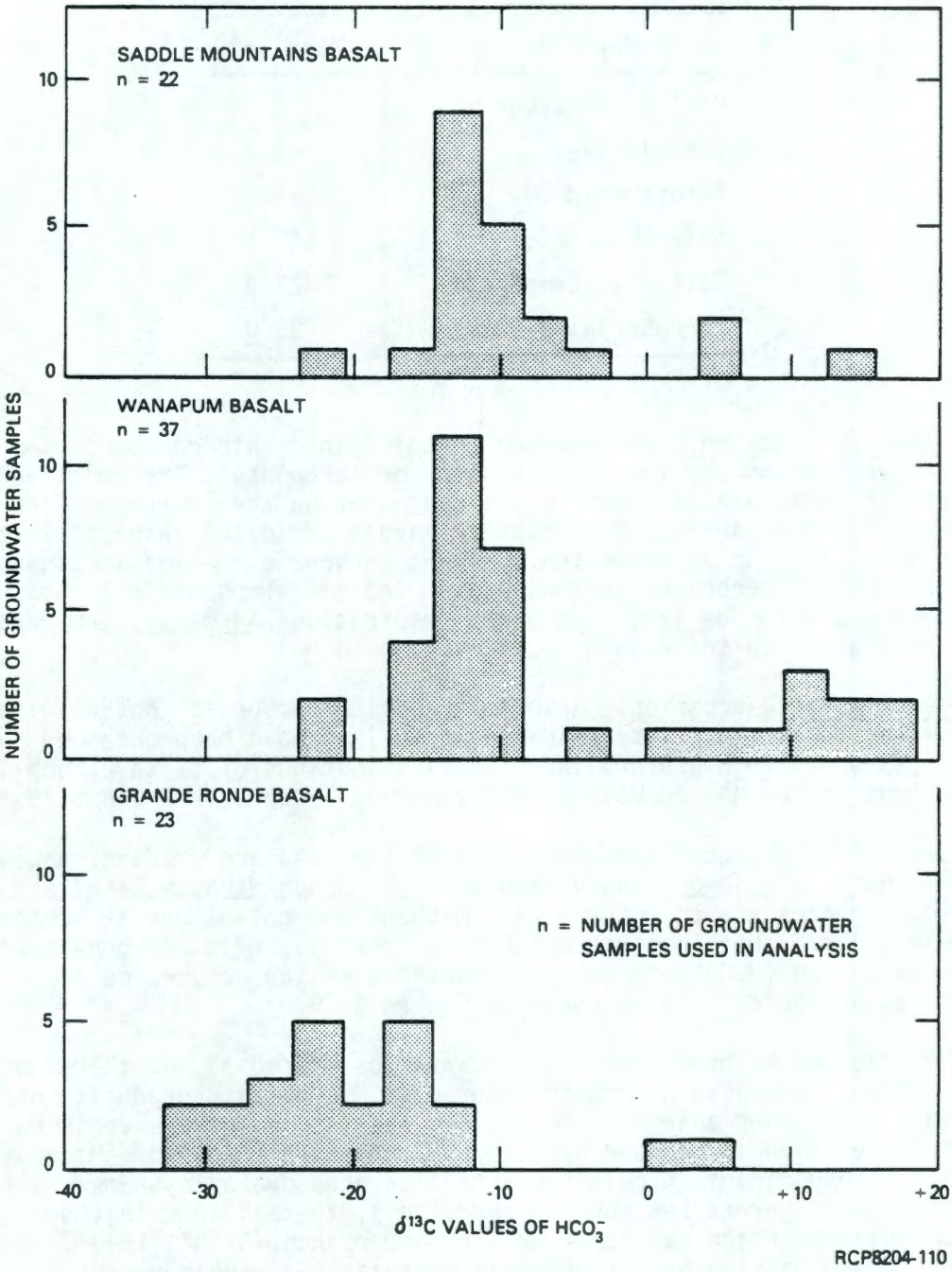

FIGURE 5-77. Distribution of Delta Carbon-13 Values of Bicarbonate Within Selected Columbia River Basalt Group Groundwaters at the Hanford Site.

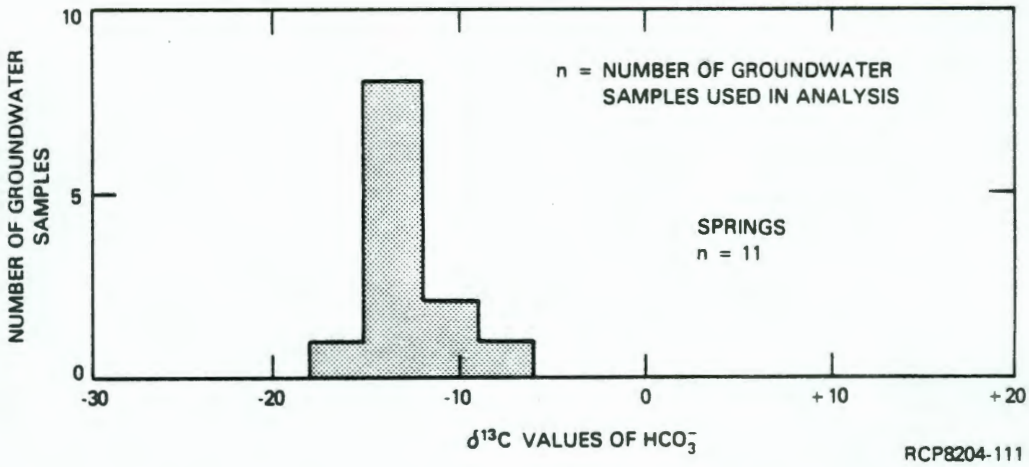

FIGURE 5-78. Distribution of Delta Carbon-13 Values of Bicarbonate for Selected Springs in the Vicinity of the Hanford Site.

This process results in very positive delta carbon-13 (HCO_3^-) values. This isotopic pattern is displayed in delta carbon-13 values shown in Table 5-39 for bicarbonate and methane within basalt groundwater at the Hanford Site. Thermocatalytic effects probably contribute minimally to the overall process, since downhole temperatures in the zones of methane accumulation are less than about 35°C. Since sulfate is relatively low in these horizons (i.e., generally less than 10 milligrams per liter), sulfate-reducing bacteria are not expected to compete successfully for the available hydrogen energy source (Carothers and Kharaka, 1979).

5.1.6.2.1.3 Sulfur-34. The sulfur-bearing species commonly found in low-temperature groundwater regimes are sulfate, bisulfide, and hydrogen sulfide. The stability of sulfur species is dependent on the pH and Eh conditions of the system. The stability of the various sulfur species as a function of Eh and pH, at standard temperature and pressure conditions is shown in Figure 5-80.

The isotopic composition of sulfur may be characterized by the ratio of sulfur-34 to sulfur-32 in standard delta units. The standard reference for sulfur isotopic analysis is the Cañon Diablo meteorite standard (Fritz and Fontes, 1980).

Sulfur normally occurs in one of three oxidation states in natural systems. In oxidizing zones, the +6 state predominates and the common ion is sulfate. Under reducing conditions, sulfur exists in the -2 valence state in the ion form of bisulfide (HS^-) in water with a pH less than about 7. In very acidic water, sulfur is in the form of hydrogen sulfide (H_2S). It should be noted that the reduction of sulfate to sulfide is a slow process. This reaction is so slow that it is undetectable unless bacteria are present to catalyze the reaction. Therefore, sulfate may be present temporarily even in strongly reducing environments.

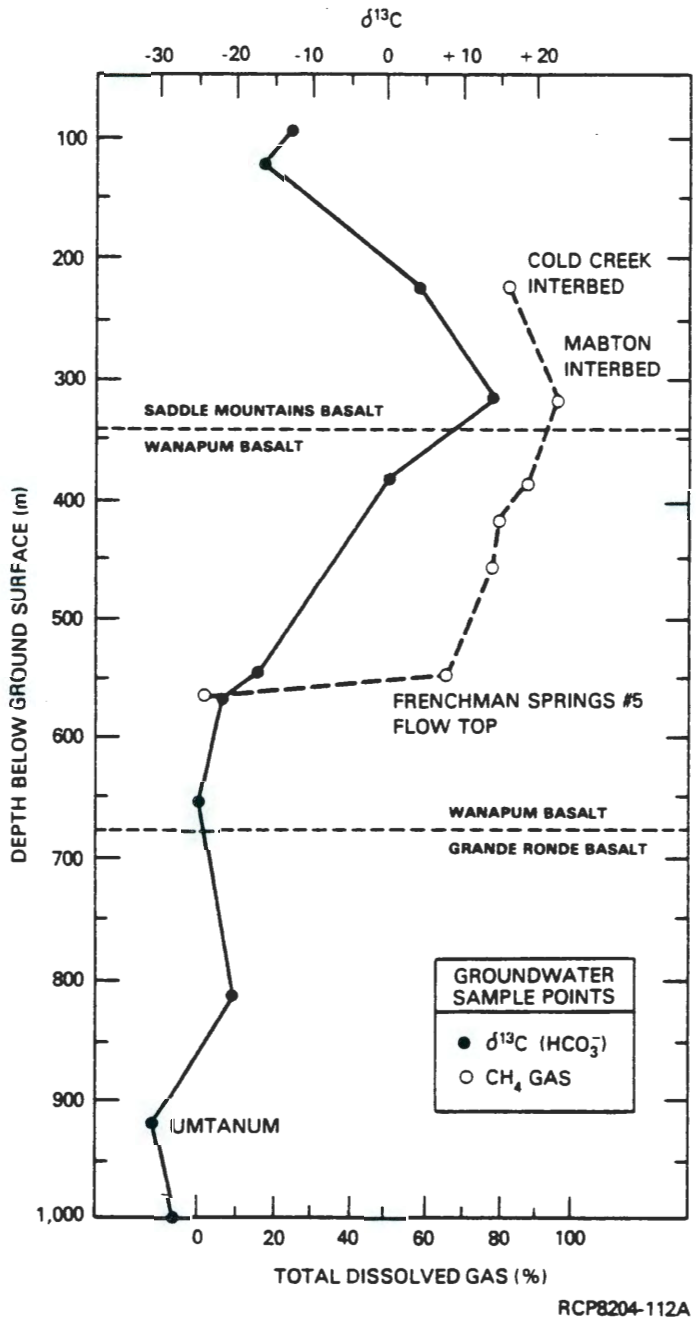

FIGURE 5-79. Relationship of Delta Carbon-13 (HCO_3^-) and Percent of Total Dissolved Gas Versus Depth in Borehole DC-15.

TABLE 5-39. Values of Delta Carbon-13 for Both Bicarbonate and Methane from Various Wells at the Hanford Site.

Well	Stratigraphic interval	$\delta^{13}C$ (HCO_3^-)	$\delta^{13}C$ (CH_4)
DC-12	Priest Rapids/Roza	+15.2	-44.00
DC-12	Roza/Frenchman Springs	+14.8	-43.66
DC-12	Frenchman Springs	+15.2	-44.15
DC-12	Frenchman Springs	+12.8	-45.57
DC-15	Cold Creek	+4.1	-63.57
DC-15	Mabton	+14.5	-46.46
DC-15	Roza flow top	+0.3	-67.06
McGee	Priest Rapids	-11.2	-51.62

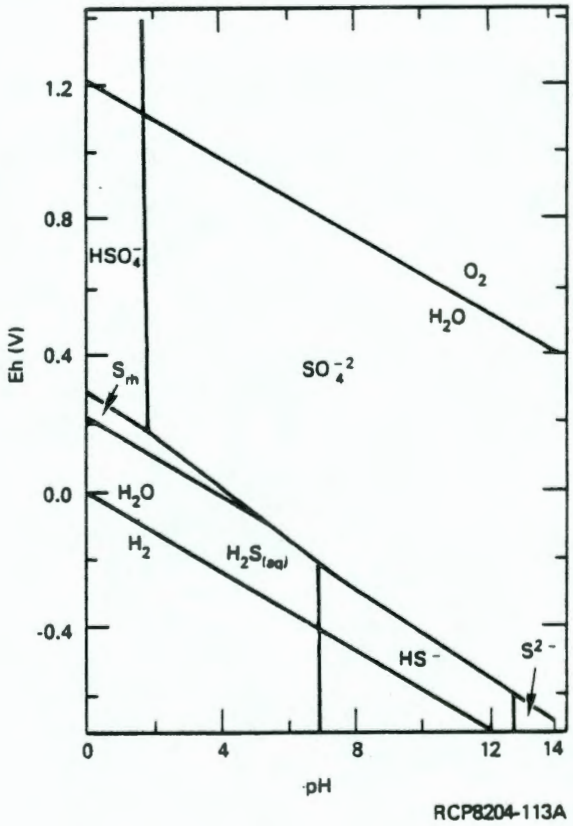

FIGURE 5-80. Eh-pH Diagram for Stable Sulfur Species at 25°C and 1 Atmosphere Total Pressure. Assumed total concentration of dissolved sulfur species is 0.001 molar (after Krauskopf, 1979).

THIS PAGE INTENTIONALLY
LEFT BLANK

9 2 1 2 4 9 5 1 0 5 5

Mean sulfur isotopic values for various sources of sulfate in groundwater are listed in Table 5-40. Sulfur isotopes may be used to determine the mineralogic origin of the sulfur species and identify the processes controlling the chemistry of sulfur in the groundwater system. Examples of this type of work have been done by Rightmire et al. (1974) and Pearson and Rightmire (1980). Sulfate in groundwater can be derived from several sources. Most commonly, sulfate is the result of evaporite-mineral dissolution and oxidation of sulfide minerals, such as pyrite. In arid regions sulfate may be derived from windblown mineral-sulfate dust obtained from soils and playas (Pearson and Rightmire, 1980). Groundwater usually contains sulfate from several sources (e.g., rainfall, evaporite dissolution, or oxidation of sulfide minerals). The range of conditions under which sulfur exists in groundwater is variable. This variability, therefore, provides additional latitude for the isotopic composition of groundwater sulfur compounds to change. Temperature and changing Eh conditions are the most common factors affecting isotopic changes in groundwater regimes.

TABLE 5-40. Sulfur Isotopic Composition for the Principal Sources of Sulfate in Groundwater (from Rightmire et al., 1974).

Source	^{34}S (o/oo)	
	Range	Mean
Seawater	+18.9 to +20.7	+20.3
Atmospheric precipitation	-1.5 to +19.4	8.1
Biogenic H_2S	-35 to +4	-15
Sedimentary rock sulfide minerals	-35 to +42	-15

Results for delta sulfur-34 analyses for basalt groundwater at the Hanford Site are presented in Figure 5-81. As shown, most basalt groundwaters have sulfur-34 values between -5 and +15 per mill. The similarity in delta sulfur-34 ranges suggests a commonality in source(s) for sulfate within groundwater in the Columbia River basalt. Because of the presence of accessory sulfide minerals, previously identified by Ames (1980) within Columbia River basalts, it is likely that oxidation of pyrite is the best source of sulfate within the basalt groundwater. The sulfur-34 content of the pyrite in the various basalt formations is currently not known.

The overall similarity in sulfur-34 ranges for all three basalt formations makes identification of separate groundwater-flow systems impossible, using this isotope alone. In addition, the presence of sulfate-reduction processes discussed in Section 5.1.5.2.1 for Saddle Mountains groundwater in the Cold Creek syncline further complicates the use of

9212495105 6

THIS PAGE INTENTIONALLY
LEFT BLANK

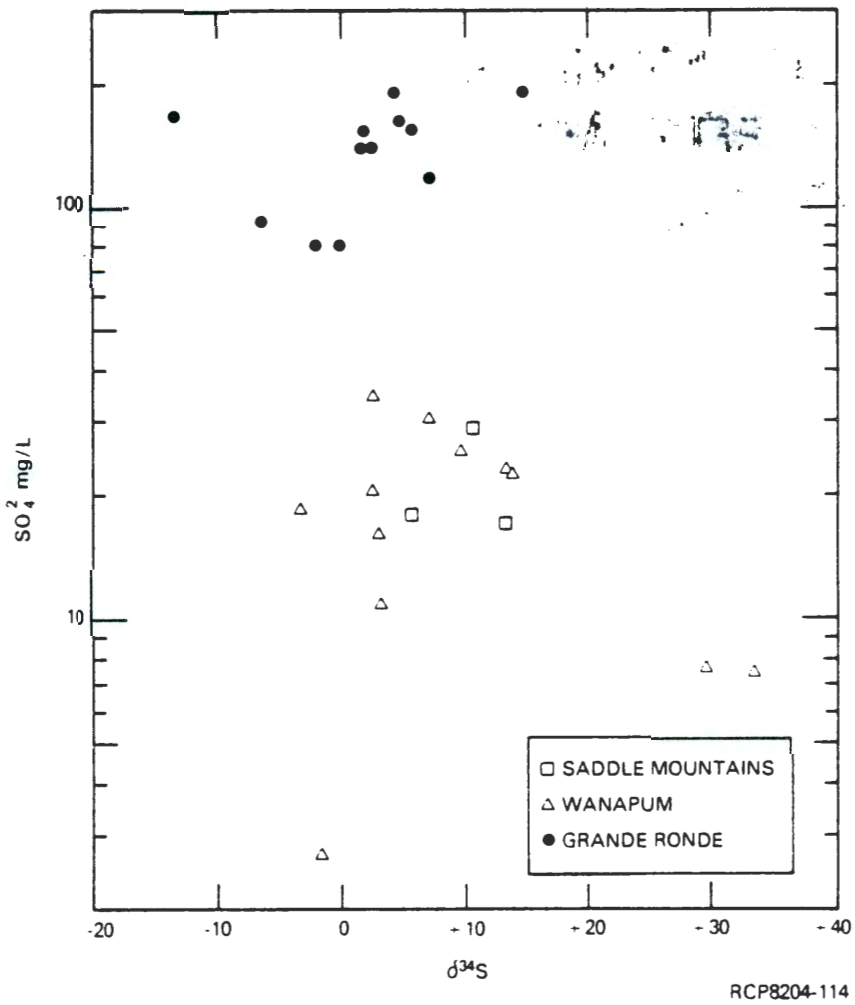

FIGURE 5-81. Sulfate Versus Delta Sulfur-34 (sulfate) for Basalt Groundwaters at the Hanford Site.

sulfur-34 in defining groundwater systems. The grouping or clustering of Grande Ronde Basalt groundwater in comparison to the overlying basalt formations is attributable solely to the presence of higher sulfate concentrations (i.e., 80 to 200 milligrams per liter) in the deeper groundwaters (Fig. 5-81). Additional areal sulfur-34 data for groundwaters and pyrite in various basalt formations are needed to more fully utilize this isotopic parameter in hydrologic characterization studies.

5.1.6.2.2 Radionuclides. Radionuclides have been used in the same manner as stable isotopes to determine flow patterns, to define recharge/discharge relationships, and as groundwater tracers. Due to radioactive-decay relationships, radionuclides have also been useful in age dating groundwater. Age dating is an important investigative tool for it provides a direct measurement of the groundwater's residence time in the geologic medium. For example, the measurement of tritium concentrations can assist the hydrologist in determining the representativeness of a water sample. Longer lived radioisotopes, such as carbon-14, are useful in both dating older groundwaters and in defining general groundwater flow patterns.

Many radionuclides have been examined for possible indicators of hydrologic age; by far the most popular and best understood is carbon-14. Other isotopes currently being used and evaluated for age dating purposes in the field of hydrology include noble gases (^{4}He, Xe, ^{81}Kr, ^{21}Ne, ^{22}Ne, and ^{40}Ar), ^{3}H, ^{32}Si, ^{36}Cl, ^{39}Ar, ^{129}I, and the ratio of ^{234}U to ^{238}U. Radionuclides used in hydrologic investigations at the Hanford Site were listed in Table 5-34.

5.1.6.2.2.1 Tritium. Tritium (^{3}H) is an isotope of hydrogen. Unlike deuterium, tritium is unstable and has a half-life of 12.35 years. The tritium content in groundwater is commonly reported in tritium units or in picocuries per liter, not as per mill. One tritium unit is equivalent to a concentration of one atom of tritium in 10^{18} atoms of hydrogen and is equal to 3.4 picocuries per liter. Tritium is produced in the upper atmosphere by cosmic-ray neutron bombardment of nitrogen nuclei. This cosmic-ray flux results in the steady-state production of tritium in the atmosphere. Tritium concentrations in the upper atmosphere amount to less than or equal to 20 tritium units.

In the early 1950s, atmospheric tritium concentrations increased dramatically with the advent of open air thermonuclear-weapons testing. Tritium concentrations in precipitation during this period increased two- to threefold. Tritium concentrations peaked in 1963 and have been declining ever since.

In groundwater studies, the following generalities are commonly made concerning tritium:

- Tritium levels less than or equal to 5 tritium units indicate groundwater was recharged prior to 1953.

- Groundwater having high tritium concentrations (i.e., greater than approximately 100 tritium units) indicates that the recharge entered the flow system after 1953.

Post-1953 groundwater is often referred to as modern- or bomb-tritium water. Groundwater with tritium concentrations between about 5 to 100 tritium units, however, may be the result of mixing of various fractions of modern and pre-bomb waters. Because of its short half-life, tritium is of limited value in age dating groundwater greater than 100 years old. Tritium, therefore, is of little use for age dating of the deep basalt groundwaters beneath the Hanford Site. Tritium's primary purpose in basalt hydrological studies at the Hanford Site has been as a natural tracer in the drilling of basalt boreholes. Drilling fluids are mixed with Columbia River water or groundwater from boreholes completed in the upper unconfined aquifers overlying the basalts. These waters have a high level of tritium that can be used as a natural spike for evaluating drilling-fluid contamination within groundwater sampled from test intervals. This procedure has been used to provide "after the fact" information concerning the groundwater's representativeness after final sample collection. At the time of actual sampling, total organic carbon, fluorescene, and lithium concentrations are used to evaluate sample representativeness.

Average tritium concentrations for the three basalt formations are usually less than 0.5 tritium unit. Average tritium values in groundwater sampled from the Saddle Mountains, Wanapum, and Grande Ronde Basalts are given in Table 5-41. For comparison, tritium values of the Columbia River, which flows adjacent to boreholes DC-14 and -15 (and which is also used for drilling "makeup" water) are listed also. Examination of Table 5-41 indicates that tritium values for respective basalt formations are low and are generally within one or two standard counting deviations. This indicates that the groundwater samples collected are representative of the formation waters.

TABLE 5-41. Mean Tritium Concentrations (in tritium units) for Columbia River Basalts from Selected Boreholes and the Columbia River.

Borehole	Basalt formation			Columbia River*
	Saddle Mountains	Wanapum	Grande Ronde	
DB-15	NA	0.2 ± 0.05	NA	Not applicable
DC-12	NA	0.05 ± 0.04	0.16 ± 0.06	Not applicable
DC-14	0.21 ± 0.05	0.21 ± 0.07	0.22 ± 0.09	40.3 ± 1.1
DC-15	0.23 ± 0.05	0.34 ± 0.07	0.63 ± 0.07	62.1 ± 1.7

NA = Not available.

*Collected from the Columbia River adjacent to borehole indicated.

5.1.6.2.2.2 Carbon-14. Radioactive decay allows carbon-14 to be useful in determining groundwater age (residence time) and flow directions. Lower carbon-14 activities in a groundwater sample are associated with greater ages. Groundwater movement can be determined by plotting carbon-14 activity for various points along a flow path. Ideally, flow will be in the direction of decreasing activity (greater ages). Carbon-14 is produced between the stratosphere and the troposphere, through conversion of nitrogen-14 atoms by a nuclear reaction between high-energy neutrons and nitrogen nuclei. This reaction is described by Libby (1965) in the following relationship:

$$^{14}N + n \longrightarrow {}^{14}C + \beta^{+} \qquad (5\text{-}7)$$

where

n = a high energy neutron

β^{+} = a proton.

Carbon-14 atoms quickly oxidize to form molecular $^{14}CO_2$, which disperses through the atmosphere and mixes with inactive atmospheric carbon dioxide. Carbon-14 is radioactive and decays with a half-life of 5,730 years to nitrogen-14 by the emission of an electron (β^{-}). Carbon-14 decay is described by the following reaction:

$$^{14}C \longrightarrow {}^{14}N + \beta^{-} \qquad (5\text{-}8)$$

The carbon-14 activity is measured by counting negative beta particles ejected during the decay process. In geologic and archaeologic studies a half-life of 5,568 years is used for carbon-14. In hydrologic studies, however, a more recent value of 5,730 (plus or minus 40) years is utilized (Mook, 1980).

The age of a groundwater sample can be determined utilizing the following equations if the initial activity (A_o) is known:

$$T = -\lambda \ln \frac{A}{A_o} \qquad (5\text{-}9)$$

or

$$T = -8{,}270 \ln \frac{A}{A_o}$$

where

T = sample age

λ = decay constant

A = sample activity

A_0 = initial sample activity.

This calculated age can be expressed either in absolute years or in a "percent modern carbon" value.

Percent modern carbon indicates the percentage difference between sample activity and that of a "modern standard." The universally accepted carbon standard is the National Bureau of Standards' oxalic-acid standard, where the carbon-14 activity of modern carbon equals 0.95 carbon-14 activity oxalic acid in 1950 (Fritz and Fontes, 1980). Percent modern carbon is calculated from the following equation:

$$A = \frac{{}^{14}C/{}^{12}C \text{ sample}}{{}^{14}C/{}^{12}C \text{ standard}} \times 100 \text{ (percent modern carbon)} \qquad (5\text{-}10)$$

In hydrogeologic studies, determining a value for the initial activity may be difficult due to the "dead" carbon that may be dissolved in the groundwater. Many workers (e.g., Pearson and White, 1967; Pearson and Hanshaw, 1970; Vogel, 1970; Tamers, 1967; Tamers and Scharpenseel, 1974; Rightmire and Hanshaw, 1973) have developed methods to determine an initial carbon-14 value. The estimated initial value can then be used in conjunction with delta carbon-13 data and carbonate analyses to provide an adjusted carbon-14 age for groundwater.

Spring waters issuing from basalts surrounding the Pasco Basin are characterized by carbon-14 ages ranging from recent (greater than 100 percent modern carbon) to approximately 23 percent modern carbon. Groundwater in the deep basalts beneath the Hanford Site is considerably older than that from springs. The average groundwater ages for Columbia River basalts are listed in Table 5-42. These carbon-14 ages are given as percent modern carbon and as a corrected age. With the exception of the Grande Ronde Basalt data, carbon-14 data show a characteristic increase in age with depth.

TABLE 5-42. Mean Carbon-14 Age Calculations for the Columbia River Basalt Groundwaters Beneath the Hanford Site.

Basalt formation	Corrected ^{14}C age (yr before present)	Percent modern carbon
Saddle Mountains	17,700	11.0
Wanapum	25,000	4.5
Grande Ronde	>32,000	<1.9

Carbon-14 data for the deep Grande Ronde Basalt groundwater provide age dates that are presently difficult to interpret. This is due to the fact that there is very little total inorganic carbon in the Grande Ronde groundwaters. Therefore, even minute sample contamination can result in anomalous carbon-14 age dates. Corrected carbon-14 ages for boreholes in the Mabton interbed are shown in Figure 5-82. The general pattern of groundwater age is that of increasing age from west to east across that portion of the Hanford Site south of the Umtanum Ridge-Gable Mountain anticline. The groundwater-flow patterns suggested by these data are consistent with plots of major inorganic species and potentiometric information. In the area of the Umtanum Ridge-Gable Mountain anticline, however, younger groundwater is encountered in the Mabton interbed (Fig. 5-82). This may be attributed to increased vertical hydraulic communication along the anticline. This hypothesis of mixing is consistent with other hydrochemical and hydraulic data. This concept is addressed in Sections 5.1.5.2, 5.1.5.3, and 5.1.5.4 dealing with the hydrochemistry of each of the Columbia River basalts as well as in Section 5.1.7.2, which discusses interrelationships between confined aquifer systems.

The two commonly used counting techniques for carbon-14 analyses require a considerably large amount of carbon for analysis. About 1.0 gram of carbon is required, which allows a 1 percent precision at a maximum age of 40,000 years (Davis, 1978). In general, a sample volume of 40 to 100 liters of water is needed to perform such an analysis.

Hufen (1974) has shown in a study of the the basalts of Hawaii that if bicarbonate concentrations were less than 50 milligrams per liter, groundwater-sample quantities in the range of 380 to 600 liters were needed. In the Grande Ronde Basalt groundwater beneath the Hanford Site, a minimum of 100 liters of sample must be collected to obtain approximately 1.0 gram of carbon.

The carbon-14 data from the Columbia River basalt groundwaters have been corrected for various inputs of "dead" carbon by two techniques. The first method to be discussed was developed by Pearson (1965), Pearson and

9 2 1 2 4 9 5 1 0 6 2

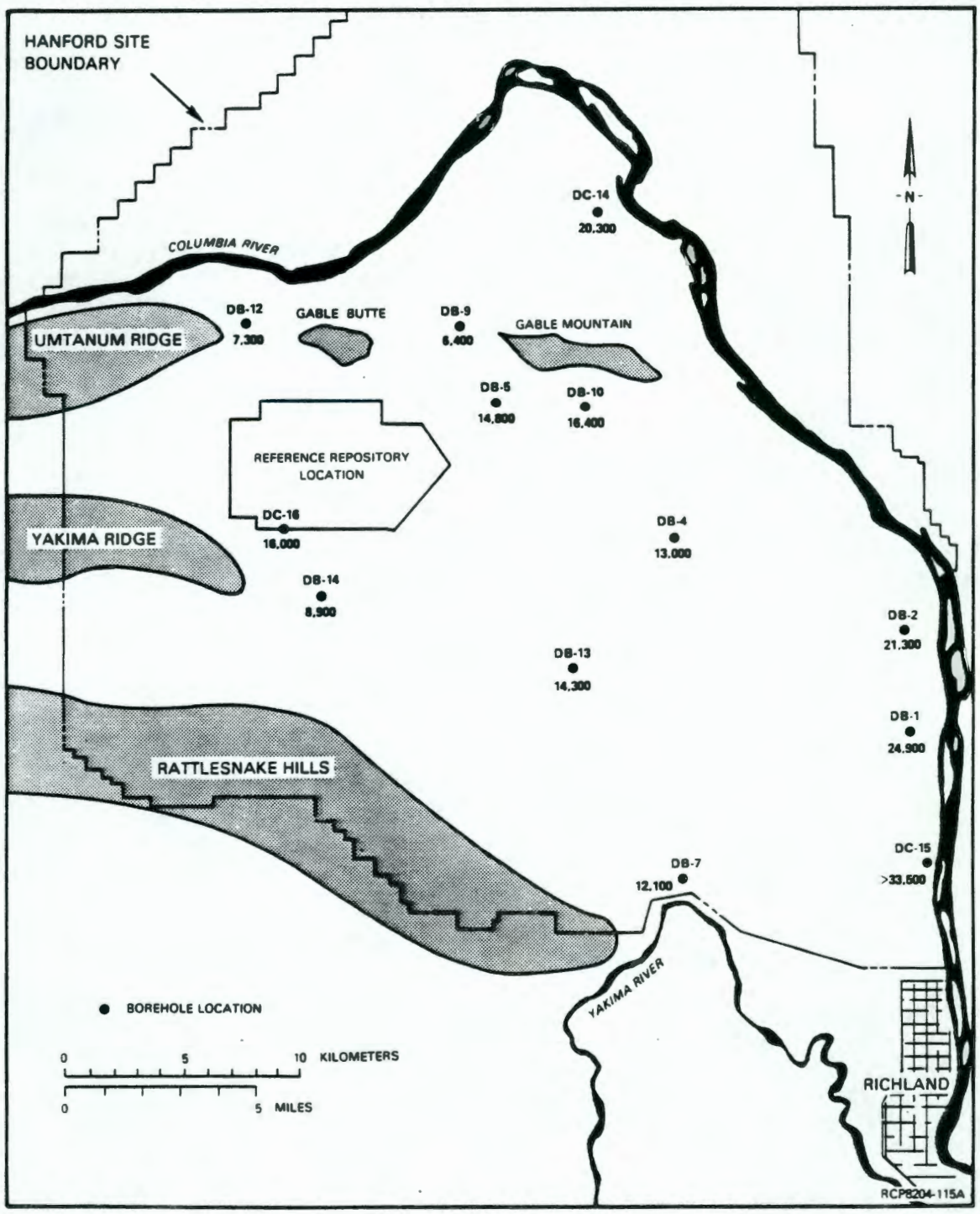

FIGURE 5-82. Areal Plot of Corrected Carbon-14 Ages for Groundwater from the Mabton Interbed.

White (1967), Pearson and Hanshaw (1970), and Pearson and Swarzenki (1974) and is based on stable isotopic content of the groundwaters. A second technique by Tamers (1976) is based on the carbonate chemistry of the groundwaters.

Pearson (1965), Pearson and White (1967), Pearson and Hanshaw (1970), and Pearson and Swarzenki (1974) attempted to adjust groundwater ages through the use of stable carbon isotopes. These isotopes are used to determine an initial carbon-14 value based on an isotope mixing model. This particular model is based on the similarities in the chemical behavior of carbon-13 and carbon-14. The carbon-13 is assumed to reflect all changes occurring to carbon-14 along a given flow path. It can therefore be used to reconstruct the changes in carbon-14 activity due to all mechanisms except radioactive decay. In general, the following equation is used to arrive at A_o:

$$A_o = \frac{\delta^{13}C_m - \delta^{13}C_{solid}}{\delta^{13}CO_2 - \delta^{13}C_{solid}} \left(A_{soil}\right) \qquad (5\text{-}11)$$

where:

A_o = initial carbon-14 activity

$\delta^{13}C_m$ = stable isotopic content of total dissolved carbon in sample

$\delta^{13}CO_2$ = stable isotopic content of soil zone CO_2; based on photosynthetic cycle of dominant vegetation type

$\delta^{13}C_{solid}$ = stable isotopic content of solid carbonate in the aquifer; usually taken to be 0 per mill

A_{soil} = activity of soil zone CO_2; usually assumed to be 100 percent modern carbon.

The delta carbon-13 of solid carbonates in an aquifer or soil are generally very close to zero versus the PDB standard, if they are of marine origin. The universally accepted carbon standard is PDB, which is a carbonate standard derived from the rostrum of Belemnitella americana from the Pee Dee Formation of South Carolina. Other sources of carbonate may be somewhat depleated or enriched in delta carbon-13 versus PDB and may very well have delta carbon-13 values greater or less than zero. It is therefore advantageous to measure this value whenever possible.

In general, Pearson's model assumes the following initial values: $\delta^{13}C_{soil}$ = -25 per mill, $\delta^{13}C_{solid}$ = 0 per mill, and the activity of the solid carbonate is zero. Under these conditions, Equation 5-11 reduces to:

$$A_o = \frac{\delta^{13}C_m}{-25\ o/oo} \times 100 \text{ (percent modern carbon).} \qquad (5\text{-}12)$$

A carbon-14 age can then be calculated using Equation 5-9. For the calculations in this report, a $\delta^{13}C_{soil}$ of -23 per mill was used for the Saddle Mountains Basalt data and a value of -25 per mill was used for the Wanapum Basalt data.

Tamers (1967 and 1975) and Tamers and Sharpenseel (1974) calculate initial carbon-14 activity using a model which takes into account the carbon speciation within the aquifer. The reasoning behind this method is that the equivalent amount of limestone diluting the total carbonate in the system is equal in quantity to half of the bicarbonate present. The remaining carbonate (0.5 HCO_3^- plus all CO_2) is that coming from plants and/or the atmosphere. An initial carbon-14 activity (A_o) based on the above relationship is obtained in the following manner:

$$A_o = \frac{mC_T - 0.5\ mHCO_3^-}{mC_T} \left(A_{soil}\right) \qquad (5\text{-}13)$$

where:

A_o = initial carbon-14 activity

mC_T = total inorganic carbon (molality)

$mHCO_3^-$ = bicarbonate present in groundwater (molality)

A_{soil} = carbon-14 activity of soil CO_2; normally assumed to be 100 percent modern carbon.

This model assumes perfect stoichometry of the reacting carbonate species and, as the Pearson model, does not account for isotope exchange. A corrected age can then be calculated using Equation 5-9.

The two methods discussed above result in corrected ages, which are normally quite similar. For the purposes of this report, the two values were averaged resulting in the ages listed.

Two studies have been conducted outside the Hanford Site related to carbon-14 age dating of groundwater in the Columbia River basalts. These were conducted by Crosby and Chatters (1965) and Silar (1969). Both studies reported groundwater ages that are consistent with those reported at the Hanford Site. Crosby and Chatters (1965) concluded that since groundwater in the basalts of the Moscow-Pullman area are of a calcium bicarbonate chemical type and the pH range is 6.8 to 7.2, there should be no additional influences on the carbon-14 ages. They concluded that the ages calculated should be actual and controlled only by radioactive decay. The data indicated that groundwater within the basalts was stratified, with an inverse relationship between elevation of the producing zone and age. Silar (1969) assumed the same equilibria controls as did Crosby and Chatters (1965). Therefore, no attempt was made to correct carbon-14 ages. The location of the wells used in Silar's study is given in Figure 5-83. Carbon-14 ages were calculated using the National Bureau of Standards' standard as the zero time reference. Silar concluded that the calculated ages, and thus groundwater flow, were affected by surface morphology; i.e., groundwater in plateau regions appeared to migrate more slowly than groundwater in valleys.

5.1.6.2.2.3. Uranium Disequilibrium. The disequilibrium occurring between uranium-234 and uranium-238 is a common phenomenon in circulating groundwater. In a closed system, the ratio of radioactivities of uranium-238 and uranium-234 should theoretically be unity. However, deviations from unity occur in nature. The exact mechanism causing isotopic disequilibrium between uranium-234 and uranium-238 is not fully understood. These variations are not attributable to mass fractionation, as with the light isotopes of hydrogen or oxygen, or to radiogenic accumulations, as is the case with lead or argon. It is apparent, however, that a dependence exists on the radiogenic origin of uranium-234 (Osmond, 1980). The magnitude and direction of this phenomenon are related to the geologic, hydrologic, and geochemical environment through which the groundwater flows.

Uranium has several oxidation states. Only the +4 and +6 states are of geologic interest. Uranium +4 is very immobile under reducing conditions. Its oxide and hydroxide are very insoluble. The +6 state of uranium is the normal ionic form in most oxidizing waters. The +6 ion is considerably more soluble than the +4 ion state. The +6 ion tends to complex readily with many anions, thus increasing the solubility of the uranium +6 valence form.

Several mechanisms have been proposed to explain the uranium-234 uranium-238 fractionation in the aqueous phase. All are related to nuclear transformations of uranium-238 to its daughters by alpha and beta decay. The processes include nuclear recoil transfer, selective leaching, autooxidation of uranium-234, and chemical fractionation of thorium-234 (Osmond, 1980). While all mechanisms may occur, the most plausible is that of recoil transfer.

9 2 1 2 4 9 5 1 0 6 6

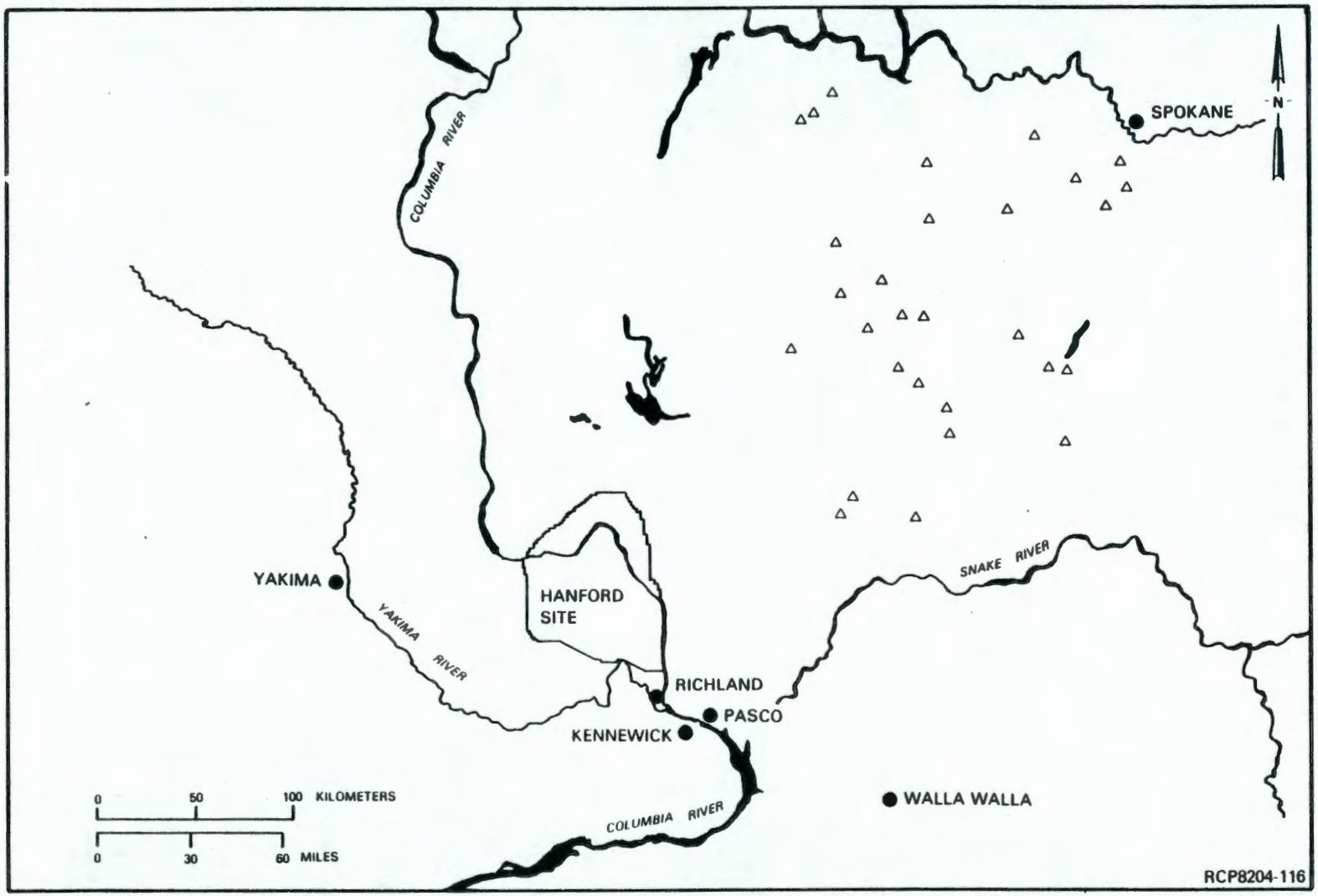

FIGURE 5-83. Location of Wells Used by Silar When Studying the Carbon-14 Age of Groundwater in Eastern Washington State (Silar, 1969).

Recoil is the name given to the process whereby the atom of a daughter isotope is suddenly ejected, due to the expulsion of an alpha particle in the opposite direction. Kigoshi (1971) proposed this mechanism, whereby the thorium-234 daughter is physically ejected across the solid/liquid interface a distance of several hundred angstrom units. Subsequent decay in the aqueous phase results in the enrichment of uranium-234 relative to its parent uranium-238.

Since the total uranium in the system is in isotopic equilibrium, an increase in the activity ratio within groundwater must be countered by a corresponding decrease within the surrounding rock. The degree of disequilibrium is the result of: (1) the isotopic ratio of uranium in the minerals of the surrounding rock to that in the groundwater, (2) relative surface area of the rock matrix, and (3) the time of coexistence of the two phases (Davis, 1978).

In terms of uranium disequilibrium, the simplest groundwater systems to study are shallow open systems. Uranium is conservative once it is leached in these environments, due to the Eh and partial-pressure conditions of carbon dioxide in the system. Deep confined groundwater systems are more difficult to characterize using uranium isotope data because of changes in Eh, pH, and CO_2 concentrations along a given flow path. The changes in these parameters result in variations of uranium concentration in both liquid and solid phases within the aquifer. Among typical uses of uranium data in hydrologic studies are mixing models, flow-system delineation, geochemical balances, age dating, uranium prospecting, and geothermal systems.

The degree of success achieved using uranium isotopes for hydrogeologic studies depends heavily on the level of understanding of both the geohydrology and geochemistry of the aquifer(s) being studied.

Water samples from springs and basalt groundwater beneath the Hanford Site have been analyzed for total uranium and uranium-234 to uranium-238 activity ratios. The distribution of total uranium and the amount of fractionation occurring for uranium-234 within basalt groundwaters is illustrated in Figure 5-84.

Results of uranium analyses for Columbia River basalt are listed in Table 5-43. Examination of data indicates that all samples exhibit very low (less than 1.0 nanogram per milliliter) total uranium concentrations, with the exception of three samples. Two of these samples represent springs obtained from oxidizing environments. The other high uranium sample was from the Rattlesnake Ridge interbed at borehole DB-15, which forms one of the uppermost confined-aquifer systems beneath the Hanford Site. The concentration of 5.62 nanograms per milliliter in DB-15 is nearly five times greater than that for other basalt groundwater. It should be noted, however, that this borehole is located in an area where vertical groundwater communication is believed to occur between the uppermost confined and unconfined-aquifer systems. The probable location and mechanism for this hydraulic communication is described in Section 5.1.7.

9 2 1 2 4 9 5 1 0 6 8

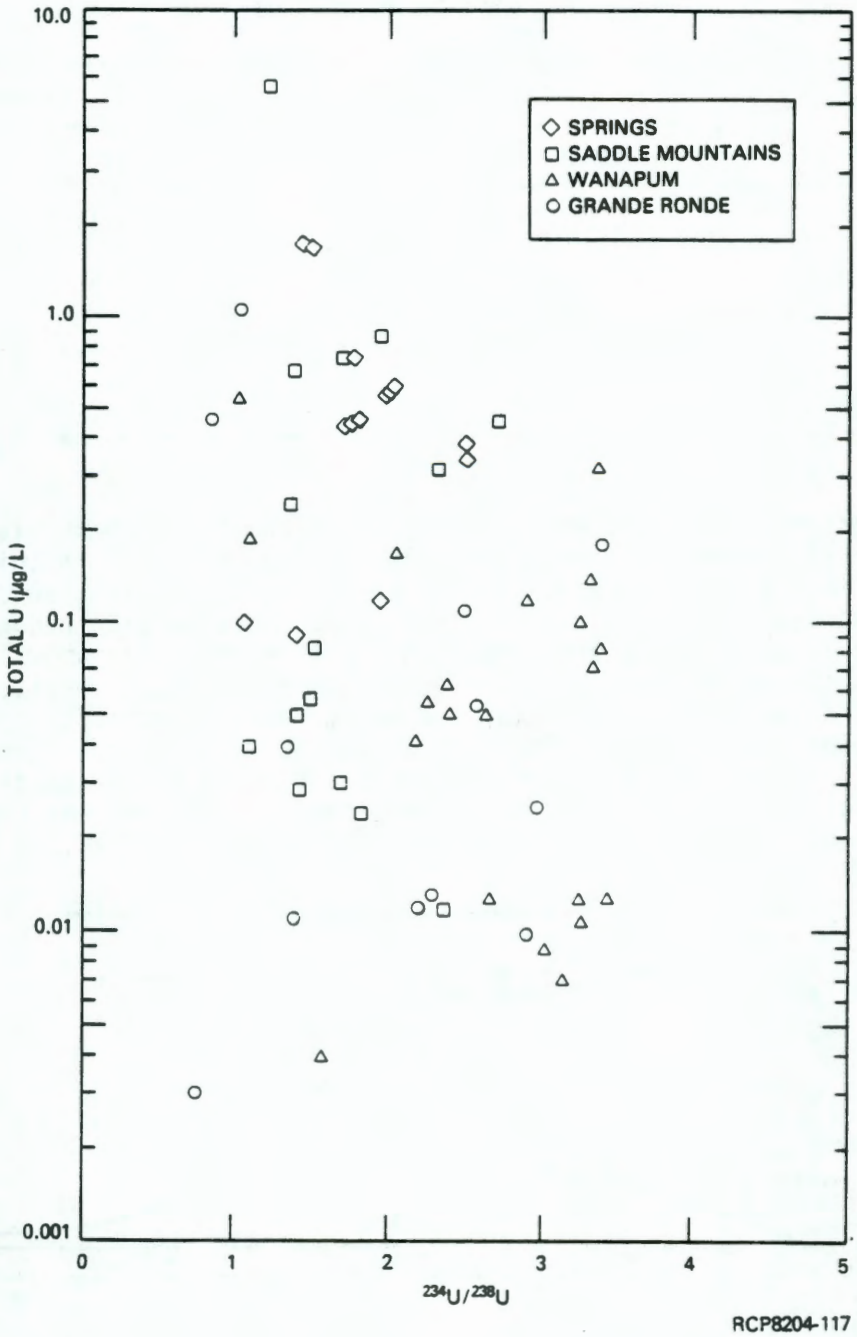

FIGURE 5-84. Total Uranium Versus Activity Ratio for the Springs and the Columbia River Basalt Groundwaters Beneath the Hanford Site.

TABLE 5-43. Range and Mean Values for Activity Ratios and Total Uranium for Spring and Groundwater Samples from Columbia River Basalts at the Hanford Site.

Basalt source	Activity ratio (%)		Total U (ng/mL)	
	Range	Mean	Range	Mean
Springs	1.1 to 2.61	1.86	0.09 to 1.77	0.61
Saddle Mountains	1.1 to 2.77	1.70	0.005 to 5.62	0.58
Wanapum	1.0 to 3.44	2.39	0.004 to 0.97	0.20
Grande Ronde	0.74 to 3.42	2.03	0.001 to 1.08	0.14

The most commonly used model to explain uranium transport along a groundwater flow path is shown graphically in Figure 5-85. In this model, uranium is mobile in the shallow oxidizing environment. As groundwater moves farther along a flow path, it encounters a decrease in redox potential. At this point along the flow-path position, the uranium valence state changes from +6 to +4 and it becomes immobile. As a result, a decrease in total dissolved uranium and an increase in activity ratio occurs in the aqueous phase. The rise in the activity ratio is the result of increased recoil transfer between the solid phase (precipitate) and groundwater. Farther along the flow path, the activity ratio within groundwater decreases due to the depletion of excess uranium-234.

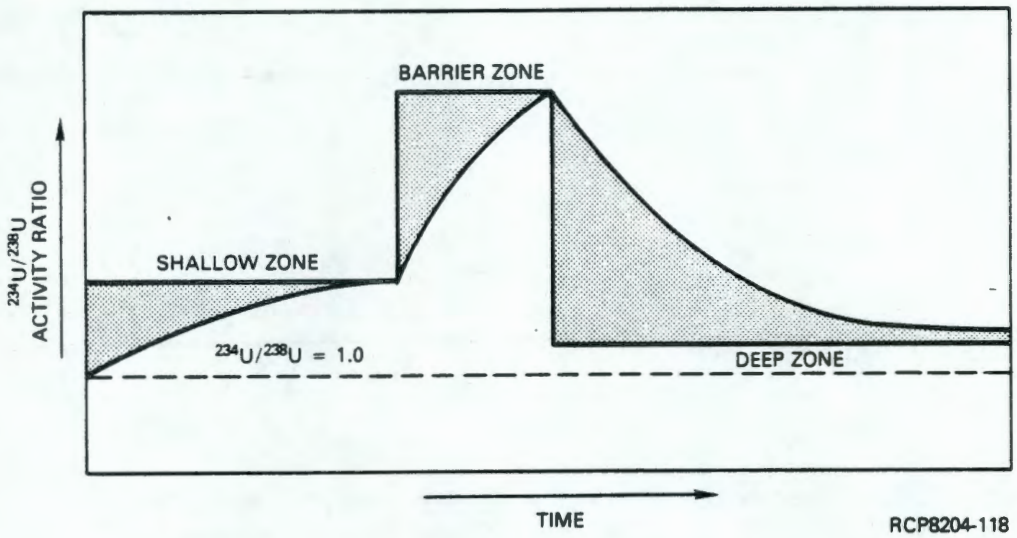

FIGURE 5-85. Possible Changes of Uranium-234/Uranium-238 as a Function of Time and Position in a Flow System (after Osmond, 1978).

Available data from Hanford do not appear to be compatible with this model. Data plotted in Figure 5-84 illustrated a large variation in total uranium concentration and a corresponding small variation in activity ratios. There is no distinct large increase in activity ratios present that would indicate the presence of a reducing barrier.

The highest total uranium concentrations are observed in spring waters and Saddle Mountains Basalt groundwater (Table 5-43). This is indicative of a shallow oxidizing environment where uranium is in the mobile +6 valence state. The groundwaters in the Wanapum and Grande Ronde Basalts are sufficiently reducing to cause uranium to change from the +6 to the +4 state. Thus, uranium would be expected to precipitate out of solution, with an accompanying significant decrease in total uranium concentration. Thermodynamic calculations indicate that there may be extremely reducing conditions at depth within the Grande Ronde Basalts. This could explain the very low total uranium concentrations present in the deep basalt groundwater. In comparing the model proposed by Osmond (1978), activity ratios for spring waters, and perhaps the Saddle Mountains groundwater, are most likely to fit within the region labeled "shallow zone" in Figure 5-85. Data for the Wanapum and Grande Ronde groundwater would be expected to occur in the region labeled "deep zone". Activity ratios are greater than unity but decreasing in the direction of flow in this zone, due to the decay of excess uranium-234. The lack of a zone of extremely high activity ratios (i.e., a reducing barrier) is believed attributable to the fact that many of the basalt groundwaters being sampled at the Hanford Site are well beyond this point in the overall flow system. Therefore, the location of the "reducing-barrier zone" for the deeper basalt groundwater may lie outside the Hanford Site.

The 250,000 year half-life of uranium-234 makes the use of this isotope attractive for dating rock and groundwater-flow systems at 10^5 to 10^6 years. Attempts have been made to use the disequilibrium of the uranium-234 to uranium-238 ratio for age dating purposes; therefore, several investigators have proposed using uranium isotopes for dating old groundwaters. The use of this technique, however, is not universally accepted. Kigoshi (1973) and Kronfeld et al. (1975) report that an increase in activity ratio should occur in groundwater in the direction of flow, due to recoil transfer. Kronfeld and Adams (1974), however, have observed a decrease in activity ratio due to decay of uranium-234. In addition, Cowart and Osmond (1974) have observed both an increase and a decrease in the activity ratio for groundwater of the Carrizo sandstone in Texas. Because of these uncertainties in uranium trends and the multitude of possible water/mineral interactions operative in a flow system, the dating of extremely old groundwaters by uranium-isotope methods is presently questionable (Osmond, 1980). As a minimum, the uranium geochemistry within the total system should be understood if worthwhile age-dating studies are to be made with uranium isotopic data in groundwater. This includes the geochemistry of both the aqueous and the rock phases for the system.

Although considerable uncertainty exists in applying uranium isotopic data directly for age-dating applications, Barr et al. (1979) have described a method whereby groundwater ages may be estimated using disequilibrium data if the decay constants and initial activity ratios of the groundwater and rock are known. To examine this technique's applicability at the Hanford Site, rock analyses are planned in conjunction with available groundwater results to calculate uranium disequilibrium age dates utilizing this method.

5.1.6.2.2.4 Chlorine-36. The potential of chlorine-36 to be used for age dating applications in hydrologic studies has been recognized for a number of years (Davis and DeWiest, 1967). Physical-detection limitations of available analytical instrumentation, however, have made the routine measurement of this isotope impractical. The development of new analytical techniques using tandem Van der Graf accelerators (such as at the University of Rochester) have recently made it practical to measure extremely low activities (i.e., one atom of chlorine-36 in 10^{14} atoms of chlorine).

Chlorine-36 is produced in the atmosphere by cosmic-ray bombardment. The isotope is long-lived, with a half-life of 3.08×10^5 years. Its long half-life, lack of apparent interferences, and conservative nature make chlorine-36 potentially useful in dating extremely old groundwater. If sufficient chlorine-36 exists in groundwater with little or no chlorine-36 production occurring in the subsurface (i.e., due to activation of chloride from neutrons released by the natural fission of uranium and thorium), then this isotope may be applied to date waters as old as 1.0×10^6 years.

At present, 10 chlorine analyses have been made on Columbia River basalt groundwaters beneath the Hanford Site. More data are needed, however, to successfully apply this method to deep-basalt hydrologic studies. Preliminary calculations indicate that the chlorine-36 method may prove particularly promising within the basalt aquifer systems.

A plot of depth below the top of basalt versus the chlorine-36 to chloride x 10^{-15} ratio in groundwater is shown in Figure 5-86. Although the data are from only three borehole sites (DC-6, -14, and -15), they do show a discernible trend. Deeper groundwaters tend to show a decrease in the chlorine-36 to chloride (total) ratio. This would be expected, since Grande Ronde Basalt groundwaters are older than the overlying groundwater. This trend, however, could also be explained by the fact that total chloride increases with depth in the basalt.

Because of the limited amount of available chlorine-36 data, more analyses are needed before quantitative interpretations can be made concerning the deep hydrology within the Columbia River basalts. In addition, mechanisms that control the in situ generation of chlorine-36 within basalts need to be examined. Whole-rock uranium analyses to be performed in the near future may provide additional insight regarding these generation processes.

9212495107 2

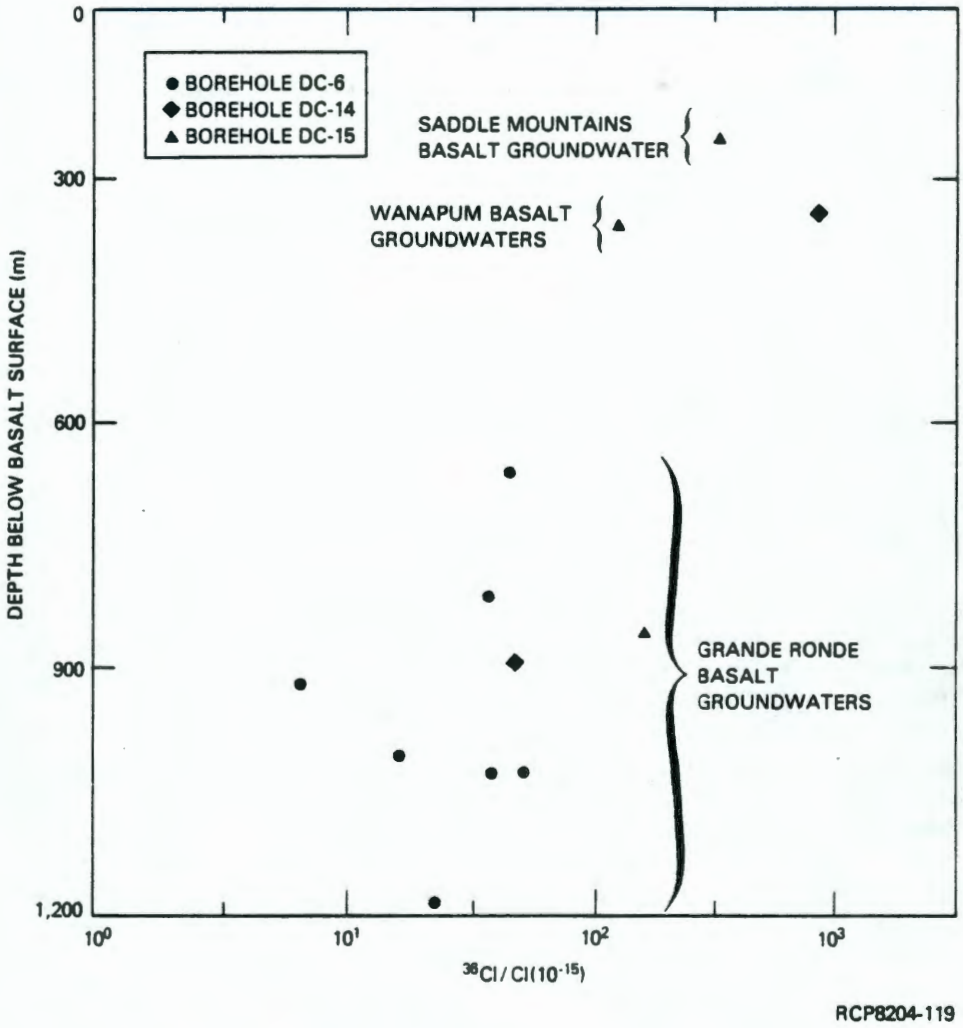

FIGURE 5-86. Distribution of Chlorine-36 to Total Chlorine with Depth for Selected Intervals Within the Columbia River Basalt Group.

5.1.7 Interrelationship of Hydrologic Systems

In this section, interrelationships between the various hydrologic systems within the Pasco Basin are discussed. Specifically, the degree of intercommunication between aquifer systems, as well as between aquifers and surface-water bodies, are examined.

5.1.7.1 Unconfined Aquifer. The hydrologic association of the unconfined aquifer with the Columbia River has been previously reported by a number of investigators (e.g., Newcomb et al., 1972; Gephart et al., 1979a). The

Columbia River forms a continuous (line-sink) discharge boundary for groundwater within the unconfined aquifer. Groundwater within this aquifer flows toward and discharges directly into the Columbia and Yakima Rivers and/or associated riverbank springs and seeps.

Due to the direct hydraulic communication between the unconfined aquifer and surface-water features, fluctuations in river-stage elevations have a profound influence on nearby water-level response within the unconfined aquifer. The hydrograph response for three wells completed in the unconfined aquifer and Columbia River elevation levels is shown in Figure 5-87. Examination of this figure indicates a close and direct association of hydrograph response to river-stage fluctuation. As expected, the amplitudes of the hydrograph responses are dampened, as well as slightly lagged, with increasing distance from the river.

Besides surface-water features, the unconfined aquifer has also been reported by Spane et al. (1980) to be in hydraulic communication with the uppermost confined aquifers of the Saddle Mountains Basalt beneath portions of the Hanford Site. Although the location(s) of hydraulic communication between the unconfined and upper confined systems is not precisely known, areas in the western section of the Hanford Site and along the southwestern edge of Gable Mountain are suspect. In these areas, overlying confining basalt flows (i.e., Elephant Mountain basalt) and/or lower Ringold Formations are not present, due to nondeposition and/or erosion. In the area immediately west and south of Gable Mountain Pond, hydraulic communication is believed to result from the presence of paleostream channels incised into the uppermost basalt formations.

While various hydrogeologic data are available that indicate some hydraulic communication, the most corroborative evidence is the presence of nitrate in groundwater within the Rattlesnake Ridge interbed at some boreholes near areas of suspected crossflow. Nitrate is a common constituent in unconfined groundwater and is the by-product of past waste-disposal practices at the Hanford Site (ERDA, 1975). The presence of nitrate at boreholes DB-14 (approximately 3 kilometers south of the 200 West Area) and DB-15 (approximately 2 kilometers east of the 200 East Area) is attributable to hydraulic communication and recharge of groundwater from the overlying unconfined aquifer.

5.1.7.2 Confined Aquifer. The association of confined aquifers with surface-water features and with other confined-aquifer systems within the Pasco Basin is discussed in this section. Large river systems are assumed to form dominant line-sink discharge boundaries for homogeneous, isotropic aquifer systems. Available hydraulic-head and hydrochemical data, however, suggest that the Columbia River does not act as a dominant discharge area along its entire course for confined-aquifer systems within the Pasco Basin (see Sections 5.1.4, 5.1.5, and 5.1.6).

Groundwater-flow patterns within the Mabton interbed were depicted in Figure 5-31. As shown, groundwater within the northern section of the Pasco Basin flow beneath the Columbia River toward a hydraulic low near Gable Mountain and Gable Butte.

9 2 1 2 4 9 5 1 0 7 4

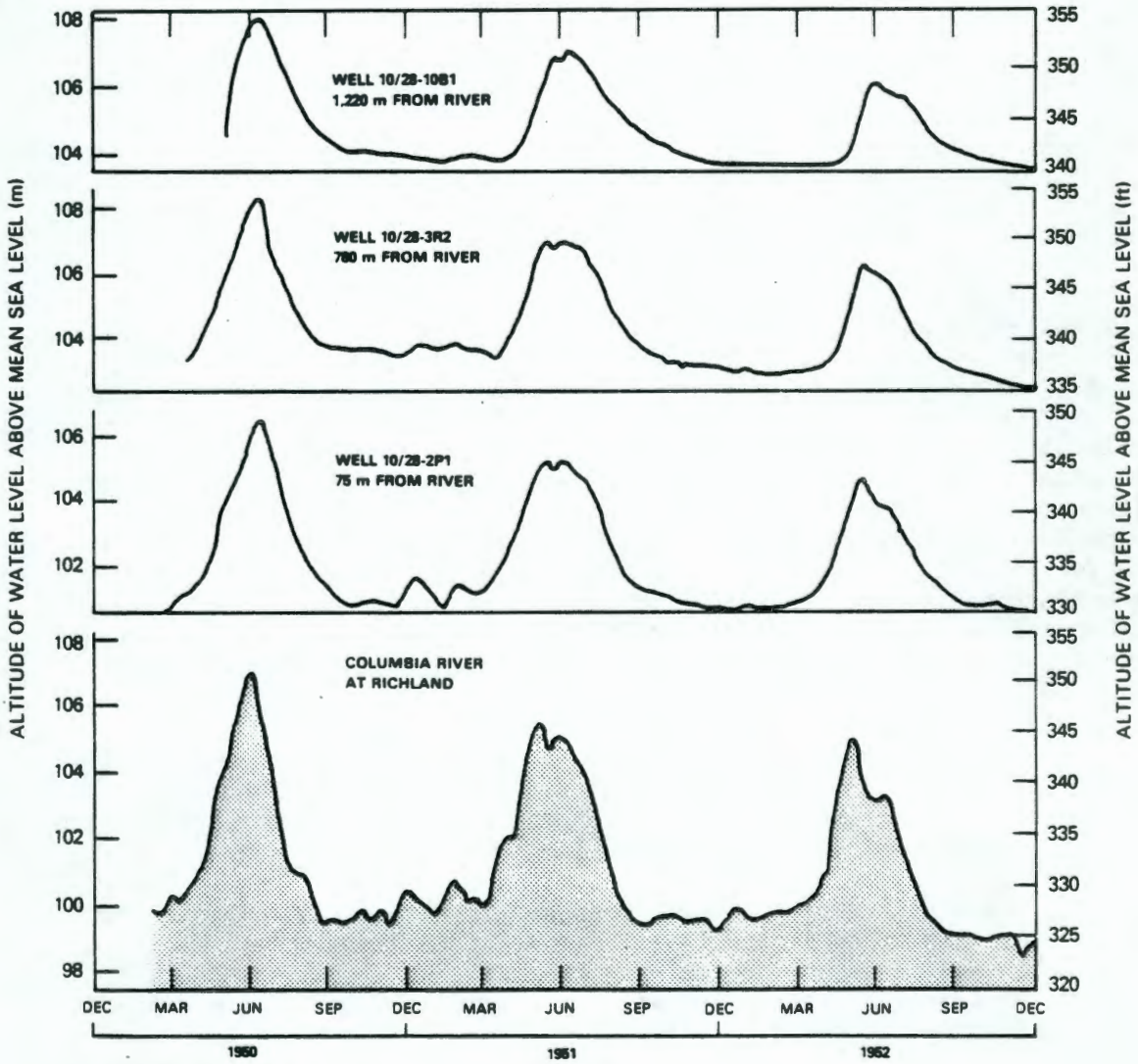

(ADAPTED FROM NEWCOMB et al., 1972)

RCP8204-120

FIGURE 5-87. Comparison of Columbia River Stage Fluctuations with Well Hydrograph Response in Three Unconfined-Aquifer Well Sites at the Hanford Site (adapted from Newcomb et al., 1972).

The vertical distribution of hydraulic head within the Columbia River Basalt Group at borehole DC-14, located adjacent to the Columbia River in the northern section of the Hanford Site, was depicted in Figure 5-38. As shown, hydraulic head increases significantly with depth to the lower Saddle Mountains Basalt. From the lower Saddle Mountains Basalt, hydraulic head decreases slightly with depth to the lower Wanapum Basalt. Near the lower Wanapum Basalt, hydraulic head decreases abruptly. Through the Grande Ronde Basalt, little head variation is shown with depth. The aforementioned description of hydraulic-head patterns at borehole DC-14 does not fit the distribution necessary for the Columbia River to be a dominant discharge area for basalt groundwaters. In fact, hydraulic head and hydrochemical patterns for lower Saddle Mountains to the Grande Ronde Basalts suggest that significant regional discharge is not occurring into the Columbia River adjacent to the Hanford Site.

The time-variant behavior of hydraulic head for confined aquifers in areas immediately adjacent to river systems at Hanford indicates no rapid hydraulic response as characteristic of the unconfined aquifer. For example, monthly streamflow rates for the Yakima and Columbia Rivers near the Hanford Site and two hydrographs for nearby boreholes completed in the Mabton interbed are given in Figure 5-88. Examination of this figure indicates that monthly variations in streamflow are not reflected by associated monthly hydraulic-head responses, even in the Mabton interbed, which is a relatively shallow unit 300 meters below ground surface. The lack of correlation concordance between streamflow and hydraulic-head patterns corroborates previously cited data which, contrary to the case of the unconfined aquifer, suggests that the Columbia River and the confined aquifers in the basalts are not in rapid hydraulic communication where depicted.

Available hydrochemical and isotopic data indicate the presence of several hydrochemical and isotopic shifts that appear coincident with major basalt formational contacts. For example, abrupt hydrochemical and isotopic breaks, which occur between Saddle Mountains and Wanapum Basalt groundwater, are discussed in Sections 5.1.5 and 5.1.6. These differences indicate the presence of different groundwater-flow-system characteristics for the two basalt formations (i.e., different recharge areas, histories, etc.). The abrupt nature of the hydrochemical and isotopic shift also suggests that little groundwater mixing is occurring across these formational contacts. As noted in previous sections, these hydrochemical breaks are evident in all of the deep boreholes drilled on the Hanford Site.

For example, selected hydrochemical data from borehole DC-15 are shown in Figure 5-89. This borehole is located next to the Columbia River in the southeast portion of the Hanford Site. In this borehole fluoride is one of several ionic species that can serve as a natural groundwater tracer. The fluoride concentration in the Saddle Mountains Basalt groundwaters is low (1 to 2 milligrams per liter). In the Wanapum, the fluoride content generally increases with depth. Fluoride concentrations in the Grande Ronde Basalt groundwaters are generally 10 milligrams per liter greater than in the Wanapum.

9 2 1 2 4 9 5 1 0 7 6

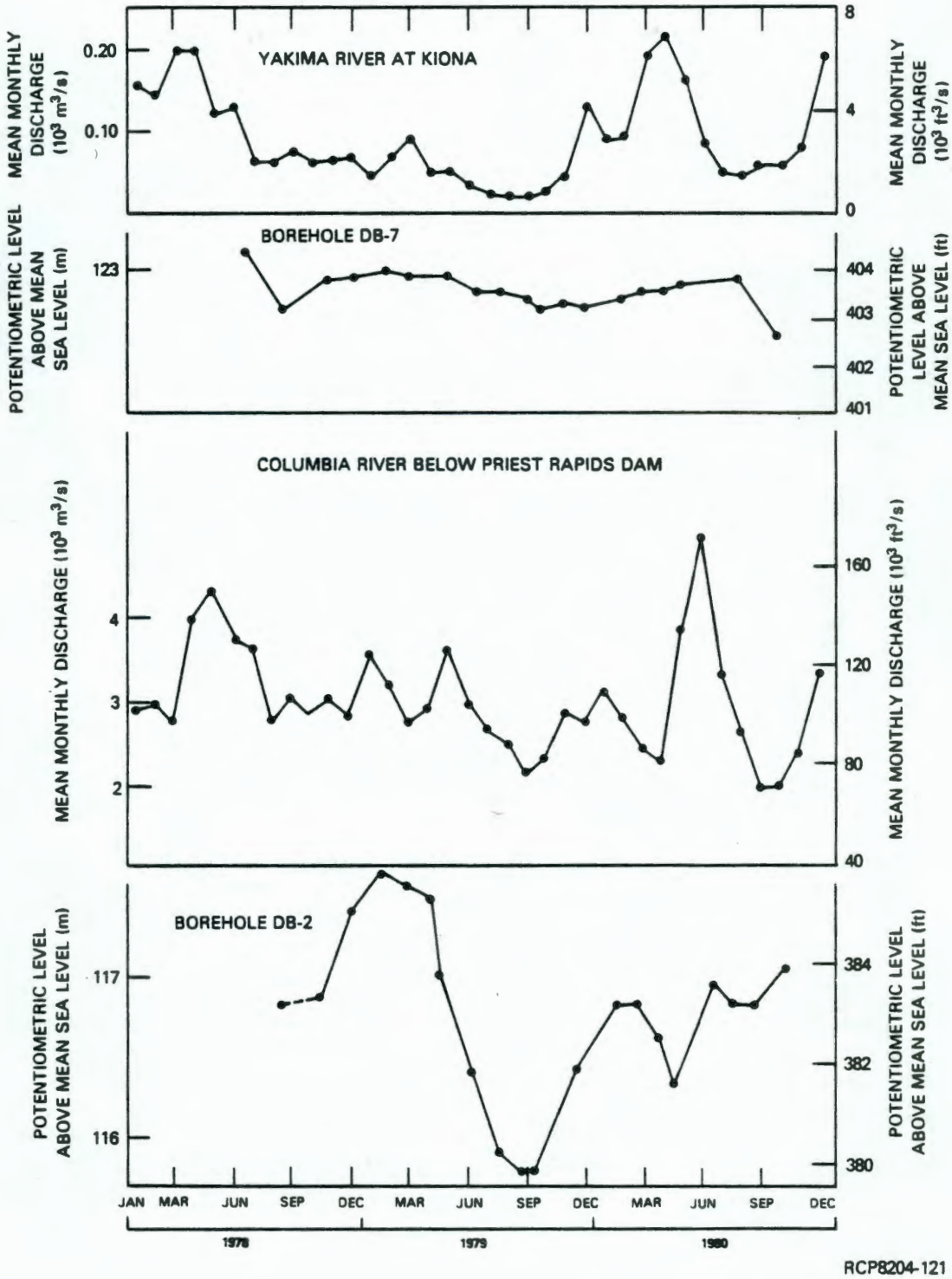

FIGURE 5-88. Streamflow Rates for the Yakima and Columbia Rivers Near the Hanford Site and Hydrographs for Two Nearby Boreholes.

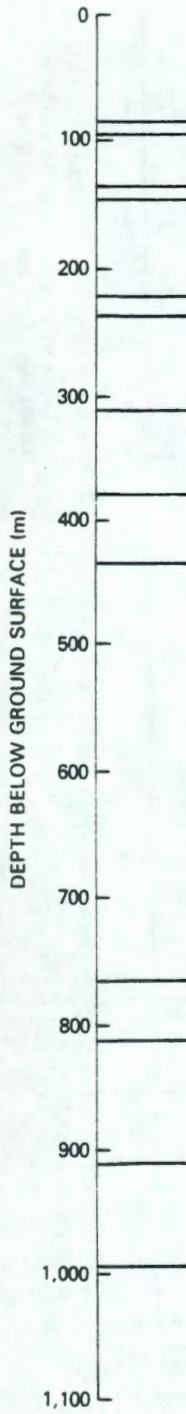

SAMPLING POINT		F (mg/L)[c]	δ^2H (% UNITS)	^{14}C % MODERN (YR BEFORE PRESENT)
LEVEY INTERBED	a	1.2	-145	12 (17,200)
RATTLESNAKE RIDGE INTERBED	a	1.0	-145	6.5 (22,000)
COLD CREEK INTERBED	a	1.1	-141	<1.4 (>34,300)
SADDLE MOUNTAINS BASALT				
MABTON INTERBED	a	2.0	-138	<1.6 (>33,500)
WANAPUM BASALT				
PRIEST RAPIDS				
ROZA	a	8.9	-139	5.9 (22,800)
	a	9.2	-137	6.7 (21,700)
FRENCHMAN SPRINGS	a	10.9	-137	<4.0 (>25,900)
	a	12.1	-137	<2.5 (>29,800)
	a	8.6	-139	<1.7 (>33,000)
GRANDE RONDE BASALT				
	a	11.5	-122	b
	a	18.4	-124	b
MIDDLE SENTINEL BLUFFS				
	a	17.5	-120	b
	a	22.9	-114	b
UMTANUM				
	a	23.5	-111	b
	a	22.7	-139	b

[a]SAMPLING POINT

[b]CARBON SOURCE TOO SMALL TO OBTAIN REASONABLE AGE DATE; THEREFORE, AGE ESTIMATED AT GREATER THAN 32,000 YEARS BEFORE PRESENT.

[c]FLUORIDE DETECTION LIMIT IS 0.1 mg/L.

RCP8204-122

FIGURE 5-89. Selected Hydrochemistry for Borehole DC-15.

Deuterium is enriched with depth. This indicates either that the paleoclimatic conditions at the recharge areas were different or that there is significant isotopic fractionation occurring with depth. However, deuterium is usually a very conservative isotope and temperatures greater than 50°C are normally needed to produce much fractionation. These temperatures are only attained at depths below about 1,000 meters.

Carbon-14 dates are given in both a percent modern value and a corrected age. The data generally indicate increasing age with depth. Groundwater samples collected in the Grande Ronde Basalt contain a carbon source that is very low, making age dating difficult. Carbonate equilibria within basalts are being studied to better evaluate these age determinations.

Dissolved-gas content also indicates the lack of significant vertical groundwater mixing at borehole DC-15. For example, within the zone 469 to 486 meters below ground surface, 65.7 percent of the dissolved gases are CH_4, while 33.8 percent are N_2. At approximately 60 meters below this (529 to 559 meters), 98.5 percent of the dissolved gases are N_2 with only 0.14 percent being CH_4.

Thus, specific ionic concentrations plus stable and radioisotopic data suggest the lack of significant vertical groundwater mixing as well as the existence of distinct flow systems at the DC-15 site. (The hydrochemical breaks for borehole DC-15 were previously shown in Figure 5-66.)

The hydrochemical and isotopic breaks evident within basalt groundwater appear areally at two different horizons. Within the Cold Creek syncline, the break occurs near the Saddle Mountains and Wanapum Basalt contact. Outside this syncline, the break is exhibited stratigraphically lower, near the Wanapum and Grande Ronde Basalt contact.

The specific reason for this difference is not presently understood. However, suspected vertical hydraulic conductivity and mixing of groundwater between the deeper, more mineralized Grande Ronde Basalt groundwater with the more dilute Wanapum Basalt groundwaters may be partly responsible. Such mixing may result from stratigraphic and/or structural discontinuities in localized areas. The potential for confined-aquifer communication along the Umtanum Ridge-Gable Mountain anticline was discussed in Section 5.1.4 and appears to be indicated by the presence of a hydraulic low (potential-discharge area) within the potentiometric map for the Mabton interbed. Areal and vertical hydraulic-head data are currently insufficient to evaluate the significance of this anticline on hydraulic communication in the area between confined aquifers within the Wanapum and Grande Ronde Basalts.

Available areal hydrochemical data for the upper Wanapum Basalt, however, suggest that mixing with deeper, more mineralized Grande Ronde Basalt groundwater may be occurring in the Gable Mountain region. For example, the hydrochemical pattern for groundwater within the Priest Rapids Member of the Wanapum Basalt at the Hanford Site is shown in Figure 5-90. Examination of the hydrochemical data indicates that Priest Rapids Member groundwater undergoes a hydrochemical-type change (i.e.,

9 2 1 2 4 9 5 1 0 7 9

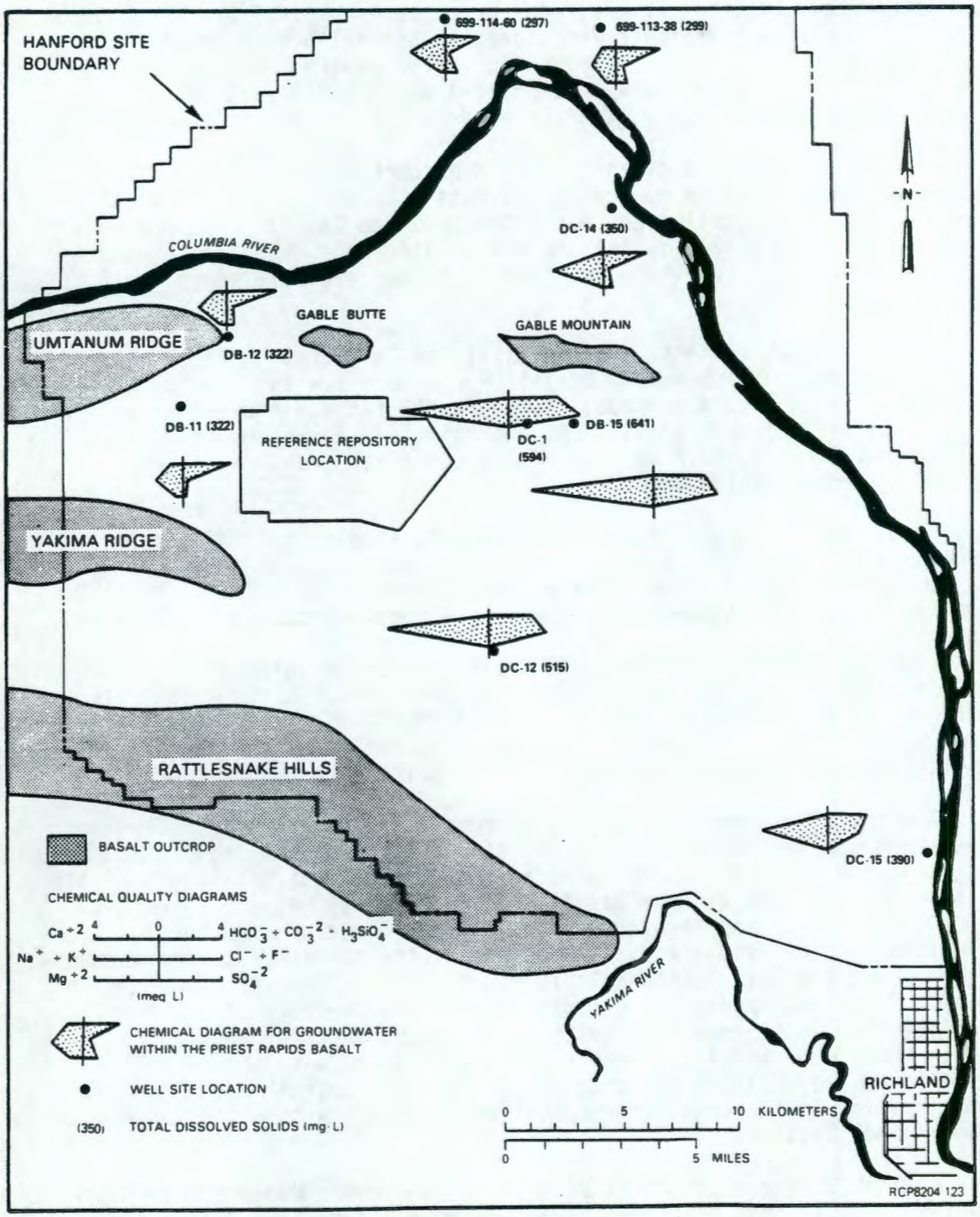

FIGURE 5-90. Areal Hydrochemical Data for Groundwater Within the Priest Rapids Member.

from sodium bicarbonate to sodium chloride) and becomes significantly more mineralized (i.e., from more than 300 to more than 600 milligrams per liter) south of Gable Mountain and east of DB-11. The impact of hydrochemical changes, attributable to mixing with deeper groundwaters, appears to decrease with distance away from this structural area. Additional hydrogeologic data are required, however, to quantitatively evaluate the impact and significance of these or other possible significant structures on the groundwater hydrology of deep basalt formations at the Hanford Site. An outline of the work required to accomplish this task is contained in Chapter 13, Work Element S.1.29.C.

5.1.8 Groundwater Velocity and Travel Times

Refer to Sections 12.4.1.1, 12.4.1.2, and 12.4.1.3 for groundwater velocity and travel time estimates.

5.1.9 Groundwater Uses

Detailed information on groundwater use within the Pasco Basin and the surrounding region can be found in several sources. Of principal interest to this section are reports by Bell and Leonhart (1980), Brown (1979), Dion and Lum (1977), Foxworthy (1979), GG/GLA (1981), Pacific Northwest River Basins Commission (1980), Stephan et al. (1979), and Wukelic et al. (1981). Additionally, numerous records are maintained in open file by state and federal agencies. In particular, the U.S. Geological Survey maintains a computerized file known as the Groundwater Site Inventory Data Base, which is a systematic digital collection of available data for permitted water wells. The BWIP has acquired digital tapes of these records corresponding to 15 counties in southeastern Washington and 4 counties in northeastern Oregon. This assemblage represents data for nearly 15,000 wells.

The matter of isolating water-use statistics for the Pasco Basin and vicinity is complicated by the lack of coincidence between physical and political boundaries. Statistical surveys performed by agencies tend to segregate data according to political divisions. For this reason, a heavy reliance was placed upon the Groundwater Site Inventory Data Base, which, because of its digital format, was better able to segregate groundwater-use data for the Pasco Basin area. It should be noted that, although this data base does not contain a complete record of all well data, its files are sufficiently complete to be considered representative of groundwater use within the Pasco Basin.

5.1.9.1 Principal Regional Groundwater Users. The Groundwater Site Inventory Data Base can be used to tally the number of wells within the region according to use designation. Although such statistics do not provide an evaluation of the quantities of water withdrawn, they can be useful in describing the dominant types of groundwater use within an area and

9 2 1 2 4 9 5 1 0 8 1

in generalizing well-construction characteristics. Such a data reduction for the Columbia Plateau and the Pasco Basin is provided in Table 5-44. Another reduction of the data in terms of generic groupings is given in Table 5-45. In reviewing these tables, it is noted that approximately 50 percent of the total number of wells within both the Columbia Plateau and the Pasco Basin are used for households (domestic); again, however, these numbers do not speak to the water volumes withdrawn, and it can be generalized that most of the wells are of relatively shallow depth (less than 150 meters). Agriculture represents one-third of the total number of wells. Industrial users are a comparatively small segment of the total number. As evident from the information given in Tables 5-44 and 5-45, the well-use distribution for the Pasco Basin is comparable to that of the Columbia Plateau as a whole.

The distribution of well uses according to selected depth intervals is shown in Figure 5-91. The histogram shows that approximately 65 percent of the wells reported in the Groundwater Site Inventory Data Base derive water from less than 60 meters below ground surface. For most locations, this depth interval may be considered to approximate the range of depth for the unconsolidated aquifers. The histogram also shows that approximately 50 percent of the wells in the Pasco Basin are used for domestic water supply.

A compilation of total groundwater quantities used in the Pasco Basin by agricultural (irrigation), municipal, industrial, and domestic groundwater users is given in Table 5-46. Figures given for agricultural and domestic groundwater users are based on 1980 data, and statistics cited for industrial and municipal groundwater users are based on 1975 data.

5.1.9.2 Hanford Groundwater Users. The principal groundwater uses within the Hanford Site are associated with the Fast Flux Test Facility and Pacific Northwest Laboratory. The Fast Flux Test Facility, a U.S. Department of Energy (DOE) research facility, operated by Hanford Engineering Development Laboratory, withdrew 350,000 cubic meters in 1980 from two wells located in the 400 Area. These wells supply water obtained from the unconfined aquifer. Pacific Northwest Laboratory, operated for the DOE by Battelle Memorial Institute, utilizes a spring on the side of Rattlesnake Mountain for a potable water source at its observatory. The springs originate from perched water tables in the Wanapum Basalt.

5.1.9.3 Impacts of Groundwater Use Activities. Throughout the Columbia Plateau region, long-term impacts of groundwater withdrawal have been predicted and observed (Foxworthy, 1979; Luzier and Burt, 1974; Luzier et al., 1968; Luzier and Skrivan, 1973; Foxworthy and Washburn, 1963; Jones and Ross, 1972; and Barker, 1979). Predictions indicate that there will be water-level declines of several meters per year in aquifers of the Wanapum and Grande Ronde Basalts. These declines are predicted for areas outside the Pasco Basin where the Wanapum and Grande Ronde Basalts are closer to the surface compared to within the Pasco Basin (Gephart et al., 1979a).

TABLE 5-44. Distribution of Wells According to Major Use Categories Within the Columbia Plateau and the Pasco Basin.

Wells	Human contact or consumption[a]	Industrial[b]	Agriculture or irrigation[c]	Total[d]
		Columbia Plateau		
Total number	7,409	312	3,158	10,879
Percentage in a given category	68.1	2.9	29.0	100
		Pasco Basin		
Total number	574	33	190	797
Percentage in a given category	72.0	4.1	23.8	100

[a]Includes wells designated as being used for bottling, domestic, medicinal, commercial, public supply, recreation, and institutional.

[b]Includes wells designated as being used for air conditioning, dewatering, fire fighting, and other industrial activities.

[c]Includes wells designated as being used for irrigation and stock watering.

[d]Includes only wells within the Groundwater Site Inventory Data Base having use designations. Wells designated as "other use" or as unused were excluded.

TABLE 5-45. Distribution of Wells Within the Columbia Plateau and Pasco Basin According to Use.

Use	Columbia Plateau wells		Pasco Basin wells	
	Total	%	Total	%
Air conditioning	2	0.0	0	0
Bottling	1	0.0	0	0
Commercial	19	0.2	2	0.2
Dewatering	19	0.2	0	0
Fire	24	0.2	0	0
Domestic	6,664	53.3	493	49.4
Irrigation	2,804	22.4	167	16.7
Medicinal	3	0.0	0	0
Industrial	267	2.1	33	3.3
Public supply	645	5.2	76	7.6
Recreation	5	0.0	1	0.1
Stock	354	2.8	23	2.3
Institutional	42	0.3	2	0.2
Unused	1,582	12.7	189	18.9
Other	64	0.5	12	1.2
Total	12,495		998	
Data base total[a]	14,566		1,820	
Percentage		85.8[b]		54.8[b]

[a]U.S. Geological Survey Groundwater Site Inventory Data Base.

[b]Percentage of the data base total for which water-use information is available.

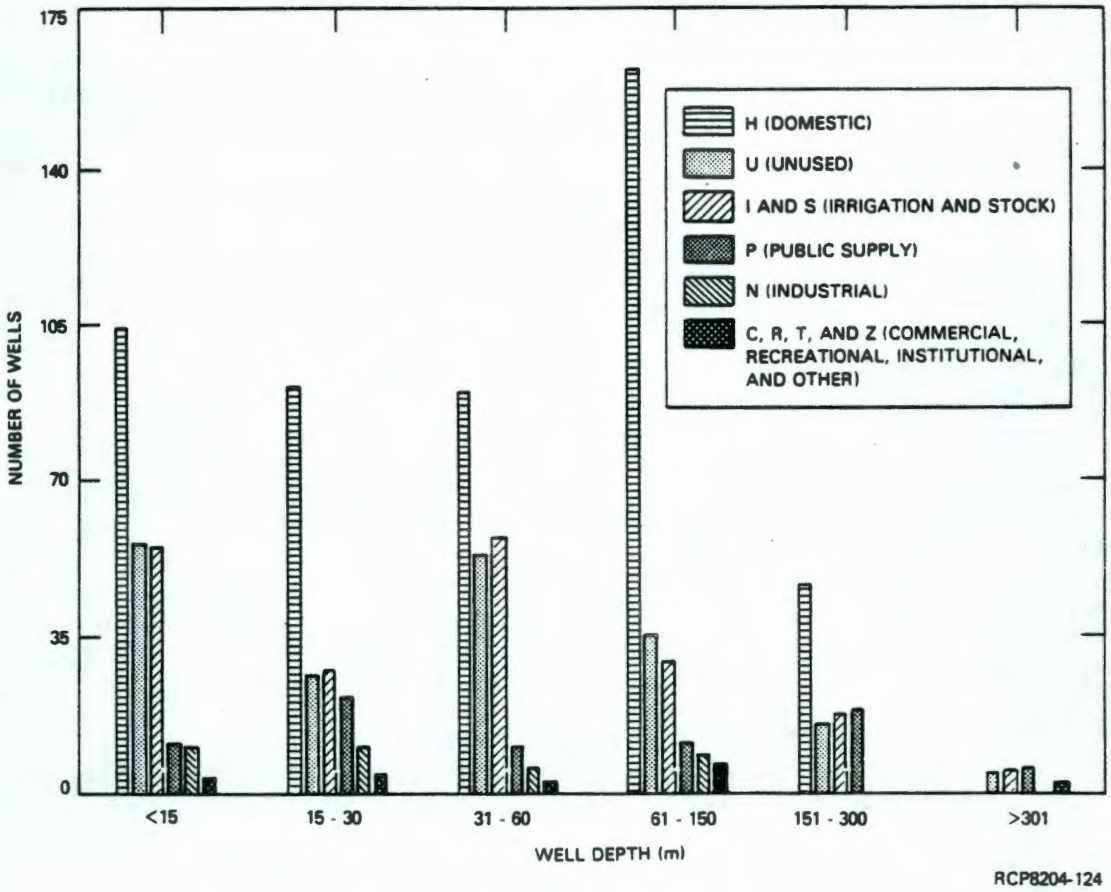

FIGURE 5-91. Frequency of Well-Use Types Listed by Depth Intervals.

TABLE 5-46. Groundwater Use in the Pasco Basin.

Groundwater users	Quantity (m^3)	Year
Agriculture (irrigation)	2.5×10^8	1980
Municipal (exclusive of industry)	1.1×10^7	1975
Industrial (self and municipally supplied)	1.9×10^{10}	1975
Domestic	7×10^5	1980

Within the Pasco Basin, a similar phenomenon is seen in the upper Cold Creek Valley, where irrigated agricultural activities have been expanding. The average water-level elevation within the Priest Rapids member in the Cold Creek Valley has declined about 10 meters over the last 3 years. In comparing present water levels in the Cold Creek Valley with figures reported by Newcomb (1961), the data show that over the last 50 years water levels have declined about 60 meters due to groundwater development.

In other areas, various activities have contributed to an increase in water-level elevations of "shallow" aquifers. Most notable is the Columbia Basin Irrigation Project, which lies north and northeast of the Pasco Basin and extends into the eastern and northern portions of the basin. Before irrigation began in the Columbia Basin Irrigation Project, there was little groundwater in the shallow sands and gravels above the basalt, and groundwater levels in the basalt were a few tens of meters below ground surface. After irrigation commenced in 1952, the upper confined aquifers of the Columbia River basalts experienced a water level rise. Water levels in typical wells drilled into the basalt aquifers underlying the Columbia Basin Irrigation Project have increased as much as 6 to 12 meters per year (Section 5.1.4). This water-level rise is due to leakage of excess irrigation water from overlying unconfined aquifers. It has been estimated that approximately 20 to 40 percent (depending on location within the project) of the water applied for irrigation undergoes deep percolation into the water table (Gephart et al., 1979a).

Artificial water recharge to the unconfined aquifer occurs at the Hanford Site from liquid-waste-disposal operations, mainly in the 200 Areas (Fig. 5-92). Although these discharges have been concentrated in the U, B, and Gable Mountain Ponds, the effects on the water levels in the unconfined aquifer have been widespread. Beneath the Hanford Site, two groundwater mounds have formed. Centered below U Pond, the water table has risen approximately 26 meters since the start of disposal operations in the mid-1940s. The peak of the eastern mound beneath B Pond indicates that the water table in this area has risen in excess of 6 meters.

Other activities that have had probable impact upon groundwater systems include several reservoirs and hydrographic modifications along the primary streams within the Columbia Plateau (Leonhart, 1980). Although the impacts of these projects generally vary according to area, their net result has been to raise the groundwater level. One project that has been studied rather intensely in this regard is that of the proposed Ben Franklin Dam, which, if constructed, would be sited along the Hanford reach of the Columbia River. The project is discussed further in Chapter 7.

9 2 1 2 4 9 5 1 0 8 6

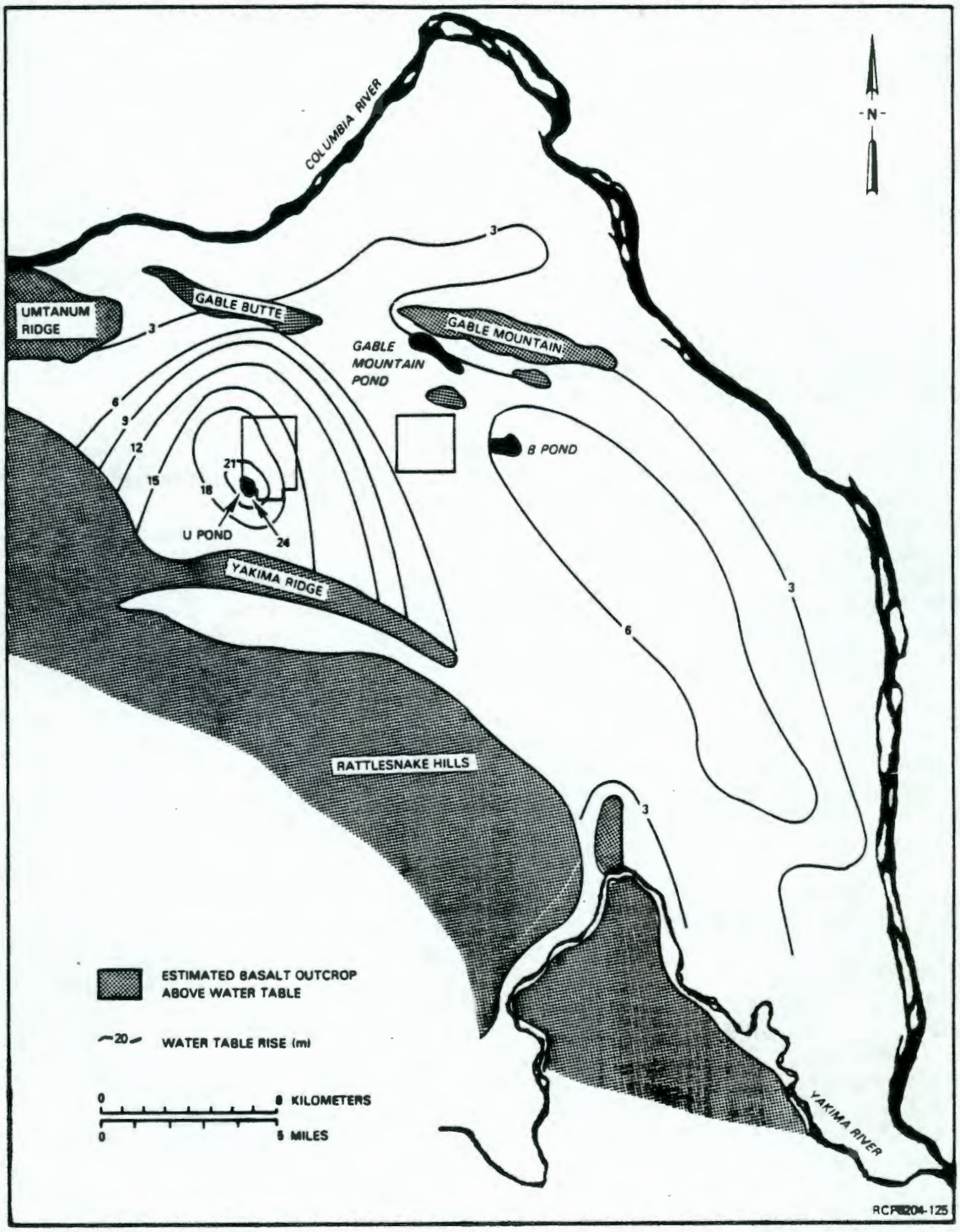

FIGURE 5-92. Water-Table Rise Beneath the Hanford Site, 1944-1978 (from Gephart et al., 1979a).

5.1.9.4 Typical Regional Well Construction.

5.1.9.4.1 Data Summary. A general evaluation of water-well construction practices within the Columbia Plateau may be obtained from two sources:

- The water-well reports available from the Washington State Department of Ecology, which are summarized within the framework of the U.S. Geological Survey Groundwater Site Inventory Data Base

- A recent survey of water-well-drilling contractors performed by the National Water Well Association (McCray, 1980; 1981).

Although these references summarized data on a national scale, data specifically for the "Columbia Lava Plateau of the Pacific Northwest" were made available to the BWIP by the National Water Well Association.

In reviewing these sources, it can be generalized that, for the Pasco Basin and most of the Columbia Plateau, wells completed in the sedimentary formations overlying the basalts are cased and screened (or open), whereas the wells that tap confined aquifers within the basalt are cased only through the sediments overlying the basalt. In many cases, the latter wells are completed in multiple zones (across sedimentary interbeds and/or flow tops) to maximize water yield. With regard to depth, most wells completed in sediments are less than 60 meters in depth and seldom deeper than 180 meters, owing to the thickness of the sediments within the Pasco Basin. Clustering of shallower wells (less than 60 meters) tends to coincide with population concentration, whereas a more dispersed distribution is seen for the deeper wells. This observation is partially explained by the fact that yield requirements and economics for household use tend to be satisfied by shallower wells, whereas well-production requirements to support irrigated agriculture necessitate the type of yield that can only be developed from the basalt aquifers.

5.1.9.5 Groundwater Management. Regulation of public groundwater within the State of Washington is an authority delegated to the Washington State Department of Ecology. Specifically, Chapter 90.44 of the Revised Code of Washington extends the applicability of the state surface-water statutes to the appropriation and beneficial use of groundwater within the state. The Washington State Department of Ecology has thus far designated two "groundwater management subareas" within the Columbia Plateau (i.e., Quincy and Odessa) under the authority of the Washington Administrative Code (WAC, 1973, Chapters 173-124; 173-128; 173-130; and 173-134) and is controlling groundwater development within certain portions of the Columbia Basin Project area (WAC, 1973, Chapter 508-14).

In general, the Washington State Department of Ecology's approach to regional groundwater management involves two activities:

(1) Reconnaissance and evaluation of groundwater conditions

(2) Regulation of use.

The reconnaissance and evaluation activities consist of annual mass (water-level) measurements that are plotted to determine the rates of water-level decline for various zones. This is used as a basis for management and regulation. As a rule of thumb, the Washington State Department of Ecology considers a situation serious when water-level declines in wells approach 9.2 meters within a 3-year period. This formula was established for the Odessa subarea and accounts for the type of agricultural practice there.

The Pasco Basin "straddles" the regional responsibility of the Washington State Department of Ecology. The Eastern Regional Office (Spokane, Washington) is responsible for groundwater-management activities east of the Columbia River, whereas the Central Regional Office (Yakima, Washington) handles the area west of the Columbia River to approximately the crest of the Cascade Range. The regulatory responsibility of the Washington State Department of Ecology does not include the Hanford Site because Hanford is a facility of the federal government.

Presently, the Eastern Regional Office of the Washington State Department of Ecology is considering a southward extension of the Odessa subarea, perhaps as far as Connell. This extension is being considered because recent water-level measurements within the area have shown declines approaching 3 meters per year. Another option being considered by the Washington State Department of Ecology is that of discontinuing groundwater withdrawals within areas where declines continue to be extreme. In contrast, there has been some consideration given to increasing permitted withdrawals in the Quincy subarea to alleviate continuing water-logging problems. The only other current management activity within the eastern region is directed toward managing the shallow unconfined aquifer in the Smith Canyon area (from Eltopia extending southwest toward the Snake River). Again, the management questions focus on artificially stored groundwaters associated with the Columbia Basin Project.

In the central region, the Washington State Department of Ecology is focusing its mass measurement activities on three areas: Moxee Valley (east of Yakima), the Naches-Tieton area (northwest of Yakima), and the lower Yakima Valley (downstream from Yakima). Within the Tri-Cities area, certain investigations have been aimed at determining the need to reserve blocks for potential future industrial developments by not permitting any additional withdrawals.

5.1.10 Reexamination of Conceptual Model

The primary basis for the conceptual hydrologic model utilized by the BWIP is described by Gephart et al. (1979a). The sophistication and level of detail in a conceptual model increase as field data become available to support or refute different concepts. The primary sources of hydrologic testing data and previous conceptual models developed are outlined in Table 5-47. New field-testing results are primarily addressed in Raymond and Tillson (1968), LaSala and Doty (1971), SAI (1978), Gephart et al. (1979a; 1979b), and Apps et al. (1979). Conceptual-model descriptions, sometimes accompanied by an extensive integration of existing data, are reported in LaSala et al. (1972), ARHCO (1976), Summers et al. (1978), Tanaka et al. (1979), Gephart et al. (1979a), and Dove et al. (1981).

The model presented by Gephart et al. (1979a) was the first major attempt to integrate the existing hydrologic-data base with the known geologic setting of the Pasco Basin and surrounding area. This model began identifying suspected recharge/discharge areas for shallow and deep basalts, examining the possibility that the Columbia River may not act as a direct line sink for all groundwater systems, suggesting a lack of major vertical mixing of groundwater in nonstructurally disrupted areas, and confirming that the basalt aquifers act as confined flow systems. However, only minimal data were available in 1979 regarding vertical or areal definitions of hydraulic heads, hydrochemistry, and hydrologic properties.

Between 1980 and 1982, several new boreholes (DB-15, DC-12, -14, -15, -16A, and RRL-2) were drilled and tested, and much additional data were collected from existing borehole sites (Section 5.1.1.1). Overviews and details of these data are given throughout this chapter.

Based on recent hydrologic information, the broad conceptual model of the flow systems beneath the Hanford Site, as noted by Gephart et al. (1979a), appears to remain supported. Many technical issues are yet unanswered; however, a plan to resolve these has been developed (Chapter 13).

Some of the key findings regarding the conceptual model are listed below and are addressed in several earlier subsections.

- Confined Flow Systems. The flow systems in the basalts are confined. This is supported by determination of storage coefficients, large horizontal hydraulic-conductivity contrasts between interbed or flow tops and the surrounding columnar basalts plus hydrochemical-type and isotopic-content shifts between individual aquifers. In addition, water-level responses in the basalts from barometric changes and distant seismic events support the concept of confined systems.

9 2 1 2 4 9 5 1 0 9 0

TABLE 5-47. Primary References for Hydrologic Testing Data and Conceptual Models. (Sheet 1 of 3)

Investigator(s), purpose of study, and work accomplished	Hydrologic properties			Hydraulic heads	Groundwater-recharge area	Groundwater-discharge area	Other
	Hydraulic conductivity (m/s)	Storativity	Porosity				
Raymond and Tillson (1968), Battelle, Pacific Northwest Laboratories In situ testing of existing borehole RSH-1. Funding from U.S. Atomic Energy Commission to measure hydrogeologic properties of basalt pertinent to radioactive waste-storage considerations. Results of geophysical logging, seven drill-stem tests, seven head measurements, and palynology studies reported.	Flow top 10^{-7} to 10^{-11} Columnar zones 10^{-10} to 10^{-11}	None given	Total porosity estimated from neutron logs to be 3 to 6% for the columnar zones.	Values questionable because the hole was open for 10 yr prior to testing. Data might suggest head decreases with depth.	Not addressed	Not addressed	Authors noted that water quality and drill-stem tests suggest that "there is a high degree of formation water isolation between major sections penetrated by the well."
LaSala and Doty (1971), U.S. Geological Survey In situ testing of existing borehole DC-1. Study done in support of U.S. Atomic Energy Commission's effort to evaluate feasibility of storing radioactive waste in basalt beneath the Hanford Site. Hydrologic tests conducted include 4 pumping, 11 fluid-injection/withdrawal, and 22 head measurements. Water samples were also collected.	Flow tops 10^{-8} to 10^{-9} No tests conducted solely across columnar zones	(Mostly composite tests) 10^{-3} to 10^{-6}	Total porosity values from core samples of flow tops ranged from 10 to 25%. Single core sample from columnar zone had 2% total porosity. Overall porosity values are poorly known.	Essentially no head gradient in Wanapum and upper Grande Ronde Basalts. Head decreases with depth below Umtanum flow of Grande Ronde Basalt.	Recharge occurs along the ridges and plateaus surrounding the Pasco Basin.	Discharge is to the Columbia River, perhaps near Wallula Gap south of the Hanford Site.	Distinct hydrochemical zonation exists. Shallow groundwaters are Na-HCO_3 chemical types, while deeper waters are Na-HCO_3,Cl types. This zonation plus small head gradients suggest, "that little, if any, vertical movement of water has occurred at the site of DC-1."
LaSala et al. (1972), U.S. Geological Survey Study of regional groundwater flow in south-central Washington as part of the the U.S. Atomic Energy Commission's research into managing radioactive wastes stored on the Hanford Site. Data are mostly from existing records and documentation. Composite groundwater samples collected from 22 existing shallow wells (150 to 450 m deep) distributed across south-central Washington.	Generally repeated data from LaSala and Doty (1971) for DC-1. Note that average hydraulic conductivity for flow tops in Wanapum and Grande Ronde Basalts was 10^{-6} m/s. "Flow tops make up a small percentage of the total basaltic rock section."			Groundwater flow controlled by topography, geologic structures, and placement of major rivers. Beneath the Hanford Site, groundwater moves southeast. Groundwater northeast and east of Hanford flows southwest toward the Columbia River.	Recharge occurs on the ridges and plateaus fringing the Pasco Basin. Water recharged during last glacial period.	Discharge is to the Columbia River south of the Hanford Site.	Intrabasin groundwater transfer not fully understood due to lack of data. Shallow basalt groundwaters of an Na,Mg-HCO_3 chemical type, while deeper groundwaters are of $NaHCO_3$,Cl type. Adjusted groundwater ages for shallow basalt waters beneath Hanford Site are 12,000 to 30,000 yr old.
ARHCO (1976), Atlantic Richfield Hanford Company Summarization of earlier studies found to be valuable in qualifying Columbia River basalt for storage of commercial radioactive waste. Work funded by the Office of Waste Isolation, Union Carbide Corporation.	Data reported principally from the above three reports, plus ERDA (1975).			Uppermost flow system in Saddle Mountains Basalt flows in east-to-southeast direction beneath Hanford Site. At DC-1, heads from 5 piezometers appear to indicate a slight upward gradient in Grande Ronde Basalt.	Recharge is from precipitation on ridges where basalt is exposed, surface runoff into coulees, and irrigation.	Discharge is to the Columbia River (no location specified).	Emphasized the need to drill and test in existing and new boreholes. Based upon these data, numerical models should be developed to better understand flow-system dynamics, as well as evaluating the potential for long-term isolation of radioactive waste in basalt. The authors noted that vertical exchange of groundwaters between different flow systems might occur along local areas near major anticlines.

TABLE 5-47. Primary References for Hydrologic Testing Data and Conceptual Models. (Sheet 2 of 3)

Investigator(s), purpose of study, and work accomplished	Hydrologic properties: Hydraulic conductivity (m/s)	Hydrologic properties: Storativity	Hydrologic properties: Porosity	Hydraulic heads	Groundwater-recharge area	Groundwater-discharge area	Other
SAI (1978), Science Applications, Inc. In situ hydrologic tests in borehole DC-2. Completed six injection tests and two head measurements. Study sponsored by the Basalt Waste Isolation Project, Rockwell Hanford Operations.	Flow tops 10^{-8} to 10^{-9} Columnar zones 10^{-8} to 10^{-13}	10^{-3} to 10^{-6}	Not addressed	Two head values across flow tops in Grande Ronde Basalt. Insufficient data to develop reliable gradient.	Not addressed	Not addressed	
Summers et al. (1978), W. K. Summers and Associates Compiled hydrologic data available from wells in Pasco Basin and summarized a conceptual model that might be inferred from these data. Study sponsored by the Basalt Waste Isolation Project, Rockwell Hanford Operations.	Flow tops and intervals 10^{-4} to 10^{-8} From composite of specific-capacity tests in irrigation wells.	10^{-3} to 10^{-4}	Referenced total porosity values given in Raymond and Tillson (1968), LaSala and Doty (1971), and Agapito et al. (1977). This last reference reports total porosities of 0.6 to 12.9% from 14 core analyses.	References existing data. From composite water levels in irrigation wells (available from Washington State Department of Ecology). The head decreases toward the Columbia and Snake Rivers. This implies groundwater flow is toward the major rivers.	Recharge occurs in the surrounding hills and mountains, plus irrigation.	Local and intermediate flow systems discharged to the nearby rivers. Regional flow system discharges west of the Pasco Basin.	Authors noted that hydrologic data within the Pasco Basin were very limited, except within the Hanford Site. Because of this, the conceptual model they developed, depicting local, intermediate, and regional flow systems, did not represent data in real space. Therefore, the model developed was, rather, that which might exist based upon hydrologic principles and the geologic setting.
Gephart et al. (1979a), Rockwell Hanford Operations Seven drill-stem tests in the Grande Ronde Basalt of borehole RSH-1. Caliper, 3-dimensional velocity, and seisviewer geophysical logs were run in selected zones. Study conducted by the Basalt Waste Isolation Project, Rockwell Hanford Operations.	Flow tops 10^{-7} to 10^{-11}	Not addressed	Not addressed	Not attempted. Reliable head measurements were not possible, since the borehole had been open for 20 yr prior to study.	Not addressed	Not addressed	Work conducted in 1977.
Tanaka et al. (1979), Washington State Department of Ecology Compiled existing hydrologic data for basalt in the Washington State portion of the Columbia Plateau. Study was sponsored by the Basalt Waste Isolation Project, Rockwell Hanford Operations.	Flow tops and interbeds 10^{-4} to 10^{-7} From composite of specific-capacity tests.	10^{-4} to 10^{-4}	Not addressed	Composite potentiometric maps suggest overall groundwater flow in Washington State portion of Columbia Plateau is toward the Pasco Basin.	Recharge is from precipitation on basalt outcrops, plus irrigation.	Discharge is to the Columbia River and its tributaries, where basalt and river are in direct contact. Water is also removed by irrigation pumping.	Intrabasin groundwater movement considered important.
Apps et al. (1979), Lawrence Berkeley Laboratory Six head measurements and one groundwater sample from Grande Ronde Basalt in borehole DC-2. Fifteen head measurements, 12 flow tests, and 1 water sample from Grande Ronde Basalt in borehole DC-6. Four head measurements from Wanapum Basalt in borehole DC-8. Study was sponsored by the U.S. Department of Energy and Basalt Waste Isolation Project, Rockwell Hanford Operations. This study was part of the feasibility study on the waste-isolation potential of basalt.	Flow tops 10^{-6} to 10^{-9}, mostly from composite flow testing	Referenced earlier reports.		Variable head pattern in Wanapum Basalt at DC-8 and Grande Ronde Basalt at DC-6. Slight head decrease with depth in Grande Ronde at DC-2. Available evidence suggests groundwater movement is parallel to the Cold Creek syncline.	Local recharge is from surrounding hills. Regional recharge is from areas outside the Pasco Basin.	Discharge is to the Columbia River at or south of the Tri-Cities.	Areas of extensive faulting and/or folding can form flow barriers to horizontal groundwater movement and maximum vertical permeability. Conceptual model consisted of two layers: an upper sedimentary layer (unconfined aquifer) and a lower layer consisting totally of basalt. Several groundwater-flow systems may exist in the basalts, each with its own geometry, recharge/discharge areas, etc. Deeper, regional systems could encompass much larger areas than shallower systems.

TABLE 5-47. Primary References for Hydrologic Testing Data and Conceptual Models. (Sheet 3 of 3)

Investigator(s), purpose of study, and work accomplished	Hydrologic properties			Hydraulic heads	Groundwater-recharge area	Groundwater-discharge area	Other
	Hydraulic conductivity (m/s)	Storativity	Porosity				
Gephart et al. (1979b), Rockwell Hanford Operations Integrated and evaluated existing hydrologic knowledge, specifically within the Pasco Basin, but also across the Washington State portion of the Columbia Plateau. New data reported included ~20 head measurements, 12 pumping tests, and hydrochemical analyses from 19, 12, and 3 well sites, respectively, in the Saddle Mountains, Wanapum, and Grande Ronde Basalts. Study conducted by the Basalt Waste Isolation Project, Rockwell Hanford Operations.	Flow tops and interbeds: Saddle Mountains 10^{-3} to 10^{-8} (median 10^{-5}) Wanapum 10^{-2} to 10^{-8} (median 10^{-3}) Grande Ronde 10^{-4} to 10^{-11} (median 10^{-8}) Columnar zones: Horizontal 10^{-9} to 10^{-14} (median 10^{-12}) Vertical 10^{-9} to 10^{-12} (model estimated)	Flow tops 10^{-3} to 10^{-4} Columnar zones 10^{-5} to 10^{-6}	Referenced same values as given by Raymond and Tillson (1968), LaSala and Doty (1971), and Agapito et al. (1977).	Potentiometric map for Mabton interbed suggests groundwater flows generally southwest across the Hanford Site. Composite potentiometric head maps for the Saddle Mountains and Wanapum Basalts across the Columbia Plateau indicate groundwater flow is toward the Pasco Basin. Within the Hanford Site, it was suggested that little head gradient existed in the Wanapum or upper Grande Ronde Basalt. Data also suggested that the Umtanum Ridge-Gable Mountain anticline forms a structural barrier to groundwater flow.	The Saddle Mountains Basalts are recharged from precipitation falling on the basalt outcrops rimming the Pasco Basin. Wanapum and Grande Ronde Basalts are recharged both locally and from surrounding basins. Artificial recharge important in areas of extensive irrigation.	Shallow flow systems discharge to the unconfined aquifer and to major rivers. Deeper, regional systems in the Wanapum and Grande Ronde Basalts discharge to rivers south of the Hanford Site, most likely near Wallula Gap.	The overall conceptual model consisted of an upper unconfined aquifer overlying confined aquifers within each of the principal basalt formations. These confined systems were thought to be categorized as local, intermediate, and regional systems. Major hydrochemical differences are evident between the Saddle Mountains and Grande Ronde groundwaters. The columnar zones of basalt flows act as low-permeability aquitards, separating higher permeable interbeds and flow tops. Little vertical groundwater mixing exists between different flow systems, except along anticlines, near major faulting, or where erosion has worn away the confining basalt units.
Dove et al. (1981), Pacific Northwest Laboratory A technical demonstration of the Assessment of Effectiveness of Geologic Isolation Systems computer-modeling technology. The study was conducted by Pacific Northwest Laboratory and sponsored by the Office of Nuclear Waste Isolation, which is managed by Battelle Memorial Institute for the U.S. Department of Energy. All data used for these simulations were published prior to 1980.	Referenced existing reports.			Composite potentiometric maps are based upon Tanaka et al. (1979). Overall groundwater-flow directions from the Columbia Plateau are toward the Pasco Basin.	Recharge is from throughout the Columbia Plateau wherever precipitation infiltrates the basalt.	Shallow and deep flow systems discharge into the unconfined aquifer and the major rivers within the Pasco Basin.	Two conceptual models were developed. The regional model for the Columbia Plateau consisted of three layers: unconfined aquifer and surface-water bodies, a composite Saddle Mountains/Wanapum layer, and a Grande Ronde layer. The Pasco Basin model had four layers: an unconfined aquifer and surface-water layer, plus three basalt layers corresponding to the Saddle Mountains, Wanapum, and Grande Ronde Basalts. Structural discontinuities were considered important to the overall understanding of groundwater flow.

- Lack of Significant Vertical Groundwater Mixing. The distinct hydrochemical types and isotopic breaks and contrast in hydraulic conductivities of flow tops versus columnar zones suggest that little vertical groundwater mixing is occurring between shallow and deep flow systems in non-structurally deformed areas. Otherwise, the waters would be more homogeneous and in areas of suspected discharge (e.g., the Columbia River), the waters would be progressively older, isotopically heavier, and have higher total dissolved contents progressing toward the surface. In addition, in many locations the vertical hydraulic heads suggest mostly lateral groundwater movement. Some vertical groundwater mixing is believed to take place along major geologic structures such as the Umtanum Ridge-Gable Mountain anticline. Future hydrologic and hydrochemical modeling will address these concepts.

- Groundwater Discharge to the Columbia River. Boreholes DC-14 and -15 were drilled adjacent to the Columbia River for examining possible regional discharge from the deep aquifers to the river. As noted in Sections 5.1.4, 5.1.5, and 5.1.6, the hydraulic heads and groundwater chemistries do not support the concept of major groundwater discharge from the deep basalts into the Columbia River at the sites tested. The principal discharge area for the deep basalts is still suspected to be south of the Hanford Site.

- Distinct Groundwater-Flow Systems. The location and extent of recharge or discharge into the Saddle Mountains, Wanapum, or Grande Ronde Basalt can be debated, but the distinct hydrochemical signatures of the groundwaters in the basalts appear to identify individual flow systems. The shallow local system appears to lie within the Saddle Mountains Basalt and the deep regional system within the Grande Ronde Basalt. The Wanapum Basalt is most closely associated with the shallow system except south of the Umtanum Ridge-Gable Mountain anticline where deeper, more mineralized waters occur in the Wanapum Basalt.

- Interbeds. The hydrologic properties of sedimentary interbeds occur within the normal distribution of permeable units tested within the Saddle Mountains or Wanapum Basalts; e.g., hydraulic conductivity is predominantly 10^{-6} to 10^{-4} meters per second. Additionally, hydrochemical breaks occur both across the Mabton interbed (the lowermost interbed in the Saddle Mountains Basalt) and in stratigraphically lower zones. The presence of interbeds has no discernible influence on vertical-head distributions. Thus, interbeds do not appear to form a significant hydraulic barrier or impediment to vertical groundwater movement. The principal confining units in the basalts are the low-permeability columnar zones of individual basalt flows.

9 2 1 2 4 9 5 1 0 9 4

- Structural Influences. The structural discontinuity trending north between the Cold Creek Valley and the reference repository location has a significant influence on local hydraulic heads and, therefore, groundwater-flow directions. The same is suggested for the Umtanum Ridge-Gable Mountain anticline. Such structural elements may also permit increased vertical movement of groundwater in localized areas, since associated fracturing is a secondary feature cutting across numerous basalt flows. Therefore, it is and will be important to understand the influence that structural discontinuities have on groundwater flow paths near the reference repository location.

- Groundwater Flow Directions. The overall groundwater flow direction for both shallow and deep basalts in the Cold Creek syncline is toward the southeast. Because of a hydraulic low near the Umtanum Ridge-Gable Mountain anticline, shallow groundwaters from the northern portion of the reference repository location may flow north rather than east to southeast; whether the hydraulic low extends to the Wanapum and Grande Ronde Basalts is an unanswered question.

- Groundwater Flow Paths. Lateral groundwater movement occurs within sedimentary interbeds and flow tops. Vertical groundwater leakage between different permeable zones takes place across the interiors of basalt flows though the extent of such leakage is presently unknown. The overall quantity of groundwater leakage across these basalt interiors is considered minimal compared to the groundwater quantity moving laterally through zones of higher permeability.

  It is presently assumed that the vertical conductivity of the basalt interiors is close to the horizontal conductivity values (less than or equal to 10^{-12} meters per second) already measured across flow interiors. Therefore, since there exists a several order-of-magnitude difference between the conductivities of flow interiors and flow tops/interbeds, the predominant quantity of groundwater movement in basalts would be laterally through these flow tops and interbeds. This concept supports the assumption that little vertical groundwater mixing occurs between flow systems (in geologically undisturbed areas).

9 2 1 2 4 9 5 1 0 9 5

THIS PAGE INTENTIONALLY
LEFT BLANK

5.2 SITE HYDROGEOLOGIC SYSTEM

This section contains information on the anticipated hydrogeology of the reference repository location. Where applicable, references are given to data presented earlier in this chapter.

5.2.1 Hydrologic Characteristics

Baseline hydraulic-property data from wells within the reference repository location are limited to the unconfined aquifer. Estimates of hydraulic characteristics (for the Columbia River basalts within the reference repository location) presented in this section are based on data contained in Section 5.1.3.

5.2.1.1 Unconfined Aquifers. Hydraulic characteristics for the unconfined aquifer are available for three well sites within the reference repository location. The location of these sites is shown in Figure 5-93. Hydraulic properties determined for the unconfined aquifer at these well sites are presented in Table 5-48. For comparison purposes, the mean and range of hydraulic-property values for the unconfined aquifer from the entire Hanford Site are also included. Pertinent well construction details for the individual well sites are contained in McGhan and Damschen (1979).

Examination of Table 5-48 indicates that transmissivity and equivalent hydraulic-conductivity values for the three unconfined-aquifer test sites in the reference repository location fall within the range of values listed for the entire Hanford Site. However, because of the limited amount of onsite hydraulic-property data, values for the unconfined aquifer within the reference repository location are likely to vary over a range similar to that reported for the entire Hanford Site.

The storativity value available within the reference repository location and the range of 10^{-2} to 10^{-1} cited for the entire Hanford Site fall within the range commonly cited by Heath and Trainer (1968) for unconfined aquifers. No effective-porosity values are currently available; however, values of less than 10 percent are expected.

5.2.1.2 Columbia River Basalts. Hydraulic-property data currently available in the reference repository location for confined aquifers within the Columbia River basalts are from boreholes RRL-2 and DC-16A as addressed in Sections 5.1.3 and 5.1.4. Information presented in this section for anticipated conditions in the reference repository location is based on these data as well as from other boreholes within the Cold Creek syncline. Plans for the acquisition of additional hydraulic-property data within the reference repository location are discussed in Chapter 13.

As discussed, confined aquifer systems within the Columbia River basalts consist of intercalated sedimentary interbeds and basalt interflow zones. Hydraulic properties for sedimentary interbeds are attributable principally to primary processes. Hydraulic properties for flow tops, in contrast, are strongly dependent on secondary processes (i.e., degree of brecciation, fracturing, secondary mineralization, etc.).

9 2 1 2 4 9 5 1 0 9 6

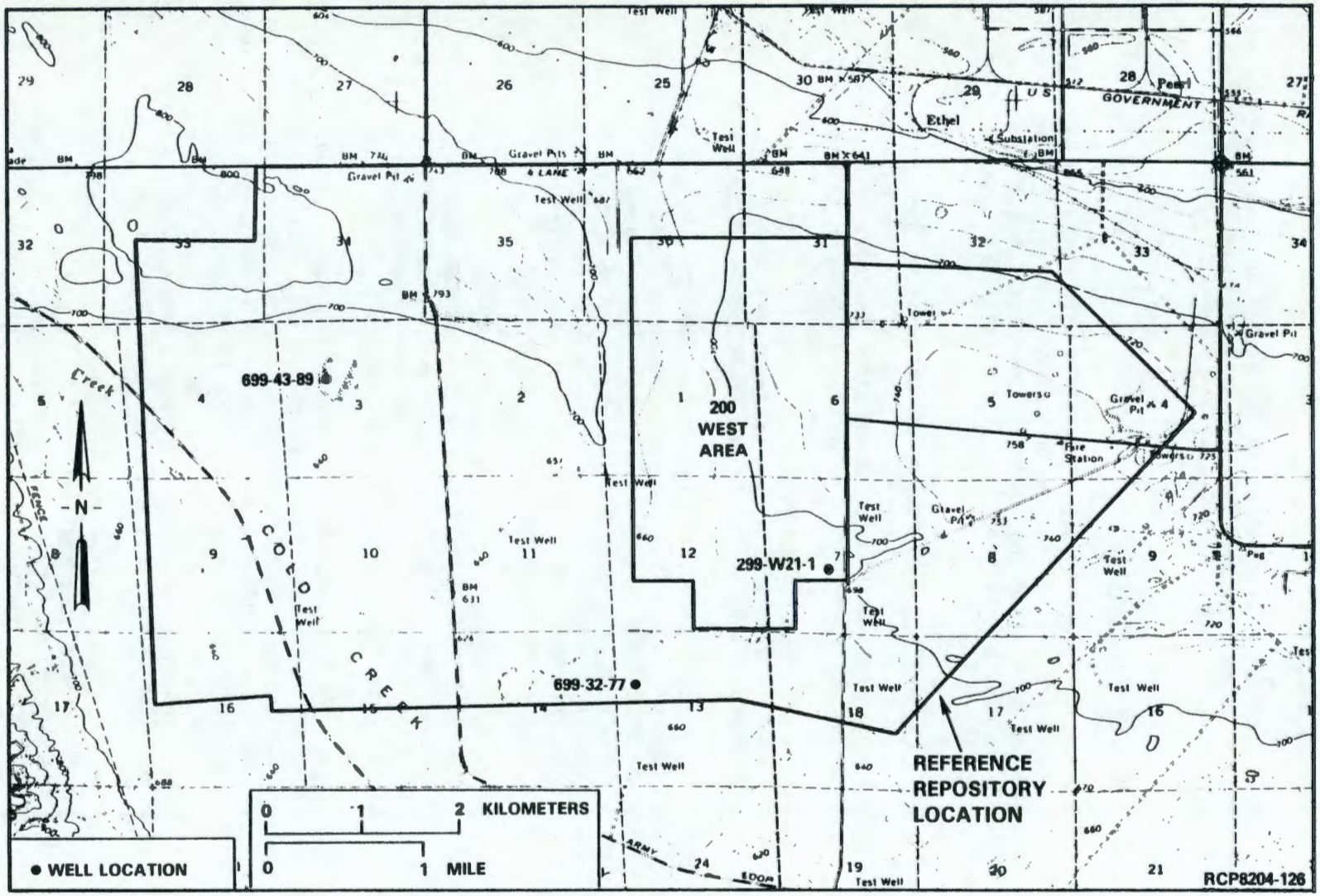

FIGURE 5-93. Location of Unconfined-Aquifer Test Sites Within the Reference Repository Location.

TABLE 5-48. Hydraulic-Property Values for the Unconfined Aquifer Within the Reference Repository Location and the Entire Hanford Site.

Hanford well site coordinates	Transmissivity (m^2/s)	Equivalent hydraulic conductivity (m/s)	Storativity (dimensionless)
299-W21-1	3.1×10^{-2}	5.3×10^{-4}	--
699-32-77	6.1×10^{-2}	9.2×10^{-4}	--
699-43-89	2.0×10^{-2}	3.0×10^{-4}	0.016
Entire Hanford Site*	($<10^{-3}$ to 10)	($<10^{-5}$ to 10^{-2})	(0.01 to 0.1)

*Values obtained from 38 test wells; range of values shown in parentheses.

Expected ranges in hydraulic-property values for confined-aquifer systems of the Columbia River basalts are presented in Table 5-49. This table indicates that the equivalent hydraulic conductivity is anticipated to vary over a wide range when comparing all flow tops. Values of hydraulic conductivity for individual flow tops are not expected to vary as widely. The diversity in hydraulic properties is a function of the degree of brecciation and secondary mineralization within the flow top and the degree of sorting and presence of clay and tuffaceous zones within sedimentary interbeds.

TABLE 5-49. Expected Range and Mean of Hydraulic-Property Values for the Columbia River Basalt Group Within the Reference Repository Location

Hydro-geologic unit	Equivalent hydraulic conductivity (m/s)		Storativity (dimensionless)		Effective porosity (%)
	Range	Mean	Range	Mean	
Interbed	10^{-9} to 10^{-4}	10^{-5}	10^{-3} to 10^{-4}	10^{-3}	<10
Flow top	10^{-10} to 10^{-2}	10^{-6}	10^{-3} to 10^{-6}	10^{-4}	<5
Entablature/ colonnade	10^{-14} to 10^{-10}	10^{-12}	--	10^{-6}	<1

9 2 1 2 4 9 5 1 0 9 8

Storativity values are expected to vary over 3 orders of magnitude (i.e., 10^{-3} to 10^{-6}) and fall within the range commonly cited for confined-aquifer systems. Estimates of effective porosity are extremely qualitative at present, but are anticipated to be less than 10 percent for sedimentary interbeds and less than 5 percent for flow tops.

The dense entablature and colonnade sections of basalt flows comprise the confining layers for the confined-aquifer systems. Hydraulic property values for these zones are expected to be considerably lower than for flow tops. As shown in Table 5-49, the mean equivalent hydraulic-conductivity values for entablature/colonnade zones are anticipated to be about 5 orders of magnitude lower than the mean value for flow tops. Estimates of storativity and effective porosity are qualitative at present, but are anticipated to be less than or equal to 10^{-6} and less than 1 percent, respectively.

5.2.2 Potentiometric Levels

Baseline potentiometric data obtained from boreholes within the reference repository location are mostly limited to geologic formations of the unconfined aquifer. Anticipated potentiometric conditions for Columbia River basalt aquifers within the reference repository location are based on the heads reported for boreholes RRL-2 and DC-16A (Section 5.1.4.2), as wells extrapolated data from other boreholes located in the Cold Creek syncline.

5.2.2.1 Unconfined Aquifer. Baseline potentiometric data for the unconfined aquifer are available for 33 well sites within the reference repository location. The location of these and surrounding well sites is shown in Figure 5-94. Potentiometric levels are monitored at these sites on a semiannual frequency or less. These measurements are reported in annual reports by the BWIP. Pertinent construction details for the individual well sites are contained in McGhan and Damschen (1979).

The potentiometric map for the unconfined aquifer within and adjacent to the reference repository location is shown in Figure 5-94. Examination of this figure indicates that synthetic recharge within the 200 West Area has a significant effect on the unconfined-aquifer potentiometric pattern. Due to the dominant recharge mound, groundwater flows radially from the 200 West Area. The major areal hydraulic gradient across the reference repository location, however, suggests that groundwater flows principally in a northeasterly to southeasterly direction.

Bierschenk (1957) and Gephart et al. (1979a) report that water levels within the unconfined aquifer in the reference repository location have increased between 10 and 25 meters since water disposal began in the mid-1940s. The areal extent and magnitude of water-table rise attributable to this practice is shown in Figure 5-95. As shown, the greatest rise in the water table is observed in the southwest corner of the 200 West Area, near the U Pond disposal facility.

9 2 1 2 4 9 5 1 0 9 9

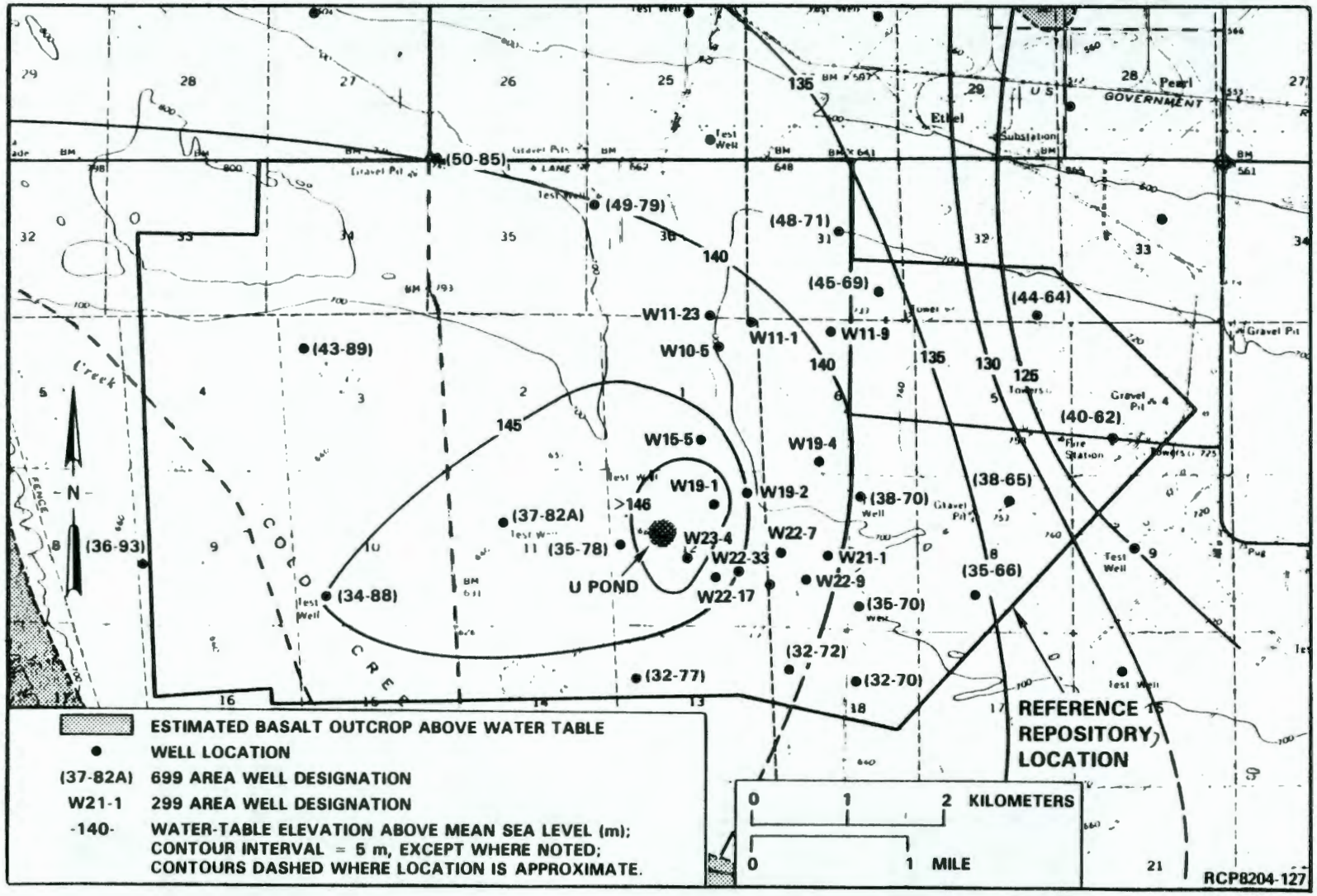

FIGURE 5-94. Water-Table Map for the Unconfined Aquifer Within the Reference Repository Location.

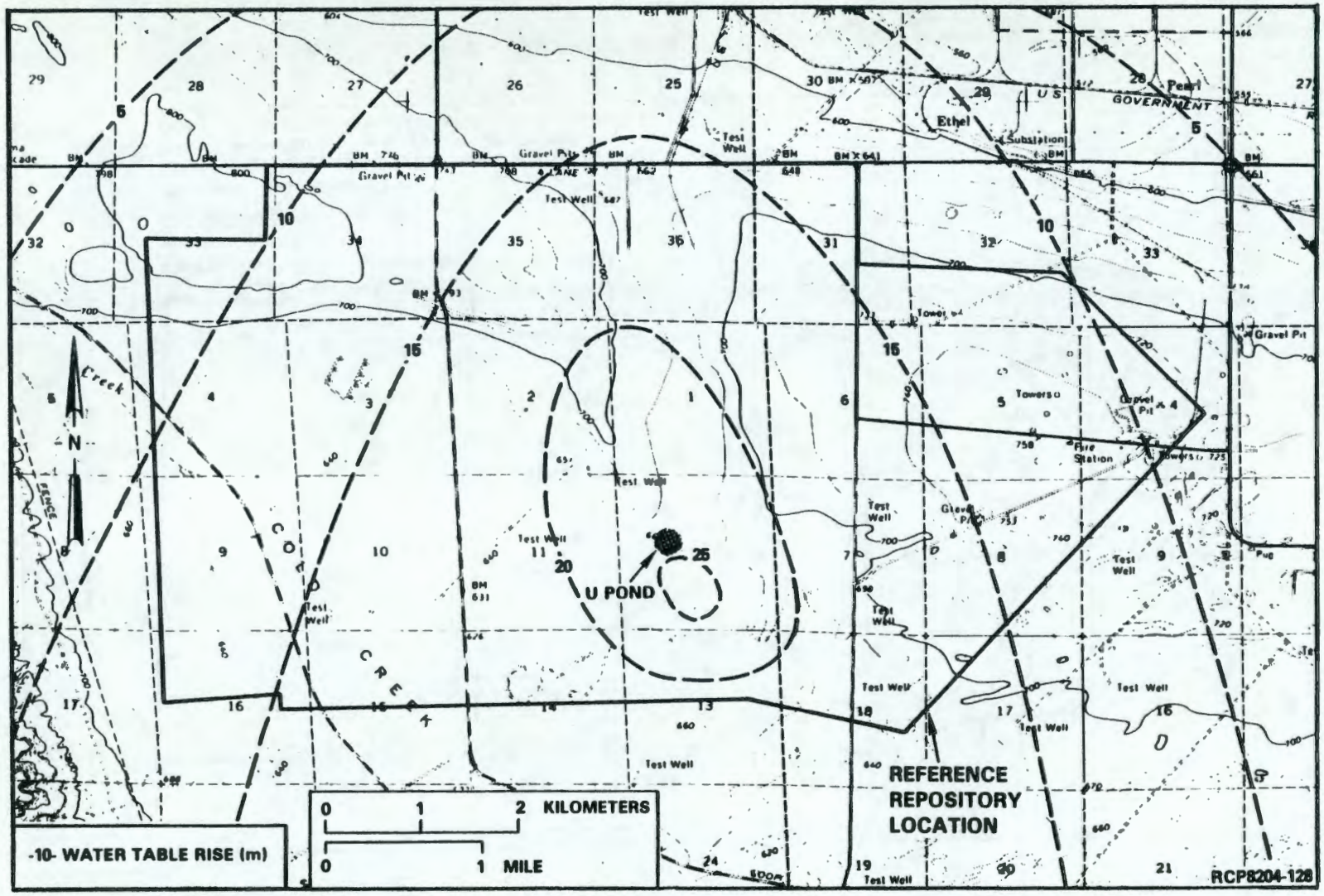

FIGURE 5-95. Water-Table Rise Within the Reference Repository Location Attributable to Water Disposal Activities (adapted from Gephart et al., 1979d).

An estimated water-table map for pre-waste-disposal conditions is shown in Figure 5-96. The map was generated by projecting back water-level data acquired between 1948 and 1952. The water-table contours indicate that a general eastward flow direction would be established if water-disposal activities were to cease in the reference repository location.

As stated previously, seasonal water-level fluctuations in the unconfined aquifer at the Hanford Site are primarily a function of the magnitude and proximity to recharge areas. Recharge factors for the unconfined aquifer include natural and synthetic sources, as well as surface-water/unconfined-aquifer interrelationships (i.e., riverbank storage). The reference repository location lies outside the boundary of recognized bank storage within the unconfined aquifer, as described by Newcomb et al. (1972). Therefore, no discernible water-table response due to Columbia and/or Yakima River stage fluctuations would be expected in this area.

Natural recharge sources to the unconfined aquifer from intrabasin areas peripheral to the Hanford Site (i.e., Rattlesnake Hills, Yakima Ridge, etc.) are believed to contribute only a small amount of the total annual recharge to the aquifer system (Newcomb et al., 1972). Therefore, no significant seasonal water-level fluctuation in the reference repository location would be expected in the unconfined aquifer from intrabasin recharge sources.

By far the most significant source of recharge to the unconfined aquifer in the Hanford Site, and specifically in the reference repository location, is from synthetic recharge sources. As shown previously in Section 5.1.4, water-disposal practices in the 200 West Area have produced a pronounced effect on water-level response in the unconfined aquifer.

In aquifer systems dominated by a single source of recharge, water-level response is a function of distance to the source area as well as the manner in which recharge is distributed with time. Water recharge from the 200 West Area is expected to be relatively uniform during the year, but may display significant year-to-year variability. This annual variability would be readily reflected in water-level response in areas adjacent to the recharge source. The effects of annual-recharge variability would be dampened with distance from the recharge area.

The response in water levels within the reference repository location, for wells adjacent to and distant from disposal areas in the 200 West Area, is shown in Figure 5-97. As expected, the hydrograph for well 299-W19-1, which is adjacent to the U Pond disposal area, displays minor seasonal and discernible annual fluctuation. In contrast, a more distant well (e.g., 699-43-89) displays a relatively uniform seasonal and annual pattern after 1969. Prior to 1969, water levels at this distance were still equilibrating to the initiation of water disposal in the 200 West Area.

9 2 1 2 4 9 5 1 1 0 2

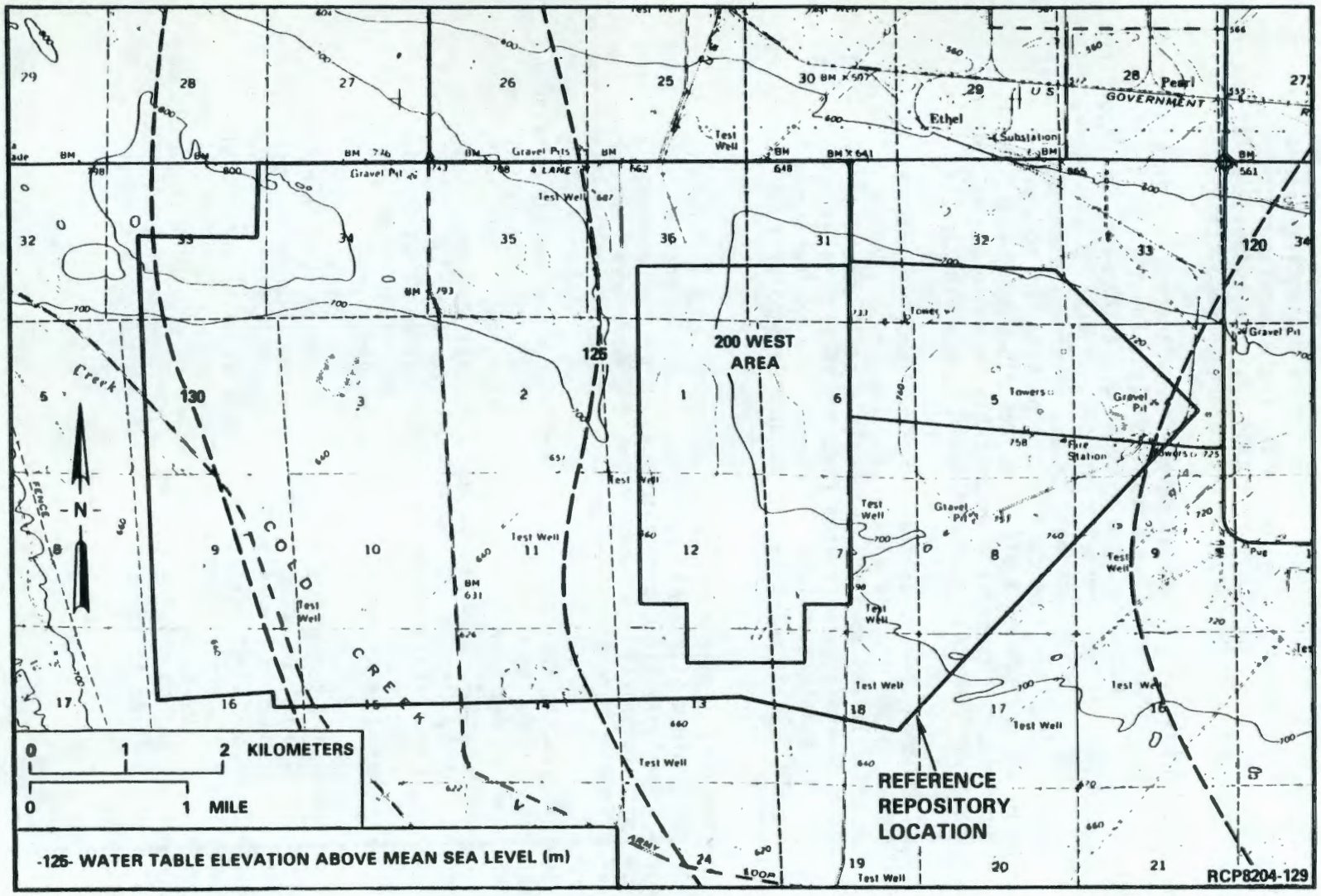

FIGURE 5-96. Estimated 1944 Water-Table Map Within the Reference Repository Location Prior to Water Disposal Activities (adapted from Gephart et al., 1979a).

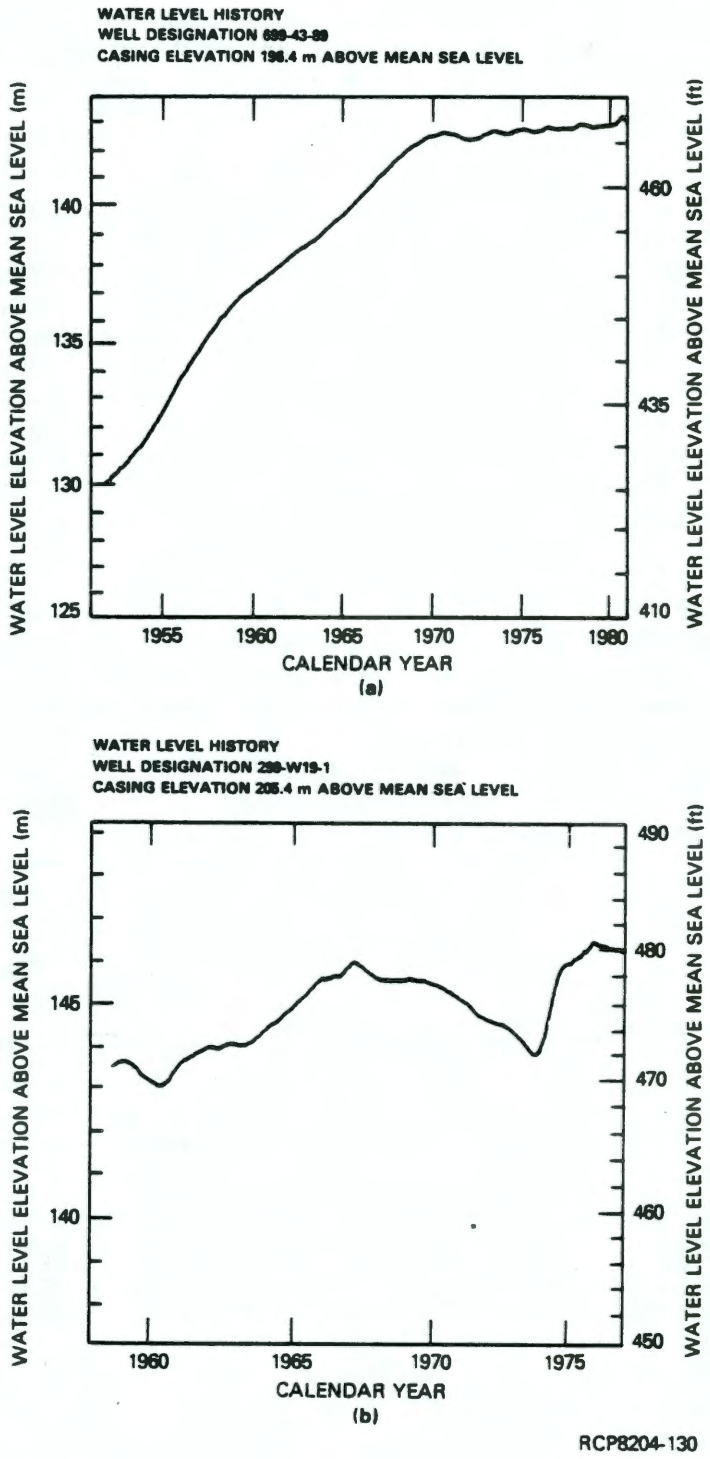

FIGURE 5-97. Unconfined Water-Level Responses in Wells Within and Adjacent to the Reference Repository Location.

9 2 1 2 4 9 5 1 1 0 4

5.2.2.2 Columbia River Basalts. Hydraulic-head data from boreholes RRL-2 and DC-16A are available in the reference repository location for confined aquifers within the Columbia River basalt. Information presented in this section for anticipated conditions in the reference repository location are based on hydraulic-head data presented in Section 5.1.4.

Expected ranges for potentiometric levels across and anticipated vertical hydraulic-head patterns for formations within the Columbia River basalts in the reference repository location are summarized in Table 5-50. As stated previously, most information at the Hanford Site is available for confined aquifers within the Saddle Mountains Basalt. As shown in Table 5-50, potentiometric levels in the Saddle Mountains Basalt are anticipated to range between 125 to 140 meters above mean sea level. The vertical hydraulic-head pattern within the formation is expected to generally decline with depth, because of recharge occurring just west of the reference repository location in the Rattlesnake Hills to Umtanum Ridge area. The effects of this recharge are reflected in the decreasing heads with depth noted for borehole DC-16A (see Section 5.1.4.2.4).

TABLE 5-50. Anticipated Hydraulic-Head Conditions Within Confined Aquifers of the Columbia River Basalt Group in the Reference Repository Location.

Basalt formation	Expected range in hydraulic head (m above mean sea level)	Vertical hydraulic-head pattern
Saddle Mountains	125 - 140	Decreasing with depth
Wanapum	120 - 130	Relatively uniform with depth
Grande Ronde	120 - 130	Relatively uniform to slightly increasing with depth

Potentiometric levels within confined aquifers of the Wanapum Basalt are expected to range between 120 to 130 meters above mean sea level across the reference repository location. The vertical hydraulic-head pattern within the formation is expected to remain relatively uniform with depth.

Potentiometric levels within confined aquifers of the Grande Ronde Basalt are expected to range between 120 to 130 meters above mean sea level across the reference repository location. The vertical hydraulic-head pattern within the formation is expected to either remain relatively uniform or increase slightly with depth.

Within the reference repository location, hydraulic heads are expected to typify artesian but not flowing artesian conditions.

9 2 1 2 4 9 5 1 1 0 5

No continuous data are available to evaluate long-term potentiometric-level fluctuations within the confined aquifer systems in the reference repository location. Based on previously given information, seasonal hydraulic-head fluctuations for confined aquifers are greatest in the Saddle Mountains and upper Wanapum Basalts. Seasonal fluctuations in these formations are attributable primarily to local natural recharge within intrabasin areas (e.g., Rattlesnake Hills, Yakima Ridge, etc.) peripheral to the Hanford Site. Due to the significant distance to outside irrigation wells and the presence of intervening hydrogeologic barriers, groundwater pumpage is expected to have a negligible impact on potentiometric levels for these aquifer systems within the reference repository location. The exception might be pumpage from irrigation wells in the Cold Creek Valley. However, the long-term effects of outside groundwater withdrawals on aquifer potentiometric levels in this area are currently not fully quantified.

Confined aquifers in the Grande Ronde and possibly the lower Wanapum Basalts are expected to display a rather uniform annual change in potentiometric levels. This behavior is expected in the reference repository location, due to the great distance to major recharge areas (located primarily outside the Pasco Basin) and the lack of groundwater development from deep aquifer sources within the Pasco Basin.

The hydrograph response for piezometers completed in Grande Ronde Basalt aquifers (over depths of 372 to 1,478 meters) at borehole DC-1 is shown in Figure 5-98. As shown, no significant seasonal fluctuations are evident in the water-level responses for individual flow-top horizons between 1975 and mid-1978. Prior to 1975, piezometers were equilibrating to formation conditions. It should be noted that piezometer #4 required substantially more time to equilibrate to formation(s) conditions. In addition, construction activities at nearby borehole DC-2 in mid-1977 may have influenced piezometric response subsequent to this construction date (piezometer #4). An evaluation of these piezometric responses is reported in Gephart et al. (1979a).

The reference repository location lies in an area where the shallow (Saddle Mountains and possibly upper Wanapum Basalts) groundwater-flow directions might be north or east, depending on the starting position. As previously shown in Figure 5-31, the hydraulic low along the Umtanum Ridge-Gable Mountain anticline would direct groundwater flow, beginning in the northern portion of the reference repository location, toward the north. However, in the southern part of the reference repository location, groundwater flow in the shallow basalts is more toward the east.

It was noted in Section 5.1.4.2 that sufficient data are not yet available to construct potentiometric maps in the Wanapum and Grande Ronde Basalts. However, existing information suggests an east to southeast areal flow direction within the Cold Creek syncline. This is also believed to be true for groundwater flow originating from the reference repository location, provided that a major hydraulic low does not exist with depth in the area of the Umtanum Ridge-Gable Mountain anticline. If such a low is present, then some northward component of groundwater flow may exist.

9 2 1 2 4 9 5 1 1 0 6

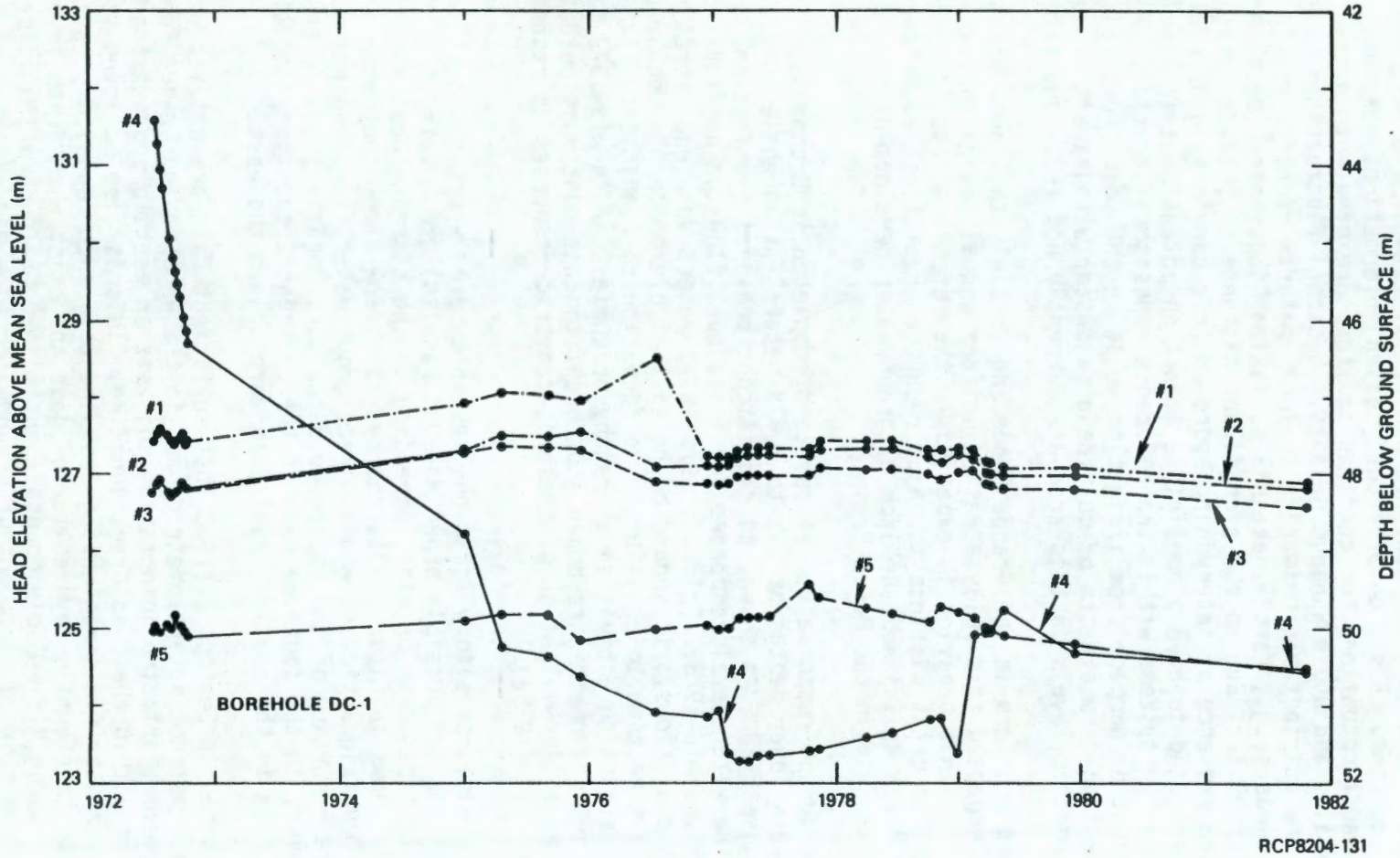

FIGURE 5-98. Hydrograph of the Water Levels in the DC-1 Piezometers from 1972 Through 1981.

5.2.3 Groundwater Hydrochemistry

Baseline hydrochemical data obtained from boreholes within the reference repository location are limited to the unconfined aquifer. (The hydrochemistry of groundwaters sampled from boreholes RRL-2 and DC-16A will be reported in the future.) Estimates of hydrochemical conditions for Columbia River basalt groundwater within the reference repository location are based on data given in Sections 5.1.5 and 5.1.6.

5.2.3.1 Unconfined Aquifer. Baseline hydrochemical data for the unconfined aquifer are available for 13 borehole sites within the reference repository location. The location of these borehole sites is shown in Figure 5-99. Data presented in this section are based on analyses performed at Hanford by the U.S. Geological Survey and Pacific Northwest Laboratory for groundwater samples collected between 1976 and 1980. Analytical results are reported in Myers (1978), Eddy (1979), and Eddy and Wilbur (1980; 1981). Pertinent well-construction details for the individual borehole sites are contained in McGhan and Damschen (1979).

5.2.3.1.1 Major Inorganic Composition. The range in concentration and mean composition for major chemical constituents within the unconfined aquifer in the reference repository location are listed in Table 5-51. For comparison, the same chemical constituents for all groundwater samples from the unconfined aquifer on the Hanford Site are also included in the table. These data indicate that a close correspondence exists in mean compositions for unconfined groundwater within the reference repository location and across the Hanford Site.

On the average, groundwater within the unconfined aquifer in the reference repository location possesses a low total dissolved solids (less than 350 milligrams per liter). Principal chemical constituents are present in the following dominance relationship (by weight): bicarbonate >calcium>silica>nitrate>sulfate>sodium>chloride>magnesium>potassium >fluoride.

The chemical composition of the 13 individual unconfined-aquifer samples is shown graphically in the trilinear diagram shown in Figure 5-100. Although the average chemical composition of unconfined groundwater is of a calcium bicarbonate chemical type, considerable variability in chemical composition is evident for individual analyses. The wide range in concentration and variability evident for major ionic constituents shown in Table 5-51 and Figure 5-100 was reported previously by Gephart et al. (1979a) to be attributable primarily to the disposal of chemical-processing and cooling waters on the Hanford Site.

Of particular interest is the presence of elevated nitrate concentrations within the unconfined aquifer. As discussed in Section 5.1.5, nitrate in the unconfined aquifer is the by-product of past water-disposal practices at the Hanford Site. Because of its mobility within aquifer systems, nitrate has been used previously by Myers (1978) to delineate the migration of contaminated groundwater within the unconfined aquifer.

9 2 1 2 4 9 5 1 1 0 8

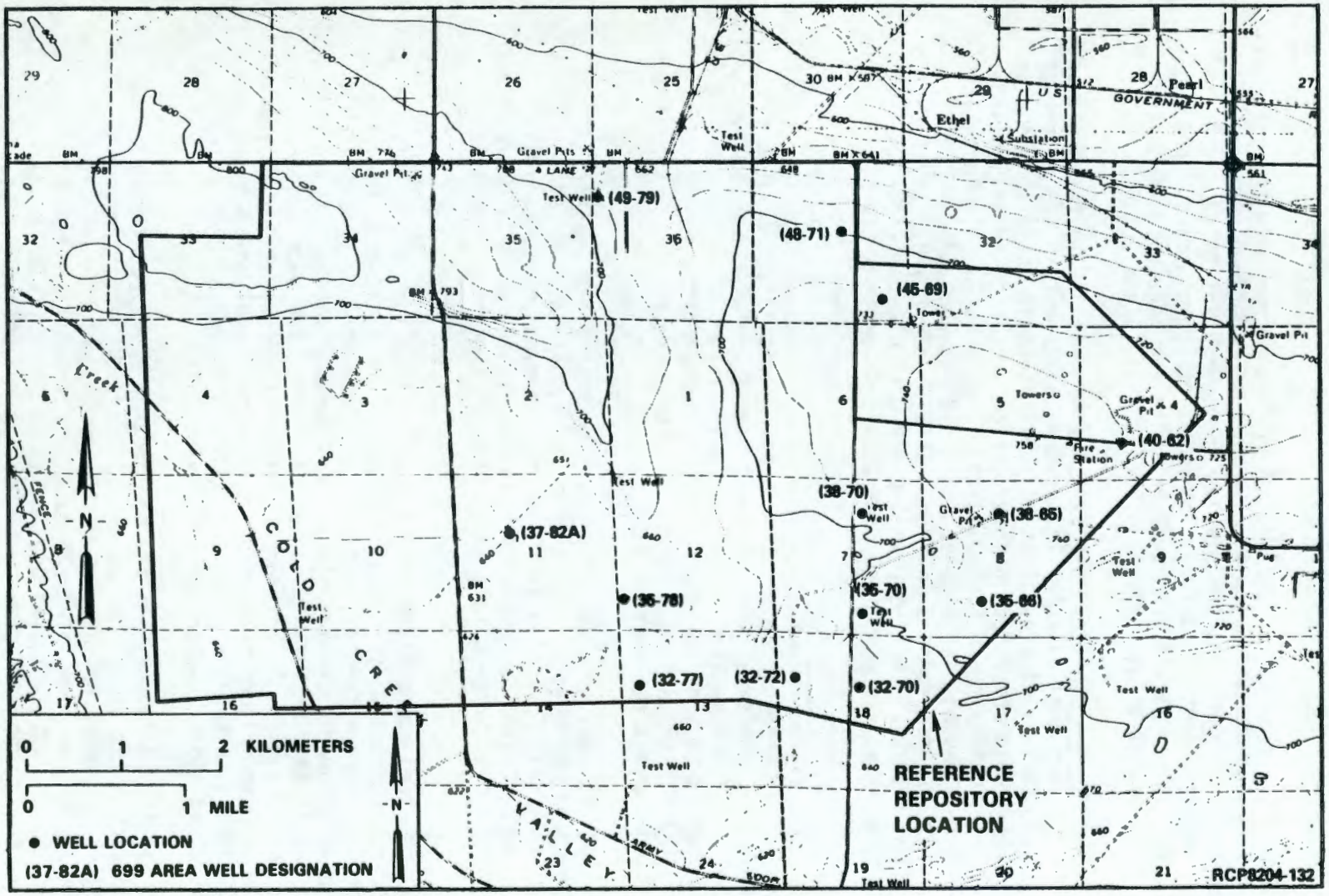

FIGURE 5-99. Location of Unconfined-Aquifer Well Sites Within the Reference Repository Location.

TABLE 5-51. Expected Range in Concentration and Mean Composition for Major Chemical Constituents for Groundwater Within the Unconfined Aquifer in the Reference Repository Location and the Entire Hanford Site.

Constituent	Concentration (mg/L)			
	Reference repository location		Entire Hanford Site*	
	Range	Mean	Range	Mean
Anions				
Alkalinity, as HCO_3^-	14 - 24	140.5	14 - 314	149
Cl^-	4.5 - 32	13.5	2.7 - 32	11
SO_4^{-2}	13 - 62	31.8	2.7 - 170	43
NO_3^-	1.1 - 256	38.4	0.1 - 270	27
F^-	0.3 - 0.8	0.4	0.1 - 1.3	0.5
Cations				
Na^+	8.7 - 28	18.3	2.9 - 69	23
K^+	3.2 - 8	5.0	2.4 - 13	6.2
Ca^{+2}	19 - 92	41	14 - 92	41
Mg^{+2}	0.4 - 29	12.7	0.4 - 30	11
SiO_2	30 - 50	40.5	8.8 - 50	35
Total dissolved solids	229 - 663	342	203 - 728	347
pH (field)	7.6 - 10.7	8.1	7.5 - 10.7	7.9
Collection temperature (°C)	15 - 21.4	19.5	14 - 39	19.0

*Data from Table 5-13.

9 2 1 2 4 9 5 1 1 1 0

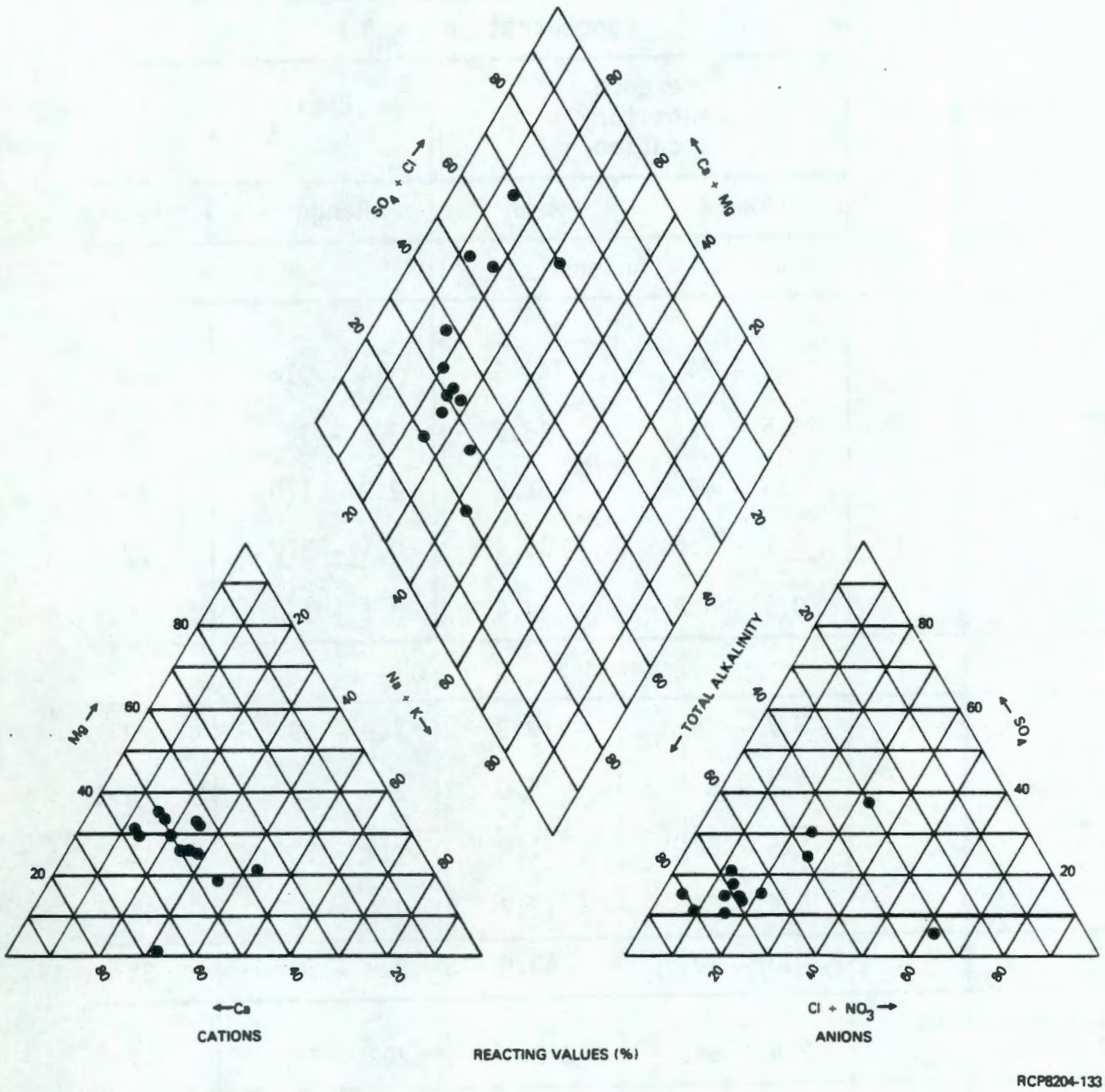

FIGURE 5-100. Chemical Composition of Groundwater Within the Unconfined Aquifer in the Reference Repository Location.

The concentration of nitrate in the unconfined aquifer within the reference repository location is shown in Figure 5-101. As shown in this figure, the highest nitrate concentration (256 milligrams per liter in borehole 699-38-70) occurs along the eastern border of the 200 West Area. The shape of the delineated nitrate plume would be expected to change slightly with incorporation of additional areal data. However, the highest concentrations would be expected to occur in the 200 West Area, with lower nitrate contents in areas surrounding the reference repository location.

A long-term data base is unavailable to evaluate possible time-dependent hydrochemical variations within the unconfined aquifer in the reference repository location. Available short-term data for the Hanford Site outside the reference repository location, however, indicate a uniform behavior in major inorganic composition. For example, the results of major inorganic analyses for well 699-27-8 (located 20 kilometers southeast of the reference repository location) between the years 1974 and 1978 are listed in Table 5-52. These data indicate that the major inorganic composition of the unconfined aquifer at this location was relatively stable over the 5-year period of record. Within the reference repository location, more temporal variability in inorganic composition would be expected, due to the close proximity to water-disposal sites within the 200 West Area.

5.2.3.1.2 Nonconservative Hydrochemical Parameters. Hydrochemical parameters discussed in this section include those nonconservative constituents that are determined in the field at or near the time of sample collection. These field-determined hydrochemical parameters include fluid temperature, pH, alkalinity, and Eh. Alkalinity results were reported in the previous section.

Fluid Temperature. The range and mean value of fluid temperatures measured at ground surface at the time of sample collection are shown in Table 5-51. Groundwater temperature for shallow aquifers is generally reflective of the local mean annual air temperature. In the reference repository location, however, unconfined-aquifer groundwater temperatures are strongly influenced by water disposal in the 200 West Area. The impact of water disposal on groundwater temperatures within the reference repository location and across the entire Hanford Site is shown in Figure 5-102. As shown, elevated groundwater temperatures attributable to this source are indicated in the 200 West Area and the eastern portion of the reference repository location. Long-term data are unavailable to evaluate the time-variant behavior of fluid temperature in the unconfined aquifer. Available short-term data listed in Table 5-52, however, indicate a relatively uniform fluid temperature with time. Considerably more variability would be expected in the unconfined aquifer at locations in proximity to known water-disposal areas within the reference repository location.

9 2 1 2 4 9 5 1 1 1 2

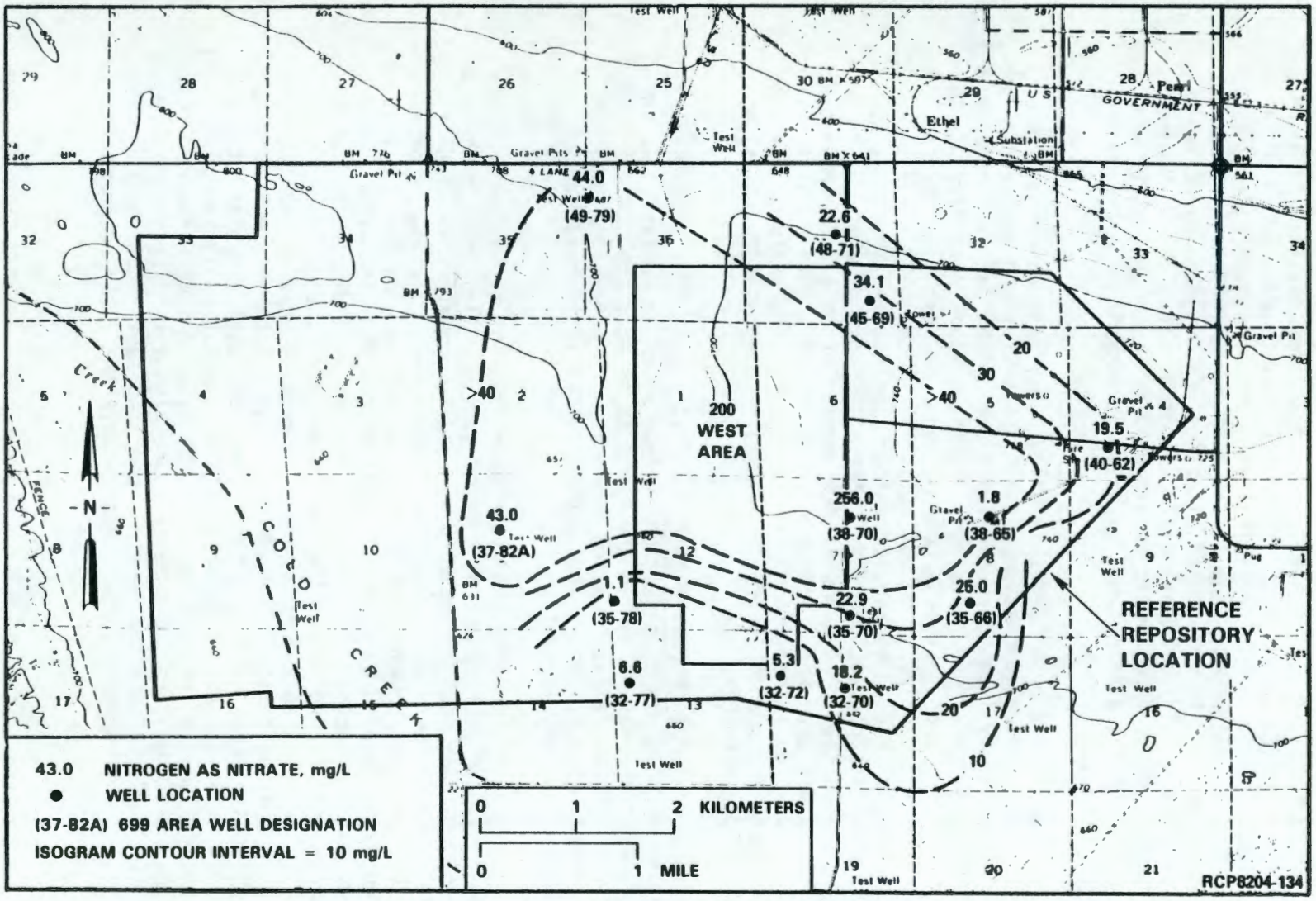

FIGURE 5-101. Nitrate Ion Distribution in Unconfined Groundwater Beneath the Reference Repository Location.

TABLE 5-52. Historic Major Inorganic- and Hydrochemical-Parameter Analyses for the Unconfined Aquifer at Well 699-27-8*.

Constituent	Concentration (mg/L) for date collected			
	11/74	4/76	4/77	4/78
Anions				
Alkalinity, as HCO_3^-	145	149	140	150
Cl^-	13	13	12	11
SO_4^{-2}	46	50	52	49
NO_3^-	58	57.4	58	58
F^-	0.2	0.3	0.3	0.3
Cations				
Na^+	19	19	20	20
K^+	6.4	6.9	6.3	6.7
Ca^{+2}	56	54	55	54
Mg^{+2}	12	11	12	13
SiO_2	36	34	36	34
Total dissolved solids	391.6	394.6	391.6	396.0
pH (field)	8.0	8.0	7.8	7.9
Collection temperature (°C)	16.5	16.3	16.5	16.4

*Well 699-27-8 is located 20 kilometers southeast of the reference repository location.

9 2 1 2 4 9 5 1 1 1 4

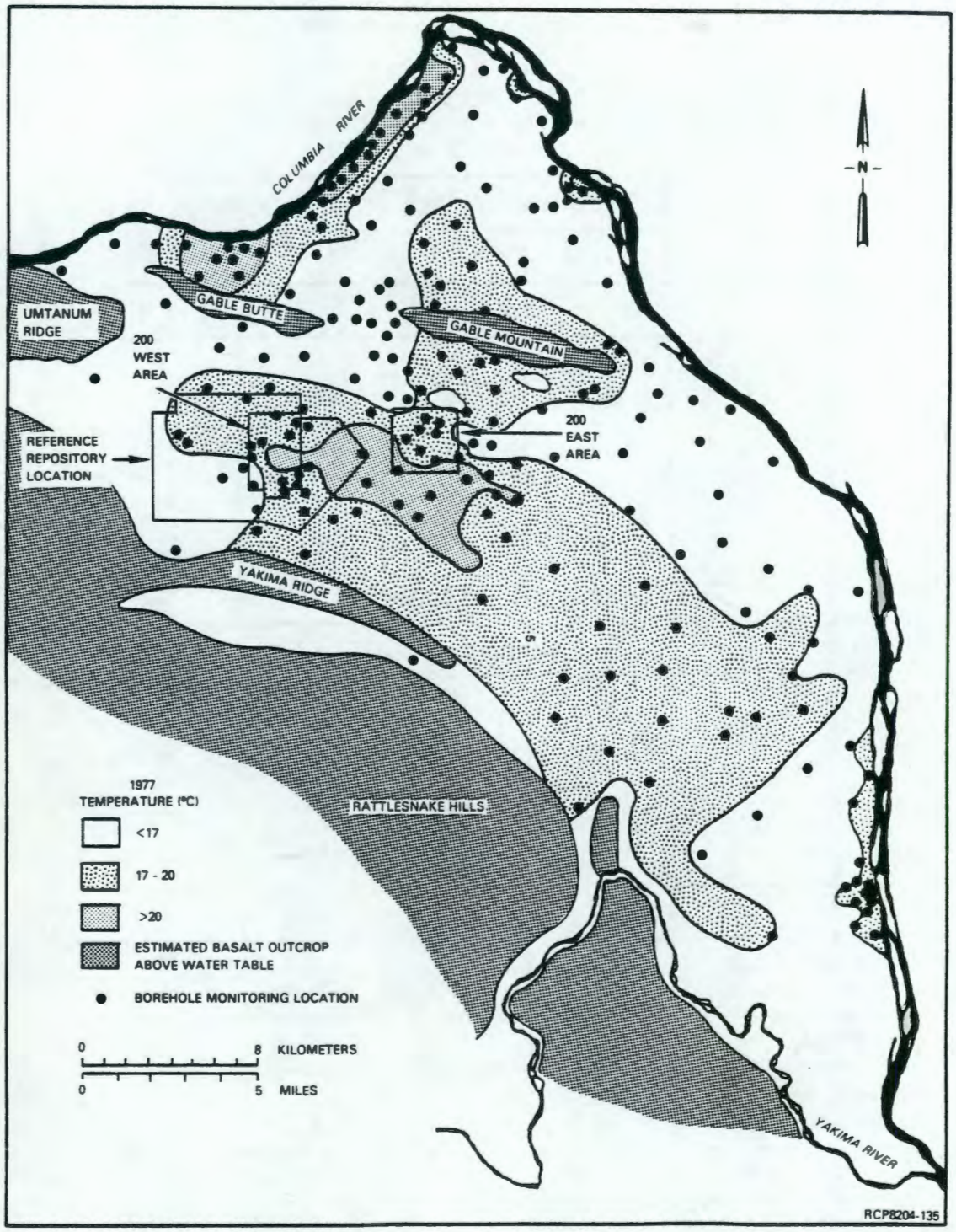

FIGURE 5-102. Temperature Distribution in Unconfined Groundwater (adapted from Myers, 1978).

pH. As indicated in Table 5-51, pH values within the unconfined aquifer range between 7.6 and 10.7, and average 8.1 for the 13 samples available. Long-term data are currently unavailable to evaluate the temporal behavior of groundwater pH within the unconfined aquifer. Available short-term data listed in Table 5-52, indicate a relatively stable pattern of pH with time. However, more variability would be expected in the unconfined aquifer in locations near water-disposal areas within the reference repository location.

Eh. Eh determinations are not currently performed on groundwater samples within the unconfined aquifer at the Hanford Site. However, Eh values for the existing pH conditions in the unconfined aquifer would be expected to range between slightly oxidizing and slightly reducing conditions.

5.2.3.1.3 Dissolved-Gas Content. Dissolved-gas analyses are unavailable for unconfined-aquifer groundwaters at Hanford. However, based on results for the uppermost confined-aquifer system beneath the Hanford Site, dissolved gas within the unconfined aquifer in the reference repository location would be expected to be in extremely low concentrations and to be predominantly nitrogen in composition.

5.2.3.1.4 Isotope Content. Isotopic analyses for the unconfined aquifer in the reference repository location are limited to radioisotopic parameters. Data for which radioisotopes are available for the unconfined aquifer at Hanford were discussed in Section 5.1.6.1. Because the majority of radioisotopic data available for the unconfined aquifer is of limited hydrologic value and is concerned primarily with monitoring contaminant migration, this section includes only a discussion of tritium.

Tritium present within the unconfined aquifer is primarily the result of water-disposal practices at the Hanford Site. Tritium values in the unconfined aquifer in the reference repository location range from less than 480 to 890,000 picocuries per liter (Eddy, 1979; Eddy and Wilbur, 1980). The distribution of tritium in the unconfined aquifer was shown previously in Figure 5-67. As with other hydrochemical parameters influenced by water-disposal activities at the Hanford Site, tritium concentrations are highest in the 200 West Area and in the eastern section of the reference repository location. Long-term data are currently unavailable to evaluate the time-dependent behavior of tritium within the unconfined aquifer. Available short-term data in the reference repository location for a well completed within (well 699-35-66) and outside (well 699-37-82A) the tritium plume in the unconfined aquifer are shown in Figure 5-103.

The plot of tritium concentrations for a well outside the contamination plume (Fig. 5-103 a) indicates a relatively stable tritium content (near detection limits) for the period of record. The tritium values from a well inside the contamination plume (Fig. 5-103 b), however,

9 2 1 2 4 9 5 1 1 1 6

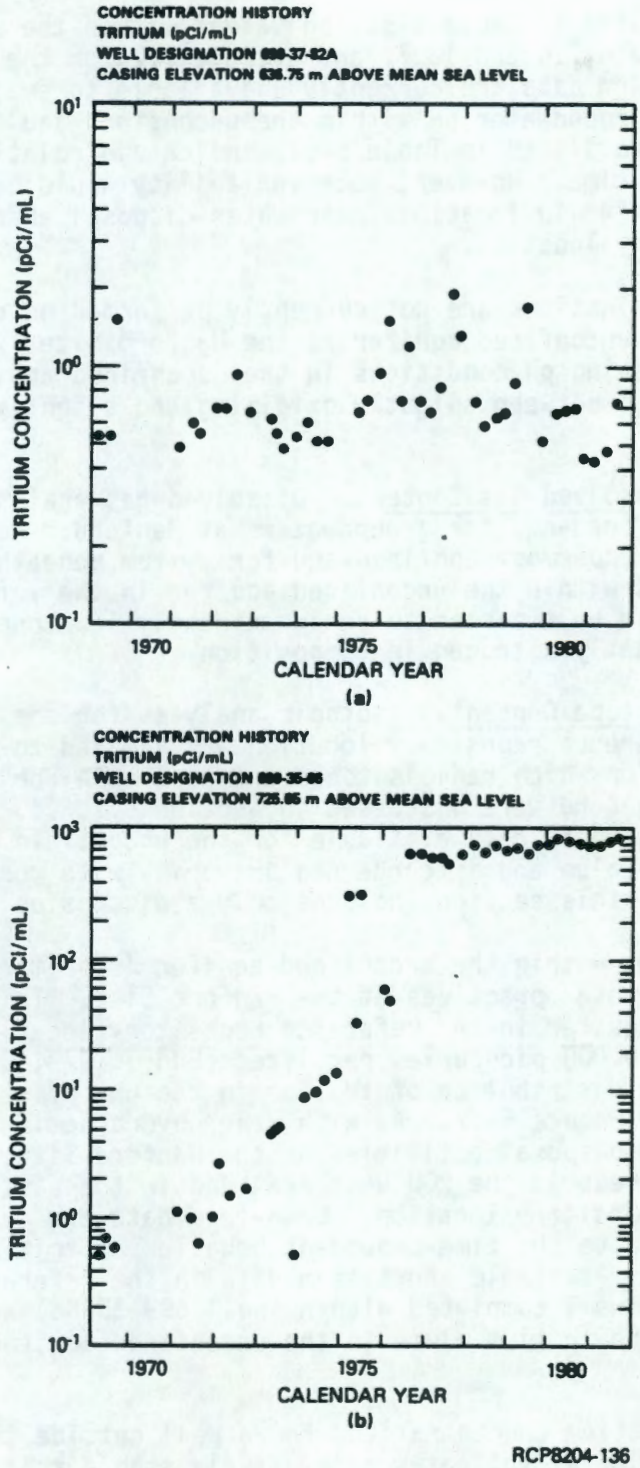

FIGURE 5-103. Tritium Hydrographs for Wells 699-35-66 and 699-37-82A Completed in the Unconfined Aquifer Within the Reference Repository Location.

9 2 1 2 4 9 5 1 1 1 7

displays a pattern of gradual buildup followed by relatively stable, elevated levels of tritium. The period of gradual buildup (i.e., 1970 to 1975) is related to the migration and extension of the tritium plume into this area of the unconfined aquifer. Future time-dependent patterns of tritium at these or other well sites within the reference repository location are dependent on water-disposal activities.

5.2.3.2 Columbia River Basalts. Hydrochemical data are now being collected at boreholes RRL-2 and DC-16A located within and adjacent, respectively, to the reference repository location. Information presented in this section for anticipated conditions in the reference repository location is based on hydrochemical data presented in Sections 5.1.5 and 5.1.6.

5.2.3.2.1 Major Inorganic Composition. The anticipated mean composition and range in concentration for major chemical constituents in Columbia River basalt groundwater in the reference repository location are listed in Table 5-53. Hydrochemical data presented in that table are based on information acquired in the Cold Creek syncline, which indicates that considerable differences in chemical type and concentrations are expected between groundwater within the Saddle Mountains and Grande Ronde Basalts. Wanapum Basalt groundwaters are anticipated to have hydrochemical characteristics that are transitional to groundwater within the upper and lower basalt formations. Hydrochemical type classifications for groundwater within the Columbia River basalts are listed below:

Basalt formation	Chemical type
Saddle Mountains	Sodium, calcium bicarbonate
Wanapum	Sodium bicarbonate-chloride
Grande Ronde	Sodium chloride

Little long-term data are available to evaluate the temporal behavior of groundwater hydrochemistry in the Columbia River basalts. Historic hydrochemical data for the McGee well, completed in the upper Wanapum Basalt in Cold Creek Valley, is presented in Table 5-54. This is a flowing artesian well located along the western border of the Hanford Site. Examination of these data indicates that little change in concentration of individual constituents is evident between samples collected over a 25-year period. Therefore, while long-term hydrochemical data are limited, the hydrochemistry of groundwater in the Columbia River basalts in the reference repository location is likely to remain relatively uniform with time.

5.2.3.2.2 Nonconservative Hydrochemical Parameters. The anticipated range and mean values for nonconservative hydrochemical parameters in Columbia River basalt groundwater within the reference repository location are shown in Table 5-53. Limitations and factors that influence the hydrochemical-parameter values listed in Table 5-53 are discussed in Section 5.1.5.

9 2 1 2 4 9 5 1 1 1 8

TABLE 5-53. Anticipated Range in Concentration and Mean Composition of Major Chemical Constituents for Columbia River Basalt Groundwaters Within the Reference Repository Location.

Constituent	Saddle Mountains Basalt		Wanapum Basalt		Grande Ronde Basalt	
	Range (mg/L)	Mean (mg/L)	Range (mg/L)	Mean (mg/L)	Range (mg/L)	Mean (mg/L)
Anions						
HCO_3^-	104 - 298	180	100 - 192	128	16 - 102	57
CO_3^{-2}	0.8 - 23	4.2	1.8 - 26	18	3.5 - 55	21
Cl^-	3.4 - 63	12	4.6 - 117	43	96 - 197	169
SO_4^{-2}	0.05 - 37	15	<0.05 - 26	11	4.2 - 199	125
NO_3^-	0.5 - 7.6	<0.5	<0.5	<0.5	<0.5	<0.5
F^-	0.03 - 8.0	1.3	0.6 - 24	8.0	13 - 42	30
$H_3SiO_4^-$	0.5 - 22	4.0	1.7 - 55	28	9.1 - 140	74
Cations						
Na^+	17 - 122	58	61 - 171	96	161 - 360	257
K^+	6.2 - 15	11	10 - 21	14	0.34 - 24	6.5
Ca^{+2}	0.5 - 42	14	1.0 - 18	3.4	0.80 - 7.8	2.4
Mg^{+2}	0.1 - 16	4.2	0.3 - 10	0.8	0.005 - 0.2	0.04
H_4SiO_4	50 - 140	97	6.2 - 152	71	39 - 132	101
Total dissolved solids	293 - 518	384	295 - 667	461	626 - 1,210	843
Eh (V) (field)	-0.09 - +0.06	-0.01	-0.18 - +0.12	+0.02	-0.217 - +0.210	-0.100
pH (field)	7.6 - 9.6	8.4	8.2 - 9.6	9.3	8.8 - 10.6	9.7
Fluid temperature (°C)	16.3 - 26.8	21.8	19.5 - 40.8	30.5	46.2 - 55.3	52.0

9 2 1 2 4 9 5 1 1 1 9

TABLE 5-54. Historic Major Inorganic and Hydrochemical Parameter Analyses for Groundwater Within the Upper Wanapum Basalt in the Cold Creek Valley.

Constituent	Concentration for date collected[a] (mg/L)	
	12/51[b]	4/77[c]
Anions		
Alkalinity, as HCO_3^-	181	170
Cl^-	4.8	4.5
SO_4^{-2}	1.6	1.4
NO_3^-	0.1	0.0
F^-	0.6	0.8
Cations		
Na^+	30	29
K^+	9.9	7.8
Ca^{+2}	17	17
Mg^{+2}	9.4	9.2
SiO_2	62	55
Total dissolved solids	316.4	294.7
pH (field)	7.8	8.0
Collection temperature (°C)	26.9	26.8

[a]Groundwater samples collected from the McGee well.

[b]Hart (1958).

[c]Myers (1978).

Fluid Temperature. Fluid temperatures listed in Table 5-53 were obtained from downhole measurements at the Hanford Site in boreholes outside the reference repository location. As discussed previously, downhole temperature measurements for specific basalt formations are largely a function of depth and the existing geothermal gradient at a particular location. As expected, the anticipated mean and ranges in fluid temperatures for basalt formations are higher with increasing stratigraphic depth. The range of mean temperature values for the reference repository location is noted in Table 5-53. No continuous long-term measurements are available to evaluate time-variant behavior of groundwater temperatures. Data presented in Table 5-54, however, suggest that no major change in fluid temperature was evident in the Wanapum Basalt over a 25-year period. Because of the dependence of fluid temperature on depth and the existing geothermal gradient, groundwater temperatures within the Columbia River basalts in the reference repository location are anticipated to be relatively uniform with time.

pH. The anticipated mean pH values for the Saddle Mountains, Wanapum, and Grande Ronde Basalts are 8.2, 9.3, and 9.7, respectively (see Table 5-53). The trend of increasing pH with stratigraphic depth is attributable to mineral-equilibria controls as discussed in Section 5.1.5. No continuous long-term measurements are available to assess the time-dependent behavior of pH in Columbia River basalt groundwaters. Due to the high buffer capacity of most basalt groundwater, however, no significant change in pH is expected for basalt groundwater in the reference repository location. Data presented in Table 5-54 support this contention and indicate that no major change in pH was exhibited at the McGee well over a 25-year period.

Eh. Only limited Eh data are available for Columbia River basalt groundwater at the Hanford Site. As indicated in Table 5-53, Eh conditions are anticipated to range from slightly oxidizing to slightly reducing conditions. Although the ranges in Eh values overlap for the various basalt formations, Eh conditions are expected to become slightly more reducing with depth.

5.2.3.2.3 Dissolved-Gas Content. Methane is the predominant dissolved-gas component by volume from the lower Saddle Mountains to the lower Wanapum Basalts. Nitrogen is the principal dissolved-gas component for upper Saddle Mountains and Grande Ronde Basalt groundwater in the eastern portion of the Cold Creek syncline. The principal dissolved-gas relationships anticipated for individual basalt formations in the reference repository location are shown in Table 5-55. Within the reference repository location, methane is expected to be the principal gas component in the Wanapum and Grande Ronde Basalts. A more detailed discussion concerning the source and areal heterogeneity of dissolved gas within basalt formations is given in Sections 5.1.5.2.4, 5.1.5.3.4, and 5.1.5.4.4.

9 2 1 2 4 9 5 1 1 2 1

TABLE 5-55. Principal Dissolved-Gas Components Anticipated in Columbia River Basalt Groundwater Within the Reference Repository Location.

Columbia River basalt formation	Principal gas component (mole %)
Saddle Mountains	Nitrogen >80
Wanapum	Methane* >90
Grande Ronde	Methane* >90

*Based on gas analyses from boreholes DC-16A and RRL-2.

5.2.3.2.4 Isotope Content. As with other hydrochemical information, no isotopic data are available for Columbia River basalt groundwater within the reference repository location. Data addressed in this section for anticipated conditions are based primarily on isotopic data presented in Section 5.1.6. Only those data that are considered to be representative of the reference repository location are included in this section. (For example, data for borehole DC-14, which occurs outside the Cold Creek syncline, are not discussed.)

Stable Isotopes. The expected range and mean values for stable isotopes within the reference repository location are listed in Table 5-56. As shown, distinct differences in isotopic content are evident, particularly between the Saddle Mountains and Wanapum Basalts. The significance and possible cause for the isotopic shifts were previously discussed.

Saddle Mountains Basalt groundwater tends to be significantly lighter isotopically, with respect to deuterium and oxygen-18 than the deeper groundwater within the Wanapum and Grande Ronde Basalts. The lighter isotopic character is attributable, in part, to the dominance and close proximity of local recharge areas for Saddle Mountains Basalt groundwater.

With respect to carbon-13 content, Grande Ronde Basalt groundwater is considerably lighter isotopically (i.e., for carbonate species) than the overlying basalt formations. This is primarily attributable to heavier carbon-13 values, which are exhibited in the lower Saddle Mountains and upper Wanapum Basalts. The presence of positive carbon-13 values in the lower Saddle Mountains and upper Wanapum Basalts appears associated with methanogenic processes that exist in these formations.

TABLE 5-56. Expected Range and Mean Values in Stable Isotopic Content for Columbia River Basalt Groundwater Within the Reference Repository Location*.

Stable isotope	Saddle Mountains		Wanapum		Grande Ronde	
	Expected range (°/oo)	Mean (°/oo)	Expected range (°/oo)	Mean (°/oo)	Expected range (°/oo)	Mean (°/oo)
Range $\delta^{18}O$	-17.9 to -16.4	-17.3	-17.8 to -14.8	-16.0	-17.7 to -12.7	-14.7
Range $\delta^{2}H$	-155 to -138	-148	-147 to -129	-139	-136 to -106	-123
Range $\delta^{13}C$	-23.8 to -14.5	-9.8	-22.1 to +17.4	+0.6	31.5 to +3.6	-19.1
Range $\delta^{34}S$	-10.3 to +23.5	+4.6	-3.0 to +33.8	+8.1	-8.2 to +15.0	+2.4

*Data from wells DB-1, -2, -7, -15, DC-6, -12, -15, S11-E12A, and McGee.

Available sulfur-34 data exhibit considerable variability and lack of distinct isotopic patterns within basalt groundwater. In addition, the extremely small amount of dissolved sulfate and sulfide concentrations have hindered measurement of sulfur-34 values for Saddle Mountains and upper Grande Ronde Basalt groundwaters. Because of these problems, the reliability of anticipated sulfur-34 values listed in Table 5-56 for the reference repository location is questionable.

Radionuclides. The expected range and mean values for radioisotopes within various Columbia River basalt groundwaters in the reference repository location are listed in Table 5-57. The radioisotopic contents shown do not exhibit the distinct differences between the various basalt formations that were evident for stable isotope distributions. Discernible differences in carbon-14 mean values are expected, however, for individual basalt-formation groundwaters.

As discussed previously in Section 5.1.6.2.2, tritium's primary application in hydrologic studies of basalt groundwater at the Hanford Site is as a trace indicator of drilling-fluid contamination within groundwater samples. Due to its relatively short half-life, tritium concentrations within uncontaminated Columbia River basalt groundwater are expected to be near analytical detection limits (i.e., 0.2 tritium unit).

As shown in Table 5-57, a considerable range in carbon-14 content is expected in basalt groundwater within the reference repository location. At a given location, however, the relative carbon-14 age would be anticipated to increase with depth. Carbon-14 activities for deep groundwater within the Grande Ronde Basalt is expected to be below standard analytical detection limits for this isotopic parameter (i.e., 1.9 percent modern carbon). Inherent problems and corrective measures for using carbon-14 in age-dating applications of deep basalt groundwater are discussed in Section 5.1.6.2.2.

Considerable variability is also expected for uranium isotopic content within basalt groundwater in the reference repository location. As indicated in Table 5-57, uranium-234 to uranium-238 ratios are anticipated to vary over approximately the same range (i.e., 0.7 to 3.4) for all basalt formations. Total uranium content, however, is expected to be greater within the Saddle Mountains Basalt. The greater total uranium content within Saddle Mountains Basalt groundwater is attributable primarily to slightly more oxidizing conditions.

Insufficient data are currently available within the Cold Creek syncline to predict the chlorine-36 content of basalt formations within the reference repository location.

TABLE 5-57. Expected Range and Mean Radioisotope Content for Columbia River Basalt Groundwaters Within the Reference Repository Location.

Basalt formation	^{3}H (tritium units)		^{14}C				$^{234}U/^{238}U$ (ratio)		^{36}Cl*
			Groundwater age (yr)		Percent modern carbon				
	Expected range	Mean	Expected range	Mean	Expected range	Mean	Expected range	Mean	
Saddle Mountains	0.07 to 0.4	0.2	20,000 to >32,000	23,700	5.2 to <1.0	4.2	1.1 to 1.8	1.5	--
Wanapum	0.07 to 0.7	0.2	20,000 to >32,000	26,500	8.0 to <1.5	3.9	1.0 to 3.4	2.0	--
Grande Ronde	0 to 0.8	0.1	30,000 to >32,000	>32,000	--	<1.8	0.7 to 2.6	1.7	--

*Insufficient data.

5.3 SUMMARY OF UNRESOLVED ISSUES

A number of technical issues regarding hydrologic-data collection and conceptual-model development remain to be resolved as part of the site characterization process. These issues and the plans for their resolution are discussed in Chapter 13.

Hydrologic modeling to assess repository performance regarding transport potential of radionuclides is discussed in Chapter 12. Issues regarding hydrologic modeling and plans for addressing these issues are covered in Chapter 16.

THIS PAGE INTENTIONALLY
LEFT BLANK

9 2 1 2 4 9 5 1 1 2 7

5.4 REFERENCES

Agapito, J. F. T., Hardy, M. P., and St. Laurent, D. R., 1977, Geo-Engineering Review and Proposed Program Outline for the Structural Design of Radioactive Waste Repository in Columbia Plateau Basalts, RHO-ST-6, Rockwell Hanford Operations, Richland, Washington, September 1977.

Ames, L. L., 1980, Hanford Basalt Flow Mineralogy, PNL-2847, Pacific Northwest Laboratory, Richland, Washington.

Apps, J., Doe, T., Doty, B., Doty, S., Galbraith, R., Kearns, A., Kohrt, B., Lons, J., Monroe, A., Narasimhan, T. N., Nelson, P., Wilson, C. R., and Witherspoon, P. A., 1979, Geohydrologic Studies for Nuclear Waste Isolation at the Hanford Reservation, LBL-8764, Vol. 2, Lawrence Berkeley Laboratory, Berkeley, California.

ARHCO, 1976, Preliminary Feasibility Study on Storage of Radioactive Wastes in Columbia River Basalts, ARH-ST-137, Atlantic Richfield Hanford Company, Richland, Washington.

ARHCO, 1977, Environmental Protection Annual Report CY-1978, ARH-LD-154, Atlantic Richfield Hanford Company, Richland, Washington.

Baas-Becking, L. G. M., Kaplan, I. R., and Moore, D., 1960, "Limits of the Natural Environment in Terms of pH and Oxidation-Reduction Potentials," Journal of Geology, Vol. 68, No. 3, pp. 243-284.

Barker, R. A., 1979, Geohydrology and Digital Simulation of the Basalt Aquifer System in the Pullman-Moscow Basin, Washington and Idaho, Water-Supply Bulletin 48, Washington State Department of Ecology, Olympia, Washington.

Barr, G. E., Lambert, S. J., and Carter, J. A., 1979, Uranium Isotope Disequilibrium in Groundwaters of Southeastern New Mexico and Implications Regarding Age-Dating of Waters, IAEA-SM-228/32, International Atomic Energy Agency, Vienna, Austria, p. 18.

Bela, J., 1979, Annotated Bibliography of the Geology of the Columbia Plateau (Columbia River Basalt) and Adjacent Areas of Oregon, RHO-BWI-C-30, Oregon Department of Geology for Rockwell Hanford Operations, Richland, Washington, January 1979.

Bell, N. M. and Leonhart, L. S., 1980, A Preliminary Evaluation of Water Resource Development and Potential Within the Pasco Basin, RHO-BWI-LD-33, Rockwell Hanford Operations, Richland, Washington, November 1980.

Benson, L. V., 1978, Secondary Minerals, Oxidation Potentials, Pressure and Temperature Gradients in the Pasco Basin of Washington State, RHO-BWI-C-34, Lawrence Berkeley Laboratory for Rockwell Hanford Operations, Richland, Washington, November 15, 1978.

Bierschenk, W. H., 1957, Hydraulic Characteristics of Hanford Aquifers, HW-48916, General Electric Company, Richland, Washington.

Brace, W. F., 1980, "Permeability of Crystalline and Argillaceous Rocks, International Journal of Rock Mechanics, Mining, Science, and Geomechanics, Vol. 17, pp. 241-251.

Brown, R. E., 1979, A Review of Water Well Data From the Unconfined Aquifer in the Eastern and Southern Parts of the Pasco Basin, RHO-BWI-C-56, R. E. Brown, Geological Consultant, for Rockwell Hanford Operations, Richland, Washington, February 5, 1981.

Burns, W. A., 1969, "New Single Well Test for Determining Vertical Permeability," Journal of Petroleum Technology, June, pp. 743-752.

Carlsson, A. and Olsson, T., 1977a, "Hydraulic Properties of Swedish Crystalline Rocks, Hydraulic Conductivity and Its Relationship to Depth," Bulletin of the Geological Institute of Uppsala, N57, Uppsala, Sweden, pp. 71-84.

Carlsson, A. and Olsson, T., 1977b, "Variations of Hydraulic Conductivity in Some Swedish Rock Types," Proceedings of Rockstore-77, First International Symposium on Storage in Excavated Rock Caverns, 2, Pergamon Press, Oxford, England, pp. 301-307.

Carothers, W. W. and Kharaka, Y. K., 1979, "Stable Carbon Isotopes of HCO_3 in Oil-Field Waters - Implications of the Origin of CO_2," Geochimica et Cosmochimica Acta, Vol. 44, pp. 323-332.

Cearlock, D. B., Cole, C. R., Foote, H. P., and Wallace, R. W., 1975, Mathematical Groundwater Model of the Ahtanum-Moxee Subbasins, Yakima County, Washington, Battelle, Pacific Northwest Laboratories, Richland, Washington.

Chebotarev, I. I., 1955, "Metamorphism of Natural Waters in the Crust of Weathering: Parts 1, 2, and 3," in Geochimica et Cosmochimica Acta, Vol. 8, pp. 22-48, 137-170, and 198-212.

Claypool, G. E. and Kaplan, I. R., 1974, "The Origin and Distribution of Methane in Marine Sediments," in Natural Gases in Marine Sediments, Kaplan, I. R. ed., Plenum Press, New York, New York, pp. 99-139.

Clayton, R. N., Goldsmith, J. R., Karol, K. J., Mayeda, T. K., and Newton, R. C., 1975, "Limits on the Effect of Pressure of Isotopic Fractionization," Geochimica et Cosmochimica Acta, Vol. 39, pp. 1197-1201.

Cowart, J. B. and Osmond, J. K., 1974, ^{234}U and ^{238}U in the Carrizo Sandstone Aquifer of South Texas, International Atomic Energy Agency, Vienna, Austria, pp. 131-149.

Craig, H., 1961, "Isotopic Deviations in Meteoric Waters," Science, Vol. 133, pp. 1702-1703.

Craig, H., 1963, "The Isotopic Geochemistry of Water and Carbon in Geothermal Areas," in Nuclear Geology of Geothermal Areas, Spoleto, Tongiorgi, E., ed., Consiglio Naz. Delle Ricerche Lab. di Nucleare, Pisa, Italy, pp. 17-53.

Crosby, J. W. and Chatters, R. M., 1965, Water Dating Techniques as Applied to the Pullman-Moscow Groundwater Basin, Bulletin 296, College of Engineering, Washington State University, Pullman, Washington.

Crosby, J. W., III, Anderson, J. V., and Kiesler, J. P., 1972, Geophysical Investigation of Wells in the Horse Heaven Hills Areas, Research Report 72/11-24, College of Engineering, Washington State University, pp. 1-9.

Dansgaard, W., 1964, "Stable Isotopes in Precipitation," Tellus, Vol. XVI, pp. 436-468.

Davis, S. N., ed., 1978, Workshop on Dating Old Groundwater, Y/OWI-Sub-78/55412, Office of Waste Isolation, Union Carbide Corporation, Oak Ridge, Tennessee.

Davis, S. N. and DeWiest, R. J. M., 1967, Hydrogeology, John Wiley & Sons, Inc., New York, New York.

Dion, N. P. and Lum, W. E., II, 1977, Municipal, Industrial and Irrigation Water Use in Washington, 1975, Open-File Report 77-308, U.S. Geological Survey, Tacoma, Washington.

Domenico, P. A., 1972, Concepts and Models in Groundwater Hydrology, McGraw-Hill, New York, New York.

Dove, F. H., Cole, C. R., Foley, M. G., Bond, F. W., Brown, R. E., Deutsch, W. J., Freshley, M. D., Gupta, S. K., Gutknecht, P. J., Kuhn, W. L., Lindberg, J. W., Rice, W. A., Schalla, R., Washburn, J. F., and Zellmer, J. T., 1981, AEGIS Technology Demonstration for a Nuclear Waste Repository in Basalt, PNL-3632, Pacific Northwest Laboratory, Richland, Washington.

Eakin, T. E., 1946, Groundwater Resources of the Waterville Area, Douglas County, Washington, Open-File Report, U.S. Geological Survey, Tacoma, Washington.

Eddy, P. A., 1979, Radiological Status of the Groundwater Beneath the Hanford Project, January-December 1978, PNL-2899, Pacific Northwest Laboratory, Richland, Washington.

Eddy, P. A. and Wilbur, J. S., 1980, Radiological Status of the Groundwater Beneath the Hanford Site, January-December 1979, PNL-3346, Pacific Northwest Laboratory, Richland, Washington.

Eddy, P. A. and Wilbur, J. S., 1981, Radiological Status of the Groundwater Beneath the Hanford Site, January-December 1980, PNL-3768, Pacific Northwest Laboratory, Richland, Washington.

ERDA, 1975, Final Environmental Statement - Waste Management Operations, Hanford Reservation, Richland, Washington, ERDA-1538, 2 Volumes, U.S. Energy Research and Development Administration, Washington, D.C., December 1975.

Foxworthy, B. L., 1962, Geology and Groundwater Resources of the Ahtanum Valley, Yakima County, Washington, Water-Supply Paper 1958, U.S. Geological Survey, Washington, D.C.

Foxworthy, B. L., 1979, Summary Appraisal of the Nation's Groundwater Resources - Pacific Northwest Region, Professional Paper 1598, U.S. Geological Survey, Washington, D.C.

Foxworthy, B. L. and Washburn, R. L., 1963, Groundwater in the Pullman Area, Whitman County, Washington, Water-Supply Paper 1655, U.S. Geological Survey, Washington, D.C.

Fried, J. J., 1975, Groundwater Pollution, Elsevier, New York, New York.

Fritz, P. and Fontes, J. C., eds., 1980, Handbook of Environmental Isotope Geochemistry, Vol. 1 - The Terrestial Environment, A, Elsevier, New York, New York.

Fritz, P., Barker, J. F., and Gale, J. E., 1979, Geochemistry and Isotope Hydrology at Groundwaters in the Stripa Granite, Results and Preliminary Interpretation, LBL-8285, Lawrence Berkeley Laboratory, Berkeley, California.

Gat, J. R., 1980, "The Isotopes of Hydrogen and Oxygen in Precipitation," in Handbook of Environmental Isotope Geochemistry, Vol. 1 - The Terrestial Environment, A, Fritz, P. and Fontes, J. C., eds., Elsevier, New York, New York, pp. 21-47.

Gelhar, L. W. and Collins, M. A., 1971, "General Analysis of Longitudinal Dispersion in Non-Uniform Flow," Water Resources Research, Vol. 7, No. 6, pp. 1511-1521.

Gephart, R. E., Eddy, P. A., Arnett, R. C., and Robinson, G. A., 1976, Geohydrologic Study of the West Lake Basin, ARH-CD-775, Atlantic Richfield Hanford Company, Richland, Washington.

Gephart, R. E., Arnett, R. C., Baca, R. G., Leonhart, L. S., and Spane, F. A., Jr., 1979a, Hydrologic Studies Within the Columbia Plateau, Washington: An Integration of Current Knowledge, RHO-BWI-ST-5, Rockwell Hanford Operations, Richland, Washington, October 1979.

Gephart, R. E., Eddy, P. A., and Deju, R. A., 1979b, Geophysical Logging and Hydrologic Testing of Deep Basalt Flows in the Rattlesnake Hills Well Number One, RHO-BWI-ST-1, Rockwell Hanford Operations, Richland, Washington, January 1979.

GG/GLA, 1981, An Evaluation of Water-Resource Economics Within the Pasco Basin, Washington, RHO-BWI-C-121, Geosciences Group and George Leaming Associates for Rockwell Hanford Operations, Richland, Washington, September 1981.

Glover, S. L., 1936, Preliminary Report on Petroleum and Natural Gas in Washington, Report of Investigations No. 4, Washington State Division of Geology, Olympia, Washington.

Graham, M. J., Hall, M. D., Strait, S. R., and Brown, W. R., 1981, Hydrology of Separations Area, RHO-ST-42, Rockwell Hanford Operations, Richland, Washington.

Grove, D. B. and Beetem, W. A., 1971, "Porosity and Dispersion Constant Calculations for a Fractured Carbonate Aquifer Using the Two Well Tracer Method," Water Resources Research, Vol. 7, No. 1, pp. 128-134.

Gutknecht, P. J., Rice, W. A., Cole, C. R., and Freshley, M. D., 1980, Pasco Basin Hydrometeorological Study, RHO-BWI-C-98/PNL-3855, Pacific Northwest Laboratory for Rockwell Hanford Operations, Richland, Washington, April 1980.

Hart, D. H., 1958, Tests of Artesian Wells in the Cold Creek Area, Washington, Open-File Report, U.S. Geological Survey, Tacoma, Washington.

Heath, R. C. and Trainer, F. W., 1968, Introduction to Groundwater Hydrology, John Wiley & Sons, Inc., New York, New York.

Hantush, M. S., 1960, "Modification of the Theory of Leaky Aquifers," Journal of Geophysical Research, Vol. 65, No. 11, pp. 3713-3726.

Hem, J. D., 1970, Study and Interpretation of Chemical Characteristics of Natural Water, Water-Supply Paper 1473, U.S. Geological Survey, Washington, D.C.

Hirasaki, G. J., 1974, "Pulse Tests and Other Early Transient Pressure Analyses for In Situ Estimation of Vertical Permeability," Transactions of 46th Annual Meeting, American Institute of Mining, Metallurgical and Petroleum Engineers, San Antonio, Texas, October 1972.

Hufen, T. H., 1974, A Geohydrologic Investigation of Honolulu's Basal Waters Based on Isotopic and Chemical Analyses of Water Samples, Ph. D. Dissertation, University of Hawaii, Honolulu, Hawaii.

Jones, R. W. and Ross, S. H., 1972, Moscow Basin Groundwater Studies, Pamphlet No. 153, Idaho Bureau of Mines and Geology, Boise, Idaho.

Kigoshi, K., 1971, "Alpha-Recoil Thorium-234: Dissolution into Water and the Uranium-234/Uranium-238 Disequilibrium in Nature," Science, Vol. 173, pp. 47-48.

Kigoshi, K., 1973, "Uranium-238/234 Disequilibrium and Age of Underground Water," International Atomic Energy Agency Panel on Application of Uranium Isotope Disequilibrium in Hydrology, Vienna, Austria, March 1973.

Kleck, W. D., 1976, Chemistry, Petrography, and Stratigraphy of the Columbia River Basalt Group in the Imnaha River Valley Region, Eastern Oregon and Western Idaho, Ph. D. Dissertation, Washington State University, Pullman, Washington.

Krauskopf, K. B., 1979, Introduction to Geochemistry, McGraw-Hill Book Company, New York, New York.

Kronfeld, J. and Adams, J. A. S., 1974, "Hydrologic Investigations of the Groundwaters of Central Texas Using U-234/U-238 Disequilibrium," Journal of Hydrology, Vol. 22, pp. 77-88.

Kronfeld, J., Gradsztajn, E., Muller, H. W., Radin, J., Yaniv, A., and Zach, R. R., 1975, "Excess ^{234}U: An Aging Effect in Confined Waters," Earth and Planetary Science Letters, Vol. 27, pp. 342-345.

Langmuir, D., 1971, "Eh-pH Determination," in Procedures in Sedimentary Petrology, Carver, R. E., ed., Wiley Interscience, New York, New York, pp. 597-635.

LaSala, A. M., Jr. and Doty, G. C., 1971, Preliminary Evaluation of Hydrologic Factors Related to Radioactive Waste Storage in Basaltic Rocks at the Hanford Reservation, Washington, Open-File Report, U.S. Geological Survey, Washington, D.C.

LaSala, A. M., Jr., Doty, G. C., and Pearson, F. J., Jr., 1972, A Preliminary Evaluation of Regional Groundwater Flow in South-Central Washington, Open-File Report, U.S. Geological Survey, Washington, D.C.

Leonhart, L. S., 1980, Assessment of the Effects of Existing Major Dams Upon a Radioactive Waste Repository Within the Hanford Site, RHO-BWI-LD-26, Rockwell Hanford Operations, Richland, Washington, June 1980.

Leonhart, L. S., Jackson, R. L., Graham, D. L., Thompson, G. M., and Gelhar, L. W., 1982, Groundwater Flow and Transport Characteristics of flood Basalt as Determined from Tracer Experiments, RHO-BW-SA-220 P, Rockwell Hanford Operations, Richland, Washington, September 15, 1982.

Libby, W. F., 1965, Radiocarbon Dating, University of Chicago Press, Chicago, Illinois.

Long, P. E., 1978, Characterization and Recognition of Intraflow Structures, Grande Ronde Basalt, RHO-BWI-LD-10, Rockwell Hanford Operations, Richland, Washington, September 1978.

Luzier, J. E. and Burt, R. J., 1974, Hydrology of Basalt Aquifers and Depletion of Groundwater in East-Central Washington, Water-Supply Bulletin 33, Washington State Department of Ecology, Olympia, Washington.

Luzier, J. E and Skrivan, J. A., 1973, Digital Simulation and Projection of Water-Level Declines in Basalt Aquifers of the Odessa-Lind Area, East-Central Washington, Water-Supply Paper 2036, U.S. Geological Survey, Washington, D.C.

Luzier, J. E., Bingham, J. W., Burt, R. J., and Barker, R. A., 1968, Groundwater Survey, Odessa-Lind Area, Washington, Water-Supply Bulletin 36, Washington State Division of Water Resources, Olympia, Washington.

MacNish, R. D. and Barker, R. A., 1976, Digital Simulation of a Basalt Aquifer System, Walla Walla River Basin, Washington and Oregon, Water-Supply Bulletin 44, Washington State Department of Ecology, Olympia, Washington.

McCray, K., 1980, "Cable Tool Drilling Today," Water Well Journal, February 1980, pp. 51-55.

McCray, K., 1981, "The Water Well Industry, A Study," Water Well Journal, January 1981, pp. 79-97.

McGhan, V. L. and Damschen, D. W., 1979, Hanford Wells, PNL-2894, Pacific Northwest Laboratory, Richland, Washington.

Mook, W. G., 1980, "Carbon-14 in Hydrogeological Studies," in Handbook of Environmental Isotope Geochemistry, Vol. 1 - The Terrestrial Environment, A, Fritz, P. and Fontes, J. C., eds., Elsevier, New York, New York, pp. 49-74.

Myers, C. W./Price, S. M., and Caggiano, J. A., Cochran, M. P., Czimer, W. J., Davidson, N. J., Edwards, R. C., Fecht, K. R., Holmes, G. E., Jones, M. G., Kunk, J. R., Landon, R. D., Ledgerwood, R. K., Lillie, J. T., Long, P. E., Mitchell, T. H., Price, E. H., Reidel, S. P., and Tallman, A. M., 1979, Geologic Studies of the Columbia Plateau: A Status Report, RHO-BWI-ST-4, Rockwell Hanford Operations, Richland, Washington, October 1979.

Myers, C. W. and Price, S. M., eds., 1981, Subsurface Geology of the Cold Creek Syncline, RHO-BWI-ST-14, Rockwell Hanford Operations, Richland, Washington, July 1981.

Myers, D. A., 1978, Environmental Monitoring Report on the Status of Groundwater Beneath the Hanford Site, January-December 1977, PNL-2624, Pacific Northwest Laboratory, Richland, Washington.

Myers, D. A., Fix, J. J., Plummer, P. J., Raymond, J. R., McGhan, V. L., and Hilty, E. L., 1976, Environmental Monitoring Report of Groundwater Beneath the Hanford Site, January-December 1975, BNWL-2034, Battelle, Pacific Northwest Laboratories, Richland, Washington.

Myers, D. A., Fix, J. J., and Raymond, J. R., 1977, Environmental Monitoring Report of Groundwater Beneath the Hanford Site, January-December 1976, BNWL-2119, Battelle, Pacific Northwest Laboratories, Richland, Washington.

Neuman, S. P. and Witherspoon, P. A., 1972, "Field Determination of the Hydraulic Properties of Leaky Multiple Aquifer Systems," Water Resources Research, Vol. 8, No. 5, pp. 1284-1298.

Newcomb, R. C., 1961, Storage of Groundwater Behind Subsurface Dams in Columbia River Basalt, Washington, Oregon and Idaho, Professional Paper 383-A, U.S. Geological Survey, Washington, D.C.

Newcomb, R. C., 1965, Geology and Groundwater Resources of the Walla Walla River Basin, Washington-Oregon, Water-Supply Bulletin 21, Washington State Division of Water Resources, Olympia, Washington.

Newcomb, R. C., 1972, Quality of the Groundwater in Basalt of the Columbia River Group, Washington, Oregon, and Idaho, Water-Supply Paper 1999-N, U.S. Geological Survey, Washington, D.C.

Newcomb, R. C., Strand, J. R., and Frank, F. J., 1972, Geology and Groundwater Characteristics of the Hanford Reservation of the U.S. Atomic Energy Commission, Washington, Professional Paper 717, U.S. Geological Survey, Washington, D.C.

Olsson, T., 1979, "Hydraulic Properties and Groundwater Balance in a Soil-Rock Aquifer System in the Jukton Area, Northern Sweden," Society Upsaliensis Pro Geologic Quaternia, Uppsala, Sweden, Striae 12.

Osmond, J. K., 1978, "Uranium and Thorium Activity Ratios Time Dependent Change in U-234/U-238 Alpha Activity Ratio (A.R.) Due to Recoil," Proceedings of Workshop on Dating Old Groundwater, David, S. N., ed., University of Arizona, Tucson, Arizona, pp. 112-114.

Osmond, J. K., 1980, "Uranium Disequilibrium in Hydrologic Studies," in Handbook of Environmental Isotope Geochemistry, Vol. 1 - The Terrestrial Environment, A, Fritz, P. and Fontes, J. C., eds., Elsevier, New York, New York, pp. 259-282.

Osmond, J. K. and Cowart, J. B., 1976, "The Theory and Uses of Natural Uranium Isotopic Variations in Hydrology," Atomic Energy Review, Vol. 14, pp. 621-679.

Pacific Northwest River Basins Commission, 1980, Irrigated Lands in the Pacific Northwest, Land Resources Committee of the Pacific Northwest River Basins Commission for the Depletions Task Force of the Columbia River Water Management Group, Vancouver, Washington.

Pearson, F. J., Jr., 1965, "Use of $^{13}C/^{12}C$ Ratios to Correct Radiocarbon Ages of Materials Initially Diluted by Limestone," in Proceedings of the 6th International Conference on Radiocarbon and Tritium Dating, Washington State University, Pullman, Washington, June 7-11, 1965, pp. 357-366.

Pearson, F. J., Jr. and Hanshaw, B. B., 1970, "Sources of Dissolved Carbonate Species in Groundwater and Their Effects on Carbon-14 Dating," Isotope Hydrology, International Atomic Energy Agency, Vienna, Austria, pp. 271-286.

Pearson, F. J., Jr. and Rightmire, C. T., 1980, "Sulphur and Oxygen Isotopes in Aqueous Sulphur Compounds," in Handbook of Environmental Isotope Geochemistry, Vol. 1 - The Terrestrial Environment, A, Fritz, P. and Fontes, J. C., eds., Elsevier, New York, New York, pp. 227-258.

Pearson, F. J., Jr. and Swarzenki, W. V., 1974, ^{14}C Evidence for the Origin of Arid Region Groundwater, Northeastern Province, Kenya, International Atomic Energy Agency, Vienna, Austria, pp. 95-109.

Pearson, F. J., Jr. and White, D. E., 1967, "Carbon-14 Ages and Flow Rates of Water in Carrizo Sand, Atascosa County, Texas," Water Resources Research, Vol. 3, pp. 251-261.

Plummer, L. N., Jones, B. F., and Truesdell, H. H., 1976, WATEQ-F, a Fortran IV Version of WATEQ, a Computer Program for Calculating Chemical Equilibrium of Natural Waters, Water Resources Investigation 76-13, U.S. Geological Survey, Washington, D.C.

Prats, M., 1970, "A Method for Determining the Net Vertical Permeability Near a Well from In Situ Measurements," Journal of Petroleum Technology, May, pp. 637-643.

Raghaven, R. and Clark, K. K., 1975, "Vertical Permeability from Limited Entry Flow Tests in Thick Formations," Transactions of 48th Annual Meeting, American Institute of Mining, Metallurgical, and Petroleum Engineers, Las Vegas, Nevada, September 1974.

Raymond, J. R., and Brown D. J., 1963, Groundwater Exchange with Fluctuating Rivers, HW-SA-3198, General Electric Company, Richland, Washington.

Raymond, J. R. and Tillson, D. D., 1968, Evaluation of a Thick Basalt Sequence in South-Central Washington, Geophysical and Hydrological Exploration of the Rattlesnake Hills Deep Stratigraphic Test Well, BNWL-776, Battelle, Pacific Northwest Laboratories, Richland, Washington.

Raymond, J. R., Myers, D. A., Fix, J. J., McGhan, V. L., and Shrotke, P. M., 1976, Environmental Monitoring Report on the Radiological Status of Groundwater Beneath the Hanford Site, January-December 1974, BNWL-1970, Battelle, Pacific Northwest Laboratories, Richland, Washington.

Reidel, S. P. and Fecht, K. R., 1981, "Wanapum and Saddle Mountains Basalts of the Cold Creek Syncline Area," in Myers, C. W. and Price, S. M., eds., Subsurface Geology of the Cold Creek Syncline, RHO-BWI-ST-14, Rockwell Hanford Operations, Richland, Washington, July 1981.

Reidel, S. P., Long, P. E., Myers, C. W., and Mase, J., 1981, New Evidence for Greater Than 3.2 Kilometers of Columbia River Basalt Beneath the Central Columbia Plateau, RHO-BWI-SA-162A, Rockwell Hanford Operations, Richland, Washington, September 1981.

Rightmire, C. T. and Hanshaw, B. B., 1973, "Relationship Between the Carbon Isotope Composition of Soil CO_2 and Dissolved Carbonate Species in Groundwater," Water Resources Research, Vol. 9, No. 4, pp. 958-967.

Rightmire, C. T., Pearson, F. J., Back, W., Rye, R. O., and Hanshaw, B. B., 1974, "Distribution of Sulfur Isotopes of Sulfate in Groundwaters from the Principal Artesian Aquifer of Florida and the Edwards Aquifer of Texas, U.S.A.," Proceedings of the Symposium on Isotope Techniques in Groundwater Hydrology, International Atomic Energy Agency, Vienna, Austria, pp. 191-207.

Robinson, J. H., 1971, Hydrology of Basalt Aquifers in the Hermiston-Ordinance Area, Umatilla and Morrow Counties, Oregon, Hydrologic Investigations Atlas HA-387, U.S. Geological Survey, Washington, D.C.

SAI, 1978, Hydrologic Testing in Borehole DC-2, RHO-BWI-C-36, Science Applications, Inc. for Rockwell Hanford Operations, Richland, Washington, September 11, 1978.

Savin, S. M., 1980, "Oxygen and Hydrogen Isotope Effects in Low-Temperature Mineral-Water Interactions," in Handbook of Environmental Isotope Geochemistry, Vol. 1 - The Terrestrial Environment, A, Fritz, P. and Fontes, J. C., eds., Elsevier, New York, New York, pp. 283-327.

Sceva, J. E., Watkins, F. A., Jr., and Schlax, W. N., Jr., 1949, Geology and Groundwater Resources of Wenas Creek Valley, Yakima County, Washington, Open-File Report, U.S. Geological Survey, Washington, D.C.

Siegenthaler, V. and Deschger, H., 1980, "Correlation of ^{18}O in Precipitation with Temperature and Altitude," Nature, Vol. 285, pp. 314-317.

Silar, J., 1969, Groundwater Studies and Ages in the Eastern Columbia Basin, Washington, Bulletin 315, College of Engineering, Washington State University, Pullman, Washington.

Smith, M. J., Anttonen, G. J., Barney, G. S., Coons, W. E., Hodges, F. N., Johnston, R. G., Kaser, J. D., Manabe, R. M., McCarel, S. C., Moore, E. L., Noonan, A. F., O'Rourke, J. E., Schulz, W. W., Taylor, C. L., Wood, B. J., and Wood, M. I., 1980, Engineered Barrier Development for a Nuclear Waste Repository Located in Basalt: An Integration of Current Knowledge, RHO-BWI-ST-7, Rockwell Hanford Operations, Richland, Washington, May 1980.

Spane, F. A., Jr., Howland, M. D., and Strait, S. R., 1980, Hydrogeologic Properties and Groundwater Chemistry of the Rattlesnake Ridge Interbed at Well 699-25-80 (DB-14), Hanford Site, RHO-LD-67, Rockwell Hanford Operations, Richland, Washington.

Stahl, W. J., 1980, "Compositional Changes and $^{13}C/^{12}C$ Fractionations During the Degradation of Hydrocarbons by Bacteria," Geochimica et Cosmochimica Acta, Vol. 44, pp. 1903-1907.

Stephan, J. G., Foote, H. P., and Coburn, V. L., 1979, Well Location and Land Use Mapping in the Columbia Plateau Area, RHO-BWI-C-61/PNL-3295, Pacific Northwest Laboratory for Rockwell Hanford Operations, Richland, Washington, October 1979.

Stiff, H. A., Jr., 1951, "The Interpretation of Chemical Water Analysis by Means of Patterns," Journal of Petroleum Technology, Vol. 3, No. 10, pp. 15-17.

Stone, W. A., Jenne, D. E., and Thorp, J. M., 1972, Climatology of the Hanford Area, BNWL-1605, Battelle, Pacific Northwest Laboratories, Richland, Washington.

Strait, S. R., 1978, Theoretical Analysis of Groundwater Flow in the Bickleton Area, Washington, M.S. Thesis, Washington State University, Pullman, Washington.

Strowd, W., 1978, Bibliography of Geologic Studies, Columbia Plateau (Columbia River Basalt) and Adjacent Areas in Idaho, RHO-BWI-C-44, Idaho Bureau of Mines and Geology for Rockwell Hanford Operations, Richland, Washington, November 1978.

Stumm, W. and Morgan, J. J., 1981, Aquatic Chemistry, 2nd ed., John Wiley & Sons, New York, New York.

Summers, W. K. and Schwab, G. E., 1978, Bibliography of the Geology and Groundwater of the Basalts of the Pasco Basin Washington, RHO-BWI-C-15, W. K. Summers and Associates for Rockwell Hanford Operations, Richland, Washington.

Summers, W. K., Weber, P. A., and Schwab, G. E., 1978, A Survey of the Groundwater Geology and Hydrology of the Pasco Basin, Washington, RHO-BWI-C-41, W. K. Summers and Associates for Rockwell Hanford Operations, Richland, Washington, October 1978.

Swanson D. A., Bentley, R. D., Byerley, G/ R., Gardner, J. N., and Wright, T. L., 1979, Preliminary Reconnaissance Geologic Maps of the Columbia River Basalt Group in Parts of Eastern Washington and Northern Idaho, Open-File Report 79-534, U.S. Geological Survey, Washington, D.C.

Swanson, D. A. and Wright, T. L., 1978, "Bedrock Geology of the Northern Columbia Plateau and Adjacent Areas," in Baker, V. R. and Nummedal, D., eds., The Channeled Scabland: Planetary Geology Program, A Guide to the Geomorphology of the Columbia Basin, Washington, Office of Space Science, National Aeronautics and Space Administration, Washington, D.C., pp. 37-57.

Tamers, M. A., 1967, "Surface-Water Infiltration and Groundwater Movement in Arid Zones of Venezuela," in Proceedings of the Symposium on Isotope in Hydrology, International Atomic Energy Agency, Vienna, Austria, pp. 339-351.

Tamers, M. A., 1975, "Validity of Radiocarbon Dates in Groundwater," Geophysical Surveys, Vol. 2, pp. 217-239.

Tamers, M. A. and Scharpenseel, H. W., 1974, Sequential Sampling of Radiocarbons in Groundwater, International Atomic Energy Agency, Vienna, Austria, pp. 241-257.

Tanaka, H. H. and Wildrick, L., 1978, Hydrologic Bibliography of the Columbia River Basalts in Washington, RHO-BWI-C-14, Washington State Department of Ecology for Rockwell Hanford Operations, Richland, Washington.

Tanaka, H. H., Barrett, G., and Wildrick, L., 1979, Regional Basalt Hydrology of the Columbia Plateau in Washington, RHO-BWI-C-60, Washington State Department of Ecology for Rockwell Hanford Operations, Richland, Washington, October 1979.

Tanaka, H. H., Hansen, A. J., Jr., and Skrivan, J. A., 1974, Digital-Model Study of Groundwater Hydrology, Columbia Basin Irrigation Project Area, Washington, Water-Supply Bulletin 40, Washington State Department of Ecology, Olympia, Washington.

Thompson, G. M., 1980, "Some Considerations for Tracer Tests in Low Permeability Formations," Proceedings of the Third Invitational Well-Testing Symposium, Lawrence Berkeley Laboratory, Berkeley, California, pp. 167-173.

Truesdell, A. H. and Jones, B. F., 1974, "WATEQ, A Computer Program for Calculating Chemical Equilibrium of Natural Waters," Journal of Research, U.S. Geological Survey, Vol. 2, No. 2, pp. 233-248.

Van Denburgh, A. S. and Santos, J. F., 1965, Groundwater in Washington; Its Chemical and Physical Quality, Water-Supply Bulletin 24, Washington Division of Water Resources, Olympia, Washington.

Vogel, J. C., 1970, Carbon-14 Dating of Groundwater, International Atomic Energy Agency, Vienna, Austria, pp. 225-237.

WAC, 1973, "Chapter 173-124 - Quincy Groundwater Management Subarea and Zones, Chapter 173-128 - Odessa Groundwater Management Subarea, Chapter 173-130 - Odessa Groundwater Subarea Management Policy, Chapter 173-134 - The Establishment of Regulations for the Administration of the Quincy Groundwater Subarea Established Pursuant to RCW 90.44.130, Chapter 173-160 - Minimum Standards for Construction and Maintenance of Water Wells, Chapter 508-14 - Columbia Basin Projects Groundrules," Washington Administrative Code, Olympia, Washington.

Walters, K. L. and Grolier, M. J., 1959, Records of Wells, Water Levels, and Quality of Groundwater in the Columbia Basin Project Area, Washington, Water-Supply Paper No. 8, Washington Division of Water Resources, Olympia, Washington.

9 2 1 2 4 9 5 1 1 3 9

Weast, R. C., ed., 1980, Handbook of Chemistry and Physics, 1980-1981, 61st ed., Chemical Rubber Company Press, Inc., Boca Raton, Florida, pp. B-258-B-342.

Webster, D. S., Proctor, J. F., and Marine, I. W., 1970, Two-Well Tracer Test in Fractured Crystalline Rock, Water-Supply Paper 1544-I, U.S. Geological Survey, Washington, D.C.

Wukelic, G. E., Foote, H. P., Blair, S. C., and Begej, C. D., 1981, Monitoring Land and Water-Use Dynamics in the Columbia Plateau Using Remote-Sensing Computer Analysis and Integration Techniques, RHO-BW-CR-122 P/PNL-4047, Pacific Northwest Laboratory for Rockwell Hanford Operations, Richland, Washington, September 1981.

Yurtsever, Y., 1975, "Worldwide Survey of Stable Isotopes in Precipitation," Proceedings of the Symposium on Isotopes in Hydrology, International Atomic Energy Agency, Vienna, Austria.

THIS PAGE INTENTIONALLY
LEFT BLANK